COMPRESSED GAS HANDBOOK

N69-26987
(ACCESSION NUMBER)
572
(PAGES)
(NASA CR OR TMX OR AD NUMBER)
(THRU)
1
(CODE)
12
(CATEGORY)
FACILITY FORM 602

NATIONAL AERONAUTICS AND SPACE ADMINISTRATION

N69-26987

CASE FILE
COPY

ERRATA

NASA Special Publication 3045

COMPRESSED GAS HANDBOOK

1969

Pages xi and 503 to 560:

Appendixes D, E, and F should be titled as follows:

Appendix D—Data on Helium
Appendix E—Data on Hydrogen
Appendix F—Data on Oxygen

Issue date: 6-20-69

NASA SP–3045

COMPRESSED GAS HANDBOOK

EDITED BY

JOHN S. KUNKLE
SAMUEL D. WILSON
RICHARD A. COTA

JOHN F. KENNEDY SPACE CENTER
KENNEDY SPACE CENTER, FLORIDA



Scientific and Technical Information Division
OFFICE OF TECHNOLOGY UTILIZATION
NATIONAL AERONAUTICS AND SPACE ADMINISTRATION
1969
Washington, D.C.

For sale by the Superintendent of Documents,
U.S. Government Printing Office, Washington, D.C. 20402

Price $4.75

Library of Congress Catalog Card No. 68–62085

TECH LIBRARY KAFB, NM
0063544

COMPRESSED GAS HANDBOOK

PREFACE

This handbook was developed to provide a complete source of the theory and data required to analyze high-pressure compressible flow systems found in space vehicle ground support equipment (GSE).

The material is presented in three sections: Theory, Part I; Application, Part II; and the Appendixes.

Part I develops the theoretical equations of fluid flow by derivation. This material is intended for those who have the time and desire to investigate the theory in depth. Practical problem solving is treated qualitatively.

Part II presents the theory without the supporting derivations and treats practical problems quantitatively. It is intended as a ready reference for analysis. A feature of this section is the inclusion of full-size working charts for the rapid solution of common compressible flow problems.

The Appendixes present a selection of basic thermodynamic data for the five gases of interest in GSE systems: Air, nitrogen, oxygen, helium, and hydrogen. The data range is as wide as possible for completeness, and special emphasis has been given to data up to 6000 psig, and from $+150°$ F to $-100°$ F.

Preceding Page Blank

ACKNOWLEDGMENTS

Appreciation is extended to the technical societies, research organizations, and manufacturers who contributed valuable data and knowledge used in the preparation of this book. Special thanks are due H. G. Zinsmeyer, A. E. Hand, and J. C. Hill for contributing much of their time and effort in the updating of the text.

J. S. KUNKLE

ABBREVIATIONS AND SYMBOLS

ABBREVIATIONS

Unit	*Description*	*Unit*	*Description*
abs	absolute	lb	pounds
atm	atmospheres	lbf	pound-force
Btu	British thermal units	lbm	pounds-mass
C	centigrade or Celsius	min	minutes
cal	calories	psia	pounds per square inch absolute
deg	degrees	psid	pounds per square inch differential
F	Fahrenheit	psig	pounds per square inch gage
ft	feet	R	Rankine
gal	gallons	rad	radians
g	grams	scfm	standard cubic feet per minute
gpm	gallons per minute	sec	seconds
in.	inches	slug	absolute mass unit
K	Kelvin	std	standard

SYMBOLS

Symbol	*Description*	*Units*	*Symbol*	*Description*	*Units*
A	Area	ft^2	c_a	actual velocity of sound	ft/sec
A'	Helmholtz function $(U-TS)$	Btu	c_0	velocity of sound at the stagnation temperature	ft/sec
A_e	flow area at the nozzle exit	ft^2			
A_t	flow area at nozzle throat	ft^2	c_p	specific heat at constant pressure	Btu/lbm-°R
A_w	wall surface area	ft^2			
a	flow area	$in.^2$	c_{pm}	molal specific heat at constant pressure	$Btu/mole_{lb}$-°R
a'	specific Helmholtz function	Btu/lbm			
B	dimensionless ratio, $(h_q A_w)/(w_1 c_r)$	dimensionless	c_r	specific heat at constant volume	Btu/lbm-°R
C	valve flow coefficient	$gpm_w/(psid)^{1/2}$	c_{rm}	molal specific heat at constant volume	$Btu/mole_{lb}$-°R
C'	partially open flow coefficient, as fraction of C_r	dimensionless			
			D	inside diameter of circular pipes, and hydraulic diameter for noncircular pipes	ft or in.
C_d	discharge coefficient	dimensionless			
C_0'	initial value of C', at displacement x_0	dimensionless			
C_{0*}	dimensionless ratio, $(W_c)w/(W_1)(c_r)$	dimensionless	d_o	equivalent sharp-edged orifice diameter, based on $K_c = 0.60$	in.
C_r	component flow coefficient	$gpm_w/(psid)^{1/2}$			
c	velocity of sound	ft/sec	E	total energy of a thermodynamic system	Btu
c^*	velocity of sound at the conditions where $M=1$	ft/sec			
			E_m	energy of a molecule	Btu

Symbol	Description	Units
e	unit total energy of a thermodynamic system or base of the natural logarithms	Btu/lbm dimensionless
F	force	lbf
F_c	combined NBS flow factor	scfm/psia or lbm/sec-psia
F_i	impulse function	lbf
F_q	NBS flow factor	scfm/psia
F_w	NBS flow factor	lbm/sec-psia
F_{wt}	weight force in earth gravity	lbf
F_{wx}	resultant of fluid force acting on the containing wall, in the opposite direction of flow	lbf
FE	flow energy	ft-lbf
f	coefficient of friction, from $\Delta P_L = f(L/D)(\rho V^2/2)$	dimensionless
$\bar{f}$	average coefficient of friction	dimensionless
f_τ	coefficient of friction from $\tau = f_\tau(\rho V^2/2)$, $f_\tau = f/4$	dimensionless
G	weight rate of flow per unit flow area, w/A	lbm/sec-ft^2
G'	Gibbs' function $(H - TS)$	Btu
GPM	volumetric flow rate	gal/min or gpm
g	acceleration due to gravity	ft/sec^2
g'	specific Gibbs' function	Btu/lbm
g_c	conversion factor relating absolute mass units (slugs) to the more commonly used weight units (lbm), $g_c = W/m = w/\dot{m} = \gamma/\rho = 32.174$	lbm/slug or ft-lbm/sec^2-lbf
H	total enthalpy	Btu
H_f	fluid static pressure head	ft
H_L or h_L	fluid pressure head loss due to friction and turbulence	ft
H_t	total fluid pressure head	ft
h	specific enthalpy	Btu/lbm
h_f	fluid static pressure head	in.
h_m	molal specific enthalpy	Btu/mole$_{lb}$
h_o	stagnation enthalpy	Btu/lbm
h_q	film coefficient of heat transfer	Btu/sec-ft^2-°R
J	mechanical energy equivalent to thermal energy, $J = 778.26$ ft-lbf/Btu	ft-lbf/Btu
K	incompressible component flow coefficient, from $\Delta P_L = K(\rho V^2/2)$	dimensionless
K'	constant of proportionality	variable
K_c	flow coefficient, $K_c = C_d/\sqrt{1 - B^4}$	dimensionless
K_t	total fluid pressure loss factor due to friction, turbulence, and area change	dimensionless
KE	kinetic energy	ft-lbf
k	specific heat ratio, $k = c_p/c_v$	dimensionless
k_s	isentropic exponent for real gases, from $Pv^{k_s} = \text{constant}$ ($k_s = k$ for perfect gas)	dimensionless
L	pipe length	ft
L_e	equivalent length of a piping component or system	ft
L_{max}	pipe length for sonic velocity at exit	ft
L/D	dimensionless pipe length based on pipe inside diameter	dimensionless
M	mach number, $M = V/c$	dimensionless
M^*	dimensionless velocity, $M^* = V/V^* = V/c^*$	dimensionless
M_w	molecular weight, $M_w = \bar{R}/R$	lbm/mole$_{lb}$
m	mass	slugs or lbf-sec^2/ft
$\dot{m}$	mass flow rate, $\dot{m} = w/g_c$	slugs/sec or lbf-sec/ft
N	number of moles of a gas	mole$_{lb}$ or mole$_{km}$
n	polytropic exponent	dimensionless
P	absolute pressure	lbf/ft^2 abs or psia
P_b	back pressure (absolute)	lbf/ft^2 abs
P_c	critical pressure of a gas	lbf/ft^2
P_e	exit pressure (absolute)	lbf/ft^2 abs
P'_e	pipe exit pressure that would occur with supersonic shockless flow	lbf/ft^2 abs
P_g	back pressure that causes a normal shock to stand in the exit, in supersonic pipe flow	lbf/ft^2 abs
P_L	pressure loss	lbf/ft^2 abs
P_r	reduced pressure (P/P_c)	dimensionless
P_t	total pressure	lbf/ft^2
PE	potential energy	ft-lbf
p	absolute pressure (static)	lbf/in.^{2} abs or psia

NOTE.—All subscripts and definitions shown above for P are applicable to p, which differs only in units.

Q	total heat transferred	Btu
Q'	heat transferred per unit mass	Btu/lbm
Q	rate of heat transfer	Btu/sec
q	volumetric flow rate	ft^3/sec

Symbol	*Description*	*Units*
R	individual gas constant, $R=\bar{R}/M_w$ (ft-lbf/mole$_{lb}$-°R)/(lbm/mole$_{lb}$)	ft-lbf/lbm-°R
$\bar{R}$	universal gas constant, $\bar{R}=1544$	ft-lbf/mole$_{lb}$-°R
R_e	Reynolds number, $R_e=DV\rho/\mu$	dimensionless
R_h	hydraulic radius, $R_h=A/$ wetted perimeter	ft
r	pressure ratio, $r=P_2/P_1=p_2/p_1$	dimensionless
S	total entropy	Btu/°R
S_A	specific gravity, based on air	dimensionless
S_w	specific gravity, based on 60° F water	dimensionless
SCFM	flow rate in standard cubic feet per minute	ft^3 std/min, or scfm
s	specific entropy	Btu/lbm-°R
T	absolute temperature (°F+460)	°R
T_c	critical temperature of a gas	°R
T_r	reduced temperature $T_r=(T/T_c)$	dimensionless
t	time	sec
U	total internal energy in a system (thermal)	Btu
u	specific internal energy	Btu/lbm
u_m	molal specific internal energy	Btu/mole$_{lb}$
V	velocity	ft/sec
$\bar{V}$	total volume	ft^3
v	specific volume, $v=1/\gamma$	ft^3/lbm
v_m	molar specific volume	ft^3/mole$_{lb}$
W	mass, in gravitational units	lbm
W_m	mass per mole	lbm/mole$_{lb}$
$(Wc)_w$	total thermal capacitance of the walls of a gas vessel	Btu/°R
Wk	mechanical work	ft-lbf
w	weight rate of flow	lbm/sec
wk	mechanical work per unit mass	ft-lbf/lbm
x	displacement or distance	ft
x_0	initial value of x, at $C'=C'_0$	dimensionless
Y_1	expansion factor for use with orifice flow	dimensionless
Y_a	expansion factor for use with nozzles or venturi tubes	dimensionless
y	distance measured perpendicular to flow direction	ft
Z	compressibility factor for a real gas, $Z=Pv/RT$	dimensionless
z	elevational distance	ft
α	linear acceleration, $\alpha=dV/dt$	ft/sec^2
β	diameter ratio, d_{throat}/d upstream pipe	dimensionless
Γ	compressibility of a fluid	
γ	weight density, $\gamma=1/v=g_c\rho$	lbm/ft^3
γ'	specific weight, $\gamma'=(g/g_c)\gamma$	lbf/ft^3
Δ	finite difference, or change, between two points or conditions	
δ	incremental quantity, such as thermal energy (δQ)	
ϵ	height of pipe wall roughness protuberances	ft
η	nozzle efficiency	dimensionless
θ	cone half angle	deg
μ	coefficient of absolute viscosity from $\tau=\mu(dV/dy)$	lbf-sec/ft^2
μ'	viscosity, $\mu'=\mu g_c=(6.72)(10^{-4}\ \mu_c)$	lbm/ft-sec
μ_c	viscosity in centipoise (100 g/cm-sec)	centipoise
μ_J	Joule-Thomson coefficient	ft^2-°R/lbf
ρ	mass density, $\rho=\gamma/g_c$	slugs/ft^3, or lbf-sec^2/ft^4
τ	fluid shear stress, $\tau=f_r(\rho V^2/2)$	lbf/ft^2
ν	kinematic viscosity, $\nu=\mu/\rho=\mu'/\gamma$	ft^2/sec
ϕ	mass flow parameter, $\phi=w/AP(\sqrt{RT/g_c})$	dimensionless
Ω	constant, PV/T	dimensionless
Ω_m	constant, $\Omega_m=Pv_m/T=\bar{R}$	ft-lbf/mole$_{lb}$-°R
ω	angular velocity	rad/sec
∞	infinity	

SUBSCRIPTS

Symbol	*Description*
0	stagnation state (where velocity is zero)
1	inlet or upstream conditions, unless otherwise specified
2	outlet or downstream conditions, unless otherwise specified
A	air at standard temperature (60° F)
a	conditions resulting from an actual process
aw	adiabatic wall conditions
b	bends
c	critical state
i	internal condition
in	conditions of entering fluid

Symbol	*Description*
J	nozzle throat conditions
L	loss
m	molal quantities
n	direction normal to the shock wave
o	overall
out	conditions of exiting fluid
P	direction parallel to the shock wave
r	reduced state (the ratio of a property to the value of that property at the critical state)
s	conditions resulting from an isentropic process
std	standard conditions of temperature (60° F) and pressure (14.7 psia)
t	total
W	water at standard temperature (60° F)
w	pipe-wall conditions
x	conditions upstream of a normal shock wave
y	conditions downstream of a normal shock wave
*	dimensionless ratio form, such as $T_* = T/T_1$ and $w_* = w/w_1$, referenced to the initial values T_1, W_1 and w_1
∞	ambient or outside condition
σ	properties of the enclosed system

SUPERSCRIPTS

Symbol	*Description*
*	conditions at the sonic point, or point of choking in adiabatic flow (where $M = 1.0$), excluding M^* which is defined otherwise
**	conditions at the point of choking in isothermal pipe flow (where $M = M^{**} = 1/\sqrt{k}$)

CONTENTS

CHAPTER		PAGE
	PART I — THEORY	
1	Fundamentals of Thermodynamics	3
2	Properties of Gases	23
3	Fundamentals of Incompressible Flow	51
4	Introduction to Compressible Flow	79
5	Adiabatic and Isentropic Flows	91
6	Shock Waves	115
7	Flow Measurement	135
8	Adiabatic Frictional Flow in Pipes	151
9	Nonadiabatic Flow in Pipes	181
10	Compressible Flow Through Components	201
11	Thermodynamics of Pressure Vessels	221
	PART II — APPLICATION	
12	Application of Fundamentals of Thermodynamics	237
13	Application of Properties of Gases	245
14	Application of Fundamentals of Incompressible Flow	273
15	Application of Compressible Flow	299
16	Application of Adiabatic and Isentropic Flows	307
17	Application of Shock-Wave Theories	325
18	Methods of Flow Measurement	343
19	Application of Adiabatic Frictional Flow in Pipes	359
20	Application of Nonadiabatic Flow in Pipes	405
21	Application of Compressible Flow Through Components	419
22	Application of Thermodynamics of Pressure Vessels	431
	Appendix A — General Engineering Data	449
	Appendix B — Data on Air	469
	Appendix C — Data on Nitrogen	485
	Appendix D — Data on ~~Oxygen~~ Helium	503
	Appendix E — Data on ~~Helium~~ Hydrogen	521
	Appendix F — Data on ~~Hydrogen~~ Oxygen	545

PART I

THEORY

CHAPTER 1

FUNDAMENTALS OF THERMODYNAMICS

Thermodynamics encompasses a broad field and is pertinent to many facets of science; this presentation, however, is primarily concerned with the thermodynamics of gases.

"Thermodynamics" is defined as "the science that treats the mechanical action or relations of heat." According to this definition, thermodynamics deals with heat and those properties of a substance that bear a relation to heat.

The study of thermodynamics is based on certain observed principles designated as the first and second laws of thermodynamics. A full understanding of these laws is basic to an understanding of thermodynamic fundamentals. These laws are presented in this chapter, preceded by definitions of the basic thermodynamic terms. A clear understanding of these terms is absolutely necessary for an understanding of subsequent material on this subject.

DEFINITION OF TERMS

Thermodynamic System

For processes involving the transfer of energy from one location to another, it is necessary to define the boundaries of these locations. One of the locations is known as the system. The system is the portion of the universe to be examined; it may be arbitrarily selected to include any portion of the universe.

This definition of a system permits a system as large or as small as the investigator desires. However, systems with sizes approaching the dimensions of the mean free path of the molecules of the substance call for special treatment and encompass the field of quantum mechanics. Since most engineering analyses are for the purpose of analyzing the gross behavior of a substance and not that of the individual molecules, the fiction of a continuous substance, or continua, is used throughout this text. The assumption of continua is valid as long as the system volume is sufficient to represent the actions of the substance and not the individual molecules which comprise the substance.

As an illustration of a thermodynamic system, consider the classical example of a gas in a cylinder fitted with a frictionless piston. If an additional weight is placed on top of the piston, the gas will be further compressed, and the weight and piston will fall to a lower position in the cylinder. If the room containing the apparatus is arbitrarily defined as the system, there has been no transfer of energy between the system and the rest of the universe. However, if the gas contained in the cylinder is selected as the system, an exchange of energy has occurred.

Preceding Page Blank

There are two types of systems considered in thermodynamics: the closed and open systems. The closed system is defined as a system that allows heat and work, but not mass, to cross the system boundary. The open system is one in which work, heat, and mass may pass the system boundary.

As stated previously, the choice of the system is arbitrary. However, the choice is an important one, since it may determine whether or not a given problem can be adequately analyzed.

Surroundings

When the system boundary has been established, the remainder of the universe is designated as the surroundings.

Thermodynamic State

A thermodynamic system always possesses a definite state. The state of the system is related to, or is determined by, the properties of the system. Properties of a system may be grouped in two general categories known as extensive properties and intensive properties. Extensive properties are functions of the amount of material or matter within the system, and intensive properties are independent of the amount of material in the system. For example, temperature, pressure, and specific volume are intensive properties, but total volume and total energy are extensive properties.

A stable system cannot be assigned arbitrary values for any number of intensive properties. For example, a pure gas such as nitrogen cannot exist at any temperature, pressure, and specific volume in a stable state. When the pressure and temperature have been chosen, the specific volume is no longer a free variable; that is, it has a definite value determined by the pressure and temperature selected. Gibbs' phase rule enables one to predict the number of intensive properties that must be specified in order to fix the state of a system. The phase rule may be stated as

$$P' + V' = G' + 2$$

where P' is the number of phases, V' the number of variants (or the number of intensive variables that must be specified before the state of a system is completely fixed), and G' the number of components. Hence, if the system is a single gas, the phase rule indicates that two intensive properties must be known to determine the state of the system. If two intensive properties, such as pressure and temperature, are specified, then all other intensive properties are invariant. As another illustration of the phase rule, stipulate that two phases of a single-component system are in equilibrium, such as liquid water and water vapor. One intensive property, such as temperature, is sufficient to determine all other intensive properties and, therefore, determine the state of the liquid-vapor system.

Property and State

Considering a given mass, a substance such as water may exist in many states. For each state there is a specific value for each property, one or more of which must change for a change in state. Properties are dependent on the state only and thereby are entirely independent of the process, or path, by which the state was obtained. In fact, a property may be defined as any quantity that is dependent on the state only.

Process

When a change in the thermodynamic properties of a system occurs, the state of the system changes from some initial state to the final state. Between these two extremes, there in an infinite number of states through which the system passes. The path traced by these intermediate states is termed the "thermodynamic process." If a system passes from an initial state through a succession of processes and reaches a final state identical to the initial state, the system has undergone a thermodynamic cycle.

Processes are often described by the fact that some thermodynamic property is held constant. Hence, an adiabatic process is one in which there is no heat transfer to or from the system. In practice, this process is approximated when the system is thermally isolated from the surroundings or when heat transfer is negligible because of a short time duration.

The isothermal process is one in which the system temperature is constant. This process is approximated in long pipelines where fluid flow rates, heat-transfer area, and heat-transfer time are such as to maintain an essentially constant fluid temperature; that is, near that of the surroundings.

The constant-volume process is a process occurring at constant system volume. An example of a constant-volume process is the heating or cooling of a gas in a storage bottle.

The constant-pressure process is a process in which system pressure is invariant. An example of this is a process in which a gas is heated in a cylinder fitted with a frictionless piston which is permitted to slide freely against a constant force.

There are two other process descriptions of a different nature from those above that need mention here: these are the quasi-static process and the reversible process. The quasi-static process is any process in which each state attained during the process is an equilibrium state. The reversible process may be defined as any process which can be carried to completion, reversed, and carried in the opposite direction back to the initial state and leave no change in system or surroundings. It can be shown that for a process to be reversible, each state must be an equilibrium state. Hence, the reversible process is also quasi-static.

Pure Substance

A pure substance may be defined as any substance with an invariant chemical composition. A substance such as water, therefore, is a pure substance, since the chemical composition is the same if the water exists as a vapor, a liquid, or a solid, or any mixture of the three. On the other hand, a substance such as air is not a pure substance, since the chemical composition will vary in a mixture of the gaseous and liquid phases. However, gaseous air exhibits many of the characteristics of a pure substance, and when no phase change is involved it can be treated as such.

As has been shown by the Gibbs' phase rule, two intensive properties are necessary to specify the state of a single phase of a pure substance. In general, then, two intensive properties, such as pressure and temperature, can be chosen as independent variables in terms of which the state and all other system properties can be defined.

Pressure Scale

The pressure on a system is defined as the force acting on the system divided by the area over which the force is in effect. If the force is measured in the gravitational unit of pounds and the area in square inches, the units of pressure are pounds per square inch (psi).

Fluid pressure is generally designated as pounds per square inch absolute (psia) or pounds per square inch gage (psig). Pressure in psig plus atmospheric pressure equals pressure in psia.

Frequently, pressures are measured in terms of the height of a column of fluid under the influence of gravity. The pressure corresponding to the weight exerted by a column of fluid will be numerically equal to the product of the height and the weight density of the fluid in a standard Earth gravity field. More exactly,

$$\Delta P = \left(\frac{g}{g_c}\right) \gamma \Delta z = \delta' \Delta z$$

Absolute pressure measurements are based on a zero reference point, the perfect vacuum. Measured from this reference, the standard atmospheric pressure at sea level is approximately 14.7 psi; however, local pressures may deviate from this standard value because of weather conditions and distance above sea level. Figure 1.1 shows graphically the relation of the various pressure terms.

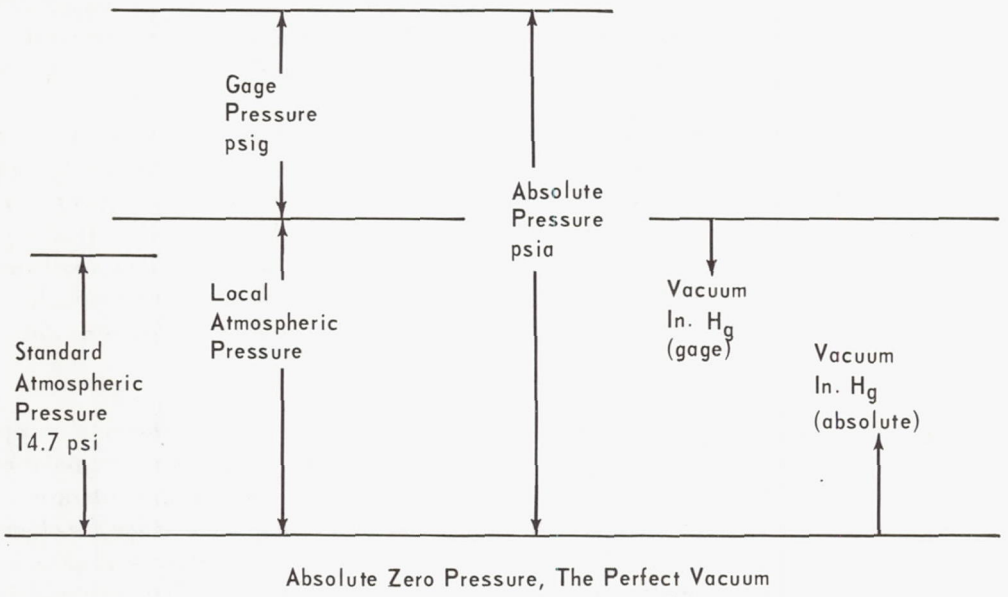


Figure 1.1. Diagram showing relation of pressure terms.

Temperature Scale

The temperature of a system is a much more difficult concept to define than pressure. Although pressure can be measured in definite units of force per unit area, temperature must be measured indirectly through its effect on the physical properties of a chosen material. Physically, temperature is an indication of the kinetic energy of molecules. It is sensed as the degree of hotness or coldness of a substance measured by arbitrary scales set up according to reference conditions. Probably the most frequently used device is based on the effect of temperature on the volume of a given quantity of liquid mercury.

To establish a numerical scale of temperature by this method, it is first necessary to decide on the increase in mercury volume (or length of column if the cross-sectional area is constant), which is to be chosen equal to a unit rise in temperature, commonly called a degree. This is an entirely arbitrary choice. The usual one is to consider the difference in length of the mercury column when the thermometer is placed in ice water and then in boiling water, maintained at standard atmospheric pressure, as equivalent to 100° C or 180° F. Any other temperature, in °C, is then defined by the following linear relation between the temperature and the length of the mercury column:

$$T\ (°\mathrm{C}) = 100\left(\frac{L - L_0}{L_{100} - L_0}\right)$$

where

L = length of mercury column at T° C
L_0 = length of mercury column at 0° C
L_{100} = length of mercury column at 100° C

Variations in physical properties other than the expansion of liquid mercury may be employed as a medium for measuring the effects of temperature. Among the properties that have been used are the following:

(1) Vapor pressure of liquids
(2) Electrical resistance of metals
(3) Electromotive force (emf) produced as a result of a junction of two dissimilar metals (thermocouple)
(4) Volume expansion of gases

The variation of the physical properties with temperature is not linear in all cases, although the temperature scales are constructed as linear subdivisions between any two reference temperatures, such as the difference between the freezing and boiling points of water. Therefore, thermometer accuracy at any other point will vary depending on the linearity of the physical properties used as the basis of the thermometer.

Hence, it is apparent that all the common methods of measuring temperature depend on evaluating the effect of temperature on the physical properties of materials, and that the temperature scale will vary with the physical property and the material used in the thermometer. A scale which is independent of the properties of the materials employed in the measuring devices, that is, a thermodynamic or absolute scale, would be desirable. The second law of thermodynamics, which is discussed later, provides the basis for establishing such a temperature scale. The international temperature scale, which has been found to be the closest approximation to the absolute or thermodynamic scale, is based on the following measuring devices:

− 190° to 660° C − platinum resistance thermometer
660° to 1063° C − platinum-rhodium thermocouple
Above 1063° C − optical pyrometer

It has been found that the temperature scale necessary to reconcile the pressure-volume-temperature (P–v–T) relationship of a perfect gas is identical with the thermodynamic temperature scale; that is, the temperature T in the perfect-gas equation of state $Pv = RT$ is

identical with the thermodynamic temperature. Although there is no truly perfect gas, many gases approach this behavior so that the gas thermometer may be used to approach closely the absolute thermodynamic temperature. In using the perfect-gas thermometer, the pressure and volume of a definite quantity of gas are measured. Then, according to the perfect-gas law, the product of these two quantities is directly proportional to the absolute temperature.

Heat

Another method of approach to the concept of temperature is to consider it as a potential for transferring energy, just as voltage is a potential for transferring energy by an electrical process. From experience, it is known that a hot body brought into contact with a cold body becomes cooler and the cold body warmer. This is a result of the transfer of heat between the two bodies. The rate of heat transfer depends on the temperature difference between the two bodies; when there is no difference in temperature, there is no transfer of energy. Therefore, "heat" can be defined as thermal energy transferred from one body to another as a result of a temperature difference. It is important to note that none of the energy stored in a body can be called heat. Only when there is a transfer of energy from one body to another does the term "heat" have any significance. Hence, heat is not a property of a body or system. The effect of the transfer of energy as heat to a system is commonly measured in terms of the change in properties of the system.

Work

In a general way, "work" may be defined as the product of a potential, or force, and an amplitude factor. If the force is mechanical and the amplitude factor is the distance through which the force operates, the result is mechanical work.

Like heat, work is energy that is transferred from one body to another. However, in the case of work, the potential involved is a force, or pressure, instead of temperature. As an illustration, consider the compression of a gas in a cylinder by the movement of a piston. The compression is accomplished by the application of a force to the piston, and this results in a transfer of energy from the piston rod to the gas. The energy so transferred is work in the thermodynamic sense. Work is not a property of a system, but is frequently measured in terms of its effect on the system properties. In the compression process just discussed, at least a portion of the work becomes a part of the internal energy of the gas and changes the value of that property of the system.

Since work results in a transfer of energy, it is associated with a source and an acceptor. Also, the work effects may take many forms, such as changes in potential energy, kinetic energy, and internal energy.

The mechanical work accompanying the change in volume of a fluid is by far the most important type that occurs in engineering thermodynamics. Work may be expressed in differential form as

$$\mathrm{d}Wk = F\ \mathrm{d}x$$

where F is the force and x is the distance through which the force acts. Since the pressure of the fluid is equal to the force divided by the area, the equation for work may be written

$$\mathrm{d}Wk = P\ \mathrm{d}\bar{V}$$

where $d\bar{V}$ is the change in volume. This is the general expression for the work done as a result of a differential expansion or compression process. It is written in differential form because the pressure may vary as the volume changes. If there is no change in volume, there can be no expansion work. However, if there is no change in pressure, the work is simply the pressure times the change in volume.

ZEROTH LAW OF THERMODYNAMICS

Practical applications of thermometry hinge on the assumption that two bodies, respectively, equal in temperature to a third body must also be equal in temperature to each other. Fortunately, this assumption is amply verified by innumerable experiments. It is sometimes called the zeroth law of thermodynamics.

FIRST LAW OF THERMODYNAMICS

The first law of thermodynamics is a statement of the often-proved principle of conservation of energy. For a system of constant mass (the closed system) undergoing a cycle, the first law may be stated thus: The amount of work done on or by a system is equal to the amount of heat transferred to or from the system. Mathematically, this is expressed

$$\oint \delta Q = \oint \delta Wk$$

where δ represents the differential form of a path-dependent function of which heat and work are examples.

Regarding the above equation, the units generally used for the quantity δQ are Btu's while ft-lbf's are generally used for the quantity δWk. Hence, for this equation to be dimensionally correct, it is necessary to introduce the quantity J, Joule's constant, which is the mechanical energy equivalent to thermal energy.

$$J = 778.26 \qquad \text{ft-lbf/Btu}$$

Hence, the previous equation written in dimensionally correct units becomes

$$\oint \delta Q = \frac{1}{J} \oint \delta Wk \tag{1.1}$$

General Statement for the Closed System

To extend the definition of the first law to a closed system undergoing a process as opposed to a cycle, consider two cycles consisting of processes A, B, and C. Cycle 1 consists of process A, which carries the system from state 1 to state 2, followed by process B, which completes the cycle along a different path (fig. 1.2). Cycle 2 consists of the same initial process A, but the process completing the cycle is along a third path C.

For cycle 1 the first law may be written

$$\oint \delta Q = \int_{1A}^{2A} \delta Q + \int_{2B}^{1B} \delta Q = \frac{1}{J} \oint \delta Wk$$

$$= \frac{1}{J} \int_{1A}^{2A} \delta Wk + \frac{1}{J} \int_{2B}^{1B} \delta Wk$$

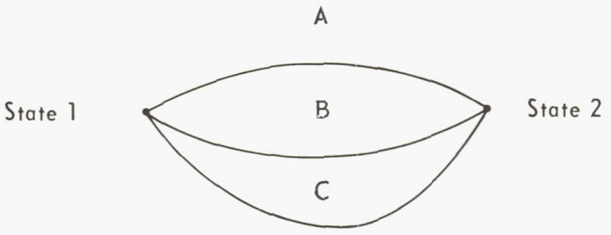


Figure 1.2. Diagram of two thermodynamic cycles with a common process.

Also for cycle 2

$$\int_{1A}^{2A} \delta Q + \int_{2C}^{1C} \delta Q = \frac{1}{J}\int_{1A}^{2A} \delta Wk + \frac{1}{J}\int_{2C}^{1C} \delta Wk$$

Since for the common process A, the integrals of δWk and δQ are equal, combining and rearranging the two equations yield

$$\int_{2B}^{1B} \delta Q - \frac{1}{J}\int_{2B}^{1B} Wk = \int_{2C}^{1C} \delta Q - \frac{1}{J}\int_{2C}^{1C} \delta Wk$$

and on integrating

$${}_2Q_1\Big|_B - \left(\frac{1}{J}\right){}_2Wk_1\Big|_B = {}_2Q_1\Big|_C - \left(\frac{1}{J}\right){}_2Wk_1\Big|_C$$

Since processes B and C are general processes, it may be concluded that the quantity $[{}_2Q_1 - (1/J)\ {}_2Wk_1]$ is independent of the path and is dependent on the state only. Hence, $[{}_2Q_1 - (1/J\ {}_2Wk_1]$ is a thermodynamic property and is called the total energy E. It follows that for the closed system undergoing a change of state, the first law may be written

$$dE_\sigma = \delta Q - \left(\frac{1}{J}\right)\delta Wk \tag{1.2}$$

This equation points out that for a closed system undergoing a change of state, the net change in the total system energy is equal to the algebraic difference between the heat transfer and the work performed.

It should be pointed out here that the convention used in this handbook regarding heat and work is to consider heat transferred to a system as positive and heat transferred from a system as negative; on the other hand, work done by a system is positive and work done on a system is negative.

General Statement for the Open System

The first law expression for the open system (one which allows mass to pass through the system boundary) may be established by considering the system shown in figure 1.3.

An amount of mass, W_{in}, enters the system and the amount, W_{out}, leaves the system. Also, the system receives an amount of heat, δQ, and does the amount of work, δWk. For these conditions, the energy change of the system, designated E_σ, is given by

$$dE_\sigma = dW_{in}e_{in} - dW_{out}e_{out} + \delta Q - \frac{1}{J}(\delta Wk - P_{in}\, d\bar{V}_{in} + P_{out}\, d\bar{V}_{out}) \tag{1.3}$$

where the symbols e_{in} and e_{out} refer to the specific energy of the mass entering and leaving the system, respectively. The $P\, d\bar{V}$ terms are flow-energy terms and will be explained here.

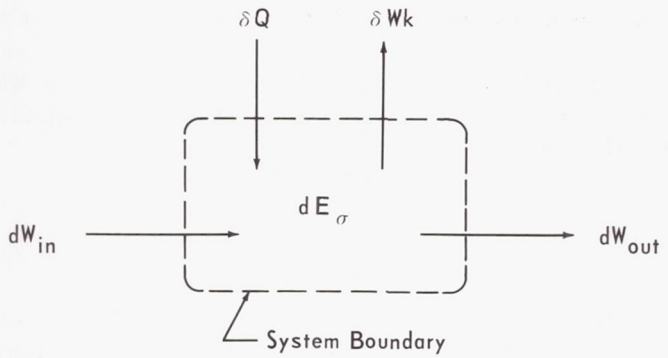


Figure 1.3. Open system with heat transfer and work being done.

Flow Energy

The energy of a system is increased or decreased as the result of fluid crossing the boundary of the system. Consider the system of figure 1.4. In order to move the mass of fluid, dW, through the pipe and past the system boundary, it is necessary to do an amount of work.

$$dWk = F\, dx = \left(\frac{F}{A}\right) A\, dx$$

It follows that the work done in moving the mass dW past the system boundary is given also by

$$dWk = P\, d\bar{V}$$

As a consequence, when the mass moves through the system boundary, the system's energy is altered by the amount $P\, d\bar{V}$. Flow energy then is the energy transmitted to a system by virtue of mass crossing the system boundary.

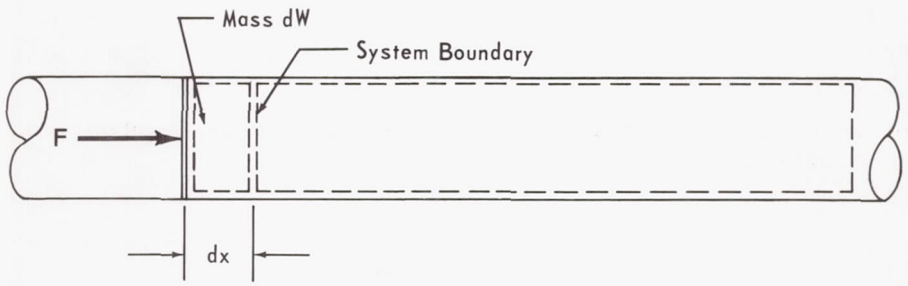


Figure 1.4. System energy is increased as a result of mass entering the system.

It is important to note that the flow energy depends on matter crossing the system boundary. Therefore, for a system which allows no matter to cross its boundary, the product $P\,d\bar{V}$, although it may be calculated, does not represent an energy term for the system.

Equation (1.3) is the general expression of the first law of thermodynamics for an open system undergoing a change of state. However, in its present form, the equation is not particularly useful because of the ambiguity of the quantities E_σ and e. For this reason, it is desirable to find expressions for the component parts that make up the total quantities E_σ and e.

In thermodynamic analysis of open systems it is most convenient to think of the quantity E_σ as being made up of three component parts: kinetic energy, KE; potential energy, PE; and internal energy, U. Mathematically,

$$E_\sigma = \frac{KE}{J} + \frac{PE}{J} + U$$

Kinetic Energy

Kinetic energy is energy a substance possesses as a result of the motion of the substance. An expression for kinetic energy may be obtained by equating it to the work done in changing the velocity of a mass, W.

$$\begin{aligned} d(KE) = d(Wk) = F\,dx &= \left(\frac{W}{g_c}\right)\alpha\,dx \\ &= \left(\frac{W}{g_c}\right)\left(\frac{dV}{dx}\right)\left(\frac{dx}{dt}\right)dx \\ &= \left(\frac{W}{g_c}\right)V\,dV \end{aligned}$$

This expression may be integrated from zero velocity to obtain

$$KE = \frac{WV^2}{2g_c}$$

Potential Energy

Potential energy is the energy a mass possesses as a result of elevation above some arbitrary datum elevation. An expression for potential energy may be obtained by equating it to the work required to raise w an incremental height dz against a gravitional acceleration, g, with no change in kinetic energy.

$$d(PE) = dWk = \left(\frac{g}{g_c}\right)W\,dz$$

This equation can be integrated from a value of $z=0$ at the datum elevation to any height z above the datum to obtain

$$PE = \left(\frac{g}{g_c}\right)Wz$$

Internal Energy

At this point, all the energy terms generally considered in thermodynamic analysis have

been discussed except internal energy. This implies that internal energy can consist of all forms of energy within a system other than kinetic, potential, and flow energies. Internal energy may consist, then, of energy associated with the movement and position of gas molecules, chemical energy such as is present in a storage battery, energy present in a charged condenser, or a number of other forms.

Internal energy is an extensive property of a fluid and is given the symbol U. In the absence of electrical, magnetic, and surface effects, the internal energy along with one other independent property will specify the state of a pure substance.

Enthalpy

This is an energy term defined as the sum of U and the product $P\bar{V}$.

$$H = U + \frac{P\bar{V}}{J}$$

Since internal energy and the product $P\bar{V}$ are dependent on the state only, it follows that enthalpy is a state-dependent function and, therefore, is a thermodynamic property. Because enthalpy is a function of flow work, it represents a useful energy term for the open system only.

Working Equations

Having defined all the components of the quantity E_σ, it is possible to rewrite the first law in more useful terms. Considering the closed system, the first law may be written

$$dE_\sigma = \delta Q - \frac{\delta Wk}{J}$$

or

$$dU + d\left(\frac{WV^2}{2g_cJ}\right) + \left(\frac{g}{g_cJ}\right) W\, dz = \delta Q - \frac{\delta Wk}{J}$$

In terms of specific quantities

$$W\left[du + d\left(\frac{V^2}{2g_cJ}\right) + \left(\frac{g}{g_cJ}\right) dz\right] = \delta Q - \frac{\delta Wk}{J}$$

or on integrating

$$W\left[(u_2 - u_1) + \frac{V_2^2 - V_1^2}{2g_cJ} + \frac{g}{g_cJ}(z_2 - z_1)\right] = {}_1Q_2 - \left(\frac{1}{J}\right){}_1Wk_2 \tag{1.4}$$

For the open system the first law is written

$$dE_\sigma = \delta Q - \frac{1}{J}(\delta Wk + P_{out}\, dV_{out} - P_{in}\, dV_{in}) + dW_{in}e_{in} - dW_{out}e_{out}$$

or, noting that $e_{in} = \dfrac{E_{in}}{W_{in}} = \dfrac{V_{in}^2}{2g_cJ} + \dfrac{gz_{in}}{g_cJ} + u_{in}$ and that $u_{in}\, dW_{in} = dU_{in}$

$$\mathrm{d}\left[U+\frac{WV^2}{2g_cJ}+\left(\frac{g}{g_c}\right)\frac{Wz}{J}\right]_\sigma=\delta Q-\frac{1}{J}\left(\delta Wk+P_{\text{out}}\,\mathrm{d}\bar{V}_{\text{out}}-P_{\text{in}}\,\mathrm{d}\bar{V}_{\text{in}}\right)$$
$$+\left[\mathrm{d}U_{\text{in}}+\frac{\mathrm{d}W_{\text{in}}V_{\text{in}}^2}{2g_cJ}+\left(\frac{g}{g_cJ}\right)\mathrm{d}W_{\text{in}}z_{\text{in}}\right]$$
$$-\left[\mathrm{d}U_{\text{out}}+\frac{\mathrm{d}W_{\text{out}}V_{\text{out}}^2}{2g_cJ}+\left(\frac{g}{g_cJ}\right)\mathrm{d}W_{\text{out}}z_{\text{out}}\right]$$

Rewriting in terms of specific quantities, noting that $\mathrm{d}\bar{V}=v\,\mathrm{d}W$,

$$\mathrm{d}\,(W_\sigma e_\sigma)=\mathrm{d}\left[Wu+\frac{WV^2}{2g_cJ}+\left(\frac{g}{g_cJ}\right)Wz\right]_\sigma$$
$$=\delta Q-\frac{\delta Wk}{J}+\mathrm{d}W_{\text{in}}\left[u_{\text{in}}+\frac{P_{\text{in}}v_{\text{in}}}{J}\right.$$
$$\left.+\frac{V_{\text{in}}^2}{2g_cJ}+\left(\frac{g}{g_cJ}\right)z_{\text{in}}\right]-\mathrm{d}W_{\text{out}}\left[u_{\text{out}}+\frac{P_{\text{out}}v_{\text{out}}}{J}\right.$$
$$\left.+\frac{V_{\text{out}}^2}{2g_cJ}+\left(\frac{g}{g_cJ}\right)z_{\text{out}}\right]$$

For a transient flow problem, this equation must be solved repeatedly for small time increments. When the input and output weight-flow quantities are continuous flow processes with relatively constant specific energy, e, the energy equation can be written as a quasi-steady-state equation

$$\frac{\mathrm{d}}{\mathrm{d}t}\left\{W\left[u+\frac{V^2}{2g_cJ}+\frac{g}{g_cJ}(z)\right]\right\}_\sigma=\dot{Q}-\frac{\dot{W}k}{J}$$
$$+w_{\text{in}}\left[u_{\text{in}}+\frac{P_{\text{in}}v_{\text{in}}}{J}+\frac{V_{\text{in}}^2}{2g_cJ}+\frac{g}{g_cJ}(z_{\text{in}})\right]$$
$$-w_{\text{out}}\left[u_{\text{out}}+\frac{P_{\text{out}}v_{\text{out}}}{J}+\frac{V_{\text{out}}^2}{2g_cJ}+\frac{g}{g_cJ}(z_{\text{out}})\right]$$

where

$$\dot{Q}=\frac{\delta Q}{\mathrm{d}t}\qquad \dot{W}k=\frac{\delta Wk}{\mathrm{d}t}\qquad w=\frac{\mathrm{d}W}{\mathrm{d}t}$$

Note that since W_{in} can be different from W_{out}, the mass of fluid, W_σ, enclosed in the system can be a variable.

If the flow rate and state of the fluid at any point in the system do not vary with time, and if the rate of heat transfer and work done do not vary with time, the flow is a steady flow, and

$$\frac{\mathrm{d}}{\mathrm{d}t}\,(We)_\sigma=W_\sigma\left(\frac{\mathrm{d}e_\sigma}{\mathrm{d}t}\right)+e_\sigma\left(\frac{\mathrm{d}W_\sigma}{\mathrm{d}t}\right)=0$$

and

$$w_{\text{in}}=w_{\text{out}}=w$$

Then

$$\frac{\dot{Q}}{w}+u_{\text{in}}+\frac{P_{\text{in}}v_{\text{in}}}{J}+\frac{V_{\text{in}}}{2g_cJ}+\frac{g}{g_cJ}\,(z_{\text{in}})=\frac{\dot{W}k}{wJ}+u_{\text{out}}+\frac{P_{\text{out}}v_{\text{out}}}{J}+\frac{V_{\text{out}}^2}{2g_cJ}+\frac{g}{g_cJ}\,(z_{\text{out}})$$

since

$$\dot{Q}=\frac{\delta Q}{\mathrm{d}t} \qquad \text{and} \qquad w=\frac{\mathrm{d}W}{\mathrm{d}t}$$

$$\frac{\dot{Q}}{w}=\frac{\delta Q}{\mathrm{d}W}=Q' \qquad \text{and} \qquad \frac{\dot{W}k}{Jw}=\frac{\delta Wk}{J\mathrm{d}W}=\frac{wk}{J}$$

The quantities Q' and wk are the heat added to the system and work done by the system per unit weight flow through the system. Substituting this and the definition of specific enthalpy, $h=u+Pv/J$, yields the steady-flow energy equation in terms of the specific or intensive properties

$$Q'+\left[h+\frac{V^2}{2g_cJ}+\frac{g}{g_cJ}\,(z)\right]_{\text{in}}=\frac{wk}{J}+\left[h+\frac{V^2}{2g_cJ}+\frac{g}{g_cJ}\,(z)\right]_{\text{out}} \tag{1.5}$$

SECOND LAW OF THERMODYNAMICS

Before considering the second law of thermodynamics, recall that the first law places no limitation on the efficiency of energy conversion or the direction in which a natural process will occur. The first law is said to be a denial of the possibility of creating a perpetual-motion machine of the first kind. That is, it is impossible to construct a device that will produce useful work with no energy input. Note that a process which consists only of the transfer of heat from a cold source to a hot sink is a valid process according to the first law. However, we know from observation that this process is not valid. For instance, a hot cup of coffee cools in the cooler environment; it never becomes warmer. This directional property of natural processes is the essence of the second law of thermodynamics. In a broader sense, the second law is a denial of the possibility of a perpetual-motion machine of the second kind. This is a machine which, when operating in a cycle, converts all the heat it receives into useful work.

The basis for the second law was established by Sadi Carnot in 1824. Carnot, through the fiction of a reversible cycle, determined that no heat engine could operate with a thermal efficiency of 100 percent. Further, Carnot showed that the thermal efficiency of the reversible ideal heat engine operating in a cycle between given temperature limits was independent of the working fluid and was dependent only on the temperature limits between which the reversible heat engine operated.

This last statement concerning thermal efficiency is very important in the field of thermodynamics because it points out the possibility of the existence of a temperature scale that is independent of the working fluid. This simply means that a direct relation between temperature and heat transferred may be proposed, and based on this relationship an absolute temperature scale may be established.

Statement of the Second Law

There are two classical statements of the second law: the Clausius statement and the Kelvin-Planck statement.

CLAUSIUS STATEMENT

It is impossible to construct a machine that, while operating in a cycle, will produce no effect other than the transfer of heat from a low-temperature body to a high-temperature body.

KELVIN-PLANCK STATEMENT

It is impossible to construct an engine that, while operating in a cycle, will absorb heat from a single reservoir and produce an equivalent amount of work.

As a consequence of the second law, there are several statements that are most important to the application of thermodynamics. Since these statements are not altogether obvious from the statements of the second law, they are listed below:

(1) The second law leads to a thermodynamic property—entropy—normally given the symbol S. More will be said about this property subsequently.

(2) The thermal efficiency of a reversible heat engine is dependent only on the temperature limits between which the reversible engine operates.

(3) All reversible heat engines operating between the same temperature limits have the same thermal efficiency.

(4) It is possible to construct a temperature scale independent of the working fluid.

(5) It is impossible to construct a heat engine more efficient than a reversible heat engine.

(6) Mathematically, the inequality of Clausius is stated

$$\oint \frac{\delta Q}{T} \leq 0$$

Physically this means that for any cycle the quantity $\delta Q/T$ is less than zero, and in the limit (the reversible process) it is equal to zero. The significance of this aspect of the second law becomes more apparent in this discussion of the thermodynamic property entropy.

Entropy—A Thermodynamic Property

In the previous discussion of the work done at the moving boundary of a system, it was found that the quantity δWk could be expressed as a function of the intensive thermodynamic property pressure and the extensive thermodynamic property volume. This relationship is expressed mathematically as

$$(\delta Wk)_{rev} = P \, d\bar{V}$$

The question arises as to the possibility of finding a similar relationship for the quantity δQ. To establish such a relationship, the most logical intensive property is the temperature T; however, there is, at this point, no extensive property to complete the pair. Therefore, it is necessary to introduce the quantity entropy. Entropy is an extensive thermodynamic property defined by the equation

$$dS = \left(\frac{\delta Q}{T}\right)_{rev}$$

Since entropy is a thermodynamic property, it, together with one other system property, defines the state of a pure substance.

The question now arises: What is the relation between the values of entropy at any

two arbitrary states? This poses two questions: What is the reference from which entropy is measured? What effect does a change in state have on entropy?

The answer to the first question is, in part, the subject of the third law of thermodynamics, which states that the absolute value of the entropy of most substances approaches zero at absolute zero temperature. Absolute values of entropy have important usage in chemical reactions. However, in the absence of such reactions, values measured relative to some convenient reference state are entirely adequate. It should be pointed out here that many tables of thermodynamic data list relative rather than absolute values of entropy.

The answer to the second question posed lies in the inequality of Clausius and a consideration of the effect of heat transfer to or from a system.

According to the inequality of Clausius:

$$\oint \frac{\delta Q}{T} \leq 0$$

If a reversible and an irreversible cycle have common end states and the reversible process

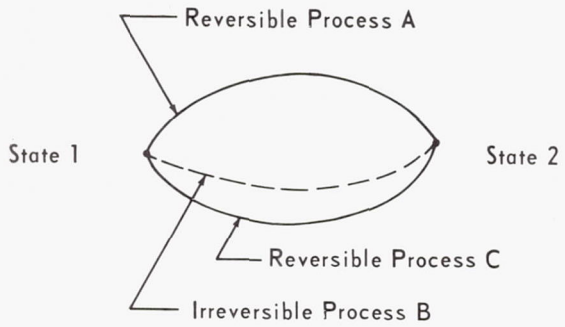


Figure 1.5. Two thermodynamic cycles with a common reversible process.

A is common to both cycles, the effect of irreversibility on entropy may be determined (fig. 1.5). Referring to figure 1.5, it is possible to write for the reversible cycle,

$$\oint \frac{\delta Q}{T} = \int_{1A}^{2A} \frac{\delta Q}{T} + \int_{2C}^{1C} \frac{\delta Q}{T} = 0$$

For the irreversible cycle,

$$\oint \frac{\delta Q}{T} = \int_{1A}^{2A} \frac{\delta Q}{T} + \int_{2B}^{1B} \frac{\delta Q}{T} < 0$$

Subtracting the second equation from the first,

$$\int_{2C}^{1C} \frac{\delta Q}{T} - \int_{2B}^{1B} \frac{\delta Q}{T} > 0$$

Since process C is reversible,

$$\int_{2C}^{1C} \frac{\delta Q}{T} = \int_{2C}^{1C} dS$$

Also, since entropy is a thermodynamic property, the change in entropy between any two states is the same regardless of the process. Therefore,

$$\int_{2C}^{1C} dS > \int_{2B}^{1B} \frac{\delta Q}{T}$$

or

$$S_2 - S_1 > \int_{1B}^{2B} \frac{\delta Q}{T}$$

This leads to the conclusion that the effect of irreversibility is to increase the entropy of a system. The effect of heat transfer on the entropy change of a system may be illustrated by considering the definition of entropy and recalling the fact that there are no negative values of absolute temperature. Hence, if heat is transferred from the system (negative),

$$dS_\sigma = -\left(\frac{\delta Q}{T}\right)_{rev} < 0$$

or the system's entropy is decreased. On the other hand, if heat is transferred to the system, δQ is positive and

$$dS_\sigma = \left(\frac{\delta Q}{T}\right)_{rev} > 0$$

Note that there are two possibilities for a constant entropy (isentropic) process for a system. These are

(1) A reversible process occurring in a system that is thermally isolated from the surroundings so that $\delta Q = 0$ (the reversible adiabatic process); and

(2) a process in which the rate of heat transfer from the system exactly offsets the entropy increase caused by irreversibilities.

Although the proof is beyond the purpose of this handbook, it must be pointed out that when system and surroundings are considered together, the net change in entropy is always greater than zero.

In closing the discussion, the following should be pointed out once again concerning the thermodynamic property, entropy:

(1) The change in entropy may be thought of as a measure of the energy unavailable for useful work, or as a measure of the degree of irreversibility connected with a given process.

(2) There are three ways of increasing a system's entropy: (*a*) transfer of mass to the system, (*b*) transfer of heat to the system, and (*c*) entropy production the result of irreversible work.

(3) When the system and its surroundings are considered together, the net change in entropy is always positive.

At this point the usefulness of entropy in quantitative analysis may not be apparent. However, as will be shown in a later section, entropy is very useful in relating thermodynamic properties of pure substances.

THERMODYNAMIC RELATIONS FOR A PURE SUBSTANCE

In this section, the origin of several useful relations between the thermodynamic properties will be summarized. It has been shown that for a closed system with negligible changes in kinetic and potential energies, the first law of thermodynamics (eq. (1.4)) becomes

$$dU = \delta Q - \frac{\delta W_k}{J}$$

If the process under consideration is reversible, the previous definition for simple expansion or compression work and the equality definition of entropy may be substituted into this equation to obtain

$$dU = T\,dS - \frac{P\,d\bar{V}}{J}$$

But since this equation is a function of properties only, it is true for any process (reversible or irreversible). Irreversibilities merely cause a discrepancy in the physical meaning of the independent terms, for example, the term $T\,dS$ is not exactly the heat transferred, and $P\,d\bar{V}$ is not exactly the work done, unless the process is reversible. Considering each unit mass of a substance as a closed system,

$$du = T\,ds - \frac{P\,dv}{J} \tag{1.6}$$

and this equation will be applicable for specific values of the related properties, regardless of the type of process or cycle considered, as long as changes in kinetic and potential energy are negligible.

A similar expression for enthalpy may be derived by combining equation (1.6) with the differential form of the equation defining enthalpy,

$$dh = du + \frac{d(Pv)}{J}$$

to obtain

$$dh = T\,ds + \frac{v\,dP}{J} \tag{1.7}$$

which is still a statement of the first law for a closed system.

While the expression for internal energy and enthalpy is most often used in formulating engineering problems, two additional properties need to be defined in order to obtain relations necessary in certain thermodynamic analyses. These properties are the Helmholtz function and the Gibbs function.

The Helmholtz function is defined as

$$A' = U - TS$$

or, in terms of specific quantities,

$$a' = u - Ts$$

By differentiating the above relation and combining it with equation (1.6), the relation

$$da' = -\frac{P\ dv}{J} - s\ dT \tag{1.8}$$

is obtained.

Similarly, the Gibbs function

$$G' = H - TS$$

or

$$g' = h - Ts$$

may be differentiated and combined with equation (1.7) to yield

$$dg' = \frac{v\ dP}{J} - s\ dT \tag{1.9}$$

Equations (1.6) through (1.9) can be used to derive a useful set of four relations for pressure, volume, temperature, and entropy known as the Maxwell relations. If a mathematical expression of the form

$$dZ = M\ dx + N\ dy$$

is an exact differential equation; then, by Green's theorem

$$\left(\frac{\partial N}{\partial x}\right)_y = \left(\frac{\partial M}{\partial y}\right)_x$$

Equations (1.6) through (1.9) are of this form, and since the variables are all thermodynamic properties having the characteristic that any two will determine all others, the exactness criterion is met. Using this theorem, the following relations may be obtained:

From equation (1.6):

$$\left(\frac{\partial T}{\partial v}\right)_s = -\left(\frac{\partial P}{\partial s}\right)_v \left(\frac{1}{J}\right) \tag{1.10}$$

From equation (1.7):

$$\left(\frac{\partial T}{\partial P}\right)_s = \left(\frac{\partial v}{\partial s}\right)_P \left(\frac{1}{J}\right) \tag{1.11}$$

From equation (1.8):

$$J\left(\frac{\partial s}{\partial v}\right)_T = \left(\frac{\partial P}{\partial T}\right)_v \tag{1.12}$$

From equation (1.9):

$$J\left(\frac{\partial s}{\partial P}\right)_T = \left(\frac{\partial v}{\partial T}\right)_P \tag{1.13}$$

Three other useful derivatives will be defined here for completeness, but the full significance and importance of these derivatives will be developed in succeeding chapters. These derivatives are:

Joule-Thomson coefficient:

$$\mu_J = \left(\frac{\partial T}{\partial P}\right)_h \tag{1.14}$$

the constant-volume specific heat:

$$c_v = \left(\frac{\partial u}{\partial T}\right)_v \tag{1.15}$$

and the constant-pressure specific heat:

$$c_p = \left(\frac{\partial h}{\partial T}\right)_P \tag{1.16}$$

325-994 O-69—3

CHAPTER 2

PROPERTIES OF GASES

Gas behavior may be expressed by two classes of parameters—the directly measurable properties such as pressure, volume, and temperature, and the thermodynamic properties such as internal energy, enthalpy, entropy, and free energy, which are not generally subject to direct measurement. This second group is useful in that it can be simply related to the heat and work effects that accompany actual thermodynamic processes.

The problem of predicting certain gas properties from known gas properties has led to the development of many property relations or, as they are commonly called, equations of state. The simplest of all the relationships developed is the perfect-gas law. Use of this law is most valuable in engineering analysis, since it affords the simplest relation between gas properties. Unfortunately, the valid range of this law is somewhat limited, so that care must be exercised in its application. In general, high pressures and low temperatures or high temperatures which cause ionization or dissociation will result in significant deviations from the perfect-gas law, in which case a different approach should be used to relate gas properties. If, because of the simplicity of approach or the lack of sufficient data, an analysis based on the perfect-gas law is used at high pressures or temperatures, it is imperative that the credibility of such an analysis be plainly understood.

When the state of a gas cannot be predicted by the perfect-gas equation of state, the gas must be treated as a real gas. There are several methods of predicting properties in the real-gas region. One method is the empirical equation of state, which is an equation for a curve fitted to experimental data. Another approach is the compressibility factor which expresses the deviation from perfect-gas behavior at a given set of conditions.

PERFECT GAS

A gas may be categorized as being perfect by different criteria. Thus, it is correct to speak of a mechanically perfect gas, a calorically perfect gas, and a thermally perfect gas. In each of these categories, certain restrictions are placed on the gas. Hence, to be classified as mechanically perfect, a gas must offer no resistance to shear. Therefore, the coefficient of viscosity is zero. More will be said regarding this subject in chapters 3 and 4. The calorically perfect gas is one which has invariant specific heats and, consequently, a fixed specific heat ratio. More regarding this subject will be discussed later in this chapter. The thermally perfect gas is categorically defined by the perfect-gas equation of state

$$Pv = RT$$

Preceding Page Blank

In this handbook, the term "perfect gas" is reserved for a gas that is both thermally and calorically perfect. If reference is intended to any other criteria of perfectness, the terms "mechanically perfect," "calorically perfect," or "thermally perfect" will be used.

Thermally Perfect Gas

The equation of state for the thermally perfect gas is a combination of the original Boyle's law and Charles' law. Boyle's law, formulated by Robert Boyle in 1662, states that the volume of a given mass of a gas varies inversely as the pressure at constant temperature. Mathematically,

$$\bar{V} \sim \frac{1}{P}$$

Charles' law states that the volume of a gas varies directly as the absolute temperature at constant pressure, hence

$$\bar{V} \sim T$$

Combining these two laws

$$\bar{V} \sim \frac{T}{P}$$

If two states of a constant mass of a gas are considered, the ratio yields

$$\frac{\bar{V}_1}{\bar{V}_2} = \frac{T_1/P_1}{T_2/P_2}$$

or on rearranging terms

$$\frac{P_1\bar{V}_1}{T_1} = \frac{P_2\bar{V}_2}{T_2}$$

It can be seen from this equation that the quantity $(P\bar{V}/T)$ is a constant for a gas regardless of the state. Therefore, the above equation may be rewritten as

$$\frac{P\bar{V}}{T} = \Omega$$

The constant Ω depends only on the gas and the units of P, $\bar{V}$, and T. The value of Ω can be established as a function of the molecular weight of the particular gas and the mass of the gas enclosed in the volume by a consideration of Avogadro's law.

Avogadro's law states that an equal number of molecules of any gas will be contained in a given volume at the same temperature and pressure. A convention has been established to relate the number of molecules to the occupied volume at an arbitrarily fixed standard temperature and pressure. The reference number of molecules is selected to be consistent with the atomic-weight scale where atomic oxygen is assigned the value of exactly 16.0. For convenience then, the reference quantity of gas is defined as that number of oxygen molecules (2 atoms per molecule) which together weigh exactly 32 units of weight in the particular system of units being used. This reference quantity of gas is called a mole and the actual quantity, or number of molecules, in a mole depends on the system of measurement (units). However, in any system of units, the number of conventional weight units in a mole

of any gas is exactly equal to (numerically) the molecular weight as obtained from the atomic-weight scale. For example, in the metric system, 1 mole_{μ} of oxygen weighs 32 grams, contains 6.02×10^{23} molecules, and occupies 22.4 liters when maintained at the arbitrarily established standard temperature and pressure. It will be seen below that the standard temperature and pressure must be universal to produce consistency between different systems of units. These standards have been established as the freezing temperature of water and standard atmospheric pressure.

In the English system, 1 mole_{lb} of molecular oxygen amounts to 32 lbm and contains a specific number of molecules. The exact volume occupied is not significant, since it depends on the particular selection of the reference temperature and pressure. The fact that the volume of a mole at some fixed temperature and pressure is the same for any gas is very significant when factored into the relationship obtained from Charles' and Boyle's laws. If v_m is the volume of 1 mole of gas at the reference temperature and pressure, then for 1 mole of any gas

$$\left(\frac{P}{T}\right)_{\text{ref}} v_m = \Omega_m = \bar{R}$$

This special value of $\Omega_m = \bar{R}$ is seen to be independent of the gas, since v_m is the same for all gases. The constant $\bar{R}$ is termed the universal gas constant and for any gas that obeys Charles' and Boyle's laws

$$P v_m = \bar{R} T \tag{2.1}$$

and for N moles having a total volume, $\bar{V} = N v_m$, the perfect-gas law becomes

$$P\bar{V} = N\bar{R}T \tag{2.2}$$

The value of $\bar{R}$ for various sets of units is shown in table 2.1

For engineering work, it is usually desirable to convert the molal specific volume term in equation (2.1) to more convenient units of volume per unit weight. This is equivalent to converting the units of weight (or mass) of the term N from moles to the standard units of weight. As stated previously in the description of a mole, the number of conventional weight units in a mole is numerically equal to the molecular weight of the gas, regardless of the system of units. Then it follows that

$$\mathbb{W} = N M_w \tag{2.3}$$

Note that this use of the molecular weight requires that it take on units of weight per mole. In the English system, it is called the pound molecular weight and has units of $\text{lbm/mole}_{\text{lb}}$. Equation (2.2) then becomes

$$P\bar{V} = \mathbb{W}\left(\frac{\bar{R}}{M_w}\right) T \qquad \text{or} \qquad P\left(\frac{\bar{V}}{\mathbb{W}}\right) = \left(\frac{\bar{R}}{M_w}\right) T$$

The quantity $\bar{V}/\mathbb{W}$ is the specific volume per unit pound mass, v, and the quantity $\bar{R}/M_w$

is the gas constant. The gas constant depends only on the molecular weight of the gas and is designated R. Mathematically,

$$R = \frac{\bar{R}}{M_w} \tag{2.4}$$

TABLE 2.1.—*Systems of Consistent Units for the Perfect-Gas Equation of State Using the Universal Gas Constant* $\bar{R}$

$P\bar{V}=N\bar{R}T$				
P	$\bar{V}$	N	$\bar{R}$	T
lbf/ft^2	ft^3	$mole_{lb}$	$1545\ \frac{ft\text{-}lbf}{mole_{lb}\ °R}$	°R
Btu		$mole_{lb}$	$1.9857\ \frac{Btu}{mole_{lb}\ °R}$	°R
lbf/in^2	ft^3	$mole_{lb}$	$10.729\ \frac{lbf\text{-}ft^3}{in^2\ mole_{lb}\ °R}$	°R
atm	cm^3	$mole_g$	$82.0567\ \frac{atm\ cm^3}{mole_g\ °K}$	°K
mm Hg	cm^3	$mole_g$	$62.363\ \frac{mm\ Hg\ cm^3}{mole_g\ °K}$	°K
kg/m^2	m^3	$mole_g$	$0.847887\ \frac{kg\ m}{mole_g\ °K}$	°K
calorie		$mole_g$	$1.9857\ \frac{cal}{mole_g\ °K}$	°K

Substituting equation (2.4) and the relation $v=\bar{V}/W$ yields the equation of state for a thermally perfect gas,

$$Pv = RT \tag{2.5}$$

Values of the gas constant R in the English system of units for several gases are shown in table 2.2.

Properties of the Perfect Gas

Having established the defining equation of state for the thermally perfect gas, it is now possible to determine the relations between the different thermodynamic properties.

TABLE 2.2.—*Values of the Gas Constant* R *for Several Gases*

Gas	$R\left(\frac{\text{ft-lbf}}{\text{lbm-°R}}\right)$
Air	53.34
Argon	38.66
Helium	386.0
Hydrogen	766.0
Methane	96.35
Nitrogen	55.15
Oxygen	48.28
Steam	85.76

Internal Energy and Enthalpy

The internal energy of a system is simply the sum of the energies of the gas molecules that comprise the system. Mathematically,

$$U_\sigma = \sum_{i=1}^{N} E_{mi}$$

where U_σ is the internal energy of the system, E_m is the energy per molecule, and N is the number of gas molecules in the system.

If the gas comprising the system is thermally perfect, it can be shown analytically that internal energy is a function of temperature only. This is accomplished by considering equation (1.6) which is the first law of thermodynamics for a closed system.

$$du = T\,ds - \frac{P\,dv}{J} \qquad [1.6]$$

Differentiating with respect to volume

$$\frac{du}{dv} = T\left(\frac{ds}{dv}\right) - \frac{P}{J}$$

Holding T constant, this equation can be written in partial differential form as

$$\left(\frac{\partial u}{\partial v}\right)_T = T\left(\frac{\partial s}{\partial v}\right)_T - \frac{P}{J}$$

From the Maxwell relation, equation (1.12), $(\partial s/\partial v)_T$ may be expressed as

$$\frac{1}{J}\left(\frac{\partial P}{\partial T}\right)_v = \left(\frac{\partial s}{\partial v}\right)_T$$

Combining the preceding two equations yields

$$\left(\frac{\partial u}{\partial v}\right)_T = T\left(\frac{\partial P}{\partial T}\right)_v \left(\frac{1}{J}\right) - \frac{P}{J}$$

For the thermally perfect gas

$$Pv = RT$$

or in differential form with the specific volume, v, held constant

$$v\ dP = R\ dT \qquad \text{and} \qquad \left(\frac{\partial P}{\partial T}\right)_v = \frac{R}{v}$$

Substituting R/v into the previous equation, it follows that for the thermally perfect gas

$$\left(\frac{\partial u}{\partial v}\right)_T = \left(\frac{1}{J}\right) T\left(\frac{R}{v}\right) - \frac{P}{J}$$

or, since $P = RT/v$,

$$\left(\frac{\partial u}{\partial v}\right)_T = 0$$

Using a similar analysis, it can be shown that all other partials of u with T held constant are zero. Hence, for the thermally perfect gas the internal energy is a function of temperature only,

$$u = f_1(T)$$

Having established the internal energy as a function of temperature only, it is a simple matter to show that enthalpy is a function of temperature only. By definition,

$$h = u + \frac{Pv}{J}$$

and for the perfect gas $Pv = RT$, hence

$$h = u + \frac{RT}{J} = f_2(T)$$

The fact that internal energy and enthalpy are functions of temperature only for a thermally perfect gas leads to the important conclusion that specifying any two of these properties is not sufficient to describe the state of a perfect gas. It is necessary, therefore, to use a combination of either u or h and P; T and P, or other thermodynamic properties which are not a function of temperature alone. Graphically, this may be illustrated on a P–v diagram such as figure 2.1.

Referring to figure 2.1, there are many possible process lines by which the temperature of the gas is changed from T_1 to T_2. Each of these lines will result in a different end state; however, the value of u_2 and h_2 will be the same for all states at temperature T_2. Hence, pairs of properties such as T and u, T and h, or u and h are not sufficient to specify the state.

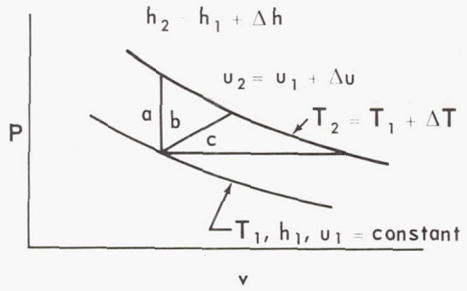


Figure 2.1. Lines of constant temperature, enthalpy, and internal energy on a pressure-volume diagram.

It must be remembered that the previous discussion is for the perfect gases only. As will be pointed out in the discussion on real gases, the internal energy and enthalpy may vary with pressure, and combinations such as h and T, or u and T may be sufficient to specify the state of the gas.

Specific Heats

The constant-volume and constant-pressure specific heats of a pure substance are defined by equations (1.15) and (1.16) as

$$c_v = \left(\frac{\partial u}{\partial T}\right)_v \qquad [1.15]$$

$$c_p = \left(\frac{\partial h}{\partial T}\right)_p \qquad [1.16]$$

It has been shown that internal energy and enthalpy of a thermally perfect gas are dependent on temperature only. It follows that the definition of the constant-volume specific heat and constant-pressure specific heat may be written for the perfect gas as total derivatives so that

$$c_v = \frac{\mathrm{d}u}{\mathrm{d}T} \qquad \text{and} \qquad c_p = \frac{\mathrm{d}h}{\mathrm{d}T}$$

From the definition of enthalpy,

$$h = u + \frac{Pv}{J}$$

or for the perfect gas,

$$h = u + \frac{RT}{J} \qquad \text{and} \qquad \mathrm{d}h = \mathrm{d}u + \frac{R\ \mathrm{d}T}{J}$$

Hence,

$$c_p - c_v = \frac{R}{J} \qquad (2.6)$$

This is an important relationship concerning the perfect gas because it shows that c_p and c_v have a common difference, the gas constant. Note, however, that the perfect-gas law places no restrictions on the absolute value of c_p or c_v. To determine the absolute value of specific heat, an analysis based on kinetic theory is used as follows.

For the monatomic gas, a fundamental kinetic theory relationship is

$$\frac{Pv_m}{J}=\frac{2}{3}\left(\frac{1}{J}\right)\frac{W_m V^2}{2g_c}=\frac{2}{3}\left(\frac{1}{J}\right)(KE)_m$$

where W_m is the mass of 1 mole_{lb} of the gas, and V is the average translational velocity of the molecules, and $(KE)_m$ is the molecular kinetic energy of a mole_{lb} of gas. For the perfect gas, using the thermal system of units, it may be written that

$$\frac{Pv_m}{J}=\left(\frac{\bar{R}T}{J}\right)=1.9857T\approx 2T$$

Combining these equations

$$\frac{2}{3}\left(\frac{1}{J}\right)\frac{W_m V^2}{2g_c}=2T$$

$$(KE)_m=3TJ$$

then

$$\mathrm{d}(KE)_m=3J\ \mathrm{d}T$$

Since the change in the translational kinetic energy of the monatomic molecules represents the change in thermal energy or internal energy,

$$\mathrm{d}(KE)_m=J\ \mathrm{d}u_m=3J\ \mathrm{d}T$$

or

$$c_{vm}=\frac{\mathrm{d}u_m}{\mathrm{d}T}=3 \qquad \frac{\text{Btu}}{\text{mole}_{\text{lb}}\text{-}^\circ\text{R}}$$

Again, from the definition of enthalpy and the perfect-gas law

$$\mathrm{d}h_m=\mathrm{d}u_m+\frac{\bar{R}\ \mathrm{d}T}{J}$$

$$=3\ \mathrm{d}T+2\ \mathrm{d}T$$

$$=5\ \mathrm{d}T$$

Hence,

$$c_{pm}=\frac{\mathrm{d}h_m}{\mathrm{d}T}=5 \qquad \frac{\text{Btu}}{\text{mole}_{\text{lb}}\text{-}^\circ\text{R}}$$

Then for a monatomic gas, the specific heat ratio, k, is

$$k=\frac{c_p}{c_v}=\frac{c_{pm}}{c_{vm}}=\frac{5}{3}=1.667$$

Plots of the specific heat ratio versus temperature show relatively good agreement with the kinetic theory prediction for monatomic gases in most instances. Figure 2.2 is a plot of specific heat ratio for gaseous helium between temperatures of −200° F and 300° F, and pressures between 14.7 and 6000 psia.

Note that for the temperature range shown in figure 2.2, the lines are relatively flat. This indicates that the specific heats are not appreciably altered by temperature changes. Also, note that the spread caused by changing pressure is small. This reflects the fact that the perfect-gas equation for helium is relatively accurate in this region; hence, the thermal energies (internal energy and enthalpy) are only weakly dependent on pressure.

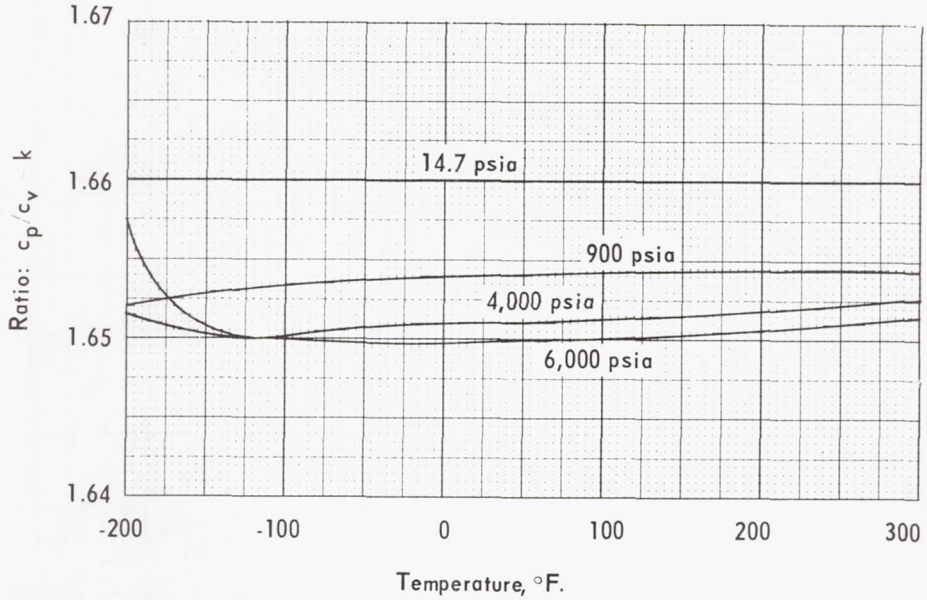


Figure 2.2. Specific heat ratio versus temperature for gaseous helium (−200° to 300° F). [*Courtesy of the Whittaker Corp.*]

Unfortunately, at temperatures below −200° F the behavior of the specific heat ratio becomes more erratic. This may be attributed to significant deviations from the perfect-gas law caused by changes in intermolecular forces and changes in the volume occupied by the gas molecules. Figure 2.3 shows significant deviations in the specific heat ratio as a result of both temperature and pressure changes.

For polyatomic molecules, the foregoing kinetic theory evaluation is not valid. This is to be expected since these molecules have energies associated with the rotational and vibrational degrees of freedom which a monatomic molecule does not possess.

Heat energy supplied to polyatomic molecules is used not only in increasing the kinetic energy of translation in the three directions, but also in increasing the energy of rotation and vibration of the atoms within the molecules. If the extra energy absorbed relative to the

translational energy is represented by X, and is independent of the process (constant volume or constant pressure), then the ratio of the specific heat will be

$$k=\frac{c_p}{c_v}=\frac{5+X}{3+X}<1.67$$

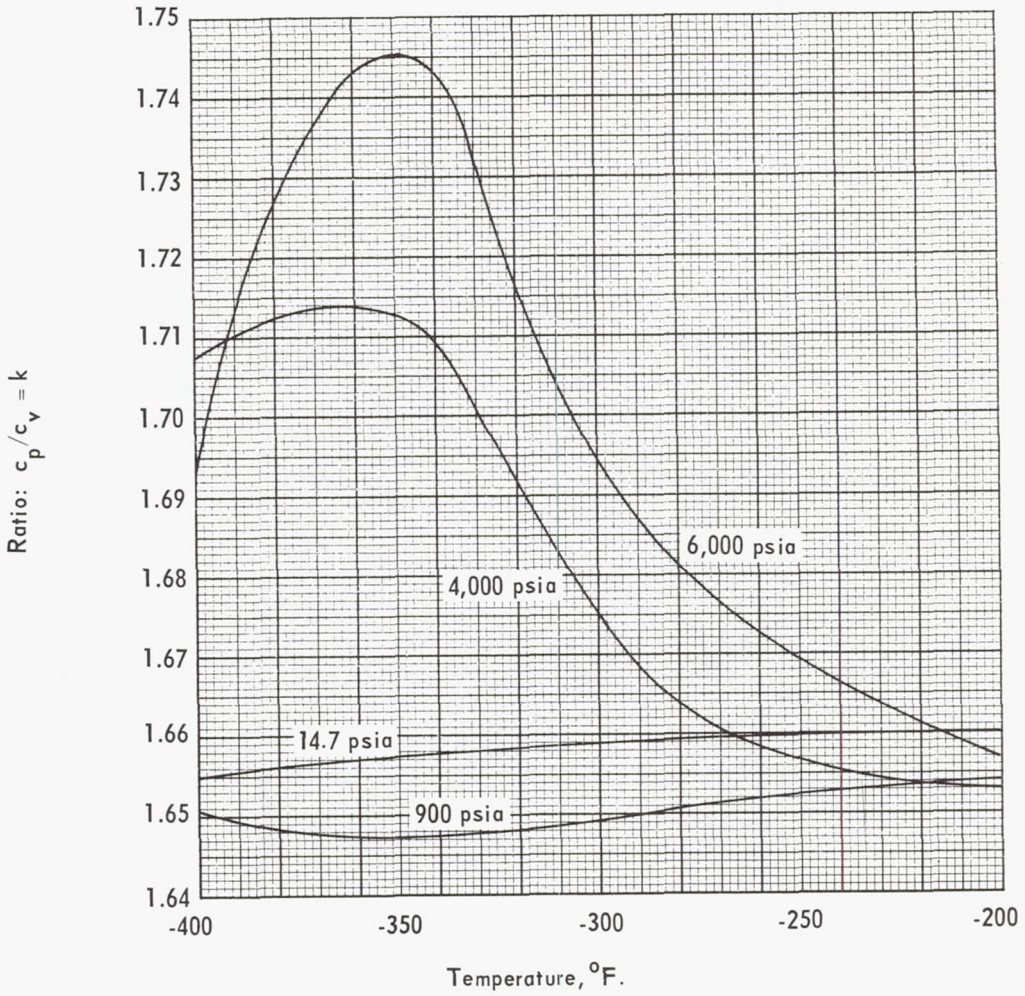


Figure 2.3. Specific heat ratio versus temperature for gaseous helium (−400° to −200° F). [*Courtesy of Whittaker Corp.*]

The ratio is less than 1.67, and with increasing complexity of the molecule, the value of X increases and the ratio k decreases but cannot become less than unity.

In those regions of temperature and pressure where the perfect-gas law $Pv=RT$ is not valid, it is necessary to resort to empirical equations or charts of experimentally determined values such as that shown in figure 2.2 or 2.3.

In regions of low pressure, where the perfect-gas law describes the state of the gas, but specific heats are variable as a function of temperature, empirical equations are often used in determining c_p. Several such equations are shown in table 2.3.

If the specific heats are constant over a given range of temperatures, then the equations

$$dh = c_p\,dT \qquad \text{and} \qquad du = c_v\,dT$$

can be integrated to yield

$$h_2 - h_1 = c_p(T_2 - T_1) \tag{2.7}$$

and

$$u_2 - u_1 = c_v(T_2 - T_1) \tag{2.8}$$

Since $k = c_p/c_v$ and $c_p - c_v = R/J$, it follows that

$$c_p = \frac{kR}{J(k-1)} \tag{2.9}$$

and

$$c_v = \frac{R}{J(k-1)} \tag{2.10}$$

Hence, for a thermally perfect gas

$$dh = \left[\frac{kR}{J(k-1)}\right] dT \tag{2.11}$$

and

$$du = \left(\frac{R}{J(k-1)}\right) dT \tag{2.12}$$

TABLE 2.3.—*Empirical Equations for Determining* c_{pm} *for Several Gases*

Gas	c_{pm}, $\frac{\text{Btu}}{\text{mole}_{\text{lb}}\text{-}^\circ\text{R}}$	Applicable range — °R	Max percent error
O_2	$c_{pm} = 11.515 - \frac{172}{\sqrt{T}} + \frac{1530}{T}$	540–5000	1.1
	$c_{pm} = 11.515 - \frac{172}{\sqrt{T}} + \frac{1530}{T} + \left(\frac{0.05}{1000}\right) T - 4000$	5000–9000	0.3
N_2	$c_{pm} = 9.47 - \frac{(3.47)10^3}{T} + \frac{(1.16)10^6}{T^2}$	540–9000	1.7
H_2	$c_{pm} = 5.76 + \left(\frac{0.578}{1000}\right) T + \frac{20}{\sqrt{T}}$	540–4000	0.8

Entropy

The equations relating entropy change of a perfect gas are derived from the two relations from chapter 1.

$$T\,ds = du + \frac{P\,dv}{J} \qquad [1.6]$$

and

$$T\,ds = dh - \frac{v\,dP}{J} \qquad [1.7]$$

Considering equation (1.6) and introducing the perfect-gas relations

$$du = c_v\,dT \qquad \text{and} \qquad Pv = RT$$

it is possible to obtain

$$ds = (c_v)\,\frac{dT}{T} + \left(\frac{R}{J}\right)\frac{dv}{v} \qquad (2.13)$$

For a thermally perfect gas

$$c_v = \frac{R}{J(k-1)}$$

so that equation (2.13) may be written as

$$ds = \left[\frac{R}{J(k-1)}\right]\frac{dT}{T} + \left(\frac{R}{J}\right)\frac{dv}{v} \qquad (2.14a)$$

If the specific heats are constant, the equation may be integrated to obtain

$$\Delta s = \left[\frac{R}{J(k-1)}\right]\ln\left(\frac{T_2}{T_1}\right) + \left(\frac{R}{J}\right)\ln\left(\frac{v_2}{v_1}\right) \qquad (2.14b)$$

Also, from equation (1.7)

$$ds = (c_p)\,\frac{dT}{T} - \left(\frac{R}{J}\right)\frac{dP}{P} \qquad (2.15)$$

By substitution, equation (1.7) may be written as

$$ds = \left[\frac{kR}{J(k-1)}\right]\frac{dT}{T} - \left(\frac{R}{J}\right)\frac{dP}{P} \qquad (2.16a)$$

and integrated for the case of constant specific heats yields

$$\Delta s = \left[\frac{kR}{J(k-1)}\right]\ln\left(\frac{T_2}{T_1}\right) - \left(\frac{R}{J}\right)\ln\left(\frac{P_2}{P_1}\right) \qquad (2.16b)$$

Perfect-Gas Processes

Constant-Volume Process

A constant volume change of state may be illustrated graphically on a temperature-versus-entropy diagram as shown in figure 2.4.

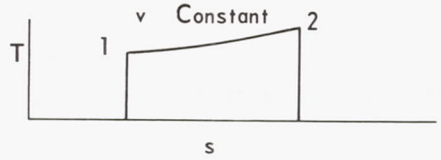


Figure 2.4. Constant-volume process on a T–s diagram.

Since volume is constant, the work done in the change of state is zero as evidenced by the equation

$$\delta wk = \int P \, dv = 0$$

For the process, the first law for a closed system is

$$dQ' = du + \frac{\delta wk}{J}$$

and since the work term is zero, the heat transfer is reflected by the change in internal energy

$$dQ' = du$$

or

$$dQ' = c_v \, dT = \left[\frac{R}{J(k-1)}\right] dT \tag{2.17}$$

Entropy change is found from equation (2.14a) by setting $dv = 0$; then

$$ds = \left[\frac{R}{J(k-1)}\right] \frac{dT}{T} \quad \text{and} \quad {}_1\Delta s_2 = \left[\frac{R}{J(k-1)}\right] \ln\left(\frac{T_2}{T_1}\right) \tag{2.18}$$

CONSTANT-PRESSURE PROCESS

This process is represented graphically on a temperature-entropy diagram as shown in figure 2.5.

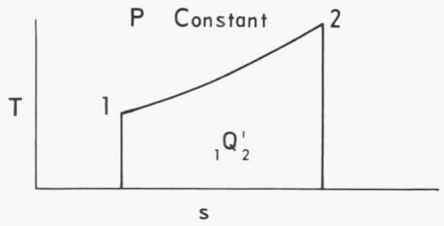


Figure 2.5. Constant-pressure process on a T–s diagram.

Since pressure is a constant, the reversible work done is given by

$${}_1wk_2 = \int_1^2 P \, dv = P(v_2 - v_1) \tag{2.19}$$

Then for the closed system the first law is written as

$$dQ' = c_v\, dT + \frac{P\, dv}{J} \tag{2.20}$$

Since $P\, dv = R\, dT$, it follows that

$$dQ' = \left(c_v + \frac{R}{J}\right) dT = c_p\, dT$$

or

$$dQ' = \left[\frac{kR}{J(k-1)}\right] dT \tag{2.21}$$

The entropy change is found from equation (2.16*a*), noting that in this case $dP = 0$; then

$$ds = \left[\frac{kR}{J(k-1)}\right] \frac{dT}{T} \quad \text{and} \quad {}_1\Delta s_2 = \left[\frac{kR}{J(k-1)}\right] \ln\left(\frac{T_2}{T_1}\right) \tag{2.22}$$

ISOTHERMAL PROCESS

The isothermal process is one which allows sufficient heat transfer to or from the system to maintain constant temperature. This process appears as a straight line on a temperature-versus-entropy diagram shown in figure 2.6.

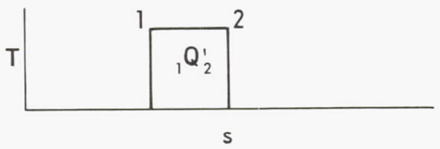


Figure 2.6. Isothermal process on a T–s diagram.

The reversible work term for the isothermal process may be evaluated by noting that at constant temperature

$$P_1v_1 = P_2v_2 = Pv = RT$$

hence,

$${}_1wk_2 = \int_1^2 P\, dv = P_1v_1 \int_1 \frac{dv}{v}$$

and finally,

$${}_1wk_2 = P_1v_1 \ln\left(\frac{v_2}{v_1}\right) = P_1v_1 \ln\left(\frac{P_1}{P_2}\right) \tag{2.23a}$$

or, since $Pv = RT$,

$${}_1wk_2 = RT \ln\left(\frac{v_2}{v_1}\right) = RT \ln\left(\frac{P_1}{P_2}\right) \tag{2.23b}$$

Also, since temperature is constant,

$$du = c_v\, dT = 0$$

It follows that the heat transferred to maintain constant temperature in the closed system is equal to the work term

$$ {}_1Q'_2 = \left(\frac{RT}{J}\right) \ln \left(\frac{P_1}{P_2}\right) = \left(\frac{RT}{J}\right) \ln \left(\frac{v_2}{v_1}\right) \tag{2.24} $$

REVERSIBLE-ADIABATIC PROCESS

The reversible-adiabatic process is an isentropic (constant entropy) process. On a temperature-versus-entropy diagram, this process plots as a straight vertical line as shown in figure 2.7.



Figure 2.7. Isentropic process on a T–s diagram.

Equation (1.6), the first law of thermodynamics for a pure substance undergoing a change in state in a closed system, may be written as

$$ du + \frac{P\,dv}{J} = T\,ds = 0 \tag{1.6} $$

For an isentropic process and a thermally perfect gas,

$$ \left[\frac{R}{J(k-1)}\right] dT + \frac{P\,dv}{J} = 0 $$

Writing the perfect-gas equation of state in differential form

$$ P\,dv + v\,dP = R\,dT $$

and substituting for $R\,dT$ in the previous equation yields

$$ \frac{1}{J(k-1)} (P\,dv + v\,dP) + \frac{P\,dv}{J} = 0 $$

$$ v\,dP + kP\,dv = 0 $$

$$ k\left(\frac{dv}{v}\right) + \frac{dP}{P} = 0 $$

If k is assumed constant, this equation may be integrated to obtain

$$ Pv^k = \text{constant} \tag{2.25} $$

From the perfect-gas equation of state, it follows that

$$\frac{T_2}{T_1}=\left(\frac{P_2}{P_1}\right)^{\frac{k-1}{k}} \tag{2.26a}$$

and

$$\frac{v_2}{v_1}=\left(\frac{T_1}{T_2}\right)^{\frac{1}{k-1}} \tag{2.26b}$$

The external work done in this process is given by

$$_1wk_2=\int_1^2 P\,\mathrm{d}v=P_1v_1{}^k\int_1^2\frac{\mathrm{d}v}{v^k}$$

$$=\left(\frac{1}{k-1}\right)(P_1v_1-P_2v_2)$$

$$=\left(\frac{R}{k-1}\right)(T_1-T_2) \tag{2.27}$$

POLYTROPIC PROCESS

A polytropic process is a general irreversible process and one in which heat is transferred to or from the system. This process requires only that its property changes be in accordance with the equation

$$P\bar{V}^n=\text{constant} \tag{2.28a}$$

or

$$Pv^n=\text{constant} \tag{2.28b}$$

where n is the constant polytropic exponent. Plotted on a graph of ln P versus ln V, the polytropic process is a straight line with slope $-n$ as shown in figure 2.8.

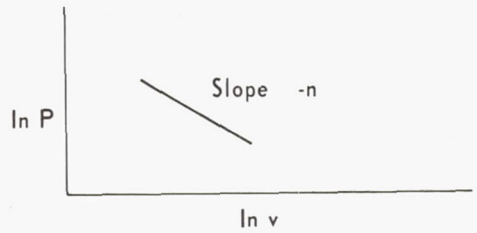


Figure 2.8. Polytropic process line.

For the perfect gas, $Pv=RT$, it follows that

$$\frac{T_2}{T_1}=\left(\frac{P_2}{P_1}\right)^{\frac{n-1}{n}} \tag{2.29}$$

and

$$\frac{T_2}{T_1}=\left(\frac{v_1}{v_2}\right)^{n-1} \tag{2.30}$$

For the closed system, the first law for this process is

$$dQ' = du + \frac{P\,dv}{J}$$

or on integrating

$${}_1Q'_2 = u_2 - u_1 + \int_1^2 \frac{P\,dv}{J}$$

Since $Pv^n = \text{constant}$, it may be written that

$$P = \frac{P_1 v_1{}^n}{v^n} = \frac{P_2 v_2{}^n}{v^n}$$

Substituting for P in the first law yields

$${}_1Q'_2 = u_2 - u_1 + \frac{P_1 v_1{}^n}{J} \int_1^2 v^{-n}\,dv$$

$$= u_2 - u_1 - \frac{P_1 v_1{}^n}{J(n-1)} \left(v_2{}^{1-n} - v_1{}^{1-n}\right)$$

$$= c_v(T_2 - T_1) - \frac{1}{J(n-1)} (P_2 v_2 - P_1 v_1)$$

$$= \frac{R}{J(k-1)} (T_2 - T_1) - \frac{R}{J(n-1)} (T_2 - T_1)$$

Finally,

$${}_1Q'_2 = \frac{R}{J} \left(\frac{1}{n-1} - \frac{1}{k-1}\right) (T_1 - T_2) \tag{2.31a}$$

and

$${}_1Q'_2 = \frac{1}{J} \left(\frac{1}{n-1} - \frac{1}{k-1}\right) (P_1 v_1 - P_2 v_2) \tag{2.31b}$$

Equations (2.31) can also be expressed as

$${}_1Q'_2 = \frac{RT_1}{J} \left(\frac{1}{n-1} - \frac{1}{k-1}\right) \left(1 - \frac{T_2}{T_1}\right) \tag{2.32}$$

and convenient forms of (T_2/T_1) are available for substitution from equations (2.29) and (2.30). Equations (2.31) and (2.32) are the expressions for the heat transfer during a polytropic process. The reversible work done during this process is obtained only from the $P\,dv$ term of the first law, yielding

$${}_1wk_2 = \frac{1}{(n-1)} (P_1 v_1 - P_2 v_2) \tag{2.33a}$$

$$ {}_1wk_2 = \frac{R}{(n-1)}(T_1 - T_2) = \frac{RT_1}{(n-1)}\left(1 - \frac{T_2}{T_1}\right) \qquad (2.33b) $$

REAL GAS

Equations of State

The perfect-gas equation of state predicts the ideal P–v–T relationship of any gas over the full temperature and pressure range. It is an experimental fact, however, that at high pressures or temperatures, or in regions near the point of condensation to the liquid phase, variations from this ideal P–v–T relationship do occur. The magnitude of these deviations depends on the particular gas and values of the temperature and pressure. As pressure is increased from zero, the deviation from the perfect-gas law increases. Also, the deviation at a given pressure will be less at higher temperatures, except when temperature is so extreme as to cause ionization or dissociation.

Numerous equations of state have been proposed that will, at least in part, compensate for the deviation from perfect-gas behavior, among these are:

(1) Van der Waals' equation

$$ \left(P + \frac{a}{v_m^2}\right)(v_m - b) = RT $$

where a and b are constants, characteristic of the particular gas.

(2) Berthelot's equation

$$ Pv_m = RT\left(1 + \frac{Pb'}{RT} - \frac{a'P}{R^2T^3}\right) $$

where a' and b' are constants.

(3) Dieterici's equation

$$ P = \left(\frac{RT}{v_m - b''}\right) e^{\frac{-a''}{RTv_m}} $$

where a'' and b'' are constants.

(4) Wohl's equation

$$ P = \frac{RT}{v_m - b'''} - \frac{a'''}{v_m(v_m - b''')} + \frac{c'''}{v_m^3} $$

where a''', b''', and c''' are constants.

(5) Keyes' equation

$$ P = \frac{RT}{v_m - \alpha} - \frac{e}{(v_m g)^2} \qquad \alpha = B(e)^{\left(\frac{-k}{v_m}\right)} $$

where B, k, e, and g are constants.

(6) Beattie-Bridgeman's equation

$$P=\frac{RT}{v_m^2}\left(1-\frac{A}{v_m T^3}\right)\left[v_m+B\left(1-\frac{D}{v_m}\right)\right]$$

$$-\frac{E}{v_m^2}\left(1-\frac{F}{v_m}\right)$$

where A, B, D, E, and F are constants.

In all these equations, v_m refers to the molal specific volume. Their accuracy in correlating experimental data depends, in general, on the number of constants that may be assigned specific values for each gas. The Beattie-Bridgeman equation of state with five such constants has been found to agree within a fraction of 1 percent with experimental data for a number of substances over a wide range of conditions. The Beattie-Bridgeman equation is complex, but it is exceedingly useful if the constants for the gas involved are known for the range of interest. B. F. Dodge's text, *Chemical Engineering Thermodynamics*, has a tabulation of Beattie-Bridgeman constants for a number of gases.

The Van der Waals equation may be expected to give better results than the perfect-gas law. However, it has only two arbitrary constants and cannot be expected to duplicate experimental data exactly, and it may be seriously in error under certain severe conditions.

The equations of Berthelot, Dieterici, Wohl, and Keyes generally are not as accurate as the Beattie-Bridgeman equation but, because of their simplicity and form, may be useful for specific types of calculations.

If it is desired to fit experimental data with great accuracy over large pressure ranges, the following equation, known as the virial form of an equation of state, is recommended because of its flexibility:

$$Pv_m=RT+\frac{B}{v_m}+\frac{r}{v_m^2}+\frac{\delta}{v_m^3}$$

where the coefficients B, r, and δ are temperature functions as follows:

$$B=RTB_0-A_0-\frac{RC}{T^2}$$

$$r=RTB_0b+aA_0-\frac{RB_0C}{T^2}$$

$$\delta=\frac{RB_0bc}{T^2}$$

This virial equation is really a condensed summary of the data. It requires a different set of coefficients for each temperature and it becomes very cumbersome for practical application.

Thermodynamic Property Diagrams

It is known from the phase rule that for a single-component system there are only two independent variables required to completely determine the state of the system. Therefore, it is not difficult to represent most of the thermodynamic properties of the single-component system by means of a table or a two-coordinate graph. Any graph or chart of thermodynamic properties is usually called a thermodynamic diagram.

In plotting thermodynamic data, the choice of coordinates is arbitrary but is influenced by the manner in which the data are to be used. Some of the diagrams in use are enthalpy-entropy, enthalpy-pressure, enthalpy-specific volume, enthalpy-temperature, and temperature-entropy. Diagrams of the enthalpy-entropy form are common and are known as Mollier diagrams. The Mollier enthalpy-entropy chart is especially useful for a reversible adiabatic expansion or compression process (since the process is isentropic, it is very simple to follow the process as a vertical line on the chart), a constant enthalpy process, and enthalpy difference between states.

Where there is more than one component involved, the portrayal of the data is more difficult. For a binary system there is a maximum of three degrees of freedom, thus requiring three coordinates. If more than two components are involved, a complete portrayal of the data is not feasible. The Keenan-Keyes steam tables and the Keenan-Kaye gas tables are good examples of thermodynamic tables.

The problems in constructing a thermodynamic diagram are determining the property values at some convenient reference state and defining the equations which govern the relation between these properties. To illustrate the extent of the problem, consider the development of the thermodynamic diagram shown in figure 2.9. The reference values of enthalpy and entropy used in the development of this chart were

$$h_r = 85.64 \text{ Btu/lbm}$$

$$s_r = 0.6152 \text{ Btu/lbm}$$

measured at atmospheric pressure and $-320.4°$ F.

The first step toward the construction of figure 2.9 was to determine the actual gas density, γ, as a function of temperature and pressure. This was accomplished by using the real-gas equation of state

$$P = RT\gamma + C_1\gamma^2 + C_2\gamma^3 + C_3\gamma^6$$

where C_1, C_2, and C_3 are temperature-dependent constants.

Dividing the above equation of state through by γ^2 and rearranging yield

$$C_1 + C_2\gamma + C_3\gamma^4 = \frac{P}{\gamma^2} - \frac{RT}{\gamma}$$

Using the notation

$$\Delta = c_1 + c_2\gamma + c_3\gamma^4 = \frac{P}{\gamma^2} - \frac{RT}{\gamma}$$

The residual function Δ can be evaluated by varying the temperature with selected values of γ held constant and a curve of Δ versus T can be plotted along lines of constant density.

Defining Z, the compressibility factor, as the factor which accounts for real gas effects in the P–v–T relationships, the foregoing equation yields

$$P=\gamma^2\Delta+RT\gamma \qquad \text{and} \qquad Z=\frac{P}{\gamma RT}=\frac{\gamma\Delta}{RT}+1$$

Using figure 2.10 and the last two equations, it is possible to solve for the compressibility factor Z, and the pressure P at each value of γ intersected by a constant-temperature line. With P, γ, Z, and T known, it is possible to plot a compressibility chart such as that shown in figure 2.11.

The next step toward compiling the Mollier chart (fig. 2.9) is to determine the value of

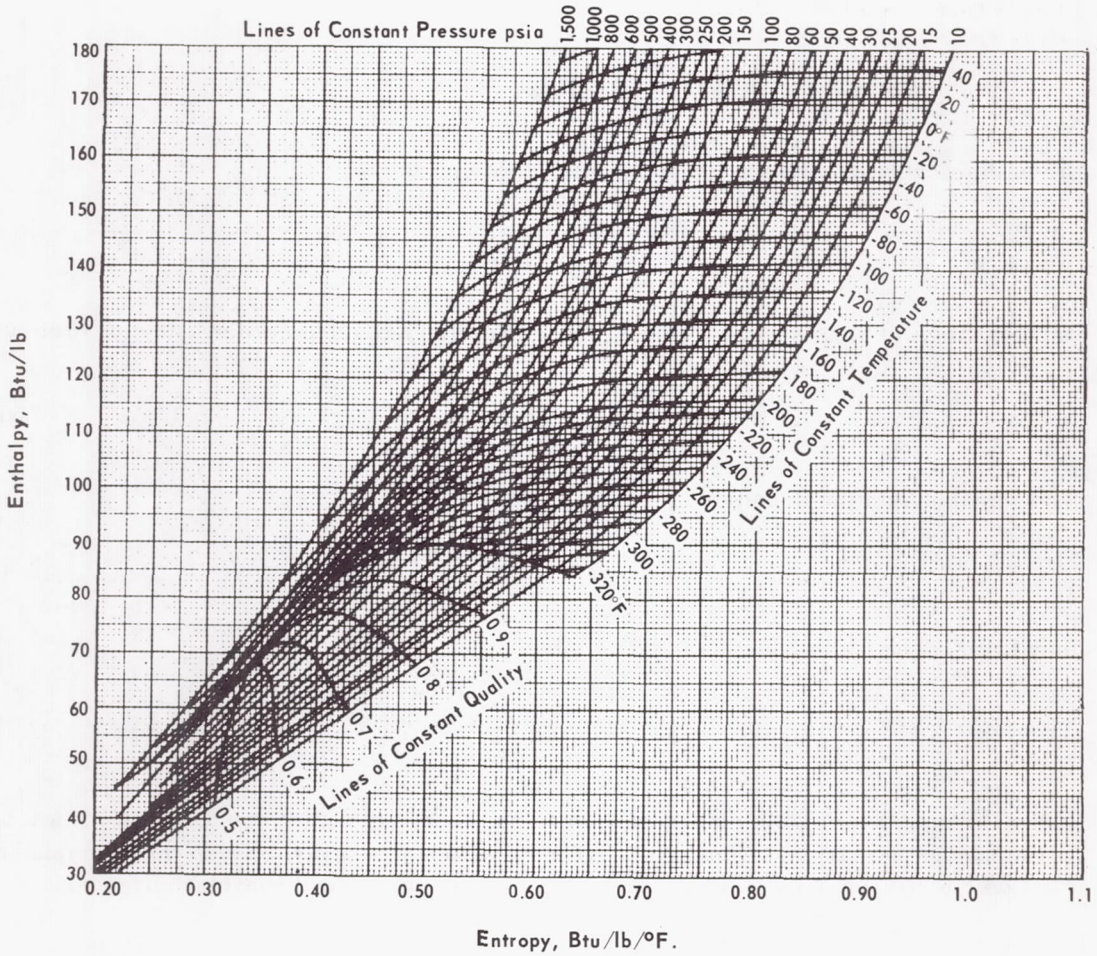


Figure 2.9. Mollier diagram for nitrogen. [*Courtesy of the Institute of Gas Technology.*]

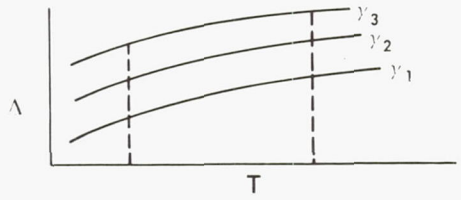


Figure 2.10. $\Delta - T$ diagram.

the two properties enthalpy and entropy at the selected values of pressure and temperature, or density and temperature. The expression for enthalpy may be written as

$$h_{T,P} = h_r + \int_{T_r}^{T} \left(\frac{\partial h}{\partial T}\right)_P dT + \int_{P_r}^{P} \left(\frac{\partial h}{\partial P}\right)_T dP \tag{2.34}$$

Since nitrogen is a pure substance, the enthalpy is defined as

$$dh = T\, ds + \frac{v\, dP}{J}$$

or, on differentiating with respect to P with T held constant,

$$\left(\frac{\partial h}{\partial P}\right)_T = T\left(\frac{\partial s}{\partial P}\right)_T + \frac{v}{J}$$

The Maxwell relation (eq. (1.13)) may be substituted into the preceding equation to obtain

$$\left(\frac{\partial h}{\partial P}\right)_T = v - T\left(\frac{\partial v}{\partial T}\right)_P \tag{2.35}$$

This equation and the definition of c_p,

$$c_p = \left(\frac{\partial h}{\partial T}\right)_P \tag{2.36}$$

may be combined with equation (2.34) to yield

$$h_{T,P} = h_r + \int_{T_r}^{T} c_p\, dT + \left(\frac{1}{J}\right) \int_{P_r}^{P} \left[v - T\left(\frac{\partial v}{\partial T}\right)_P\right]_T dP \tag{2.37}$$

Since the equation of state employed is in terms of density rather than pressure, it will be advantageous to rearrange equation (2.37) as a function of density. To do this, the relation $Pv = ZRT$ is written in differential form with the temperature held constant. Hence,

$$\int_{P_r}^{P} v_T\, dP = RT \int_{Z_{r=1}}^{Z} dZ - \int_{v_{r=\infty}}^{v} P\, dv$$

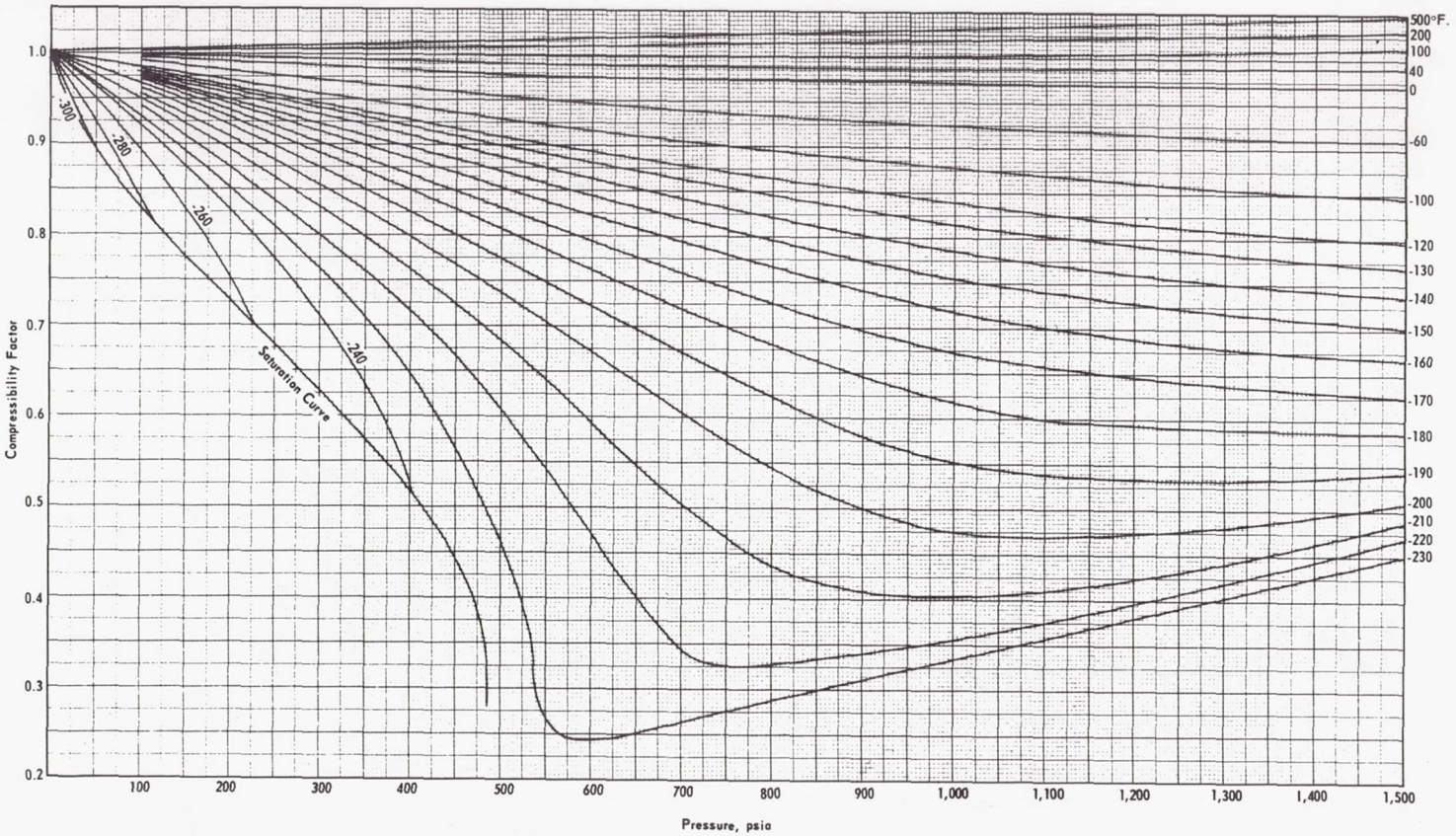


Figure 2.11. Compressibility factor for gaseous nitrogen. [*Courtesy of the Institute of Gas Technology.*]

and

$$\int_{P_r}^{P} v_T \, dP = RT(Z-1) - \int_{v_r}^{v} P \, dv \tag{2.38}$$

Next, the thermodynamic relation

$$\left(\frac{\partial v}{\partial T}\right)_P = -\left(\frac{\partial v}{\partial P}\right)_T \left(\frac{\partial P}{\partial T}\right)_v$$

substituted with equation (2.38) into equation (2.37) yields

$$h_{T,P} = h_r + \int_{T_r}^{T} c_p \, dT + (Z-1)\frac{RT}{J} - \left(\frac{1}{J}\right)\int_{v_r}^{v}\left[P - T\left(\frac{\partial P}{\partial T}\right)_v\right]_T dv \tag{2.39}$$

Introducing the relations $v = 1/\gamma$ and $dv = -d\gamma/\gamma^2$, equation (2.39) becomes

$$h_{T,P} = h_r + \int_{T_r}^{T} c_p \, dT + (Z-1)\frac{RT}{J} - \left(\frac{1}{J}\right)\int_{0}^{\gamma}\left[\frac{P}{\gamma^2} - \frac{T}{\gamma^2}\left(\frac{\partial P}{\partial T}\right)_\gamma\right]_T d\gamma \tag{2.40}$$

Using an analogous process, it may be shown that

$$s_{\gamma,T} = s_r + \int_{T_r}^{T} c_p \, d\,(\ln T) + \frac{1}{J}\int_{0}^{\gamma}\left[\frac{P}{\gamma} - \frac{\left(\frac{\partial P}{\partial T}\right)_\gamma}{\gamma^2}\right]_T d\gamma - \left(\frac{R}{J}\right)\ln\left(\frac{P}{Z}\right) \tag{2.41}$$

By using the compressibility chart (fig. 2.11) and equations (2.40) and (2.41), it is now possible to construct the Mollier diagram shown in figure 2.9. The procedure is as follows:

(1) Holding pressure constant, evaluate h from equation (2.40) and s from equation (2.41) at preselected values of temperature. Repeat for as many lines of constant pressure as required.

(2) Plot the values of h and s along the constant-pressure lines.

(3) Cross-plot lines of constant temperature on the constant-pressure lines.

Law of Corresponding States

There is yet another method of coping with real-gas deviation from perfect-gas behavior. This method is based on the law of corresponding states. The deviation of the volume of real gases from that predicted by the perfect-gas law can be simply represented by plotting the ratio of the actual volume to that predicted by the perfect-gas law versus the pressure or, in other words,

$$\frac{v}{\frac{RT}{P}} = \frac{Pv}{RT} = Z = \text{compressibility factor}$$

is plotted as the ordinate and pressure as the abscissa, for lines of constant temperature.

The law of corresponding states provides an avenue for determining the compressibility factor, z, in a generalized form that is applicable to all gases.

As previously stated, the extent of deviation from perfect-gas behavior increases as the region of condensation is approached. The law of corresponding states postulates that all

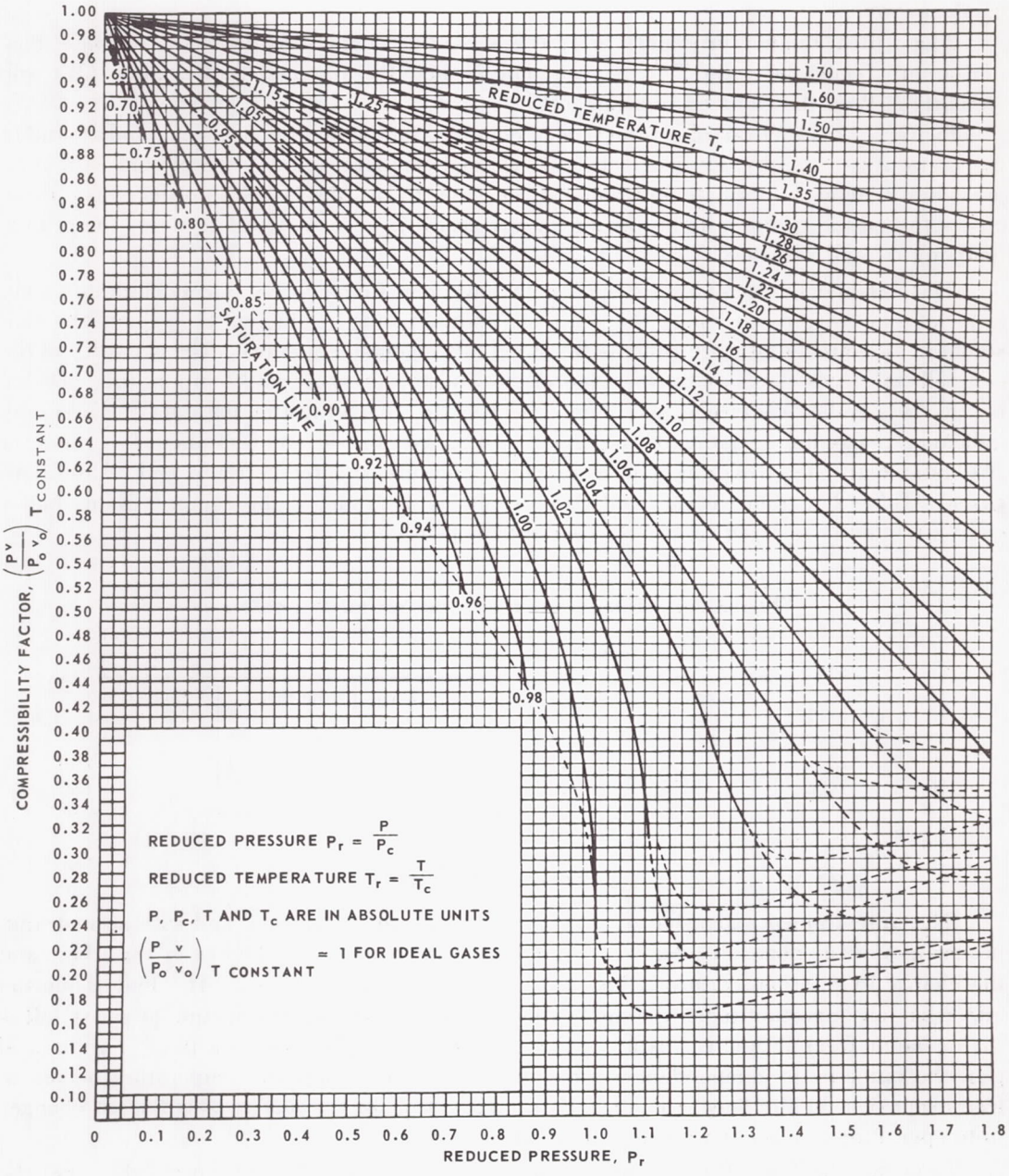


Figure 2.12. Compressibility factor for gases. [*Courtesy of the American Society of Mechanical Engineers.*]

gases have the same P–v–T behavior at the same reduced conditions. Hence, the behavior of all gases is correlated, not by using actual temperature and pressure but by using ratios of those values to the temperature and pressure at the critical point. In other words, the deviation of two gases may be very different at the same temperature and pressure, but may be the same if considered at the same temperature and pressure relative to the region of condensation.

The critical temperature and pressure are used as characteristics of the region of condensation. Thus the ratio T/T_c is commonly called the reduced temperature (T_r) and similarly P/P_c is the reduced pressure (P_r).

Figure 2.12 is an example of the type of compressibility factor charts commonly found in the literature; generally, lines of constant reduced temperature, T_r, are plotted with compressibility factor as ordinate and reduced pressure, P_r, as abscissa. In order to use these charts to find the compressibility factor for any gas, it is necessary to know only the critical temperature and pressure.

This method of correlating P–v–T data has been found to be of considerable value, especially in those cases where the available information is insufficient to evaluate the constants in an equation of state such as the Beattie-Bridgeman equation. The accuracy of the generalized charts depends on the type of gas and the pressure and temperature. Dodge has made a rather comprehensive comparison of the charts with actual data. His results indicate a maximum deviation of 15 percent and an average deviation of about 2 percent for 263 individual cases covering a wide range of pressure and temperature and 18 different gases. Table 2.4, from Getman and Daniels, shows the value of the compressibility factor chart (frequently referred to as "Hougen and Watson chart").

TABLE 2.4.—*Comparison of Compressibility Factors*

	Pv/RT for nitrogen at 1000 atm				
Temperature, °C	Observed	Ideal	Van der Waals	Berthelot	Hougen and Watson chart
0	2.0632	1.0000	2.426	0.731	2.10
50	1.9285	1.0000	2.182	1.071	1.95

Joule-Thomson Effect

The unrestrained expansion of a gas is known as free expansion, and with no restraint, no useful work is done. Under flow conditions, free expansion is known as throttling, and the change in gas temperature is known as the Joule-Thomson effect. The Joule-Thomson effect has an important industrial application in the cooling and liquefaction of gases. It is the deviation from perfect-gas behavior that makes these applications possible. For an ideal gas, the enthalpy is independent of pressure; hence, no change in temperature occurs in free expansion for the flow or nonflow case. However, for the real gas, significant changes in temperature may occur with free expansion.

Consider the flow of a real gas through the orifice restriction of figure 2.13. For the system shown, there is no work crossing the system boundary, and it is reasonable to neglect

heat transfer. For this system, the first law energy equation may be written in the form

$$h_1+\frac{V_1^2}{2g_cJ}=h_2+\frac{V_2^2}{2g_cJ}$$

where the subscript 1 denotes upstream conditions and the subscript 2 denotes downstream conditions.

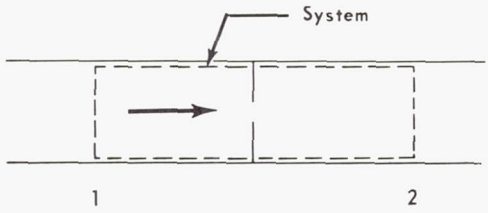


Figure 2.13. Gas flowing through an orifice in a pipe.

As the gas flows through the restriction, there is a decrease in pressure and an increase in specific volume with a corresponding increase in kinetic energy; however, the increase in kinetic energy is often negligible. For a situation where changes in kinetic energy are negligible, the throttling process may be considered isenthalpic.

$$h_1=h_2=\text{constant}$$

It is for this process that the Joule-Thomson coefficient is significant.

The Joule-Thomson experiment consists essentially of an adiabatic expansion of a gas through a line restriction. The experiment shows that though the enthalpy is constant for the process, a change in temperature accompanies the expansion. The temperature change is found to be equal to the change in pressure across the restriction multiplied by the Joule-Thomson coefficient, which is defined by the equation

$$\mu_j=\left(\frac{\partial T}{\partial P}\right)_h$$

The Joule-Thomson coefficient is the change in temperature with respect to pressure during an isenthalpic process.

Consider the expansion of a gas from point A to point B along the constant enthalpy line of figure 2.14. The changes in temperature and pressure between points A and B may be related by the expression

$$\Delta T_{AB}=(M_{AB})\Delta P_{AB} \tag{2.42}$$

For a given pressure change along the constant enthalpy line, the change in temperature will be positive or negative, depending on the sign of the slope M. The slope M of the line joining points A and B is the mean value of the Joule-Thomson coefficient between these points.

$$\mu_j(\text{mean})=M=\frac{T_B-T_A}{P_B-P_A}$$

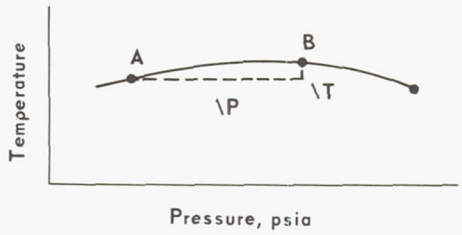


Figure 2.14. Constant enthalpy line for a real gas.

If lines of constant enthalpy are plotted on a $P-T$ diagram (fig. 2.15), it follows that the $(\partial T/\partial P)_h$ is the slope of the tangent to the constant enthalpy line.

Observing the line of constant enthalpy, it is evident that the slope of the curve can be positive, negative, or zero. The points on the constant-enthalpy lines, where the slope equals zero, are the inversion points, and the curve joining these points is the inversion curve. The physical significance of the inversion curve is that it shows that at a given pressure there exists a temperature above which it is impossible to have a positive Joule-Thomson coefficient. To illustrate, consider the pressure P_a of figure 2.15. If the temperature corresponding to this pressure is lower than T_a, it is possible to have a positive value of μ_j, as at point b on curve 1. If the temperature is above T_a, it is impossible to have positive value of μ_j, as is illustrated by point c on curve 3. This is to say, T_a is the maximum temperature the gas can have at the pressure P_a and have a positive Joule-Thomson coefficient.

The physical significance of the inversion curve is that positive Joule-Thomson coefficients occur to the left of the curve and negative coefficients occur to the right of the curve.

The inversion curve also shows the existence of a maximum inversion temperature for each gas. This temperature is represented by point d of figure 2.15 and is the temperature above which it is impossible to cool the gas by expansion.

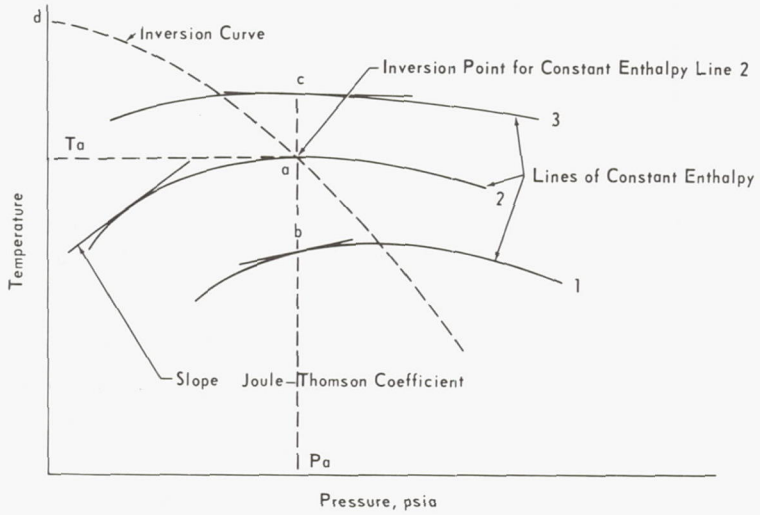


Figure 2.15. Temperature versus pressure for an actual gas.

CHAPTER 3

FUNDAMENTALS OF INCOMPRESSIBLE FLOW

The term "fluid" is applied to substances which, by the nature of their internal structure, offer comparatively little resistance to a change in form. Incompressible fluids, however, offer great resistance to volume change.

No fluid is capable of any internal adjustment which will enable it to maintain equilibrium at rest while subjected to a shear stress. If a shearing force is applied to any fluid, the fluid will continue to move as long as the force is applied. There will invariably be some movement in which the velocity is proportional to the applied shear stress. The relation between force and velocity depends on, among other things, that property of fluids known as viscosity.

An ideal or perfect fluid is merely one which, for purposes of developing theory or making a mathematical demonstration, is conveniently assumed to be nonviscous or incompressible, or both. Such fluids do not exist, and theory based on such assumption is subject in its application to correction for the effect of these physical properties that have been neglected.

In this chapter, only the flow of incompressible fluids is considered. The effects of work, heat addition or removal, and change in sonic velocity are neglected. In an incompressible fluid, an increase in pressure will not cause a significant increase in density. The assumption that liquids are incompressible usually does not introduce an appreciable error. The assumption that gases are incompressible, for flows below a mach number of 0.2, introduces only very slight error. Beyond this point, gases should be treated as compressible fluids.

MASS DENSITY AND SPECIFIC WEIGHT

"Mass density" is defined as the mass of a substance per unit volume. Specific weight is the gravitational force per unit volume exerted by the mass subjected to a given acceleration due to gravity. In this text, units for density are slugs per cubic foot or pounds mass per cubic foot, and specific weight has units of pounds force per cubic foot. The relation between these quantities is determined from Newton's first law written in terms of gravity.

$$F_{wt} = mg \tag{3.1a}$$

or

$$F_{wt} = \left(\frac{W}{g_c}\right) g \tag{3.1b}$$

If both sides of equations (3.1*a*) and (3.1*b*) are divided by the total volume $\bar{V}$, it follows that

$$\frac{F_{wt}}{\bar{V}}=\left(\frac{W}{\bar{V}}\right)\frac{g}{g_c}=\frac{mg}{\bar{V}}=\rho g \tag{3.2}$$

In this system, g_c must have the units of lbm/slug or lbm-ft/lbf-sec^2. Using equation (3.2), the following definitions are

Mass density = $\rho=\frac{m}{\bar{V}}$ slugs/ft^3 or lbf-sec^2/ft^4 (3.3*a*)

Weight density = $\gamma=\frac{W}{\bar{V}}$ lbm/ft^3 (3.3*b*)

Specific weight = $\gamma'=\frac{F_{wt}}{\bar{V}}$ lbf/ft^3 (3.3*c*)

Rewriting equation (3.2) in terms of the above three definitions, the following relationships are obtained:

$$\gamma=\rho g_c \tag{3.4a}$$

and

$$\gamma'=\rho g=\gamma\left(\frac{g}{g_c}\right) \tag{3.4b}$$

VISCOSITY OF FLUIDS

Viscosity is the property of a substance by which it offers resistance to shearing stresses. In a Newtonian fluid, the viscosity is in linear proportion to the ability of the fluid to resist such shearing stresses.

All substances, both liquids and gases, have viscosity. Because of this, the property should be explained by one or more physical properties common to all fluids, such as molecular activity. Because of molecular activity, there is a constant interchange of molecules and, therefore, of momentum between adjacent layers of the fluid. If adjacent layers are moving with different velocities, this constant interchange of momentum sets up a resistance to any relative motion of the two layers. As a result of this resistance, energy is transformed into heat; and to maintain the velocity, a steady force is required.

The viscosity of a liquid decreases with an increase in temperature. The interchange of momentum is accelerated with an increase in temperature, but the viscosity of a liquid must be regarded as the combined effect of cohesion and interchange of momentum. Cohesion is the force with which like molecules of a substance attract each other. A change in temperature has opposite effects on cohesion and molecular activity, with the effect of cohesion being more pronounced so that as temperature is decreased, viscosity is increased in a liquid. Because of low cohesive forces in gases, viscosity of gases increases with temperature.

When a shearing force or stress is applied to elastic bodies, there is a definite deformation which is proportional to the force. A shearing force applied to a viscous fluid causes an unlimited and continuous deformation of the material. The rate at which the deformation takes place is proportional to the force. The rate of deformation or shear becomes a measure of the viscosity of the fluid. The behavior of a substance under the influence of shearing stresses is the criterion by which it may be classified as a fluid or solid. Any material in which a continuous deformation is caused by a shearing force, however small, is a fluid.

In considering the effect of viscosity on fluid flow, it is necessary to introduce two fundamental assumptions which become the basis for the theory of viscosity. These assumptions are:

(1) There is no relative motion between a solid boundary and the layer of fluid in contact with it.

(2) The shearing stress between layers of fluid, of infinitesimal thickness, is proportional to the rate of angular deformation of the fluid (Newtonian fluids).

Consider two parallel plates (fig. 3.1); one fixed and one suspended on a layer of fluid. After applying a force F to the upper plate, the plate and the adjacent particles of fluid will acquire a steady velocity ΔV.

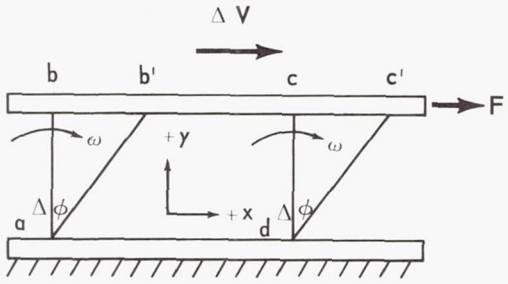


Figure 3.1. Deformation resulting from shear.

During some time interval, Δt, the fluid element, $abcd$, will change to the shape $ab'c'd$. If the point b moves to b' in time Δt with a velocity ΔV, then the distance bb' is equal to $\Delta V \Delta t$. The fluid particles along line ab are moved during time Δt to line ab', and the angular deformation can be expressed as

$$\Delta\phi \approx \tan \Delta\phi = \frac{bb'}{ab} = \frac{\Delta V \Delta t}{ab}$$

The fluid at any position between the plates has a velocity proportional to the distance from the lower plate. If the deformation takes place in a time Δt, the time rate of angular deformation of line ab is

$$\omega = \frac{\Delta\phi}{\Delta t} = \frac{\Delta V \Delta t}{ab \Delta t} = \frac{\Delta V}{ab} = \frac{\Delta V}{\Delta y}$$

NOTE: $ab = \Delta y$.

In the limit, where the fluid layer is very thin ($\Delta y \rightarrow 0$), the rate of angular deformation becomes just the velocity gradient,

$$\omega = \frac{dV}{dy}$$

where V is the velocity in the x direction and y is the displacement coordinate perpendicular to both the flow and the bounding surfaces of the layer.

Then, for a Newtonian fluid the shear stress, τ, at a given layer is, by definition, proportional to the rate of angular deformation or velocity gradient at that layer, so that

$$\tau = \mu \left(\frac{dV}{dy}\right) \tag{3.5}$$

The term μ is the coefficient of proportionality and is called the absolute viscosity or coefficient of absolute viscosity.

In the English system of units, equation (3.5) requires that the units of viscosity be lbf-sec/ft^2.

An alternate form of expressing the viscosity of liquids is the kinematic viscosity, which is defined by the equation

$$\nu = \frac{\mu}{\rho} = \frac{\mu g_c}{\gamma} = \frac{\mu'}{\gamma} \tag{3.6}$$

From equation (3.6) it follows that the units for kinematic viscosity in the English system are ft^2/sec. The use of kinematic viscosity is convenient in incompressible flow analyses (only), since it combines two fluid property constants into one.

Figure 3.2 shows a plot of viscosity versus temperature for liquid oxygen. Similar charts are presented in the appendixes for several liquids and for gases at low pressures. For extremely high gas pressures, viscosity no longer varies with temperature alone; pressure effects on viscosity may be appreciable. Therefore, viscosity data based on temperature considerations only may lead to significant error when dealing with high-pressure gases. This subject will be considered in more detail in chapter 4.

RELATION OF PRESSURE TO ELEVATION

The effect of change in elevation can have a very significant effect on fluid-flow calculations. The effect of elevation on pressure can be determined by considering the forces acting on a free body of the fluid. Consider a vertical fluid element of cross-sectional area A, such as shown arbitrarily as a right cylinder in figure 3.3.

The only vertical forces acting on the free body are the forces F_1, F_2 and the weight, F_{wt}. Summing forces in the vertical direction yields

$$\Sigma F = 0$$

$$F_1 - F_2 - F_{wt} = 0$$

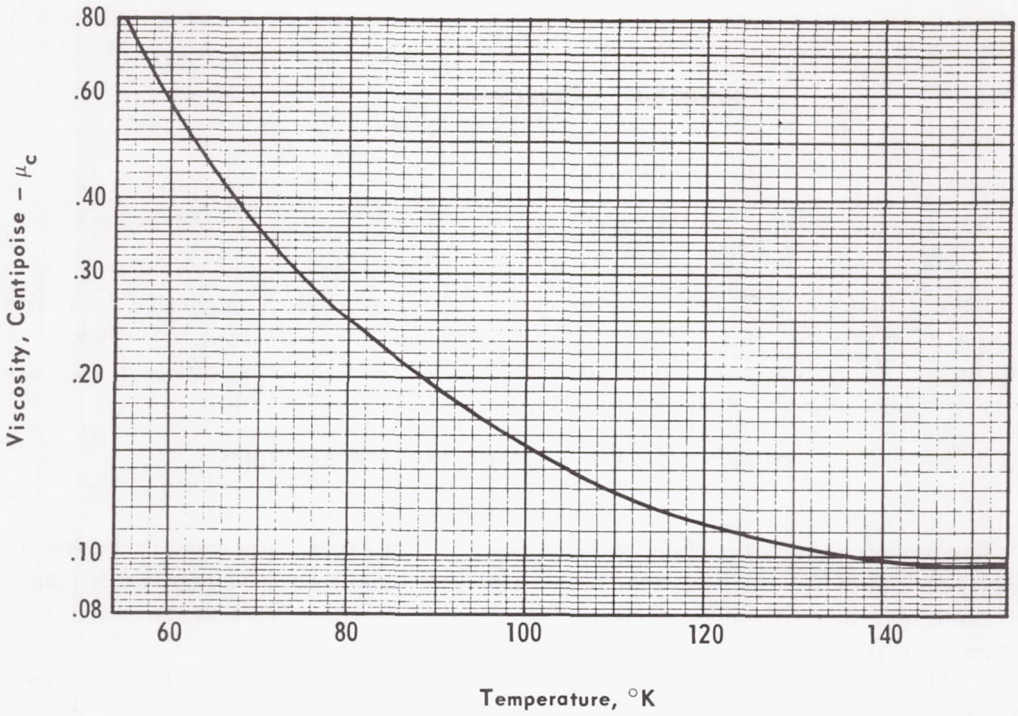


Figure 3.2. Viscosity of liquid oxygen.

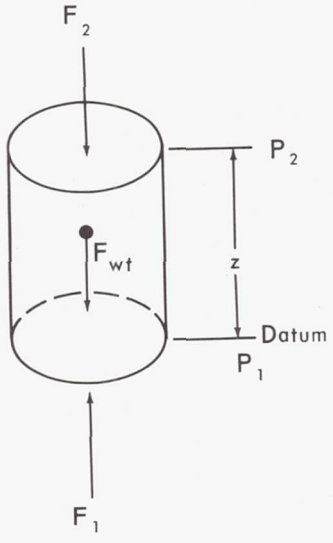


Figure 3.3. Forces acting on a fluid column.

Since the end forces are simply the fluid pressure multiplied by the area over which the pressure is acting and the weight force F_{wt} of the column is $\gamma'\bar{V}$ or $\gamma' Az$, the above relation reduces to

$$P_1 A - P_2 A - \gamma' Az = 0$$

or

$$P_1 - P_2 = \gamma' z = \left(\frac{g}{g_c}\right)\gamma z \tag{3.7}$$

This shows that the difference in pressures between two points separated by a vertical distance, z, is equal to the specific weight multiplied by the difference in elevation. Note that the specific weight term is proportional to density and can also vary with local gravity and other superimposed vertical accelerations that are summed up here as g.

STEADY-FLOW STREAMLINES AND STREAM TUBES

Steady Flows

The motion of a fluid is classified as steady, provided that at any point in the stream the velocity and all fluid properties remain invariant with time. This means that the conditions prevailing at a given fixed cross section of the flow (not moving with the stream) do not change with time. For a flow to be steady

(1) The mass rate of flow into the system is constant and equal to the mass flow rate out of the system

(2) The fluid is uniform in composition, state, and velocity at the entrance and exit of the system, and these do not vary with time

(3) The state of the fluid found at any point within the system is the same at all times

(4) The rate at which heat and work cross the boundary is constant.

Streamlines and Stream Tubes

In the usual case of steady flow, streamlines correspond with the paths of fluid particles. Also, the local direction of a streamline is the velocity direction of the particles as they pass the location. In this idealized concept, all particles entering the path described by a streamline will follow that streamline throughout its length. Except for the ideal frictionless fluid, this type of flow corresponds only with a highly laminar and viscous movement of fluid which is moving so slowly that no eddies are formed. However, even in the turbulent high-speed flow of a real fluid, streamlines can be defined as lines drawn everywhere tangent to the local mean velocities.

It is possible to consider a set of streamlines which form an imaginary enclosure within the flow field defined as a stream tube, as illustrated by figure 3.4. Because of the definition of the streamline, no fluid crosses the streamline boundaries of the stream tube, and the flow behaves as though it were restrained within the stream tube, except for friction. The stream tube lends itself to very convenient application of the equations of continuity and momentum.

CONTINUITY EQUATION

Since, by definition, no fluid can enter or leave a stream tube across the walls, it is possible to write an equation expressing the continuity of flow along a stream tube. Consider

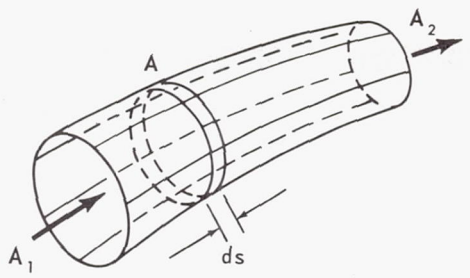


Figure 3.4. The stream tube.

the flow conditions at the arbitrary station where the flow cross-sectional area is A (fig. 3.4). The fluid passing through the cross section traverses a distance, ds, in a time interval, dt. Therefore, the volume of fluid passing through the cross section in time dt is just A ds. The mass of fluid represented by A ds is γA ds, and the mass flow rate per unit time is simply

$$\frac{\mathrm{d}W}{\mathrm{d}t}=\frac{\gamma A\,\mathrm{d}s}{\mathrm{d}T}=\gamma AV$$

since $\mathrm{d}s/\mathrm{d}t=V$, the nominal velocity of flow through A.

If w represents mass flow per unit time, the law of conservation of mass requires that, for a steady flow, w in a stream tube be a constant, or

$$w=\gamma_1 A_1 V_1=\gamma_2 A_2 V_2=\gamma AV \tag{3.8}$$

since there can be no accumulation between stations.

In incompressible fluid flow, where pressure changes do not cause changes in density, the continuity equation can be written simply as

$$\frac{w}{\gamma}=A_1V_1=A_2V_2=AV=\text{constant} \tag{3.9}$$

The result is that the velocity in a stream tube is inversely proportional to the local cross-sectional flow area.

BERNOULLI EQUATION

To obtain an equation for describing steady, constant-energy, frictionless flow, consider the differential length of the stream tube shown in figure 3.5. Flow is caused in this stream tube by the difference in pressure acting along the stream tube axis.

If the axial forces on the stream tube are summed, it follows from Newton's second law, $\Sigma F=m\alpha$, that

$$PA+\left(P+\frac{\mathrm{d}P}{2}\right)(A+\mathrm{d}A-A)-(A+\mathrm{d}A)(P+\mathrm{d}P)-mg\sin\theta=m\alpha$$

Neglecting all terms which are products of differentials, since they are vanishingly small in comparison to the other terms, yields

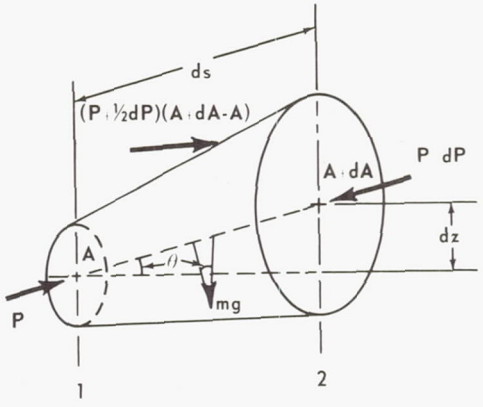


Figure 3.5. Forces acting on a stream-tube element in steady flow.

$$-A\ dP - mg\ \sin\theta - m\alpha = 0$$

Making the following substitutions

$$\alpha = \frac{dV}{dt} = \left(\frac{dV}{ds}\right)\frac{ds}{dt} = \frac{V\,dV}{ds} = \frac{1}{2}\left[\frac{d(V^2)}{ds}\right]$$

and

$$\sin\theta = \frac{dz}{ds}$$

and simplifying yields

$$A\ dP\ ds + mg\ dz + \left(\frac{m}{2}\right) d(V^2) = 0$$

This is an energy relation which states that in a frictionless system, work done by a force (in this case, the force due to the differing pressures on the stream tube elements) is balanced by equivalent changes in potential energy, $mg\ dz$, and kinetic energy, $m d(V^2)/2$, of the mass acted on. Dividing by mg yields

$$\frac{A.ds\ dP}{mg} + dz + \frac{d(V^2)}{2g} = 0$$

Since $mg = Wg/g_c$, it follows from the definition of specific volume that

$$\frac{A\ ds}{W\dfrac{g}{g_c}} = V\left(\frac{g_c}{g}\right)$$

neglecting second-order differentials. Therefore, substituting this relation into the flow relation yields

$$V\left(\frac{g_c}{g}\right)dP + dz + \frac{d(V^2)}{2g} = 0 \tag{3.10}$$

which integrates, at constant specific volume, to

$$\frac{P}{\gamma'} + z + \frac{V^2}{2g} = \text{constant} \qquad \text{ft} \tag{3.11a}$$

This is the familiar Bernoulli equation for steady, frictionless incompressible flow, in terms of fluid head. Multiplying through by (g/g_c) converts the terms to energy quantities so that

$$\frac{P}{\gamma} + \left(\frac{g}{g_c}\right)z + \frac{V^2}{2g_c} = \text{constant} \qquad \text{ft-lbf/lbm} \tag{3.11b}$$

MOMENTUM EQUATION

Newton's second law states that the resultant force applied to a free body can be equated to the rate of change of momentum of the body. Mathematically,

$$\Sigma\mathbf{F} = \frac{d}{dt}(\mathbf{MV}) \tag{3.12a}$$

which can also be written as the impulse-momentum principle,

$$\Sigma\mathbf{F}\ dt = d(\mathbf{MV}) \tag{3.12b}$$

This principle is often applied in the analysis of a wide variety of fluid dynamics problems. For example, in the more common case of a steady flow in a continuous flow conduit, such as in a stream tube (or more practically, in a conduit), the continuity equation can be substituted into the momentum term for an incremental quantity of fluid, dm, passing any station in the stream. Then $dm = \dot{m}\,dt = \rho A V\,dt$. Also, for the fixed station, the velocity is a constant so that

$$d(\mathbf{mV}) = \mathbf{V}\,d\mathbf{m}$$

Then the change in momentum that the increment of fluid experiences between any two stations in the stream is

$$\Delta(\mathbf{mV}) = (\mathbf{V}\ d\mathbf{m})_2 - (\mathbf{V}\ d\mathbf{m})_1$$

and the resulting force that must be applied to the increment of fluid between the stations must be

$$\Sigma\mathbf{F}\ dt = (\rho_2 \mathbf{A}_2 \mathbf{V}_2^2\ dt) - (\rho_1 \mathbf{A}_1 \mathbf{V}_1^2\ dt) \tag{3.13a}$$

or

$$\Sigma\mathbf{F} = (\rho_2 \mathbf{A}_2 \mathbf{V}_2^2) - (\rho_1 \mathbf{A}_1 \mathbf{V}_1^2)$$

Also, since the continuity equation holds throughout the length of the stream tube or conduit,

the resultant accelerating and turning force can be evaluated in terms of the mass flow rate and the vector difference in velocity by

$$\Sigma \mathbf{F} = \dot{m}(\mathbf{V}_2 - \mathbf{V}_1) \tag{3.13b}$$

This method of determining resultant forces on nozzles, piping systems, turbine blades, and so forth, offers the great advantage of evaluating only the inlet and outlet flow conditions and direction, rather than the integration of very complex pressure distributions within the flow section of interest.

REYNOLDS NUMBER

The flow and heat-transfer behavior of fluids can often be conveniently described or categorized by dimensionless parameters. One of the more widely used of these parameters is the Reynolds number, R_e. The Reynolds number can be rationally derived from dimensional analysis and has as its defining equation

$$R_e = \frac{VL\rho}{\mu} \tag{3.14a}$$

For the circular cross section, the length dimension is the diameter so that equation (3.14*a*) becomes

$$R_e = \frac{VD\rho}{\mu} \tag{3.14b}$$

The physical significance of the Reynolds number is that it represents the ratio of the inertial to the viscous forces acting in the fluid stream. This ratio, in turn, has a definite effect on such factors as heat-transfer coefficients and the coefficient of viscous friction. It is also possible to describe types of flow in terms of the Reynolds number. For low Reynolds numbers the viscous forces predominate, and the flow is termed "viscous flow," or "laminar flow." The Reynolds number for laminar flow is generally 2000 or less. The upper limit for laminar flow, however, is subject to some extent to vibrational effects and perturbations in the flow stream. For a steady, laminar flow in a horizontal circular pipe, the velocity profile is parabolic with a maximum velocity at the pipe centerline of

$$V_{\max} = \left(\frac{\Delta P_L}{L}\right)\frac{r^2}{4\mu}$$

and an average velocity of

$$V_{\text{avg}} = \left(\frac{1}{2}\right) V_{\max}$$

where $\Delta P_L/L$ is the pressure drop per unit pipe length, and r is the pipe radius. Figure 3.6 shows a typical velocity profile for laminar flow in a circular pipe. For Reynolds numbers of 4000 and above, the flow is governed primarily by inertial forces, and the velocity profile is no longer parabolic. The velocity profile has a tendency to become blunt and almost a straight line across the entire pipe cross section, as shown in figure 3.7.

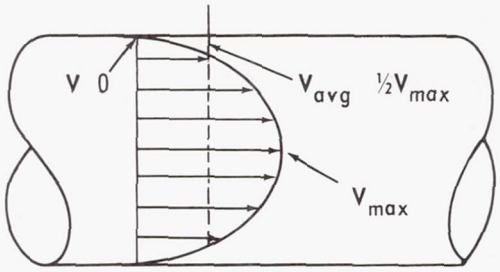


Figure 3.6. Velocity distribution in laminar flow.

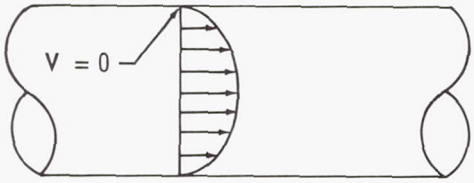


Figure 3.7. Velocity distribution in turbulent flow.

Between Reynolds numbers of 2000 and 4000, the flow is termed "transitional flow." In this region the flow can be either laminar or turbulent, or mixed. Above about 2100 if the system is disturbed, or if there are any irregularities, the flow will change from laminar to turbulent. In general, when the Reynolds number is above 2000, the flow is considered turbulent to some degree.

HYDRAULIC RADIUS

The major part of all piping in flow systems is of round cross section, but in some instances, this is not the case. Therefore, it is necessary to develop an equivalent diameter for these noncircular pipes. This equivalent diameter is primarily for use in computing the Reynolds number and is known as the hydraulic diameter. This hydraulic diameter of any cross section is defined as four times the hydraulic radius, defined in turn as

$$R_h = \frac{\text{cross-sectional area}}{\text{wetted perimeter of cross section}} = \frac{D}{4} \tag{3.15a}$$

For a differential length of pipe, the wetted area is

$$dA_w = (WP)\ dL$$

and it follows that

$$WP = \frac{dA_w}{dL}$$

Substituting this value into equation (3.15*a*) yields

$$R_h = A\left(\frac{dL}{dA_w}\right)$$

Now, by definition, the hydraulic diameter, D, is $4R_h$ so that

$$D = 4R_h = 4A\left(\frac{dL}{dA_w}\right) \tag{3.15b}$$

FLOW OF FLUIDS IN PIPES

Fluid flowing in a pipe is constrained laterally by pressure forces at the walls, so that the net fluid motion in the lateral direction is always zero. Conversely, axial velocity of the fluid is controlled by axial forces on the fluid, the predominant ones being differential pressure, viscous friction at the wall, acceleration, and gravity forces. The Bernoulli equation was developed earlier in this chapter to describe the steady-flow conditions in the ideal stream tube. The primary difference between stream-tube flow and practical pipe flow is the irreversible losses of energy that occur in pipes due to friction. When the Bernoulli equation is applied to pipe flow, the loss in energy is reflected as a deviation from equation (3.11*b*). The summation of the energy terms is no longer a constant at all points in the pipe. Rather, the summation decreases progressively at points taken farther downstream. In the case of incompressible flow, the static pressure term is the only term that can reflect the change in total energy of the stream.

The phenomenon can best be described by means of the Bernoulli equation, (3.11*b*), after multiplying through by the fluid weight density γ. This multiplication converts each term of the equation to units of pressure so that

$$P + g\left(\frac{\gamma}{g_c}\right)z + \left(\frac{\gamma}{2g_c}\right)V^2 = P_t$$

or

$$P + g\rho z + \left(\frac{1}{2}\right)\rho V^2 = P_t \qquad \text{lbf/ft}^2 \tag{3.16}$$

Here P_t is defined as the total pressure of the incompressible stream. Note that $g\rho z$ is the pressure resulting from elevational head, z, above some datum plane. Its magnitude is dependent on the fluid density and the local acceleration resulting from gravity (plus any superimposed accelerations that are being experienced by the entire system). The term $(\frac{1}{2})\rho V^2$ is the dynamic pressure resulting from velocity. It was shown in the case of the ideal stream-tube flow that there can be interchanges between the three pressure terms, but the total pressure is a constant. In the case of pipe flow, the interchange between the different forms of pressure terms also occurs as flow area (and, therefore, velocity) and elevational head changes. However, the total of the terms diminishes persistently because of friction and turbulence losses, and the loss is always reflected as a reduction in static pressure, P. The interchange of pressures and the loss in total pressure may be better understood by study of a pressure diagram such as figure 3.8, drawn for a typical section in a pipeline. Certain features of the pressure diagram should be noted and compared to the governing Bernoulli equation, equation (3.16).

(1) The elevation head pressure line becomes zero at the point where the pipe centerline intersects the horizontal elevation datum plane. This line is straight only because the pipe centerline was drawn straight.

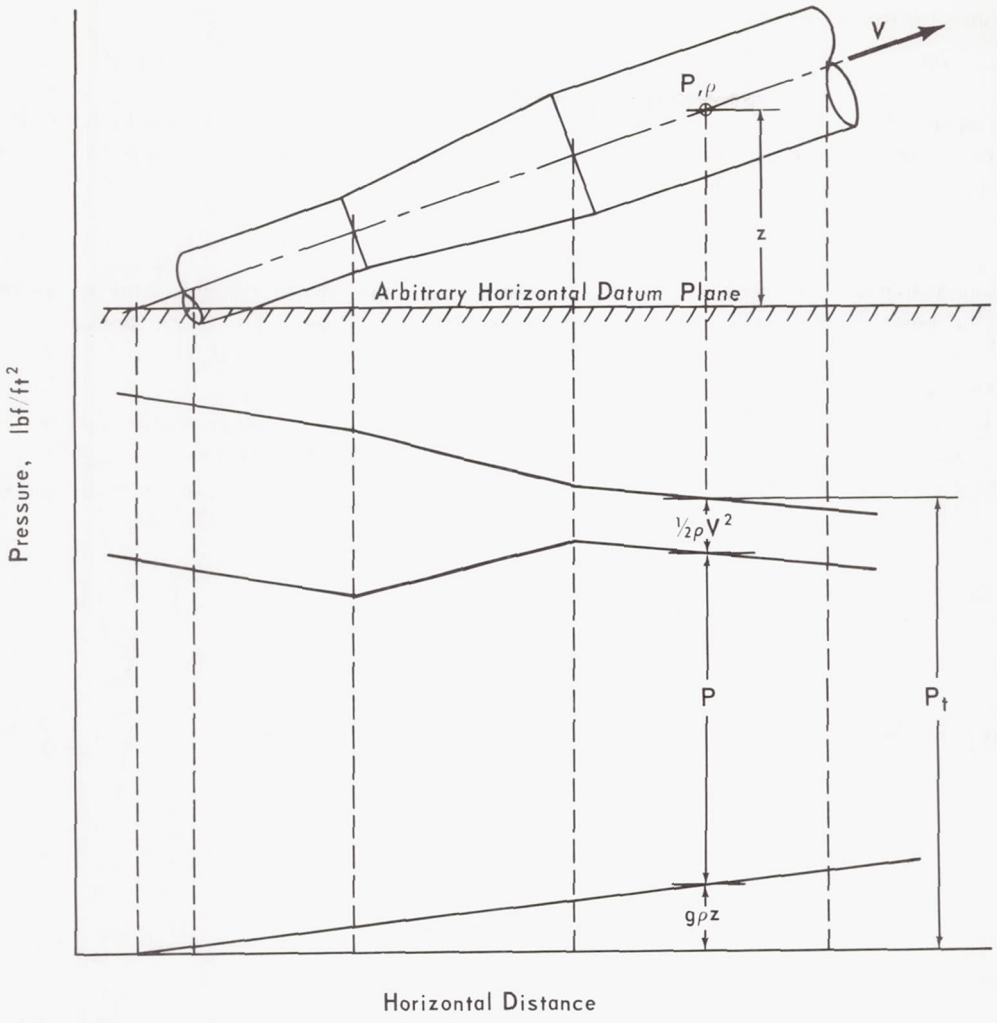


Figure 3.8. Pipeline section, flow with friction.

(2) The dynamic pressure term is constant in the constant-flow area sections, since continuity requires constant velocity for incompressible flow with constant area.

(3) The total pressure loss is due to viscous friction alone in the constant-area sections. In the variable-area section, the loss is due to additional turbulence and possibly boundary-layer separation, as well as friction. In such a diffusing section, the total pressure loss and the static pressure recovery are greatly dependent on design.

(4) It should be especially noted that even though there may be a significant loss in total pressure across a diffusing section (as shown) with a sudden expansion, there may be a net increase in static pressure due to the recovery of dynamic pressure.

A reinspection of equation (3.16) shows that for the common case of steady incompressible fluid flow in a constant-area pipe, the dynamic pressure is constant. Then the loss in total

pressure between two points in the pipe can be expressed as

$$P_{t1} - P_{t2} = P_1 + g\rho z_1 - P_2 - g\rho z_2$$

Also, since the loss is due only to viscous friction, the elevation terms are insignificant in an evaluation of friction losses. Therefore, the pipe can be assumed horizontal for the purpose of this investigation and

$$P_{t1} - P_{t2} = P_1 - P_2$$

This establishes that the loss in total pressure in steady incompressible flow in constant-area, horizontal pipes is just equal to the static pressure loss. The static pressure losses can be determined as the product of the frictional length parameter, $f(L/D)$, and the dynamic pressure as follows.

In the incompressible flow case, there can be no velocity change in the constant-area pipe, and, therefore, no acceleration. Thus, the static pressure forces on a fluid element of length dL can be equated directly to the viscous shear forces at the pipe wall. Then

$$PA - (P + dP)A = \tau\, dA_w$$

clearing and substituting the expression for shear stress,

$$\tau = f_\tau(\tfrac{1}{2}\rho V^2)$$

the relation between the two friction factors, derived subsequently as equation (8.17) (ch. 8).

$$f_\tau = \frac{f}{4}$$

and (equation 3.15*b*)

$$dA_w = 4A\left(\frac{dL}{D}\right)$$

yields

$$-dP = \left(\frac{f\rho V^2}{2D}\right) dL \tag{3.17}$$

Integrating the pressure change over the pipe length, L, yields the pressure loss due to viscous friction.

$$\Delta P_L = P_1 - P_2 = \left[f\left(\frac{L}{D}\right)\right]\left(\frac{1}{2}\right)\rho V^2 = \left[f\left(\frac{L}{D}\right)\right]\frac{\gamma V^2}{2g_c} \tag{3.18}$$

Equation (3.18) is the basis for computing frictional pressure losses for incompressible flow in constant-area pipes. This theory applies well over a wide range of flow conditions; however, it will be seen later on that an accurate estimation of the friction factor involves a thorough evaluation of the pipe and the prevailing flow condition as described by the Reynolds number.

For the case of completely laminar flow ($R_e < 2000$), an exact solution for the pressure loss can be obtained from the predictable velocity distribution in the pipe. The result is

the Hagen-Poiseuille equation, written as

$$\Delta P_L = \frac{32\mu LV}{D^2} \tag{3.19}$$

Substituting the definition of the Reynolds number $R_e = DV\rho/\mu$ and rearranging yields the common form for computing flow pressure loss in pipes

$$\Delta P_L = \left(\frac{64}{R_e}\right)\left(\frac{L}{D}\right)\left[\left(\frac{1}{2}\right)\rho V^2\right] = \left(\frac{64}{R_e}\right)\left(\frac{L}{D}\right)\left(\frac{\gamma V^2}{2g_c}\right) \tag{3.20}$$

FRICTION FACTOR

Equation (3.20) represents the loss in pressure because of viscous friction. In this equation the value of the friction factor is given by

$$f = \frac{64}{R_e} \qquad R_e < 2000$$

which holds for viscous, or laminar, flow only. In turbulent flow, the above relation for f does not hold, and the friction factor must be determined in a manner so that equation (3.18) correctly yields the pressure loss. In turbulent flow, f is found to be a more complex function of the Reynolds number and certain characteristics of the wall roughness that are signified by ϵ, ϵ', and m. These symbols are defined: ϵ is a measure of the size of the roughness projections and has dimensions of a length; ϵ' is a measure of the arrangement of spacing of the roughness elements and also has dimensions of a length; m is a form factor depending on the shape of the individual roughness elements and is dimensionless. The term f, instead of being a simple constant, is a factor that depends on seven quantities, or

$$f = f_1(V, D, \rho, \mu, \epsilon, \epsilon', m)$$

Since f is a dimensionless factor, it must depend on the grouping of these quantities into dimensionless parameters. For smooth pipes $\epsilon = \epsilon' = m = 0$, leaving f dependent on the first four quantities. They can be arranged in only one way to make them dimensionless; namely, $VD\rho/\mu$, which is the Reynolds number. For rough pipes the ϵ terms may be made dimensionless by dividing by D. Therefore, in general,

$$f = f_2\left(\frac{VD\rho}{\mu}, \frac{\epsilon}{D}, \frac{\epsilon'}{D}, m\right)$$

L. F. Moody has constructed one of the most convenient charts for determining friction factors in clean, commercial pipe. This chart, presented in figure 3.9 and, to a larger scale, in chapter 14, is the basis for many flow calculations requiring the friction factor in all ranges of the Reynolds number.

There is a less frequently used friction factor (shown in fig. 3.10) found in the literature. This factor is called the Stanton friction factor and is defined by the equation relating fluid shear stress

$$f_\tau = \frac{\tau}{\frac{\rho V^2}{2}}$$

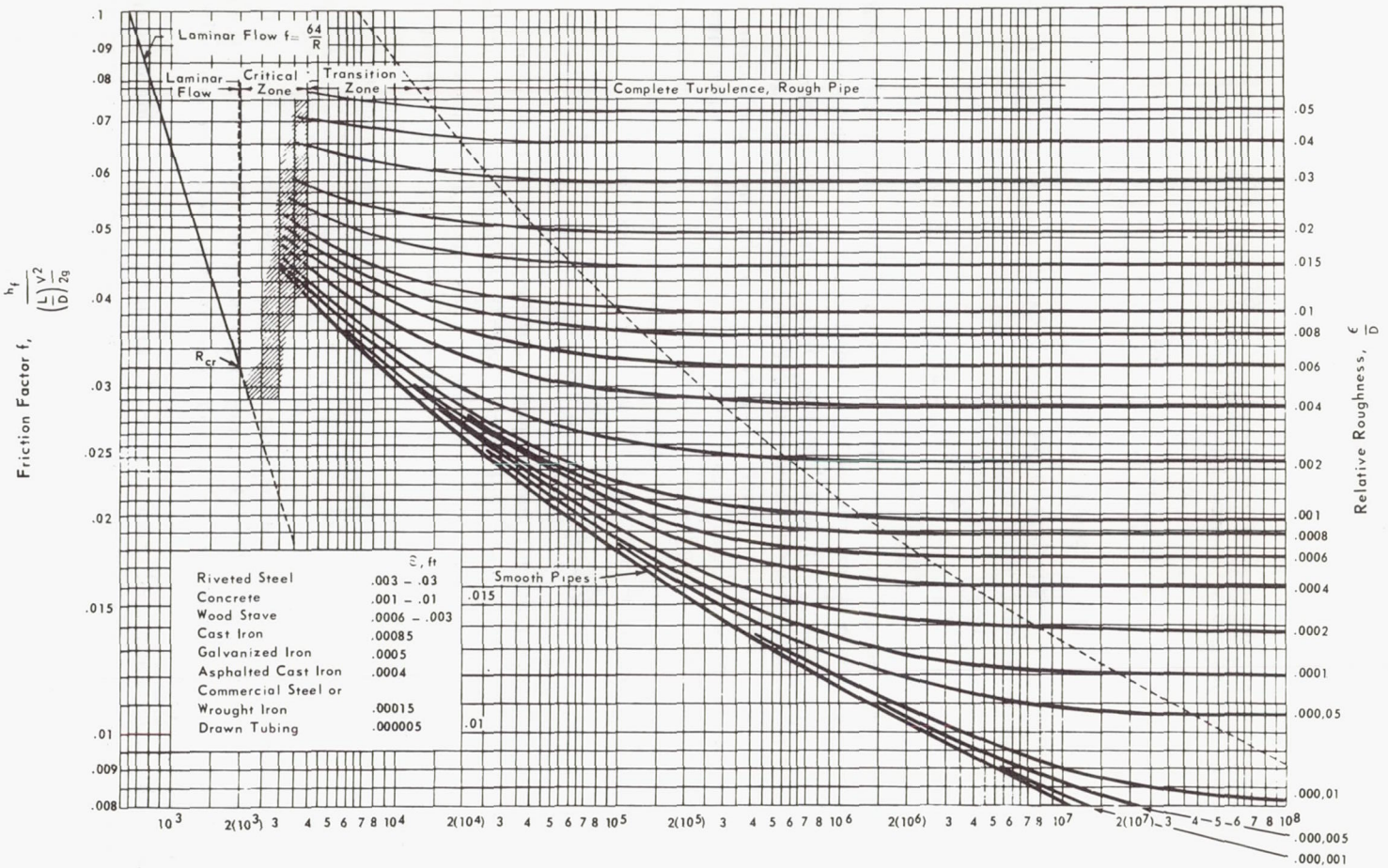


Figure 3.9. Moody friction factor diagram. [*Courtesy of the American Society of Mechanical Engineers.*]

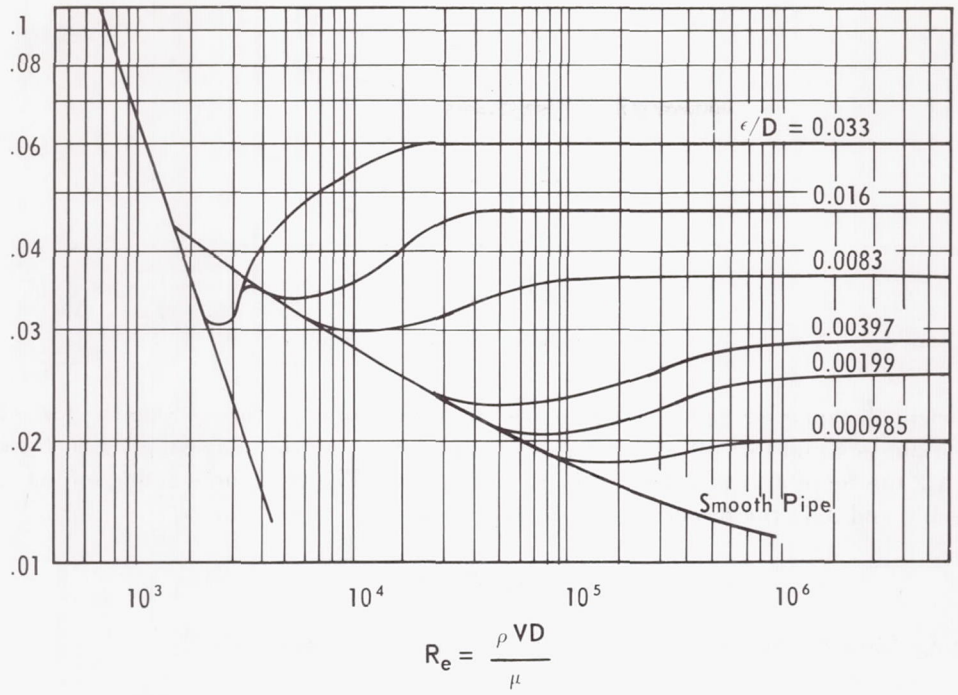


Figure 3.10. Stanton diagram. [*Courtesy of the American Society of Mechanical Engineers.*]

It will be shown in chapter 8 that the relation between the Moody and the Stanton friction factors is

$$f_\tau = \frac{f}{4} \tag{3.21}$$

where f is the Moody friction factor and f_τ is the Stanton friction factor. For a more detailed discussion of the relation between these two friction factors, refer to chapter 8, "Working Relations."

PRESSURE LOSSES IN PIPING SYSTEMS

There are numerous sources of pressure loss in piping systems in addition to that of fluid friction. As fluid flowing through a pipeline is caused to undergo a change in direction or velocity, a loss in pressure is experienced due to the turbulent conversion of energy to heat. The amount of this loss can, in some instances, be approximated by analytical calculation, but in most cases it must be determined experimentally.

Sudden Enlargement in Cross-Sectional Area

The pressure drop caused by a sudden area increase can be found by determining the forces acting on a system in the neighborhood of the area change. In figure 3.11 the pressure upstream of the area change is P_1 and that downstream is P_2.

At section 1 just downstream of the area change, the pressure is still equal to P_1 due to

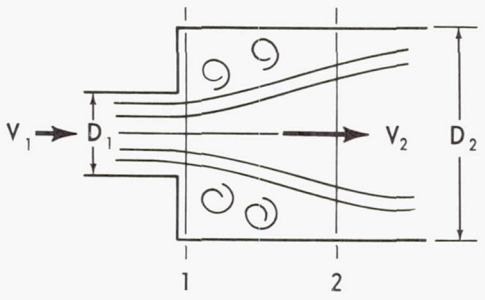


Figure 3.11. Sudden area increase.

insufficient distance for significant pressure drop to occur. At this section the force acting to the right is equal to P_1A_2. Further downstream the pressure has dropped to P_2, and at section 2 the force acting to the left is equal to P_2A_2. The total force acting on the section between 1 and 2, in the direction of flow, is given by

$$F = A_2(P_1 - P_2)$$

Equating this force to the momentum change, using equation (3.13*b*)

$$(P_1 - P_2)A_2 = \dot{m}(V_2 - V_1)$$

or

$$P_1 - P_2 = \rho V_2(V_2 - V_1)$$

Applying the Bernoulli equation from equation (3.16) between points 1 and 2 and solving for the loss in total pressure yield

$$\Delta P_{tL} = P_{t1} - P_{t2} = (P_1 - P_2) + \tfrac{1}{2}\rho(V_1^2 - V_2^2)$$

Now, substituting the value of $(P_1 - P_2)$ from the previous equation into the Bernoulli equation yields after combining and clearing

$$\Delta P_{tL} = \left(1 - \frac{V_2}{V_1}\right)^2 (\tfrac{1}{2}\rho V_1^2) \tag{3.22}$$

The velocity ratio V_2/V_1 can be expressed exactly as the area ratio A_1/A_2 in incompressible flow and also as the diameter ratio $(D_1/D_2)^2$. With this substitution the expression for total pressure loss becomes the product of a geometrical factor and the dynamic pressure

$$\Delta P_{tL} = \left(1 - \frac{A_1}{A_2}\right)^2 (\tfrac{1}{2}\rho V_1^2) = \left[1 - \left(\frac{D_1}{D_2}\right)^2\right]^2 (\tfrac{1}{2}\rho V_1^2) \tag{3.23}$$

This is of the same general form as the pattern established by equation (3.18), the pipe frictional pressure-loss equation. The coefficient of the dynamic pressure term is generally defined as the total pressure-loss coefficient K_t, so that for constant-area frictional pipes,

$K_t = f(L/D)$ and for sudden expansions,

$$K_t = \left(1 - \frac{V_2}{V_1}\right)^2 = \left(1 - \frac{A_1}{A_2}\right)^2 = \left[1 - \left(\frac{D_1}{D_2}\right)^2\right]^2 \tag{3.24}$$

The K_t value for a sudden expansion as defined by equation (3.24) is plotted versus the ratio of upstream to downstrean pipe diameter in figure 3.12. Also shown in this figure is a plot for the sudden contraction in the flow stream. The data for the second curve, however, cannot be determined by analytical means, but were determined from experimental data. Note that the K_t factors plotted in figure 3.12 are always based on dynamic pressure in the smaller diameter pipe. This can be seen by observing that the defining equation for K_t (eq. 3.23) is based on the velocity, V_1. If it is desired to convert the published K_t factor so as to be used with the dynamic pressure in the larger diameter pipe, the new factor must be defined as

$$\Delta P_{tL} = K_{t'}\left(\frac{1}{2}\rho V_2^2\right) \tag{3.25}$$

Then, by an analysis similar to the foregoing

$$K_{t'} = \frac{(V_1 - V_2)^2}{V_2^2} = \frac{(V_1 - V_2)^2}{V_1^2}\left(\frac{V_1}{V_2}\right)^2$$

and

$$K_{t'} = K_t\left(\frac{V}{V_2}\right)^2 = K_t\left(\frac{D_2}{D_1}\right)^4 \tag{3.26}$$

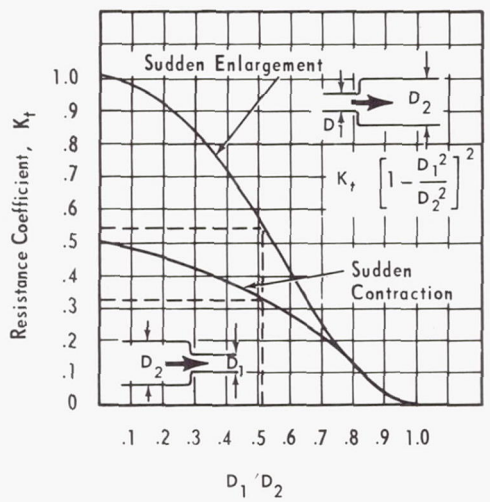


Figure 3.12. Loss resulting from sudden area change. [*Courtesy of Crane Co.; reproduced from Tech. Paper No. 410, Flow of Fluids.*]

Resistance of Bends

The resistance of bends to the flow of an incompressible fluid can be attributed to three factors (loss mechanisms).

The first of these three loss mechanisms is the frictional forces acting on the fluid over the length of the bend, as in the case of straight pipe frictional flow.

The second loss is the result of a condition known as secondary flow. This is a rotating motion circulating at right angles to the pipe axis caused by the combined effect of pipe-wall friction and centrifugal force.

The third loss is simply the excess loss in the portion of pipe just downstream of the bend. This loss is the result of the increased turbulence induced by the bend.

As in the case of friction loss and sudden area changes, the total pressure loss in bends has been found empirically to vary proportionally with the local dynamic pressure, over the wide range of turbulent flow conditions. Then

$$\Delta P_{tL} = K_{tb}\left(\frac{1}{2}\rho V^2\right)$$

where K_{tb} is the overall bend loss factor for the three combined loss mechanisms discussed above. In the case of bends, it has been found convenient to consider the loss factor as an equivalent frictional length parameter, $f(L/D)$. In this way the loss factor can be separated into two parts—that attributed to centerline length pipe friction and that attributed to the curvature (induced secondary flow and downstream turbulence). Then, in terms of the friction factor and dimensionless lengths

$$K_{tb} = \left[f\left(\frac{L}{D}\right)\right]_b = f\left(\frac{L_b}{D}\right) + f_{\text{tur}}\left(\frac{L}{D}\right)_e$$

The length, L_b, is the centerline length of the bend, and f should be evaluated for the particular pipe condition (ϵ/D) and flow condition (R_e), using the Moody diagram. The length L_e is the equivalent additional length that should be added to account for curvature losses. The value of L_e depends on the radius of centerline curvature, and the empirical variation has been plotted nondimensionally on figure 3.13 as bend resistance. The friction factor f_{tur} that should be assigned to the bend equivalent length is that of complete turbulent flow (the horizontal part of the Moody diagram curve at high value of R_e) at the pertinent pipe wall roughness factor, ϵ/D. This is due to the observed fact that the bend resistance portion of the total bend loss is largely unaffected by changes in the Reynolds number.

Figure 3.13 provides the necessary data for evaluating 90° bend losses and shows the breakdown of the two separate composite loss factors, as well as the total. A large-scale plot for both continuous and miter bends is included in chapter 14.

For continuous bends it has been found that the total resistance is less than that caused by a number of 90° bends, comprising the continuous bend. This is reasonable, since the loss in downstream tangent occurs only once in the continuous bend. However, reasonable accuracy and conservative results can be attained for continuous bends by considering the bend as being the sum of the required number of 90° bends.

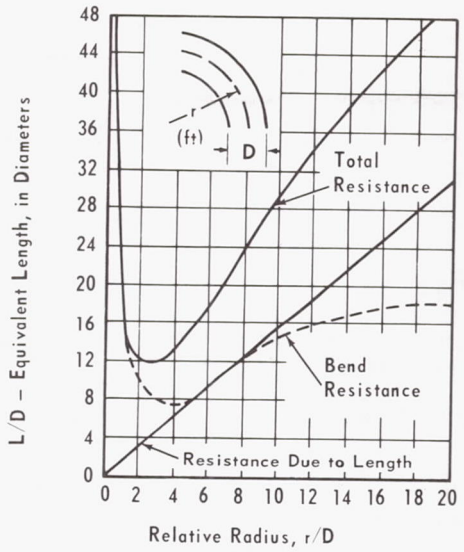


Figure 3.13. Resistance of bends. [*Courtesy of Crane Co.; reproduced from Tech. Paper No. 410, Flow of Fluids.*]

Entrance and Exit Losses

Losses due to pipe entrance and exit are the result of turbulence in the fluid stream caused by the entrance or exit configuration. Since there is no length involved with an entrance or exit, there is no effect caused by pipe roughness. Hence, for incompressible flows, relative size of entrance and exit does not affect the loss, and loss factors are dependent solely on the configuration of the entrance or exit.

Once again, the total pressure loss is found to increase linearly with dynamic pressure in the pipe and is proportional to a configuration pressure-loss factor. Then

$$\Delta P_{tl} = K_t \left(\frac{1}{2}\rho V^2\right) = \frac{K_t}{2g_c\gamma}$$

where V is the velocity just downstream of an entrance or just upstream of an exit. Values of K_t for several configurations are shown below in figure 3.14, and more are included in chapter 14, "Viscosity of Fluids." The reader is reminded that the static pressure changes across an entrance or exit must be evaluated with a consideration of the changes in dynamic pressure, per equation (3.16). For example, the static pressure loss across an entrance is the sum of the total pressure loss and the dynamic pressure inside the pipe entrance. Likewise, the static pressure loss across an exit into a large reservoir is zero.

Valves and Fittings

The pressure loss caused by standard fittings and valves installed in a pipeline varies with the internal configuration of the component. Variation due to fluid temperature and pressure has been found to be slight, and variation with the Reynolds number in the turbulent

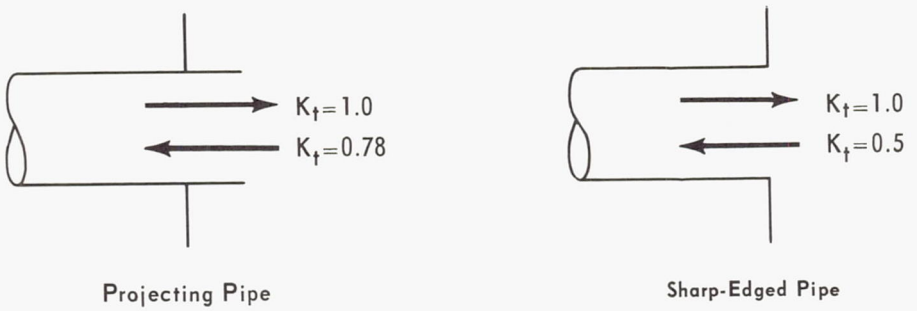


Figure 3.14. Resistance because of pipe entrance and exit. [*Courtesy of Crane Co.; reproduced from Tech. Paper No. 410, Flow of Fluids.*]

flow region is insignificant. However, in the laminar flow region the loss factor must be altered to account for an increased viscous effect.

Pressure-loss factors of valves and fittings are generally given in terms of an empirical K_t or an equivalent pipe length, based on the inside diameter of the pipe for which the component is constructed. The method of determining K_t consists of determining the loss across the component, measuring the velocity in the pipe adjoining the component, and solving for the equivalent K_t or L/D for the component from the equations

$$K_t = \frac{\Delta P_{tL}}{\frac{1}{2}\rho V^2}$$

or

$$\left(\frac{L}{D}\right)_e = \frac{\Delta P_{tL}}{f(\frac{1}{2}\rho V^2)}$$

where f is the Moody friction factor read at high (fully turbulent) Reynolds number for the adjacent pipe. Table 3.1 shows various L/D values found for several components by different investigators. K_t and other tables of L/D values for various components are to be found in "Viscosity of Fluids." The variations in published L/D and K_t values for given components reflect the wide differences that can occur in the design of valves in the same general category.

The equivalent lengths shown in table 3.1 are based on the pipe size for which the component was designed. It has been shown by tests that the pressure-drop variations resulting from mating the component to different thicknesses of the same nominal pipe size are small within reasonable limits. However, for calculational purposes, if the pipe size is altered, the value of L/D for the valve must also be altered. It follows that since pressure drop varies as the second power of the velocity, which varies as the second power of the diameter, the relation between the two L/D values is

$$\frac{L}{D} = \left(\frac{L}{D}\right)_{\text{std}} \left(\frac{D}{D_{\text{std}}}\right)^4 \tag{3.27}$$

The relations between the several commonly used flow factors for components are derived and presented in chapter 10. The most important are, for incompressible flow,

$$K_t = f\left(\frac{L}{D}\right) = \left(5472\,\frac{A}{C_v}\right)^2$$

TABLE 3.1.—*Equivalent Lengths of Valves and Fittings*

Type component	L/D [a]	L/D iron pipe [b]	L/D copper tubing [b]	K_f [c]	L/D [d]	K_f [e]	L/D [e]	K_f [f]
Angle valve conventional	145–200			2.1–3.1	165–204	3	170	
Angle poppet unobstructed with stem 45° from line of pipe								2.75
Angle poppet with stem 60° from line of pipe								3.4
Angle poppet in 90° pipe bend								6.5
Butterfly valve 6 in. and larger	20							
Butterfly valve 7 percent thick								.13
Butterfly valve 35 percent thick								.60
Check valve conventional swing	135							2.5
Check valve clear way swing	50							.95
Check valve in line ball	150							
Recessed swing check								
Gate valve conventional	13	12.5	17.5	0.05–0.19		0.13	7	
Gate valve pulp stock	17							
Globe valve conventional	340–450	300.0	425.0	5.2–10.3	335–448	6.0	300	
Globe valve Y-pattern	145–175							
Bend 180° return close pattern	50			0.75–2.2		1.7	75	
Bend 180° medium return						1.2	50	
Bend flanged return composed of 2 90° elbows				0.38				
Bend flanged return long radius				0.26				
Cock 3-way flow straight through	44							
Cock 3-way flow through branch	140							
Coupling reducing		10.0	10.0					
45° elbow	16	17.8	17.8			.3	15	
45° long radius flange				0.14–0.23				
90° elbow standard radius	30	25.4	25.4		32	.74	32	
90° elbow medium radius	20	12.4	12.4			.60	26	
90° elbow long radius						.46	20	
90° elbow standard screw				0.56–0.90				
90° elbow long radius screw				0.22–0.60				
90° elbow standard flange				0.21–0.30				
Square-edged inlet				0.47–0.56				
Tee used as elbow entering run						1.3	60	
Tee used as elbow entering branch						1.9	90	
Standard tee flow through	20							
Standard tee flow through branch	60	45.0	30.0		65–96	1.3	60	
Standard screw tee flow through				40		1.9	90	
Standard screw tee flow through branch				0.85–1.30				
Long radius screw tee flow through branch				0.37–0.80				
Long radius screw tee flow through				0.50–0.52				
Reducer bell mouth				0.04–0.05				
Coupling and unions				0.02–0.07				

[a] Crane Corp., 1957.
[b] Jennings, 1958.
[c] Dahle, 1958.
[d] Kent, 1950.
[e] Perry, 1959.
[f] Society of Automotive Engineers, 1962.

Analysis of test data on the effect of end connections indicates there is little, if any, justification for assigning different resistance coefficients to a given valve or fitting with varying types of end connections. The difference between flanged, screwed, and welded ends, in this respect, has been found to be insignificant. The pressure drop resulting from unions, couplings, and flanged joints is likewise insignificant in incompressible flow.

Divergent Branches

The loss in total pressure resulting from flow through divergent branches in piping systems has been found experimentally to depend on the split in mass flow rate, the flow areas involved, and the branch angle. The empirical total pressure-loss data are presented in figure 3.15, along with a sketch showing the system of locating the pressure points and branch angles. The total pressure loss is plotted versus the ratio of mass velocities for the two sections of interest, with the branch angle as a parameter. The angle of the third branch has insignificant effect. Then the total pressure loss between stations 1 and 2 of the divergent branch is

$$\Delta P_{tL} = {}_1K_{t2}\left(\frac{1}{2}\rho V_1^2\right) = \frac{{}_1K_{t2}}{2g_c\gamma}\left(\frac{w_1}{A_1}\right)^2 \tag{3.28}$$

Convergent Branches

Convergent branches, as depicted in figure 3.16, are handled in similar fashion, except that the evaluation of K_t requires a computation using the approximate equation

$${}_1K_{t3} = \lambda + \left(\frac{G_3}{G_1}\right)^2 - 2\left(\frac{A_1}{A_3}\right)\cos\beta' - \left(\frac{G_2}{G_1}\right)^2\left[2\left(\frac{A_2}{A_3}\right)\cos\delta'\right] \tag{3.29}$$

Each of the variables or groups of variables is evaluated from the data of figure 3.16, and the total pressure loss is computed by

$$\Delta P_{tL} = {}_1K_{t3}\left(\tfrac{1}{2}\rho V_1^2\right) = \frac{{}_1K_{t3}}{2g_c\gamma}\left(\frac{w_1}{A_1}\right)^2 \tag{3.30}$$

OVERALL LOSS FACTORS

Lines in Series

If pipes of different sizes are connected in series as shown in figure 3.17, an overall total pressure-loss coefficient for the system can be derived. Adding the total pressure losses, resulting from both friction and area change, in the circuit yields

$$\Delta P_{tL} = \left[f\left(\frac{L}{D}\right)\right]_1 \left(\tfrac{1}{2}\rho V_1^2\right) + K_{t1}\left(\tfrac{1}{2}\rho V_1^2\right) + \left[f\left(\frac{L}{D}\right)\right]_2 \left(\tfrac{1}{2}\rho V_2^2\right) + K_{t3}\left(\tfrac{1}{2}\rho V_3^2\right) + \left[f\left(\frac{L}{D}\right)\right]_3 \left(\tfrac{1}{2}\rho V_3^2\right) + \cdots$$

Dividing through by the dynamic pressure term for the first section of pipe $(\frac{1}{2}\rho V_1^2)$ and applying the continuity equation for incompressible flow yield

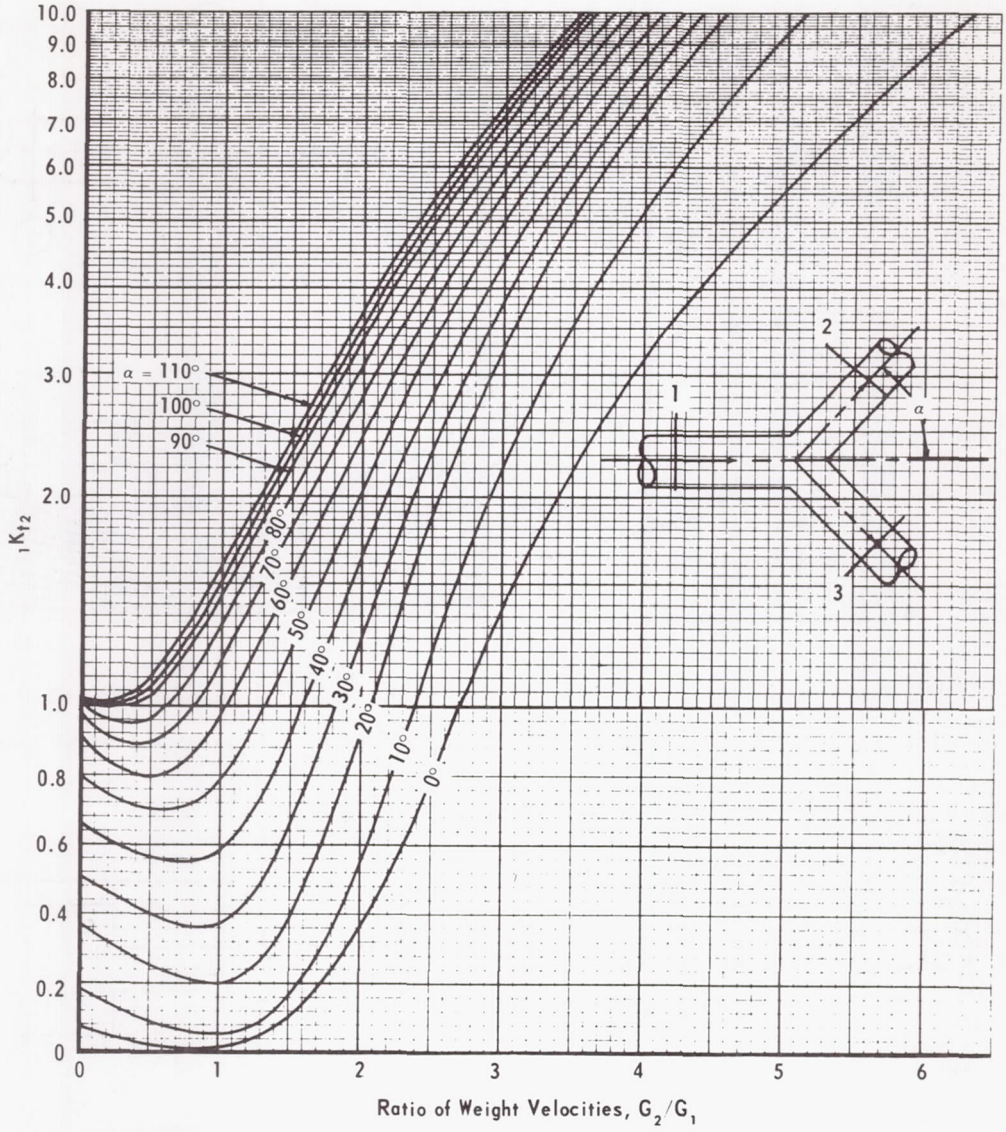


Figure 3.15. Divergent branch—loss coefficient, $G_2/G_1 < 1$. [*Courtesy of the Society of Automotive Engineers.*]

$$\frac{\Delta P_{tl}}{\frac{1}{2}\rho V_1^2} = \left[f\left(\frac{L}{D}\right)\right]_1 + K_{t1} + \left[f\left(\frac{L}{D}\right)\right]_2 \left(\frac{D_1}{D_2}\right)^4 + K_{t3}\left(\frac{D_1}{D_3}\right)^4 + \left[f\left(\frac{L}{D}\right)\right]_3 \left(\frac{D_1}{D_3}\right)^4 + \cdots$$

Then, in general terms, the overall coefficient for total pressure loss, based on the dynamic pressure in the first section of pipe, is

$$\frac{\Delta P_{tl}}{\frac{1}{2}\rho_1 V_1^2} = K_{to} = \sum \left(f\frac{L}{D}\right)_n \left(\frac{D_1}{D_n}\right)^4 + \sum K_{ts}\left(\frac{D_1}{D_s}\right)^4 \tag{3.31}$$

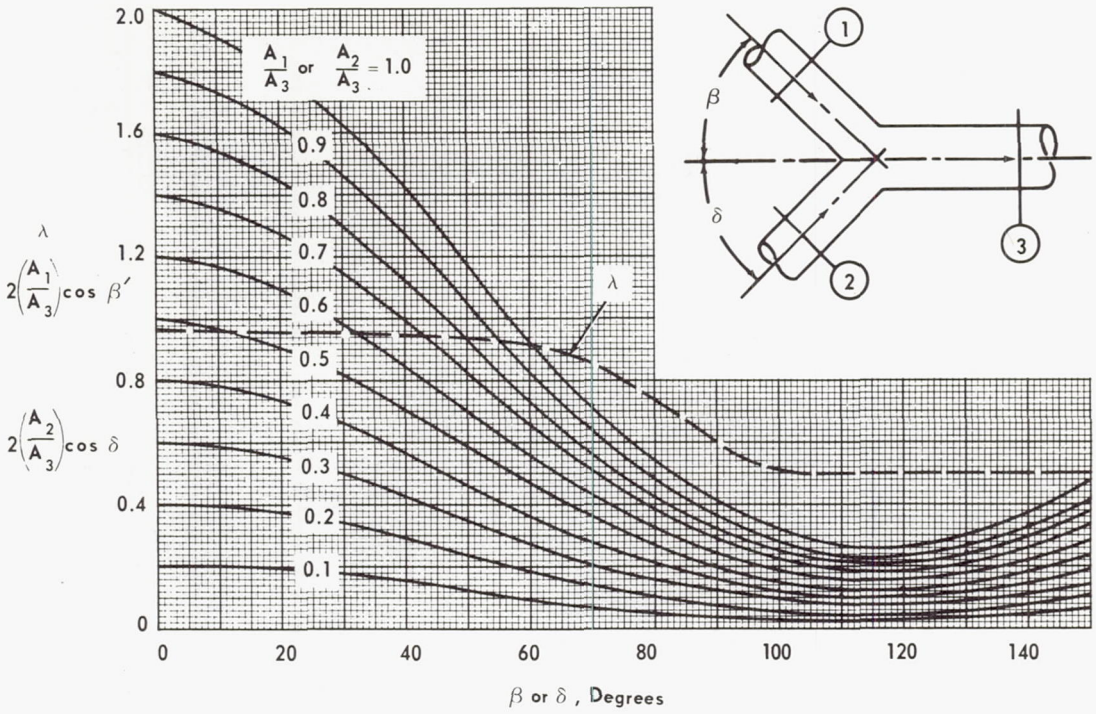


Figure 3.16. Convergent branch—functions for computing loss coefficient. [*Courtesy of the American Society of Automotive Engineers.*]

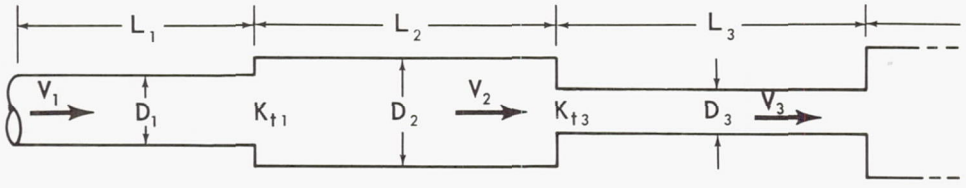


Figure 3.17. Lines in series.

Here, s indicates the smaller of the two pipes at the sudden area change, and K_{ts} is read from figure 3.12. Other types of fittings and valves can be included into the overall coefficient in the same manner, by including the diameter ratio factor when the device is of a different size than the reference size.

Lines in Parallel

In the case of series lines above, the loss in total pressure for the system was found to be the sum of the losses in the separate parts. In the case of parallel lines connected into common reservoirs on both ends as in figure 3.18, the loss in total pressure is equal in all the lines. Then

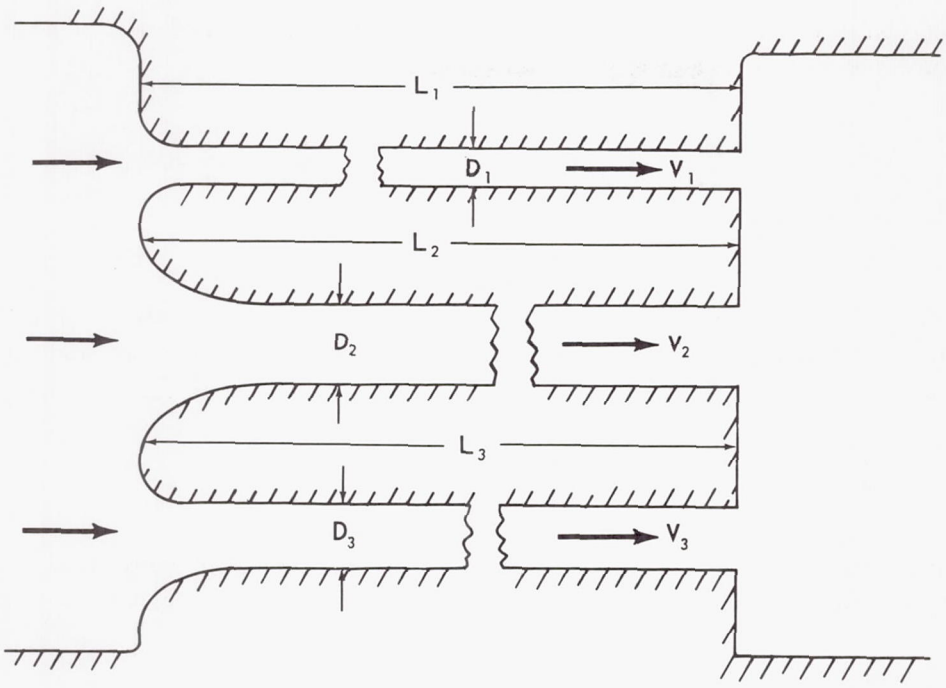


Figure 3.18. Parallel lines.

$$\Delta P_{tL} = K_{t1}(\tfrac{1}{2}\rho V_1^2) = K_{t2}(\tfrac{1}{2}\rho V_2^2) = K_{tn}(\tfrac{1}{2}\rho V_n^2) = \cdots$$

Also, the total mass flow rate is the sum of the flow rates in each line so that

$$w_t = w_1 + w_2 + \cdots + w_n + \cdots$$

It should be noted here that each of the parallel lines may be a complex series line having fittings, valves, and different-size pipes as discussed in "Pressure Loss in Piping Systems." If so, the individual K_t factors mentioned here are the overall values for each series line K_{to} as may be obtained by means of equation (3.31).

Proceeding, the individual mass flow rates can be expressed by means of the pressure-loss relationships above. Substituting and solving for mass flow rate in one line yield

$$w = A\sqrt{\frac{2g_c\gamma\Delta P_{tL}}{K_t}} \tag{3.32}$$

so that the total mass flow rate w_t is

$$w_t = \sqrt{2g_c\gamma\Delta P_{tL}}\left[\left(\frac{A}{\sqrt{K_t}}\right)_1 + \left(\frac{A}{\sqrt{K_t}}\right)_2 + \cdots + \left(\frac{A}{\sqrt{K_t}}\right)_n + \cdots\right]$$

The total flow rate can also be conveniently expressed as a ratio of the flow in some arbitrary reference line such as line 1. Then

$$\frac{w_t}{w_1}=1+\left(\frac{A_2}{A_1}\right)\sqrt{\frac{K_{t1}}{K_{t2}}}+\cdots+\left(\frac{A_n}{A_1}\right)\sqrt{\frac{K_{t1}}{K_{tn}}}+\cdots$$

and for N pipes

$$\frac{w_t}{w_1}=\sum_1^N\left(\frac{D_n}{D_1}\right)^2\sqrt{\frac{K_{t1}}{K_{tn}}} \tag{3.33}$$

Equation (3.32) can be written for line 1, substituted into equation (3.33), and solved for ΔP_{tL} as

$$\Delta P_{tL}=\left(\frac{K_{t1}}{2g_c\gamma}\right)\left[\frac{w_t}{A_1\sum_1^N\left(\frac{D_n}{D_1}\right)^2\sqrt{\frac{K_{t1}}{K_{tn}}}}\right]^2 \tag{3.34}$$

It is also convenient to define an overall total pressure-loss coefficient in the usual terms, and involving quantities that are generally known. The most convenient form is

$$\Delta P_{tL}=K_{to}\left(\frac{1}{2}\rho V_t^2\right)=\frac{K_{to}}{2g_c\gamma}\left(\frac{w_t}{A_t}\right)^2 \tag{3.35}$$

where the fictitious total or overall velocity is defined as

$$V_t=\frac{w_t}{\gamma A_t}$$

and A_t is the total flow area of all the lines. After combining and equating with equation (3.34), the overall loss factor is found in terms of only the piping system description as

$$K_{to}=K_{t1}\left[\frac{\sum_1^N\left(\frac{D_n}{D_1}\right)^2}{\sum_1^N\left(\frac{D_n}{D_1}\right)^2\sqrt{\frac{K_{t1}}{K_{tn}}}}\right]^2 \tag{3.36}$$

where

$$\sum_1^N\left(\frac{D_n}{D_1}\right)^2=\frac{A_t}{A_1}$$

Then for a given total flow rate and the piping system description, the loss in total pressure (which is also the loss in static pressure between reservoirs in this case) can be computed using equations (3.35) and (3.36). Likewise, when the pressure loss is known, equation (3.35) can be solved explicitly for total mass flow rate.

It should be noted that when all the parallel lines have identical values of D and K_t, equation (3.36) predicts an overall loss factor equal to each of the individual loss factors.

CHAPTER 4

INTRODUCTION TO COMPRESSIBLE FLOW

Compressible flow is characterized by variation in fluid density along the flow path. In a compressible flow there are several parameters which are most convenient in relating fluid property changes along the flow path. These parameters are the speed of sound, the mach number, and the dimensionless flow parameter ϕ. In addition, the Reynolds number and viscosity are also used in compressible flows in characterizing flows and determining frictional lengths of piping systems.

Also involved in compressible flows are effects caused by high pressure. As will be illustrated herein, high pressure causes variation in viscosity and hence Reynolds numbers as well as significant variation in pressure-drop-flow rate relations. In this chapter, the fundamental concepts of compressible flow are illustrated, and also high-pressure effects on fluid flow are explained.

CLASSIFICATION OF FLOWS

In problems concerning fluid flow, the ratio of the flow velocity to the velocity of sound in the media is a most convenient parameter for classifying flow. This classification is necessary, since the characteristic equations which describe the fluid properties along the flow path vary according to the magnitude of the ratio

$$M=\frac{V}{c}$$

where M is a dimensionless ratio termed the mach number, V is the flow velocity, and c is the speed of sound in the fluid at the local flowing conditions. The several classifications of flow may be illustrated graphically by considering the first law energy equation in the form

$$h+\frac{V^2}{2g_cJ}=h_o=\text{constant}$$

Using the perfect-gas relations

$$dh=c_p\,dT,\ c=\sqrt{kg_cRT} \qquad \text{and} \qquad c_p=\frac{kR}{k-1}$$

it follows that

$$\frac{c^2}{(k-1)}+\frac{V^2}{2g_cJ}=\frac{c_0^2}{(k-1)}$$

where c_o is the maximum sonic velocity, which occurs at the stagnation ($V=0$) condition. The foregoing equation plots as an ellipse as shown in figure 4.1 and, when so plotted, the curve represents all the possible flow velocities attainable from $V=0$ to $V=V_{max}$. Also, since the mach number M varies in direct proportion to the velocity, this curve represents all mach numbers attainable from $M=0$ to $M=M_{max}$.

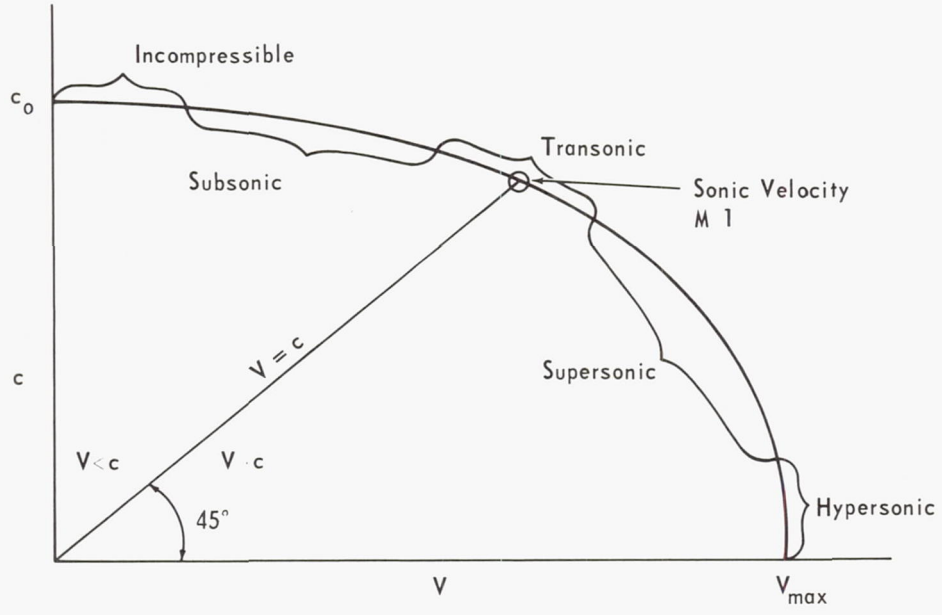


Figure 4.1. Adiabatic steady-flow ellipse.

As shown in the above figure, the different flow regimes are:

(1) *Incompressible flow.*—In this region, flow velocity is small as compared to sonic velocity. This region is applicable for incompressible fluids and for compressible fluids when $M \leq 0.3$. Note that V and c changes are small in the region.

(2) *Subsonic flow.*—Flow velocities in this region are higher than those for incompressible flow, but the velocity ratio M is still small, varying between $0.3 \leq M = 1$. Figure 4.1 shows that in this region changes in mach number are primarily caused by changes in velocity V, with changes in c being relatively small.

(3) *Transonic flow.*—Flow in the immediate area where $M \simeq 1$. Differences in V and c are small, and changes in M may be attributed to changes in both V and c.

(4) *Supersonic flow.*—Flow at velocities greater than sonic, $M > 1$. In this region, significant changes in both c and V occur causing M variation.

(5) *Hypersonic flow.*—Region of high mach flow. In this region, changes in V are relatively small compared to changes in c. Mach number changes are almost exclusively the result of changes in c.

VELOCITY OF SOUND IN A FLUID

The velocity of sound in a media is simply the velocity of propagation of a pressure disturbance through the media. Consider the system shown in figure 4.2 which shows a pipe filled with a fluid and fitted with a piston in one end.

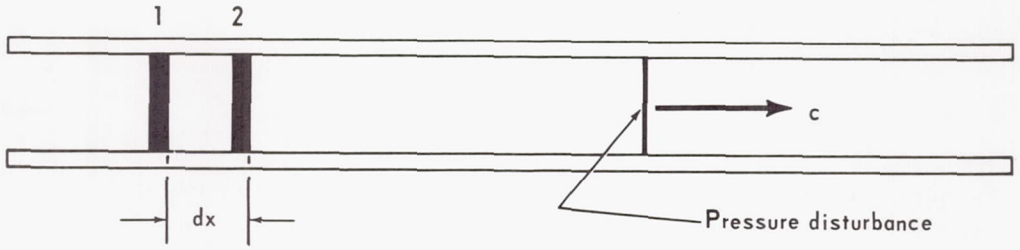


Figure 4.2. Pressure disturbance propagated by a sudden movement.

If the piston is suddenly moved to the right an incremental distance dx, a pressure disturbance is created which propagates to the right with a velocity c. An equivalent arrangement is to consider the wavefront stationary and the gas flowing to the left with a velocity c, as shown in figure 4.3.

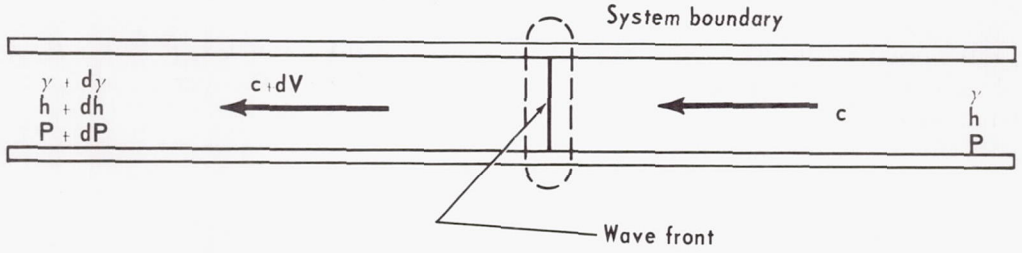


Figure 4.3. Fluid properties change after flowing through wave front.

After passing through the wavefront, the gas properties have changed a differential amount, and the gas is flowing with a new velocity $(c+dV)$. Writing the first law of thermodynamics for the system shown

$$(h+dh)+\frac{(c+dV)^2}{2g_cJ}=h+\frac{c^2}{2g_cJ}$$

or by rearranging terms and neglecting the higher order differential term $(dV)^2$,

$$dh+\frac{c\,dV}{Jg_c}=0 \tag{4.1}$$

For a steady flow, the continuity equation yields

$$(\gamma+d\gamma)A(c+dV)=\gamma Ac \tag{4.2}$$

or

$$\gamma c+\gamma\,dV+c\,d\gamma+dV\,d\gamma=\gamma c$$

neglecting the higher order differential term it follows that

$$c\,d\gamma+\gamma\,dV=0$$

Substituting for dV in equation (4.1) yields

$$dh - \frac{c^2\, d\gamma}{J g_c \gamma} = 0 \tag{4.3}$$

For the pure substance, the first law of thermodynamics of an open system is

$$dh = T\, ds + \left(\frac{1}{\gamma}\right) \frac{dP}{J}$$

Substituting, equation (4.3) may be rewritten as

$$T\, ds + \left[\left(\frac{1}{\gamma}\right) \frac{dP}{J} \right] - \frac{c^2\, d\gamma}{J g_c \gamma} = 0$$

Since the pressure disturbance is small, the process is nearly reversible, and since the time involved is very small, the process is nearly adiabatic. Hence, the entropy is essentially constant (that is, $ds \approx 0$), and the previous relationship reduces to

$$c^2 = g_c \left(\frac{dP}{d\gamma}\right)$$

or

$$c^2 = g_c = \left(\frac{\partial P}{\partial \gamma}\right)_s = \left(\frac{\partial P}{\partial \rho}\right)_s \tag{4.4}$$

Equation (4.4) is the expression for the velocity of sound in a pure substance.

The value of the quantity $(\delta P/\delta \gamma)_s$ can often be obtained with sufficient accuracy from an equation of state that relates the properties p and γ at constant entropy. The simplest equation relating these two properties is the perfect-gas equation of state. For a perfect gas undergoing an isentropic process

$$\left(\frac{P}{\gamma^k}\right) = \text{constant}$$

or, in logarithmic differential form

$$\frac{dP}{P} - k \left(\frac{d\gamma}{\gamma}\right) = 0$$

Hence,

$$\left(\frac{\partial P}{\partial \gamma}\right)_s = \frac{dP}{d\gamma} = \frac{kP}{\gamma} \qquad \text{and} \qquad c^2 = (k g_c) \frac{P}{\gamma}$$

For the perfect gas, $P/\gamma = RT$ and

$$c = \sqrt{k g_c R T} \tag{4.5}$$

Equation (4.5) shows that the velocity of sound in a perfect gas is a function of temperature and the specific heat ratio only and is not affected by pressure.

For the real gas the simple expression (eq. (4.5)) does not hold and may lead to serious error in calculating the velocity of sound. In regions of temperature and pressure where real-gas effects are appreciable, more difficult P–v–T relations must be used to determine the velocity of sound. As an example, consider the real-gas equation of state

$$Z=\frac{P}{\rho RT}=1+B_pP+C_pP^2+D_pP^3$$

where B_p, C_p, and D_p are temperature-dependent constants. Using this equation of state, the following expression for velocity of sound is obtained:

$$\frac{1}{c^2}=\frac{1}{Z^2RT}\left[Z-P\left(\frac{\partial Z}{\partial P}\right)_T-\frac{\left[Z+T\left(\frac{\partial Z}{\partial T}\right)_P\right]^2}{J\left(\frac{c_{po}}{R}\right)-T\left(\frac{\mathrm{d}}{\mathrm{d}T}\left\{\int_0^P\left[Z-1+T\left(\frac{\partial Z}{\partial T}\right)_P\right]\frac{\mathrm{d}P}{P}\right\}\right)_P}\right]$$

It is evident from the complex nature of this equation that a computer solution is necessary and that data must be tabulated or plotted before this equation will be useful for computations. Graphs of velocity of sound for various gases in the regions where real-gas equations of state must be used are given in the appendixes.

If charts for velocity of sound in a real gas are not available, it is possible to determine approximate values from a Mollier diagram, or other thermodynamic charts. The method consists of determining an exponent k_s, which forces the relation

$$Pv^{k_s}=\text{constant} \tag{4.6}$$

to hold along a constant entropy path. The value of k_s thus determined is then substituted into the equation

$$c_a=\sqrt{k_sg_cZRT} \tag{4.7}$$

The quantity k_s is termed the isentropic exponent and is simply a number which forces the P–v relation of equation (4.6) to approximate accurately the local real-gas region for a small isentropic expansion or compression. It is not a thermodynamic property and should not be associated with the actual specific heats or the actual specific heat ratio for the real gas.

Useful expressions for k_s can be found by writing equation (4.6) in logarithmic form and differentiating to obtain

$$\frac{\mathrm{d}P}{P}+k_s\left(\frac{\mathrm{d}v}{v}\right)=0$$

Rearranging yields

$$k_s=-\frac{\frac{\mathrm{d}P}{P}}{\frac{\mathrm{d}v}{v}}=-\frac{v}{P}\left(\frac{\mathrm{d}P}{\mathrm{d}v}\right)=-\frac{v}{P}\left(\frac{\partial P}{\partial v}\right)_s \tag{4.8}$$

From the definition of density, we have

$$v = \gamma^{-1}$$

and on differentiating

$$dv = -\gamma^{-2}\, d\gamma$$

Substituting for v and dv in equation (4.8) yields an equivalent relationship in terms of density.

$$k_s = \frac{\gamma}{P}\left(\frac{\partial P}{\partial \gamma}\right)_s \tag{4.9}$$

If k_s is assumed to be constant over a short isentropic process between points 1 and 2, equations (4.8) and (4.9) can be integrated to yield

$$k_s = \frac{\ln\left(\frac{P_2}{P_1}\right)}{\ln\left(\frac{\gamma_2}{\gamma_1}\right)} = \frac{\ln\left(\frac{P_2}{P_1}\right)}{\ln\left(\frac{v_1}{v_2}\right)} \tag{4.10}$$

Good approximate values can be obtained from points read directly from expanded thermodynamic charts using equation (4.10) if the pressure change between points 1 and 2 is small.

It must be pointed out that the accuracy of this method in predicting velocity of sound is greatly dependent on the accuracy of the thermodynamic chart used and the care with which data points are extracted.

The value of k_s is more readily computed using equation (4.7) when the actual sonic velocity is known. A limited amount of actual sonic velocity data is presented in the appendixes.

MACH NUMBER

Flow characteristics in compressible flow have been found to vary as a function of the ratio of the velocity of stream flow to that of the velocity of sound. This ratio is termed the mach number and is defined by the equation

$$M = \frac{V}{c} \tag{4.11}$$

where

M = mach number

V = flow velocity at a point in the flow stream

c = speed of sound in the media measured at the fluid conditions existing at the point where V is measured

Other convenient forms of the mach number may be derived by consideration of the continuity equation

$$w = \gamma A V \tag{4.12a}$$

Solving for velocity and substituting into equation (4.11) yield

$$M = \left(\frac{w}{\gamma A}\right)\frac{1}{c} \tag{4.12b}$$

If the gas is perfect,

$$c=\sqrt{kg_cRT} \qquad \text{and} \qquad P=\gamma RT$$

Hence, equation (4.12*b*) can be written for the perfect gas as

$$M=\left(\frac{w}{A}\right)\left(\frac{1}{P}\right)\sqrt{\frac{RT}{kg_c}} \tag{4.12c}$$

Since for circular pipe

$$A=\frac{\pi D^2}{4}=\frac{\pi}{4}\left(\frac{D^2}{144}\right) \qquad \text{and} \qquad P=(144)P$$

Equation (4.12*c*) may be written as

$$M=0.2245\left(\frac{w}{D^2}\right)\frac{1}{p}\sqrt{\frac{RT}{k}} \tag{4.12d}$$

When the flow rate is known in terms of standard cubic feet per minute (SCFM),

$$M=15.21\left(\frac{\text{SCFM}}{1000\,pD^2}\right)\sqrt{\frac{T}{kR}} \tag{4.12e}$$

If flow is measured in cubic feet per second, we have the relation $V=q/A$ and the mach-number expression becomes

$$M=\frac{\frac{q}{A}}{c}=\frac{\frac{q}{A}}{\sqrt{kg_cRT}} \tag{4.12f}$$

For real gases, the mach number is determined from

$$M=\frac{V}{c_a}=\frac{\frac{q}{A}}{c_a}=\frac{\frac{w}{A}}{\gamma c_a} \tag{4.13a}$$

Using the real-gas equation of state $P=\gamma ZRT$, the mach-number expression for a real gas becomes

$$M=\frac{w}{A}\left(\frac{ZRT}{P}\right)\frac{1}{c_a} \tag{4.13b}$$

or when written for circular pipe and pressure in psia

$$M=1.273\left(\frac{w}{D^2}\right)\left(\frac{ZRT}{pc_a}\right) \tag{4.13c}$$

If the flow units are in SCFM, the mach-number expression becomes

$$M=86.4\left(\frac{\text{SCFM}}{1000}\right)\frac{ZT}{pD^2c_a} \tag{4.13d}$$

In equations (4.13), the actual speed of sound can be found from charts of speed of sound for the gas, or in the absence of such charts, c_a may be determined from equation (4.7).

REYNOLDS NUMBER

The Reynolds number for pipes was defined in chapter 3 by the equation

$$R_e = \frac{VD\rho}{\mu} \qquad [3.14b]$$

To extend the discussion in chapter 3 to compressible fluids, it is only necessary to establish convenient relations for determining the Reynolds number. Starting with the continuity equation and solving for the velocity,

$$V = \frac{w}{\gamma A}$$

Substituting this relationship into the defining equation for the Reynolds number yields

$$R_e = \left(\frac{w}{\gamma A}\right)\frac{D\rho}{\mu}$$

Noting that for the usual case of circular pipes

$$A = \frac{\pi D^2}{4} \qquad \text{and} \qquad \frac{\rho}{\gamma} = \frac{1}{g_c}$$

the above relations reduce to

$$R_e = \left(\frac{4}{\pi g_c}\right)\frac{w}{\mu D}$$

and since

$$\mu' = \mu g_c$$

R_e becomes

$$R_e = \left(\frac{4}{\pi}\right)\frac{w}{\mu' D} \qquad (4.14)$$

VISCOSITY

Quantitative knowledge of viscosity is required in many engineering problems which involve heat-transfer, mass-transfer, or pressure-loss relationships. In analysis of high-pressure gas systems, experimental viscosity data are often not available for the gas in the region of pressure and temperature under investigation. To fill this gap in the data, a generalized method of estimating viscosity has been developed which is based on the critical viscosity of the gas.

At low pressure, where the perfect-gas law is applicable, the viscosity of a gas is primarily dependent on temperature, and is little affected by pressure. However, as the pressure greatly increases, the viscosity increases, though not nearly in proportion.

If the viscosity of several gases is plotted in the low-pressure region versus reduced temperature, a family of curves results. If each curve is replotted as a reduced viscosity

(by dividing all data by the individual viscosities at the respective critical points of the gases), all data are reduced to a single curve. From this curve the low-pressure viscosity of any gas with known critical temperature may be determined if only the viscosity is known at the critical point. The same procedure can be repeated at a constant high value of reduced pressure, yielding a single curve showing the reduced viscosity of all gases. By this means, it is possible to combine the low-pressure generalized viscosity curve with similar dimensionless correlations for high pressures, thereby expressing high-pressure effects for all gases on a single chart. Such a plot is shown in figure 4.4. All that is required to determine the viscosity from this figure is a knowledge of the critical temperature, critical pressure, and the viscosity at the critical point for the particular gas. Figure 4.4 is reproduced to a large scale in chapter 15 along with the required critical pressure, temperature, and viscosity data. For convenience, viscosity data extracted from figure 4.4 on the five gases—air, nitrogen, helium, hydrogen, and oxygen—are plotted in the applicable appendix.

HIGH-PRESSURE EFFECTS ON FLOW

The effects of high pressure on flow can best be understood by comparing these effects to an analysis based on a perfect gas. To facilitate such a comparison, it is convenient to utilize a slightly modified form of the dimensionless parameter, mach number. This parameter is given the symbol ϕ and is found for the perfect gas by multiplying both sides of equation (4.12*b*) by the square root of the specific heat ratio to obtain

$$\phi = \sqrt{k}\,(M) = \left(\frac{w}{A}\right)\left(\frac{1}{P}\right)\sqrt{\frac{RT}{g_c}} \tag{4.15}$$

This form is convenient since ϕ can be determined from readily measurable gas properties, and independently of k and its variations. Also, it is shown in chapters 5 and 8 that this parameter can be simply related to (A_2/A_1) and the frictional length, $f(L/D)$, respectively, and the ratio of downstream to upstream pressure, r. The relation between the three quantities ϕ, A_2/A_1 or $f(L/D)$, and r can then be plotted for discrete values of k.

The effect of high pressure on the flow parameter ϕ is limited, therefore, to the deviation in gas density in the high-pressure region from that predicted by the perfect-gas law. A correction for density can be made by using the modified perfect-gas expression

$$\gamma = \frac{P}{ZRT}$$

in the development of equation (4.12*b*). Combining this with the real-gas equation (4.7) yields

$$\phi = (M)\sqrt{k_s} = \left(\frac{w}{A}\right)\left(\frac{1}{P}\right)\sqrt{\frac{ZRT}{g_c}} \tag{4.16}$$

As can be seen by examining the right side of equations (4.15) and (4.16), the only difference between the two is the compressibility factor Z, appearing in the numerator of equation (4.16). Hence, any value of $Z > 1$ will cause the actual ϕ value to be greater than the perfect-gas value. As can be seen from figures 8.11 through 8.28 (ch. 8), increases in ϕ are accompanied by decreases in the pressure ratio r and increases in pressure loss.

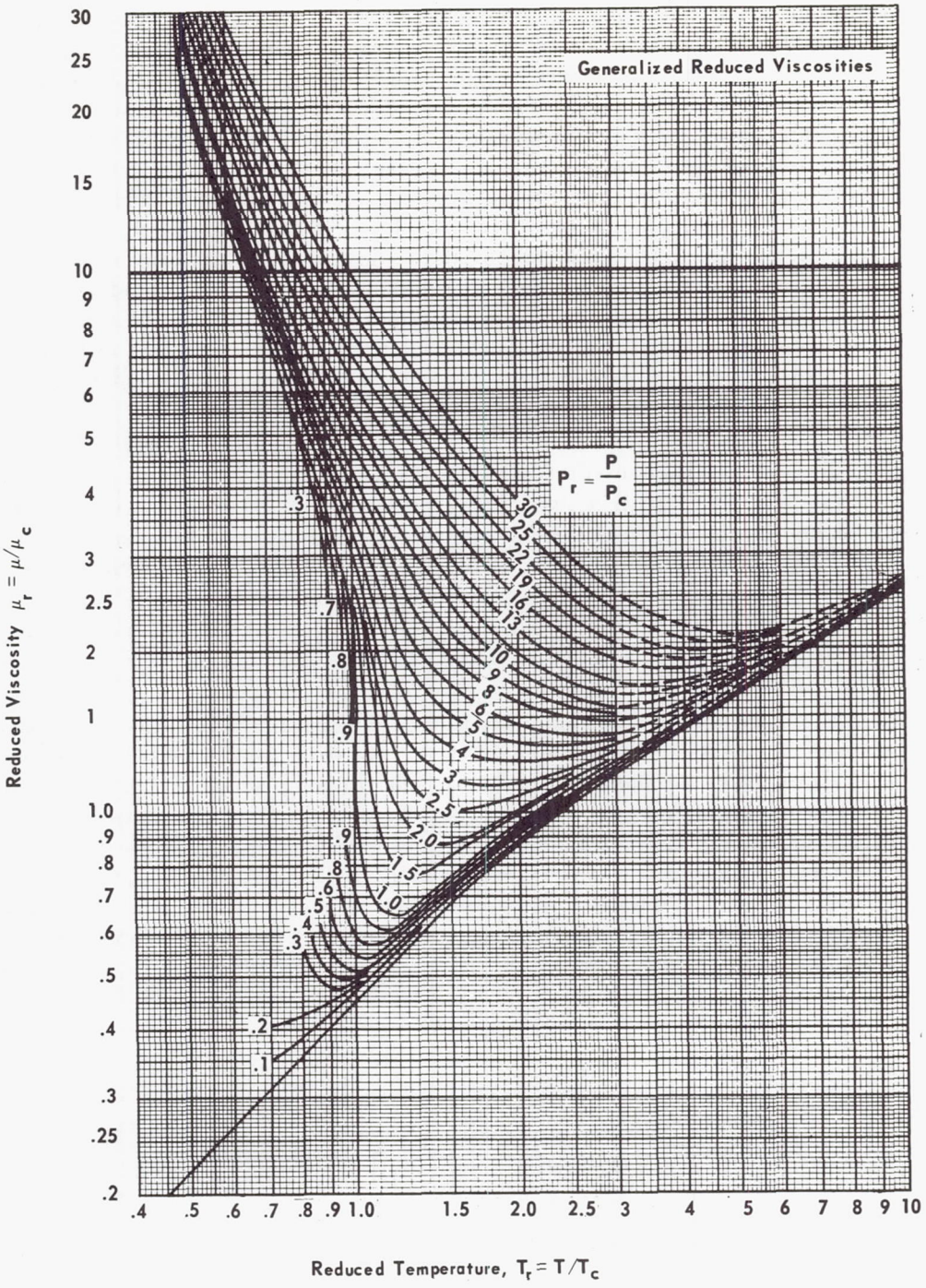


Figure 4.4. Generalized viscosity diagram. [*Reprinted from National Petroleum News, copyright McGraw-Hill, Inc., 1967.*]

Note, however, that the ϕ chart for the correct k or k_s value must be used to determine the proper pressure ratio for a given ϕ. It can be seen further from figures 8.11 through 8.28 that increases in k or k_s that usually accompany increases in Z have an opposite and more pronounced effect on the pressure ratio. Therefore, the end result of high-pressure effects on high-speed compressible flow is a lesser pressure drop (greater pressure ratio) for a given mass flow rate.

CHAPTER 5

ADIABATIC AND ISENTROPIC FLOWS

It is often convenient and realistic in dealing with compressible flow problems to assume the flow to be isentropic and one dimensional. In this chapter, the conditions necessary for the proper application of this type of analysis will be discussed, and the governing relations for adiabatic and isentropic flow of both real and perfect gases will be derived. The usual practice of referring to a reversible adiabatic flow as isentropic will be followed. It should be noted that the analysis developed here is generally applicable only to adiabatic and isentropic flows, and is not applicable to any other process.

By assuming an isentropic process, it is also assumed that heat transfer to the fluid is negligible (adiabatic), and there are no irreversibilities caused by friction or turbulence. The assumption of one-dimensional flow implies that fluid velocity and properties are constant across any cross section in the pipe.

Adiabatic flow can be assumed when there is a negligible change in the stagnation enthalpy of the fluid during the process. This assumption is usually made when the flow path is short relative to the flow velocity or when the pipe-wall temperature is approximately equal to the gas temperature.

The assumption that the flow is reversible can be made only in the absence of shock waves and when there is a negligible amount of irreversible pressure loss resulting from friction or turbulence. This assumption requires that the flow passage be relatively short and smooth, and that there is no abrupt change in cross-sectional shape which will cause flow separation and turbulence. Because of boundary-layer characteristics, more abrupt changes in cross section can be tolerated in nozzles than in diffusers. For this reason, subsonic convergent nozzles may have rather sudden reductions in area without flow separation, while subsonic diffusers must be limited to small rates of area increase to prevent flow separation and turbulence and stagnation pressure loss.

The assumption of one-dimensional flow can be made when the rate of change of fluid properties normal to the stream direction is negligible compared with the rate of change in the flow direction. In the limit, when an infinitesimal stream tube is considered, the flow is exactly one dimensional. However, since it is known that the fluid properties do vary over the pipe cross section, certain average properties will be considered in making the one-dimensional flow assumption. The resulting error will be small if

(1) The change in flow area is gradual with respect to distance along the pipe axis

(2) The radius of curvature of the pipe is large relative to the diameter

Preceding Page Blank

(3) The velocity and temperature profile shapes are relatively unchanged from section to section along the axis of the pipe

GENERAL FEATURES OF ISENTROPIC FLOW

In investigating isentropic flow it is useful to define certain reference properties that are constant throughout the flow. The most useful of these reference properties are the stagnation properties.

The stagnation properties are defined as the fluid properties that would be observed if the fluid were brought to rest in a reversible adiabatic process. Using this definition, the following governing physical equations may be written for a control volume extending between the stagnation section and any other section in the pipe as shown in figure 5.1.

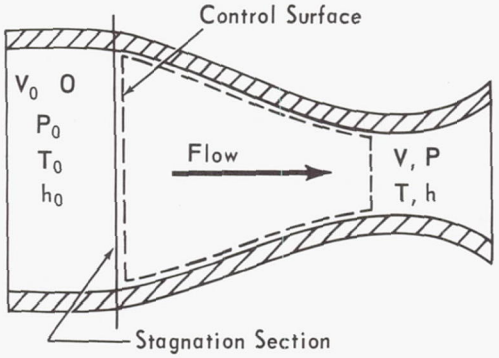


Figure 5.1. Control surface between the stagnation section and any other section.

The steady-flow energy equation for an adiabatic process with no work and no change in elevation of the fluid is

$$h_0 = \frac{V^2}{2g_c J} + h = \text{constant} \tag{5.1}$$

The second law of thermodynamics for a reversible adiabatic process is

$$s_0 = s = \text{constant} \tag{5.2}$$

The continuity equation for steady flow is

$$\frac{w}{A} = \gamma V = g_c \rho V \tag{5.3}$$

The equation of state for the given gas may be expressed in the form of charts, tables, or algebraic equations. In general, any property can be defined by any other two independent properties for a pure substance. For example,

$$\begin{aligned} h &= h(s, P) \\ \rho &= \rho(s, P) \end{aligned} \tag{5.4}$$

The definition of mach number is

$$M=\frac{V}{c}=\frac{V}{\left(\frac{\partial P}{\partial \rho}\right)_s^{1/2}} \tag{5.5}$$

These equations define the conditions along an isentropic line as illustrated in figure 5.2.

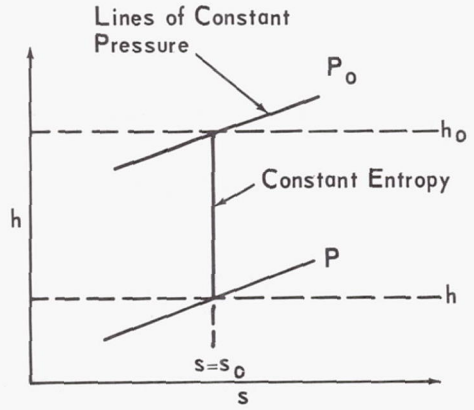


Figure 5.2. Isentropic process on a Mollier chart.

With a knowledge of two thermodynamic properties and the velocity at any point on this process line, the conditions at all other points may be computed from equations (5.1) through (5.5). For example, if in addition to the velocity the temperature and pressure are known, then the other properties (ρ, s, h) can be determined from the equations of state, and the stagnation enthalpy, weight flow, and mach number can be determined from equations (5.1), (5.3), and (5.5). Stagnation conditions other than the enthalpy can be determined from equations (5.4), since two properties are known, h_0 and s_0. The flow condition at any other point in the flow can be related to the stagnation conditions in the same manner, and the properties along the isentropic line can be found to vary as shown in figure 5.3. The value

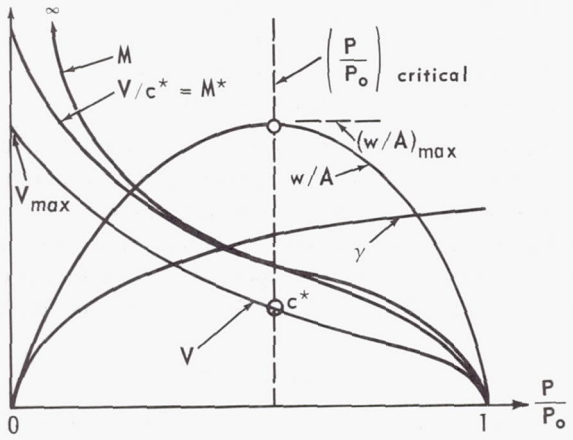


Figure 5.3. Typical trends in flow properties with isentropic flow.

of the pressure ratio that corresponds to the maximum weight flow per unit area is called the critical pressure ratio. It will be shown later that, although all states shown in figure 5.3 are thermodynamically possible, a certain pipe shape and flow area change are required to reach the described flow conditions.

The effect of area change on isentropic flow can be investigated by using the differential form of Euler's equation for a frictionless flow, neglecting changes in elevation

$$-\mathrm{d}P = \rho V\,\mathrm{d}V \tag{5.6}$$

and the logarithmic differential form of the continuity equation for a constant-mass flow rate,

$$\frac{\mathrm{d}\rho}{\rho} + \frac{\mathrm{d}A}{A} + \frac{\mathrm{d}V}{V} = 0 \tag{5.7}$$

to obtain

$$\frac{\mathrm{d}A}{A} = \frac{\mathrm{d}P}{\rho}\left(\frac{1}{V^2} - \frac{\mathrm{d}\rho}{\mathrm{d}P}\right)$$

Since an isentropic process is being considered, it may be written that

$$\frac{\mathrm{d}P}{\mathrm{d}\rho} = \left(\frac{\partial P}{\partial \rho}\right)_s = c^2$$

so that

$$\frac{\mathrm{d}A}{A} = \frac{\mathrm{d}P}{\rho V^2}\left(1 - \frac{V^2}{c^2}\right) = \left(\frac{1 - M^2}{\rho V^2}\right)\mathrm{d}P = -(1 - M^2)\frac{\mathrm{d}V}{V} \tag{5.8}$$

Now, the results of area change may be noted by analyzing the effect of equations (5.6) and (5.8). Equation (5.6) requires that the pressure always decreases in an accelerating flow and increases in a decelerating flow. This may be stated as $\mathrm{d}P/\mathrm{d}V < 0$, indicating that the differentials of P and V are always opposite in sign. Using this result in conjunction with equation (5.8), the following conclusions can be reached:

(1) For subsonic flow ($M < 1$), $\mathrm{d}A/\mathrm{d}P > 0$; $\mathrm{d}A/\mathrm{d}V < 0$

(2) For supersonic flow ($M > 1$), $\mathrm{d}A/\mathrm{d}P < 0$; $\mathrm{d}A/\mathrm{d}V > 0$

(3) For sonic speeds ($M = 1$), $\mathrm{d}A/\mathrm{d}P = 0$; $\mathrm{d}A/\mathrm{d}V = 0$

The flow conditions described by (1) and (2) above are shown schematically in figure 5.4. Condition (3) indicates that the area is at a minimum when the mach number is unity for a constant-weight flow rate in a one-dimensional isentropic flow.

It can be concluded from the effect of area variations on the flow conditions investigated that to accelerate a fluid from subsonic to supersonic velocities requires a passage that converges for $M < 1$, reaches a minimum area at $M = 1$, and diverges for $M > 1$.

ADIABATIC FLOW

Before restricting the discussion to a reversible adiabatic flow, it is desirable to determine what general relationships can be obtained for any adiabatic flow and with a constant-weight flow rate. The discussion is restricted to the perfect gas and the following equations

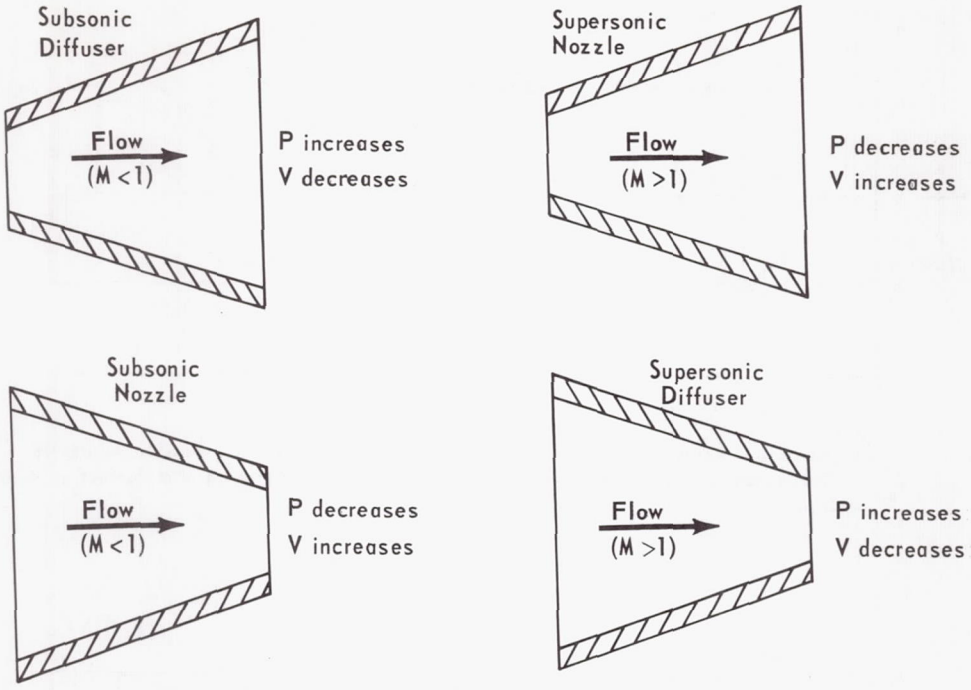


Figure 5.4. Effects of area change on isentropic flow.

as derived in chapter 2. Discussion of adiabatic flows for constant-area pipes will be continued in chapters 8 and 10.

$$Pv = RT$$

$$dh = c_p\, dT$$

$$c_p - c_v = \frac{R}{J}$$

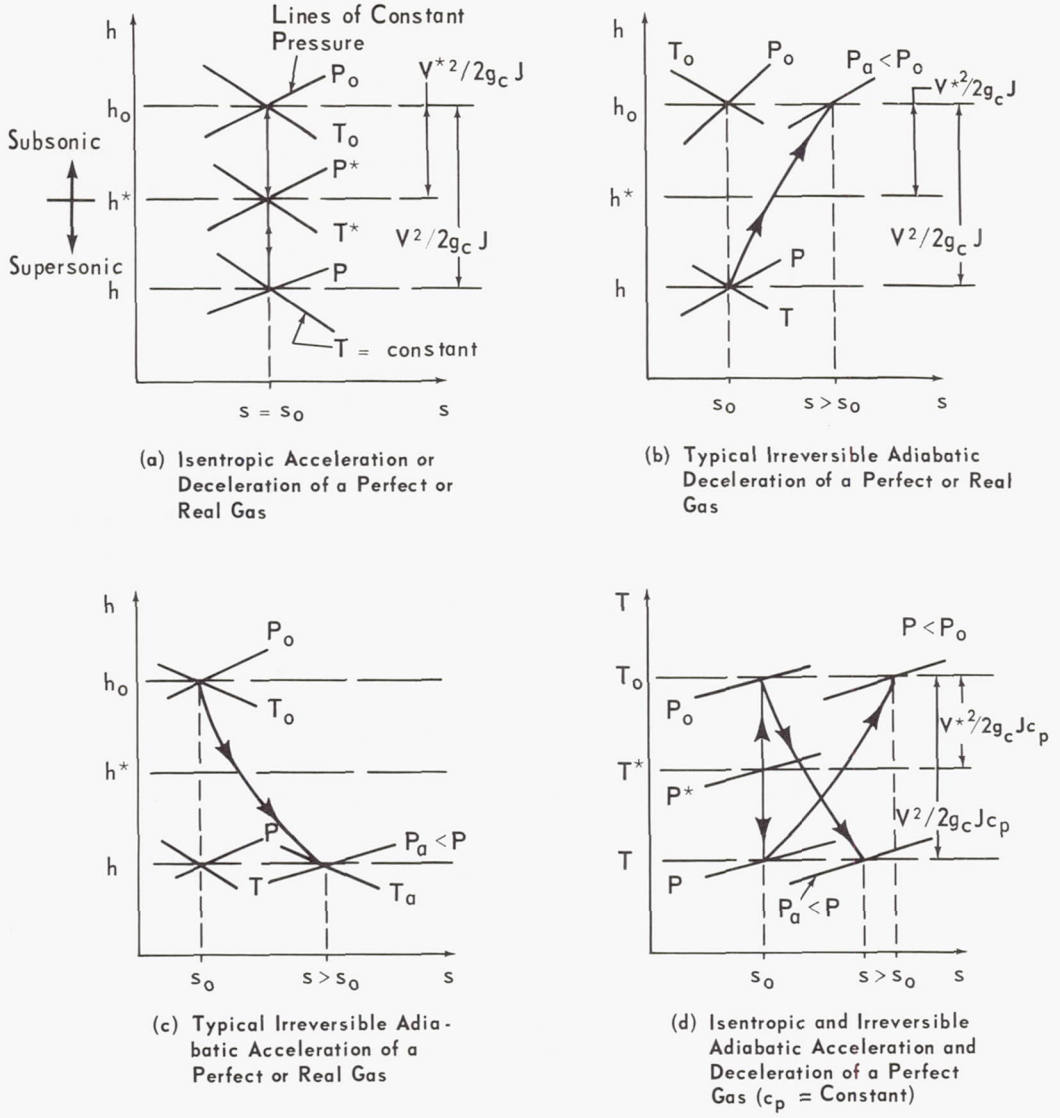
$$\frac{c_p}{c_v} = k$$

$$\frac{R}{c_p J} = \frac{k-1}{k}$$

The differences between the thermodynamic states attained during isentropic versus irreversible adiabatic flow processes are shown in figure 5.5. The conditions with the subscript 0 refer to the isentropic stagnation location, and the conditions with the superscript * refer to the location where $M = 1$. It should be noted that irreversible adiabatic deceleration to zero velocity produces a lower actual pressure P_a than the isentropic stagnation pressure.

Using the steady-flow energy equation (5.1), the velocity at any point may be defined as

$$V = [2g_c J(h_0 - h)]^{1/2}$$



(a) Isentropic Acceleration or Deceleration of a Perfect or Real Gas

(b) Typical Irreversible Adiabatic Deceleration of a Perfect or Real Gas

(c) Typical Irreversible Adiabatic Acceleration of a Perfect or Real Gas

(d) Isentropic and Irreversible Adiabatic Acceleration and Deceleration of a Perfect Gas (c_p = Constant)

Figure 5.5. Typical adiabatic flow processes.

and for a perfect gas

$$V = [2g_c J c_p (T_0 - T)]^{1/2}$$
$$= \left[\left(\frac{2k}{k-1}\right) g_c R (T_0 - T)\right]^{1/2} \tag{5.9}$$

This equation shows that, for a given stagnation enthalpy (sometimes called total enthalpy), all states that have the same enthalpy have the same velocity.

Stagnation Temperature Ratio

For a perfect gas, a useful equation defining the stagnation temperature (sometimes called total temperature) ratio may be obtained by rearranging equation (5.9) to

$$\frac{T_0}{T}=1+\left(\frac{k-1}{2}\right)\frac{V^2}{g_c k R T}$$

Since $c^2=g_c k R T$, the simple form is obtained:

$$\frac{T_0}{T}=1+\left(\frac{k-1}{2}\right)M^2 \tag{5.10}$$

which is valid for any adiabatic flow of a perfect gas, including irreversible flows.

Three Reference Velocities

Certain reference velocities which are constant throughout an adiabatic flow process have been found to be convenient in analysis and presentation of compressible flow problems. These velocities are defined as follows for a perfect gas:

(1) Maximum obtainable velocity by expansion to absolute zero temperature:

$$V_{\max}=\left[\left(\frac{2k}{k-1}\right)g_c R T_0\right]^{1/2}=(2g_c J c_p T_0)^{1/2} \tag{5.11}$$

(2) Speed of sound at stagnation temperature:

$$c_0=(g_c k R T_0)^{1/2} \tag{5.12}$$

(3) Speed of sound at the conditions where $M=1$:

$$V^*=c^*=(g_c k R T^*)^{1/2} \tag{5.13}$$

Equation (5.13) can be rearranged by substituting equation (5.10) evaluated at $M=1$

$$\frac{T_0}{T^*}=\frac{k+1}{2} \tag{5.14}$$

to obtain

$$V^*=c^*=\left[\left(\frac{2k}{k+1}\right)g_c R T_0\right]^{1/2} \tag{5.15}$$

Kinematic Form of the Energy Equation

The energy equation for adiabatic flow (eq. (5.1)) can be written for a perfect gas in the form

$$V^2+2g_c J c_p T=2g_c J c_p T_0$$

Using a perfect gas

$$g_c J c_p T = \left(\frac{c_p J}{kR}\right) g_c k R T = \left(\frac{1}{k-1}\right) c^2$$

Combining these relations and evaluating the energy equation at the conditions of zero speed, zero temperature, and sonic speed, the energy equation involving V, c, and k can be obtained.

$$V^2 + \left(\frac{2}{k-1}\right) c^2 = \left(\frac{2}{k-1}\right) c_0^2 = V_{max}^2 = \left(\frac{k+1}{k-1}\right) c^{*2} \tag{5.16}$$

The Dimensionless Velocity

Although the mach number is often a convenient parameter, it has the disadvantages that it is not proportional to velocity alone and tends toward infinity as V approaches V_{max}. To overcome these disadvantages, a useful dimensionless velocity can be defined by

$$M^* = \frac{V}{c^*} = \frac{V}{V^*} \tag{5.17}$$

From this definition, the following relationship can be obtained:

$$M^{*2} = M^2 \left(\frac{c^2}{c^{*2}}\right)$$

In this equation, V is the fluid velocity at the point under investigation and c^* is the speed of sound at the section where the velocity is sonic ($c^* = V^*$). This equation can be used with equation (5.16) to obtain the following relations between M and M^* for a perfect gas:

$$M^{*2} = \frac{\left(\frac{k+1}{2}\right) M^2}{1 + \left(\frac{k-1}{2}\right) M^2} \tag{5.18}$$

$$M^2 = \frac{\left(\frac{2}{k+1}\right) M^{*2}}{1 - \left(\frac{k-1}{k+1}\right) M^{*2}} \tag{5.19}$$

Figure 5.3 illustrates the relative magnitudes of M and M^* in subsonic and supersonic flow. Where M goes to infinity at $V = V_{max}$, M^* has the value

$$M^*_{max} = \frac{V_{max}}{c^*} = \left(\frac{k+1}{k-1}\right)^{1/2} \tag{5.20}$$

Adiabatic Weight Flow Relations

To obtain the mass flow per unit area for a real gas, the continuity equation is written using the enthalpy difference to specify the velocity.

$$\frac{w}{A}=\gamma V=\gamma[2g_cJ(h_0-h)]^{1/2} \tag{5.21}$$

In order to evaluate this relation, it is necessary to have charts or tables of the thermodynamic properties and to know the stagnation enthalpy and two thermodynamic properties at the location of interest.

For a perfect gas, the continuity equation can be rearranged using the perfect-gas law and definition of mach number to relate the weight flow rate and fluid static properties to the mach number.

$$\frac{w}{A}=\gamma V=\left(\frac{P}{RT}\right)Mc=\left(\frac{P}{RT}\right)M(kg_cRT)^{1/2}$$

Then

$$\left(\frac{w}{A}\right)\left(\frac{1}{P}\right)\sqrt{\frac{RT}{kg_c}}=M \tag{5.22}$$

The temperature term can be converted to the stagnation value by substituting equation (5.10), yielding the adiabatic flow parameter.

$$\left(\frac{w}{A}\right)\left(\frac{1}{P}\right)\sqrt{\frac{RT_0}{kg_c}}=M\left[1+\left(\frac{k-1}{2}\right)M^2\right]^{1/2} \tag{5.23}$$

ISENTROPIC FLOW

Before discussing isentropic flow, it should be emphasized that the relations discussed above are applicable to any adiabatic flow process where no work is performed on or by the fluid. Therefore, they are applicable to isentropic (reversible adiabatic) flow, since this is a special case of adiabatic flow.

The use of the isentropic flow assumption for the analysis of real gases provides some simplification over the adiabatic flow assumption. Only one thermodynamic property or the velocity is required to completely specify the conditions at a point once the stagnation enthalpy and the entropy are known, since these properties are both constants throughout the flow process. However, it is still not convenient to write additional equations that will describe the fluid properties along lines of constant entropy on the thermodynamic chart of a real gas. For a perfect gas, the first law of thermodynamics can be used to establish the explicit relationships that describe the relative changes in fluid properties in an isentropic process. For a closed system,

$$dQ'=T\,ds=du+\frac{P\,dv}{J}=0$$

Substituting the perfect-gas relationships

$$du = c_v \, dT$$

$$p = \left(\frac{1}{v}\right) RT$$

$$\frac{R}{J} = c_p - c_v$$

yields

$$\frac{dT}{T} = -(k-1)\frac{dv}{v}$$

This equation can be integrated between any two points, 1 and 2, along the isentropic process line yielding

$$\frac{T_2}{T_1} = \left(\frac{\gamma_2}{\gamma_1}\right)^{k-1} = \left(\frac{v_1}{v_2}\right)^{k-1} \tag{5.24}$$

Substituting equation (5.24) into the perfect-gas equation of state to eliminate the temperature parameter produces

$$\frac{P_2}{P_1} = \left(\frac{\gamma_2}{\gamma_1}\right)^{k} = \left(\frac{v_1}{v_2}\right)^{k} \tag{5.25}$$

Also, equation (5.25) solved for v_1/v_2 is

$$\frac{v_1}{v_2} = \left(\frac{P_2}{P_1}\right)^{1/k} \tag{5.26}$$

and when substituted into equation (5.24), the direct relation between temperature and pressure results:

$$\frac{T_2}{T_1} = \left(\frac{P_2}{P_1}\right)^{\frac{k-1}{k}} \tag{5.27}$$

Equations (5.24), (5.25), and (5.27) can now be used to relate the static properties of a flowing perfect gas at any point to the isentropic stagnation values

$$\frac{T}{T_0} = \left(\frac{\gamma}{\gamma_0}\right)^{k-1} = \left(\frac{v}{v_0}\right)^{-(k-1)} = \left(\frac{P}{P_0}\right)^{\frac{k-1}{k}} \tag{5.28}$$

$$\frac{P}{P_0} = \left(\frac{\gamma}{\gamma_0}\right)^{k} = \left(\frac{v}{v_0}\right)^{-k} = \left(\frac{T}{T_0}\right)^{\frac{k}{k-1}} \tag{5.29}$$

$$\frac{\gamma}{\gamma_0} = \left(\frac{v}{v_0}\right)^{-1} = \left(\frac{P}{P_0}\right)^{\frac{1}{k}} = \left(\frac{T}{T_0}\right)^{\frac{1}{k-1}} \tag{5.30}$$

These equations can be combined with the previously established perfect-gas relationships involving mach number to produce the following very useful isentropic flow equations for a perfect gas.

Temperature, Pressure, and Density Ratios

Combining equations (5.29) and (5.30) with the adiabatic temperature ratio of equation (5.10)

$$\frac{T_0}{T}=1+\left(\frac{k-1}{2}\right)M^2$$

results in

$$\frac{P_0}{P}=\left[1+\left(\frac{k-1}{2}\right)M^2\right]^{\frac{k}{k-1}} \tag{5.31}$$

and

$$\frac{\gamma_0}{\gamma}=\frac{v}{v_0}=\left[1+\left(\frac{k-1}{2}\right)M^2\right]^{\frac{1}{k-1}} \tag{5.32}$$

Equations (5.10), (5.31), and (5.32) when evaluated at $M=1$ yield the ratios which are referred to as the critical flow ratios. (This should not be confused with the thermodynamic properties of a substance at the critical point.) From equation (5.10), it follows that

$$\frac{T^*}{T_0}=\frac{2}{k+1} \tag{5.33}$$

and from equations (5.31) and (5.32), respectively,

$$\frac{P^*}{P_0}=\left(\frac{2}{k+1}\right)^{\frac{k}{k-1}} \tag{5.34}$$

and

$$\frac{\gamma^*}{\gamma_0}=\left(\frac{2}{k+1}\right)^{\frac{1}{k-1}} \tag{5.35}$$

Isentropic Weight Flow Relations

The adiabatic flow parameter (eq. (5.23)) can be converted entirely to terms of stagnation properties. Substituting equation (5.31) into equation (5.23), it follows that

$$\left(\frac{w}{A}\right)\left(\frac{1}{P_0}\right)\sqrt{\frac{RT_0}{kg_c}}=M\left[1+\left(\frac{k-1}{2}\right)M^2\right]^{-\frac{k+1}{2(k-1)}} \tag{5.36}$$

This equation shows that for a given mach number the flow is directly proportional to stagnation pressure and inversely proportional to the square root of the stagnation temperature. For this reason, the performance data for compressors, turbines, and the other components are often plotted using the quantity $(w\sqrt{T_0})/P_0$ as the flow parameter.

325-994 O-69—8

Since it has been shown that for isentropic one-dimensional flow, the area is at a minimum when $M=1$, the maximum flow rate per unit area w/A can be obtained from equation (5.36) by setting $M=1$. This yields

$$\left(\frac{w}{A}\right)_{\max}=\frac{w_{\max}}{A^*}=P_0\sqrt{\frac{kg_c}{RT_0}}\left(\frac{2}{k+1}\right)^{\frac{k+1}{2(k-1)}} \tag{5.37}$$

Combining equations (5.36) and (5.37), a ratio can be obtained of the flow area at any point to the area at the section where $M=1$.

$$\frac{A}{A^*}=\frac{\frac{w}{A^*}}{\frac{w}{A}}=\frac{1}{M}\left\{\frac{2}{k+1}\left[1+\left(\frac{k-1}{2}\right)M^2\right]\right\}^{\frac{k+1}{2(k-1)}} \tag{5.38}$$

This area ratio is always equal to or greater than 1. Subsequent detailed discussions in "Working Charts and Tables" and "Choking in Isentropic Flow" will show that for every value of A/A^* there are two values of M—one for supersonic flow and the other for subsonic flow.

The Impulse Function

In order to analyze the force on pipe walls, it is convenient to define a quantity F_i called the impulse function.

$$F_i=PA+\rho AV^2 \tag{5.39}$$

The usefulness of this function can be illustrated by applying the momentum equation to the control volume shown in figure 5.6.

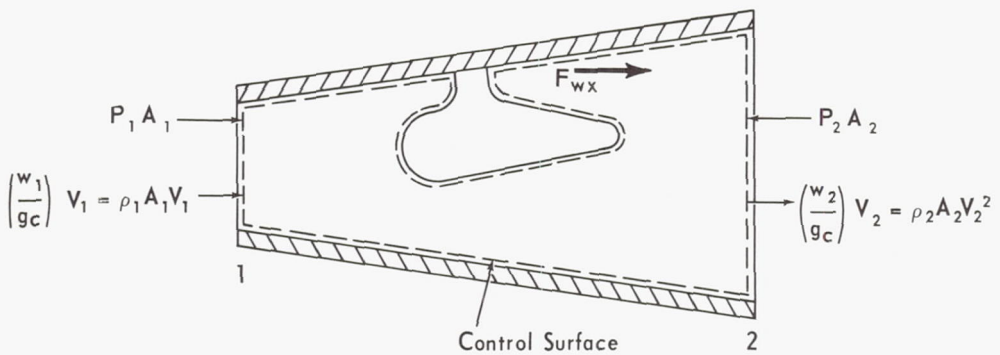


Figure 5.6. Control surface for analyzing the impulse function.

The sum of all forces on control volume is equal to the momentum out minus the momentum in. Then letting F_{wx} be the force exerted by the wall on the fluid,

$$F_{wx}+P_1A_1-P_2A_2=\rho_2A_2V_2^2-\rho_1A_1V_1^2$$

or

$$F_{wx} = (P_2A_2 + \rho_2A_2V_2^2) - (P_1A_1 + \rho_1A_1V_1^2)$$
$$= F_{i2} - F_{i1}$$

In this sign convention, F_{wx} is the x component of the force exerted on the fluid by the wall, so the force exerted on the wall by the fluid will be in the opposite direction. Therefore, the force on the pipe by the fluid opposite to the flow direction is equal to the downstream value of F_i minus the upstream value of F_i. If F_{i1} is larger than F_{i2}, then the force on the pipe is in the same direction as the flow. The protuberance in the flow was included in the figure to emphasize that the result is independent of wall shape so long as the pressure and velocity are constant across the cross sections under consideration. Of course, if the wall shape or protuberances cause irreversibilities that cannot be neglected, then the isentropic portion of the succeeding analysis cannot be applied.

For a perfect gas

$$\rho V^2 = \frac{PV^2}{g_cRT} = \frac{PkV^2}{kg_cRT}$$

and since $c^2 = g_ckRT$ and $M = V/c$

$$\rho V^2 = kPM^2$$

which when substituted in equation (5.39) yields

$$F_i = PA(1 + kM^2) \tag{5.40}$$

If consideration is restricted to isentropic flow, the following dimensionless impulse function ratio can be obtained with the use of equations (5.31), (5.34), and (5.38).

$$\frac{F_i}{F_i^*} = \frac{1 + kM^2}{M\left\{2(k+1)\left[1 + \left(\frac{k-1}{2}\right)M^2\right]\right\}^{1/2}} \tag{5.41}$$

WORKING CHARTS AND TABLES

To simplify computations, the values of certain isentropic ratios for perfect gases have been charted and tabulated in various references as a function of mach number. Figure 5.7 shows the characteristic shape of these isentropic flow relationships. In addition, expanded working charts are presented in chapter 16. It should be noted in these charts that the changes in density are very small up to mach number of approximately 0.3. Therefore, at low velocities, good accuracy is obtained in engineering calculations when gases are considered incompressible.

The ratios presented are referenced either to the stagnation conditions or to the conditions where $M = 1$, which are constant in a given isentropic flow situation. Therefore, the ratio of two ratios, evaluated at different points in the same flow field, will produce the property change between the two points. For example, in an isentropic flow, if the pressure and mach number are known at location (1), and the pressure is known at location (2), the mach number and all other changes in properties can be determined between the two locations as follows:

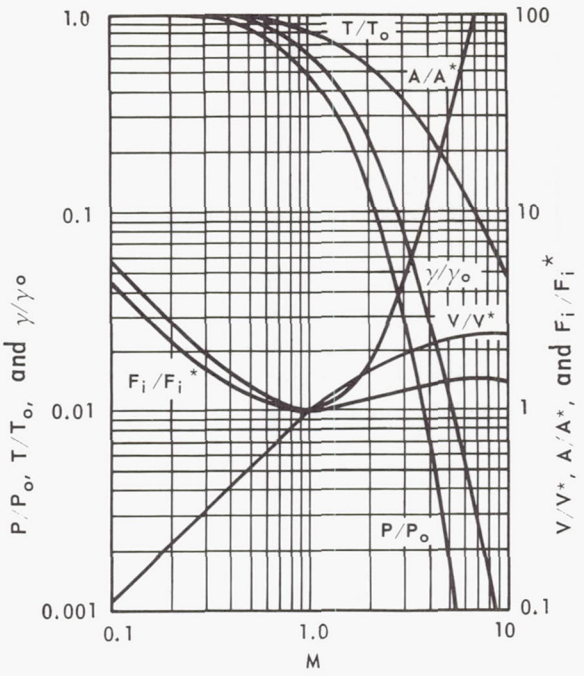


Figure 5.7. Chart for isentropic flow with $k = 1.4$.

(1) Read P_1/P_0 at M_1 and compute $P_0 = P_1/(P_1/P_0)$

(2) Compute P_2/P_0, and at that value read M_2

(3) At M_2, read any other property rates desired

(4) Then if, for example, the temperature change is desired, read T_1/T_0 and T_2/T_0 at M_1 and M_2, respectively, and compute

$$\frac{T_2}{T_1} = \frac{(T_2/T_0)}{(T_1/T_0)}$$

Any of the other property and function changes are obtained in the same manner.

CHOKING IN ISENTROPIC FLOW

The previous observation that the weight flow per unit area goes through a maximum at $M = 1$ is associated with an important phenomenon called choking. It was also stated previously that for every possible numerical value of (A/A^*), there are either two solutions for mach number (for $A/A^* > 1$) which are physically possible or no solutions at all (for $A/A^* < 1$). The analysis of this situation can be facilitated by considering several area ratios between two locations having mach number of M_1 and M_2 using figure 5.8 which was derived from equation (5.38). For a particular upstream mach number M_1, and an area ratio $A_1/A_2 > 1$, there are, in all cases, two possible solutions for M_2; but for an area ratio $A_1/A_2 < 1$, there are some values of M_1 for which there are no solutions for M_2.

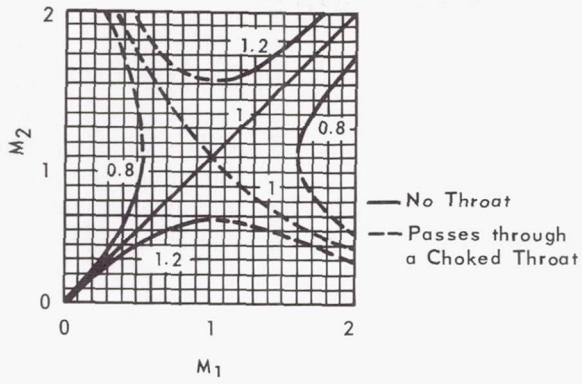


Figure 5.8. Typical curves of M_2 versus M_1 for fixed values of area ratio A_2/A_1 as noted.

In the cases where there are two possible values of M_2, the one which occurs will depend on the shape of the passage. Since it is necessary to have a minimum area in order to have sonic flow, a minimum area section (throat) is necessary to go from subsonic to supersonic velocity or to go from supersonic to subsonic velocity (in the absence of a normal shock which is nonisentropic). Therefore, if there is no minimum area, that is, the flow passage continuously converges, then both M_1 and M_2 must be either subsonic or supersonic. If M_1 is subsonic, and the passage is convergent-divergent so that minimum area is present, then M_2 may be subsonic as in a venturi or supersonic as in a rocket nozzle. The solution which actually occurs will depend on the pressure ratio between the two points and will be discussed further in "Operation of Nozzles" and "Normal Shock Waves." If M_1 is supersonic and the passage is convergent-divergent, then M_2 may be either subsonic or supersonic depending on the flow system and pressures involved. This problem is complex and appears to have no application in pneumatic systems. Therefore, it will not be discussed further.

In the cases where there is no solution for M_2 using the selected values of A_1/A_2 and M_1, the solution is imaginary in the mathematical sense. When this occurs, it is always for a case of reducing area. This lack of a solution signifies that $A_2 < A^*$; that is, sonic velocity would be reached at a location upstream of location (2) in the converging section where $A = A^*$. Since w/A is a maximum, w/A_2 would have to be greater than the maximum flow rate per unit area, which is physically impossible. This phenomenon is called choking and may be summarized as follows:

> For steady flow in a pipe with a given area reduction, there is a maximum initial subsonic mach number or minimum initial supersonic mach number which can occur upstream of the minimum area. These conditions can be identified in terms of the mach numbers which will produce $M = 1$ at the minimum section.

OPERATION OF NOZZLES

In this discussion, the performance of both convergent and convergent-divergent nozzles will be investigated along with the effects of choking discussed previously.

Convergent Nozzles

Consider the nozzle shown in figure 5.9, with the back pressure in the discharge chamber controlled by a valve. It is assumed that the upstream area is sufficiently large so that the property values at station 0 are the stagnation properties which will remain constant throughout the assumed isentropic flow. This further implies that the upstream supply is sufficient to maintain the upstream conditions at that constant value regardless of flow. The pressure in the exit is P_e and the back pressure in the exhaust chamber is P_b.

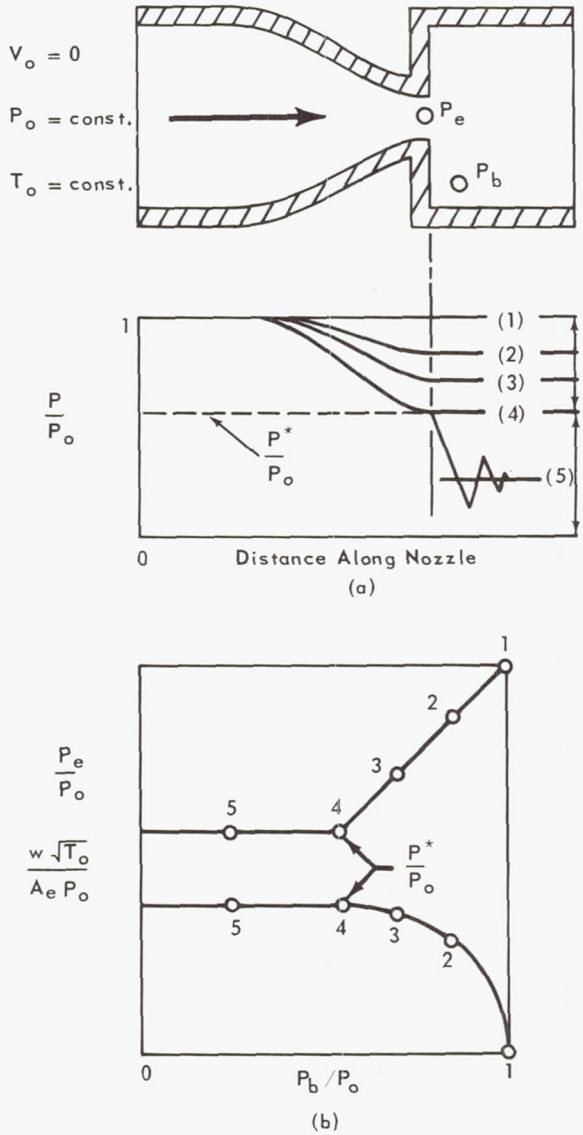


Figure 5.9. Characteristics of convergent nozzle operation.

The effects of lowering the back pressure P_b on the pressure throughout the nozzle, and the weight flow rate, will be investigated. These effects, shown graphically in figures 5.9*a* and 5.9*b*, are:

(1) When the exhaust valve is closed, there is no flow and the pressure is constant throughout as noted by point 1 on the graphs.

(2) When the back pressure is reduced slightly, flow begins and the pressure in the nozzle throat drops as the flow accelerates in the convergent section. The exit pressure P_e is equal to P_b, except for small secondary flow effects which will be neglected.

(3) Further reduction of the exhaust pressure to point 3 causes increased flow rate and velocity, but since P_b/P_0 is still greater than the critical pressure ratio P^*/P_0, the flow is still subsonic throughout and $P_e = P_b$.

(4) If the back pressure is reduced further, the critical pressure ratio can be reached where $P_b = P_e = P^*$. The flow is entirely subsonic in the nozzle and sonic at the exit.

(5) Further reduction in back pressure to values of $P_b < P^*$ has no effect on the flow in the nozzle. Since the nozzle is entirely convergent, the exit velocity corresponding to sonic velocity is the maximum velocity that can be achieved. The exit pressure remains equal to the critical pressure ($P_e = P^*$), and the weight flow is independent of the exhaust pressure P_b. Under these conditions, the nozzle is choked. Analysis of the supersonic expansion of the free jet outside the nozzle cannot be treated using one-dimensional analysis and has been shown here as a jagged line.

It has been shown that after a nozzle is choked, further reduction in back pressure has no effect on the flow rate, but it cannot be concluded that a choked nozzle passes a fixed flow rate. Changes in the upstream conditions of pressure and temperature can still cause changes in the flow rate by changing the gas density and the speed of sound in the gas.

Convergent-Divergent Nozzles

It should be noted that conditions discussed here are not generally applicable to pneumatic systems and are included in this text only to give a more complete understanding of the characteristics of isentropic flow.

For convergent-divergent nozzles an experiment similar to the one just discussed will be considered through the use of figure 5.10. The stagnation condition at station 0 will be assumed fixed once again, and the effects of reduction of the back pressure P_b on the nozzle performance will be noted for steady flow.

(1) When the exhaust valve is closed, there is no flow and the pressure is uniform throughout the pipe.

(2) When the back pressure is reduced slightly, flow stabilizes after the initial pressure disturbances, and the flow is subsonic throughout. As with a convergent nozzle, when the flow is subsonic, the exit pressure is equal to the back pressure.

(3) Further reduction in the back pressure causes increased flow velocities and weight flow, but since $P_e > P^*$, the flow is still subsonic throughout the system with the divergent section acting as a subsonic diffuser, and $P_e = P_b$.

(4) With sufficient reduction in the back pressure, the flow rate increases until the pressure at the throat is equal to the critical pressure P^*. When this condition is initially achieved, the back pressure is still higher than the throat pressure, so the divergent portion of the nozzle still acts as a subsonic diffuser to increase the pressure of the stream to the back

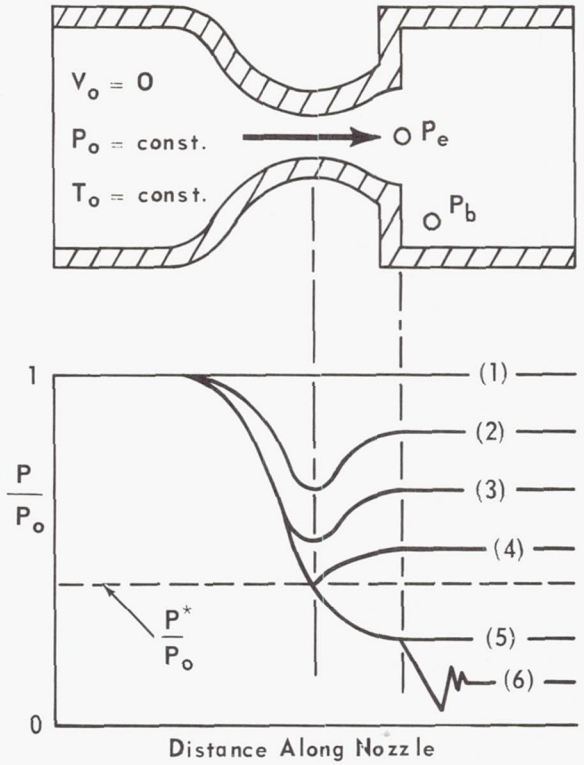


Figure 5.10. Characteristics of convergent-divergent nozzle operation.

pressure. At this point, the pressure ratio $(P_e/P_0)_4$ corresponds to the subsonic mach number defined by A_e/A^* and $P_e = P_b$. Since the maximum weight flow per unit area has been reached at the throat, further reduction in the back pressure will not change the flow rate or the pressure distribution in the convergent portion of the nozzle.

(5) Between the pressures corresponding to points 4 and 5, the flow pattern cannot fulfill the conditions for one-dimensional isentropic flow. In this case, a normal shock wave will stand in the divergent section, and a discussion of these conditions is presented in chapter 6. When the back pressure reaches point 5, the gas expands supersonically in the divergent portion of the nozzle, and the pressure ratio $(P_e/P_0)_5$ corresponds with the supersonic mach number defined by A_e/A^*.

(6) Further reduction in back pressure below P_5 has no effect on the flow in any part of the nozzle. As with the convergent nozzle, the supersonic expansion outside of the nozzle cannot be treated one-dimensionally, and this expansion is shown here by a jagged line.

The question raised in "Choking in Isentropic Flow" can now be answered as to which of the two downstream mach numbers (subsonic or supersonic) applies when there is a given subsonic upstream mach number and area ratio between two points connected by a convergent-divergent pipe. It is seen that the choice depends on the back pressure. Therefore, it is necessary to know something about the back pressure in addition to a knowledge of the upstream mach number M_1 and the area ratio A_1/A_2 in order to select the proper solution

for M_2. Solutions for conditions with back pressures between the pressures represented by P_4 and P_5 in this example are discussed in chapter 6.

PERFORMANCE OF REAL NOZZLES

Since flow in real nozzles is not exactly one dimensional and reversible, the performance of real nozzles differs somewhat from the performance predicted using isentropic relations. This discussion will consider nozzle efficiency, nozzle discharge coefficients, sharp-edged orifices, and a useful adiabatic relation for determining the flow conditions downstream of a choked real nozzle.

Nozzle Efficiency

Nozzle efficiency is used to relate the velocity increase in an actual nozzle to the velocity increase in an ideal isentropic nozzle. If the inlet stagnation condition is designated with the subscript 0, the actual adiabatic exit conditions with the subscript a, and the ideal isentropic exit conditions with the subscript s, the nozzle efficiency can be defined as the ratio of actual-to-ideal exit kinetic energy.

$$\eta = \frac{V_a^2}{V_s^2}$$

Using the steady-flow energy equation (5.1), this equation can be put in the form

$$\eta = \frac{h_0 - h_a}{h_0 - h_s} \tag{5.42}$$

The enthalpies h_a and h_s are evaluated at the nozzle-exit pressure P_e, as indicated in figure 5.11. If analysis is restricted to perfect gases, equation (5.42) may be rearranged to any of the following forms:

$$\eta = \frac{\dfrac{V_a^2}{2g_cJ}}{c_p(T_0 - T_s)} = \frac{\dfrac{V_a^2}{2g_cJc_pT_0}}{\left(1 - \dfrac{T_s}{T_0}\right)}$$

And since for a perfect gas

$$c^2 = kg_cRT \qquad \text{and} \qquad c_pJ = R\left(\frac{k}{k-1}\right)$$

$$\eta = \frac{\left(\dfrac{k-1}{2}\right)\left(\dfrac{V_a}{c_0}\right)^2}{1 - \dfrac{T_s}{T}} = \left(\frac{k-1}{2}\right)\left(\frac{V_a}{c_0}\right)^2 \left[1 - \left(\frac{P_s}{P_0}\right)^{\frac{k-1}{k}}\right]^{-1} \tag{5.43}$$

The efficiency of nozzles is usually high, but the efficiency is greatly affected by boundary-layer effects. Since the boundary-layer thickness depends on the Reynolds number and on the rate of change of pressure in the nozzle, no simple expression for efficiency can be derived for nozzles in general. Well-designed nozzles may have efficiencies as high as 99 percent in

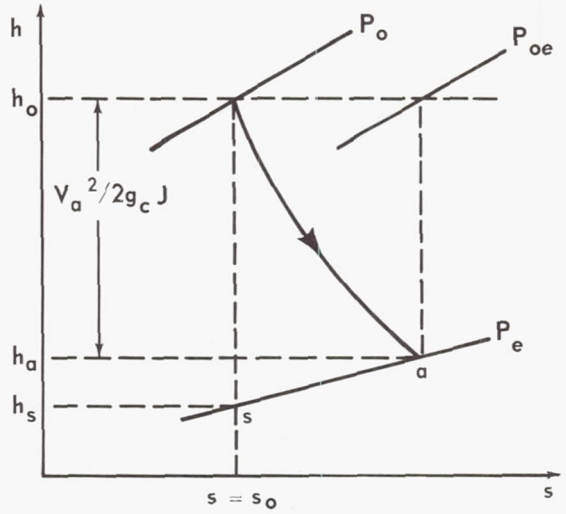


Figure 5.11. Illustration of a real-nozzle process.

certain cases. However, when the nozzle's diameter is small and the boundary layer nearly fills the passage, the efficiency may be greatly reduced.

Nozzle Discharge Coefficient

The nozzle discharge coefficient is the ratio of actual nozzle weight flow to the ideal isentropic weight flow.

$$C_d = \frac{w_a}{w_s} \tag{5.44}$$

If the nozzle is operating with back pressures that cause sonic (choked) conditions at the minimum area station (see "Operation of Nozzles"), then the isentropic weight flow used in the above equation is computed using the choked isentropic flow equation (5.37). If the pressures are such that subsonic velocity occurs at the minimum area station, then the isentropic weight flow is determined using the isentropic equation (5.36), evaluated at either the throat or the exit stations. The mach number can be evaluated at the selected station using known pressures at that location and equation (5.31).

As in the case of nozzle efficiency, the discharge coefficient is a function of the Reynolds number, and values of discharge coefficients for some nozzles are presented in chapter 7.

Sharp-Edged Orifices

The flow characteristics of the sharp-edged orifice differ considerably from those of the nozzle with the well-rounded approach. In a properly designed nozzle, the actual flow passage very nearly approaches a minimum at the point where the nozzle area approaches a minimum, and the actual effective flow area does not vary significantly from the nozzle-throat area. In a sharp-edged orifice the effective flow area is at a minimum in the vena contracta downstream of the orifice, as shown in figure 5.12. For turbulent flow ($R_e > 10^4$) and small orifice-diameter-to-pipe-diameter ratios, the size of the vena contracta is essentially constant

at 61 percent of the orifice area. However, it increases in size as the pressure ratio across the orifice decreases, to values less than the critical pressure. Therefore, since the discharge coefficient of the orifice is computed based on the constant area of the orifice opening rather than the effective flow area, the discharge coefficient and weight flow will continue to increase somewhat as downstream pressure is reduced to values below that of the critical pressure ratio. The practical aspects of this characteristic are discussed in chapter 7.

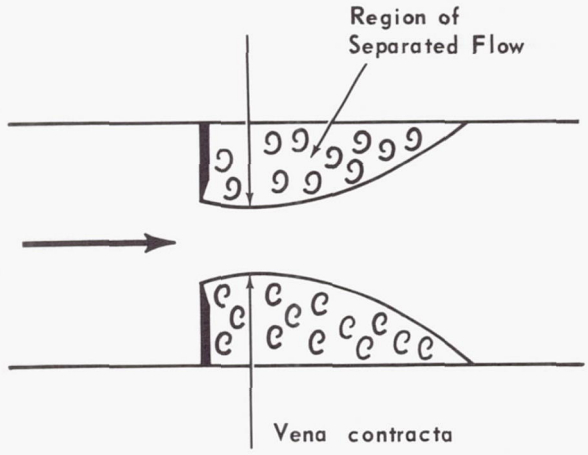


Figure 5.12. *Representation of flow pattern through a sharp-edged orifice.*

Adiabatic Relations

When a convergent nozzle is installed in a pipe as shown in figure 5.13*a*, it can be hypothesized that the flow goes through a process somewhat like that shown by figure 5.13*b*. If the nozzle is properly designed, the expansion in the nozzle from the inlet condition (1) to the throat condition t is nearly isentropic, but the expansion into the pipe causes stagnation pressure losses as a result of flow separation and turbulence. Even though the flow is not isentropic, an expression using isentropic functions can be obtained to estimate the conditions in the pipe downstream of the nozzle if the nozzle is choked.

Equation (5.37) can be modified by the discharge coefficient so that the actual weight flow is defined at the throat as

$$\frac{w}{A_t} = C_d P_{01} \sqrt{\frac{kg_c}{RT_{01}}} \left(\frac{2}{k+1}\right)^{\frac{k+1}{2(k-1)}}$$

Equation (5.23), which is applicable to any adiabatic flow regardless of irreversibilities, can be written for the point 2 in the pipe downstream of the nozzle.

$$\frac{w}{A_2} = P_2 \sqrt{\frac{kg_c}{RT_{02}}} (M_2) \left[1 + \left(\frac{k-1}{2}\right) M_2^2\right]^{1/2}$$

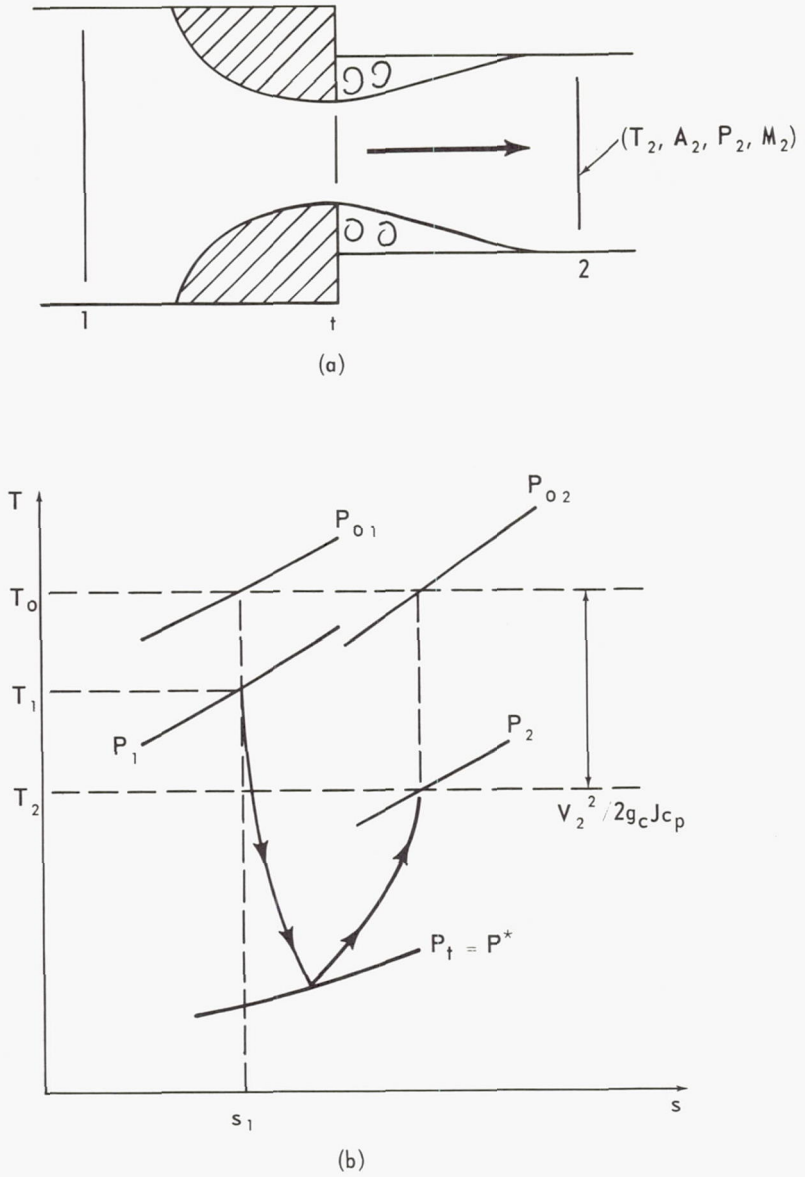


Figure 5.13. Typical flow process for a nozzle installed in a pipe.

Dividing the two equations yields

$$\left(\frac{1}{C_d}\right)\frac{\frac{A_2}{A_t}}{\frac{P_{01}}{P_2}}=\frac{\left(\frac{2}{k+1}\right)^{\frac{k+1}{2(k-1)}}}{M_2\left[1+\left(\frac{k-1}{2}\right)M_2^2\right]^{1/2}} \tag{5.45}$$

since for adiabatic flow, $T_0=T_{01}=T_{02}$. The right side of equation (5.45) is exactly the same

expression that results from dividing the isentropic relation for $(A/A^*)_2$ (eq. (5.38)), by the isentropic pressure ratio $(P_0/P)_2$ (eq. (5.31)). Therefore

$$\left(\frac{1}{C_d}\right)\left(\frac{A_2}{A_t}\right)\left(\frac{P_2}{P_{01}}\right)=\left[\left(\frac{A}{A^*}\right)_2\left(\frac{P}{P_0}\right)_2\right]_{\text{isen}}$$

$$=\frac{\left(\frac{2}{k+1}\right)^{\frac{k+1}{2(k-1)}}}{M_2\left[1+\left(\frac{k-1}{2}\right)M_2^2\right]^{1/2}} \tag{5.46}$$

Graphic or tabulated solutions of equation (5.46) are useful in establishing the mach number and the other flow conditions at the downstream location using the known (or measurable) terms of the left side of the equation. P_{01} is the isentropic stagnation pressure at the nozzle inlet; P_2 is the actual static pressure at the downstream location where the area is A_2; and A_t is the nozzle-throat area. The user is cautioned to apply this technique only when choked flow at the minimum area can be ensured.

CHAPTER 6

SHOCK WAVES

In this chapter the characteristics of normal and oblique shock waves are discussed. Shock waves are discontinuities in fluid properties which can occur in supersonic flow. As the names imply, normal shock waves are discontinuities normal to the streamlines, while oblique shock waves are similar discontinuities which are not normal to the streamlines.

NORMAL SHOCK WAVES

For the purpose of the following discussion, a normal shock wave may be considered a pure discontinuity occurring normal to the direction of fluid flow; that is to say, a normal shock wave may be considered an extremely rapid change in fluid properties occurring normal to the direction of flow of the fluid stream and taking place over an extremely short distance.

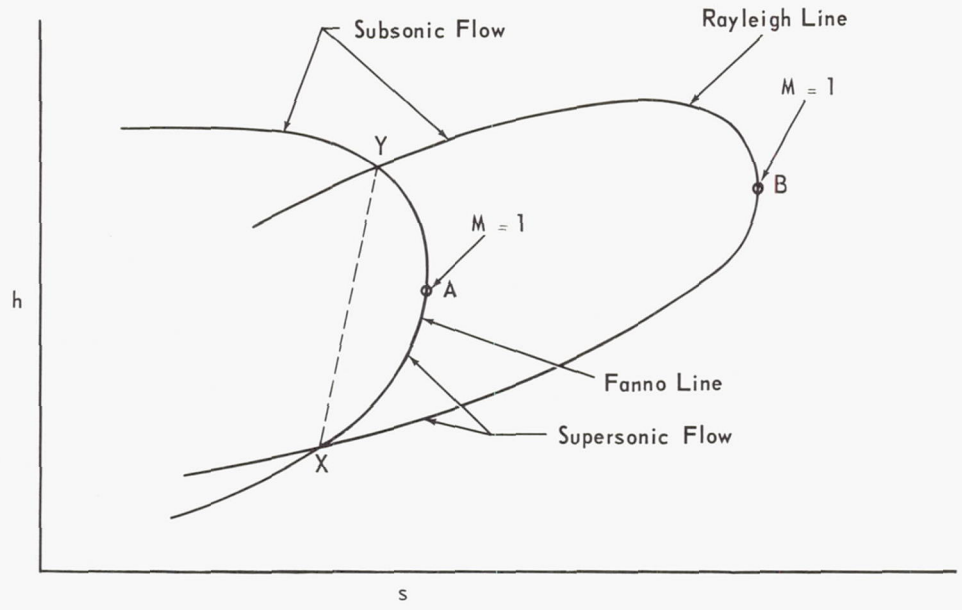
Description

A normal shock must simultaneously satisfy the steady-flow energy equation for an adiabatic process, the continuity equation, the momentum equation, and the equation of state of the fluid.

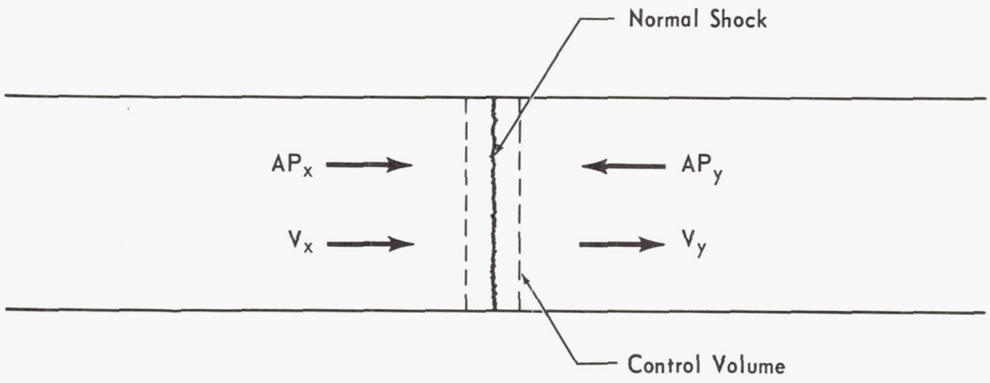
Combining the steady-flow energy equation for an adiabatic process, the continuity equation, written for constant area, and the equation of state yield a locus of points called the Fanno line. Combination of the continuity equation, the momentum equation, and the equation of state yields a locus of points called the Rayleigh line. When two of these lines are plotted on an h–s diagram, there are two points of intersection, points X and Y in figure 6.1a. Since these two points satisfy all four of the equations that the normal shock must satisfy, it can be concluded that the two intersections of the Rayleigh and Fanno lines represent the initial and final states of the gas passing through the normal shock.

As will be shown later, the mach number at points A and B, the points of maximum entropy of the Fanno and Rayleigh lines, is unity. Further, it can be shown that the lower branches of these two lines represent supersonic velocities and the upper branches represent subsonic velocities. Finally, it will be shown that point X represents the initial state of the fluid passing through the shock and that fluid velocity always proceeds from supersonic to subsonic across the shock.

Preceding Page Blank



(a) Thermodynamic States Before and After Normal Shock.



(b) Control Volume for a Normal Shock.

Figure 6.1. Normal shocks in pipes.

In the preceding discussion, normal shock waves were discussed from a qualitative point of view. It was stated that the normal shock must simultaneously satisfy four equations: the first law of thermodynamics, the continuity equation, the momentum equation, and the equation of the fluid. These equations can be combined into functions which describe the fluid property changes across the normal shock. In general, the equations can be used for both the perfect or real gas. However, to continue the discussion on a quantitative basis, it is desirable to restrict the analysis to perfect gas.

The Fanno Line

In this chapter only the Fanno-line relations necessary for an understanding of shock waves will be developed. A more extensive analysis of the Fanno line is presented in chapter 8.

Since the Fanno line is the locus of points describing the irreversible adiabatic flow of a gas at constant mass flow per unit area, the adiabatic relations developed in "Adiabatic Flow" (ch. 5) can be applied. Referring to the notation of figure 6.1*b*, the steady-flow energy equation for an adiabatic process can be written as

$$h_{ox} = h_{oy}$$

or, for a perfect gas

$$T_{ox} = T_{oy} \tag{6.1}$$

Combining equation (6.1) with equation (5.10)

$$\frac{T_o}{T} = 1 + \left(\frac{k-1}{2}\right) M^2 \qquad [5.10]$$

yields

$$\frac{T_y}{T_x} = \frac{1 + \left(\frac{k-1}{2}\right) M_x^2}{1 + \left(\frac{k-1}{2}\right) M_y^2} \tag{6.2}$$

Since the area is the same on both sides of the shock, the continuity equation yields

$$\frac{m}{A} = \rho_x V_x = \rho_y V_y \qquad \text{or} \qquad \frac{w}{A} = \gamma_x V_x = \gamma_y V_y \tag{6.3}$$

Combining equation (6.3) with the perfect-gas equation of state yields

$$\frac{T_y}{T_x} = \frac{P_y V_y}{P_x V_x}$$

and since $M = V/\sqrt{g_c k R T}$, it follows that

$$\frac{T_y}{T_x} = \left(\frac{P_y M_y}{P_x M_x}\right) \sqrt{\frac{T_y}{T_x}}$$

Solving this equation for the temperature ratio

$$\frac{T_y}{T_x} = \left(\frac{P_y}{P_x}\right)^2 \left(\frac{M_y}{M_x}\right)^2 \tag{6.4}$$

and combining with equation (6.2) yields

$$\frac{P_y}{P_x}=\left(\frac{M_x}{M_y}\right)\sqrt{\frac{1+\left(\frac{k-1}{2}\right)M_x^2}{1+\left(\frac{k-1}{2}\right)M_y^2}} \tag{6.5}$$

Equation (6.5) is the equation of the Fanno line in terms of P and M.

To prove that point A in figure 6.1a is the point where $M=1$, consider an adiabatic process very close to point A. For such an adiabatic process, the steady-flow energy equation may be written as

$$\mathrm{d}h+\frac{V\,\mathrm{d}V}{g_cJ}=0 \tag{6.6}$$

and the continuity equation for constant area

$$\mathrm{d}(\gamma V)=0$$

or

$$\gamma\,\mathrm{d}V+V\,\mathrm{d}\gamma=0 \tag{6.7}$$

The first law of thermodynamics yields

$$T\,\mathrm{d}s=\mathrm{d}h-\frac{\mathrm{d}P}{J\gamma}$$

and for an infinitesimal process at point A, the entropy goes through a maximum. Therefore, $\mathrm{d}s=0$ and

$$\mathrm{d}h=\frac{\mathrm{d}P}{J\gamma} \tag{6.8}$$

Substituting equations (6.7) and (6.8) into equation (6.6) and solving for V results in

$$V=\sqrt{g_c\left(\frac{\mathrm{d}P}{\mathrm{d}\gamma}\right)}=\sqrt{\frac{\mathrm{d}P}{\mathrm{d}\rho}}$$

Since entropy is constant for this infinitesimal process, a more exact expression is

$$V=\sqrt{\left(\frac{\partial P}{\partial\rho}\right)_s} \tag{6.9}$$

Equation (6.9) is the definition of the velocity of sound, so that the velocity at the point of maximum entropy is equal to the speed of sound and $M=1$.

The Rayleigh Line

The Rayleigh line is the locus of points describing a frictionless flow at constant area with heat transfer. If frictional effects are neglected, the forces acting on the fluid consist of pressure forces only, and the forces in the flow direction can be equated with the change in momentum of the fluid. Referring to the notation of figure 6.1*b*, the momentum equation is

$$AP_x - AP_y = \dot{m}V_y - \dot{m}V_x$$

Rearranging terms and substituting using the continuity equation for a constant area yield

$$P_x + \rho_x V_x^2 = P_y + \rho_y V_y^2 \tag{6.10}$$

For a perfect gas, substituting $\rho V^2 = kPM^2$ in equation (6.10) yields the Rayleigh-line expression

$$\frac{P_y}{P_x} = \frac{1 + kM_x^2}{1 + kM_y^2} \tag{6.11}$$

By an analysis similar to that shown for the Fanno line, it can be shown that the point of maximum entropy on the Rayleigh line (point B, fig. 6.1*a*) is the point where $M = 1$.

Changes in Properties Across a Normal Shock

The changes in pressure and temperature across a normal shock are obtained using the relationships developed for either the Fanno or Rayleigh lines, but first an expression relating the upstream and downstream mach numbers which simultaneously satisfies both functions must be obtained. This is done by equating equations (6.5) and (6.11) and rearranging to obtain

$$\frac{M_x \sqrt{1 + \left(\frac{k-1}{2}\right) M_x^2}}{1 + kM_x^2} = \frac{M_y \sqrt{1 + \left(\frac{k-1}{2}\right) M_y^2}}{1 + kM_y^2} \tag{6.12}$$

To obtain an explicit relationship for the downstream mach number, equation (6.12) is solved and the two following solutions are obtained

$$M_y = M_x \tag{6.13}$$

and

$$M_y^2 = \frac{M_x^2 + \frac{2}{k-1}}{\left(\frac{2k}{k-1}\right) M_x^2 - 1} \tag{6.14}$$

The first solution, equation (6.13), is trivial since it expresses the fact that conditions at x and y are the same if no shock occurs. The second solution, equation (6.14), expresses the condition that must be satisfied between the two sides of the shock. A useful relation

between M_x^* and M_y^* may be obtained by substituting equation (5.19) into equation (6.14) to yield

$$M_x^* M_y^* = 1 \tag{6.15}$$

or since $c_x^* = c_y^*$ for an adiabatic process

$$V_x V_y = c^{*2}$$

From this, it is evident that if the flow at X is supersonic, the flow at Y must be subsonic, and vice versa.

Using the relation between upstream and downstream mach numbers, relationships can be obtained for the property change across the shock in terms of the upstream mach number.

To obtain the pressure ratio, equation (6.14) is substituted into either equation (6.5) or (6.11) to give

$$\frac{P_y}{P_x} = \left(\frac{2k}{k+1}\right) M_x^2 - \frac{k-1}{k+1} \tag{6.16}$$

The temperature ratio is obtained by substituting equation (6.14) into equation (6.2) to give

$$\frac{T_y}{T_x} = \frac{\left[1 + \left(\frac{k-1}{2}\right) M_x^2\right]\left[\left(\frac{2k}{k-1}\right) M_x^2 - 1\right]}{\left[\frac{(k+1)^2}{2(k-1)}\right] M_x^2} \tag{6.17}$$

Using equations (6.16) and (6.17), the density ratio may be obtained from the perfect-gas equation of state

$$\frac{\gamma_y}{\gamma_x} = \frac{\rho_y}{\rho_x} = \frac{\frac{P_y}{P_x}}{\frac{T_y}{T_x}} \tag{6.18}$$

and this equation combined with equation (6.3) yields the relation for the velocity ratio

$$\frac{V_y}{V_x} = \frac{\gamma_x}{\gamma_y} = \frac{\frac{T_y}{T_x}}{\frac{P_y}{P_x}} \tag{6.19}$$

Since the normal shock process is irreversible, there is a loss in stagnation pressure across the shock. To obtain the stagnation pressure change across the shock, note that $P_{oy}/P_{ox} = (P_{oy}/P_y)(P_y/P_x)/(P_{ox}/P_x)$. Using equation (5.31) to define P_{ox}/P_x and P_{oy}/P_y,

equation (6.16) for P_y/P_x, and equation (6.14) to eliminate M_y, after simplification the following is obtained:

$$\frac{P_{oy}}{P_{ox}} = \frac{\left[\dfrac{\left(\dfrac{k+1}{2}\right)M_x^2}{1+\left(\dfrac{k-1}{2}\right)M_x^2}\right]^{\frac{k}{k-1}}}{\left[\left(\dfrac{2k}{k+1}\right)M_x^2 - \dfrac{k-1}{k+1}\right]^{\frac{1}{k-1}}} \tag{6.20}$$

The downstream stagnation pressure can be related to the upstream static pressure by substituting the isentropic pressure relationship, equation (5.31), into equation (6.20), yielding

$$\frac{P_{oy}}{P_x} = \frac{\left[\left(\dfrac{k+1}{2}\right)M_x^2\right]^{\frac{k}{k-1}}}{\left[\left(\dfrac{2k}{k+1}\right)M_x^2 - \dfrac{k-1}{k+1}\right]^{\frac{1}{k-1}}} \tag{6.21}$$

To evaluate the increase in entropy across a shock, the first law of thermodynamics for a perfect gas is used

$$T\ \mathrm{d}s = c_p\ \mathrm{d}T - \left(\frac{v}{J}\right)\mathrm{d}P$$

division through by $T = Pv/R$ gives

$$\mathrm{d}s = c_p\left(\frac{\mathrm{d}T}{T}\right) - \frac{R}{J}\left(\frac{\mathrm{d}P}{P}\right)$$

Integrating from condition X to Y yields

$$s_y - s_x = c_p \ln\left(\frac{T_y}{T_x}\right) - \left(\frac{R}{J}\right)\ln\left(\frac{P_y}{P_x}\right) \tag{6.22}$$

Further substitution using the perfect-gas relation,

$$\frac{R}{J} = c_p\left(\frac{k-1}{k}\right)$$

yields

$$s_y - s_x = c_p \ln\left[\frac{\dfrac{T_y}{T_x}}{\left(\dfrac{P_y}{P_x}\right)^{\frac{k-1}{k}}}\right] \tag{6.23}$$

Using the equations for T_o/T and P_o/P (eqs. (5.10) and (5.31)) an expression for the entropy increase in terms of the stagnation conditions can be obtained

$$s_y - s_x = c_p \ln \left[\frac{\frac{T_{oy}}{T_{ox}}}{\left(\frac{P_{oy}}{P_{ox}}\right)^{\frac{k-1}{k}}} \right] \tag{6.24}$$

In the present case, $T_{oy} = T_{ox}$ since the flow is adiabatic so that

$$\frac{s_y - s_x}{\frac{R}{J}} = -\ln \left(\frac{P_{oy}}{P_{ox}}\right) \tag{6.25}$$

Or, after substituting the value of P_{ox}/P_{oy} given in equation (6.20),

$$\frac{s_y - s_x}{\frac{R}{J}} = \left(\frac{k}{k-1}\right) \ln \left[\frac{2}{(k+1)M_x^2} + \frac{k-1}{k+1} \right] + \left(\frac{1}{k-1}\right) \ln \left[\left(\frac{2k}{k+1}\right) M_x^2 - \frac{k-1}{k+1} \right] \tag{6.26}$$

If equation (6.26) is analyzed, it will be seen that for a gas with $1 < k < 1.67$, the entropy change is positive when M_x is greater than unity and negative when M_x is less than unity. Since the second law demands that the entropy cannot decrease in the absence of heat transfer, the fluid velocity can change only from supersonic to subsonic across the normal shock. Also, by observing equation (6.25) with $s_y > s_x$, it can be seen that there is always a decrease in the isentropic stagnation pressure across a shock.

Convergent-Divergent Nozzles

The isentropic flow of a perfect gas through a convergent-divergent nozzle is described in chapter 5. However, a specific range of nozzle outlet pressures between process lines (4) and (5) in figures 5.10 and 6.2 was excluded, since these values cannot be achieved with isentropic flow throughout the nozzle. It will be shown here that a shock wave occurs somewhere within the supersonic portion of the nozzle, which separates two isentropic processes.

Consider the case of an intermediate nozzle-exit pressure P_e, as indicated on figure 6.2. The flow tends to be isentropic in the smooth nozzle, but since the end pressure P_e cannot be achieved in an isentropic process, the process must obviously follow some irreversible path. With the virtual absence of the usual irreversibilities caused by friction and turbulence, the shock provides the only remaining irreversible mechanism in a smooth-flow nozzle. In general, a normal shock will stand somewhere within the supersonic nozzle (diverging region), producing an abrupt change in properties. In figure 6.2 this change is reflected by a step change in static pressure from the supersonic isentropic line (5), to a subsonic isentropic line that terminates at P_e at the nozzle-exit location. The entire irreversibility occurs essentially at a point along the nozzle-length dimension. Therefore, the locations just upstream of the normal shock x_x and just downstream of the shock x_y are the same ($A_x = A_y$). Also, the isentropic flow relationships can be used for both processes on either side of the shock.

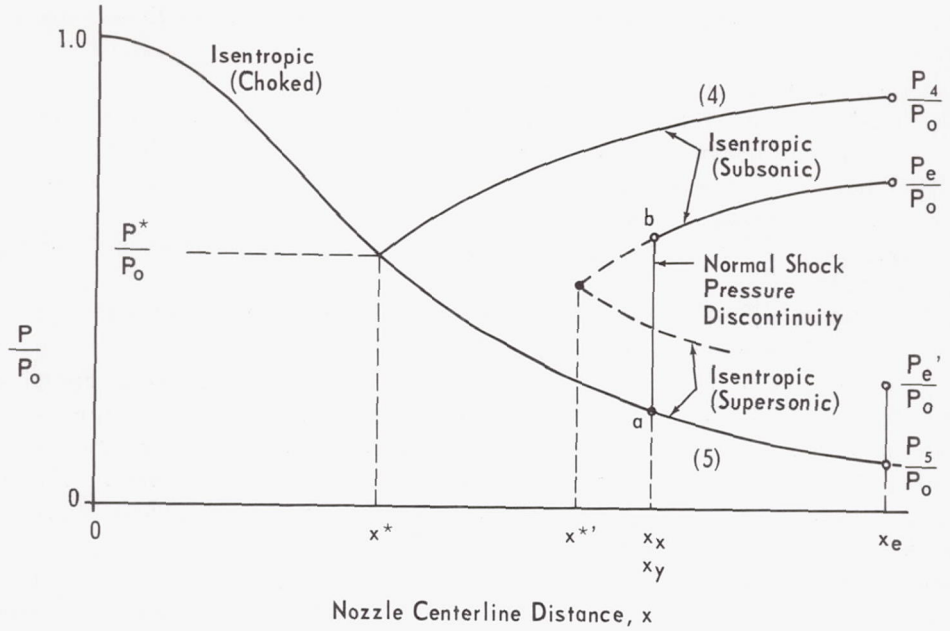


Figure 6.2. *Convergent-divergent nozzle flow with internal normal shock.*

The one-dimensional isentropic flow relationships developed in chapter 5, combined with the normal shock functions developed in this chapter, provide the means for determining the flow conditions throughout the smooth nozzle and identification of the location of the normal shock. Specifically, for a nozzle of known dimensions, the flow area is known as a function of the nozzle-length parameter x. Then the nozzle area ratio (A/A^*) can be established for all locations ahead of the shock wave by the isentropic relationship (eq. (5.38)). On the upstream side of the shock, depicted by point a in figure 6.2, the supersonic area ratio is

$$\frac{A_x}{A^*}=\frac{1}{M_x}\left\{\left(\frac{2}{k+1}\right)\left[1+\left(\frac{k-1}{2}\right)M_x^2\right]\right\}^{\frac{k+1}{2(k-1)}} \tag{6.27}$$

On the downstream side of the shock, point b, the flow is subsonic, but equation (5.38) applies once again. However, a different and fictitious throat area $A^{*\prime}$ must be considered for the new subsonic isentropic line which passes through point b and terminates at P_e. For the two points of interest on this line, the area ratios are

$$\frac{A_y}{A^{*\prime}}=\frac{1}{M_y}\left\{\left(\frac{2}{k+1}\right)\left[1+\left(\frac{k-1}{2}\right)M_y^2\right]\right\}^{\frac{k+1}{2(k-1)}} \tag{6.28}$$

where $A_x=A_y$ and

$$\frac{A_e}{A^{*\prime}}=\frac{1}{M_e}\left\{\left(\frac{2}{k+1}\right)\left[1+\left(\frac{k-1}{2}\right)M_e^2\right]\right\}^{\frac{k+1}{2(k-1)}} \tag{6.29}$$

For example, for a given nozzle geometry and upstream reservoir condition, the mach number and fluid conditions can be established throughout the nozzle by the procedure outlined below, if the shock location is known or assumed. Graphic or tabulated solutions

to the isentropic flow and normal shock functions are required, such as those found in chapters 16 and 17:

Compute A_x/A^* from the known areas.

Read M_x from a graphic or tabulated solution of equation (6.27), which is just equation (5.38) with the applicable subscripts. (See fig. 16.6, ch. 16.)

Obtain M_y as a function of M_x using the normal shock wave, equation (6.14), or its graphic or tabulated solution. (See fig. 17.1, ch. 17.)

Obtain $A_y/A^{*\prime}$ at M_y by equation (6.28), or use the solved equation (5.28) (fig. 16.6, ch. 16).

Obtain $A_y/A^{*\prime} = (A_e/A_x)(A_y/A^{*\prime})$ and read M_e for the area ratio $A_e/A^{*\prime}$, once again using the solution of equation (5.38). (See fig. 16.6, ch. 16.)

Using a similar procedure, all of the fluid properties can be established throughout the nozzle. The isentropic flow functions (tabulated or plotted) of chapter 16 are used in the two isentropic regions, remembering that in those two regions the stagnation properties are constant and the static properties are dependent on local mach number. The changes in stagnation properties across the normal shock are established by the normal shock equations of this chapter, or their graphic or tabulated solutions.

For the more common case, where the nozzle-exit pressure is specified, and the shock location is unknown, a trial-and-error solution is required. The procedure is exactly the same as outlined above, except that the computation is carried out with assumed shock locations (or more specifically, assumed values of A_x). The procedure is repeated until the value of A_x that will produce the known exit pressure is identified.

There is a limiting exit pressure which will cause the normal shock to stand at the nozzle exit. For this case, $x_x = x_e$ (or $A_x = A_e$), and the limiting exit pressure can be easily established for a given nozzle by the same procedure outlined above, noting that $P'_e = P_y$.

When the exit pressure is reduced below P'_e, the normal shock leans outward, pivoting at the nozzle-exit lip, and becomes an oblique shock wave. There can be no variation in flow conditions within the nozzle as a result of changes in exit pressure below P'_e. The flow stream outside the nozzle cannot be analyzed using one-dimensional theory when $P_e < P'_e$ because of the existence of oblique (two-dimensional) shock waves.

Ideal nozzle operation occurs when the back pressure is exactly that at the end point of the supersonic isentropic line (5). This pressure and the other fluid properties at the exit are fixed by the specific nozzle area ratio (A_e/A^*), the gas constants, and the supersonic exit mach number identified by equation (5.38).

Nozzles operating with back pressures greater than P_5 are said to be overexpanded, and when the back pressure is less than P_5 the nozzle is said to be underexpanded.

OBLIQUE SHOCK WAVES

Although it is improbable that the use of oblique shock-wave analysis would ever be required in the design of a pneumatic system, an understanding of the characteristics of oblique shock waves is desirable in understanding compressible flow and evaluating conditions which may occasionally occur in practice. Oblique shock waves are a general form of discontinuity in supersonic flow and in the limit they approach the normal shock wave which was discussed in the previous section. Oblique shock waves are inclined to the flow direc-

tion, and they occur when a supersonic flow undergoes a change in direction requiring a compression (fig. 6.3). The converse case in which a supersonic flow undergoes an expansion during a change in direction will not be considered, but it should be noted that a shock wave is not possible in this case since it would require an increase in entropy.

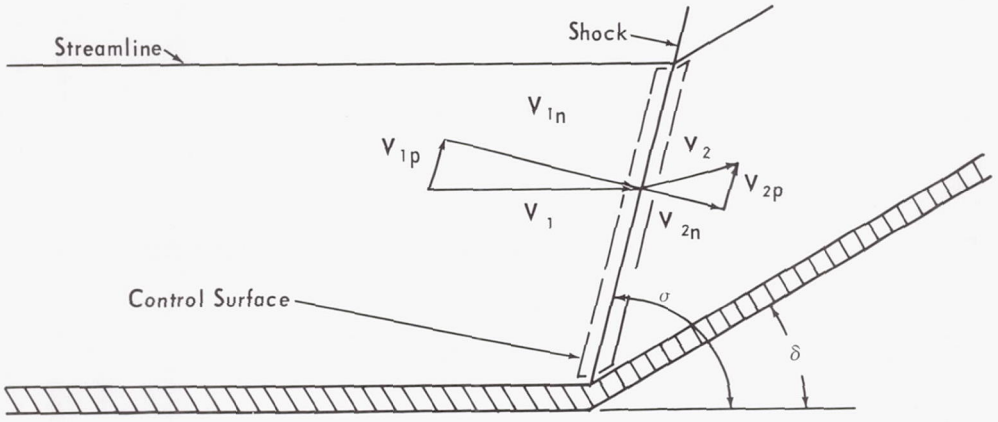


Figure 6.3. Control volume for oblique-shock analysis.

Governing Relations

In order to derive the governing relations for oblique shocks, the control volume of figure 6.3 will be used. It should be noted that the mass flow across the boundary of a control volume must always be evaluated using the velocity component normal to the control volume surface. In addition, it should be noted that, although there is a pressure force in the normal (n) direction due to the pressure rise across the shock wave, there is no pressure force in the parallel (p) direction. With these points in mind, one can write the following basic relations:

From continuity

$$\rho_1 V_{1n} = \rho_2 V_{2n} \tag{6.30}$$

The change in momentum in the p direction, where there are no unbalanced pressure forces

$$(\rho_1 V_{1n}) V_{1p} = (\rho_2 V_{2n}) V_{2p}$$

Therefore,

$$V_{1p} = V_{2p} = V_p \tag{6.31}$$

Equating momentum changes in the n direction to pressure forces results in

$$P_2 - P_1 = \rho_1 V_{1n}^2 - \rho_2 V_{2n}^2 = \rho_1 V_{1n}^2 \left(1 - \frac{\rho_2 V_{2n}^2}{\rho_1 V_{1n}^2}\right) \tag{6.32}$$

The energy equation for adiabatic flow (from eq. (6.6)) across the oblique shock yields

$$h_1 - h_2 = \frac{V_2^2 - V_1^2}{2g_c J} \tag{6.33}$$

Geometrical consideration of figure 6.3 requires that

$$V_2^2 - V_1^2 = (V_{2n}^2 + V_{2p}^2) - (V_{1n}^2 + V_{1p}^2) = V_{2n}^2 - V_{1n}^2 \tag{6.34}$$

$$V_{1p} = V_1 \cos \sigma \qquad V_{2p} = V_2 \cos (\sigma - \delta) \tag{6.35}$$

$$V_{1n} = V_1 \sin \sigma \qquad V_{2n} = V_2 \sin (\sigma - \delta) \tag{6.36}$$

If only perfect gases are considered, the energy equation (6.33) may be rearranged using

$$h = c_p T = \frac{c_p}{R}\left(\frac{P}{\gamma}\right) = \left(\frac{1}{Jg_c}\right)\left(\frac{k}{k-1}\right)\frac{P}{\rho}$$

and equation (6.34) to obtain

$$\frac{k}{k-1}\left(\frac{P_2}{\rho_2} - \frac{P_1}{\rho_1}\right) = \frac{V_{1n}^2 - V_{2n}^2}{2} \tag{6.37}$$

In order to obtain a relation between the pressure and density before and after the shock, it is necessary to rearrange equation (6.32) by substituting equation (6.30) to yield

$$P_2 - P_1 = \rho_1 V_{1n}^2 \left(1 - \frac{\rho_1}{\rho_2}\right) \tag{6.38}$$

from which

$$V_{1n}^2 = \left(\frac{P_2 - P_1}{\rho_2 - \rho_1}\right)\left(\frac{\rho_2}{\rho_1}\right) \tag{6.39}$$

Similarly, for the downstream normal velocity, the following may be obtained

$$V_{2n}^2 = \left(\frac{P_2 - P_1}{\rho_2 - \rho_1}\right)\left(\frac{\rho_1}{\rho_2}\right) \tag{6.40}$$

Equations (6.39) and (6.40), when substituted in equation (6.37), yield the following relations between the pressure and density ratios before and after the shock:

$$\frac{P_2}{P_1} = \frac{\left(\frac{k+1}{k-1}\right)\left(\frac{\rho_2}{\rho_1}\right) - 1}{\frac{k+1}{k-1} - \frac{\rho_2}{\rho_1}} = \frac{\left(\frac{k+1}{k-1}\right)\left(\frac{\gamma_2}{\gamma_1}\right) - 1}{\frac{k+1}{k-1} - \frac{\gamma_2}{\gamma_1}} \tag{6.41a}$$

Equation (6.41*a*) solved for density ratio is

$$\frac{\gamma_2}{\gamma_1}=\frac{\rho_2}{\rho_1}=\frac{\left(\frac{k+1}{k-1}\right)\left(\frac{P_2}{P_1}\right)+1}{\frac{k+1}{k-1}+\frac{P_2}{P_1}} \tag{6.41b}$$

Other relations for the pressure and density before and after the shock may be obtained as a function of the shock and deflection angles and the mach numbers. To obtain these additional relations, equations (6.31) and (6.35) are combined to yield

$$\frac{V_2}{V_1}=\frac{\cos\sigma}{\cos(\sigma-\delta)} \tag{6.42}$$

and equation (6.30) is combined with equation (6.36) to obtain

$$\rho_1 V_1 \sin\sigma=\rho_2 V_2 \sin(\sigma-\delta) \tag{6.43}$$

Combining equations (6.42) and (6.43) yields

$$\frac{\gamma_2}{\gamma_1}=\frac{\rho_2}{\rho_1}=\left(\frac{V_1}{V_2}\right)\frac{\sin\sigma}{\sin(\sigma-\delta)}=\left[\frac{\cos(\sigma-\delta)}{\cos\sigma}\right]\left[\frac{\sin\sigma}{\sin(\sigma-\delta)}\right]=\frac{\tan\sigma}{\tan(\sigma-\delta)} \tag{6.44}$$

Since $\rho_1 V_1^2=P_1 k M_1^2$ may be written for a perfect gas, equation (6.38) may be solved for the pressure ratio as a function of the mach number using the relation of equation (6.36).

$$\frac{P_2}{P_1}=1+k\left(1-\frac{\gamma_1}{\gamma_2}\right)M_1^2\sin^2\sigma \tag{6.45}$$

Similarly, it can be shown that

$$\frac{P_1}{P_2}=1+k\left(1-\frac{\gamma_2}{\gamma_1}\right)M^2\sin^2(\sigma-\delta) \tag{6.46}$$

There are four equations ((6.41), (6.44), (6.45), and (6.46)) which may be used to relate the six variables σ, δ, M_1, M_2, (P_2/P_2), and (γ_2/γ_1). Consequently, these equations can be solved simultaneously and solutions plotted against any two independent variables.* Typical graphs are presented as figures 6.4 through 6.7.

The temperature change across the oblique shock is also of interest and can be obtained from energy considerations of the adiabatic process. Equation (6.33) can be rewritten as

$$c_p(T_2-T_1)=\left(\frac{1}{2Jg_c}\right)(V_1^2-V_2^2)$$

and

$$T_1\left(\frac{T_2}{T_1}-1\right)=\frac{V_1^2}{2Jg_c c_p}\left[1-\left(\frac{V_2}{V_1}\right)^2\right]$$

*This is not completely true, since P_2/P_1 and γ_2/γ_1 cannot be chosen as the independent variables.

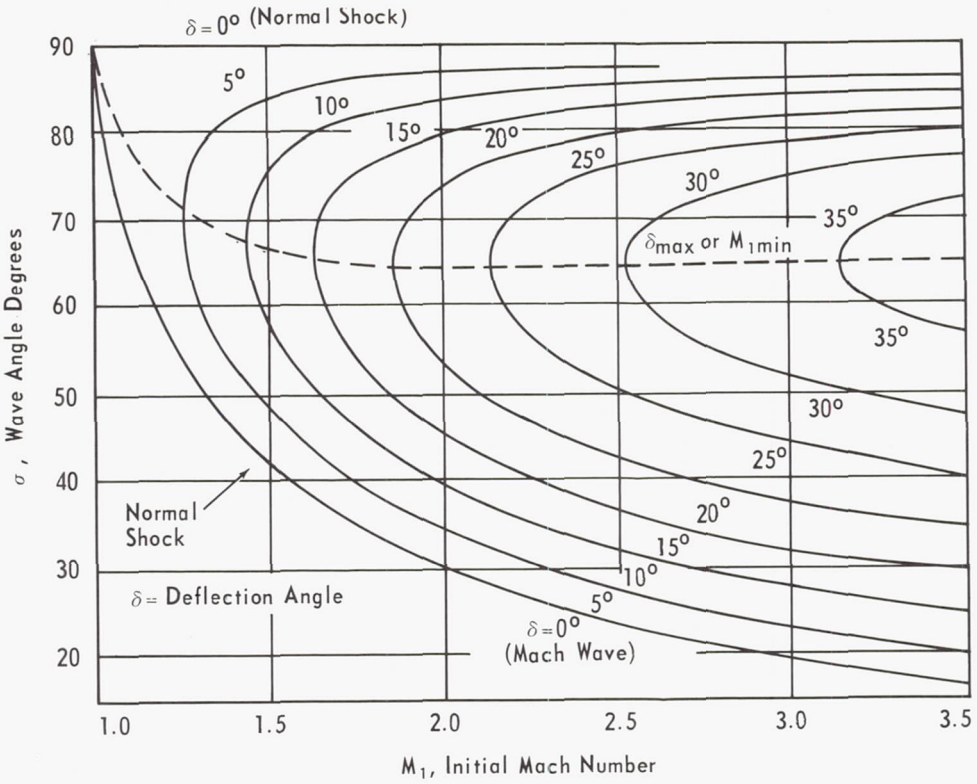


Figure 6.4. Wave-angle variances with initial mach number.

Substituting the definition of mach number M_1 and the perfect gas relationship

$$\frac{R}{c_p J} = \frac{k-1}{k}$$

yields

$$\frac{T_2}{T_1} = 1 + \left(\frac{k-1}{2}\right) M_1^2 \left[1 - \left(\frac{V_2}{V_1}\right)^2\right]$$

Equation (6.42) can be used to replace the velocity ratio so that

$$\frac{T_2}{T_1} = 1 + \left(\frac{k-1}{2}\right) M_1^2 \left[1 - \frac{\cos^2 \sigma}{\cos^2 (\sigma - \delta)}\right] \tag{6.47}$$

It is often convenient when working with oblique shocks to transform the coordinate system so that the normal shock tables may be used for oblique shock. This can be done by setting $M_1 \sin \sigma$ equal to M_x in a normal shock table so that P_y/P_x, γ_y/γ_x, T_y/T_x, and P_{oy}/P_{ox} are, respectively, the values of P_2/P_1, γ_2/γ_1, T_2/T_1, and P_{o2}/P_{o1} for an oblique shock with an inclination of σ and an approach mach number of M_1. In addition, the mach number downstream of the equivalent normal shock M_y is equal to $M_2 \sin (\sigma - \delta)$ for the oblique shock.

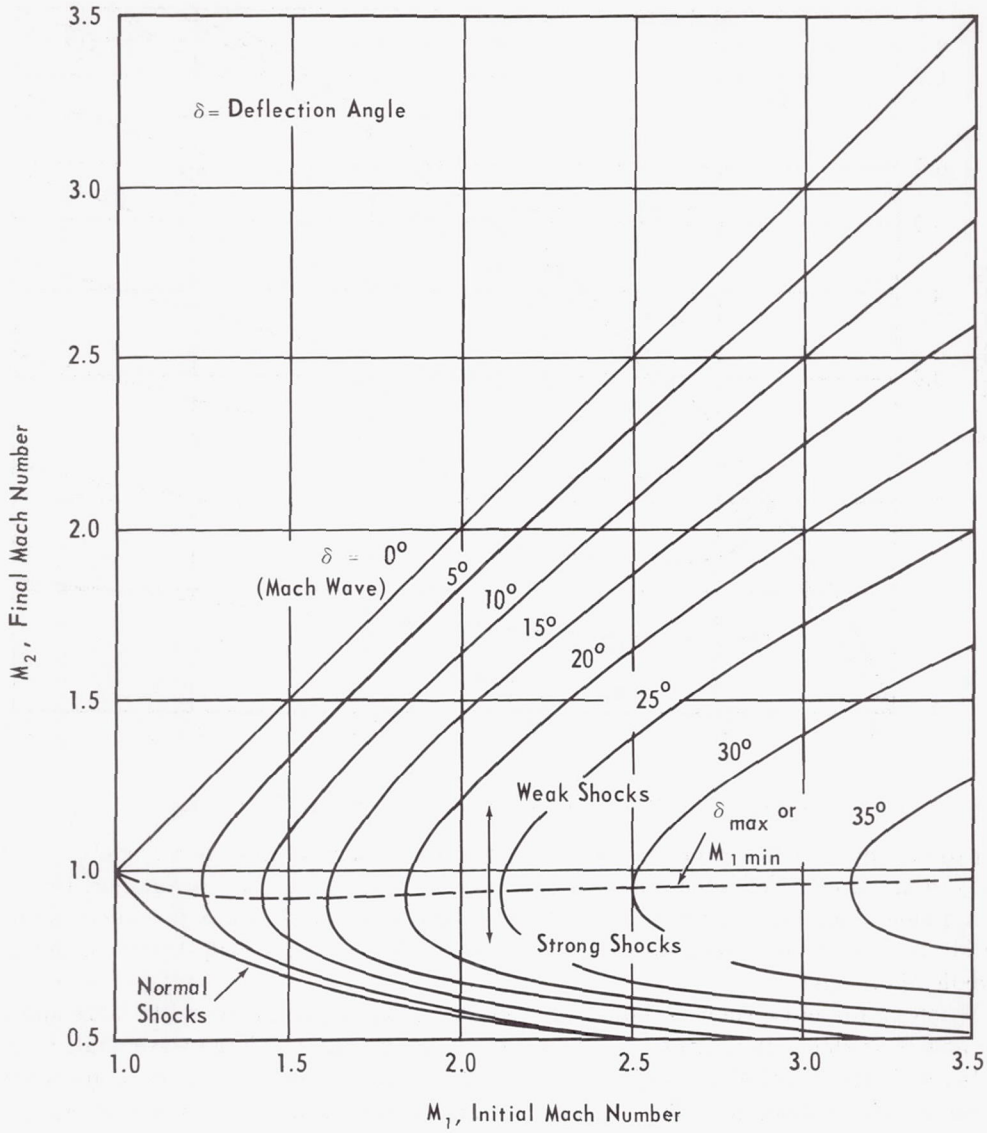


Figure 6.5. Final mach-number variances with initial mach number.

Characteristics of Oblique Shock Waves

In examining the characteristics of oblique shock waves, it should first be noted that the flow deflection angle is not necessarily equal to the deflection angle of the bounding surface. Although this is the case for a two-dimensional surface as shown in figure 6.3, it is not true, for example, on a cone as shown in figure 6.8. In any case, however, the initial flow deflection caused by the shock is δ, as defined by the oblique shock relations at the observed shock angle. Consider the oblique shock relationships shown in figures 6.4 through 6.7 for $k = 1.4$. It may be seen from these figures that a single solution for a particu-

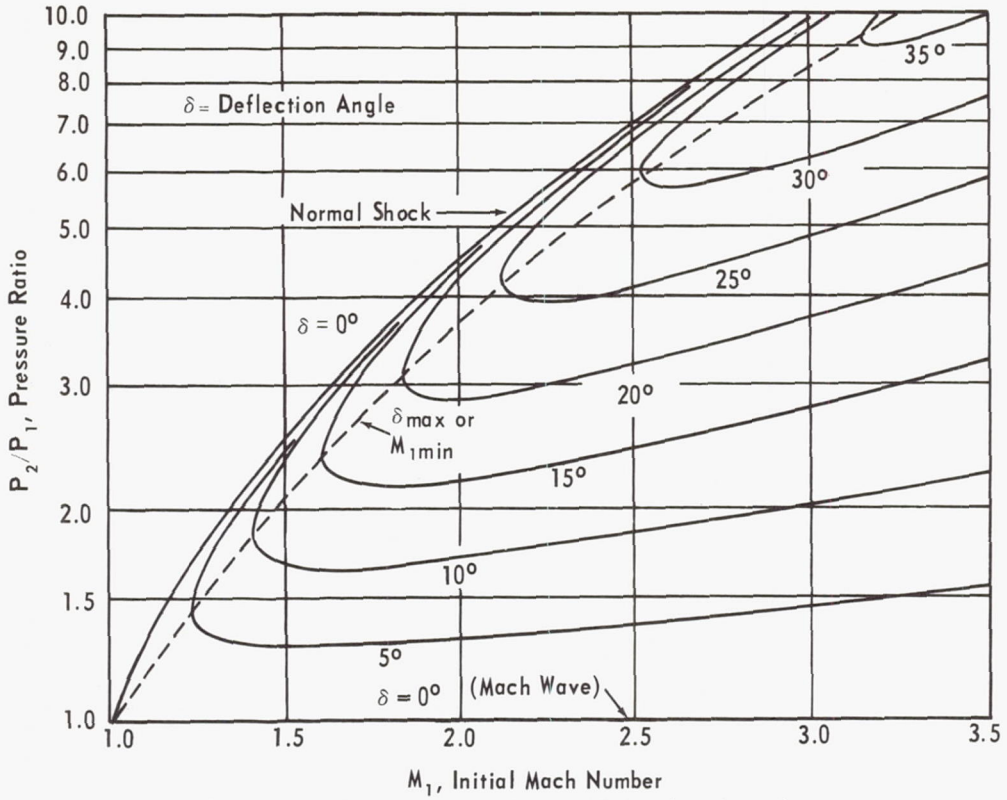


Figure 6.6. Pressure ratio variances with initial mach number.

lar upstream mach number occurs only for one particular flow deflection angle δ_{max}. Conversely, a given flow deflection angle is associated with only one mach number, which will give a single solution. In most cases likely to be encountered in practice then, there will be either two shock-wave solutions or no solutions at all for any given upstream mach number and deflection angle.

When two oblique shock solutions are possible, they will correspond to large and small wave angles as shown in figure 6.9. The solution with a relatively large wave angle is termed the "strong" shock solution, while the shock with a relatively small wave angle is termed the "weak" shock solution. The component of the mach number normal to the shock wave, $M_1 \sin \sigma$, is much larger for the strong shock so it corresponds to a normal shock at a higher mach number than does the weak solution. Therefore, the entropy loss and static pressure rise are larger for the strong shock than the corresponding values for the weak shock solution. There is no simple, clear-cut answer as to which of the two solutions will occur. The solution which occurs will depend, at least in part, on the flow conditions downstream of a shock. If an oblique shock were to occur in a pipe, for example, the back pressure could control the strength of the shock. If the back pressure were high, the strong shock solution would occur. It has been observed that when a wedge-shaped airfoil is used in flight, only the weak shock solution occurs. It should be noted in figure 6.5 that the weak shock solution is usually followed by supersonic flow downstream and the strong shock solution usually produces subsonic flow downstream.

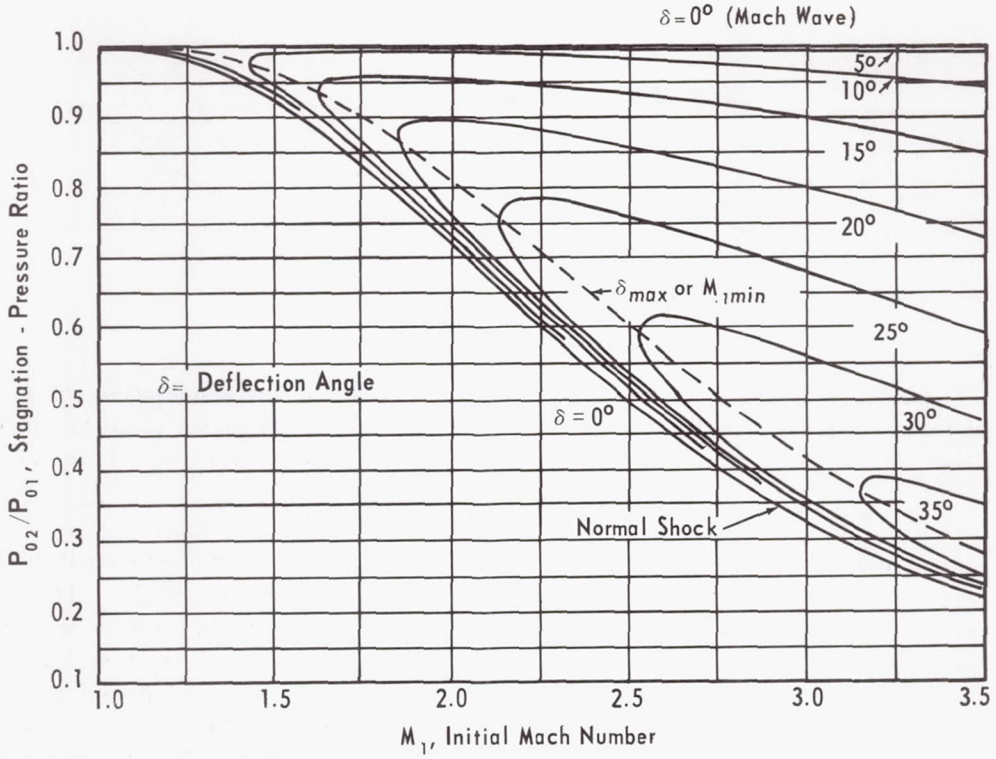


Figure 6.7. Stagnation pressure ratio variances with initial mach number.

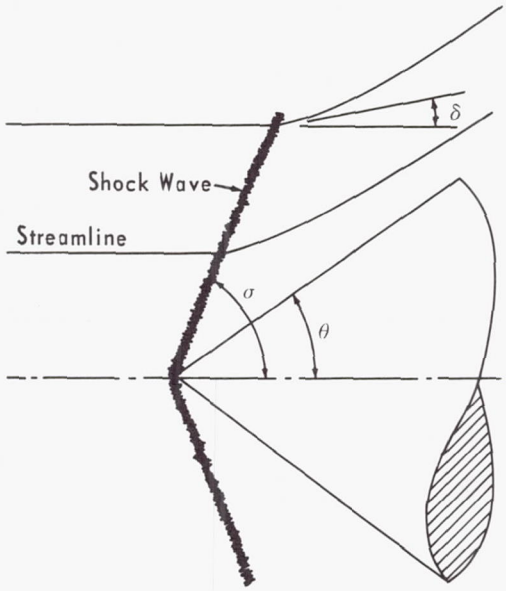


Figure 6.8. Oblique shock on a cone.

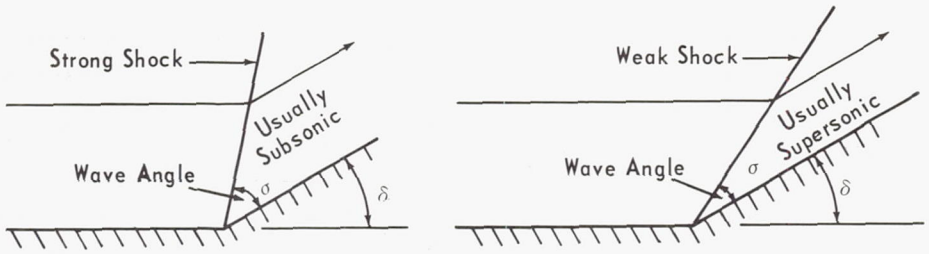


Figure 6.9. Comparison of strong and weak shocks.

For the cases in which there is no oblique shock solution, the shock wave will be detached from the point of deflection and will generally be curved as shown in figure 6.10. The values of M_1 and δ for which solutions are possible are shown in figure 6.11 for $k = 1.4$.

Occurrence of Oblique Shocks in Pipes

In pneumatic systems the flow is normally fully developed and turbulent so that the flow field is not uniform as was assumed in the previous discussion of oblique shocks. Therefore, there is no simple way of describing exactly how oblique shocks might occur in pneumatic systems. However, it may be said that if supersonic flow occurs in the system due to the variation in flow area in components and fittings, oblique shocks in some form will generally have an important role in reducing the flow back to the subsonic condition. Even the simple concept of a normal shock does not actually occur in practice when a thick boundary layer is present. The effect of boundary-layer thickness on the normal shock in a pipe is shown in figure 6.12*a*. Even with a thin boundary layer, the normal shock will not extend to the wall. The rise in pressure across the normal shock tends to thicken the boundary layer and thereby reduces the mass flow per unit area near the wall. The necessary deflection and compression of the supersonic flow near the boundary layer to accommodate this changing flow pattern occurs through a pair of oblique shocks extending from the normal shock in a forked pattern. For thicker boundary layers, a series of shock patterns with progressively shorter normal shocks occurs before the stream is completely subsonic, as illustrated in figure 6.12*b*. With this thicker boundary layer, the pressure rise across the shocks produces

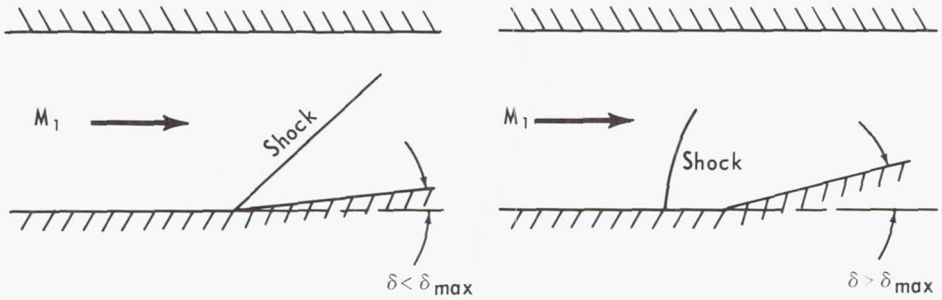


Figure 6.10. Concave corner with attached and detached shocks.

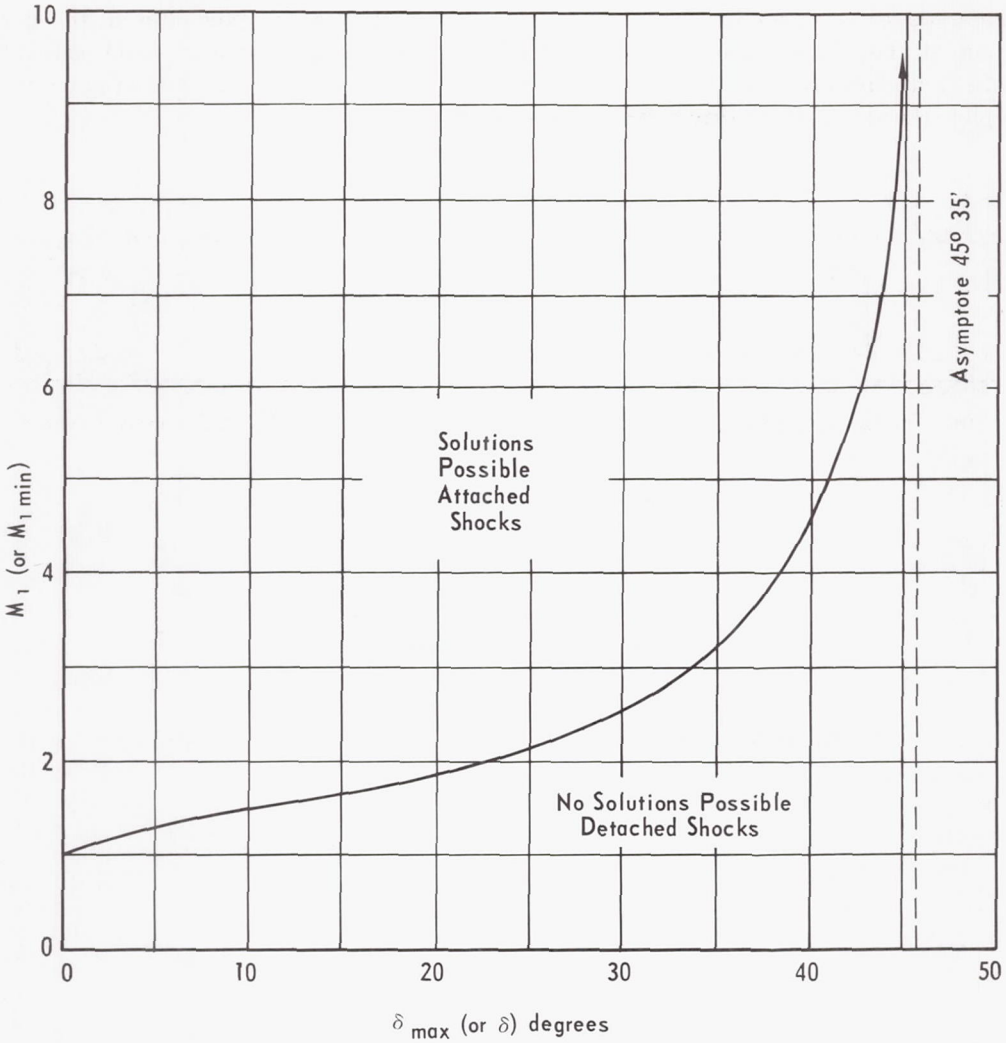


Figure 6.11. Conditions for attached shocks ($k = 1.4$).

boundary-layer separation. As still thicker boundary layers are encountered, the normal portion of the shocks disappears completely because of the boundary-layer separation. As the boundary layer increases in supersonic flow in a pipe, the pipe length necessary to complete the shock pattern increases.

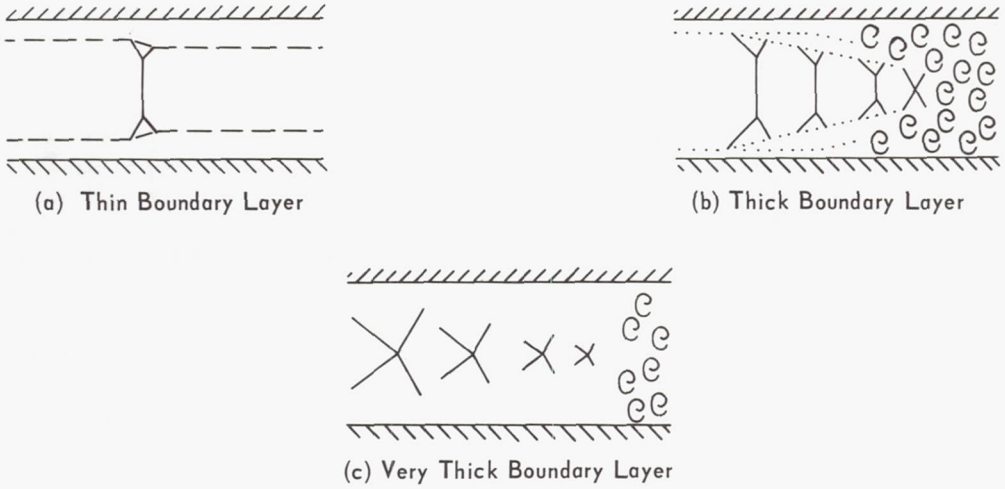


Figure 6.12. Effect of boundary layer thickness on a shock in a pipe.

CHAPTER 7

FLOW MEASUREMENT

Measurement of the rate of flow of fluid through a pipe is often accomplished with one of four devices: the venturi tube, the flow nozzle, the orifice, or the turbine meter.

The first two devices mentioned are elements which gradually restrict the flow passage to a minimum called the throat. This area reduction increases the fluid velocity, and the associated reduction in static pressure can be measured and used to compute the mass flow rate. The third device mentioned, the orifice, is also a restrictive element in the flow stream but, in this case, the area change is abrupt. The turbine meter does not operate on pressure drop, but measures flow velocity and mass flow rate by recording the speed of rotation of turbine blades placed in the stream.

The equations that predict the change in fluid properties caused by a restriction placed in the flow path are derived from the first law of thermodynamics when the flowing fluid is compressible and Bernoulli's equation when the flowing fluid is incompressible. These equations predict the theoretical rate of flow and must be modified by empirical flow coefficients to obtain the actual rate.

The value of the flow coefficient used with either of the above-mentioned equations depends, in part at least, on the geometry of the particular device being used for flow-measurement purposes. It will be found that the coefficient used in conjunction with the venturi tube is very near unity, which indicates that the theory employed to calculate venturi flow rate gives very good accuracy. The flow coefficient required with the flow nozzle is also near unity, but not so near as that of the venturi tube. The coefficient used with the orifice deviates considerably from unity, indicating that simple theory alone does not adequately describe the flow through an orifice.

THE HYDRAULIC EQUATION

The flow of an incompressible fluid through a constant-area passage into which a venturi tube, a nozzle, or an orifice has been inserted can be calculated by observation of Bernoulli's equation. The assumptions necessary are a steady, fully developed flow and no sensible heat transfer.

To begin the analysis, consider the system shown in figure 7.1. Bernoulli's equation applied between sections 1 and 2 gives

$$P_1+\frac{\gamma_1 V_1^2}{2g_c}=P_2+\frac{\gamma_2 V_2^2}{2g_c}$$

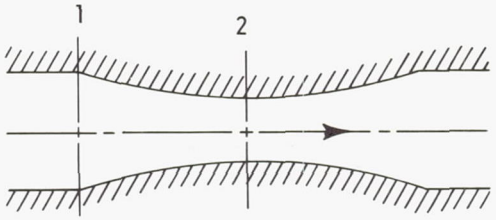


Figure 7.1. Flow system.

Solving for the change in pressure

$$P_1 - P_2 = \frac{\gamma_2 V_2^2 - \gamma_1 V_1^2}{2g_c}$$

Since for an incompressible fluid γ is constant, the preceding equation is rewritten as

$$P_1 - P_2 = \left(\frac{\gamma}{2g_c}\right)\left(V_2^2 - V_1^2\right) \tag{7.1}$$

For a steady incompressible flow, the continuity equation gives

$$A_1 V_1 = A_2 V_2$$

and solving for V_1 yields

$$V_1 = \left(\frac{A_2}{A_1}\right) V_2$$

Substituting this relation into equation (7.1)

$$P_1 - P_2 = \frac{\gamma}{2g_c}\left[V_2^2 - \left(\frac{A_2}{A_1}\right)^2 V_2^2\right]$$

or

$$V_2 = \left\{\frac{(P_1 - P_2)2g_c}{\left[1 - \left(\frac{A_2}{A_1}\right)^2\right]\gamma}\right\}^{1/2} \tag{7.2}$$

Defining

$$\beta = \frac{d_2}{d_1} \qquad \beta^2 = \frac{A_2}{A_1}$$

Equation (7.2) becomes

$$V_2 = \left(\frac{2g_c}{\gamma}\right)^{1/2}\left(\frac{P_1 - P_2}{1 - \beta^4}\right)^{1/2}$$

Writing the equation for the weight rate of flow in terms of conditions at section 2, the minimum cross section

$$w = \gamma A_2 V_2$$

or

$$w = A_2\left[\frac{2g_c\gamma(P_1 - P_2)}{1 - \beta^4}\right]^{1/2} \tag{7.3}$$

Equation (7.3) is known as the hydraulic equation, and it expresses the theoretical mass flow rate in terms of the three measurable variables: pressure, area, and mass density.

THE COMPRESSIBLE FLOW EQUATION

The equation for theoretical rate of flow of a compressible fluid through a venturi tube, nozzle, or an orifice is found in a manner similar to that for incompressible flow. The assumptions necessary for this analysis are a perfect gas and steady, reversible, adiabatic flow. To begin the analysis, consider the system shown in figure 7.1. For the system shown, the first law of thermodynamics can be written in the form

$$h_1+\frac{V_1^2}{2g_cJ}=h_2+\frac{V_2^2}{2g_cJ} \tag{7.4}$$

Rearranging terms yields

$$\frac{V_2^2-V_1^2}{2g_cJ}=h_1-h_2$$

and since the gas is perfect,

$$h_1-h_2=c_p(T_1-T_2) \qquad \text{and} \qquad Pv=RT$$

It follows that

$$h_1-h_2=\frac{c_p}{R}(P_1v_1-P_2v_2)$$

and since the process is adiabatic,

$$c_p=\frac{kR}{(k-1)}$$

which, when substituted into the foregoing equation, yields

$$\frac{V_2^2-V_1^2}{2g_c}=\frac{k}{(k-1)}(P_1v_1-P_2v_2) \tag{7.5}$$

For a steady flow, the continuity equation can be written as

$$\gamma_1A_1V_1=\gamma_2A_2V_2$$

and solving for V_1 yields

$$V_1=\left(\frac{\gamma_2A_2}{\gamma_1A_1}\right)V_2$$

Substituting for V_1 in equation (7.5)

$$\frac{1}{2g_c}\left[V_2^2-\frac{\gamma_2^2}{\gamma_1^2}\left(\frac{A_2^2}{A_1^2}\right)V_2^2\right]=\frac{k}{k-1}(P_1v_1-P_2v_2)$$

Solving for the throat velocity gives

$$V_2^2 = \frac{\left(\frac{k}{k-1}\right) 2g_c(P_1v_1 - P_2v_2)}{1 - \left(\frac{\gamma_2}{\gamma_1}\right)^2 \beta^4} \tag{7.6}$$

where

$$\beta^2 = \frac{A_2}{A_1}$$

For an isentropic process

$$\frac{P_1}{\gamma_1^k} = \frac{P_2}{\gamma_2^k}$$

or

$$\frac{\gamma_2}{\gamma_1} = \left(\frac{P_2}{P_1}\right)^{1/k}$$

which, when substituted into equation (7.6), gives

$$V_2^2 = \frac{\left(\frac{k}{k-1}\right) 2g_c(P_1v_1 - P_2v_2)}{1 - (r)^{2/k}\beta^4} \tag{7.7}$$

where

$$r = \frac{P_2}{P_1}$$

From the relation for an isentropic process

$$P_1v_1^k = P_2v_2^k$$

it can be shown that

$$p_1v_1r^{(k-1)/k} = P_2v_2 \tag{7.8}$$

which, when substituted into equation (7.7), yields

$$V_2 = \left[\frac{\left(\frac{k}{k-1}\right) 2g_c(P_1v_1)\,(1 - r^{(k-1)/k})}{1 - r^{2/k}\beta^4}\right]^{1/2} \tag{7.9}$$

Writing the equation for mass flow rate in terms of conditions at section 2 of figure 7.1,

$$w = \gamma_2 A_2 \left[\frac{\left(\frac{k}{k-1}\right) 2g_c(P_1v_1)\,(1 - r^{(k-1)/k})}{1 - r^{2/k}\beta^4}\right]^{1/2} \tag{7.10}$$

and again employing the isentropic flow relation

$$\frac{P_2}{\gamma_2^k}=\frac{P_1}{\gamma_1^k}$$

Equation (7.10) becomes

$$w=\gamma_1 r^{1/k} A_2 (P_1 v_1)^{1/2} (2g_c)^{1/2} \left[\frac{\frac{k}{k-1}(1-r^{(k-1)/k})}{1-(r)^{2/k}\beta^4}\right]^{1/2}$$

or the perfect gas

$$\gamma_1=\frac{P_1}{RT_1}$$

and the above relation becomes

$$\frac{w}{A_2 P_1}\sqrt{\frac{RT_1}{g_c}}=\left[\frac{\left(\frac{2k}{k-1}\right) r^{1/k}(r^{1/k}-r)}{1-(r)^{2/k}\beta^4}\right]^{1/2} \tag{7.11}$$

Equation (7.11) is the theoretical equation for the mass rate of flow of a perfect gas undergoing a reversible adiabatic process. This equation is in terms of the upstream pressure and temperature, the pressure ratio, area ratio, and the specific heat ratio.

It is possible to re-derive the theoretical weight rate equation to obtain it in another very useful form. To accomplish this, equation (7.11) is rewritten in the form

$$w=A_2\left(\frac{P_1}{\sqrt{RT_1}}\right)\left[\frac{2g_c\left(\frac{k}{k-1}\right) r^{2/k}(1-r^{(k-1)/k})}{1-(r)^{2/k}\beta^4}\right]^{1/2}$$

From the perfect gas law

$$P_1=\gamma_1 RT_1$$

therefore

$$w=A_2\left(\frac{P_1}{\sqrt{P_1/\gamma_1}}\right)\left[\frac{2g_c\left(\frac{k}{k-1}\right) r^{2/k}(1-r^{(k-1)/k})}{1-(r)^{2/k}\beta^4}\right]^{1/2}$$

or

$$w=A_2\left[\frac{\gamma_1 P_1 2g_c\left(\frac{k}{k-1}\right) r^{2/k}(1-r^{(k-1)/k})}{1-(r)^{2/k}\beta^4}\right]^{1/2} \tag{7.12}$$

and noting that

$$P_1-P_2=P_1(1-r) \qquad P_1=\frac{P_1-P_2}{1-r}$$

Equation (7.12) becomes

$$w = A_2\left[\frac{2g_c\gamma_1(P_1-P_2)}{1-\beta^4}\right]^{1/2}\left[(r)^{2/k}\left(\frac{k}{k-1}\right)\left(\frac{1-r^{(k-1)/k}}{1-r}\right)\left(\frac{1-\beta^4}{1-(r)^{2/k}\beta^4}\right)\right]^{1/2} \tag{7.13}$$

Note that equation (7.13) is simply the hydraulic equation modified by the factor Y_a, where

$$Y_a = \left[r^{2/k}\left(\frac{k}{k-1}\right)\left(\frac{1-r^{(k-1)/k}}{1-r}\right)\left(\frac{1-\beta^4}{1-(r)^{2/k}\beta^4}\right)\right]^{1/2} \tag{7.14}$$

The value of Y_a depends on the pressure ratio r; the diameter ratio β; and the specific heat ratio k. If the specific heat ratio is constant, it is possible to plot a family of curves to represent Y_a over the pressure ratio range from $r=1$ to $r=$ pressure ratio at which sonic velocity occurs at the throat. Such a curve is shown in figure 7.2 for k values between 1.0 and 1.8. A large-scale working chart of Y_a also appears in chapter 18. It is important to note at this point that the value Y_a, just discussed, applies only to the measurement of a perfect gas using either the venturi tube or the flow nozzle. It does not apply to the thin-plate orifice. The value Y_a used in the equation to calculate flow through a thin-plate orifice is empirically determined and cannot be found by theoretical considerations.

THE VENTURI TUBE

The venturi tube consists of a short converging section followed by a short constant-area section called the throat and then a diverging section. The purpose of the venturi tube is to accelerate temporarily the fluid in order that measurement of the change in static pressure, caused by the velocity change, can be obtained. Pressure taps are located in the pipeline just upstream of the converging section and at the venturi throat. The static pressure is measured at the two pressure taps, and the change in pressure is used in the appropriate equation to calculate the rate of fluid flow.

One of the notable characteristics of the venturi tube is its small pressure loss. This is a result of the gradual area change and the diverging section which acts to decelerate the fluid with a small amount of turbulence. The report of the ASME Research Committee on Fluid Meters points out that the overall pressure loss through the venturi tube will be approximately 10 to 20 percent of the difference between the upstream static pressure and the throat static pressure. In other words, between 80 and 90 percent of the venturi pressure differential is restored in the diverging cone. This committee also points out that the percent of pressure loss decreases as the speed of flow increases or as the size of the venturi tube is increased. Figure 7.3 shows a typical section of a venturi tube and a pressure history through the entire section.

For incompressible fluids, equation (7.3) gives the theoretical rate of flow through a venturi tube. For compressible fluids, equations (7.11) through (7.14) are applicable. To obtain the actual rate of flow, it is necessary to introduce the discharge coefficient C_d where

$$C_d = \frac{\text{actual weight rate of flow}}{\text{theoretical weight rate of flow}}$$

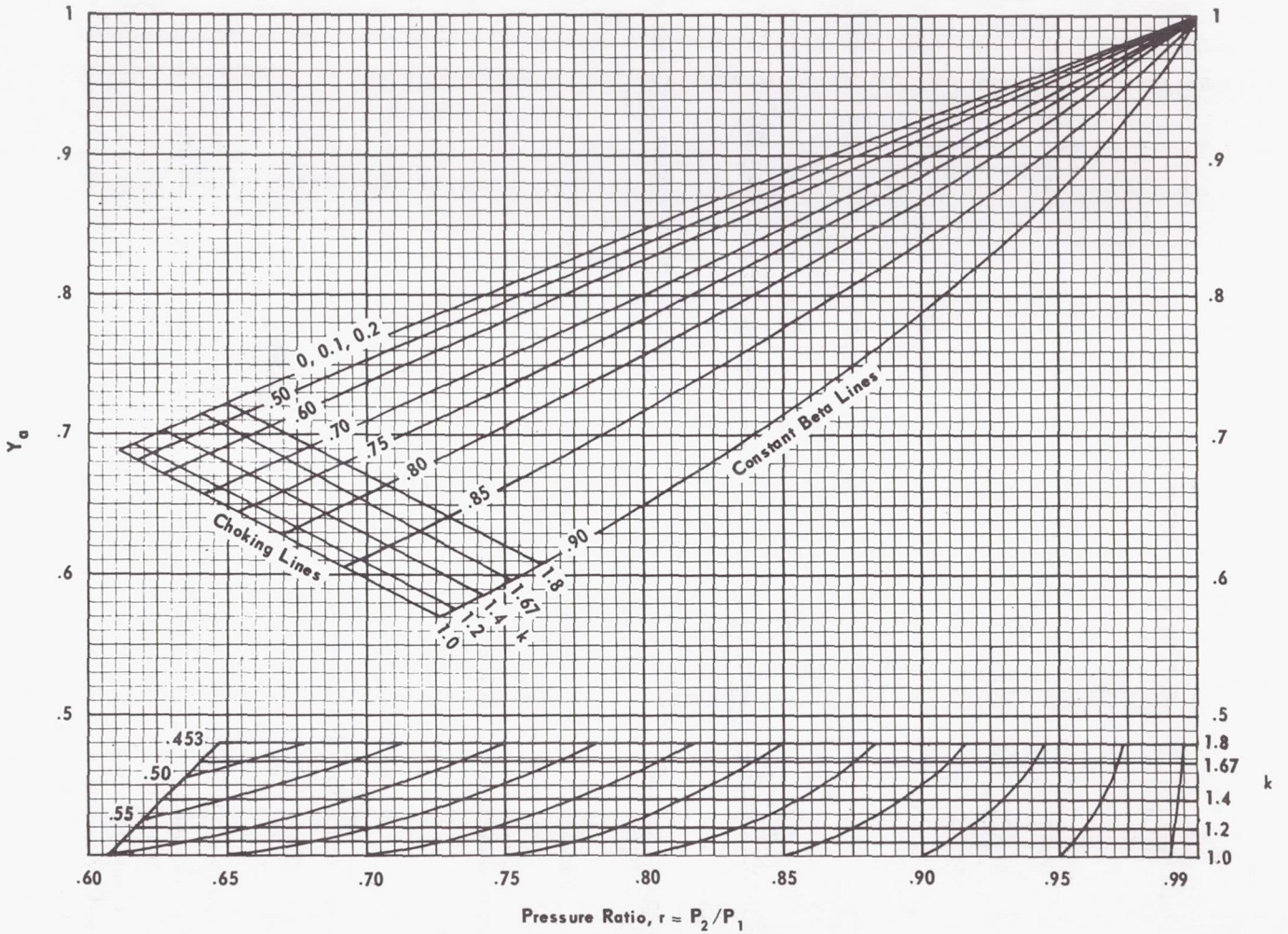


Figure 7.2. Expansion factor for venturi tubes and nozzles.

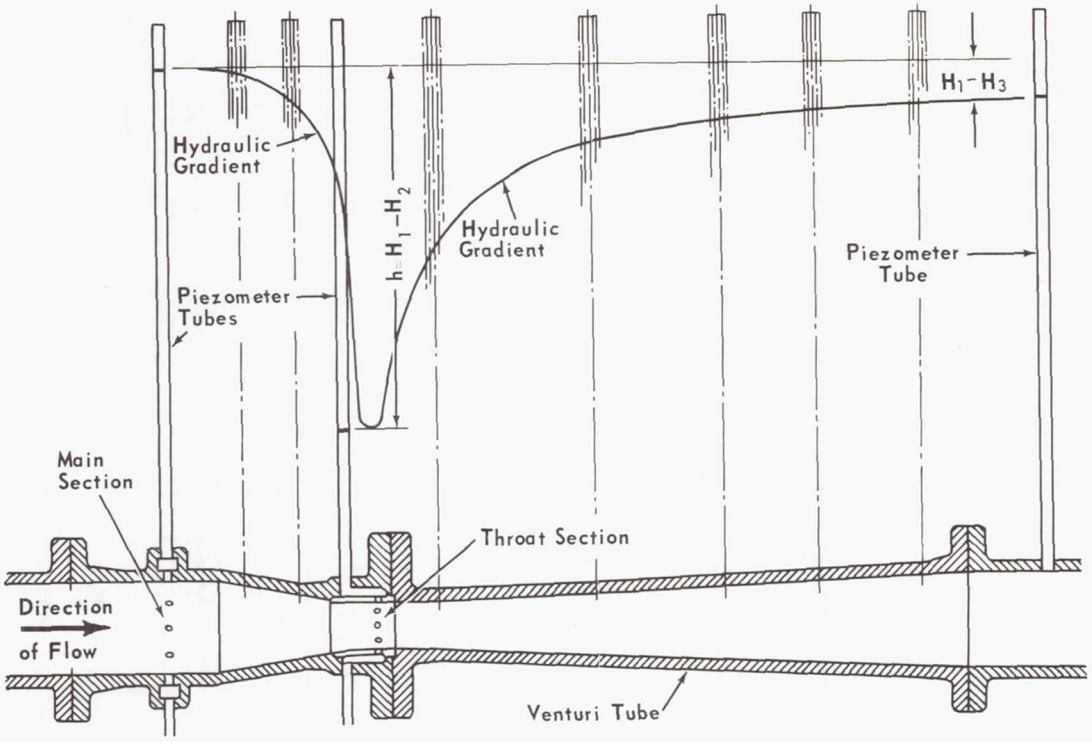


Figure 7.3. Venturi tube. [*Courtesy of the American Society of Mechanical Engineers.*]

The actual weight rate of flow then is given by

$$w = C_d A_2 \left[\frac{2g_c\gamma(P_1-P_2)}{1-\beta^4}\right]^{1/2} \tag{7.15}$$

for an incompressible fluid, and

$$w = C_d Y_a A_2 \left[\frac{2g_c\gamma_1(P_1-P_2)}{1-\beta^4}\right]^{1/2} \tag{7.16}$$

for a compressible fluid.

The discharge coefficient C_d should be determined by direct calibration whenever possible. When it is not possible to determine C_d by direct calibration, the use of curves of C_d versus pipe Reynolds number is suggested. These curves are constructed from data gathered by testing a large group of venturi tubes of a specific design. It should be noted here that any such curve will be for a particular variation of the basic venturi tube, and the value of C_d found with these curves should not be used with any type venturi tube except the type for which the chart was constructed. ASME constructed such a curve, for the Herschel venturi, which is reprinted as figure 7.4 and is also reprinted to a larger scale in chapter 21. Although the curve, figure 7.4, is limited to pipe sizes 2 inches (I.D.) and larger, it is feasible to use the values obtained from this curve for pipe sizes smaller than 2 inches,

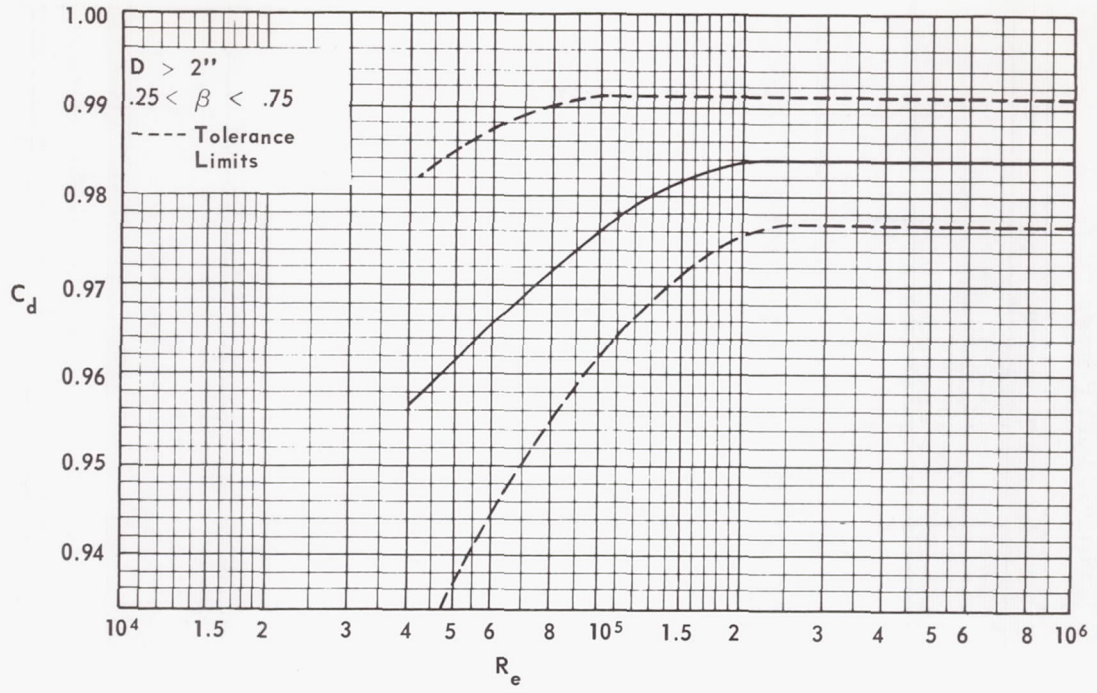


Figure 7.4. Discharge coefficient for venturi tubes. [*Courtesy of the American Society of Mechanical Engineers.*]

especially since no definite trend in the discharge coefficient with pipe size has been identified by the tests.

THE FLOW NOZZLE

A flow nozzle may be described as a short cylinder, one end of which is flared to form a flange that can be clamped between pipe flanges. This flared end forms a curved entrance leading smoothly into a cylindrical section called the throat. The flow nozzle performs the same function as the converging section and the throat of the venturi tube; that is, it accelerates the fluid so that the static-pressure difference can be measured and used to compute flow rate in an appropriate equation.

Because of the absence of the diverging section, the pressure loss through the nozzle is greater than through the venturi tube. The overall pressure loss for flow nozzles ranges from about 30 to 95 percent of the inlet-to-throat pressure drop as the throat-to-pipe-diameter ratio decreases from 0.8 to 0.2, as shown by figure 7.5.

The actual weight rate of flow through a flow nozzle can be calculated with equation (7.15) for an incompressible fluid and with equation (7.16) for a compressible fluid. The coefficient C_d to be used with the flow equations for a flow nozzle is different from that used with the venturi tube, although, as in the case of the venturi tube, the value of C_d will vary with the design of the flow nozzle.

Figure 7.6 is a graphic representation of the ASME long-radius flow nozzle which is the flow nozzle for which the values of C_d listed in chapter 18 are applicable.

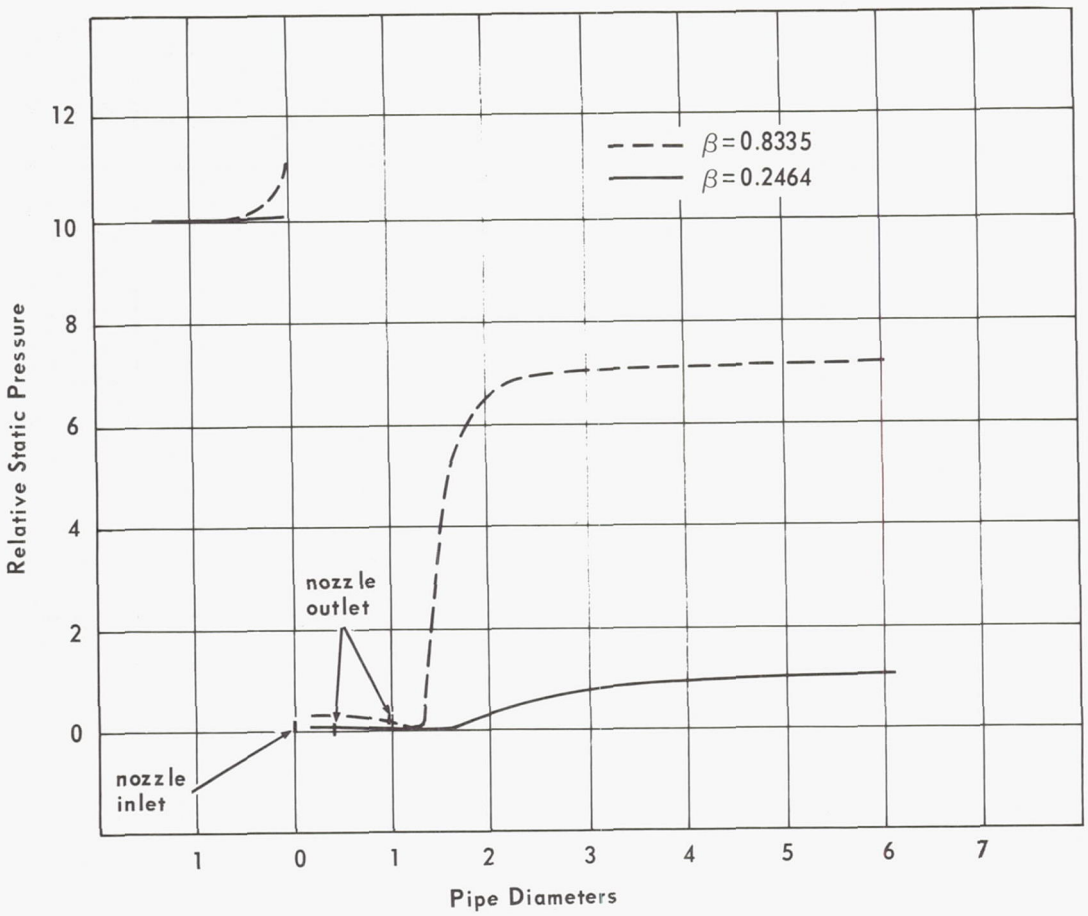
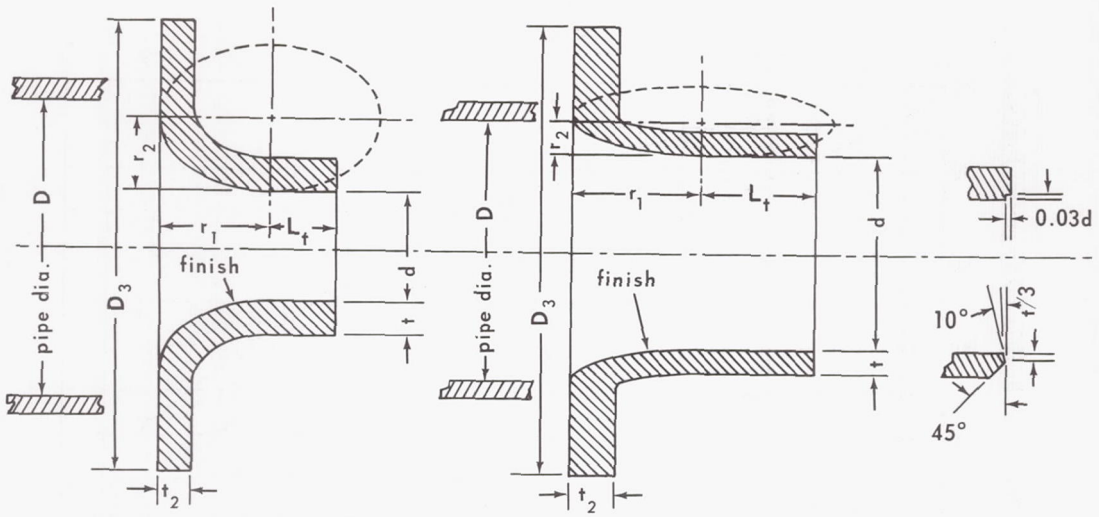


Figure 7.5. Qualitative representation of pressure gradients through flow nozzle. [*Courtesy of the American Society of Mechanical Engineers.*]

THE ORIFICE

The orifice in its simplest form is a thin, flat plate into which a small circular hole has been bored. As in the case of the venturi tube and the flow nozzle, there are many forms of the orifice. Attention in this handbook, however, is focused entirely on the concentric, thin-plate, square-edged orifice as shown in figure 7.7.

If manometers are connected to a series of static-pressure holes made in the pipe on both sides of the orifice, these manometers will show the variation in static pressure along the pipe in the region of the orifice. The lower part of figure 7.7 illustrates the average static-pressure gradient in the vicinity of an orifice. Close to the inlet side of the orifice, the static pressure in the pipe increases slightly and reaches its maximum value at the entrance to the orifice. The pressure of the fluid drops abruptly as it flows through the orifice, and on the outlet side, the pressure continues to decrease slightly. The minimum value is reached at a short distance from the outlet side of the orifice. Beyond this minimum point, the pressure increases again to a second maximum several pipe diameters beyond the orifice plate. Since no guiding of the stream occurs on either the inlet or the outlet side of an



Low β Series $\beta < 0.5$

$r_1 = d$

$r_2 = 2/3\ d$

$L_t = 0.6\ d$

$1/8'' \leq t \leq 1/2''$

$1/8'' \leq t_2 \leq 0.15\ D$

High β Series $\beta > 0.25$

$r_1 = 1/2\ D$

$r_2 = 1/2\ (D-d)$

$L_t \leq 0.6\ d$ or $L_t \leq 1/3\ D$

$2t \leq D-(d + 1/8'')$

$1/8'' \leq t_2 \leq 0.15D$

Optional Designs of Nozzle Outlet

Figure 7.6. ASME long-radius flow nozzle. [*Courtesy of the American Society of Mechanical Engineers.*]

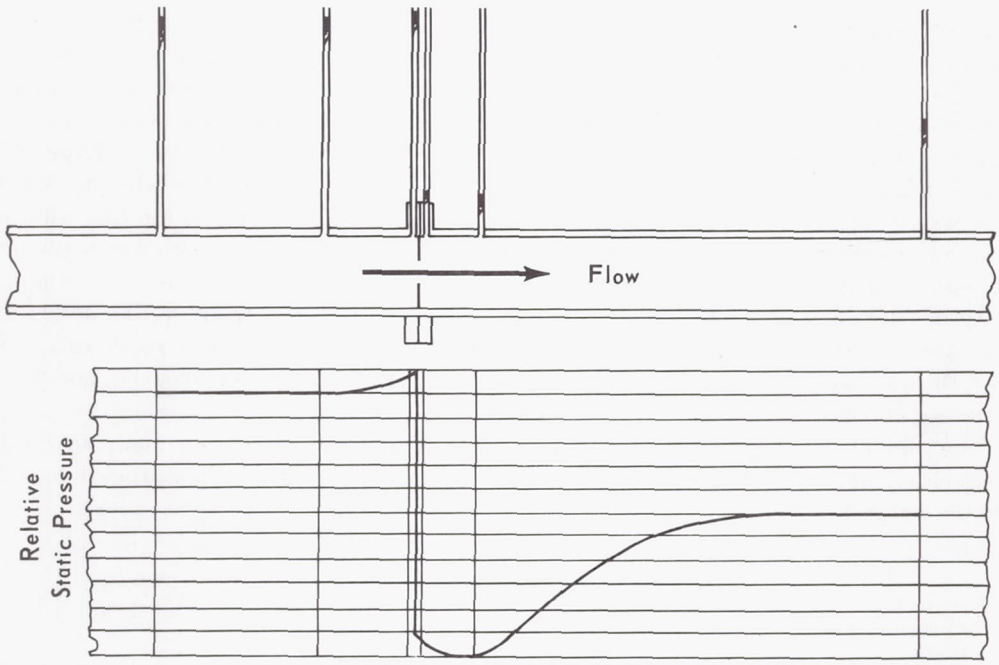


Figure 7.7. ASME standard orifice installation. [*Courtesy of the American Society of Mechanical Engineers.*]

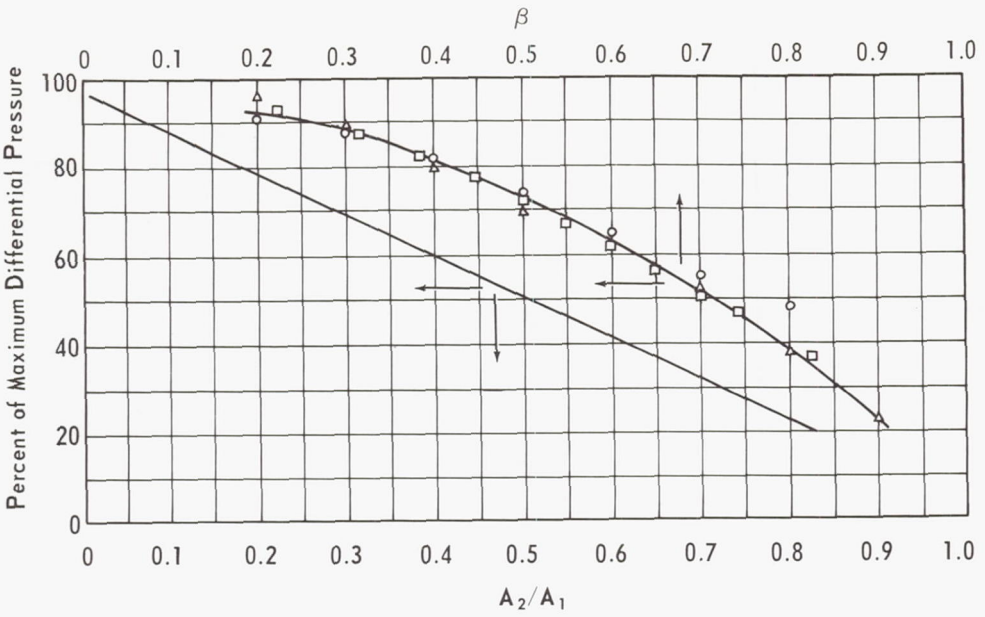


Figure 7.8. Overall pressure loss across a thin-plate orifice. [*Courtesy of the American Society of Mechanical Engineers.*]

orifice, the acceleration and deceleration of the fluid stream, which the pressure gradient manifests, is accompanied by considerable turbulence and dissipation of pressure energy, especially on the outlet side. Consequently, for the same diameter ratio, the downstream maximum pressure is much lower for an orifice than for a venturi tube, and only slightly lower than for a flow nozzle. In other words, for the same diameter ratio and measuring differential pressure, the overall pressure loss through a square-edged orifice and a flow nozzle are nearly the same, while that through a venturi tube is much less. Experiments seem to indicate that, with liquids having low viscosity, such as water, and with gases having the pressure ratio, P_2/P_1, not far from unity, the overall pressure loss ratio (the difference between the minimum pressure above the orifice and the maximum pressure below the orifice expressed as a fraction of the drop from the upstream minimum to the downstream minimum) is very nearly equal to $1-\beta^2$. This relation holds approximately true for β values of up to about 0.85 and is illustrated in figure 7.8, which is based on several groups of tests. With gases, the overall pressure loss ratio increases as the rate of flow is increased, and the rate of increase in the pressure loss ratio is augmented by increases in β.

The weight rate of flow through an orifice can be calculated from modified forms of equations (7.15) and (7.16) and are reprinted here for convenience. Note the change from Y_a to the empirical factor Y_1 for orifices.

$$w = C_d A_2 \left[\frac{2g_c\gamma(P_1-P_2)}{1-\beta^4}\right]^{1/2} \tag{7.15}$$

$$w = C_d Y_1 A_2 \left[\frac{2g_c\gamma_1(P_1-P_2)}{1-\beta^4}\right]^{1/2} \tag{7.16}$$

It is possible to rearrange terms in equations (7.15) and (7.16) and thereby obtain

$$w = K_c A_2 [2 g_c \gamma (P_1 - P_2)]^{1/2} \tag{7.17}$$

and

$$w = K_c A_2 Y_1 [2 g_c \gamma_1 (P_1 - P_2)]^{1/2} \tag{7.18}$$

where K_c is a flow coefficient defined as the product of the discharge coefficient and the velocity of approach factor, $1/\sqrt{1-\beta^4}$

$$K_c = \frac{C_d}{\sqrt{1-\beta^4}}$$

Equation (7.17) then is to be used to calculate the mass rate of flow of an incompressible fluid through a sharp-edged orifice, and equation (7.18) is to be used with compressible fluids.

The determination of the coefficients K_c and Y_1 to be used in equations (7.17) and (7.18) involves a very lengthy discussion, the details of which are beyond the purpose of this handbook. In general, K_c and Y_1 are functions of the Reynolds number, the shape of the orifice, and the compressibility of the fluid. The shape of the orifice is given by 11 parameters; this number, however, has been reduced by standardization of many of the orifice shape variables. As a result of the above-mentioned standardization, it is possible to write for an incompressible fluid

$$K_c = f(R_e, \beta, D)$$

and for the compressible fluid

$$K_c = f(R_e, \Gamma, \beta, D)$$

where Γ (gamma) is the compressibility of the fluid.

The equations which relate the factors listed above are empirical in nature and are based on the experimental values reported by the joint American Gas Association-ASME Committee on Orifice Coefficients.

The value of Y_1 to be used in equation (7.18) for noncritical flow has also been determined by the ASME Research Committee on Fluid Meters, and for a complete discussion the reader is referred to page 79, *Fluid Meters, Their Theory and Application*, ASME, 1959.

The expansion factor Y_1 for corner taps, $1\text{–}D$ and $\frac{1}{2}\text{–}D$ taps, and vena contracta taps is given by

$$Y_1 = 1 - (0.41 + 0.35\beta^4)^{x/k}$$

and for pipe taps

$$Y_1 = 1 - [0.333 + 1.145(\beta^2 + 0.7\beta^5 + 12\beta^{13})]^{x/k}$$

where

$$x = \frac{P_1 - P_2}{P_1} \qquad k = \frac{c_p}{c_v}$$
$$= 1 - r$$

Plotted values of K_c and Y_1 can be found in chapter 18.

CRITICAL FLOW THROUGH ORIFICES

The existence of a maximum possible flow rate of a compressible fluid through a nozzle was discussed in chapter 5. It was pointed out that for a gas having $k=1.4$, the maximum flow occurs at a ratio of static to total pressure equal to approximately 0.53. It was further shown that in nozzle flow this pressure ratio occurs at the minimum throat cross section, and that sonic flow conditions exist at the nozzle throat for this maximum flow condition.

It is an experimental fact that flow through a thin-plate orifice does not obey the ideal flow law, as does flow through a nozzle. The most significant deviation being that flow rates through an orifice continue to increase for pressure ratios below the critical. Flows at ratios less than the critical are termed "critical," or in some texts, "supercritical" flows. In this region the characteristic equations for determining such factors as the flow coefficient K_c and expansion factor Y_1 vary considerably from the equations predicting these same quantities in the subcritical region. This phenomenon of increasing flow rates is attributed to the efflux from the orifice, unlike a nozzle, being unconfined. Thus, the minimum area of the flow stream, the vena contracta, just downstream of the orifice is free to move axially, or to experience area change. It can be shown that as the pressure ratio decreases in the critical flow region, the vena contracta size approaches the orifice size. This change in vena contracta area is reflected by changes in the discharge coefficient C_d, and consequently the fluid flow rate.

The flow of a perfect gas through an orifice in a pipeline has been shown to be a function of the flow area, the Reynolds number, diameter ratio, pipe diameter, specific heat ratio, upstream and downstream pressures, and the absolute gas temperature. Hence,

$$w=f(A, R_e, \beta, D, k, P_1, P_2, T)$$

Restricting the discussion to high Reynolds numbers (when flow does not vary with the Reynolds number variations) and further requiring small β ratios, the mass flow rate of a given perfect gas can be shown to vary as a function of A, k, P_1, P_2, and T. The relation between the fluid flow rate and the quantities mentioned above may be expressed

$$\frac{w\sqrt{T_1}}{A_2P_1}=f(r) \tag{7.19}$$

where r is the ratio P_2/P_1.

By test, it is possible to plot a curve of $(w\sqrt{T_1})/(A_2P_1)$ versus r for a particular gas. Such a curve is shown for low-pressure air in figure 7.9. This graph shows a plot of the theoretical flow of a gas through an ideal nozzle and a plot of test data for flow through a sharp-edged orifice.

To determine a relation between the flow coefficient K_c, the coefficient of expansion Y_1, and the pressure ratio, the basic flow equation given by ASME is used where

$$w=0.668\,A_2K_cY_1\sqrt{\gamma(P_1-P_2)}$$

Since a perfect gas is being considered, combining $P=\gamma RT$ and the previous relation yields

$$\frac{w\sqrt{T_1}}{A_2P_1}=0.668\,K_cY_1\left(\sqrt{\frac{1-r}{R}}\right)$$

or

$$K_c Y_1 = \frac{w\sqrt{T_1}}{A_2 P_1}\left(\frac{1}{0.668}\right)\sqrt{\frac{R}{1-r}} \tag{7.20}$$

From equation (7.20) and figure 7.9, it is possible to plot the product $K_c Y_1$ as a function of r. Such a plot is shown in figure 7.10 for air. Notice that for this gas the product $K_c Y_1$ is a linear function of r in both the subcritical (B) and supercritical (A) regions, but the functions have different slopes.

Now, by use of numerical methods, it is possible to determine an analytical solution for $K_c Y_1$ as a function of the pressure ratio r. As an example, J. A. Perry, 1949, determined the weight flow equation for air as

$$w = 0.668A(0.410 + 0.220r)\sqrt{\gamma \Delta P} \tag{7.21}$$

It should be pointed out that equation (7.21) applies only to air at low pressure and moderate temperatures with a negligible velocity of approach factor (β near zero).

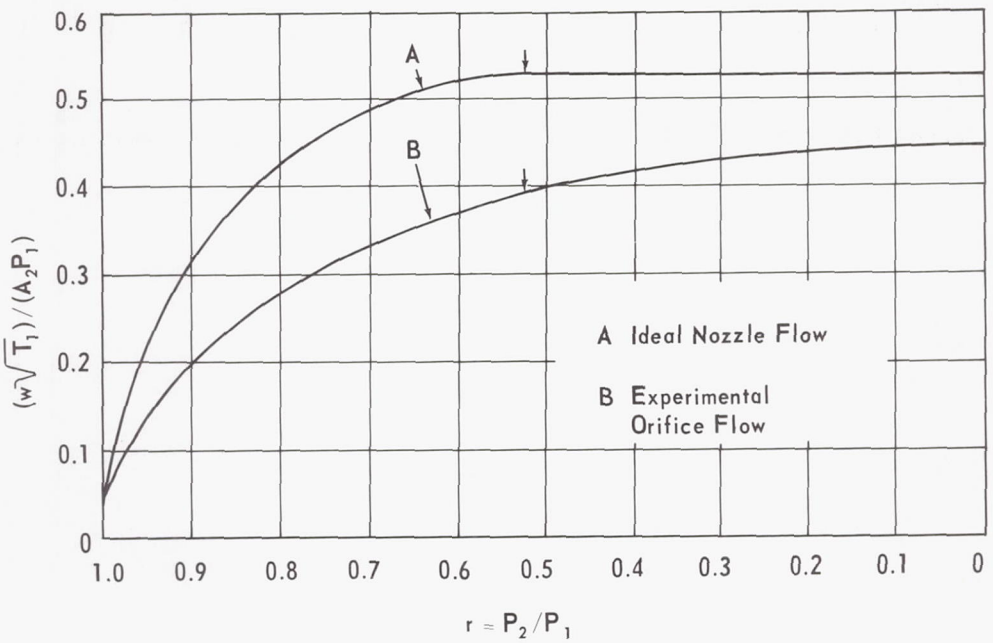


Figure 7.9. Flow comparison chart. [*Courtesy of the American Society of Mechanical Engineers.*]

325-994 O-69—11

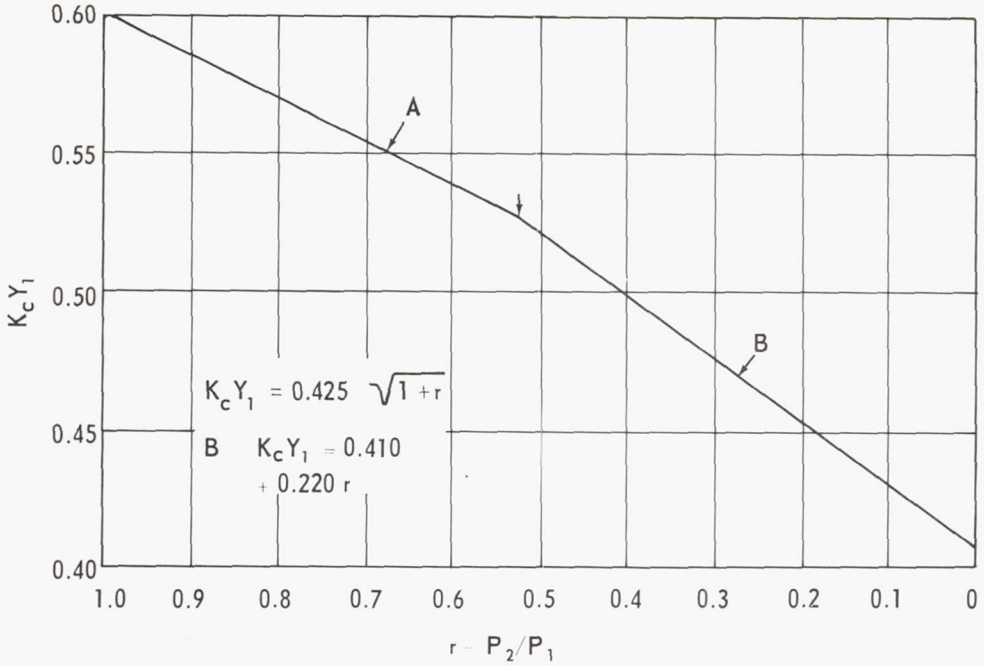


Figure 7.10. Variation in K_cY_1 product. [*Courtesy of the American Society of Mechanical Engineers.*]

CHAPTER 8

ADIABATIC FRICTIONAL FLOW IN PIPES

GENERAL PIPE-FLOW CONSIDERATIONS

In general, the property changes that occur in a compressible fluid flowing steadily through a constant-area pipeline are dependent on a variety of factors. The most important factors are:

(1) Characteristics of the gaseous fluid
(2) Mach number of the flow (a generalized mass flow parameter)
(3) Fluid friction acting on the pipe wall
(4) Existence of shock waves
(5) Elevational change
(6) Presence of pipe fittings, valves, and other components
(7) Heat transfer through the pipe wall

This chapter includes only the evaluation of the effects of items (1), (2), (3), and (4). The effects of changes in elevation are generally negligible in compressible flow as a result of the low gas densities and will, therefore, be neglected here. When very high densities and great elevational changes occur, the effect on static pressure can be approximated by using an average density to compute the static-pressure change. This is then added algebraically to the other losses.

The presence of pipe fittings, valves, and other components is not specifically considered in this chapter, since a complete discussion of the flow characteristics of components is found in chapter 10. However, it is general practice to assign equivalent nondimensional lengths (L/D) of straight pipe to fittings and simple components. The equivalent-length values are based on empirical data and are to be treated as extra pipe. This technique is considered acceptable in compressible flow problems only if the pressure loss across the component is a small percentage of the absolute pressure and if the gas velocities are relatively low (corresponding to a mach number of approximately 0.3 or less).

When heat is transferred between the fluid and the pipe wall, straightforward solutions can be obtained for special cases. These nonadiabatic flows are the subject of chapter 9.

The characteristics of the fluid are usually represented by the perfect-gas law, the knowledge of the specific heat ratio, and the molecular weight. This simple description of a real gas is found to be satisfactory for conditions of high temperature and low pressure (relative to the critical values for the particular gas). In this chapter, the analysis of the pipe flow phenomenon will be based on the perfect-gas relationships. It should be noted,

however, that in the region of low temperature and/or high pressure, the deviation from the perfect-gas characteristics can be very significant. These deviations are discussed in detail in chapters 2 and 4, and methods of accounting for them in pipe flow calculations are included in chapter 19.

The mach number is the general mass flow rate parameter in pipe flow analysis. The mach number also serves to factor into the analysis the molecular weight of the gas and the base levels of temperature and pressure.

When the effects of fluid friction on the pipe wall are considered in the analysis, the frictional pipe-length parameter $f(L/D)$ defines the frictional characteristics of the pipe. The friction factor f depends on the turbulent nature of the flow, and also serves to factor into the analysis the effects of fluid viscosity and pipe inside-wall roughness. The friction factor is basically a function of the Reynolds number. The common case of frictional flow in an adiabatic pipe is the primary subject of this chapter.

The compressible flow functions developed in this chapter do not automatically account for choked flow conditions or shock waves. However, the solutions identify the choked conditions, and a discussion of choking and shock waves resulting from friction in constant-area pipes is presented in "Choking Because of Friction."

FEATURES OF ADIABATIC FRICTIONAL FLOW

The flow of compressible fluids through pipes may be treated as adiabatic (the change in stagnation enthalpy is negligible) only when the pipe length is short and/or when insulation has been employed to inhibit heat transfer. The analytical developments of this paragraph are based on the following assumptions, consistent with the introductory discussion in this chapter.

(1) The flow is steady and subject to viscous friction in a constant-area pipe, tube, or duct.

(2) The characteristics of the fluid can be described by the perfect-gas laws.

(3) The effects of elevational change, if present, are negligible compared with frictional effects.

(4) The pipe is straight and without fittings and components.

(5) There is no appreciable heat exchange between the fluid and the pipe relative to the total heat capacity of the flowing stream.

(6) There is no external work done by the fluid.

The changes in fluid properties in adiabatic frictional flow at constant area are defined fundamentally by the Fanno equation. Combination of the first law total energy equation, with no external work or heat transfer, and the continuity equation for flow at constant area yields the Fanno equation in terms of enthalpy and density.

$$h = h_0 - \frac{V^2}{2g_c J} \qquad \text{First law}$$

$$G = \frac{W}{A} = \gamma V = \frac{V}{v} \qquad \text{continuity equation}$$

$$h = h_0 - \frac{G^2 v^2}{2g_c J} \qquad \text{Fanno equation}$$

Figures 8.1 and 8.2 illustrate the general shape of Fanno lines on h–v and h–s diagrams and are helpful in illustrating the effect of wall friction on fluid properties. Figure 8.2 is possible, since, for a pure substance, entropy can be defined by the two properties, h and v. When real-gas effects are significant, these plots can be made on the thermodynamic chart for the particular gas.

It was shown in the paragraph on normal shocks in chapter 6 that point A, the point of maximum entropy, represents the point where the mach number is unity. Also, it was shown that the lower portion of the curve (X to A) represents flow at supersonic velocity, and the upper portion (Y to A) represents subsonic velocities. Furthermore, it can be shown that frictional effects are, in general, necessary to pass from point to point along the Fanno line to satisfy the momentum equation.

The foregoing facts used in conjunction with the second law of thermodynamics lead to the following conclusions concerning adiabatic frictional flow through constant-area pipes.

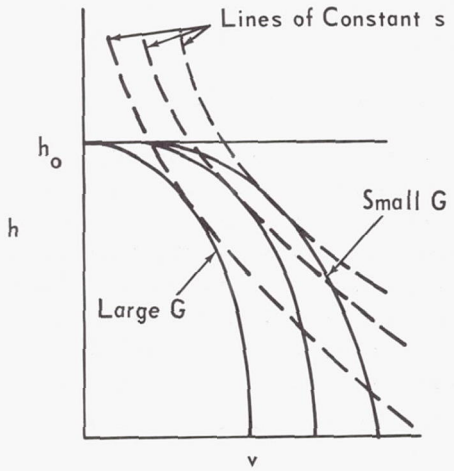


Figure 8.1. Fanno lines on h–v diagram.

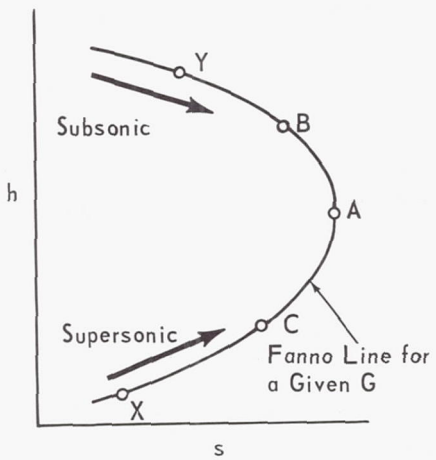


Figure 8.2. Fanno lines on h–s diagram.

Flow initially supersonic. — If point *C* (fig. 8.2) represents the state of the fluid as it enters the pipe, there are two directions in which the fluid properties may progress; that is, from *C* to *X* or from *C* to *A*. The second law states that for an adiabatic process, the change in entropy must be positive; hence, the process from *C* to *X* is impossible and the process from *C* to *A* occurs. For this shock-free process, the mach number diminishes from its initial supersonic value to unity at point *A*. There can be no further decrease in velocity without violating the second law. Hence, if the flow is initially supersonic, the effect of friction is to cause a velocity decrease and a corresponding pressure increase.

Flow initially subsonic. — As in the preceding paragraph, the entropy must increase for the adiabatic process. Therefore, for flow initially subsonic, the process must be from point *B* toward point *A* on the Fanno line, rather than toward point *Y*. In order to satisfy the second law, the maximum velocity attainable with initial subsonic flow is sonic velocity. Thus, the effect of friction for subsonic flows is to increase velocity with a corresponding decrease in pressure. The effects of friction on velocity, mach number, and pressure are, therefore, seen to be opposite for subsonic and supersonic flows.

THE FANNO-LINE EQUATIONS

In order to proceed with the discussion of adiabatic flow with constant area, it is necessary to derive equations for the fluid properties along the pipe and to determine the quantitative effect of friction on these properties for supersonic and subsonic flow. The equations are derived from the perfect-gas law relationships, the definition of mach number, and from the laws of conservation of energy, mass, and momentum. The result is five simultaneous differential equations that relate six differential variables. These include the fluid static properties, fluid velocity, mach number, and the frictional pipe length. These equations are then solved simultaneously and integrated to produce the desired direct relationships.

The changes in the flow conditions within the differential length of pipe, as shown on figure 8.3, are evaluated as follows:

The equation of state for a perfect gas in logarithmic form is

$$\ln P = \ln \gamma + \ln R + \ln T$$

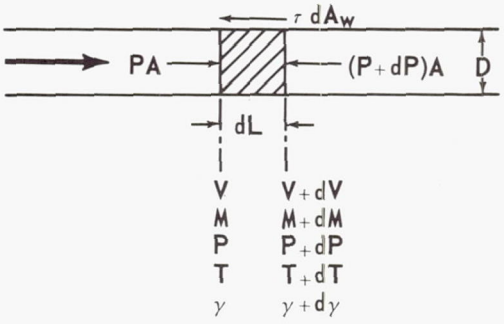


Figure 8.3. Pipe flow element.

which can be written in differential form as

$$\frac{dP}{P}=\frac{d\gamma}{\gamma}+\frac{dT}{T} \tag{8.1}$$

The definition of mach number,

$$M^2=\frac{V^2}{c^2}=\frac{V^2}{kg_cRT}$$

which in logarithmic differential form is

$$\frac{dM^2}{M^2}=\frac{dV^2}{V^2}-\frac{dT}{T} \tag{8.2}$$

From the total energy equation

$$h_0=h+\frac{V^2}{2g_cJ}=\text{constant}$$

which in differential form, for a perfect gas, is

$$c_p\ dT+d\left(\frac{V^2}{2g_cJ}\right)=0$$

and dividing by c_pT,

$$\frac{dT}{T}+\left(\frac{1}{2g_cJ}\right)\left(\frac{1}{c_pT}\right)\ d(V^2)=0$$

Substituting into this equation the value of T from the definition of mach number

$$T=\frac{V^2}{kg_cRM^2}$$

and the value of c_p obtained from the perfect-gas relationships, $c_p-c_v=R/J$ and $k=c_p/c_v$

$$c_p=\frac{kR}{(k-1)J}$$

yields

$$\frac{dT}{T}+\left(\frac{k-1}{2}\right)M^2\left(\frac{dV^2}{V^2}\right)=0 \tag{8.3}$$

From the continuity equation

$$G=\frac{w}{A}=\gamma V \qquad \text{and} \qquad d(\gamma V)=dG$$

Since G is constant,

$$V\ d\gamma+\gamma\ dV=0 \qquad \text{or} \qquad \frac{d\gamma}{\gamma}+\frac{dV}{V}=0$$

Combining this with the mathematical identity

$$\frac{dV^2}{2V^2}=\left(\frac{1}{2V^2}\right)2V\ dV=\frac{dV}{V}$$

yields

$$\frac{dV^2}{2V^2}+\frac{d\gamma}{\gamma}=0 \tag{8.4}$$

Now, consider the forces on the element of fluid in the pipe, where τ is the wall shear stress acting on the fluid and dA_w is the differential wetted surface area of the pipe element. Summing these forces yields the change in momentum of the flowing stream between the ends of the pipe element

$$PA-(P+dP)A-\tau\ dA_w=\dot{m}\ dV=\left(\frac{W}{g_c}\right)dV$$

and

$$-A\ dP-\tau\ dA_w=\dot{m}\ dV$$

The coefficient of friction, defined as

$$f_\tau=\frac{\tau}{\rho\left(\frac{V^2}{2}\right)}$$

and the hydraulic diameter, defined as

$$D=\frac{4\text{ (flow area)}}{\text{wetted perimeter}}=\frac{4A}{\left(\frac{dA_w}{dL}\right)}$$

are substituted into the momentum equation to convert the friction term into more useful terms, resulting in

$$-A\ dP-\left(\frac{f_\tau\rho V^2}{2}\right)\left[\left(\frac{4A}{D}\right)dL\right]=\dot{m}\ dV$$

Substituting $\dot{m}=\rho AV$ from continuity and dividing through by PA yields

$$-\frac{dP}{P}-\left(\frac{4f_\tau\rho V^2}{2DP}\right)dL=\left(\frac{\rho V^2}{P}\right)\frac{dV}{V}$$

The perfect-gas law can be written as

$$\frac{\rho}{P}=\frac{k}{kg_cRT}=\frac{k}{c^2}$$

so that

$$\frac{\rho V^2}{P}=\frac{kV^2}{c^2}=kM^2$$

Introducing this relation into the momentum equation yields

$$\frac{dP}{P}+\frac{kM^2}{2}\left(\frac{4f_\tau}{D}\right)dL+kM^2\left(\frac{dV}{V}\right)=0$$

Substituting once again the mathematical identity

$$\frac{dV}{V}=\frac{1}{2}\left(\frac{dV^2}{V^2}\right)$$

yields

$$\frac{dP}{P}+\frac{kM^2}{2}\left(\frac{4f_\tau}{D}\right)dL+\frac{kM^2}{2}\left(\frac{dV^2}{V^2}\right)=0 \tag{8.5}$$

Equations (8.1) through (8.5) comprise the five necessary simultaneous differential equations in the six differential variables: dP/P, $d\gamma/\gamma$, dT/T, dM^2/M^2, dV^2/V^2, and $4f_\tau\,(dL/D)$. It is desirable to include in the analysis, at this point, the evaluation of changes in stagnation pressure, impulse function, and entropy, which increase the problem to one of eight equations and nine differential variables.

From equation (5.31) the isentropic stagnation pressure is defined as

$$P_0=P\left[1+\left(\frac{k-1}{2}\right)M^2\right]^{\frac{k}{k-1}}$$

Then

$$\ln P_0=\ln\left\{P\left[1+\left(\frac{k-1}{2}\right)M^2\right]^{\frac{k}{k-1}}\right\}$$

which, in differential form, is

$$\frac{dP_0}{P_0}=\frac{dP}{P}+\left[\frac{\frac{kM^2}{2}}{1+\left(\frac{k-1}{2}\right)M^2}\right]\frac{dM^2}{M^2} \tag{8.6}$$

The definition of impulse function, from equation (5.40), is

$$F_i=PA(1+kM^2)$$

which, when written in logarithmic differential form for constant-area pipes, is

$$\frac{dF_i}{F_i}=\frac{dP}{P}+\left(\frac{kM^2}{1+kM^2}\right)\frac{dM^2}{M^2} \tag{8.7}$$

The final equation is written to obtain the entropy change. Applying the first law to a unit mass of fluid moving through the pipe element

$$ds=\frac{du}{T}+\left(\frac{1}{J}\right)\left(\frac{P}{T}\right)dv$$

For a perfect gas,

$$du = c_v\, dT \qquad \text{and} \qquad \frac{P}{T} = \frac{R}{v}$$

so that

$$ds = c_v \left(\frac{dT}{T}\right) + \left(\frac{R}{J}\right) \frac{dv}{v}$$

Substituting the perfect-gas law written in logarithmic differential form as

$$\frac{dP}{P} + \frac{dv}{v} = \frac{dT}{T}$$

yields

$$ds = c_v \left(\frac{dT}{T}\right) + \frac{R}{J} \left(\frac{dT}{T} - \frac{dP}{P}\right)$$

And for a perfect gas, $c_p - c_v = R/J$, $k = c_p/c_v$, and $R/J = c_p[(k-1)/k]$. Substitution and clearing yield

$$\frac{ds}{c_p} = \frac{dT}{T} - \left(\frac{k-1}{k}\right) \frac{dP}{P} \tag{8.8}$$

By selecting $4f_\tau(dL/D)$ as the independent variable, the remaining variables can be defined explicitly in terms of M and $4f_\tau(dL/D)$. This is accomplished by the simultaneous solution of the eight numbered equations (8.1) through (8.8), resulting in the following:

$$\frac{dP}{P} = -kM^2 \left[\frac{1 + (k-1)M^2}{2(1-m^2)}\right] 4f_\tau \left(\frac{dL}{D}\right) \tag{8.9}$$

$$\frac{dM^2}{M^2} = kM^2 \left[\frac{1 + \left(\frac{k-1}{2}\right) M^2}{(1-M^2)}\right] 4f_\tau \left(\frac{dL}{D}\right) \tag{8.10}$$

$$\frac{dV}{V} = \left[\frac{kM^2}{2(1-M^2)}\right] 4f_\tau \left(\frac{dL}{D}\right) \tag{8.11}$$

$$\frac{dT}{T} = -\left[\frac{k(k-1)M^4}{2(1-M^2)}\right] 4f_\tau \left(\frac{dL}{D}\right) \tag{8.12}$$

$$\frac{d\gamma}{\gamma} = -\left[\frac{kM^2}{2(1-M^2)}\right] 4f_\tau \left(\frac{dL}{D}\right) \tag{8.13}$$

$$\frac{dP_0}{P_0} = -\left(\frac{kM^2}{2}\right) 4f_\tau \left(\frac{dL}{D}\right) \tag{8.14}$$

$$\frac{dF_i}{F_i} = -\left[\frac{kM^2}{2(1+kM^2)}\right] 4f_\tau \left(\frac{dL}{D}\right) \tag{8.15}$$

$$\frac{ds}{c_p} = \left(\frac{k-1}{2}\right) M^2 4f_\tau \left(\frac{dL}{D}\right) \tag{8.16}$$

Integration of equations (8.9) through (8.16) will produce the explicit relation between the fluid properties, frictional length, mach number, velocity, and impulse function. But first, it is advantageous to study the equations in the differential form to identify the direction of change of the various properties as the fluid progresses down the pipe for subsonic and supersonic flow. Table 8.1 summarizes these changes.

TABLE 8.1.—*Fluid Property Changes*

If $M > 1$ (supersonic)—			If $M < 1$ (subsonic)—		
$dM < 0$	M	decreases	$dM > 0$	M	increases
$dT > 0$	T	increases	$dT < 0$	T	decreases
$dV < 0$	V	decreases	$dV > 0$	V	increases
$d\gamma > 0$	γ	increases	$d\gamma < 0$	γ	decreases
$dP > 0$	P	increases	$dP < 0$	P	decreases
$dP_0 < 0$	P_0	decreases	$dP_0 < 0$	P_0	decreases
$dF_i < 0$	F_i	decreases	$dF_i < 0$	F_i	decreases
$ds > 0$	s	increases	$ds > 0$	s	increases

Equation (8.16), and the second law requirement that ds be positive, establishes that the coefficient of friction must always be positive. It should be noticed that the quantities defined by those equations which contain the factor $(1-M^2)$ experience opposite changes under supersonic conditions than when under subsonic conditions. This includes the mach number itself, which is seen always to tend toward unity. Therefore, for any given upstream condition with subsonic or supersonic flow, there is a maximum downstream pipe length, L_{max}, associated with that condition such that the mach number would be unity at the end of the pipe. The theoretical results for supersonic flows are usually subject to inaccuracy stemming from the viscous behavior of real fluids that cause the formation of boundary layers and shock waves within the pipe. A more complete discussion of these effects can be found in chapter 6.

WORKING RELATIONS

To arrive at working relations, the mach number is specified as the independent variable, and equations (8.9) through (8.16) are integrated. Equation (8.10) is integrated directly to obtain the explicit relation between M and $4f_\tau(L/D)$. Equation (8.10) is also solved for $4f_\tau(dL/D)$ and substituted into each of the other equations so that all parameters can be integrated with respect to the common mach number.

It is desirable first to convert the coefficient of friction f_τ, since coefficient of friction data is usually found in terms of f rather than f_τ (such as the Moody diagram). The conversion between these two coefficients can be obtained as follows, by definition of f for a differential length of pipe dL

$$f = \frac{\Delta P_L}{\frac{dL}{D}\left[\rho\left(\frac{V^2}{2}\right)\right]}$$

By definition

$$f_\tau = \frac{\tau}{\left[\rho\left(\frac{V^2}{2}\right)\right]}$$

so that

$$\frac{f}{f_\tau} = \left(\frac{D}{\tau}\right)\frac{dP_L}{dL}$$

Summing pressure and shear forces on the incompressible fluid element yields

$$A\ dP_L = \tau\ dA_w$$

Note that $dP_L = -dP$, relative to figure 8.3. From the definition of hydraulic diameter, $dA_w = 4A\ dL/D$, so that

$$\frac{dP_L}{dL} = \frac{4\tau}{D}$$

Substituting this into the expression for the ratio of friction factors above yields the following direct conversion between f and f_τ

$$f = 4f_\tau \tag{8.17}$$

Substituting equation (8.17) into equation (8.10) and rearranging yields the following integrable equation for $f(L/D)$ in terms of the more common friction factor f

$$\int_0^{L_{max}} f\left(\frac{dL}{D}\right) = \int_M^1 \left\{\frac{1-M^2}{kM^4\left[1+\left(\frac{k-1}{2}\right)M^2\right]}\right\} dM^2$$

The lower limits of integration are selected at a point along the pipe where the mach number is M and where $L=0$, the zero reference for pipe-length measurement. The upper limit is selected as the point where the mach number is unity and the distance corresponding to $M=1$ is the maximum pipe length, L_{max}, mentioned previously. Integrating equation (8.10) and clearing yields

$$\bar{f}\left(\frac{L_{max}}{D}\right) = \frac{1-M^2}{kM^2} + \left(\frac{k+1}{2k}\right)\ln\left\{\frac{(k+1)M^2}{2\left[1+\left(\frac{k-1}{2}\right)M^2\right]}\right\} \tag{8.18}$$

where $\bar{f}$ is the mean friction coefficient between 0 and L_{max}, defined by

$$\bar{f} = \frac{1}{L_{max}}\int_0^{L_{max}} f\ dL$$

The friction factor is usually found to vary only slightly over the length of the pipe. The average value will always be assumed, hereafter, and the bar over the symbol will be omitted for simplicity. The variation should be checked using the Moody diagram (ch. 3).

Eliminating the frictional length parameter from the remaining equations, using equation (8.10) and integrating results in the following explicit relationships

$$\frac{P}{P^*}=\frac{1}{M}\sqrt{\frac{k+1}{2\left[1+\left(\frac{k-1}{2}\right)M^2\right]}} \tag{8.19}$$

$$\frac{V}{V^*}=M\sqrt{\frac{k+1}{2\left[1+\left(\frac{k-1}{2}\right)M^2\right]}} \tag{8.20}$$

$$\frac{T}{T^*}=\frac{c^2}{c^{*2}}=\frac{k+1}{2\left[1+\left(\frac{k-1}{2}\right)M^2\right]} \tag{8.21}$$

$$\frac{\gamma}{\gamma^*}=\frac{V^*}{V}=\frac{1}{M}\sqrt{\frac{2\left[1+\left(\frac{k-1}{2}\right)M^2\right]}{k+1}} \tag{8.22}$$

$$\frac{P_0}{P_0^*}=\frac{1}{M}\sqrt{\left\{\frac{2\left[1+\left(\frac{k-1}{2}\right)M^2\right]}{k+1}\right\}^{\frac{k+1}{k-1}}} \tag{8.23}$$

$$\frac{F_i}{F_i^*}=\frac{1+kM^2}{M\sqrt{2(k+1)\left[1+\left(\frac{k-1}{2}\right)M^2\right]}} \tag{8.24}$$

$$\frac{s-s^*}{c_p}=\ln\left(M^2\sqrt{\left\{\frac{k+1}{2M^2\left[1+\left(\frac{k-1}{2}\right)M^2\right]}\right\}^{\frac{k+1}{k}}}\right) \tag{8.25}$$

Equations (8.18) through (8.25) are the Fanno-line equations. The superscript * denotes the properties where the flow is sonic, at the end of a pipe having a length, L_{max}. The usual problem is to determine the change in fluid properties in a shockless flow between two pipe locations, 1 and 2, separated by a frictional distance, $f(L/D)$, which is less than $f(L_{max}/D)$. Note that the choked flow properties are established without knowledge of $f(L_{max}/D)$. Then, for a given pipe system and a specified flow condition, there can be only one set of choked flow conditions, and these superscripted (*) quantities are the same, regardless of what upstream location is used to establish them. Conversely, the specification of flow conditions at any location fixes conditions throughout the pipe. The additional relationship of equation (8.18) establishes the frictional distance between the known upstream point and the location of choking. Then, with reference to figure 8.4,

$$L=(L_{max})_1-(L_{max})_2$$

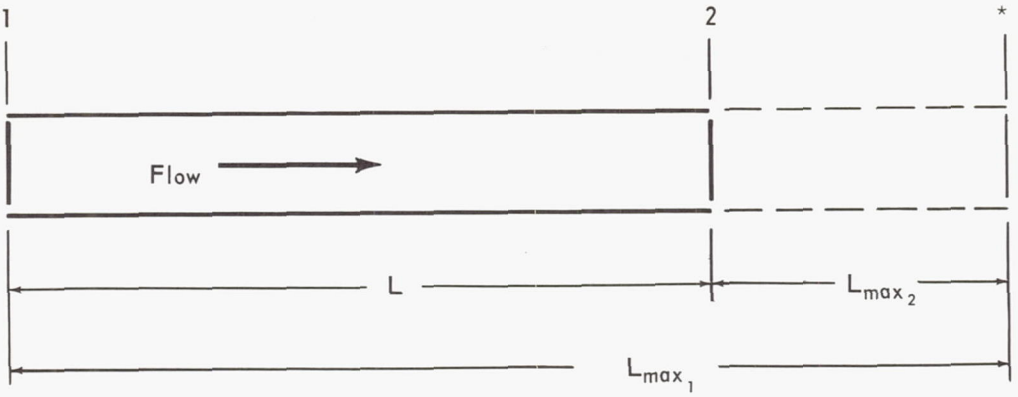


Figure 8.4. Pipe-length measurements.

so that

$$f\left(\frac{L}{D}\right)=\left[f\left(\frac{L_{\max}}{D}\right)\right]_1-\left[f\left(\frac{L_{\max}}{D}\right)\right]_2 \tag{8.26}$$

Likewise, since the choked values of the properties are the same, regardless of the upstream point used to establish them, the entropy change from location 1 to 2 is found by

$$\frac{s_2-s_1}{c_p}=\left(\frac{s-s^*}{c_p}\right)_2-\left(\frac{s-s^*}{c_p}\right)_1 \tag{8.27}$$

Since the other properties are related to the choked value as a ratio, a ratio form of equation is needed. The change in pressure, for example, between locations 1 and 2 is found by

$$\frac{P_2}{P_1}=\frac{\left(\frac{P}{P^*}\right)_2}{\left(\frac{P}{P^*}\right)_1} \tag{8.28}$$

All the other property changes are found by using the form of equation (8.28).

Figure 8.5 is a graphic representation of the most important of the working equations, evaluated for perfect gases having a value of $k=1.4$. More exact graphs for these and other gases are presented in chapter 19. Solutions for the equations can also be found tabulated in Keenan and Kaye (1948), Ames (1953), and Pratt & Whitney Aircraft (1963).

It must be emphasized that the Fanno-line equations describe only that flow in pipes which can theoretically exist and that which is chockless. For example, in subsonic flow, $f(L/D)$ cannot exceed $f(L_{\max}/D)$. If $f(L/D)$ is computed to be larger than the $f(L_{\max}/D)$ associated with the mach number of the flow, either the mach number is too large for the frictional pipe length or the length is too large for the upstream mach number. In supersonic flow with $L<L_{\max}$, pipe-exit back pressures equal to or greater than a specific pressure (P_g) will cause a normal shock to exist somewhere in the pipe. The Fanno equations describe flow only on either side of the shock, but not across it. P_g is the pressure just downstream of a normal shock that stands in the pipe exit with a shockless flow upstream. With $L>L_{\max}$ in

supersonic flow, a normal shock exists somewhere in the pipe, and the Fanno equations apply only in the shockless regions once again. A detailed description of this phenomenon is presented in "Choking Because of Friction."

The usual procedure for computing the change in gas properties between two points in a pipe with the graphic or tabulated solution is as follows. The mach number is computed for the point in the pipe where the flow rate and fluid properties are known. A convenient form is

$$M=\left(\frac{W}{A}\right)\left(\frac{1}{P}\right)\sqrt{\frac{RT}{kg_c}} \tag{8.29}$$

The point of known conditions may be either upstream (1) or downstream (2), as shown in figure 8.4. The frictional length parameter, $f(L_{max}/D)$, and the fluid property ratios of interest, such as (P/P^*), are read from the graphs or tables at the computed mach number. The fric-

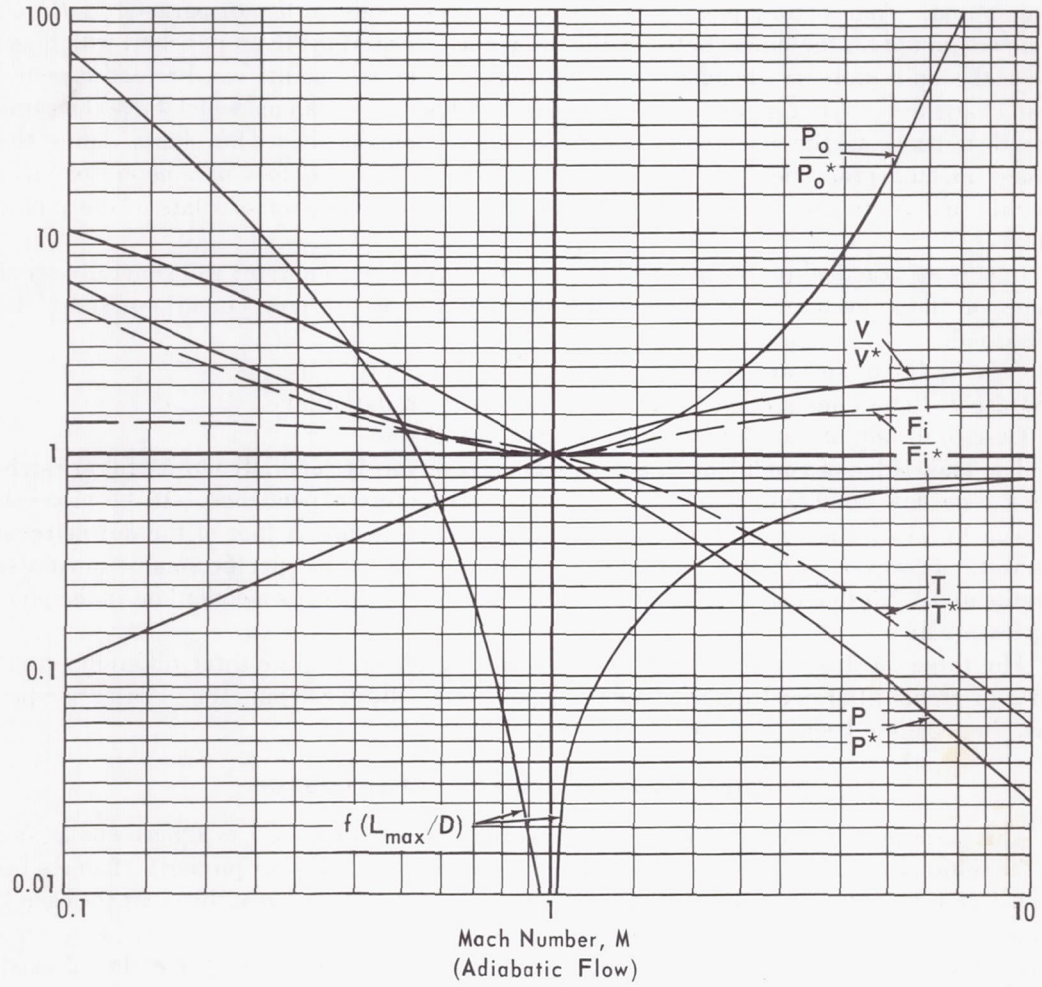


Figure 8.5. Graphic solution of the important Fanno-line equations for $k=1.4$.

tional length $f(L/D)$ between the points 1 and 2 is computed from the pipe description and combined with the value of $f(L_{max}/D)$ as read from the charts in accordance with equation (8.26). This computation establishes the value of $f(L_{max}/D)$ for the other point in the pipe, which, in turn, identifies the associated mach number and fluid property ratios for that location by means of the charts. The changes in properties between the two points are then evaluated by means of equations (8.27) and (8.28) and others of that form.

DIRECT GRAPHIC METHODS—SUBSONIC FLOW

The adiabatic frictional flow equations can be derived and integrated in the subsonic range between two specific locations in the piping system to produce solutions that can be charted. These charts then provide direct methods for calculating the compressible fluid property changes between various locations in a piping system. For example, if the mass flow rate and fluid properties are known at a point in the pipe, the mass flow parameter can be computed. And if the piping system is defined, the frictional length parameters $f(L/D)$ can be computed for the piping between the two points. Entering the proper chart with these values, the fluid property changes that occur between the two points can be read directly. These charts are graphic solutions of exact compressible flow equations which have the same theoretical basis as the Fanno-line equations derived previously. The charts define the changes in fluid properties that occur as a function of dimensionless parameters of mass flow rate and frictional pipe length measured at (or between) specific points in the piping system.

In solving practical problems, the known (reference) flow conditions will generally occur in one of three locations, relative to the location where the flow conditions are to be established.

Case 1: Conditions are known at an upstream point in the pipe.

Case 2: Conditions are known at a downstream point in the pipe.

Case 3: Conditions are known in an upstream reservoir.

The knowledge of conditions in a downstream reservoir is generally not useful in establishing pipe flow conditions since there is no necessary interdependence. If the pipe-exit flow can be proven to be subsonic, then the pipe-exit pressure is that of the downstream reservoir. However, in such a case, the pipe-exit temperature or specific volume must also be estimated. This changes the problem to one of known downstream conditions in the pipe, as in case 2 above.

The three locations where the flow conditions are known require three different sets of charts to prevent the need for trial-and-error solutions. In developing the necessary equations, the location designations will follow that of figure 8.6.

Conditions Known in an Upstream Pipe Location

The basic pipe flow equations are developed for the section from 1 to 2, based on known flow conditions at 1. By assuming various flow conditions, the fluid property changes between 1 and 2 can be computed for selected values of $f(L/D)$ to produce the chart for case 1. As discussed previously, for any assumed flow condition and piping system, the properties of the fluid are fixed throughout the pipe and the upstream reservoir, if one should exist, regardless of the location of the known flow conditions. Therefore, the data required to produce the charts for cases 2 and 3 are obtained by modifying the flow parameters and fluid

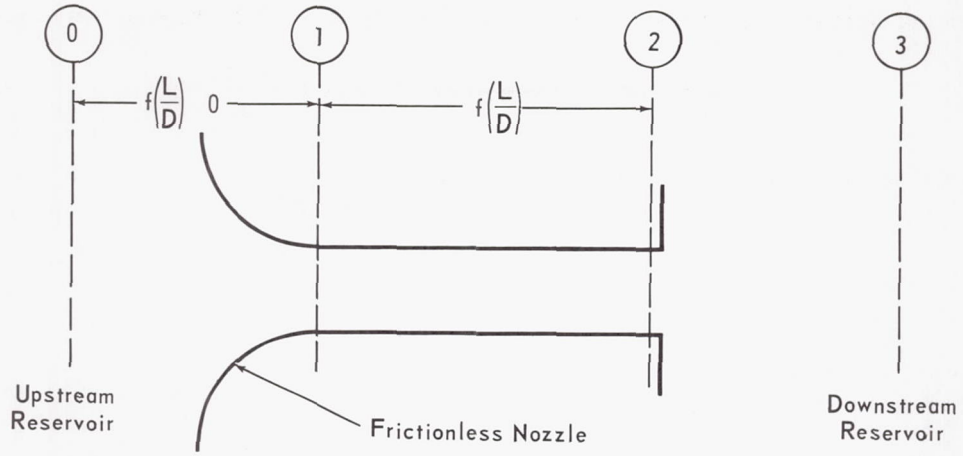


Figure 8.6. Direct pipe flow solutions (conditions known in an upstream pipe location).

property changes to reflect the change in the reference location from 1 to 2 and to 0, respectively. The pipe is assumed to be connected to the upstream reservoir with a frictionless isentropic nozzle to simplify the analysis. The significance of the frictionless nozzle is that isentropic flow can be assumed to relate the conditions between locations 0 and 1. The use of the nozzle also permits the use of the charts of case 3 to relate downstream conditions with stagnation conditions at location 1. In a practical problem, a square-edged entrance would be accommodated by increasing the effective pipe-length parameter $f(L/D)$.

Proceeding with the analysis of case 1, the equation of state which describes the state of the fluid as it progresses through the pipe is established by noting that the total specific enthalpy of the fluid is constant if the flow is adiabatic. Then

$$\mathrm{d}\left(\frac{V^2}{2g_c}\right)+J\ \mathrm{d}h=\mathrm{d}\left(\frac{V^2}{2g_c}\right)+J\ \mathrm{d}u+\mathrm{d}(Pv)=0 \tag{8.30}$$

For a perfect gas, it has been established previously (ch. 2) that

$$\mathrm{d}u=c_v\ \mathrm{d}T \qquad\qquad c_p-c_v=\frac{R}{J}$$

and

$$\mathrm{d}(Pv)=R\ \mathrm{d}T \qquad\qquad k=\frac{c_p}{c_v}$$

These equations can be combined to obtain

$$J\ \mathrm{d}u=\frac{\mathrm{d}(Pv)}{k-1}$$

Substituting this into equation (8.30) yields

$$\mathrm{d}(Pv)=-\left(\frac{k-1}{k}\right)\mathrm{d}\left(\frac{V^2}{2g_c}\right) \tag{8.31}$$

Integrating equation (8.31) between points 1 and 2 in the pipe yields the equation of state

$$Pv+\left(\frac{k-1}{2kg_c}\right)V^2=P_1v_1+\left(\frac{k-1}{2kg_c}\right)V_1^2=P_2v_2+\left(\frac{k-1}{2kg_c}\right)V_2^2 \tag{8.32}$$

which can be rearranged as

$$P_2v_2=P_1v_1+\left(\frac{k-1}{2kg_c}\right)V_1^2\left[1-\left(\frac{V_2}{V_1}\right)^2\right]$$

From continuity

$$w=\gamma_1A_1V_1=\gamma_2A_2V_2$$

and for a constant-area pipe

$$\frac{V_2}{V_1}=\frac{\gamma_1}{\gamma_2}=\frac{v_2}{v_1}$$

Also, by definition of the mach number for the upstream location

$$V_1^2=M_1^2c^2=M_1^2kg_cP_1v_1$$

Substituting these into the equation of state yields the equations relating the fluid property changes to the upstream mach number.

$$\frac{P_2}{P_1}=\frac{v_2}{v_2}\left\{1-\left[\left(\frac{k-1}{2}\right)M_1^2\right]\left[\left(\frac{v_2}{v_1}\right)^2-1\right]\right\} \tag{8.33}$$

Also, since

$$\frac{P_2}{P_1}\left(\frac{v_2}{v_1}\right)=\frac{T_2}{T_1}$$

$$\frac{T_2}{T_1}=1-\left[\left(\frac{k-1}{2}\right)M_1^2\right]\left[\left(\frac{v_2}{v_1}\right)^2-1\right] \tag{8.34}$$

An additional equation is needed to relate these fluid property changes to the frictional length of the pipe. From an intermediate stage in the derivation of equation (8.5), the following equation can be written

$$\frac{\gamma V^2\,\mathrm{d}V}{g_cV}+\mathrm{d}P+f\left(\frac{\gamma V^2}{2g_c}\right)\frac{\mathrm{d}L}{D}=0 \tag{8.35}$$

An alternate form of this equation is the Bernoulli theorem, obtained by substituting $\mathrm{d}V^2=2V\,\mathrm{d}V$

$$\mathrm{d}\left(\frac{V^2}{2g_c}\right)+v\,\mathrm{d}P+f\left(\frac{V^2}{2g_c}\right)\frac{\mathrm{d}L}{D}=0 \tag{8.36}$$

By substituting the mathematical identity

$$v\,\mathrm{d}P=\mathrm{d}(Pv)-P(\mathrm{d}v)$$

and the value of $d(Pv)$ from equation (8.31), equation (8.36) can be rewritten as

$$\frac{dV}{V}-\frac{kg_c}{V^2}(Pv)\frac{dv}{v}+\left(\frac{kf}{2D}\right)dL=0$$

Further substitution of the value of Pv from equation (8.32) yields

$$\frac{dV}{V}-kg_c\left[P_1v_1+\frac{k-1}{2kg_c}\left(V_1^2-V^2\right)\right]\frac{dv}{vV^2}+\left(\frac{kf}{2D}\right)dL=0$$

For steady flow in a constant-area pipe, continuity requires that

$$G=\frac{w}{A}=\frac{V}{v}=\text{constant}$$

which can be written once again in logarithmic differential form as

$$\frac{dV}{V}=\frac{dv}{v}$$

Substituting this and clearing yield the following integrable equation

$$(k+1)\int_{V_1}^{V_2}\frac{dV}{V}-\left[2kg_cP_1v_1+(k-1)V_1^2\right]\int_{V_1}^{V_2}\frac{dV}{V^3}+\frac{kf}{D}\int_0^L dL=0$$

Carrying out the integration and substituting the definitions of sonic velocity and mach number yield the equation that relates the frictional length $f(L/D)$, measured between the two pipe locations, to the fluid properties and mach number

$$f\left(\frac{L}{D}\right)=\frac{1}{k}\left[\frac{2+(k-1)M_1^2}{2M_1^2}\right]\left[1-\left(\frac{v_1}{v_2}\right)^2\right]-\left(\frac{k+1}{2k}\right)\ln\left(\frac{v_2}{v_1}\right)^2 \tag{8.37}$$

Equations (8.33) and (8.37) can be solved simultaneously to produce the charts for case 1, which consist of separate charts for each value of k that is to be represented. Figure 8.7 represents the chart for $k=1.4$ and case 1. Note that the mass flow parameter ϕ_1 has been chosen as

$$\phi_1=\sqrt{k}(M_1)=\left(\frac{w}{A}\right)\left(\frac{1}{P_1}\right)\sqrt{\frac{RT_1}{g_c}} \tag{8.38}$$

Comparing equations (8.38) and (8.29) shows that ϕ is merely a modified mach number, made independent of $k[\phi=(\sqrt{k})M_1]$. This selection is made to provide easier interpolation between charts for uneven values of k. For example, for any value of k, ϕ_1 needs to be calculated only once, and the charts drawn for all specific values of k can be entered using the same value of ϕ_1. It can be shown by cross-plotting the data versus k that linear interpolation between the charts for any in-between values of k yields good accuracy.

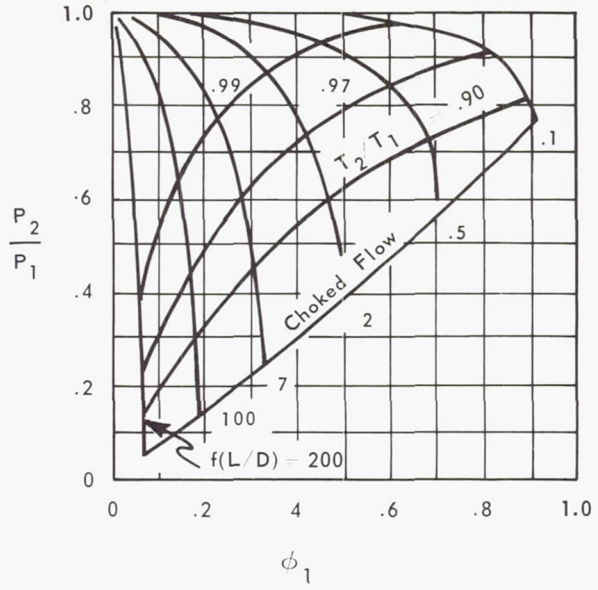


Figure 8.7. Direct pipe flow solutions (conditions known in an upstream pipe location).

Although equation (8.34) can be used to compute the temperature change (T_2/T_1) for each assumed flow condition used in computing points on the chart, it must be modified to produce the parametric curves for selected even values of (T_2/T_1). This modification requires substitution of $(v_2/v_1)=(T_2/T_1)\,(P_2/P_1)^{-1}$ into equation (8.34), resulting in

$$\frac{P_2}{P_1}=\frac{T_2}{T_1}\left[\frac{1-\dfrac{T_2}{T_1}}{\left(\dfrac{k-1}{2}\right)M_1^2}+1\right]^{-1/2} \tag{8.39}$$

Equations (8.38) and (8.39) establish the variation of (P_2/P_1) versus ϕ_1 along lines of constant (T_2/T_1). That this equation is indeterminant for $k=1.0$ is insignificant, since for $k=1.0$, the temperature is constant over the entire chart, and no lines of constant (T_2/T_1) exist.

The critical flow conditions are plotted on the chart to identify the limiting (maximum) subsonic flow, which occurs when the velocity at the pipe exit becomes sonic. The sonic flow line is described by the previously derived equation (8.19), which can be rewritten as

$$\frac{P^*}{P_1}=M_1\sqrt{\frac{2+(k-1)M_1^2}{k+1}}=\phi_1\sqrt{\frac{2+\left(\dfrac{k-1}{k}\right)\phi_1^2}{k(k+1)}} \tag{8.40}$$

Conditions Known in a Downstream Pipe Location

The charts for case 2 can be plotted from the calculated data of case 1 simply by defining the flow parameter for the downstream pipe location

$$\phi_2 = \sqrt{k}\,(M_2) = \left(\frac{w}{A}\right)\left(\frac{1}{P_2}\right)\sqrt{\frac{RT_2}{g_c}} \tag{8.41}$$

The conversion relating ϕ_1 and ϕ_2 is obtained by combining equations (8.38) and (8.41)

$$\phi_2 = \phi_1\left(\frac{\phi_2}{\phi_1}\right) = \phi_1\frac{\sqrt{\frac{T_2}{T_1}}}{\left(\frac{P_2}{P_1}\right)} \tag{8.42}$$

The (P_2/P_1) data computed for the flow conditions used in establishing the charts for case 1 can now be plotted versus ϕ_2 using equation (8.42), producing the charts for case 2. The case 2 chart for $k = 1.4$ is shown in figure 8.8. The lines of constant (T_2/T_1) are derived by substituting into equation (8.34) the relationship

$$\frac{v_2}{v_1} = \left(\frac{T_2}{T_1}\right)\left(\frac{P_2}{P_1}\right)^{-1}$$

from the perfect-gas law, and

$$M_1^2 = M_2^2\frac{\left(\frac{P_2}{P_1}\right)^2}{\left(\frac{T_2}{T_1}\right)}$$

obtained from combination of equations (8.38), (8.41), and (8.42). Clearing and solving for

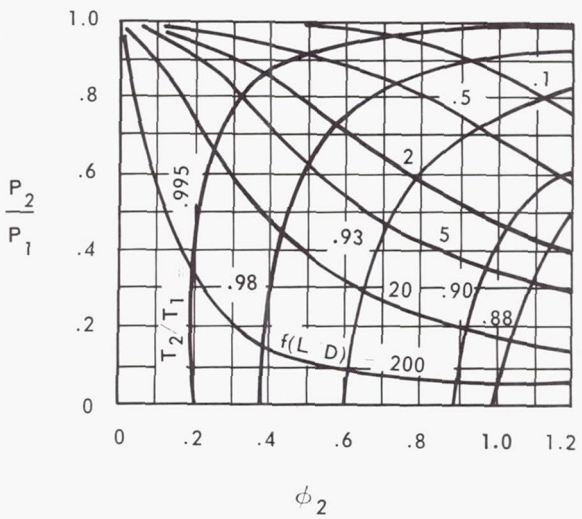


Figure 8.8. Direct pipe flow solutions (conditions known in a downstream pipe location).

(P_2/P_1) yield the necessary relationship to define the lines of constant (T_2/T_1) on the charts of case 2.

$$\frac{P_2}{P_1}=\left(\frac{T_2}{T_1}\right)\left[1-\frac{\left(\frac{T_1}{T_2}\right)-1}{\left(\frac{k-1}{2k}\right)\phi_2^2}\right]^{1/2} \tag{8.43}$$

The sonic flow line occurs as a vertical line on the charts of case 2, since the choked condition occurs at the pipe exit, where the flow parameter ϕ_2 is computed. And since M_2 is unity, the sonic flow line is described using equation (8.41) as

$$\phi_2=\sqrt{k} \tag{8.44}$$

Conditions Known in an Upstream Reservoir

To extend the analysis to case 3, which accounts for a reservoir ahead of the pipe, it has been found convenient to assume a frictionless nozzle at the pipe inlet. This permits the use of the isentropic flow relationships to define the changes in properties between the upstream reservoir location 0 and the pipe inlet 1. Therefore, these charts are also applicable for computation between two pipe locations, when the upstream stagnation properties in the pipe are known. The pipe inlet corresponds with the nozzle throat. Then, for this section, the pressure and temperature ratios across the nozzle are obtained directly from equation (8.38) and the previously derived isentropic relationships of equations (5.31) and (5.10)

$$\frac{P_1}{P_0}=\left[1+\left(\frac{k-1}{2}\right)M_1^2\right]^{-\frac{k}{k-1}} \tag{8.45}$$

$$\frac{T_1}{T_0}=\left[1+\left(\frac{k-1}{2}\right)M_1^2\right]^{-1} \tag{8.46}$$

By using equations (8.45) and (8.46) and the data computed previously for the charts of case 1, the pressure and temperature change data required for the charts of case 3 can be computed. This is possible since for a given flow condition and piping system

$$\frac{P_2}{P_0}=\left(\frac{P_2}{P_1}\right)\left(\frac{P_1}{P_0}\right) \tag{8.47}$$

and

$$\frac{T_2}{T_0}=\left(\frac{T_2}{T_1}\right)\left(\frac{T_1}{T_0}\right) \tag{8.48}$$

The flow parameter for case 3 is defined as

$$\phi_0=\left(\frac{w}{A}\right)\left(\frac{1}{P_0}\right)\sqrt{\frac{RT_0}{g_c}} \tag{8.49}$$

and ϕ_0 is equivalent to ϕ_1 and ϕ_2, except that no real mach number can be associated with

the stagnation conditions of the upstream reservoir. ϕ_0 is related to ϕ_1, by combining equations (8.38) and (8.49)

$$\phi_0 = \phi_1 \left(\frac{\frac{p_1}{P_0}}{\sqrt{\frac{T_1}{T_0}}} \right) = (\sqrt{k}) M_1 \left(\frac{\frac{p_1}{p_0}}{\sqrt{\frac{T_1}{T_0}}} \right) \tag{8.50}$$

Since the process between the reservoir and throat is isentropic,

$$\left(\frac{T_1}{T_0} \right) = \left(\frac{P_1}{P_0} \right)^{\frac{k-1}{k}}$$

and equation (8.50) can be simplified to

$$\phi_0 = \phi_1 \left(\frac{P_1}{P_0} \right)^{\frac{k+1}{2k}} = \sqrt{k} (M_1) \left(\frac{P_1}{P_0} \right)^{\frac{k+1}{2k}} \tag{8.51}$$

Equations (8.45) through (8.51), when combined with the data computed for case 1, can be used to compute the data for the charts of case 3. Figure 8.9 is the case 3 chart plotted for $k = 1.4$.

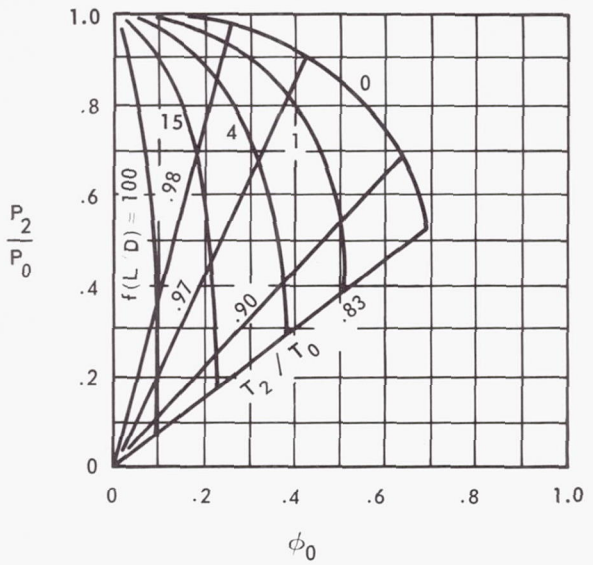


Figure 8.9. Direct pipe flow solutions (conditions known in an upstream reservoir).

Note that in the case of an upstream reservoir, the chart includes a curve for $f(L/D) = 0$. This curve corresponds with the isentropic flow from the upstream reservoir to the throat of a smooth nozzle, which is also the upstream pipe location in this case. The $f(L/D) = 0$

curves are readily obtained from the isentropic flow functions of chapter 5. The adiabatic flow parameter of equation (5.36) is recognized as $\phi_0/\sqrt{k}$ and was obtained by referring the local mach number, defined by equation (5.22) or (8.29), to the stagnation conditions. Then, for the nozzle-throat location

$$\phi_0 = (\sqrt{k})\, M_1 \frac{\left(\frac{P_1}{P_0}\right)}{\sqrt{\frac{T_1}{T_0}}}$$

Substituting the isentropic flow relationship of equation (5.28) to eliminate the temperature and equation (5.31) to eliminate M_1 yields the explicit formula ϕ_0 in terms of pressure ratio

$$\phi_0[f(L/D)=0] = \sqrt{\frac{2k}{k-1}\left[\left(\frac{P_1}{P_0}\right)^{\frac{2}{k}} - \left(\frac{P_1}{P_0}\right)^{\frac{(k+1)}{k}}\right]} \tag{8.52}$$

The lines of constant (T_2/T_0) are obtained by substituting into equation (8.34) the relationships

$$\frac{v_2}{v_1} = \frac{T_2}{T_1}\left(\frac{P_2}{P_1}\right)^{-1}$$

(T_2/T_1) from equation (8.48), (T_1/T_0) from equation (8.46), and M_1 from equation (8.50). The resulting equation solved for (P_2/P_0) is

$$\frac{P_2}{P_0} = \phi_0\left(\frac{T_2}{T_0}\right)\sqrt{\frac{\frac{k-1}{2k}}{1-\frac{T_2}{T_0}}} \tag{8.53}$$

The form of equation (8.53) indicates a straight-line relationship between (P_2/P_0) and ϕ_0 for constant values of (T_2/T_0).

The sonic flow line can be derived by substituting into equation (8.19) the relationships

$$P^*/P_1 = (P^*/P_0)/(P_1/P_0)$$

M_1 from equation (8.51), and (P_1/P_0) from equation (8.45), resulting in

$$\frac{P^*}{P_0} = \phi_0\sqrt{\frac{2}{k(k+1)}} \tag{8.54}$$

An alternate method for obtaining equation (8.54) is to substitute the critical temperature ratio from equation (5.14)

$$\frac{T^*}{T_0} = \frac{2}{k+1}$$

into equation (8.53). This relationship can be used for case 3 because the upstream temperature is the stagnation temperature, and because the equation has been shown in chapter 5 to apply to any adiabatic flow, regardless of irreversibilities. It is also possible to obtain the relationship of equation (5.14) independently by equating equations (8.53) and (8.54) (evaluated for the choked condition where $T_2 = T^*$ and $P_2 = P^*$).

Expanded working charts for cases 1, 2, and 3, plotted for values of $k = 1.0$, 1.4, 1.67, 1.8, 2.5, and 4.0, are placed in chapter 19. Values of $k > 1.67$ are included to account for real-gas effects, in which case k represents k_s, the isentropic exponent discussed in chapter 4, rather than the specific heat ratio. These charts are plotted on logarithmic scales to improve readability in the ranges commonly encountered in practice.

CHOKING AS A RESULT OF FRICTION

It has been determined that for a given upstream mach number and specific heat ratio, there exists a maximum frictional length, $f(L_{max}/D)$, as defined by equation (8.18), which causes sonic velocity at the pipe exit. Further, it has been shown that there can be no transition within the pipe from supersonic to subsonic velocity in the absence of shocks, and there can be no transition from the subsonic to supersonic velocity within the constant-area pipe. The question often arises, when dealing with subsonic flow, as to the effect of an increase in pipe length to a value greater than L_{max} for the particular upstream flow condition. For flow initially subsonic, such an increase in pipe length will reduce the mach number and, hence, reduce the mass flow. The reduced upstream mach number will have a value that corresponds to the increased value of $f(L_{max}/D)$. Choking in subsonic flow can also be produced by reducing the back pressure at the exit of a fixed pipe, thereby increasing the flow rate to achieve choked flow conditions.

Supersonic flow in pipes is generally produced by an upstream converging-diverging nozzle operating with sufficiently low back pressure. An important difference is that in the supersonic case, the flow rate (w/A) is constant, as controlled by the upstream conditions and the size of the choked converging-diverging nozzle upstream. The flow conditions are defined by a single Fanno line, as long as the back pressure is maintained low enough to choke the nozzle. Therefore, the concept of choking is slightly different in supersonic flow and is associated with the formation of normal shock waves within the pipe, rather than a limit on flow rate and/or pipe length. Shock waves can be caused by excessive back pressure or excessive pipe lengths, or both. An important similarity to subsonic flow is the existence of a maximum pipe length at which the flow will become sonic $(M = 1)$ at the exit with shockless flow.

The choking phenomenon can be analyzed in detail most conveniently by studying the changes that occur when the back pressure at the pipe exit is varied. To facilitate the analysis, it is necessary to divide the discussion into two parts: (1) subsonic, such as for pipes fed by converging nozzles; and (2) supersonic, such as for pipes fed by converging-diverging nozzles.

Subsonic Flow

Flow in a pipe fed by a reservoir and a converging nozzle must be subsonic, with static pressure decreasing with pipe length. Consider the flow through the pipe of the system shown in figure 8.10. Assume the back pressure P_b to be variable beginning with an initial

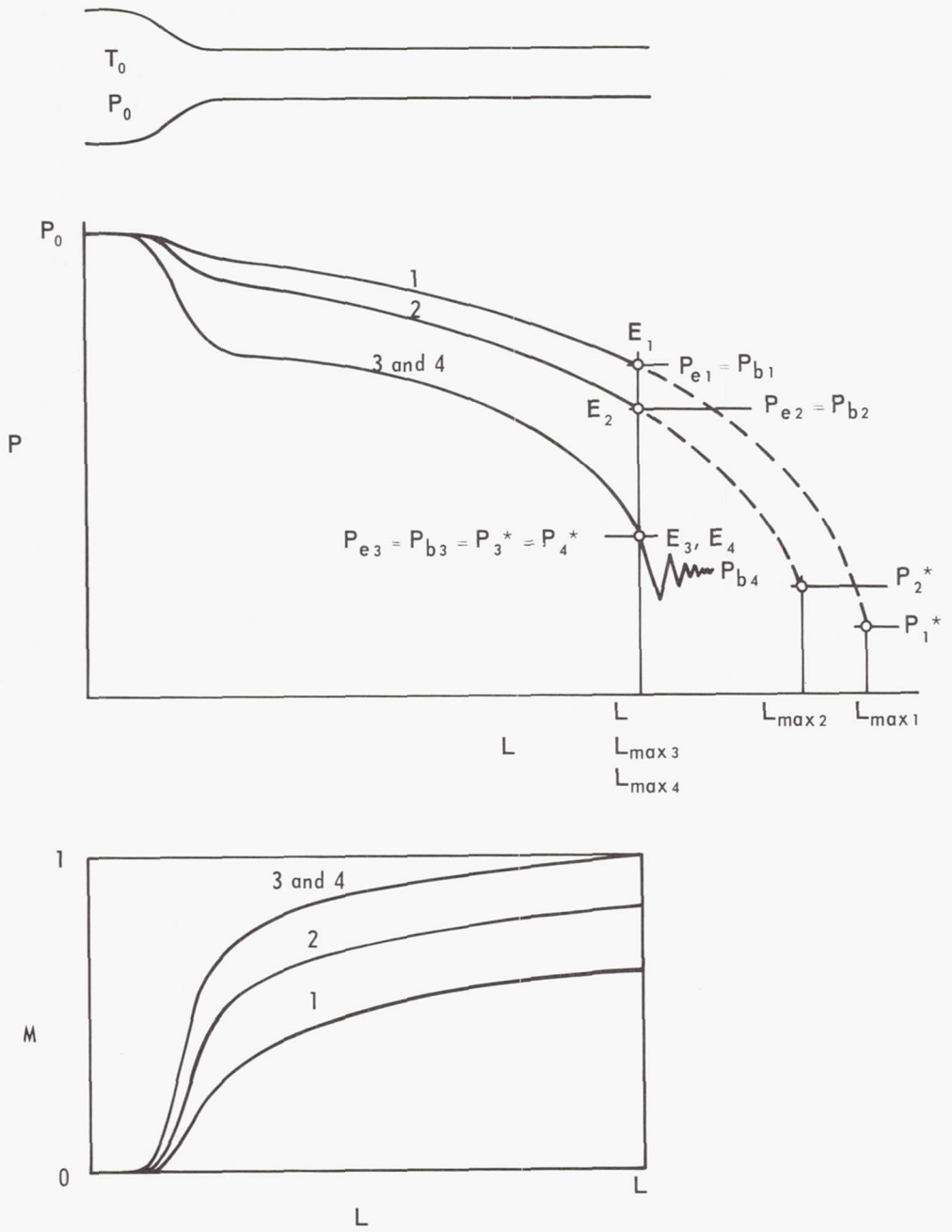


Figure 8.10. Choking because of friction with subsonic adiabatic pipe flow.

value of P_0, the same as the supply pressure, and decreasing through the whole range of pressures to essentially zero pressure.

$P_0 > P_{b1} > P_1^*$ (curve 1, fig. 8.10)

When the back pressure is less than P_0, there is a certain mass flow through the pipe and a certain value of M at the pipe entrance. For this situation, the flow velocity increases through the pipe, but the flow is entirely subsonic and $P_{e1} = P_{b1}$.

$P_0 > P_{b2} > P_2^*$ but $P_{b2} < P_{b1}$ (curve 2, fig. 8.10)

Qualitatively curve 2 is the same as curve 1. The only difference to be observed is an increase in mass flow, mach number, and velocity and a decrease in L_{max}.

$P_{b3} = P_3^*$ (curve 3, fig. 8.10)

When the back pressure is decreased to P_3^*, which is the value of the back pressure that causes sonic velocity at the pipe exit, the pipe is said to be choked. The exit mach number is unity, the inlet mach number is maximum, and $P_{e3} = P_{b3} = P_3^*$.

$P_{b4} < P_3^* = P_4^*$ (curve 4, fig. 8.10)

Dropping the back pressure below P_3^* has no effect on the flow anywhere in the pipe. For this condition, $P_{e4} = P_{e3} = P_3^*$. Also, $P_{b4} < P_{e4}$ and the drop in pressure from P_{e4} to P_{b4} takes place by expansion outside the pipe in the form of oblique expansion waves.

It should be noted that the choked pressures, P^*, are different for curves having different mass flow per unit area, since the Fanno curves are different.

Supersonic Flow

Flow in a pipe fed by a reservoir and a converging-diverging nozzle will produce supersonic pipe flow if the back pressure is maintained sufficiently low. For this case, as shown in figure 8.11, it is necessary to consider two classes of flow; namely, flow in a pipe having a lesser length than L_{max} and flow in a pipe with L greater than L_{max}.

It should be noted that the flow per unit area with all the supersonic flow cases to follow is a constant, as fixed by the choked condition of the upstream converging-diverging nozzle. Therefore, contrary to the subsonic behavior, there can be only a single Fanno curve and a

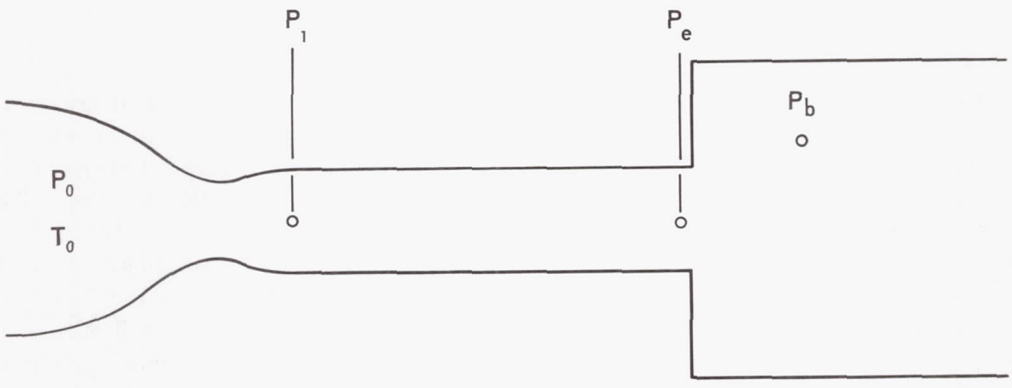


Figure 8.11. Choking because of friction with supersonic adiabatic pipe flow.

single choked flow pressure P^*, regardless of the back pressure, so long as supersonic flow is maintained and the upstream stagnation conditions are unchanged.

CLASS 1: $L < L_{max}$

This implies that the pressure in the pipe exit with shockless flow designated as P'_e must be less than the choked flow pressure P^*, identified by the Fanno-line equations.

CASE 1.1: $P_b < P'_e$

When the back pressure is less than the shockless exit pressure, the process will follow the supersonic part of the Fanno line until the exit pressure $P_e = P'_e$, as shown in figure 8.12. Expansion from P_e to P_b will occur outside the pipe with oblique expansion waves. There can be no shock, since this would cause the process to jump to the subsonic part of the Fanno curve, and then with subsonic flow, the exit pressure would have to match the back pressure. To reach that back pressure, as specified to be less than P'_e from the subsonic part of the Fanno curve, would require a process of decreasing entropy along the Fanno line. This violates the second law of thermodynamics and will not occur.

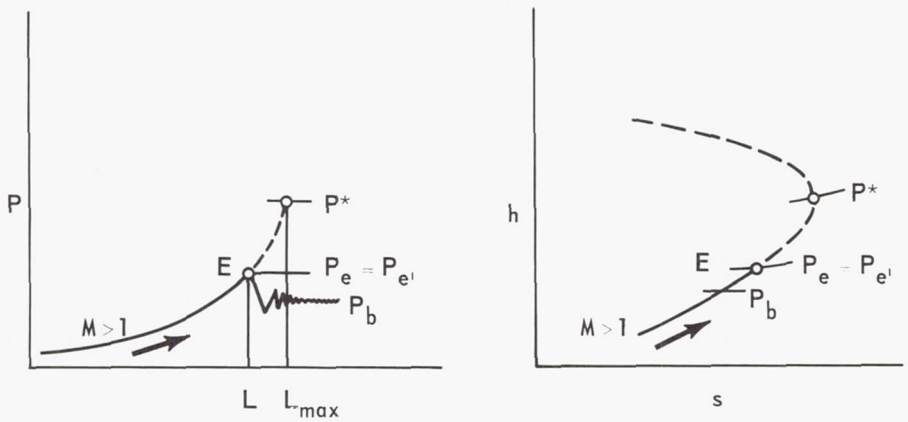


Figure 8.12. Case 1.1, frictional choking with supersonic flow when $L < L_{max}$ and $P_b < P'_e$.

CASE 1.2: $P_g > P_b > P'_e$

If the back pressure is increased from that of case 1.1 to something slightly greater than P'_e, the oblique expansion waves outside the pipe exit are replaced by oblique shocks which serve to raise the pressure of the supersonic flow to the back pressure. Otherwise, case 1.2 is identical with case 1.1 in that $P_e = P'_e$ and no shock wave occurs within the pipe. There is a limit, however, as to how high P_b can be raised without causing the external oblique shocks to retract to the pipe exit and form a normal shock, as shown as a heavy dotted line on figure 8.13. This limiting back pressure is designated P_g and identifies the threshold of back pressures that cause internal shocks. Then P_g is the pressure that will occur downstream of a normal shock standing in the pipe exit and whose upstream shock condition is that resulting from shockless supersonic flow in the pipe up to the exit. The pressure just upstream of the normal shock would be P'_e.

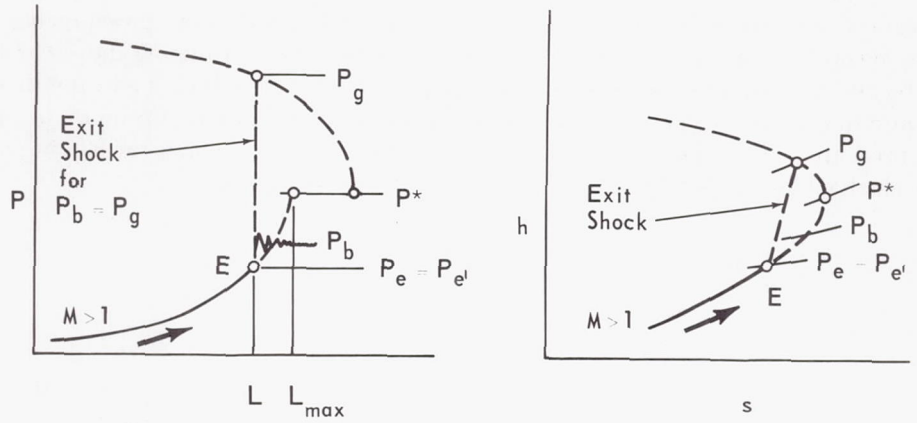


Figure 8.13. Case 1.2, frictional choking with supersonic flow when $L < L_{max}$ and $P_g > P_b > P'_e$.

CASE 1.3: $P_b > P_g$

When the back pressure is increased to a value equal to P_g, as described in case 2, a normal shock stands in the pipe exit. Further increases in P_b will cause the normal shock to move upstream into the pipe, resulting in subsonic flow between the shock and the exit. The exit pressure of the subsonic flow will adjust to the back pressure so that $P_e = P_b$, as shown in figure 8.14. Progressive increases in back pressure will simply move the shock farther upstream in the pipe and subsequently into the nozzle, until subsonic flow exists throughout the system.

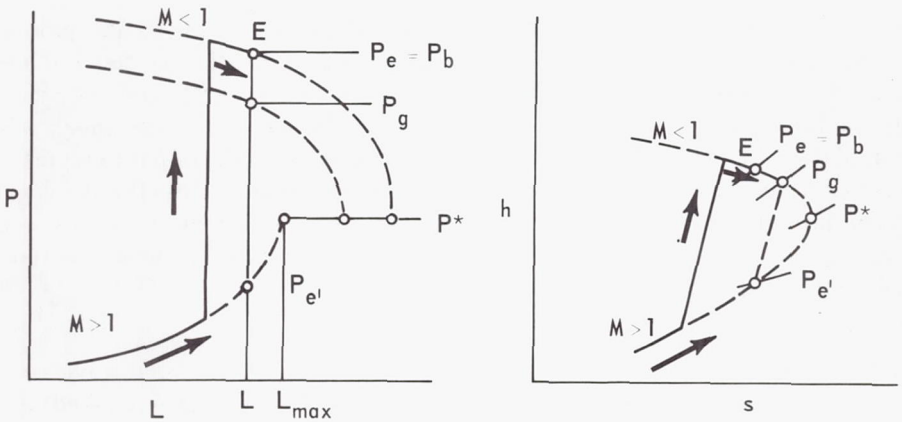


Figure 8.14. Case 1.3, frictional choking with supersonic flow when $L < L_{max}$ and $P_b > P_g$.

CLASS 2: $L > L_{max}$

When the flow possibilities of $L < L_{max}$ were considered, the shockless flow exit pressure P'_e was found to be actually attainable for some values of back pressure. When $L > L_{max}$, the existence of P'_e, as defined, is impossible, since this would require the existence of a flow process beyond the sonic point on the supersonic pressure curve, as shown on the pres-

sure diagram of figure 8.15. It has already been established that the flow process cannot progress beyond the sonic point in a constant area pipe without violating the second law of thermodynamics. This violation is reflected by the process of reducing entropy that would be required to progress around the knee of the Fanno curve of figure 8.15 from P^* to any other greater pressure. Therefore, P_e' is nonexistent when $L > L_{max}$, which further implies that there is no shockless path to points beyond L_{max} in supersonic flow.

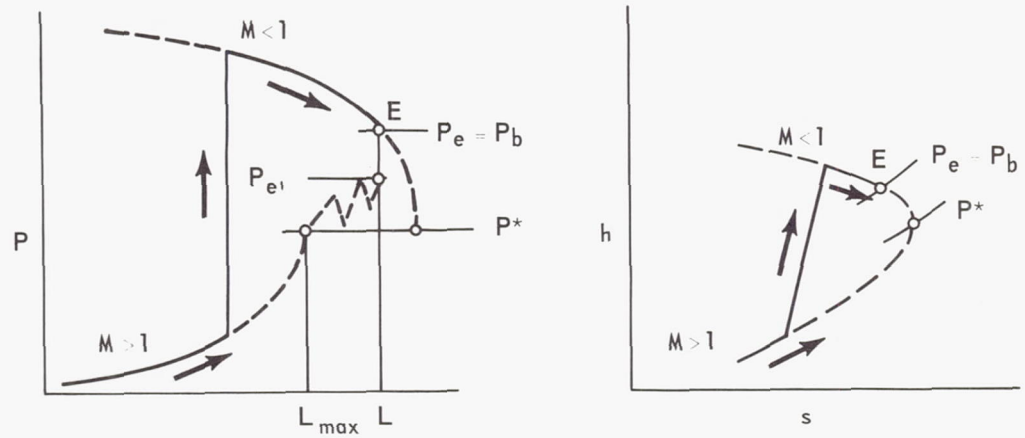


Figure 8.15. Case 2.1, frictional choking with supersonic flow when $L > L_{max}$ and $P_b > P^*$.

CASE 2.1: $P_b > P^*$

In view of the above discussion, the existence of a shock wave in the pipe upstream of L_{max} is apparent for any back pressure that allows supersonic flow at the pipe inlet. The flow process is described by figure 8.15 for the case where $P_b > P^*$, and the exit pressure adjusts to the back pressure, as in all subsonic flow. The location of the shock wave in the pipe is established by the back pressure and the required matching of fluid property changes in the supersonic and subsonic regions with the changes occurring across the shock. Increasing the back pressure moves the shock upstream, as in case 1.3, until the flow is subsonic in the entire pipe. Also, as long as $P_b > P^*$, the subsonic flow in the downstream region will remain unchoked at the exit.

CASE 2.2: $P_b < P^*$

When the back pressure is reduced to P^* with $L > L_{max}$, the shock wave moves to its farthest possible downstream location and the subsonic flow becomes choked at the exit. Any further decreases in back pressure will be ineffective in changing the flow conditions anywhere in the pipe. Then $P_e = P^*$, and the expansion from P_e to P_b will occur once again as oblique expansion waves outside the end of the pipe, as indicated in figure 8.16.

In closing, it should be mentioned that the foregoing analysis was developed from the idealized theory of shock waves as plane discontinuities. It must be remembered in practice that the change from supersonic to subsonic flow is likely to extend over a considerable distance within the pipe as a result of boundary-layer effects, and this phenomenon is described in some detail in chapter 6.

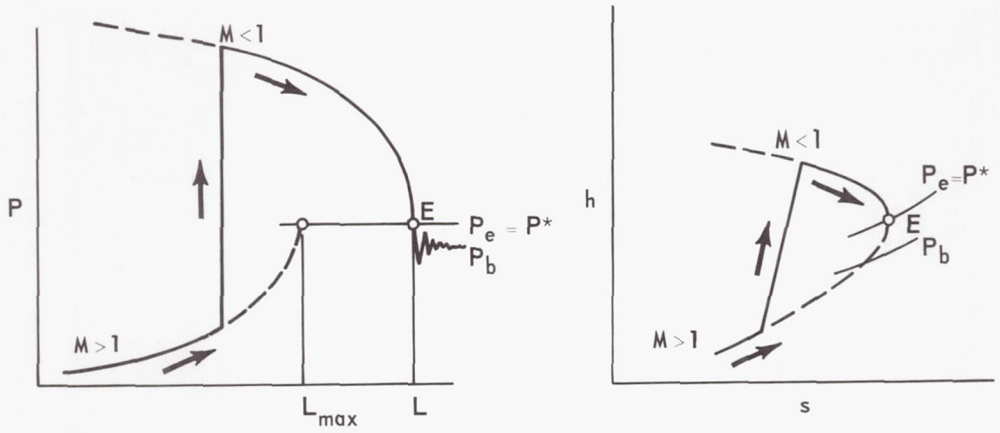


Figure 8.16. Case 2.2, frictional choking with supersonic flow when $L > L_{max}$ and $P_b < P^*$.

CHAPTER 9

NONADIABATIC FLOW IN PIPES

As mentioned in the general discussion of pipe flow in chapter 8, straightforward analytical solutions are available for special cases of compressible pipe flow with heat transfer. The most common of these is the case of isothermal flow (constant temperature) with friction, which generally applies to very long pipelines with relatively low mach-number flow. A second case is that of relatively short pipes with high heat transfer (usually deliberate) and in which the frictional effects are assumed to be negligible, relative to the heating or cooling effects. A third case is one in which the effects of both friction and heat transfer are significant, resulting in a more complex problem that requires the use of the special techniques.

ISOTHERMAL FRICTIONAL FLOW IN PIPES

Features of Isothermal Pipe Flow

When gases are transported over long distances in pipes, the static temperature tends to remain at the surrounding ambient temperature as a result of heat transfer from the surroundings. This tendency toward constant temperature is increased by long pipe length, low gas velocity, and absence of thermal insulation. In such pipelines, the total frictional pressure loss is generally high, and to assume incompressible flow (constant density) would usually result in poor calculational accuracy, in spite of low mach numbers. In this section, therefore, the same assumptions are made as in adiabatic frictional flow, except that sufficient heat is assumed to be added to maintain constant temperature.

Governing Equations

Equations (8.1) and (8.2) of chapter 8 reduce to the following for isothermal flow:

$$\frac{dP}{P}=\frac{d\gamma}{\gamma} \tag{9.1}$$

$$\frac{dM^2}{M^2}=\frac{dV^2}{V^2}=2\left(\frac{dV}{V}\right) \tag{9.2}$$

Equations (8.4) and (8.5) remain unchanged as

$$\frac{d\gamma}{\gamma}=-\frac{1}{2}\left(\frac{dV^2}{V^2}\right)=-\frac{dV}{V} \tag{9.3}$$

325-994 O-69—13

Preceding Page Blank

and

$$\frac{dP}{P}+\left(\frac{kM^2}{2}\right)f\left(\frac{dL}{D}\right)+\frac{kM^2}{2}\left(\frac{dV^2}{V^2}\right)=0 \tag{9.4}$$

Proper combination of these four equations yields the explicit differential relation between the frictional length and mach number

$$\frac{dM^2}{M^2}=\left(\frac{kM^2}{1-kM^2}\right)f\left(\frac{dL}{D}\right) \tag{9.5}$$

An important difference between adiabatic and isothermal flow can be identified by comparing equation (9.5) with the equivalent adiabatic flow equation (8.10). For adiabatic flow, the choked condition can be identified at the point where the factor $(1-M^2)$ approaches zero at $M=1$. In the case of isothermal flow, the equivalent factor is $(1-kM^2)$ which establishes the choked condition at a value of $M=1/\sqrt{k}$, rather than unity.

It is convenient to establish the limits of integration of equation (9.5) from some upstream reference point of distance measurement where $L=0$, and the mach number is M, to a point downstream where the mach number reaches the choked value, $M=M^{**}=1/\sqrt{k}$. This point is selected since it can be shown that M tends toward this value from either the subsonic or supersonic flow conditions in the same way M tends toward the value of unity in adiabatic pipe flow. This condition can be reached, therefore, only at the end of the pipe, which is said to be at a distance L_{max} from the arbitrary reference point.

Integrating

$$\int_0^{L_{max}} f\left(\frac{dL}{D}\right)=\int_{M^2}^{1/k}\left(\frac{1-kM^2}{kM^4}\right)dM^2$$

yields

$$f\left(\frac{L_{max}}{D}\right)=\frac{1-kM^2}{kM^2}+\ln kM^2 \tag{9.6}$$

The equation can also be applied to a length of pipe L between two real points by subtracting the distances in the same manner described in chapter 8 and in accordance with figure 8.4 and equation (8.26).

Substitution of equation (9.6) into equation (8.26) yields

$$f\left(\frac{L}{D}\right)=\frac{1-kM_1^2}{kM_1^2}-\frac{1-kM_2^2}{kM_2^2}+\ln\left(\frac{M_1^2}{M_2^2}\right) \tag{9.7}$$

It is possible to convert equation (9.7) into a more useful form which directly relates mass flow rate, the pressures at points 1 and 2, and the frictional distance. The flow properties which occur at the choked location, L_{max}, are utilized since these values are fixed independently of the chosen upstream locations 1 and 2 and are, therefore, a fixed constant for a given pipe flow. These properties are designated by the superscript **.

From the definition of local mach number and for constant temperature, M varies only

with velocity and is directly proportional to it. The conditions at an upstream point can be related directly to the conditions at L_{max} by

$$\frac{M}{V}=\frac{\sqrt{\frac{1}{k}}}{V^{**}} \qquad \text{and} \qquad \frac{V}{V^{**}}=(\sqrt{k})M$$

From the continuity equation applied to constant-area pipes,

$$\gamma V=\gamma^{**}V^{**}$$

From the perfect-gas law with T constant,

$$\frac{P}{P^{**}}=\frac{\gamma}{\gamma^{**}}$$

Combining yields

$$\frac{P}{P^{**}}=\frac{\gamma}{\gamma^{**}}=\frac{V^{**}}{V}=\frac{1}{(\sqrt{k})M} \tag{9.8}$$

Therefore, since P^{**} is constant for any given flow condition, the pressure and mach numbers at points 1 and 2 are related by

$$\frac{P_1}{P_2}=\frac{M_2}{M_1} \tag{9.9}$$

Solving equation (9.9) for M_2 and substituting into equation (9.7) yield the following explicit equation for M_1:

$$M_1^2=\frac{1}{k}\left[\frac{1-\left(\frac{P_2}{P_1}\right)^2}{f\left(\frac{L}{D}\right)-\ln\left(\frac{P_2}{P_1}\right)^2}\right] \tag{9.10}$$

The flow parameter ϕ_1 is also completely defined since, as in chapter 8,

$$\phi_1=(\sqrt{k})M_1$$

so that

$$\phi_1=\frac{w}{A}\left(\frac{1}{P_1}\right)\sqrt{\frac{RT_1}{g_c}}=\left[\frac{1-\left(\frac{P_2}{P_1}\right)^2}{f\left(\frac{L}{D}\right)-\ln\left(\frac{P_2}{P_1}\right)^2}\right]^{1/2} \tag{9.11}$$

Equation (9.11) produces solutions for isothermal flow in any perfect gas, regardless of the specific heat ratio. The solutions are found to coincide exactly with that of adiabatic flow of a gas having a value of $k=1.0$, as established by the direct graphic methods of chapter 8, "Direct Graphic Methods—Subsonic Flow," and case 1.

For cases when the downstream conditions are known, the isothermal flow equation can be rewritten in terms of the downstream conditions by means of equations (8.41), (8.42), and (9.11).

$$\phi_2 = \frac{w}{A}\left(\frac{1}{P_2}\right)\sqrt{\frac{RT_2}{g_c}} = \left[\frac{\left(\frac{P_2}{P_1}\right)^{-2} - 1}{f\left(\frac{L}{D}\right) - \ln\left(\frac{P_2}{P_1}\right)^2}\right]^{1/2} \tag{9.12}$$

Equation (9.12) also produces solutions which exactly coincide with the charts computed for adiabatic flow of a gas having a value of $k = 1.0$, as established for case 2 (ch. 8). Therefore, the evaluation of static pressure changes for isothermal, frictional pipe flow of any perfect gas can be made without approximation using the charts that describe adiabatic flow of a gas having $k = 1.0$. The choked flow lines also apply since $P_2/P_1 = M_1/M_2$ and $M_2 = 1/\sqrt{k}$ at the choked condition. When an upstream reservoir enters the problem, the property changes at the pipe entrance normally cannot be considered isothermal due to the abrupt change, and the case 3 chart for $k = 1.0$ is not generally applicable to the isothermal flow of all perfect gases. However, for the usual case of unheated isothermal flow, the isothermal assumption is valid only with low mach-number flows. Also, the entrance effects are described as an equivalent value of $f(L/D)$ which usually never exceeds unity. The case 3 chart data indicate that for low values of ϕ_0 and for $f(L/D)$ values less than 1.0, the fluid temperature change is very small, and the pressure ratio is essentially independent of k. Therefore, the case 3 chart for $k = 1.0$ can be used for the isothermal flow of any perfect gas with little error if the mach number (and ϕ_0) is relatively low and the pipe is long, which is usually the case in isothermal flow.

In addition to static pressure changes, the changes in fluid density and stagnation temperatures and pressures are also of interest. The perfect-gas law requires that

$$\frac{\gamma_2}{\gamma_1} = \frac{P_2}{P_1}$$

for the isothermal flow, which is already available from the charts.

The isentropic stagnation temperature was established by equation (5.10), chapter 5.

$$T_0 = T\left[1 + \left(\frac{k-1}{2}\right)M^2\right] \tag{5.10}$$

For the isothermal case, equation (5.10) can be written in logarithmic differential form as

$$\frac{dT_0}{T_0} = \left\{\frac{(k-1)M^2}{2\left[1 + \left(\frac{k-1}{2}\right)M^2\right]}\right\}\frac{dM^2}{M^2} \tag{9.13}$$

Likewise, the isentropic stagnation pressure was established by equation (5.31) as

$$P_0 = P\left[1 + \left(\frac{k-1}{2}\right)M^2\right]^{\frac{k}{k-1}} \tag{5.31}$$

which, when written in logarithmic differential form, is

$$\frac{dP_0}{P_0}=\frac{dP}{P}+\left\{\frac{kM^2}{2\left[1+\left(\frac{k-1}{2}\right)M^2\right]}\right\}\frac{dM^2}{M^2} \tag{9.14}$$

By properly combining equations (9.1), (9.2), (9.3), (9.4), (9.13), and (9.14), the differential equations for fluid property changes can be obtained in terms of the frictional pipe length.

$$\frac{dP}{P}=\frac{d\gamma}{\gamma}=-\frac{dV}{V}=-\frac{1}{2}\left(\frac{dM^2}{M^2}\right)=-\left[\frac{kM^2}{2(1-kM^2)}\right]f\left(\frac{dL}{D}\right) \tag{9.15}$$

$$\frac{dP_0}{P_0}=\left\{\frac{kM^2\left[1-\left(\frac{k+1}{2}\right)M^2\right]}{2(kM^2-1)\left[1+\left(\frac{k-1}{2}\right)M^2\right]}\right\}f\left(\frac{dL}{D}\right) \tag{9.16}$$

$$\frac{dT_0}{T_0}=\left\{\frac{k(k-1)M^4}{2(1-kM^2)\left[1+\left(\frac{k-1}{2}\right)M^2\right]}\right\}f\left(\frac{dL}{D}\right) \tag{9.17}$$

These equations show the direction of change in the fluid properties as the fluid progresses down the pipe isothermally. (See table 9.1.)

TABLE 9.1.—*Fluid Property Changes*

	$M<1/\sqrt{k}$	$M>1/\sqrt{k}$
Pressure and density	Decreases	Increases
Velocity, mach number and stagnation temperature	Increases	Decreases
Stagnation pressure	Decreases	Increases for $M<\sqrt{2/(k+1)}$ Decreases for $M>\sqrt{2/(k+1)}$

The mach number tends toward the value of $1/\sqrt{k}$, which represents the limit for continuous isothermal flow. As indicated by stagnation temperature change, heat must be added to the stream when M is less than $1/\sqrt{k}$, and heat must be removed when M is greater than $1/\sqrt{k}$.

Equation (9.15) was previously integrated as equation (9.5) to produce equation (9.6). Substituting equation (9.5) into equations (9.16) and (9.17) to eliminate $f(dL/D)$ and integrating between the same limits as before result in

$$\frac{P_0}{P_0^{**}}=\left[\frac{1}{(\sqrt{k})M}\right]\left\{\left(\frac{2k}{3k-1}\right)\left[1+\left(\frac{k-1}{2}\right)M^2\right]\right\}^{\frac{k}{k-1}} \tag{9.18}$$

and

$$\frac{T_0}{T_0^{**}}=\left(\frac{2k}{3k-1}\right)\left[1+\left(\frac{k-1}{2}\right)M^2\right] \tag{9.19}$$

Once again, the superscript ** refers to the choked flow condition at the end of the maximum length pipe (L_{max}), where $M = M^{**} = 1/\sqrt{k}$. The changes which occur between two specific points in the pipe can be obtained using the techniques outlined for adiabatic flow using equations of the form of equation (8.28).

Required Heat Transfer

The heat added between two points in the pipe can be computed from the change in stagnation temperature.

$$Q'_{1-2} = c_p(T_{02} - T_{01}) \tag{9.20}$$

The stagnation temperature change is obtained from

$$\frac{T_{02}}{T_{01}} = \frac{\left(\frac{T_0}{T_0^{**}}\right)_2}{\left(\frac{T_0}{T_0^{**}}\right)_1} = \frac{1 + \left(\frac{k-1}{2}\right) M_2^2}{1 + \left(\frac{k-1}{2}\right) M_1^2} \tag{9.21}$$

Substitution of equations (9.21) and (9.9) into equation (9.20) produces the direct means for computing the heat transfer required to maintain the isothermal flow condition. Then

$$\frac{Q'_{1-2}}{c_p T_{01}} = \frac{\left(\frac{k-1}{2}\right)\left[\left(\frac{P_2}{P_1}\right)^{-2} - 1\right]}{\frac{1}{M_1^2} + \frac{k-1}{2}} \tag{9.22}$$

and

$$\frac{Q'_{1-2}}{c_p T_{02}} = \frac{\left(\frac{k-1}{2}\right)\left[1 - \left(\frac{P_2}{P_1}\right)^2\right]}{\frac{1}{M_2^2} + \frac{k-1}{2}} \tag{9.23}$$

where M can be replaced by ϕ using $\phi = (\sqrt{k})M$.

Equations (9.22) and (9.23) apply when upstream and downstream flow conditions are known, respectively, and the necessary pressure data can be taken from the direct graphic solutions of chapter 8, "Direct Graphic Methods – Subsonic Flow," for $k = 1.0$. Also, note that equations (9.22) and (9.23) predict that no heat transfer is required for the isothermal flow of a gas having $k = 1.0$, as expected.

It must be remembered that as M approaches the choked value, the heat transfer required to maintain constant temperature becomes very high and will not occur without deliberate heating. Similarly, large and sudden pressure losses in piping components cannot be expected to occur isothermally.

FRICTIONLESS FLOW IN PIPES WITH HEAT EXCHANGE

This section considers the change in properties of a fluid in a nonadiabatic, constant-area, frictionless pipe. Physically, a simple heating or cooling process is seldom achieved. However, in cases where a large temperature difference is maintained between the pipe

wall and the moving stream, frictional effects will be relatively unimportant compared to the heating effect, and the conclusions reached in this paragraph will have a high degree of validity.

As in chapter 8, the analysis is made on the assumption of one-dimensional flow and that of the perfect gas.

The Rayleigh Line

Assuming no frictional effect and no area change, the continuity equation is, as before

$$\gamma V = \frac{w}{A} = G = \text{constant}$$

Because of the momentum considerations of the frictionless constant-area flow, the impulse function defined by equation (5.39) is found to be constant. Then

$$P + \rho V^2 = P + \left(\frac{\gamma}{g_c}\right) V^2 = \frac{F_i}{A} = \text{constant}$$

which, when combined with the continuity equation, yields the Rayleigh-line equation.

$$P + \frac{G^2}{g_c \gamma} = P + \left(\frac{G^2}{g_c}\right) v = \frac{F_i}{A} \tag{9.24}$$

The Rayleigh line can be plotted as a diagram of h–s, as shown in figure 9.1, in the same manner as was the Fanno line of chapter 8.

Once again, the point of maximum entropy is the point where the mach number is unity.

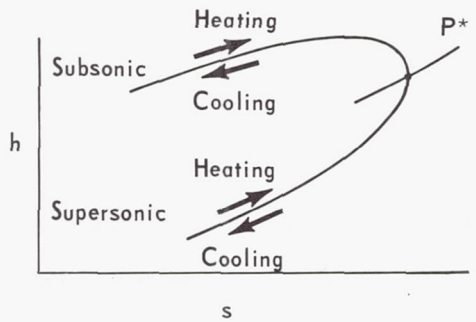


Figure 9.1. Rayleigh line on h–s diagram.

The second law of thermodynamics requires that entropy increase with heat addition and decrease with cooling. As on the Fanno line, the upper portion of the Rayleigh line corresponds with subsonic flow and the lower portion corresponds with supersonic flow. With either subsonic or supersonic flow, heat addition takes the flow process toward mach number of unity at which point the flow is said to become choked. Heat addition greater than that which will cause choking at the pipe exit will result in a reduced flow rate (and upstream mach number) and the process will be defined by a different Rayleigh line. The reduced upstream mach number will be consistent with the heat transfer and choked flow.

Governing Equations

The Rayleigh-line equations that establish the fluid property changes are based on the usual definitions of a perfect gas and mach number and the conservation laws. It is found most convenient, once again, to relate all fluid property changes to the common mass flow parameter, the mach number. Proceeding with reference to the nonadiabatic frictionless pipe model of figure 9.2, the continuity equation for constant area is

$$\gamma_1 V_1 = \gamma_2 V_2 = \frac{w}{A} = \text{constant} \tag{9.25}$$

In the absence of friction, conservation of momentum requires that

$$P_1 A + \rho_1 A V_1^2 = P_2 A + \rho_2 A V_2^2$$

and when combined with equation (9.25)

$$P_1 - P_2 = \frac{w}{g_c A}(V_2 - V_1)$$

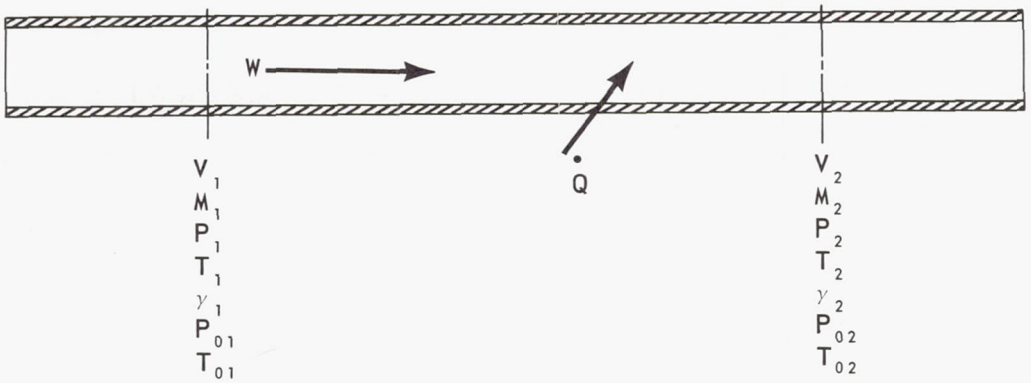


Figure 9.2. Frictionless pipe flow with heat transfer.

Also, since for a perfect gas, $\rho V^2 = kPM^2$, the static-pressure change can be defined by

$$\frac{P_2}{P_1} = \frac{1 + kM_1^2}{1 + kM_2^2} \tag{9.26}$$

By the perfect-gas law,

$$\frac{P_2}{P_1} = \frac{\gamma_2 T_2}{\gamma_1 T_1} \tag{9.27}$$

The definition of mach number yields

$$\frac{M_2}{M_1} = \frac{c_1 V_2}{c_2 V_1} = \frac{V_2}{V_1}\left(\sqrt{\frac{T_1}{T_2}}\right) \tag{9.28}$$

Equations (9.25) through (9.28) can be combined and solved for T_2/T_1, yielding the static temperature change

$$\frac{T_2}{T_1}=\left[\frac{M_2(1+kM_1^2)}{M_1(1+kM_2^2)}\right]^2 \tag{9.29}$$

The density ratio is obtained by combining equations (9.26), (9.27), and (9.29), yielding

$$\frac{\gamma_2}{\gamma_1}=\frac{V_1}{V_2}=\left(\frac{M_1}{M_2}\right)^2\left(\frac{1+kM_2^2}{1+kM_1^2}\right) \tag{9.30}$$

Applying the first law of thermodynamics, the change in entropy can be established as

$$\frac{s_2-s_1}{c_p}=\ln\left[\frac{\dfrac{T_2}{T_1}}{\left(\dfrac{P_2}{P_1}\right)^{\frac{k-1}{k}}}\right]$$

Substituting equations (9.26) and (9.29) yields

$$\frac{s_2-s_1}{c_p}=\ln\left[\left(\frac{M_2}{M_1}\right)^2\left(\frac{1+kM_1^2}{1+kM_2^2}\right)^{\frac{k+1}{k}}\right] \tag{9.31}$$

The stagnation pressure change is obtained using the defining equation (5.31) and the static-pressure ratio of equation (9.26)

$$\frac{P_{02}}{P_{01}}=\left(\frac{1+kM_1^2}{1+kM_2^2}\right)\left[\frac{1+\left(\dfrac{k-1}{2}\right)M_2^2}{1+\left(\dfrac{k-1}{2}\right)M_1^2}\right]^{\frac{k}{k-1}} \tag{9.32}$$

Finally, the stagnation temperature change is obtained from the defining equation (5.10)

$$\frac{T_{02}}{T_{01}}=\left(\frac{T_2}{T_1}\right)\left[\frac{1+\left(\dfrac{k-1}{2}\right)M_2^2}{1+\left(\dfrac{k-1}{2}\right)M_1^2}\right]$$

Substituting T_2/T_1 from equation (9.29) yields

$$\frac{T_{02}}{T_{01}}=\left[\frac{M_2(1+kM_1^2}{M_1(1+kM_2^2)}\right]^2\left[\frac{1+\left(\dfrac{k-1}{2}\right)M_2^2}{1+\left(\dfrac{k-1}{2}\right)M_1^2}\right] \tag{9.33}$$

It should be noted, at this point, that all the fluid property changes are established in terms of changes in the mach number and without a specification of the heat transferred between the two pipe locations 1 and 2. A key relationship is required to associate the heat transfer to the change in mach number. This key relationship can be obtained in terms of the stagnation temperatures from the first law of thermodynamics applied to the open system. In the absence of elevational change and work, the steady-flow energy equation, (1.5), reduces to

$$Q' = h_2 - h_1 + \frac{V_2^2 - V_1^2}{2g_c J} = h_{02} - h_{01}$$

Also for perfect gases,

$$Q' = c_p(T_2 - T_1) + \frac{V_2^2 - V_1^2}{2g_c J} = c_p(T_{02} - T_{01})$$

which can be rearranged as

$$\frac{T_{02}}{T_{01}} = 1 + \frac{Q'}{c_p T_{01}} \tag{9.34}$$

It is often desirable to convert this equation to a form which involves total heat-transfer rate and weight flow rates by noting that

$$Q' = \frac{\frac{dQ}{dt}}{w} = \frac{\dot{Q}}{w}$$

Then the required temperature ratio becomes

$$\frac{T_{02}}{T_{01}} = 1 + \frac{\dot{Q}}{w c_p T_{01}} \tag{9.35}$$

which is generally computable when the heat-transfer rate and the flow conditions at one of the pipe locations are known.

The use of the Rayleigh-line equations, as derived above, is usually prohibitively complex due to the complex functions involving mach number. It has been found convenient, once again, to normalize the equations by referencing the conditions that exist where $M = 1$, which is a constant for any particular flow. Location 1 is chosen as the point where $M = 1$ and, according to usual convention, the various parameters are designated by an * at that location. The downstream pipe location becomes any location in general and the subscript 2 is deleted. The Rayleigh-line equations can be rewritten in simpler form as follows:

$$\frac{P}{P^*} = \frac{k+1}{1+kM^2} \tag{9.36}$$

$$\frac{T}{T^*} = \left[\frac{(k+1)M}{1+kM^2}\right]^2 \tag{9.37}$$

$$\frac{V}{V^*}=\frac{\gamma^*}{\gamma}=\frac{(k+1)M^2}{1+kM^2} \tag{9.38}$$

$$\frac{s-s^*}{c_p}=\ln\left[M^2\left(\frac{k+1}{1+kM^2}\right)^{\frac{k+1}{k}}\right] \tag{9.39}$$

$$\frac{P_0}{P_0^*}=\left(\frac{k+1}{1+kM^2}\right)\left\{\frac{2\left[1+\left(\frac{k-1}{2}\right)M^2\right]}{k+1}\right\}^{\frac{k}{k-1}} \tag{9.40}$$

$$\frac{T_0}{T_0^*}=\frac{2(k+1)M^2\left[1+\left(\frac{k-1}{2}\right)M^2\right]}{(1+kM^2)^2} \tag{9.41}$$

TABLE 9.2.—*Heat-Transfer Effects*

	Heating		Cooling	
	$M<1$	$M>1$	$M<1$	$M>1$
T_0	Increases	Increases	Decreases	Decreases
M	Increases	Decreases	Decreases	Increases
P	Decreases	Increases	Increases	Decreases
T	[a]	Increases	[b]	Decreases
V	Increases	Decreases	Decreases	Increases
P_0	Decreases	Decreases	Increases	Increases

[a] Increases for $M<1/\sqrt{k}$, and decreases for $M>1/\sqrt{k}$.
[b] Decreases for $M<1/\sqrt{k}$, and increases for $M>1/\sqrt{k}$.

Equations (9.36) through (9.41) are plotted in figure 9.3 and in more readable form as a working chart in chapter 20.

The plotted solutions in figure 9.3 show the effects of heat transfer, as reflected in a change in T_0, for flow initially supersonic and subsonic. For brevity, these effects are listed in table 9.2.

It can be seen that heating always reduces the stagnation pressures. Also notice that the curve for T/T^* of figure 9.3 goes through a maximum at $M=1/\sqrt{k}$. This corresponds to the point of maximum h on the Rayleigh line of figure 9.1. In this case of $k=1.4$, for example, for flows with a mach number between 0.85 and 1, heat addition reduces the stream temperatures, and cooling increases the stream temperature.

Since the conditions at $M=1$, superscripted *, are constant, the change between any two points can be obtained in the same manner as described for the Fanno-line equations in chapter 8. For example,

$$\frac{T_{02}}{T_{01}} = \frac{\left(\frac{T_0}{T_0^*}\right)_2}{\left(\frac{T_0}{T_0^*}\right)_1} \tag{9.42a}$$

and

$$\frac{s_2 - s_1}{c_p} = \left(\frac{s - s^*}{c_p}\right)_2 - \left(\frac{s - s^*}{c_p}\right)_1 \tag{9.42b}$$

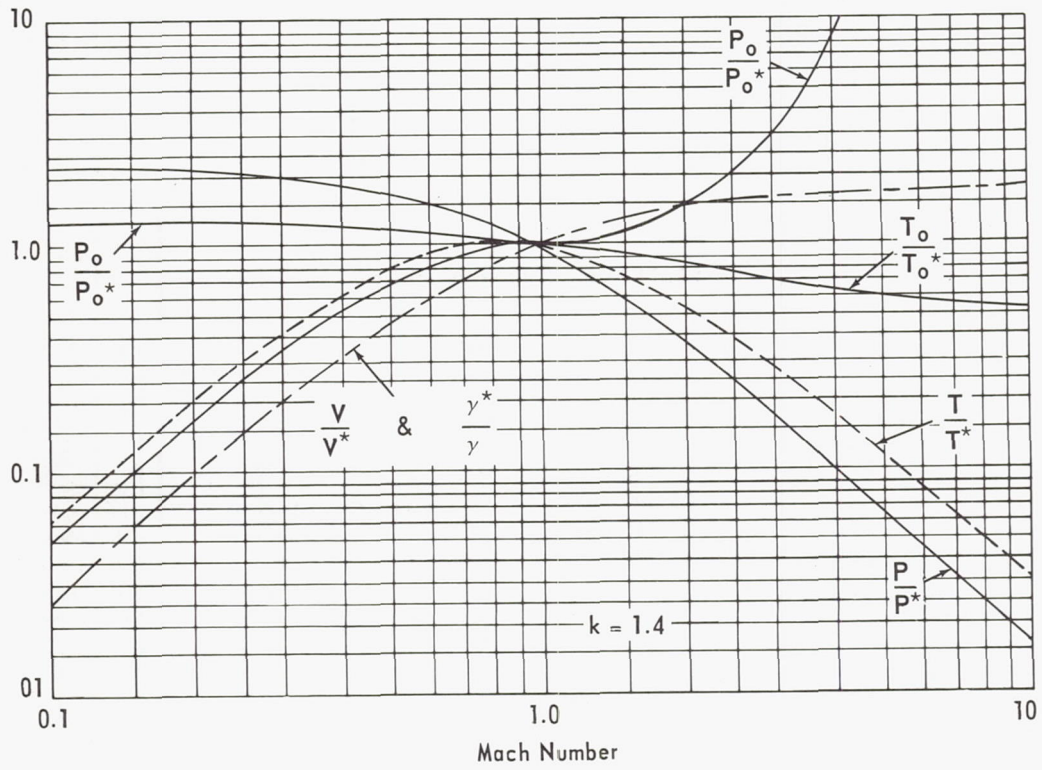


Figure 9.3. Rayleigh line equations (simple T_0 change).

A typical problem might require a calculation of the change in fluid conditions between an upstream location (designated by the subscript 1), where all the flow conditions are known, and a downstream location (designated by the subscript 2) due to heat transfer that occurs between the two locations. The solution can be obtained as follows. Compute (T_{02}/T_{01}) by equation (9.35) and read $(T_0/T_0^*)_1$ at M_1 from the tabulated or charted solution of equation (9.41). Compute $(T_0/T_0^*)_2$ by equation (9.42*a*) and read M_2 from the same solution of equation (9.41). With both M_1 and M_2 established, all the other property changes can be obtained using the known conditions. charted data, and equations of the form of equations (9.42).

Choking Effects of Heating

Although shockless supersonic pipe flow without friction can be choked by a cooling

process, the usual problems of choking due to heat transfer are associated with heating. For the case of heating a subsonic flow at constant area, the Rayleigh line requires that the mach number of the flow must increase. However, the amount of increase is limited since the exit mach number cannot exceed unity. If a greater amount of heat is transferred than that necessary to cause an exit mach number of unity, the flow will become choked and the flow rate will be reduced correspondingly so that $M=1$ at the exit. This process is analogous to the subsonic Fanno process (adiabatic frictional flow in pipes) in which the frictional length of pipe is increased beyond L_{max}, the choking length. For flow initially supersonic, heat addition reduces the flow mach number; and once again, there is a limit as a result of the limiting value of $M=1$ at the exit. Since the supersonic flow is generally supplied by a choked converging-diverging nozzle, the reduction in mach number occurs as a result of changes in fluid conditions, rather than the mass flow per unit area. The fluid condition changes result from the formation of a normal shock in the diverging section of the nozzle, which, in turn, causes the pipe flow downstream to become subsonic.

There are other interesting aspects of the simple heating flow process that include considerations of various combustion processes and condensation shocks. These topics are withheld as beyond the purpose of this handbook. Interested readers are directed to the presentations of Shapiro, 1953, for a more complete treatment of the subject.

PIPE FLOW WITH COMBINED FRICTION AND HEAT EXCHANGE

The mechanisms of friction and heat transfer are so similar that, in general, one cannot exist entirely without the other. To calculate fluid property changes in heat exchangers, for example, it is necessary to take into account heat transfer as well as friction, since the effects of both are significant. It is assumed that area, specific heat, and molecular weight are constant for the respective gas.

General Analysis

For a pipe element of infinitesimal length, dL, the rate of heat transfer is expressed by means of the energy equation in terms of the increase in stagnation enthalpy. It can also be expressed by means of the coefficient of heat transfer h_q, in terms of $(T_w - T_{aw})$.

$$w\ dQ' = \gamma A V c_p\ dT_0 = h_q\ dA_w (T_w - T_{aw}) \tag{9.43}$$

The adiabatic wall temperature T_{aw} is the wall temperature achieved with high-speed gas flow in a thermally insulated pipe. This temperature is dependent on the static temperature of the flowing gas and the mach number. The adiabatic wall temperature usually lies between T and T_0, and for subsonic flow in pipes, T_{aw} can be determined with generally acceptable accuracy as

$$T_{aw} = T\left[1 + 0.90\left(\frac{k-1}{2}\right)M^2\right]$$

For subsonic flow, the adiabatic wall temperature does not differ appreciably from the stagnation temperature, T_0. Moreover, the error in substituting T_0 for T_{aw} will be small if the wall temperature T_w is considerably in excess of T_{aw}. In the following it is assumed that this substitution is permissible, which is equivalent to the assumption that the recovery factor

is unity rather than 0.90. Substituting T_0 for T_{aw} and the definition of hydraulic diameter, $dA_w = 4A\,dL/D$, into equation (9.43) yields

$$\frac{dT_0}{T_w - T_0} = \left(\frac{4h_q}{V c_p \gamma}\right) \frac{dL}{D} \tag{9.44}$$

Equation (9.44) can be simplified further using the Reynolds analogy between the coefficients of friction and heat transfer. Experiments show that this analogy, which relates the heat-transfer and friction coefficients according to

$$\frac{h_q}{V c_p \gamma} = \frac{f}{8}$$

is accurate within a small percentage for fully developed turbulent gas flow. Substituting in equation (9.44) yields

$$\frac{dT_0}{T_w - T_0} = \left(\frac{f}{2D}\right) dL \tag{9.45}$$

The steady-flow energy equation can be applied to the pipe element yielding the following equation in the absence of work

$$dQ = dh + \left(\frac{1}{g_c J}\right) d\left(\frac{V^2}{2}\right) = dh_0 = c_p\, dT_0$$

Substituting the perfect-gas relationships and the definition of mach number yields

$$\frac{dQ}{c_p T} = \frac{dT}{T} + \left(\frac{k-1}{2}\right) M^2 \left(\frac{dV^2}{V^2}\right) \tag{9.46}$$

The isentropic stagnation temperature has been established as

$$T_0 = T\left[1 + \left(\frac{k-1}{2}\right) M^2\right]$$

which can be written in logarithmic differential form as

$$\frac{dT_0}{T_0} = \frac{dT}{T} + \left[\frac{\left(\frac{k-1}{2}\right) M^2}{1 + \left(\frac{k-1}{2}\right) M^2}\right] \frac{dM^2}{M^2} \tag{9.47}$$

In chapter 8, equations (8.1), (8.2), (8.4), and (8.5) were written for adiabatic frictional flow in pipes. These equations were based on the definitions of a perfect gas and mach number and the considerations of continuity and momentum. These equations also apply to this investigation which includes heat transfer and, when combined with equations (9.46) and (9.47) above, comprise six differential equations in eight differential variables.

A simultaneous solution of the six equations can be performed to yield the following differential relation among mach number, stagnation temperature, and frictional length

$$\frac{dM^2}{M^2}=\frac{(1+kM^2)\left[1+\left(\frac{k-1}{2}\right)M^2\right]}{1-M^2}\left(\frac{dT_0}{T_0}\right)+\left\{\frac{kM^2\left[1+\left(\frac{k-1}{2}\right)M^2\right]}{1-M^2}\right\}f\left(\frac{dL}{D}\right) \tag{9.48}$$

The coefficients of dT_0/T_0 and $f(dL/D)$ are referred to as "influence coefficients." These are only two of several that can be identified in a more general analysis that includes mass injection, work, area change, and so forth. The magnitudes of the influence coefficients reflect the strength of the effects of a given independent variable on the dependent variable, such as dM^2/M^2 in this particular case.

Equation (9.45) relates the frictional length parameter to the stagnation temperature change by a formulation of the heat transfer and use of the Reynolds analogy. Combining with equation (9.48) to eliminate $f(dL/D)$ yields

$$\frac{dM^2}{M^2}=\left\{\frac{(1+kM^2)\left[1+\left(\frac{k-1}{2}\right)M^2\right]}{1-M^2}+\left(\frac{kM^2\left[1+\left(\frac{k-1}{2}\right)M^2\right]}{1-M^2}\right)\left(\frac{2T_0}{T_w-T_0}\right)\right\}\frac{dT_0}{T_0} \tag{9.49}$$

Equations (9.45) and (9.49) provide the general means of solving the pipe-flow problems involving friction and heat transfer. Additional equations are necessary, however, to convert the solutions obtained in the form of M, T_0, and $f(L/D)$ to the other fluid properties. The necessary equations can be obtained from the perfect-gas law, continuity equation for constant flow rate and area, and the definitions of the mach number and stagnation properties.

$$\frac{P_2}{P_1}=\left(\frac{M_1}{M_2}\right)\sqrt{\frac{T_2}{T_1}} \tag{9.50}$$

$$\frac{\gamma_2}{\gamma_1}=\left(\frac{M_1}{M_2}\right)\sqrt{\frac{T_1}{T_2}} \tag{9.51}$$

$$\frac{V_2}{V_1}=\frac{\gamma_1}{\gamma_2} \tag{9.52}$$

$$\frac{T_2}{T_1}=\left(\frac{T_{02}}{T_{01}}\right)\left[\frac{1+\left(\frac{k-1}{2}\right)M_1^2}{1+\left(\frac{k-1}{2}\right)M_2^2}\right] \tag{9.53}$$

$$\frac{P_{02}}{P_{01}}=\left(\frac{P_2}{P_1}\right)\left[\frac{1+\left(\frac{k-1}{2}\right)M_2^2}{1+\left(\frac{k-1}{2}\right)M_1^2}\right]^{\frac{k}{k-1}} \tag{9.54}$$

The solution of a specific pipe-flow problem having friction and heat transfer using the above analysis requires a further specification of the heat-transfer process. The following sections will include the treatment of the cases of constant pipe-wall temperature and constant heat flux.

Constant Wall Temperature

In some practical applications the pipe-wall temperature can be assumed constant. For example, when the pipe or tube is a good thermal conductor, surrounded by a constant pressure bath of condensing vapor or a boiling liquid, the tube wall can generally be considered at the constant temperature of the bath throughout its submerged length. Then, since T_w is independent of location in the pipe, equation (9.45) can be integrated directly from the upstream pipe location (1) where $L=0$, to the downstream location where $L=L_2$, yielding

$$f\left(\frac{L_2}{D}\right)=2\ln\left(\frac{T_w-T_{01}}{T_w-T_{02}}\right)=2\ln\left(\frac{\frac{T_w}{T_{01}}-1}{\frac{T_w}{T_{01}}-\frac{T_{02}}{T_{01}}}\right) \tag{9.55a}$$

which can also be solved explicitly for (T_{02}/T_{01}) as

$$\frac{T_{02}}{T_{01}}=\frac{T_w}{T_{01}}-\left(\frac{T_w}{T_{01}}-1\right)e^{-\frac{fL_2}{2D}} \tag{9.55b}$$

Equation (9.55*a*) provides the explicit relationship between the frictional pipe length and change in stagnation temperature, when the initial conditions (at location 1) and pipe-wall temperature and friction factor are known. It can be seen from equation (9.55*b*) that for large pipe lengths, the downstream stagnation temperature approaches the wall temperature.

Evaluation of any other fluid properties at the downstream location requires a solution of equation (9.49) for the change in mach number. Equation (9.49) cannot be integrated in closed analytical form because of its complexity and must be integrated numerically or graphically with the aid of equations (9.55). Conventional methods of finite difference approximations, applied to short pipe segments, or small changes in T_0 can be used with an iterative procedure to produce an accurate solution for M_2. A digital-computer solution is recommended. Once the value of M_2 is established, all the other fluid property changes can be obtained using equations (9.50) through (9.54).

An approximate solution can be obtained in closed analytical form when the mach number is low, thereby eliminating the lengthy numerical method for the more common case of $M \leq 0.3$. It was shown previously that equations (8.1), (8.2), (8.4), and (8.5) can be applied to frictional pipe flow with heat transfer as well as to adiabatic flow. Likewise, the definitions of stagnation pressure and temperature, as written in logarithmic differential form as equations (8.6) and (9.47), also apply. The equations can be combined to produce

$$\frac{dP_0}{P_0}=-\frac{kM^2}{2}\left[\frac{dT_0}{T_0}+f\left(\frac{dL}{D}\right)\right]$$

Further substitution of dT_0 from equation (9.45) yields

$$\frac{dP_0}{P_0}=\frac{d\left(\frac{P_0}{P_{01}}\right)}{\frac{P_0}{P_{01}}}=-kM^2\left(\frac{f}{2D}\right)\left(\frac{T_w-T_0}{2T_0}+1\right)dL \tag{9.56}$$

Generalizing the downstream conditions (removing the subscript 2) and combining equations (9.50), (9.53), and (9.54) yield

$$M^2=\left(\frac{P_{01}}{P_0}\right)^2\left(\frac{T_0}{T_{01}}\right)\left[\frac{1+\left(\frac{k-1}{2}\right)M^2}{1+\left(\frac{k-1}{2}\right)M_1^2}\right]^{\frac{k+1}{k-1}}M_1^2 \tag{9.57}$$

Substituting this expression of M^2 into equation (9.56) yields

$$-\left(\frac{P_0}{P_{01}}\right)d\left(\frac{P_0}{P_{01}}\right)=\left(\frac{k}{2}\right)M_1^2\left[\frac{1+\left(\frac{k-1}{2}\right)M^2}{1+\left(\frac{k-1}{2}\right)M_1^2}\right]^{\frac{k+1}{k-1}}\frac{f}{2D}\left(\frac{T_w}{T_{01}}+\frac{T_0}{T_{01}}\right)dL \tag{9.58}$$

The left side of equation (9.58) is easily integrated, but the right side can be integrated only if simplifying assumptions can be made. Expanding the factor involving M in a binomial expansion yields

$$\left[1+\left(\frac{k-1}{2}\right)M^2\right]^{\frac{k+1}{k-1}}\approx 1+\left(\frac{k-1}{2}\right)M^2+\cdots$$

Inspection of this equation reveals that for small values of M, the function of M is nearly constant. Hence, if the function is assumed to have constant mean value over the interval of integration, the relative error in evaluating the change in P_0 will be only a small percentage if $M \lesssim 0.3$.

Integrating over the pipe length L (between locations 1 and 2) yields

$$1-\left(\frac{P_{02}}{P_{01}}\right)^2=kM_1^2\left[\frac{1+\left(\frac{k-1}{2}\right)M^2}{1+\left(\frac{k-1}{2}\right)M_1^2}\right]_{\text{avg}}^{\frac{k+1}{k-1}}\frac{f}{2D}\int_0^{L_2}\left(\frac{T_w}{T_{01}}+\frac{T_0}{T_{01}}\right)dL$$

The average value of the mach-number term is found by taking the average of the term evaluated with $M=M_1$ and $M=M_2$. When $M=M_1$, the term is unity. When $M=M_2$, the term is found to be equal to

$$\left(\frac{P_{02}}{P_{01}}\right)^2\left(\frac{T_{01}}{T_{02}}\right)\left(\frac{M_2}{M_1}\right)^2.$$

with the aid of equations (9.50) through (9.54). Then the average value

$$\left[\frac{1+\left(\frac{k-1}{2}\right)M^2}{1+\left(\frac{k-1}{2}\right)M_1^2}\right]_{\text{avg}}^{\frac{k+1}{k-1}}=\frac{1}{2}\left[1+\left(\frac{P_{02}}{P_{01}}\right)^2\left(\frac{T_{01}}{T_{01}}\right)\left(\frac{M_2}{M_1}\right)^2\right] \tag{9.59}$$

and the stagnation-pressure equation becomes

$$\left(\frac{P_{02}}{P_{01}}\right)^2=1-\left(\frac{k}{2}\right)M_1^2\left[1+\left(\frac{P_{02}}{P_{01}}\right)^2\left(\frac{T_{01}}{T_{02}}\right)\left(\frac{M_2}{M_1}\right)^2\right]\frac{f}{2D}\int_0^{L_2}\left(\frac{T_w}{T_{01}}+\frac{T_0}{T_{01}}\right)dL \tag{9.60}$$

Equation (9.55*b*) can be generalized by replacing T_{02} with the length-dependent T_0, and the pipe length L_2 with the variable pipe length L, resulting in

$$\frac{T_0}{T_{01}}=\frac{T_w}{T_{01}}-\left(\frac{T_w}{T_{01}}-1\right)e^{-\left(\frac{f}{2D}\right)L}$$

This value of T_0 can be substituted into equation (9.60) and integrated over the pipe length resulting in the following equation for stagnation-pressure ratio

$$\left(\frac{P_{02}}{P_{01}}\right)^2=1-\left(\frac{k}{2}\right)M_1^2\left[1+\left(\frac{P_{02}}{P_{01}}\right)^2\left(\frac{T_{01}}{T_{02}}\right)\left(\frac{M_2}{M_1}\right)^2\right]\left[f\left(\frac{L_2}{D}\right)\left(\frac{T_w}{T_{01}}\right)+\left(\frac{T_w}{T_{01}}-1\right)\left(e^{-\frac{fL_2}{2D}}-1\right)\right] \tag{9.61}$$

Although the equation does not define P_{02}/P_{01} explicitly and the value of M_2 remains unknown, a brief trial-and-error solution produces both unknown quantities, P_{02}/P_{01} and M_2/M_1. A first trial can be made by assuming the average value of the mach-number term of equation (9.59) to be unity. This eliminates the unknown terms of equation (9.61), and an approximate value of P_{02}/P_{01} can be computed. In the second and following trials, T_{01}/T_{02} is computed by equation (9.55*b*), P_{02}/P_{01} is that computed in the previous trial, and M_2/M_1 is obtained by equation (9.57) in which $M=M_2$, $P_0=P_{02}$, and $T_0=T_{02}$. Although equation (9.57) cannot be solved explicitly for M_2, a fortunate coincidence occurs in that the solution of the isentropic area ratio function can be used in this solution. Specifically, because of the similarity of the two functions, the value of M_2 can be established at a value of $(A/A^*)M_2$ computed as

$$\left(\frac{A}{A^*}\right)_{M_2}=\frac{\left(\frac{A}{A^*}\right)_{M_1}\left(\frac{P_{02}}{P_{01}}\right)}{\sqrt{\frac{T_{02}}{T_{01}}}} \tag{9.62}$$

The isentropic area ratios can be read directly from the plotted solutions found in chapter 16.

The iterative solution of equation (9.61) should be carried out until an acceptable agreement is reached between the assumed value of P_{02}/P_{01} and the calculated value that results. The associated value of M_2 is then correct and can be used to establish the changes in all the

other fluid properties using equations (9.50) through (9.54). The amount of heat transferred can be readily computed from the stagnation temperature change by

$$Q' = c_p(T_{02} - T_{01}) = c_p T_{01}\left(\frac{T_{02}}{T_{01}} - 1\right) \qquad \text{Btu/lbm}$$

and as a heat-transfer rate

$$\dot{Q} = wQ' \qquad \text{Btu/sec} \tag{9.63}$$

Constant Heat Flux

For this case it is assumed that the heat flux per unit pipe wall area is the same throughout the length of pipe under consideration. Such a situation can result when the pipe or tube is electrically heated. Then with constant heat flux, the heat-transfer equation (eq. (9.43)) requires that the temperature difference $(T_w - T_{aw})$, which is essentially $T_w - T_0$, must be a constant when h_q is constant. Then for constant h_q

$$T_w - T_0 = T_{w1} - T_{01}$$

and equation (9.45) becomes

$$\frac{dT_0}{T_{w1} - T_{01}} = \left(\frac{f}{2D}\right) dL \tag{9.64}$$

Equation (9.64) can be integrated directly to produce the change in stagnation temperature with distance along the pipe.

$$\frac{T_{02} - T_{01}}{T_{w1} - T_{01}} = \frac{fL_2}{2D} \tag{9.65}$$

As in the case of constant wall temperature, the mach number must be evaluated at the downstream location before the changes in all the other fluid properties can be established. Once again, equation (9.49) must be integrated numerically or graphically over the pipe length, with the aid of equation (9.65), using finite difference methods and a lengthy iterative process.

For low mach numbers, an approximate procedure can be written equivalent to that developed previously for the constant wall temperature problem. When this procedure is carried out, the following equation, equivalent to equation (9.61), is obtained.

$$\left(\frac{P_{02}}{P_{01}}\right)^2 = 1 - \left(\frac{k}{2}\right) M_1^2 \left[1 + \left(\frac{P_{02}}{P_{01}}\right)^2 \left(\frac{T_{01}}{T_{02}}\right) \left(\frac{M_2}{M_1}\right)^2\right] \left(\frac{fL_2}{2D}\right) \left[\frac{T_{w1}}{T_{01}} + \left(\frac{fL_2}{4D}\right) \left(\frac{T_{w1}}{T_{01}} - 1\right)\right] \tag{9.66}$$

The procedure for solving equation (9.66) is identical to that outlined for solving equation (9.61), including the use of the isentropic area ratio solutions.

CHAPTER 10

COMPRESSIBLE FLOW THROUGH COMPONENTS

This analysis of flow through components is directed primarily to the flow characteristics of fully open valves. The more complex variable operating characteristics of flow-control valves are beyond the scope of this handbook, although brief discussions of valve-opening characteristics and pressure regulators are presented in the next two sections.

COMPONENT PRESSURE LOSS AND FLOW CAPACITY

The pressure loss through a fixed-orifice pneumatic component, such as a fully open valve, usually cannot be established from a purely theoretical approach. The difficulty stems from the complex flow paths and the wide variations that exist in the many designs that are available. Component manufacturers have established empirical equations which describe the flow capacity of their components in terms of the pressures, pressure drop, and the gas properties. Invariably, some type of flow coefficient, which is used as a measure of the overall capacity of the component, is factored into each of the equations. Unfortunately, a relatively large number of slightly different equations has come into use that incorporates several uniquely defined flow coefficients. Lack of standardization has resulted in serious problems for pneumatic system designers. After considerable research and industry consultation, Slawsky et al. (1955) of the Pneumatics Laboratory of the National Bureau of Standards have suggested a standard for defining flow capacity and pressure drop across flow components.

The NBS Flow Factor for Air

It has been found experimentally that the standard temperature airflow characteristics of fully open valves and similar flow-restricting components can be described approximately by the expression

$$(\text{SCFM})_A = K'\sqrt{P_1^2 - P_1^2} \qquad \text{scfm of air} \tag{10.1}$$

where K' is a constant of proportionality, depending on the fluid properties, the flow path geometry, and the fluid friction offered by the component. Note that pressures are measured specifically in the common units of lbf/in.^{2} abs (psia). Defining the ratio of downstream to upstream pressure as $r = P_2/P_1$ yields

$$(\text{SCFM})_A = K' p_1 \sqrt{1 - r^2}$$

Preceding Page Blank

The experimental data also reveal that for perfect gases the empirical constant of proportionality K' is independent of the upstream absolute pressure p_1. Therefore, a K' factor which is evaluated at one pressure can be used at any pressure if the inlet air temperature is held constant. If the new pressure is sufficiently different from the tested pressure such that the compressibility factor ($Z=Pv/RT$) or the specific heat ratio of the air is changed appreciably, treatment of the gas as a real gas is recommended. The necessary corrections will be outlined subsequently along with temperature corrections. Since K' is independent of p_1, the pressure and flow terms can be combined so that

$$\frac{(\text{SCFM})_A}{p_1}=K'\sqrt{1-r^2} \qquad \text{scfm/psia}$$

Based on this equation, the flow characteristics of a component can theoretically be defined by a single, airflow test which establishes K' for the test gas at the test temperature.

When the flow test is performed with air at standard temperature (60° F) and at a pressure ratio ($r=1/2$), the value of flow rate per unit upstream absolute pressure measured at that flow condition is defined as the "National Bureau of Standards flow factor, F_q or F_w." The value of F_q represents the approximate maximum capacity of the component, using air at standard temperature as the reference gas, since the flow rate increases at pressure ratios less than one-half are generally slight. Then the constant K' can be evaluated in terms of F_q

$$K'=\frac{F_q}{\sqrt{1-\left(\frac{1}{2}\right)^2}}=F_q\sqrt{\frac{4}{3}}$$

and the characteristic flow equation for the component becomes

$$\frac{(\text{SCFM})_A}{p_1}=F_q\sqrt{\frac{4}{3}(1-r^2)} \tag{10.2}$$

The flow factor is not dimensionless and can be specified in any air mass flow rate and pressure units such as the commonly used scfm/psia for F_q and lbm/sec-psia for F_w. The conversion between standard cubic feet and mass flow units is obtained from the perfect-gas law evaluation of volume at standard temperature and pressure.

$$\bar{V}_{\text{std}}=\left(\frac{T}{P}\right)_{\text{std}}Rw$$

Then the relation between the two common units of flow rates is obtained by differentiating with respect to time and substituting the standard values of the pressure and temperature, yielding

$$\text{SCFM}=60\left[\frac{520}{(144)(14.7)}\right]Rw$$

or

$$\text{SCFM} = 14.75Rw \qquad \text{scfm} \tag{10.3}$$

It should be noted that the conversion is dependent on the gas constant R, resulting in a different conversion factor for each gas. For air, where $R = 53.36$ ft-lbf/lbm-°R

$$(\text{SCFM})_A = (14.75)(53.36)w_A$$

and

$$\frac{(\text{SCFM})_A}{w_A} = 786 \qquad \frac{\text{scfm}}{\text{lbm/sec}} \qquad \text{for air}$$

Likewise, since the flow factor F_q is defined for air only, the conversion between F units is equal to the same constant as the flow unit conversion. Then

$$F_q = 786F_w$$

These conversions can be substituted into equation (10.2) to demonstrate the general nature of the pressure ratio function.

$$\frac{(\text{SCFM})_A}{F_q p_1} = \frac{w_A}{F_w p_1} = \sqrt{\frac{4}{3}(1 - r^2)} \tag{10.4}$$

It was stated that, theoretically, the flow factor can be established by a single flow test. However, to obtain accuracy, the flow test should cover a wide range of pressure ratios, r, and the best curve of the pressure ratio function should be fitted to produce the most accurate value of F_q for the range of expected flow rates.

Extensive study of experimental data from the National Bureau of Standards has verified that equation (10.4) yields a conservative prediction of flow rates through components in that the actual pressure drop is usually equal to or slightly less than the prediction. On the opposite extreme, the following similar pressure ratio function can be used to predict the maximum flow rates at a given pressure ratio.

$$\frac{(\text{SCFM})_A}{F_q p_1} = 2\sqrt{r(1 - r)} \tag{10.5}$$

Equation (10.5) is an approximation of the isentropic flow formula and represents components which cause very little loss of stagnation pressure.

A third equation has been written which predicts flow rates between those of equations (10.4) and (10.5)

$$\frac{(\text{SCFM})_A}{F_q p_1} = \sqrt{\left(\frac{8}{5}\right) r(1 - r)(3 - r)} \tag{10.6}$$

Finally, there is a fourth empirical equation in wide use

$$(\text{SCFM})_A = 33.75 d_0^2 \sqrt{r(r^{0.43} - r^{0.71})}$$

which, when converted into the general terms of F_q, is

$$\frac{(\mathrm{SCFM})_A}{F_q p_1} = \sqrt{15.3\,(r^{1.43} - r^{1.71})} \tag{10.7}$$

Note that the NBS flow factor (F_q or F_w) is applicable to each of these equations according to its definition, since

$$\frac{(\mathrm{SCFM})_A}{p_1} = F_q$$

when

$$r = \frac{1}{2}$$

The normalized equations (10.4) through (10.7) have been plotted in figure 10.1 for comparison. Most test data fall within the band defined by equations (10.4) and (10.5). Therefore, the intermediate curve of equation (10.6) can be expected to predict flow rates and pressure drops that are as accurate as can be expected from an empirical curve applied to all fully open components in general. The reader is cautioned against overconfidence in using these equations for predicting flow through untested components. For example, it is known that for valves having low-resistance flow characteristics because of internal port sizes approaching that of the inside diameter of its associated pipe, the choking pressure ratio will be well above $r = 0.5$. Therefore, cases can be expected where the characteristic curve will fall even farther to the right on figure 10.1 than that of equation (10.7). When numerous components are connected in parallel, the combined system flow factor is determined as the sum of the flow factors of the individual components. Hence, for components connected in parallel

$$F_c = F_1 + F_2 + F_3 + \cdots$$

When equation (10.4) is used for each of a number of components connected in series, the combined flow factor F_c can also be computed for the series in terms of the individual flow factors. The series of components can then be treated as a single component, and the pressure ratio corresponds to the pressures upstream of the first component and downstream of the last component. For a two-component series, the combined flow factor can be determined from equation (10.4) to be

$$F_c = \frac{F_1 F_2}{\sqrt{F_1^2 + F_2^2}}$$

Similarly, for three and four components, respectively,

$$F_c = \frac{F_1 F_2 F_3}{\sqrt{(F_1 F_2)^2 + (F_2 F_3)^2 + (F_1 F_3)^2}}$$

and

$$F_c = \frac{F_1 F_2 F_3 F_4}{\sqrt{(F_1 F_2 F_3)^2 + (F_2 F_3 F_4)^2 + (F_1 F_3 F_4)^2 + (F_1 F_2 F_4)^2}}$$

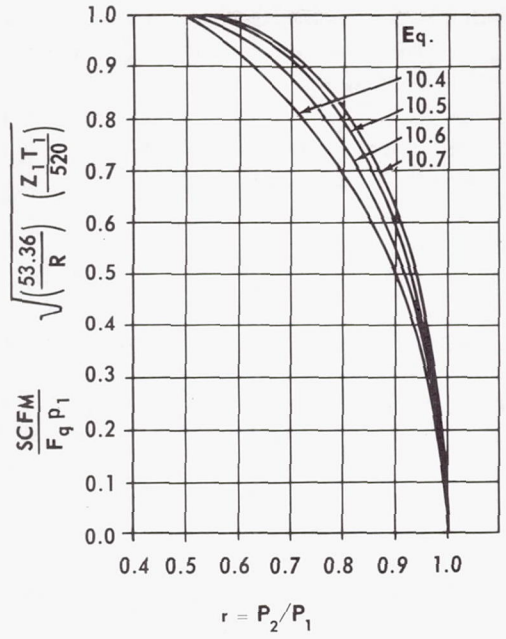


Figure 10.1. Normalized component flow characteristic curves.

Note that the arrangement of terms in each of the equations is such that F_c is independent of the order in which the components are installed. The equation for F_c can easily be extended to describe the overall flow factor for a series of any number of components.

Perfect Gases Other Than Air at Standard Temperature

Since the NBS flow factor is established for airflow at standard temperature, a means of correcting for different temperatures and for gases other than standard air is needed. While there is no exact means of correcting the empirical equations, it has been suggested that corrections developed for nozzles and orifices should be applied. In chapter 7, equation (7.11) was developed to describe isentropic flow through nozzles and orifices installed in pipes. Rearranging slightly to incorporate the area A_1 in the mass flow parameter instead of A_2, equation (7.11) becomes

$$\frac{w}{A_1 P_1}\sqrt{\frac{RT_1}{g_c}}=\left[\left(\frac{2k}{k-1}\right)\frac{r^{1/k}(r^{1/k}-r)}{\beta^{-4}-r^{2/k}}\right]^{1/2}=f_1(r, k, \beta)$$

Likewise, the direct graphic solutions of frictional adiabatic pipe flow derived in chapter 8 indicate the existence of a complex but explicit relationship involving the same dimensionless flow parameter.

$$\phi_1=\frac{w}{A_1 P_1}\sqrt{\frac{RT_1}{g_c}}=f_2\left[r, k, f\left(\frac{L}{D}\right)\right]$$

In each of these adiabatic flow cases, the flow parameter varies with pressure ratio, specific heat ratio, and a geometrical factor which describes the flow path. If the adiabatic flow through components is assumed to be affected by changes in the gas constant and upstream temperature in the same manner as is shown analytically for adiabatic nozzles and pipes, then the same simple corrections can be applied to the component flow equation for standard temperature air, which was written as

$$\frac{(\text{SCFM})}{F_q p_1} = \frac{w_A}{F_w p_1} = f(r)$$

In this empirical equation, the flow area and geometrical factor are combined into the NBS flow factors F_q and F_w, and k is not represented at all.

The correction for different gas constants and changes in upstream temperature can be determined for any given upstream pressure and fixed values of k, r, and the geometrical factor. Note that with either the nozzle equation or pipe flow equation

$$w\sqrt{RT_1} = (w\sqrt{RT_1})_{\text{any ref gas}} = \text{constant}$$

Applying this to component flow by substituting the expression for w_A yields

$$w\sqrt{RT_1} = (w_A\sqrt{R_A T_1})_{\text{std temp air}} = [F_w P_1 f(r)]\sqrt{(53.36)\,(520)}$$

so that

$$\left(\frac{w}{F_w}\right)\left(\frac{1}{p_1}\right)\sqrt{\left(\frac{R}{53.36}\right)\left(\frac{T_1}{520}\right)} = f(r) \tag{10.8}$$

for any perfect gas having the same value of k as air (1.4). Since the specific heat ratio term does not exist in the empirical component flow equation, corrections for variations in k cannot be made. This discrepancy is not considered serious, however, except in the high pressure-drop range. Only here have changes in k been found to be effective with adiabatic nozzles and adiabatic pipe flow. Also, because of the approximate nature of the empirical equations associated with the NBS flow factor, a rigorous evaluation of the small effects of changes in k is not justified except in cases of conditions that approach choked flow in the component.

Equation (10.8) can be converted to units of scfm by substituting equation (10.3) and the associated relationship

$$\frac{F_q}{F_w} = \frac{(\text{SCFM})_A}{w_A} = (14.75)\,(53.36)$$

which yields the general expression for SCFM

$$\frac{\text{SCFM}}{F_q}\left(\frac{1}{p_1}\right)\sqrt{\left(\frac{53.36}{R}\right)\left(\frac{T_1}{520}\right)} = f(r) \tag{10.9}$$

Note that the conversion from mass flow rate units to units of standard volumetric flow rate (which is also a mass flow rate) inverts the gas constant ratio under the radical. The

gas constant ratio can also be converted to ratios of specific gravity (relative to air) or molecular weight since

$$S_A=\frac{R_A}{R}=\frac{\gamma}{\gamma_A}=\frac{M_w}{M_{w_A}} \tag{10.10}$$

Real-Gas Effects

When gases are used at high pressure and/or at low temperature, the behavior is not accurately described by the perfect-gas law. Therefore, the corrections derived from the exact flow relationships for adiabatic nozzles and pipe flow must be further modified to account for the real-gas effects. A detailed analysis of real-gas effects on pipe flow can be found in chapters 4 and 8. Specifically, if the real-gas effects on the flow characteristics of components are assumed to be the same as the effects on the flow characteristics of nozzles and pipes, then the same modifications can be applied to the empirical relationships of equations (10.8) and (10.9). Therefore, just as equations (8.55*a*) and (8.55*b*) of chapter 19 were modified for real gases to produce equations (8.55*f*) and (8.55*g*), equations (10.8) and (10.9) modified for real gases with the compressibility factor become

$$\left(\frac{w}{F_w p_1}\right)\sqrt{\left(\frac{Z_1 R}{53.36}\right)\left(\frac{T_1}{520}\right)}=f(r) \tag{10.11}$$

and

$$\frac{\text{SCFM}}{F_q p_1}\sqrt{\left(\frac{53.36}{R}\right)\left(\frac{Z_1 T_1}{520}\right)}=f(r) \tag{10.12}$$

The function $f(r)$ still represents any of the four functions defined by equations (10.4) through (10.7). The means for accounting for any gas other than air at standard temperature is seen to involve only a generalization of the flow parameter. The variation of the isentropic exponent k_s for real gases, which is usually accounted for as the additional variable in the pressure ratio function, is neglected once again as was k with perfect gases. The error involved is not expected to be significant for the usual range of pressure ratios which are greater than approximately 0.85. When accurate pressure-drop characteristics are required for untested components, especially those intended for service at very high pressure and/or low temperature, actual testing of the components is recommended. The tests should be performed, preferably, with the gas to be used and at gas conditions that duplicate as closely as possible the expected operating conditions.

Conversion Factors Relating Flow Coefficients

There are three widely used flow coefficients that are different from the NBS flow factor, F_q or F_w. These three—C_v, d_0, and K—which will be defined in order, describe the major portion of available components. Only conversions between these and the NBS factor will be examined here.

C_v is a coefficient based on incompressible fluid flow and is defined as the rate of flow of 60° F water, in gallons per minute, that will exist in the component with a differential pressure of 1 psid across the component. C_v is based on the water flow formula

$$(\text{GPM})_W=C_v\sqrt{p_1-p_2}$$

or

$$(\text{GPM})_W = C_v\sqrt{p_1(1-r)} \qquad \text{gpm of } 60^\circ \text{ F water} \tag{10.13}$$

For incompressible flow of any fluid, the volumetric flow rate can be obtained from the Bernoulli equation, modified by the flow coefficient, as in chapter 7. Writing equation (7.15) in terms of volumetric flow rate yields

$$q = AK_c\sqrt{2g_c\left(\frac{144\Delta p_L}{\gamma}\right)} \qquad \text{ft}^3/\text{sec}$$

In terms of gallons per minute,

$$\text{GPM} = (q,\ \text{ft}^3/\text{sec})\,(7.48,\ \text{gal}/\text{ft}^3)\,(60,\ \text{sec}/\text{min})$$

or

$$\text{GPM} = 448.8(q) \qquad \text{gpm}$$

Then by substitution, for any incompressible fluid,

$$\text{GPM} = 12(448.8)AK_c\sqrt{2g_c\left(\frac{\Delta p_L}{\gamma}\right)} \qquad \text{gpm}$$

The ratio of airflow (A) to water flow (W) for a given component, Δp_L, and discharge coefficient is, in terms of gpm,

$$\frac{(\text{GPM})_A}{(\text{GPM})_W} = \sqrt{\frac{\gamma_W}{\gamma_A}} = \sqrt{\frac{\gamma_W R_A T_1}{P_1}}$$

and

$$(\text{GPM})_A = \sqrt{\left(\frac{\gamma_W R_A T_1}{p_1}\right)}\,(\text{GPM})_W$$

Substituting equation (10.13) for $(\text{GPM})_W$ and converting P to p yield

$$(\text{GPM})_A = \sqrt{\frac{\gamma_W R_A T_1}{144 p_1}}\,C_v\,\sqrt{p_1(1-r)}$$

or

$$(\text{GPM})_A = \frac{C_v}{12}\sqrt{\gamma_W R_A T_1(1-r)} \qquad \text{gpm}$$

This flow is converted to units of scfm by

$$(\text{SCFM})_A = [(\text{GPM})_A,\ \text{gal/min}]\left(\frac{1}{7.48},\ \text{ft}^3/\text{gal}\right)\left(\frac{\gamma_A}{\gamma_{A_{\text{std}}}},\ \frac{\text{lbm}/\text{ft}^3}{\text{lbm}/\text{ft}^3_{\text{std}}}\right)$$

where, from the perfect-gas law,

$$\frac{\gamma_A}{\gamma_{A_{std}}} = \left(\frac{P_1}{P_{std}}\right)\left(\frac{T_{std}}{T_1}\right) = \left(\frac{p_1}{p_{std}}\right)\left(\frac{T_{std}}{T_1}\right)$$

The conversion is being performed for the NBS flow factor defined for air at standard temperature only. Therefore,

$$T_1 = T_{std} = 520^\circ \text{ R} \qquad \text{and} \qquad \frac{T_{std}}{T_1} = 1$$

Finally,

$$(\text{SCFM})_A = \left(\frac{1}{7.48}\right)\left(\frac{p_1}{p_{std}}\right)\left(\frac{C_v}{12}\right)\sqrt{\gamma_W R_A T_1 (1-r)} \qquad \text{scfm}$$

Then for $T_1 = 520^\circ$ R and $\gamma_W = 62.4$ lbm/ft^3

$$(\text{SCFM})_A = p_1\left(\frac{C_v}{12}\right)\left[\frac{1}{(7.48)(14.7)}\right]\sqrt{(62.4)(53.36)(520)(1-r)}$$

or

$$(\text{SCFM})_A = 0.997 C_v p_1 \sqrt{1-r} \qquad \text{scfm of air at } 60^\circ \text{ F} \tag{10.14}$$

By the definition of F_q

$$(\text{SCFM})_A = p_1 F_q f(r)$$

where $f(r)$ can be any of the functions defined by equations (10.4) through (10.7). Equating the two expressions yields the conversion between the NBS flow factor and the C_v factor established from water flow tests.

$$\frac{F_q}{C_v} = 0.997\left(\frac{\sqrt{1-r}}{f(r)}\right) \tag{10.15}$$

Before equation (10.15) can be used, a decision must be reached regarding the pressure ratio at which the compressible and incompressible equations should be tied together. In accordance with the NBS convention, all functions $f(r)$ must have a value of 1.0 at $r = 1/2$, since a given component should flow a fixed quantity of fluid per unit upstream pressure at that pressure ratio, regardless of the function used to describe it. On this erroneous basis, the reference pressure ratio for use in equation (10.15) should be $r = 0.5$, and the corresponding value of $f(0.5)$ will be unity, regardless of the function used. Then

$$\left(\frac{F_q}{C_v}\right) = 0.997\left(\frac{\sqrt{1-0.5}}{1}\right)$$
$$= 0.705$$

The use of this conversion factor with all the empirical functions will result in their uniform, but erroneous, prediction of like flow capacity at $r=1/2$ for a given C_v value. Also, this flow capacity will correspond with that predicted by the incompressible equation (10.14), which is not accurate in predicting airflow at $r=1/2$.

Equation (10.14) and, therefore, equation (10.15) also are valid only when the value of r is set to unity, since equation (10.14) was derived on the basis of an incompressible fluid only. In effect, the two equations tie together the compressible flow equation and the incompressible flow equation, and these relationships can be simultaneously valid only in the low pressure-drop region, where r is essentially unity.

It is also evident from equation (10.15) that, on this basis, the conversion between F_q and C_v is dependent on the particular empirical pressure ratio function assumed for the component flow characteristic. For the relationship of equation (10.4)

$$\left(\frac{F_q}{C_v}\right)=0.997\left.\frac{\sqrt{1-r}}{\sqrt{\left(\frac{4}{3}\right)(1-r^2)}}\right|_{r=1}$$

$$=0.997\left.\frac{\sqrt{1-r}}{\sqrt{\left(\frac{4}{3}\right)(1-r)(1+r)}}\right|_{r=1}$$

and

$$\left(\frac{F_q}{C_v}\right)=0.6105 \tag{10.16a}$$

Similarly, for equations (10.5), (10.6), and (10.7), respectively,

$$\left(\frac{F_q}{C_v}\right)=0.4985 \tag{10.16b}$$

$$\left(\frac{F_q}{C_v}\right)=0.5580 \tag{10.16c}$$

$$\left(\frac{F_q}{C_v}\right)=0.482 \tag{10.16d}$$

The conversions from the equivalent orifice diameter, d_o, and the head loss factor, K, can be done in a similar fashion. However, since these factors are also derived from water flow tests, they can be related directly to an equivalent value of C_v. This equivalent C_v is then converted to F_q by means of equations (10.16a) through (10.16d).

It was shown in the preceding development that for any incompressible fluid

$$\text{GPM}=12\,(448.8)AK_c\sqrt{2g_c\left(\frac{\Delta p_L}{\gamma}\right)} \qquad \text{gpm}$$

The equivalent orifice of diameter d_o is measured in inches and is based on an assumed flow coefficient K_c. Then for convenience, consider water flowing at 60° F

$$(\text{GPM})_W = 12\,(448.8)K_c\left(\frac{\pi}{4(144)}\right)\sqrt{\frac{2(32.2)}{62.4}}_{o}(d^2)\sqrt{\Delta p_L}$$

$$= 29.8K_c\, d_0^2\sqrt{\Delta p_L} \qquad \text{gpm}$$

Also, by the definition of C_v,

$$(\text{GPM})_W = C_v\sqrt{\Delta p_L}$$

Equating the two separate equations yields the conversion factor

$$C_v = 29.8K_c\, d_0^2$$

Since the general practice is to define the equivalent orifice as one with a flow coefficient of $K_c = 0.60$, the conversion factor becomes

$$C_v = 17.9d_0^2 \tag{10.17}$$

The direct conversion between d_0 and F_q is obtained by substituting the expression for C_v into equations (10.16).

The head loss factor K, which can also be written in terms of an equivalent pipe length and the fully turbulent friction factor $K = f(L/D)$, can be related to C_v by a similar procedure. By definition, for incompressible flow

$$K = f(L/D) = \frac{\Delta P_L}{\frac{\rho V^2}{2}} = \frac{144\Delta p_L}{\frac{\gamma V^2}{2g_c}}$$

Substituting $V = q/A$ and solving for q yields

$$q = 12A\sqrt{\frac{2g_c\Delta p_L}{\gamma K}} \qquad \text{ft}^3/\text{sec}$$

Using the previously developed relationship $\text{GPM} = 448.8(q)$, the foregoing expression is rewritten as

$$\text{GPM} = 12(448.8)A\sqrt{\frac{2g_c\Delta p_L}{\gamma K}}$$

For 60° F water, $\gamma = 62.4$ lbm/ft^3 and

$$(\text{GPM})_W = 12(448.8)A\sqrt{\frac{2(32.2)\Delta p_L}{62.4K}}$$

or

$$(\text{GPM})_W = 5472 \frac{A}{\sqrt{K}} \sqrt{\Delta p_L}$$

Equating this to the definition of C_v yields the conversion

$$C_v = 5472 \left(\frac{A}{\sqrt{K}} \right)$$

and in terms of the inside diameter of a circular pipe D measured in inches

$$C_v = 29.8 \frac{D^2}{\sqrt{K}} = 29.8 \left[\frac{D^2}{\sqrt{f \left(\frac{L}{D} \right)}} \right] \tag{10.18}$$

Note that the flow area A (or the pipe inside diameter D) on which K is empirically based must be known before the conversion can be made to any of the other flow factors. K is generally based on the inside diameter of the pipe to which the component is connected. Equation (10.18) can also be substituted into equation (10.16) to obtain the direct conversion between K and F_q.

Combining equations (10.17) and (10.18) produces the direct relation between d_o and K.

$$d_o = 17.48 \frac{\sqrt{A}}{(K)^{1/4}} = 1.29 \left[\frac{D}{(K)^{1/4}} \right] \tag{10.19}$$

Other well-defined flow coefficients can be converted to F_q by similar procedures. It is especially desirable to convert all flow coefficients of a group of series-connected components to the NBS flow factor. If this is done, the combined system flow factor F_c, based on the pressure ratio function of equation (10.4), can be computed and the whole series can then be treated as a single unit.

Component flow and capacity coefficients are subject to wide variations even among components of the same general type. Coefficients taken from several sources are tabulated in chapter 14. When a need exists for great accuracy in predicting pressure drop and flow capacity, the components should be subjected to testing at conditions which closely duplicate the important flow conditions. When less accuracy is required, the tabulated values are recommended. The wide variation found in the tabulated values indicates that good engineering judgment should be exercised in selecting values so that realistic, but conservative, predictions will result. Valve-flow factors should be obtained from the manufacturer whenever possible.

Component Equivalence With Frictional Pipes

An additional method of correlating the compressible flow characteristics of components lies in the possible equivalence with some specific length of adiabatic frictional pipe. A similar procedure is widely accepted for the analysis of incompressible flow, in which the component head loss factors and flow coefficients are expressed as equivalent lengths of

straight pipe, to which the completely turbulent friction factor must be applied, $K=f(L/D)$. These correlations have been demonstrated in chapter 3 and in this chapter in the paragraph describing flow coefficient conversions. In fact, the incompressible flow factors [$K, f(L/D)$, C_v and d_o] have already been applied to the compressible flow problem in terms of the NBS flow factor and the four associated pressure ratio functions (eqs. (10.4) through (10.7)). These applications of the incompressible flow coefficients to the compressible flow problem are considered acceptable because the factors were assumed equivalent only in the incompressible flow range (where the compressible flow pressure ratio is essentially unity and the flow is essentially zero).

It will now be shown that the use of the direct graphic solutions, developed in chapter 8 for the compressible flow in pipes, merely substitutes the more rigorous pressure ratio functions in place of the strictly empirical component flow functions of equations (10.4) through (10.7). The exact equivalence in the incompressible flow regime (pressure ratios near unity) between the ϕ_1 charts of chapter 19 and incompressible flow theory can be proven as follows. For incompressible flow

$$\Delta P_L = P_1 - P_2 = P_1\left(\frac{1-P_2}{P_1}\right) = \left[f\left(\frac{L}{D}\right)\right]\frac{\rho V^2}{2} = \left[f\left(\frac{L}{D}\right)\right]\frac{\gamma V^2}{2g_c}$$

By substituting V from the continuity equation $V=w/\gamma A$, and rearranging, the incompressible flow equation can be written precisely in terms of the compressible flow parameter

$$\phi_1 = \left(\frac{w}{AP_1}\right)\sqrt{\frac{P_1 v}{g_c}} = \frac{w}{A}\sqrt{\frac{1}{g_c P_1 \gamma}} = \sqrt{\frac{2\left(1-\frac{P_2}{P_1}\right)}{f\left(\frac{L}{D}\right)}} \approx \sqrt{\frac{2\Delta P_L}{P_1\left[f\left(\frac{L}{D}\right)\right]}} \tag{10.20}$$

Superimposing a plot of equation (10.20) on the logarithmic charts of ϕ_1 in chapter 19 reveals that the incompressible data plot into a straight line having a slope of exactly two. The straight lines are also found to coincide exactly with the compressible pipe flow solutions in the high pressure ratio (incompressible) region of the charts. Therefore, the flow coefficient $f(L/D)$, as used in the incompressible flow equation, is seen to be equivalent to the compressible frictional length parameter (described by the same symbols) as it occurs in the more complex compressible-flow solutions for adiabatic pipes.

Then, in the incompressible flow range, the flow-versus-pressure-drop predictions obtained from the incompressible flow theory, the empirical compressible flow functions associated with the NBS flow factor, and the compressible pipe flow charts are all identical and valid. However, as the pressure drop and flow are increased, the compressible flow solutions for a given $f(L/D)$ deviate from the straight-line variation (on the logarithmic ϕ_1 plot) with increasing slope, which accounts for the increasing velocity, and the slope becomes infinite at the point of choking. The point of infinite slope occurs with the empirical formulas of equations (10.4), (10.5), and (10.6) at pressure ratios $P_2/P_1=0$, 0.5, and 0.451, respectively. A study of the ϕ_1 charts indicates that the choking-pressure ratio for pipes is a variable depending strongly on the value of $f(L/D)$ and the specific heat ratio. Specifically, the choking-pressure ratio decreases with increases in either (or both) $f(L/D)$ and k. It can also be shown that the lines of constant $f(L/D)$ approach the straight lines (incompressible)

325-994 O-69—15

of equation (10.20) as a limit, as k, or the isentropic exponent k_s (for real gases) is increased to large values.

Although the direct application of the pipe flow charts to component flow is expected to yield satisfactory correlations well into the compressible flow regimes, great accuracy cannot be expected at conditions approaching the point of choking and beyond. This is because of the usual existence of a reduced flow area somewhere in the component which will choke at a lower flow rate than that of an equivalent constant-area pipe. The choking-pressure ratio is primarily dependent on the minimum flow area within the component relative to the flow area of the connecting piping, as in the case of smooth nozzles, and also on the pressure-recovery characteristics afforded by the flow-path geometry downstream of the minimum area. The choking-pressure ratio should not be expected to be as well defined as that of smooth nozzles as a result of the pressure recovery within the component and the possible variation in flow-stream contraction. Stream contraction downstream of the minimum area, as occurs with choked sharp-edged orifices at the vena contracta, may have a significant effect on the compressible flow characteristics of components near and above the apparent choked flow conditions.

The equivalent pipe-length method using the ϕ_1 charts offers additional advantages by providing established means for compensating for the variation in specific heat ratio and the real-gas effects experienced at high pressures, as discussed in chapters 4 and 8. The method also permits the component to be included in a pipeline analysis simply as additional pipe.

Based on the above discussion, the equivalent pipe-length method of correlating the compressible flow characteristics of fully open components, such as valves, consists of the direct application of the graphic solutions for compressible pipe flow developed in chapter 8. Application should be limited to flow rates which are significantly less than that which will cause choking in the minimum flow area region of the component. This choking flow rate may be considerably less than that predicted for straight pipes, as indicated by the choked flow lines on the ϕ_1 charts. The component flow parameter, written in the most general form to include real-gas effects, is the same as equation (8.55) of chapter 19. Repeating,

$$\phi_1 = (\sqrt{k})\, M_1 = \frac{w}{AP_1}\sqrt{\frac{Z_1RT_1}{g_c}} = 0.2245\left(\frac{w}{P_1D^2}\right)\sqrt{Z_1RT_1} \tag{10.21a}$$

and in terms of standard cubic feet per minute

$$\phi_1 = 15.21\left(\frac{\text{SCFM}}{1000\, p_1D^2}\right)\sqrt{\frac{Z_1T_1}{R}} \tag{10.21b}$$

where A and D are that of the connecting piping.

The values of equivalent $f(L/D)$ can be obtained by rearranging the flow coefficient conversions developed previously as equations (10.16a), (10.17), (10.18), and (10.19).

$$f\left(\frac{L}{D}\right)k = 332\left(\frac{D^4}{F_q^2}\right) = 890\left(\frac{D^4}{C_v^2}\right) = 2.77\left(\frac{D}{d_o}\right)^4 \tag{10.22}$$

Then, at a given upstream flow condition identified by equations (10.21), and the equivalent frictional length parameter obtained from equation (10.22) for the component, the downstream-to-upstream pressure ratio is read directly on the appropriate ϕ_1 chart selected on the basis of k or k_s.

Repeating an earlier statement for emphasis, when very accurate pressure-drop characteristics are required for components, especially when intended for service at very high pressure, actual flow tests should be performed. Preferably, the tests should be performed at conditions that accurately duplicate the important flow conditions in every respect. The test data reduction to the general form of the ϕ_1 charts is recommended so that any equivalence with straight pipe can be identified, and so that the generalized characteristics can be applied to other gases and flow conditions.

VALVE OPENING FLOW CHARACTERISTICS

Valves are often designed to provide a special characteristic curve of flow versus position of the valve stem or operator. These valves are generally of the globe valve configuration consisting of an orifice which is closed by insertion of a stem-mounted plug. The flow through the partially open valve is controlled by providing a shaped extension to the plug so that the flow is throttled through the annular space between the shaped plug and the orifice port. The shape of the plug extension establishes the flow characteristics of the valve as shown on figure 10.2.

Linear Valves

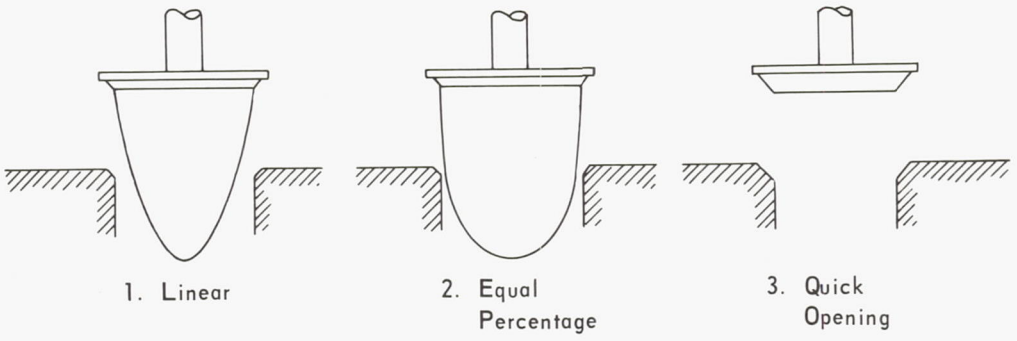
The plug contour of a valve having linear characteristics is shown as sketch 1 of figure 10.2. The associated characteristic curve of flow-versus-plug travel is curve 1 on the accompanying graph. The flow is seen to be directly proportional to the stem travel from the closed position.

Equal Percentage Valves

Sketch 2 describes a plug extension which will produce equal percentage changes in flow for a given increment of stem travel, regardless of the particular initial position (except for positions very near the closed position). The percentage changes are based on the flow at the initial valve position, and are not percentages of the fully open flow capacity. By defining the variable flow capacity C, as the fraction of the fully open capacity C_v, and the stem travel x, as the fraction of the maximum stem travel, the flow characteristic of the equal percentage valve is defined mathematically as

$$\frac{dC}{C} = K' \, dx \tag{10.23}$$

Mathematically, such a valve will never close completely, so the characteristic curve of a practical design is interrupted near the closed position by placing a shoulder and seat on the plug which affords a quick closure from that point. The constant of proportionality, defined here as K', relates the incremental percentage change in C with the incremental change in position dx. The value of K' will be established by the selection of any arbitrary lower end point (C_0, x_0) of the characteristic curve. Since the curve must pass through the



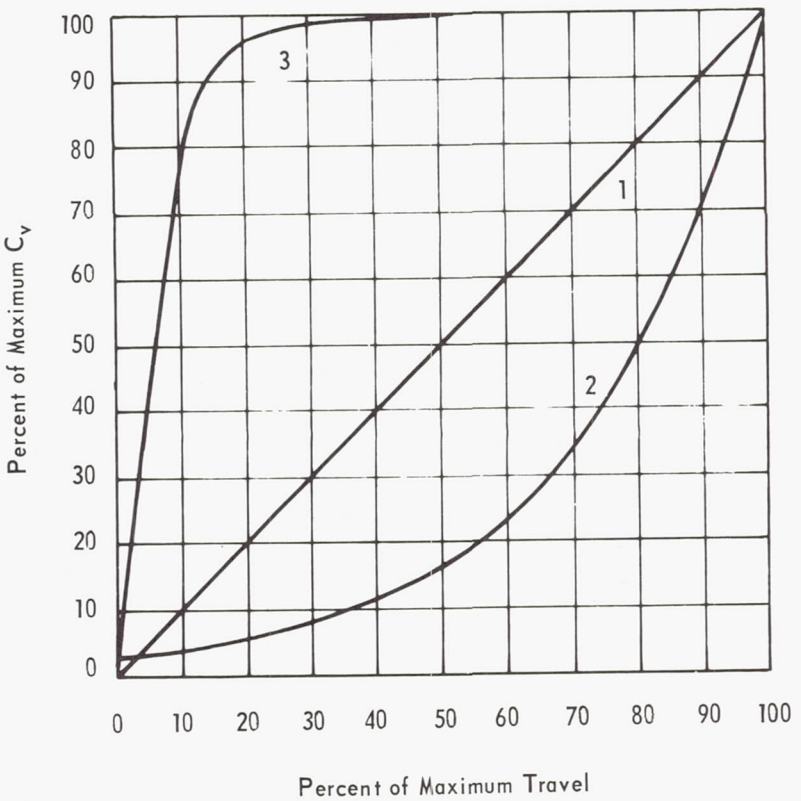


Figure 10.2. Valve opening flow characteristics.

100-percent value of each, C and x, the upper limits of integration of equation (10.23) are established as unity. Then

$$\int_C^1 \frac{dC}{C} = K' \int_x^1 dx$$

Then, integrating

$$\ln\left(\frac{1}{C}\right) = K'(1-x) \qquad \text{and} \qquad \ln C = K'(x-1)$$

At the lower end point (C_0, x_0),

$$\ln C_0 = K'(x_0 - 1)$$

so that

$$K' = \frac{\ln C_0}{x_0 - 1}$$

Therefore,

$$\ln C = \left(\frac{x-1}{x_0-1}\right) \ln C_0 = \ln (C_0)^{(x-1/x_0-1)}$$

and

$$C = C_0^{(x-1/x_0-1)} = C_0^{(1-x/1-x_0)} \tag{10.24}$$

The position-dependent valve coefficient is then

$$C_v(x) = CC_v = C_v C_0^{(1-x/1-x_0)} \tag{10.25}$$

Curve 2 of figure 10.2 is a plot of equation (10.24) with $x_0 = C_0 = 0.03$. Valves having equal percentage characteristics provide uniform flow sensitivity to stem movements over the entire range of stem travel beyond x_0. Equal percentage characteristics are desirable for precise flow control and in applications where large and fast changes in valve flow rate must be avoided.

Quick-Opening Valves

The plug of a quick-opening valve has no plug extension, and a typical plug of this type is shown in sketch 3. A characteristic flow curve is identified as curve 3 which shows the rapid rate of increase in flow with stem travel. The initial portion of the curve is linear and reflects the straight-line variation of flow area with plug displacement from the seat. For this configuration, where the flow area of the entrance channel is equal to the area of the orifice formed by the valve seat, a plug displacement of one-fourth the seat diameter will provide a flow area equal to that of the wide open orifice. Plug movement beyond that point increases flow only slightly.

Plug extensions can be shaped to provide a variety of characteristics, depending on the particular application. It should be noted that the characteristics are often based on the water flow test for C_v. Therefore, any application of such valves to compressible flow circuits must be subjected to a consideration of the complexities of converting the C_v factor to the compressible flow characteristics described in "Component Pressure Loss and Flow Capacity."

PRESSURE REGULATORS

Pressure regulators are specialized apparatus that perform an active role in pneumatic systems. As the name implies, pressure regulators are generally used to produce automatically a constant (regulated) pressure gas source, over a wide range of flow rates, from a source of higher and variable pressure.

Operation

Pressure regulators consist of three functional elements: the restricting element, the measuring element, and the loading element.

The restricting element throttles the flow in varying degrees to produce the required flow with fixed downstream pressure. This element is often of the same general configuration as a globe valve with variable stem (or plug) position.

The measuring element senses the downstream pressure and feeds back this pressure information in terms of a mechanical force acting on the movable stem of the restricting element. Downstream pressure tends to close the valve of the restricting element, usually by means of the diaphragm or piston of the measuring element.

The loading element provides a mechanical force that opposes the force of the measuring element. The loading force can be provided by a deadweight, a spring, an independently provided pressure acting on a diaphragm or piston, and so forth. The loading element is usually designed so that the loading force is essentially constant during normal operation, yet is adjustable to suit particular applications.

The measuring element tends to close the valve, and the loading element tends to open the valve. In steady-state flow operation the two opposing forces are just balanced, as required to maintain the valve stem motionless in a partially open position. In the better regulator designs, the variable differential pressure forces acting on the restricting element (plug) are counterbalanced separately so that these otherwise unbalanced forces will not affect the position of the stem. The restricting element is then free to virtually float throughout the entire range from full closed to full open, with corresponding variation in flow rate, while always maintaining the balanced condition between the loading and measuring elements. Then any imbalance that occurs between the constant loading force and the opposing force developed by the measured outlet pressure will cause valve-stem movement in the direction necessary to restore the balance. For example, a decrease in outlet pressure, caused by an increase in flow demand downstream, opens the valve to whatever position necessary to restore the outlet pressure and rebalance the regulator forces at the increased flow rate.

Flow Characteristics

The fully open flow characteristics of a regulator can be plotted in the same manner as that of ordinary valves, as shown in figure 10.3 in the most general form. The partially open flow curves are even subdivisions of the 100-percent-capacity curve. Therefore, if the partial open-flow characteristics of the plug are known from a plot such as figure 10.2, the actual plug position can also be established.

For given upstream conditions and flow rate, the plotted flow parameter can be computed. For a constant upstream pressure, the pressure ratio P_2/P_1 will remain constant due to the action of the regulator in maintaining P_2 constant. Therefore, the operation of the regulator with constant upstream conditions will be described ideally by a vertical line on figure 10.3,

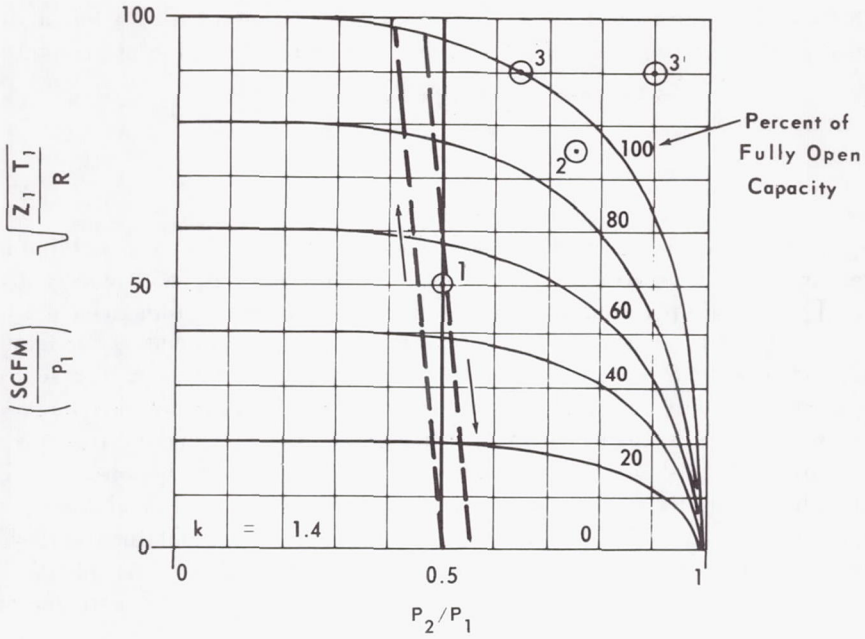


Figure 10.3. Pressure regulator flow characteristics.

as shown. If the upstream pressure is reduced, the operating line must be shifted to the right, reflecting the change in P_1 and (P_2/P_1). Also, if the mass flow rate and the other upstream conditions are held constant, the change in P_1 causes the operating point to be at a higher value of the flow parameter as well. Therefore, reducing the upstream pressure shifts the operating point up and to the right, causing the regulator to operate nearer its full capacity, even though the mass flow rate is unchanged. This important characteristic will be demonstrated by the following example using the hypothetical curves of figure 10.3.

Assume the regulator is flowing 50 percent of the maximum capacity flow (based on $P_2/P_1 = 0$) with an upstream pressure of 6000 psia and a regulated downstream pressure of 3000 psia. The operating point, 1, occurs on the line at $P_2/P_1 = 0.5$ and at about 52 percent of full capacity at that pressure ratio. Now assume that the upstream pressure falls to 4000 psia, and all other conditions, including flow rate, remain unchanged. The change in P_1 increases (P_2/P_1) to 0.75, since the outlet pressure remains constant and increases the generalized flow parameter by a factor of 6000/4000 to a value of 75. The relatively small variation in Z and k for a real gas is neglected for simplicity. The new operating conditions, point 2, require the regulator to operate at about 90 percent of its capacity, even though the mass flow rate and downstream conditions are largely unchanged.

If the upstream pressure falls to 3333 psia with unchanged flow rate, the flow parameter is increased to a value of 90, and the regulated pressure ratio should be 0.90. However, note that this operating point, 3, falls outside the maximum capacity curve. Consequently, the regulator cannot regulate at these flow conditions, and if the flow rate is still maintained

constant, the actual operating point, 3, will occur on the maximum capacity line at an unregulated value of P_2/P_1. In this case, $P_2/P_1 = 0.65$. The unregulated outlet pressure is

$$P_2 = 0.65(3333)$$
$$= 2167 \text{ psia}$$

which is less than the set pressure of 3000 psia.

The operating curve on figure 10.3 has been drawn ideally as a vertical line indicating perfect pressure regulation over the entire range of flow capacity with constant upstream conditions. The actual operating line usually deviates somewhat from the ideal in various ways depending on the particular design. For example, if the loading element consists of a spring, the loading forces decrease with stem displacement from the seat at a rate dependent on the spring constant. Therefore, the loading force, and consequently the outlet pressure, decreases slightly with increased flow rate causing the operating line, as plotted on figure 10.3, to slant slightly to the left with a high negative slope.

Frictional forces acting on the stem cause the operating lines obtained during increasing flow processes to lie at a slightly lower value of P_2/P_1 than those obtained with decreasing flow processes. The resulting curves are similar to hysteresis curves that identify a narrow range or deadband of outlet pressures that can result with an actual regulator at a given setting.

Flow Capacity

The flow capacity of regulators is best determined from the various manufacturers' sizing charts since designs vary widely, and the quoted flow factors are often not standardized nor well defined. In general, the charts are constructed so that the chart can be entered at the most difficult fluid flow conditions (highest flow rate at lowest upstream pressure) to identify the model and orifice size required for the particular application.

CHAPTER 11

THERMODYNAMICS OF PRESSURE VESSELS

The most frequently used approach to the problem of determining the state of a gas in a tank undergoing either a charging or discharging operation is to obtain expressions for the state of the fluid from a pure thermodynamic analysis that excludes the complication of heat transfer. In many cases, however, neglecting the effects of heat transfer can lead to substantial error in the prediction of system behavior. In this chapter a variety of system analyses are developed in which heat transfer between the enclosed gas and the receiver walls is considered. The two types of flow most commonly encountered are analyzed; that is, the constant mass flow process and blowdown through a critical flow nozzle.

In sections "Adiabatic Charging" and "Adiabatic Discharging," adiabatic cases are analyzed for the perfect gas. Sections "Nonadiabatic Charging" and "Nonadiabatic Discharging" present solutions of gas properties for a perfect gas undergoing processes that include heat transfer as well as mass transfer, and these analytical methods are based upon those of Reynolds and Kays (1958).

The basic theory describing the processes of pneumatic pressure vessels is the first law of thermodynamics. Since the gas bottle processes are generally associated with a mass transfer, the first law written for the open system is found to apply. The following general equation was written in chapter 1 in the development of equation (1.5).

$$d(W_\sigma e_\sigma) = d\left[Wu + \frac{WV^2}{2g_cJ} + \left(\frac{g}{g_cJ}\right)Wz\right]_\sigma = \delta Q - \frac{\delta Wk}{J}$$

$$+ dW_{in}\left[u + \frac{Pv}{J} + \frac{V^2}{2g_cJ} + \left(\frac{g}{g_cJ}\right)z\right]_{in} - dW_{out}\left[u + \frac{Pv}{J} + \frac{V^2}{2g_cJ} + \left(\frac{g}{g_cJ}\right)z\right]_{out}$$

The analysis of pneumatic vessels (see fig. 11.1) usually permits the following assumptions to be made with accuracy:

(1) The specific energy for the system e_σ consists only of the internal-energy term u_σ.

(2) The work done, δWk, is zero (δWk does not include flow work).

(3) The potential-energy term z is negligible.

Also, since $u + Pv/J + V^2/2g_cJ = h + V^2/2g_cJ = h_0$ the first law energy equation reduces to

$$d(Wu) = \delta Q + h_{0\,in}\, dW_{in} - h_{0\,out}\, dW_{out} \tag{11.1}$$

where the subscript σ denoting properties of the gas of the system is dropped for simplicity.

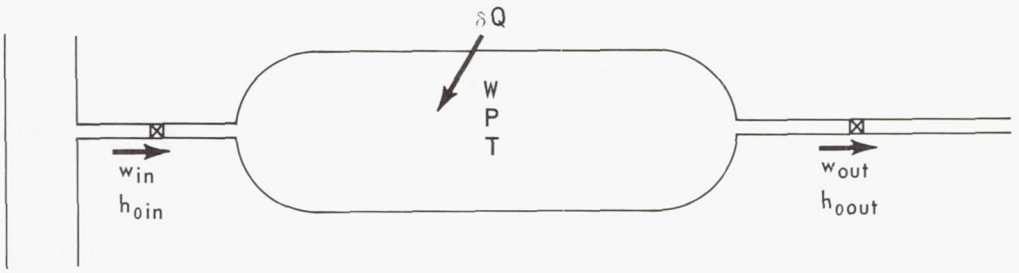


Figure 11.1. Typical pneumatic pressure vessel.

ADIABATIC CHARGING

Adiabatic charging can be assumed only when the process occurs over a short time interval so that the heat transfer will be insignificant in spite of the temperature differences.

Evacuated Receivers

The simplest charging process is that of charging an initially evacuated tank under adiabatic conditions. For this case, $dW_{out} = \delta Q = 0$, and if the inlet stagnation enthalpy is constant, the energy equation reduces to the integrable form

$$\int_{(Wu)_1}^{(Wu)_2} d(Wu) = h_{0\,in} \int_0^{W_{in}} dW_{in}$$

resulting in

$$(Wu)_2 - (Wu)_1 = h_{0\,in} W_{in}$$

Also, since the receiver was initially empty, the mass in the system, W, is just the mass injected, W_{in}, so that $W_1 = 0$ and

$$u_2 = h_{0\,in} \tag{11.2}$$

For calorically perfect gases (constant specific heats)

$$c_v T_2 = c_p T_{0\,in}$$

or

$$T_2 = k\, T_{0\,in} \tag{11.3a}$$

and

$$P_2 = \left(\frac{W_{in}}{\bar{V}}\right) kRT_{0\,in} \tag{11.3b}$$

Therefore, it is seen that since k is usually greater than unity, the gas temperature in an initially evacuated receiver will be greater than the charging gas temperature and, specifically, higher by the factor k for calorically perfect gas.

Partially Filled Receivers

If at the start of the charging operation the gas receiver (system) contains a mass of fluid $\mathcal{W}_1$ at an internal energy level u_1, the result remains

$$(\mathcal{W}u)_2-(\mathcal{W}u)_1=h_{0\text{ in}}\mathcal{W}_{\text{in}}$$

The change in $\mathcal{W}$ is just $\mathcal{W}_{\text{in}}$ so that

$$\mathcal{W}_2u_2-\mathcal{W}_1u_1=h_{0\text{ in}}(\mathcal{W}_2-\mathcal{W}_1) \tag{11.4}$$

which can be reduced to

$$\frac{\mathcal{W}_2}{\mathcal{W}_1}=1+\frac{\mathcal{W}_{\text{in}}}{\mathcal{W}_1}=\frac{h_{0\text{ in}}-u_1}{h_{0\text{ in}}-u_2} \tag{11.5}$$

If the gas is calorically perfect,

$$\frac{\mathcal{W}_2}{\mathcal{W}_1}=\frac{kT_{0\text{ in}}-T_1}{kT_{0\text{ in}}-T_2}=\frac{\dfrac{kT_{0\text{ in}}}{T_1}-1}{\dfrac{kT_{0\text{ in}}}{T_1}-\dfrac{T_2}{T_1}} \tag{11.6a}$$

which can also be solved for T_2/T_1 as

$$\frac{T_2}{T_1}=\frac{kT_{0\text{ in}}}{T_1}-\frac{\left(\dfrac{kT_{0\text{ in}}}{T_1}\right)-1}{\dfrac{\mathcal{W}_2}{\mathcal{W}_1}} \tag{11.6b}$$

Equations (11.6) are plotted as figure 11.2 for $k=1.4$.

The perfect-gas law $\mathcal{W}=P\bar{V}/RT$ can be substituted into equation (11.4) so that for a thermally and calorically perfect gas, the relation between temperature and pressure can be established as

$$\frac{T_2}{T_1}=\frac{\dfrac{P_2}{P_1}}{\left(\dfrac{T_1}{kT_{0\text{ in}}}\right)\left(\dfrac{P_2}{P_1}-1\right)+1} \tag{11.7a}$$

Equation (11.7a) can also be solved explicitly for pressure ratio as

$$\frac{P_2}{P_1}=\frac{\left(\dfrac{T_2}{T_1}\right)\left(\dfrac{T_1}{kT_{0\text{ in}}}-1\right)}{\left(\dfrac{T_1}{kT_{0\text{ in}}}\right)\left(\dfrac{T_2}{T_1}\right)-1} \tag{11.7b}$$

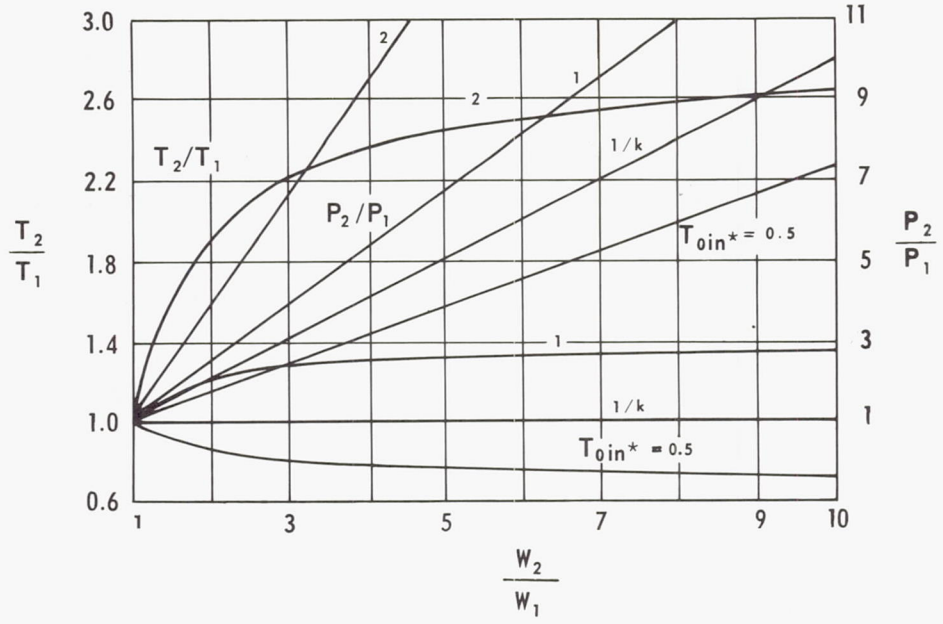


Figure 11.2. Adiabatic charging of partially filled vessel, $k = 1.4$.

Equations (11.7) identify the temperature and pressure changes based on initial conditions and inlet gas stagnation temperature. These relationships are also included in figure 11.2. For the special case where the inlet stagnation temperature is the same as the initial system temperature, equations (11.7) further reduce to

$$\frac{T_2}{T_1} = \frac{k\left(\frac{P_2}{P_1}\right)}{\left(\frac{P_2}{P_1}\right) + k - 1} \tag{11.8a}$$

and

$$\frac{P_2}{P_1} = \frac{(k-1)\left(\frac{T_2}{T_1}\right)}{k - \left(\frac{T_2}{T_1}\right)} \tag{11.8b}$$

Equations (11.8) are plotted as figure 11.3 for various values of k and correspond with the lines of constant, $T_{0in}/T_1 = 1$ in figure 11.2. The change in mass can be obtained by $W_2/W_1 = (P_2/P_1)/(T_2/T_1)$, or by using figure 11.2. Accurate working charts of these functions for various values of k are presented in chapter 22.

NONADIABATIC CHARGING

When the charging process occurs over a significant time interval, the heat exchange between the enclosed gas and the containing vessel should not be neglected.

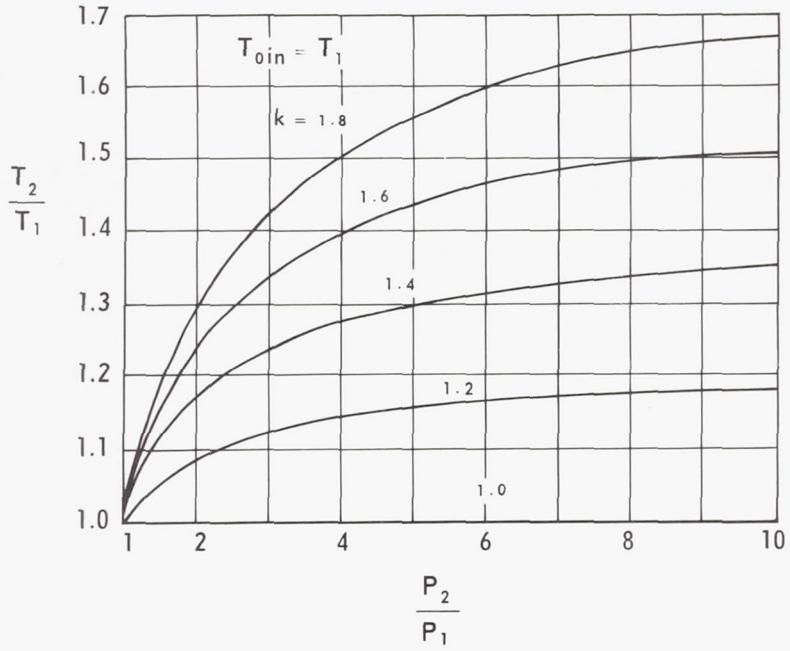


Figure 11.3. Adiabatic charging of a partially filled vessel $T_{0\,\mathrm{in}} = T_1$.

General Analysis

Equation (11.1) can be written for the nonadiabatic charging process as the following rate equation if the inlet conditions are constant. With reference to the sign convention of figure 11.4,

$$\frac{\mathrm{d}}{\mathrm{d}t}(Wu) = -\dot{Q}_i + w_{\mathrm{in}} h_{0\,\mathrm{in}} \tag{11.9}$$

Note that, because of the expected direction of heat transfer, the heat-transfer term is changed in sign so that $\mathrm{d}Q/\mathrm{d}t = -\dot{Q}_i$. An energy balance of the receiver wall can be written as

$$\frac{\mathrm{d}U_w}{\mathrm{d}t} = (Wc)_w \left(\frac{\mathrm{d}T_w}{\mathrm{d}t}\right) = \dot{Q}_i - \dot{Q}_\infty \tag{11.10}$$

where $(Wc)_w$ is the total or effective heat capacitance of the container walls.

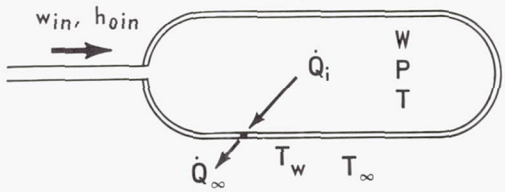


Figure 11.4. Pneumatic vessel—charging.

The heat-transfer terms can be defined in terms of the film coefficients. For the inside surface

$$\dot{Q}_i = (h_q A_w)_i (T - T_w) \tag{11.11}$$

Similarly, for the outside surface (uninsulated wall of high conductivity)

$$\dot{Q}_\infty = (h_q A_w)_\infty (T_w - T_\infty) \tag{11.12}$$

Combining equations (11.9), (11.11), and the definition $w_{\text{in}} = w = \mathrm{d}W/\mathrm{d}t$ yields

$$wW\left(\frac{\mathrm{d}T}{\mathrm{d}W}\right) + \left[\frac{(h_q A_w)_i}{c_v}\right](T - T_w) + w(T - kT_{0\ \text{in}}) = 0 \tag{11.13}$$

Similarly, combining equations (11.10), (11.11), and (11.12) yields

$$w\left(\frac{\mathrm{d}T_w}{\mathrm{d}W}\right) + \left[\frac{(h_q A_w)_i + (h_q A_w)_\infty}{(Wc)_w}\right] T_w - \left[\frac{(h_q A_w)_i}{(Wc)_w}\right] T - \left[\frac{(h_q A_w)_\infty}{(Wc)_w}\right] T_\infty = 0 \tag{11.14}$$

Equations (11.13) and (11.14) can be written in dimensionless form as follows. Equation (11.13) divided by $w_1 T_1$ yields

$$w_* W_* \left(\frac{\mathrm{d}T_*}{\mathrm{d}W_*}\right) + B_i(T_* - T_{w*}) + w_*(T_* - kT_{0\ \text{in}*}) = 0 \tag{11.15}$$

and equation (11.14) multiplied by $W_1/w_1 T_1$ yields

$$w_*\left(\frac{\mathrm{d}T_{w*}}{\mathrm{d}W_*}\right) + \left(\frac{B_1 + B_\infty}{C_{0*}}\right) T_{w*} - \left(\frac{B_i}{C_{0*}}\right) T_* - \left(\frac{B_\infty}{C_{0*}}\right) T_{\infty *} = 0 \tag{11.16}$$

The dimensionless ratios depicted by the subscript $*$ are defined as follows, where the subscript 1 indicates initial conditions,

$$B = \frac{(h_q A_w)}{(w_1 c_v)}$$

$$C_{0*} = \frac{(Wc)_w}{W_1 c_v}$$

$$T_* = \frac{T}{T_1}$$

$$T_{w*} = \frac{T_w}{T_1}$$

$$T_{0\,\text{in}*}=\frac{T_{0\,\text{in}}}{T_1}$$

$$T_{\infty *}=\frac{T_\infty}{T_1}$$

$$w_*=\frac{w}{w_1}$$

$$W_*=\frac{W}{W_1}$$

Equations (11.15) and (11.16) can be solved generally only by numerical methods and are subject to the initial conditions that at $W_*=1$, then $T_*=1$ and $T_{w*}=T_{w1}/T_1$. The equations are linear only if the flow rate is independent of the temperature. Therefore, the solution of equations (11.15) and (11.16) requires a further specification of the problem, such as in the cases treated below, after which solutions can be produced in terms of temperatures and contained mass. From this information, the pressures can be obtained from the perfect-gas law, $P_*=T_*W_*$, where $P_*=P/P_1$.

The solution of the simultaneous differential equations (eqs. (11.15) and (11.16)) for charging processes cannot be obtained unless the mass flow rate is a constant. Methods of solution are discussed by Reynolds and Kays (1958).

Isothermal Charging

Isothermal behavior is obtained when $C_{o*}=\infty$ and $B_i=\infty$, or if $B_i=B_\infty=\infty$. The first criterion is for isothermal behavior obtained by receivers having large thermal capacitance, $(Wc)_w$, accompanied by a high value of heat-transfer coefficient, $(h_qA_w)_i$. The latter criterion for isothermal behavior is for cases where the mass flow rate is extremely low. The isothermal charging solution is rather trivial, except in the above identification of necessary criteria, since the temperature is a constant and the pressure-mass relationship is just

$$\frac{P_2}{P_1}=\frac{W_2}{W_1} \tag{11.17a}$$

and for real gases

$$\frac{P_2}{P_1}=\left(\frac{Z_2}{Z_1}\right)\frac{W_2}{W_1} \tag{11.17b}$$

Charging at Constant Mass Flow Rate With Heat Transfer to an Isothermal Sink

For most systems the thermal capacitance of the metal receiver walls is much greater than that of the enclosed gas. Therefore, the temperature change of the walls is much less than that of the gas. A solution is possible for the limiting case of constant wall (sink) temperature; in which case, $C_{o*}=\infty$ and $T_{w*}=\text{constant}$. For constant mass flow rate, $w_*=1$, and equation (11.15) can be integrated to

$$T_*=\frac{kT_{0\,\text{in}*}+B_iT_{w*}-(kT_{0\,\text{in}*}-1-B_i+B_iT_{w*})W_*^{-(B_i+1)}}{B_i+1} \tag{11.18}$$

Equation (11.18) and pressure from $P_* = W_* T_*$ are plotted as figure 11.5 for $T_{0\,in*} = 1$, $T_{w*} = 1$, and $k = 1.4$.

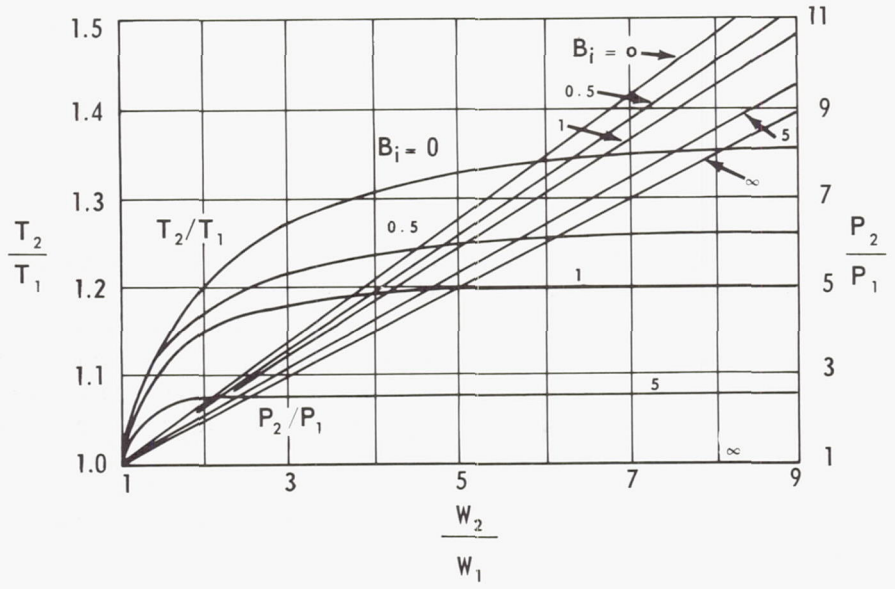


Figure 11.5. Charging at constant mass flow with heat transfer to an isothermal sink, $T_{0\,in*} = 1$, $T_{w*} = 1$, and $k = 1.4$.

Charging at Constant Mass Flow Rate With Inside Resistance Negligible

When the inside resistance approaches zero, the coefficient B_i approaches ∞. Very large values of B_i can be obtained practically if the mass flow rate is very low, if the inside heat conductance is high, if the heat-transfer area is large, or any combination of these. The importance of this solution is that it establishes the effect of thermal capacitance of the containing vessel on the thermodynamic behavior of the contained gas. For $B_i = \infty$, the other terms of equation (11.15) become negligible, and $T_* = T_{w*}$. The variation of T_* (and T_{w*}) can be obtained from equation (11.16), but only after B_i has been eliminated by combining with equation (11.15). The resulting equation written for constant mass flow rate ($w_* = 1$) is

$$(W_* + C_{0*}) \frac{dW_*}{dT_*} + (1 + B_\infty) T_* - kT_{0\,in*} - B_\infty T_{\infty*} = 0 \tag{11.19}$$

Equation (11.19) can be integrated to produce the following closed solution

$$T_* = T_{w*} = \left(\frac{1}{1+B_\infty}\right)\left[(1 + B_\infty - kT_{0\,in*} - B_\infty T_{\infty*}) \left(\frac{C_{0*}+1}{C_{0*}+W_*}\right)^{1+B_\infty} + kT_{0\,in*} + B_\infty T_{\infty*} \right] \tag{11.20}$$

Equation (11.20) is plotted in figure 11.6, along with $P_* = W_* T_*$, for low external heat transfer ($B_\infty = 0$), $T_{0\text{in}*} = 1$, and $k = 1.4$.

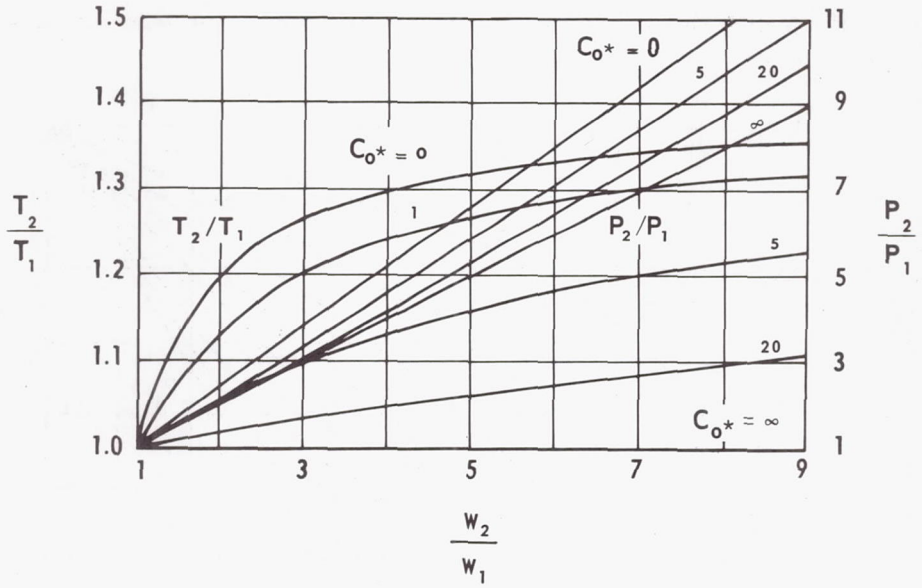


Figure 11.6. Charging at constant mass flow with inside resistance negligible, $T_{0\text{ in}}/T_1 = 1$, $B_\infty = 0$, and $k = 1.4$.

ADIABATIC DISCHARGING

When the gas in a receiver is permitted to flow out at a rapid rate, the gas remaining in the receiver can be assumed to expand reversibly and adiabatically (isentropically). Therefore, the isentropic relationships of equations (5.24) through (5.27) can be applied directly and are repeated here for convenience. However, the enclosed mass term is included since, in this case, the total volume is a constant, and the mass term is of interest. Therefore,

$$\gamma = \frac{W}{\bar{V}}$$

and since $\bar{V}$ is a constant,

$$\frac{\gamma_2}{\gamma_1} = \frac{W_2}{W_1}$$

Then the isentropic equations for pneumatic pressure vessels and perfect gases become

$$\frac{T_2}{T_1} = \left(\frac{\gamma_2}{\gamma_1}\right)^{k-1} = \left(\frac{W_2}{W_1}\right)^{k-1} = \left(\frac{v_1}{v_2}\right)^{k-1} = \left(\frac{P_2}{P_1}\right)^{k-1/k} \tag{11.21}$$

$$\frac{P_2}{P_1} = \left(\frac{\gamma_2}{\gamma_1}\right)^{k} = \left(\frac{W_2}{W_1}\right)^{k} = \left(\frac{v_1}{v_2}\right)^{k} = \left(\frac{T_2}{T_1}\right)^{k/k-1} \tag{11.22}$$

$$\frac{W_2}{W_1}=\left(\frac{\gamma_2}{\gamma_1}\right)=\left(\frac{v_1}{v_2}\right)=\left(\frac{P_2}{P_1}\right)^{1/k}=\left(\frac{T_2}{T_1}\right)^{1/k-1} \tag{11.23}$$

Figure 11.7 is the plotted solution that relates the temperature and pressure changes to the change in enclosed mass.

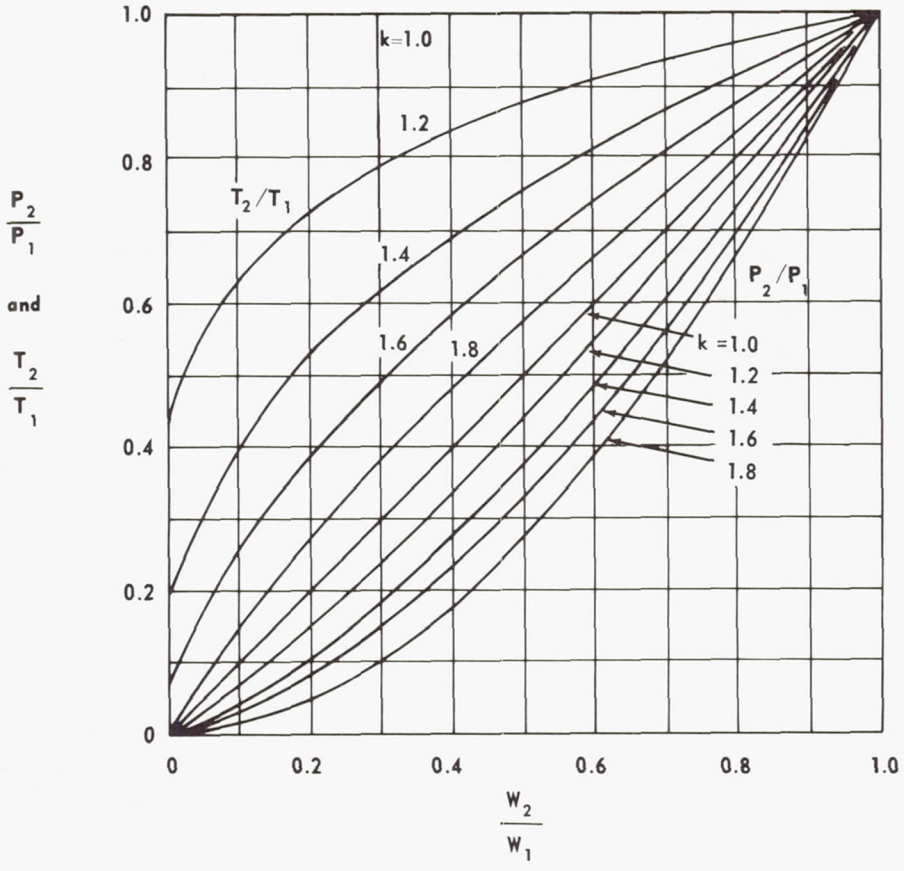


Figure 11.7. Adiabatic discharging (isentropic).

NONADIABATIC DISCHARGING

The differential equations governing the thermodynamics of the pressure vessel discharging process can be developed by an application of the first law of thermodynamics similar to that applied to the charging process.

General Analysis

In this case, since the mass flow is in an outward direction,

$$w=-\frac{\mathrm{d}W}{\mathrm{d}t} \tag{11.24}$$

Applying the energy balance of equation (11.1) to the open system, written in terms of a time-rate equation, yields

$$\frac{\mathrm{d}}{\mathrm{d}t}(Wu)=\dot{Q}_i-h_{0\ \mathrm{out}}\,w_{\mathrm{out}} \tag{11.25}$$

The sign convention is in accordance with figure 11.8 which is established once again to match the expected changes.

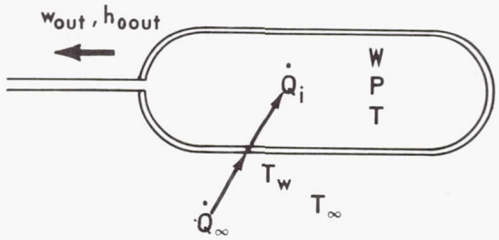


Figure 11.8. Pressure vessel discharging.

Likewise, an energy balance of the receiver walls can be written as

$$\frac{\mathrm{d}U_w}{\mathrm{d}t}=(Wc)_w\left(\frac{\mathrm{d}T_w}{\mathrm{d}t}\right)=\dot{Q}_\infty-\dot{Q}_i \tag{11.26}$$

The heat-transfer rates are described by

$$\dot{Q}_i=(h_qA_w)_i(T_w-T) \tag{11.27}$$

$$\dot{Q}_\infty=(h_qA_w)_\infty(T_\infty-T_w) \tag{11.28}$$

Combination of equations (11.24) through (11.28) yields the following two differential equations describing the thermal behavior of the enclosed gas and its containing vessel

$$wW\left(\frac{\mathrm{d}T}{\mathrm{d}W}\right)-\left[w(k-1)+\frac{(h_qA_w)_i}{c_v}\right]T+\left[\frac{(h_qA_w)_i}{c_v}\right]T_w=0 \tag{11.29}$$

$$w\left(\frac{\mathrm{d}T_w}{\mathrm{d}W}\right)-\left[\frac{(h_qA_w)_i+(h_qA_w)_\infty}{(Wc)_w}\right]T_w+\left[\frac{(h_qA_w)_i}{(Wc)_w}\right]T+\left[\frac{(h_qA_w)_\infty}{(Wc)_w}\right]T_\infty=0 \tag{11.30}$$

Equations (11.29) and (11.30) can be written in dimensionless form as

$$w_*W_*\left(\frac{\mathrm{d}T_*}{\mathrm{d}W_*}\right)-[(k-1)w_*+B_i]T_*+B_iT_{w*}=0 \tag{11.31}$$

and

$$w_*\left(\frac{\mathrm{d}T_{w*}}{\mathrm{d}W_*}\right)-\left(\frac{B_i+B_\infty}{C_{0*}}\right)T_{w*}+\left(\frac{B_i}{C_{0*}}\right)T_*+\left(\frac{B_\infty}{C_{0*}}\right)T_{\infty*}=0 \tag{11.32}$$

where the dimensionless ratios subscripted with an $*$ are identical to those defined previously for equations (11.15) and (11.16). As in the case of the dimensionless equations describing charging, solution of equations (11.31) and (11.32) is subject to the requirement that when $\dot{W}_*=1$, then $T_*=1$ and $T_{w*}=T_{w1}/T_1$. Once again, the equations can be solved generally only by numerical methods. They can be solved for closed solutions only if the mass flow rate is a constant, and when the problem is further specified, as in the following cases.

Discharging at Constant Mass Flow Rate With Heat Transfer From an Isothermal Source

For many systems, the thermal capacitance of the metal receiver walls far exceeds the thermal capacitance of the gas. If so, the temperature change of the walls is very small compared to that of the gas. A solution of equation (11.31) can be made for the limiting case, where C_{0*} is essentially infinite, and the only heat transfer is between the gas and the isothermal source (wall). Then for constant mass flow rate and wall temperature, equation (11.31) integrates directly to

$$T_*=\frac{(k-1+B_i-B_iT_{w*})W_*^{(k-1+B_i)}+B_iT_{w*}}{k-1+B_i} \tag{11.33}$$

This relationship is plotted in figure 11.9, along with the associated pressure ratio, for $w_*=1$, $T_{w*}=1$ and $k=1.4$.

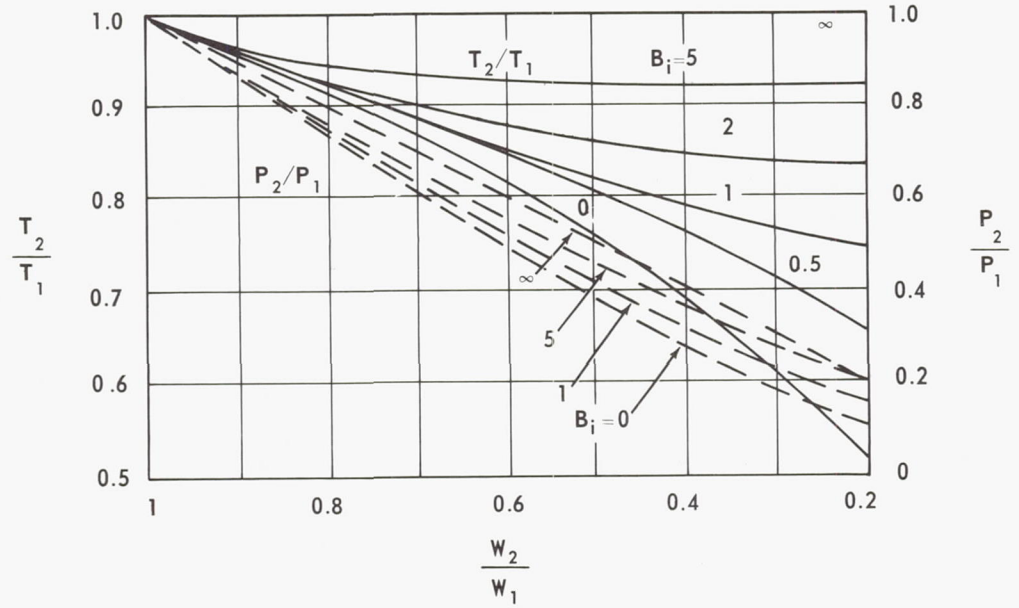


Figure 11.9. Discharge at constant mass flow with heat transfer from an isothermal source, $T_{w*}=1$ and $k=1.4$.

Discharging Through a Critical Flow Nozzle With Heat Transfer From an Isothermal Source

The mass flow rate through a critical flow nozzle can be written in dimensionless form as

$$w_* = W_* \sqrt{T_*} \tag{11.34}$$

for a discharging receiver. Substituting this into equation (11.31) along with the criterion for a constant source temperature, T_{w*}, yields

$$W_* \left(\frac{dT_*}{dW_*}\right) - (k-1)T_* + \frac{B_i(T_{w*} - T_*)}{W_* \sqrt{T_*}} = 0 \tag{11.35}$$

Since the flow rate is a variable, it should be remembered that B_i (by definition) is still established by the initial flow rate. Equation (11.35) is seen to be nonlinear, and closed solutions are not possible. However, since the case is a very common one, numerical solutions have become available and are plotted, along with pressure change, in figure 11.10 for $T_{w*} = 1$ and $k = 1.4$. Note that the temperature decreases initially, as in the constant flow rate case but eventually begins to increase once again. This is because the ever-decreasing mass flow rates cause the cooling effects by expanison to be overcome by the heating effects of the walls.

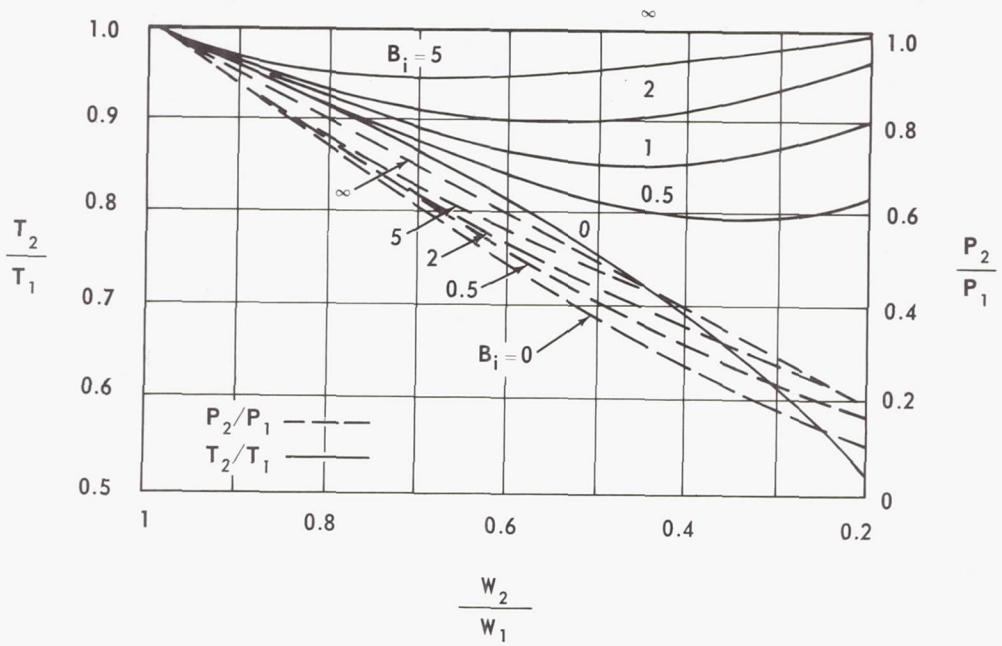


Figure 11.10. Discharging through a critical-flow nozzle with heat transfer from an isothermal source, $T_{w*}=1$ and $k = 1.4$.

Discharge at Constant Mass Flow Rate With Inside Resistance Negligible

If the assumption can be made that $B_i = \infty$, a closed-form solution of the thermal equations can be made. The value of B_i is made very large when the mass flow rate is very small

and/or the heat-transfer coefficient-area product is very high. In the limit when $B_i = \infty$, equation (11.31) reduces to $T_* = T_{w*}$, which means that the temperatures of the enclosed gas and the containing wall vary together. The variation can be established using equation (11.32) by simultaneous solution with equation (11.31) to eliminate B_i, resulting in the following when $w_* = 1$

$$(C_{0*} + w_*) \frac{dT_*}{dW_*} - (k - 1 + B_\infty) T_* + B_\infty T_{\infty *} = 0 \tag{11.36}$$

Equation (11.36) integrates to

$$T_* = T_{w*} = \left[\frac{1}{k - 1 + B_\infty}\right] \left[(k - 1 + B_\infty - B_\infty T_{\infty *}) \left(\frac{W_* + C_{0*}}{1 + C_{0*}}\right)^{(k-1+B_\infty)} + B_\infty T_{\infty *} \right] \tag{11.37}$$

Equation (11.37) is plotted in figure 11.11, along with $P_* = W_* T_*$, for $w_* = 1$ and $k = 1.4$.

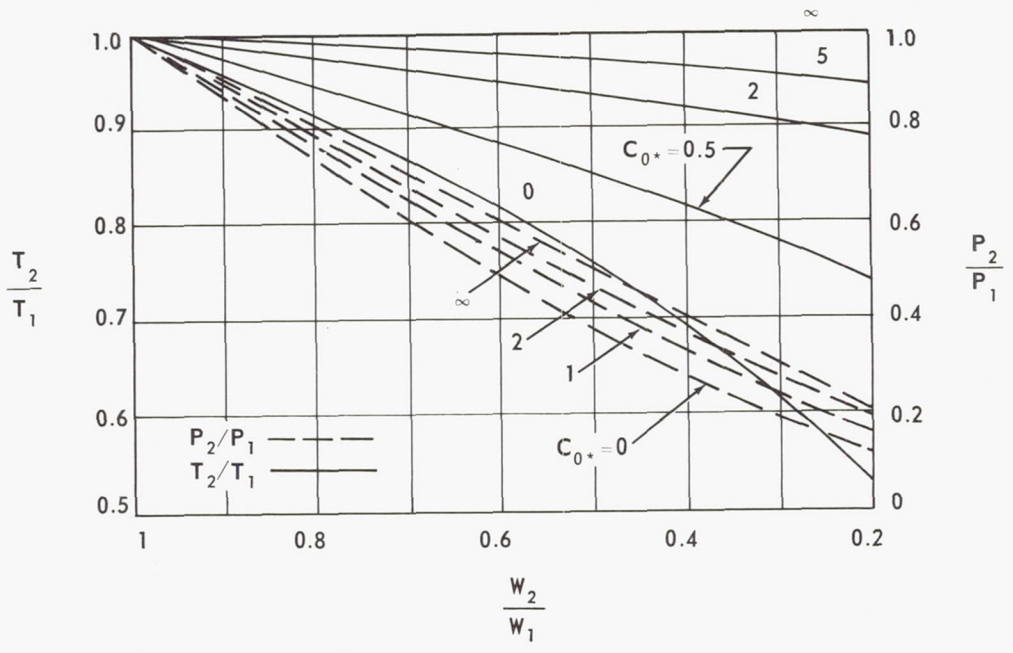


Figure 11.11. Discharge at constant mass flow with inside resistance negligible, $B_\infty = 0$ and $k = 1.4$.

PART II

APPLICATION

CHAPTER 12

APPLICATION OF FUNDAMENTALS OF THERMODYNAMICS

Thermodynamics is the science which treats the mechanical actions or relations of heat. In this handbook, emphasis is on the thermodynamics of gases or gas systems.

The study of thermodynamics is based on certain observed principles, termed the zeroth, first, second, and third laws of thermodynamics. (See ch. 1.) In this chapter the application of the first law to various flow situations is illustrated along with a brief discussion of temperature and pressure. Also presented in this chapter are abbreviated definitions of several of the more basic terms used in the science of thermodynamics.

DEFINITIONS OF TERMS

(1) *System.*—That portion of the universe to be examined.

(2) *Closed system.*—System which allows energy, but not mass, to cross the system boundary.

(3) *Open system.*—System which allows both energy and mass to cross the system boundary.

(4) *Surroundings.*—The universe, exclusive of the system.

(5) *State.*—A unique set of physical conditions under which the system exists.

(6) *Property.*—Physical quantity which determines the state.

(7) *Extensive property.*—Property of a system which is a function of the amount of material, as well as the physical state.

(8) *Intensive property.*—Property of a system which is independent of the amount of material, but dependent only on the particular substance and its state.

(9) *Process.*—The path traced by the succession of states between some initial state and some final state through which a system passes.

(10) *Quasi-static process.*—A process in which each state attained during the process is an equilibrium state.

(11) *Reversible process.*—A process which can be carried to completion and returned to its original state without changing the system or surroundings.

(12) *Pure substance.*—A substance with an invariant chemical composition.

DETERMINATION OF THE STATE

The state of a substance is determined by the values of the independent properties at that state. The number of properties required to fix the state can be determined by

Preceding Page Blank

Gibbs' phase rule. This rule may be stated mathematically as

$$P' + V' = C' + 2$$

where P' is the number of phases, V' is the number of intensive variables (independent properties), and C' is the number of components. As an example, determine the number of independent properties required to specify the state of gaseous nitrogen. Since there is only one component (nitrogen) and one phase (gaseous), Gibbs' phase rule gives

$$1 + V' = 1' + 2 \qquad \text{or} \qquad V' = 2$$

According to Gibbs' phase rule then, the state of a single phase of a pure substance is completely defined when the value of two independent properties is specified.

PRESSURE SCALE

Pressure is defined as the force acting on the system divided by the area over which the force is in effect.

$$p = \frac{F}{a}\left(\frac{\text{lbf}}{\text{in.}^2}\right) \qquad P = \frac{F}{A}\left(\frac{\text{lbf}}{\text{ft}^2}\right)$$

The common conversion between pressure measurements in lbf/ft^2 and lbf/in.^2 is as follows:

$$p\left(\frac{\text{lbf}}{\text{in.}^2}\right) = P\left(\frac{\text{lbf}}{\text{ft}^2}\right) \qquad \frac{1}{144}\left(\frac{\text{ft}^2}{\text{in.}^2}\right) = \frac{P}{144}\left(\frac{\text{lbf}}{\text{in.}^2}\right)$$

Pressure is measured relative to an absolute zero datum, the perfect vacuum. Figure 12.1 shows the relation of the various pressure terms to the datum, zero pressure, and to each other.

Pressures above atmospheric are most often measured in pounds force per square inch or, for low positive pressures in inches of fluid, usually mercury. Pressure measurements are generally accomplished with a Bourdon-tube gage or a mercury manometer.

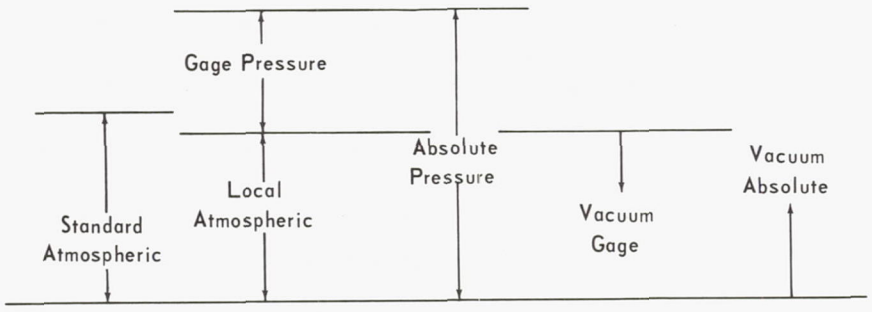


Figure 12.1. Relation of pressure terms.

Both of these instruments are shown in figure 12.2. The relation between pressure measurements in pounds force per square inch and height of a fluid column can be found by summing the forces acting on the fluid of a manometer connected to a pressure source as in figure 12.3.

$$\Sigma F = 0$$

$$p_1 a = p_2 a + h_f a \left(\frac{\gamma'}{1728}\right) \tag{12.1a}$$

$$h_f = \frac{(p_1 - p_2)(1728)}{\gamma'} \qquad \text{(inches of fluid)}$$

In feet of fluid, this equation becomes

$$H_f = \frac{(p_1 - p_2)(144)}{\gamma'} \qquad \text{(feet of fluid)} \tag{12.1b}$$

TEMPERATURE SCALE

Temperature is a measure of the kinetic energy of the molecules of a substance. It is sensed by the degree of hotness or coldness and is measured by determining its effect on the physical properties of some measuring substance. The most common method of

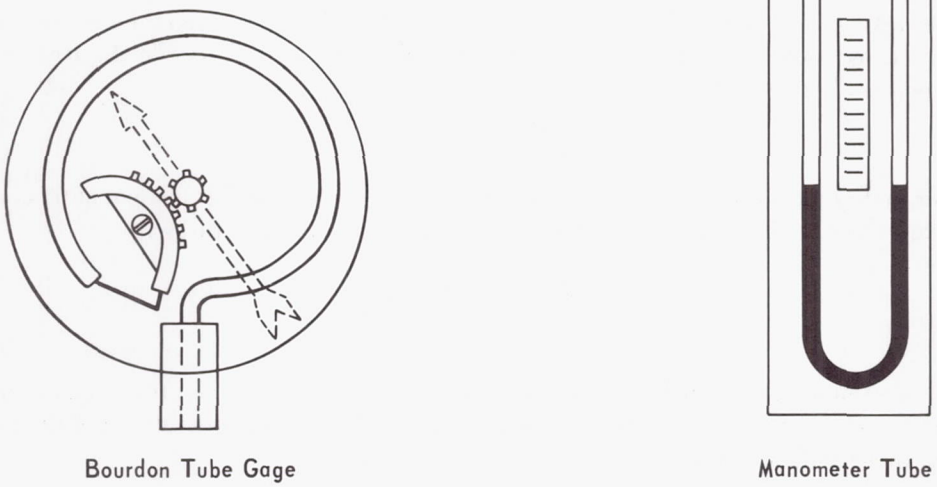


Figure 12.2. Pressure measurement devices.

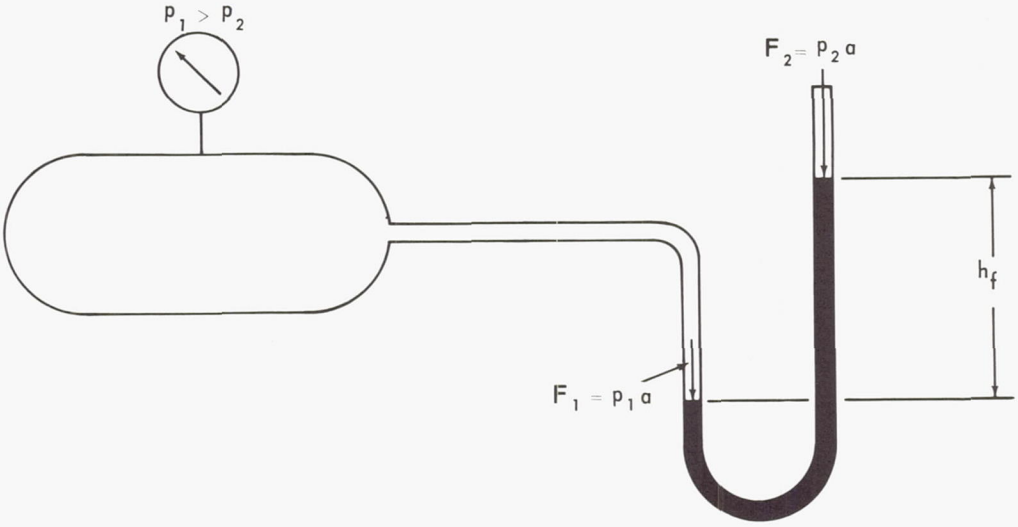


Figure 12.3. Relation between pressure and head.

temperature measurement is the mercury thermometer. This method of temperature measurement consists of determining the difference in height of a constant area mercury column when placed in boiling water and an ice bath, both at the same pressure. The difference in length between these two datum points is taken as 100° C (180° F). It is then assumed that the relation between temperature and length of mercury column (thermal expansion) is linear. In the centigrade scale, 0° C is defined as the freezing point of water (where $L = L_0$) so that the temperature can be computed by

$$T, °C = (100)\frac{L' - L'_0}{L'_{100} - L'_0}$$

The relation between the Fahrenheit and centigrade scales can be determined by noting that, as shown by figure 12.4, there are 180° F or 100° C between the freezing and boiling points of water. Hence,

$$1° C = 1.8° F$$

However, note that on the Fahrenheit scale the freezing point is at 32° instead of 0° as on the centigrade scale. Therefore, the relation between the two temperatures is

$$\frac{T, °C}{100} = \frac{T, °F - 32}{180}$$

For thermodynamic analysis, the most frequently used temperature scales are the absolute temperature scales. These are the Kelvin and the Rankine scales, and the relation between these scales and the Fahrenheit and centigrade scales is

$$T, °R = T, °F + 460 \qquad \text{and} \qquad T, °K = T, °C + 273$$

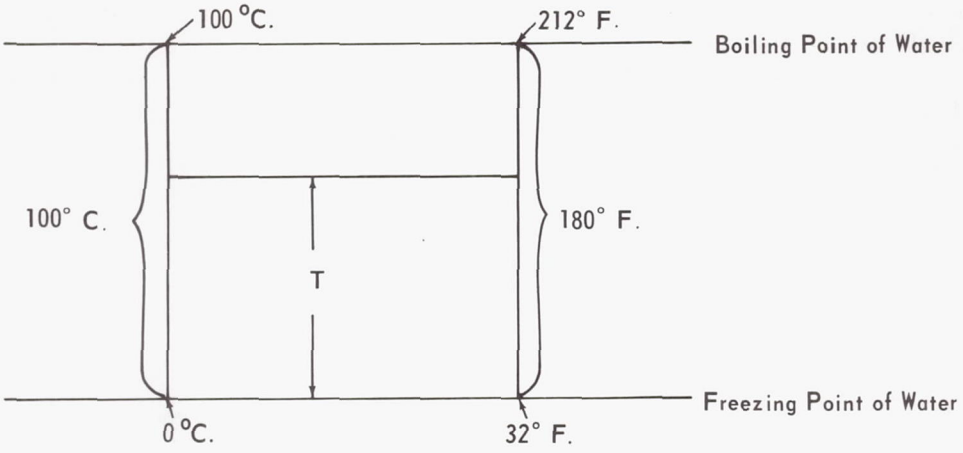


Figure 12.4. Relation between Fahrenheit and centigrade scales.

FIRST LAW OF THERMODYNAMICS

The first law of thermodynamics is an expression of the law of conservation of energy, applied to a thermodynamic system.

In analytical form, the first law relates the change in the properties of a system to the amount of heat transferred to or from the system and the amount of work done by or on the system. The application of the first law is subject to the type of system being analyzed, open or closed.

Consider the generalized open system shown in figure 12.5. This system has an amount of heat, δQ, transferred to it and does an amount of work, δWk. The mass of fluid W_{in} enters the system, and the mass W_{out} leaves. For this system, the change in the total system energy, $dE\sigma$, is given by

$$dE_\sigma = \delta Q - \frac{1}{J}(\delta Wk + P_{out}\, d\bar{V}_{out} - P_{in}\, d\bar{V}_{in}) + E_{in} - E_{out} \tag{12.2}$$

where E is the energy of the masses entering and leaving, at their respective entrance and exit conditions. The term $(P\, d\bar{V})/J$ is a flow-work term which represents the change in

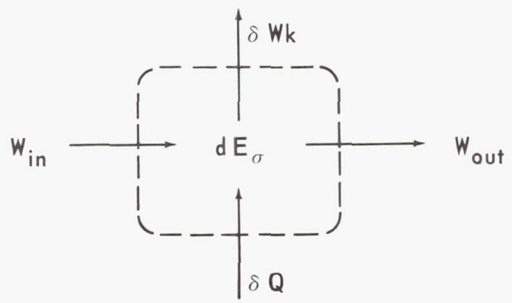


Figure 12.5. Thermodynamic open system.

system energy due to mass crossing the system boundary. Hence, it represents an energy term for the open system only.

In thermodynamic analysis, the energy term E can represent three forms of energy as listed below:

$$\text{Kinetic energy} = \frac{WV^2}{2g_cJ}$$

$$\text{Potential energy} = \left(\frac{g}{Jg_c}\right)Wz$$

$$\text{Internal energy} = U$$

Hence,

$$E = \frac{WV^2}{2g_cJ} + \left(\frac{g}{Jg_c}\right)Wz + U \tag{12.3a}$$

or by defining the energy per unit mass as e, it follows that

$$e = \frac{E}{W} = \frac{V^2}{2g_cJ} + \left(\frac{g}{Jg_c}\right)z + u \tag{12.3b}$$

These total energy definitions apply to both the enclosed system material and the material crossing the system boundaries.

The stepwise form of equation (12.2), supplemented by equation (12.3), lends itself well to the solution of highly transient problems. Each step can be made sufficiently small, with conditions changing each time.

When the process is of a more continuous nature, the equation is best used as a quasi-steady-state rate equation. This is obtained by differentiating with respect to time, holding all intensive properties constant, which yields the following,

$$\frac{dE_\sigma}{dt} = \frac{d}{dt}\left\{W\left[u + \frac{V^2}{2g_cJ} + \left(\frac{g}{g_cJ}\right)z\right]\right\}_\sigma = \dot{Q} - \frac{\dot{W}k}{J} + w_{in}\left[u + \frac{Pv}{J} + \frac{V^2}{2g_cJ} + \left(\frac{g}{g_cJ}\right)z\right]_{in} - w_{out}\left[u + \frac{Pv}{J} + \frac{V^2}{2g_cJ} + \left(\frac{g}{g_cJ}\right)z\right]_{out} \tag{12.4}$$

A mass balance of the system yields

$$\frac{dW_\sigma}{dt} = w_{in} - w_{out}$$

Equation (12.4) also makes use of the following definitions:

$$\frac{dW}{dt} = w = \text{mass flow rate, lbm/sec}$$

$$\frac{\delta Q}{dt} = \dot{Q} = \text{rate of heat transfer, Btu/sec}$$

$$\frac{\delta Wk}{dt} = \dot{W}k = \text{rate of doing work, ft-lbf/sec}$$

$$\frac{dV}{dt} = \frac{dWv}{dt} = wv = \text{rate of volume change, } \frac{ft^3}{sec}$$

A steady-flow process requires that:

(1) The flow rate into the system is equal to that out of the system and neither varies with time

(2) The rate of heat transfer and the rate of work do not vary with time

(3) The state of the fluid at any point in the system does not vary with time. Then, for the steady-flow process, the following relations apply:

$$\frac{dE_\sigma}{dt} = \frac{d(W_\sigma e_\sigma)}{dt} = 0$$

$$w_{in} = w_{out} = wt$$

and the energy equation for the open system simplifies to

$$\frac{\dot{Q}}{w} + \left[u + \frac{Pv}{J} + \frac{V^2}{2g_cJ} + \left(\frac{g}{g_cJ}\right) z \right]_{in} = \frac{\dot{W}k}{wJ} + \left[u + \frac{Pv}{J} + \frac{V^2}{2g_cJ} + \left(\frac{g}{g_cJ}\right) z \right]_{out} \tag{12.5}$$

Substituting the quantities Q' and wk, defined as

$$Q' = \frac{\dot{Q}}{w} \quad \text{Btu/lbm} \quad \text{and} \quad wk = \frac{\dot{W}k}{w} \quad \text{ft-lbf/lbm}$$

and the standard definition of the thermodynamic property, enthalpy,

$$h = u + \frac{pv}{J}$$

into equation (12.5) yields the first law expression for the open system under steady-state conditions

$$\left[\frac{V_2^2}{2g_cJ} + \left(\frac{g}{Jg_c}\right) z_2 + h_2 \right]_{in} + Q' = \left[\frac{V_1^2}{2g_cJ} + \left(\frac{g}{Jg_c}\right) z_1 + h_1 \right]_{out} + \frac{wk}{J} \tag{12.6}$$

In many cases, the change in elevation is negligible, and the work term is zero. Hence, this further simplification yields

$$\left(\frac{V_2^2}{2g_cJ} + h_2 \right)_{in} + Q' = \left(\frac{V_1^2}{2g_cJ} + h_1 \right)_{out} \tag{12.7}$$

or

$$h_{0\,in} + Q' = h_{0\,out}$$

Now if the flow is also adiabatic, Q' is zero, and

$$\left(\frac{V_2^2}{2g_cJ}+h_2\right)_{\text{in}}=\left(\frac{V_1^2}{2g_cJ}+h_1\right)_{\text{out}} \tag{12.8}$$

or

$$h_{0\ \text{in}}=h_{0\ \text{out}}$$

which means it is a constant enthalpy stagnation process.

The first law expression for the closed system may be obtained similarly from equation (12.2), except that all terms involving energy of the mass transferred are set to zero. Then

$$\mathrm{d}E_\sigma=\delta Q-\frac{\delta Wk}{J}=\mathrm{d}(W_\sigma e_\sigma)$$

and since W_σ is a constant,

$$\mathrm{d}u+\mathrm{d}\left(\frac{V^2}{2g_cJ}\right)+\left(\frac{g}{g_cJ}\right)\mathrm{d}z=\frac{\delta Q}{W_\sigma}-\frac{\delta Wk}{W_\sigma J}=Q'-\frac{wk}{J} \tag{12.9}$$

On integrating, the changes in conditions can be computed by

$$u_2-u_1+\frac{V_2^2-V_1^2}{2g_cJ}+\frac{g}{g_cJ}(z_2-z_1)={}_1Q_2'-{}_1\left(\frac{wk}{J}\right)_2 \tag{12.10}$$

Very often in closed systems the velocity changes and elevation changes are negligible; in which case,

$$u_2-u_1={}_1Q_2'-{}_1\left(\frac{wk}{J}\right)_2 \tag{12.11}$$

CHAPTER 13

APPLICATION OF PROPERTIES OF GASES

PERFECT GAS

The thermally perfect gas is, by definition, a gas whose state is described by the equation

$$Pv = RT \qquad [2.5]$$

or in terms of total volume

$$P\bar{V} = WRT \qquad [2.5a]^*$$

where R is a gas constant for a particular gas, R values are shown in table 13.1. Also, since the weight of gas is given by

$$W = NM_w$$

it follows that

$$P\bar{V} = NM_wRT \qquad \text{or} \qquad P\bar{V} = N\bar{R}T$$

where

$$R = \frac{\bar{R}}{M_w}$$

The quantity $\bar{R}$ is a universal gas constant that can be used for all thermally perfect gases. Dividing by the number of moles N, the perfect-gas equation of state can be written as

$$Pv_m = \bar{R}T$$

where v_m is the volume of 1 mole of a gas. Values of the universal gas constant $\bar{R}$ for several consistent sets of units are shown in table 13.2.

*This equation is a variation of equation (2.5) and does not appear in ch. 2.

TABLE 13.1—*Data on Gases*

Gas	Properties of gases					
	Chemical symbol	Gas constant R, ft-lbf/lbm-°R	Specific heat ratio, c_p/c_v	Critical temp, °F	Boiling point, °F	Critical pressure, atm
Helium	He	386.30	1.66	−405.20	−452.00	2.26
Argon	A	38.70	1.67	−187.70	−302.50	48.00
Air	.....	53.30	1.40	−220.30	−317.60	37.20
Oxygen	O_2	48.31	1.40	−181.80	−297.20	−181.80
Nitrogen	N_2	55.16	1.40	−232.80	−320.40	33.50
Hydrogen	H_2	766.80	1.40	−399.80	−422.90	12.80
Nitric oxide	NO	51.52	1.40	−136.70	−239.80	65.00
Carbon monoxide	CO	55.19	1.41	−220.30	−313.60	34.53
Hydrochloric acid	HCl	42.41	1.40	124.50	−121.00	81.60
Steam	H_2O	85.81	1.28	705.45	.....	218.50
Carbon dioxide	CO_2	35.13	1.28	88.00	−109.30	73.00
Nitrous oxide	N_2O	35.12	1.26	97.70	−129.10	71.70
Sulfur dioxide	SO_2	24.13	1.25	315.00	14.00	77.70

Ammonia	NH_3	90.77	1.29			
Acetylene	C_2H_2	59.40	1.38			
Methyl chloride	CH_3Cl	30.62	1.20	289.60	−10.25	65.80
Methane	CH_4	96.37	1.26	−116.50	258.30	45.80
Ethylene	C_2H_4	55.11	1.22			

TABLE 13.2.—*Systems of Consistent Units for the Perfect-Gas Equation of State Using the Universal Gas Constant* $\bar{R}$

$P\bar{V}=N\bar{R}T$				
P	$\bar{V}$	N	$\bar{R}$	T
lbf/ft²	ft³	mole_{lb}	$1545\ \frac{\text{ft-lbf}}{\text{mole}_{lb}\ °R}$	°R
Btu		mole_{lb}	$1.9857\ \frac{\text{Btu}}{\text{mole}_{lb}\ °R}$	°R
lbf/in.²	ft³	mole_{lb}	$10.729\ \frac{\text{lbf-ft}^3}{\text{in.}^2\ \text{mole}_{lb}\ °R}$	°R
atm	cm³	mole_{g}	$82.0567\ \frac{\text{atm cm}^3}{\text{mole}_{g}\ °K}$	°K
mm Hg	cm³	mole_{g}	$62\,363\ \frac{\text{mm Hg cm}^3}{\text{mole}_{g}\ °K}$	°K
kg/m²	m³	mole_{g}	$0.847887\ \frac{\text{kg m}}{\text{mole}_{g}\ °K}$	°K
calorie		mole_{g}	$1.9857\ \frac{\text{cal}}{\text{mole}_{g}\ °K}$	°K

PROPERTIES OF THE PERFECT GAS

Internal Energy and Enthalpy

The internal energy of a system represents the sum of the kinetic energy of the gas molecules that comprise the system. For the perfect gas, internal energy is a function of temperature only. To illustrate the proof of this statement, consider the first law expression for a closed system.

$$du = T\,ds - \frac{P\,dv}{J} \qquad [1.6]$$

Differentiating this expression with respect to the volume change, holding T constant, and substituting from the Maxwell relation, equation (1.12), for $(\partial s/\partial r)_T$, it follows that

$$\left(\frac{\partial u}{\partial v}\right)_T = \frac{T}{J}\left(\frac{\partial P}{\partial T}\right)_v - \frac{P}{J}$$

Writing the perfect-gas equation of state in differential form with v held constant yields

$$\left(\frac{\partial P}{\partial T}\right)_v = \frac{R}{v}$$

Substituting for $(\partial P/\partial T)_v$ in the previous equation yields

$$\left(\frac{\partial u}{\partial v}\right)_T = \frac{T}{J}\left(\frac{R}{v}\right) - \frac{P}{J}$$

or, from the perfect-gas law

$$\left(\frac{\partial u}{\partial v}\right)_T = \frac{RT}{Jv} - \frac{RT}{Jv} = 0$$

Using a similar approach, it can be shown that all other partials of u with T held constant are zero. Hence, for the perfect gas, internal energy is a function of temperature only.

Enthalpy is, by definition, the sum of the internal energy and the flow-work term. In mathematical form

$$h = u + \frac{Pv}{J}$$

Since the product Pv can represent the flow work or the change in system energy as a result of mass crossing the system boundary, it follows that enthalpy generally represents an energy term for the open system only. Since enthalpy is a function of internal energy which is a temperature-dependent quantity, it follows that the enthalpy is also a function of temperature only, since

$$\begin{aligned} h &= u + \frac{Pv}{J} \\ &= f_1(T) + \left(\frac{R}{J}\right) T \\ &= f_2(T) \end{aligned}$$

Having established that internal energy and enthalpy are dependent on temperature only, it follows that at any given temperature, internal energy and enthalpy are single values and independent of pressure. Hence, as shown in figure 13.1, specifying temperature and

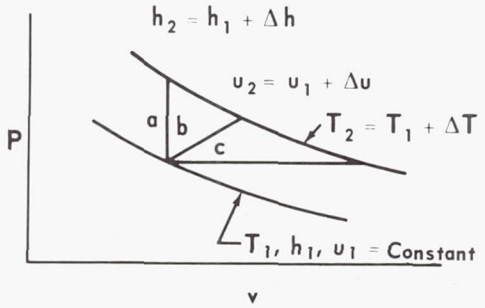


Figure 13.1. Lines of constant temperature, enthalpy, and internal energy on a pressure-volume diagram.

enthalpy or temperature and internal energy does not specify the state of a perfect gas. To adequately describe the state, it is necessary to specify pressure or some other temperature-independent property and either T, u, or h.

Specific Heats—The specific heats of a pure substance at constant volume and constant pressure are defined as

$$c_v = \left(\frac{\partial u}{\partial T}\right)_v \qquad [1.15]$$

and

$$c_p = \left(\frac{\partial h}{\partial T}\right)_p \qquad [1.16]$$

Since internal energy and enthalpy for a perfect gas are quantities dependent on temperature only, it follows that the specific heats for a perfect gas may be expressed as

$$c_v = \frac{du}{dT} \qquad (1.15a)^*$$

and

$$c_p = \frac{dh}{dT} \qquad (1.16a)^\dagger$$

An important relation between the two specific heats can be found from the definition of enthalpy of a perfect gas written in differential form,

$$dh = du + \frac{R\,dT}{J}$$

By substituting

$$du = c_v\,dT \qquad \text{and} \qquad dh = c_p\,dT$$

it follows that

$$c_p\,dT = c_v\,dT + \frac{R\,dT}{J}$$

or

$$c_p - c_v = \frac{R}{J} \qquad [2.6]$$

The above relation is very important in thermodynamic analysis, since it shows that for a perfect gas the difference between the two specific heat quantities is a constant, regardless of the absolute values of these quantities.

---

*This equation is a variation of equation (1.15) and does not appear in chapter 1.

†This equation is a variation of equation (1.16) and does not appear in chapter 1.

If the specific heats are constant, the ratio of these two quantities is a constant, and from equation (2.6)

$$1-\frac{c_v}{c_p}=\frac{R}{Jc_p} \qquad c_p=\frac{kR}{J(k-1)} \qquad [2.9]$$

and

$$\frac{c_p}{c_v}-1=\frac{R}{c_v} \qquad c_v=\frac{R}{J(k-1)} \qquad [2.10]$$

where k is the ratio c_p/c_v. With the specific heats constant, equations (1.15a) and (1.16a) may be simply integrated to yield

$$\Delta u=u_2-u_1=c_v\Delta T=\frac{R}{J(k-1)}\,\Delta T$$

and

$$\Delta h=h_2-h_1=c_p\Delta T=\frac{kR}{J(k-1)}\,\Delta T$$

The value of the specific heat and the specific heat ratio k depends on the complexity of the molecular structure of the gas molecule. For a monatomic gas, such as helium, the kinetic theory predicts values of c_{vm} and c_{pm} to be 3 and 5 Btu/mole$_{lb}$-°R, respectively, and a k value of 1.67. For gases with more complex structure, the value of k decreases but can never be less than unity. Values of k for several gases are shown in table 13.1.

The normal specific heat values tabulated in table 13.1 are obtained from equations (2.8) and (2.9) and are often termed the constant pressure zero pressure specific heat and the constant volume zero pressure specific heat. This is because they are accurate for moderate temperature and low pressure only. In low-pressure regions the specific heats of actual gases are only weakly dependent on pressure, and deviations from the normal k values listed in table 13.1 can be considered a result of temperature only. Several empirical equations for determining the real-gas specific heats at constant pressure are shown in table 2.3 (ch. 2). In higher pressure regions, the specific heats vary considerably with pressure variation. Also, the extent of this variation with pressure is affected by the temperature range. In some ranges of temperature, pressure of 6000 psia does not cause excessive changes in specific heats; however, in other temperature ranges, variation with pressure may be extreme. Plotted values of c_p and c_v for five gases are shown in appendixes B through F. The reader is cautioned against the use of a value of k computed from the real-gas values of specific heats as an isentropic exponent in the perfect-gas relationships. (See ch. 4 for more on this subject.)

EXAMPLE PROBLEM 13.1

The tank shown in figure 13.2 has a water volume of 10.65 ft^3 and is thermally insulated. Initially, it contains gaseous nitrogen at 85.3 psig and 70° F. If the solenoid valve connecting the tank and the supply line is opened and the tank is charged with gaseous nitrogen at 750 psia and 0° F, determine:

(1) Final mass of gas in the tank

(2) Final temperature of the gas in the tank after charging

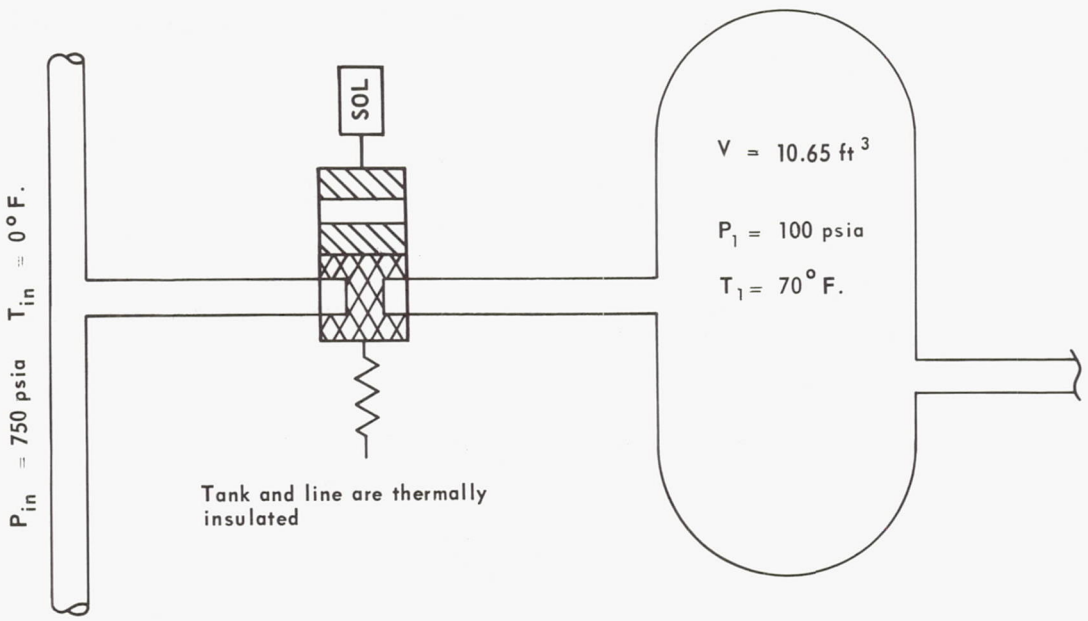


Figure 13.2. Gas storage system schematic.

(3) Heat required to bring gas temperature to 200° F
(4) Pressure after required amount of heat is added

Treat the gas as a perfect gas.

SOLUTION

Considering the tank contents as the system, equation (12.2) may be written as

$$dE_\sigma = E_{in} - E_{out} + \frac{(P\bar{V})_{in}}{J} - \frac{(P\bar{V})_{out}}{J}$$

Denoting the initial and final tank conditions by the subscripts 1 and 2, respectively, the following relation is obtained

$$E_2 - E_1 = E_{in} - E_{out} + \frac{(P\bar{V})_{in}}{J} - \frac{(P\bar{V})_{out}}{J}$$

Since no fluid leaves the system, it follows that

$$E_2 - E_1 = E_{in} + \frac{(P\bar{V})_{in}}{J}$$

Neglecting the kinetic energy and potential energy terms, equation (12.3*a*) becomes

$$E = U \qquad \text{or} \qquad E = Wu$$

hence,

$$W_2u_2 - W_1u_1 = W_{in}u_{in} + \frac{W_{in}(Pv)_{in}}{J}$$

Also, from the definition of enthalpy

$$h = u + \frac{Pv}{J}$$

therefore,

$$W_2u_2 - W_1u_1 = W_{in}h_{in}$$

Since no flow leaves the system,

$$W_{in} = W_2 - W_1$$

it follows that

$$(W_2 - W_1)h_{in} = W_2u_2 - W_1u_1$$

$$W_2(h_{in} - u_2) = W_1(h_{in} - u_1)$$

therefore,

$$W_2 = \frac{W_1(h_{in} - u_1)}{h_{in} - u_2}$$

Since the gas is perfect, the internal energy may be expressed

$$du = c_v\,dT$$

and for a constant c_v over the temperature range from T_r to T_2,

$$u_2 - u_r = c_v(T_2 - T_r)$$

where u_r is the internal energy at the reference temperature T_r. Choosing the reference internal energy as zero, at T_r of 0° R, the above equation reduces to

$$u_2 = c_vT_2$$

Since

$$\bar{V} = Wv \qquad \text{and} \qquad Pv = RT$$

the temperature may be expressed as

$$T = \frac{\bar{V}P}{RW} \qquad \text{and} \qquad u_2 = c_v\left(\frac{\bar{V}P_2}{RW_2}\right)$$

By substituting this last equation into the equation relating W_2 and W_1 and solving for W_2, it follows that

$$W_2 = W_1 \left(1 - \frac{u_1}{h_{in}}\right) + \frac{c_v}{h_{in}} \left(\frac{P_2 \bar{V}}{R}\right)$$

Since the gas is perfect, W_1 can be evaluated at $P = 100$ psia and $T = 70°$ F as

$$\begin{aligned} W_1 &= \frac{P_1 \bar{V}}{RT_1} \\ &= \frac{(100)(144)(10.65)}{55.2(70+460)} \\ &= 5.24 \text{ lbm} \end{aligned}$$

Also, u_1 can be evaluated at $T = 70°$ F from

$$\begin{aligned} u_1 &= c_v T_1 \\ &= 0.177(460+70) \\ &= 93.8 \text{ Btu/lbm} \end{aligned}$$

Similarly,

$$\begin{aligned} h_{in} &= c_p T_{in} \\ &= 0.248(460) \\ &= 114 \text{ Btu/lbm} \end{aligned}$$

Substituting these values into the previous equation

$$\begin{aligned} W_2 &= 5.24 \left(1 - \frac{93.8}{114.0}\right) + \left(\frac{0.117}{114.0}\right) \frac{(750)(144)(10.65)}{55.2} \\ &= 33.264 \text{ lbm} \end{aligned}$$

The final temperature may now be evaluated by

$$\begin{aligned} T &= \frac{P\bar{V}}{WR} \\ &= \frac{(750)(144)(10.65)}{33.264(55.2)} \\ &= 627° \text{ R} \\ &= 167° \text{ F} \end{aligned}$$

To determine the heat needed to bring the tank to the required temperature, the first law energy equation is used. Since there is no work done and no mass enters or leaves, the first law requires that

$$dQ = dU = W_2 \, du = W_2 c_v \, dT \qquad \text{or} \qquad \Delta Q = W_2 c_v (\Delta T)$$

$$\begin{aligned} \Delta Q &= 33.264(0.177)(200-167) \\ &= 194.5 \text{ Btu} \end{aligned}$$

At the new temperature, the new system pressure is given by

$$P=\frac{\mathbb{W}RT}{\bar{V}}$$
$$=\frac{33.3(55.2)(660)}{10.65}$$
$$=113\,200 \text{ psf}$$

$$p=\frac{P}{144}=\frac{113\,200}{144}$$
$$=788 \text{ psia}$$

Entropy—Two general expressions for the change in entropy of a perfect gas can be found from the two first law expressions

$$T\,ds=du+\frac{P\,dv}{J} \qquad [1.6]$$

and

$$T\,ds=dh-\frac{v\,dP}{J} \qquad [1.7]$$

Utilizing the perfect-gas relations

$$du=c_v\,dT=\left(\frac{R}{J(k-1)}\right)dT, \qquad dh=c_p\,dT=\left(\frac{kR}{J(k-1)}\right)dT \qquad \text{and} \qquad Pv=RT$$

the above relations become

$$ds=(c_v)\,\frac{dT}{T}+\left(\frac{R}{J}\right)\frac{dv}{v} \qquad [2.13]$$

$$ds=\left[\frac{R}{J(k-1)}\right]\frac{dT}{T}+\left(\frac{R}{J}\right)\frac{dv}{v} \qquad [2.14a]$$

or

$$\Delta_s=\left[\frac{R}{J(k-1)}\right]\ln\left(\frac{T_2}{T_1}\right)+\left(\frac{R}{J}\right)\ln\left(\frac{v_2}{v_1}\right) \qquad [2.14b]$$

Also, by equation (1.7),

$$ds=(c_p)\,\frac{dT}{T}-\left(\frac{R}{J}\right)\frac{dP}{P} \qquad [2.15]$$

or

$$ds=\left[\frac{kR}{J(k-1)}\right]\frac{dT}{T}-\left(\frac{R}{J}\right)\frac{dP}{P} \qquad [2.16a]$$

$$\Delta_s=\left[\frac{kR}{J(k-1)}\right]\ln\left(\frac{T_2}{T_1}\right)-\left(\frac{R}{J}\right)\ln\left(\frac{P_2}{P_1}\right) \qquad [2.16b]$$

Perfect-Gas Processes

Constant-Volume Process—Since there is no volume change for this process, the work given by $\delta Wk = P\ d\bar{V}$ is zero. Since the work term is zero, the heat transferred during the process is reflected by the change in internal energy; hence, for the closed system

$$dQ' = c_v\ dT = \left[\frac{R}{J(k-1)}\right] dT \qquad [2.17]$$

or

$$\Delta Q' = c_v\ \Delta T = \left[\frac{R}{J(k-1)}\right] \Delta T$$

The entropy change for this process is given by equation (2.14*a*) with $d\gamma = 0$ as

$$ds = \left[\frac{R}{J\ (k-1)}\right] \frac{dT}{T} \qquad [2.18]$$

or

$${}_1\Delta s_2 = \left[\frac{R}{J\ (k-1)}\right] \ln\left(\frac{T_2}{T_1}\right)$$

Constant-Pressure Process—Since pressure is a constant for this process, the reversible work done is given by

$${}_1wk_2 = \int_1^2 P\ dv = P(v_2 - v_1) \qquad [2.19]$$

Then, for the closed system the heat transfer is found as the sum of the internal energy and the work, in accordance with the first law, equation (1.7)

$$dQ' = c_p\ dT - \frac{v\ dP}{J} \qquad [2.20]$$

Then, for the case of constant pressure,

$$dQ' = \left[\frac{kR}{J(k-1)}\right] dT = c_p\ dT \qquad [2.21]$$

or

$$\Delta Q' = \left[\frac{kR}{J(k-1)}\right] \Delta T = c_p\ \Delta T$$

For the entropy change, the general equation (2.15) is selected so that for the constant-pressure process

$$ds = \left[\frac{kR}{J(k-1)}\right] \frac{dT}{T} = \int c_p \left(\frac{dT}{T}\right) \qquad [2.22]$$

or

$${}_1\Delta s_2 = \left[\frac{kR}{J(k-1)}\right] \ln\left(\frac{T_2}{T_1}\right) = c_p \ln\left(\frac{T_2}{T_1}\right)$$

Isothermal Process—The isothermal process is a process occurring at constant temperature, so that for the perfect gas

$$Pv = \text{constant} = P_1 v_1 = RT$$

and as a result, the following equations taken from equations (2.23*a*) and (2.23*b*) show that the work may be evaluated as

$$_1wk_2 = \int_1^2 P\,dv = P_1 v_1 \int_1^2 \frac{dv}{v}$$

$$= P_1 v_1 \ln\left(\frac{v_2}{v_1}\right) = RT \ln\left(\frac{v_2}{v_1}\right)$$

$$= P_1 v_1 \ln\left(\frac{P_1}{P_2}\right) = RT \ln\left(\frac{P_1}{P_2}\right)$$

Also, since the temperature is a constant, it follows from the first law that the heat transfer for this process is equal to the work done. Hence, for a constant-temperature process of a perfect gas in a closed system,

$$_1Q_2' = \left(\frac{RT}{J}\right) \ln\left(\frac{P_1}{P_2}\right) = \left(\frac{RT}{J}\right) \ln\left(\frac{v_2}{v_1}\right) \qquad [2.24]$$

Reversible-Adiabatic Process—The reversible-adiabatic process is a constant-entropy process; hence, the first law for a closed system undergoing a reversible-adiabatic process may be written for this process as

$$du + \frac{P\,dv}{J} = T\,ds = 0 \qquad [1.6]$$

If the gas is thermally perfect, it follows that

$$\left[\frac{R}{J(k-1)}\right] dT + \frac{P\,dv}{J} = 0$$

By writing the perfect-gas equation of state in differential form and substituting for dT in the foregoing equation, the following very useful relation can be obtained

$$k\left(\frac{dv}{v}\right) + \frac{dP}{P} = 0$$

which integrates for constant k values to yield

$$Pv^k = \text{constant} \qquad [2.25]$$

Also, by use of the perfect-gas equation of state, it may be shown that the following relations hold

$$\frac{T_2}{T_1}=\left(\frac{P_2}{P_1}\right)^{\frac{k-1}{k}} \qquad [2.26a]$$

and

$$\frac{v_2}{v_1}=\left(\frac{T_1}{T_2}\right)^{\frac{1}{k-1}} \qquad [2.26b]$$

Since the process is adiabatic, the heat transfer is zero. The work term is

$$\begin{aligned} {}_1wk_2 &= \int_1^2 P\,\mathrm{d}v = P_1v_1^k \int_1^2 \frac{\mathrm{d}v}{v^k} \\ &= \left(\frac{1}{k-1}\right)(P_1v_1 - P_2v_2) \\ &= \left(\frac{R}{k-1}\right)(T_1 - T_2) \end{aligned} \qquad [2.27]$$

Polytropic Process—A polytropic process is a general irreversible process in which there is heat transfer. The analysis of this general process requires only that the properties can be defined by the equation

$$Pv^n = \text{constant} \qquad [2.28b]$$

Then, where n is a constant, it follows, as in the isentropic process, that

$$\frac{T_2}{T_1}=\left(\frac{P_2}{P_1}\right)^{n-1/n} \qquad [2.29]$$

and

$$\frac{T_2}{T_1}=\left(\frac{v_1}{v_2}\right)^{n-1} \qquad [2.30]$$

The first law for a closed system undergoing a polytropic process may be written

$${}_1Q_2' = u_2 - u_1 + \int_1^2 \frac{P\,\mathrm{d}v}{J}$$

Utilizing the perfect-gas relation

$$u = h - \frac{Pv}{J}$$

$$Pv^n = \text{constant}$$

$$\mathrm{d}h = \left[\frac{kR}{J\,(k-1)}\right]\mathrm{d}T \qquad \text{and} \qquad Pv = RT$$

the foregoing relation becomes

$$ {}_1Q_2' = \frac{R}{J}\left(\frac{1}{n-1} - \frac{1}{k-1}\right)(T_1 - T_2) \qquad [2.31a] $$

$$ {}_1Q_2' = \frac{1}{J}\left(\frac{1}{n-1} - \frac{1}{k-1}\right)(P_1v_1 - P_2v_2) \qquad [2.31b] $$

$$ {}_1Q_2' = \frac{RT_1}{J}\left(\frac{1}{n-1} - \frac{1}{k-1}\right)\left(1 - \frac{T_2}{T_1}\right) \qquad [2.32] $$

From an intermediate step in the derivation of equation (2.31), the reversible work term may be shown to be

$$ {}_1wk_2 = \frac{1}{n-1}(P_1v_1 - P_2v_2) \qquad [2.33a] $$

$$ {}_1wk_2 = \frac{R}{(n-1)}(T_1 - T_2) = \frac{RT_1}{n-1}\left(1 - \frac{T_2}{T_1}\right) \qquad [2.33b] $$

Table 13.3 summarizes the equation applicable to each of the perfect-gas processes discussed.

REAL GAS

Equations of State

The perfect-gas equation of state predicts the ideal relationship of any gas over the full range of temperature and pressure. It is an experimental fact, however, that at high pressures or high temperatures or in regions near the point of condensation of the liquid phase, variations from this ideal relationship do occur. The magnitude of these deviations depends on the particular gas and the values of the temperature and pressure. As pressure is increased from zero pressure, the deviation from the perfect-gas law increases. Also, the deviation at a given pressure will be less at higher temperatures, except when temperature is so extreme as to cause ionization or dissociation.

Numerous equations of state have been proposed that will, at least in part, compensate for the deviation from perfect-gas behavior, among these are:

(1) Van der Waals' equation:

$$ \left(P + \frac{a}{v_m^2}\right)(v_m - b) = RT $$

where a and b are constants, characteristic of the particular gas.

(2) Berthelot's equation:

$$ Pv_m = RT\left(1 + \frac{Pb'}{RT} - \frac{a'P}{R^2T^3}\right) $$

where a' and b' are constants.

(3) Dieterici's equation:

$$ P = \left(\frac{RT}{v_m - b''}\right)e^{-a''/RTv_m} $$

TABLE 13.3.—*Perfect-Gas Processes and Equations*

Gas processes	Equations	Final pressure	Final volume	Final temperature	Heat added, Btu	External work, ft-lbf
Isothermal:		$P_2 = P_1\left(\frac{v_1}{v_2}\right)$	$v_2 = v_1\left(\frac{P_1}{P_2}\right)$	$T_2 = T_1$	$\left(\frac{RT_1}{J}\right)\ln\left(\frac{v_2}{v_1}\right)$	$RT_1 \ln\left(\frac{v_2}{v_1}\right)$
$T = C$	$Pv = C$				or	or
$n = 1$		Decreases	Increases	No change	$\left(\frac{P_1v_1}{J}\right)\ln\left(\frac{v_2}{v_1}\right)$	$P_1v_1 \ln\left(\frac{v_2}{v_1}\right)$
Adiabatic constant entropy:		$P_2 = P_1\left(\frac{v_1}{v_2}\right)^k$	$v_2 = v_1\left(\frac{P_1}{P_2}\right)^{\frac{1}{k}}$	$T_2 = T_1\left(\frac{v_1}{v_2}\right)^{k-1}$		$\frac{P_1v_1 - P_2v_2}{k-1}$
$n = k$	$Pv^k = C$				None	or
No heat exchanges		$P_2 = P_1\left(\frac{T_2}{T_1}\right)^{\frac{k}{k-1}}$	$v_2 = v_1\left(\frac{T_1}{T_2}\right)^{\frac{1}{k-1}}$	$T_2 = T_1\left(\frac{P_2}{P_1}\right)^{\frac{k-1}{k}}$		$c_vJ(T_1 - T_2)$
		Decreases	Increases	Decreases		
Isobaric:	$P = C$	$P_2 = P_1$	$v_2 = v_1\left(\frac{T_2}{T_1}\right)$	$T_2 = T_1\left(\frac{v_2}{v_1}\right)$	$c_p(T_2 - T_1)$	$P_1(v_2 - v_1)$
$n = 0$					or	or
$P = C$	$v = CT$	No change	Increases	Increases	$\frac{P_2k(v_2 - v_1)}{(k-1)J}$	$R(T_2 - T_1)$

Charles' law: $n=1$ $V=C$	$v=C$ $p=CT$	$P_2=\frac{P_1T_2}{T_1}$ Increases	$v_2=v_1$ No change	$T_2=\frac{P_2T_1}{P_1}$ Increases	$c_p(T_2-T_1)$ or $\frac{v_1(P_2-P_1)}{(k-1)J}$	None
Polytropic: $n=\frac{r-1+a}{a}$ External work = a loss in intrinsic energy	$Pv^n=C$	$P_2=P_1\left(\frac{v_1}{v_2}\right)^n$ $P_2=P_1\left(\frac{T_1}{T_2}\right)^{\frac{n}{n-1}}$ Decreases	$v_2=v_1\left(\frac{P_1}{P_2}\right)^{\frac{1}{n}}$ $v_2=v_1\left(\frac{T_1}{T_2}\right)^{\frac{n-1}{n}}$ Increases	$T_2=T_1\left(\frac{V_1}{V_2}\right)^{n-1}$ $T_2=T_1\left(\frac{P_2}{P_1}\right)^{\frac{n-1}{n}}$ Decreases	$(P_1v_1-P_2v_2)\left(\frac{1}{n-1}-\frac{1}{k-1}\right)$ or $c_v(T_1-T_2)\left(\frac{k-1}{n-1}-1\right)$	$\frac{P_1v_1-P_2v_2}{n-1}$ or $\frac{R(T_1-T_2)}{n-1}$

Values of constants:

$R=1544/M_w$ (M_w = molecular weight).

$k=1.4$ for diatomic gases.

$k=1.3$ for triatomic gases.

where a'' and b'' are constants.

(4) Wohl's equation:

$$P=\frac{RT}{v_m-b'''}-\frac{a'''}{v_m(v_m-b''')}+\frac{c'''}{v_m^3}$$

where a''', b''', and c''' are constants.

(5) Keyes' equation:

$$P=\frac{RT}{v_m-\alpha}-\frac{e}{(v_m g)^2} \qquad \alpha=Be^{-k/v_m}$$

where B, k, e, and g are constants.

(6) Beattie-Bridgeman's equation:

$$P=\frac{RT}{v_m^2}\left(1-\frac{A}{v_m T^3}\right)\left[v_m+B\left(1-\frac{D}{v_m}\right)\right]-\frac{E}{v_m^2}\left(1-\frac{F}{v_m}\right)$$

where A, B, D, E, and F are constants.

In all these equations, v_m refers to the molal specific volume. Their accuracy in correlating experimental data depends, in general, on the number of constants (listed beneath each equation) that may be assigned specific values for each gas. The Beattie-Bridgeman equation of state with five such constants has been found to agree within a fraction of 1 percent with experimental data for a number of substances over a wide range of conditions. The Beattie-Bridgeman equation is complex, but it is exceedingly useful if the constants for the gas involved are known for the range of interest. B. F. Dodge's text on *Chemical Engineering Thermodynamics* (1944) has a tabulation of Beattie-Bridgeman constants for a number of gases.

The Van der Waals equation may be expected to give better results than the perfect-gas law. However, it has only two arbitrary constants and cannot be expected to duplicate experimental data exactly, and it may be seriously in error under certain severe conditions.

The equations of Berthelot, Dieterici, Wohl, and Keyes generally are not as accurate as the Beattie-Bridgeman equation but, owing to their simplicity and form, may be useful for specific types of calculations.

If it is desired to fit experimental data with great accuracy over large pressure ranges, the following equation known as the virial form of an equation of state is recommended because of its flexibility

$$Pv_m=RT+\frac{B}{v_m}+\frac{r}{v_m^2}+\frac{\delta}{v_m^3}$$

where the coefficients B, r, and δ are temperature functions as follows

$$B=RTB_0-A_0-\frac{RC}{T^2}$$

$$r=RTB_0b+aA_0-\frac{RB_0C}{T^2}$$

$$\delta=\frac{RB_0bc}{T^2}$$

This virial equation is really a condensed summary of the data. It requires a different set of coefficients for each temperature, and it becomes very cumbersome for practical application.

Law of Corresponding States

There is yet another method of coping with real-gas deviation from perfect-gas behavior. This method is based on the law of corresponding states. The deviation of the volume of real gases from that predicted by the perfect-gas law can be simply represented by plotting the ratio of the actual volume to that predicted by the perfect-gas law versus the pressure, or in other words,

$$\frac{v}{\frac{RT}{P}}=\frac{Pv}{RT}=Z=\text{compressibility factor}$$

is plotted as the ordinate, and pressure as the abscissa, for lines of constant temperature. The law of corresponding states provides an avenue to a method of determining the compressibility factor Z in a generalized form applicable to all gases.

It was stated previously that the extent of deviation from perfect-gas behavior increased as the region of condensation was approached. The law of corresponding states postulates that all gases have the same P–v–T behavior at the same reduced conditions. Hence, the behavior of all gases is correlated, not by using actual temperature and pressure but by using ratios of those values to the temperature and pressure at the critical point. In other words, the deviation of two gases may be very different at the same temperature and pressure, but may be the same if considered at the same temperature and pressure relative to the region of condensation.

The critical temperature and pressure are used as characteristics of the region of condensation. Thus, the ratio T/T_c is commonly called the reduced temperature (T_r), and similarly P/P_c is the reduced pressure (P_r).

This method of correlating P–v–T data has been found to be of considerable value, especially in those cases where the available information is insufficient to evaluate the constants in an equation of state such as the Beattie-Bridgeman equation. The accuracy of the generalized charts, such as those shown in figure 13.3, depends on the type of gas and the pressure and temperature. Dodge has made a rather comprehensive comparison of the charts with actual data. His results indicate a maximum deviation of 15 percent and an average deviation of about 2 percent for 263 individual cases covering a wide range of pressure and temperature and 18 different gases. Table 13.4 (from Getman and Daniels) shows the value of compressibility factor chart (frequently referred to as "Hougen and Watson chart").

TABLE 13.4.—*Comparison of Compressibility Factors*

Pv/RT for nitrogen at 1000 atm					
Temperature, °C	Observed	Ideal	Van der Waals	Berthelot	Hougen and Watson chart
0	2.0632	1.0000	2.426	0.731	2.10
50	1.9285	1.0000	2.182	1.071	1.95

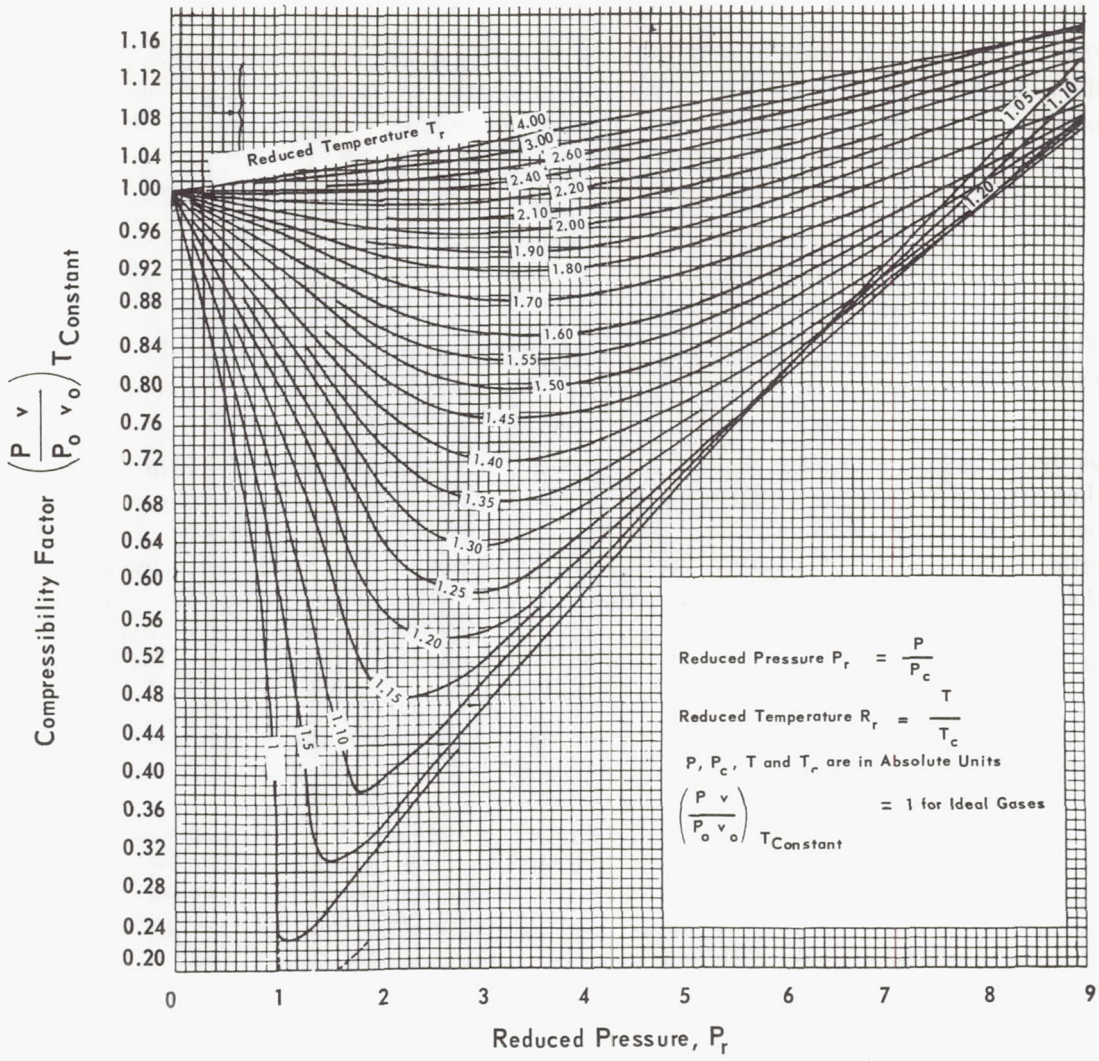
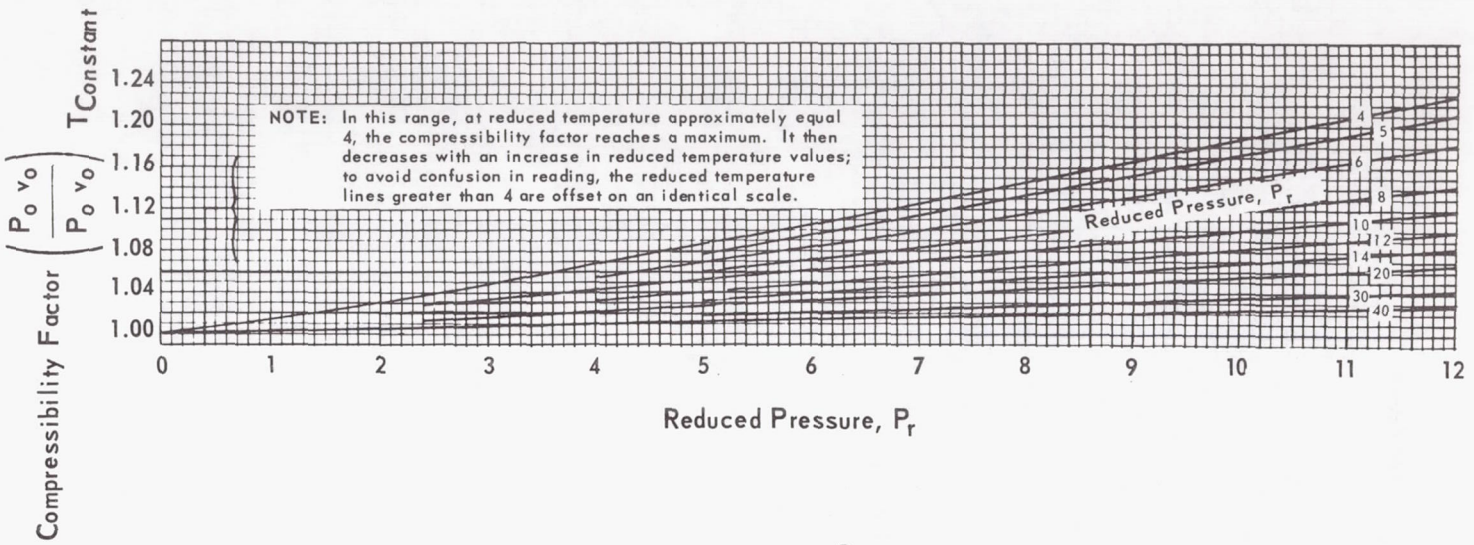


Figure 13.3. Compressibility factor for gases. [*Courtesy of the American Society of Mechanical Engineers.*]



$$\text{Reduced Pressure } P_r = \frac{P}{P_c}$$

$$\text{Reduced Temperature } R_r = \frac{T}{T_c}$$

P, P_c, T and T_c are in Absolute Units

$$\left(\frac{P\ v}{P_o\ v_o}\right)_{T\,Constant} = 1 \text{ for Ideal Gases}$$

Figure 13.3. Compressibility factor for gases.—Continued. [*Courtesy of the American Society of Mechanical Engineers.*]

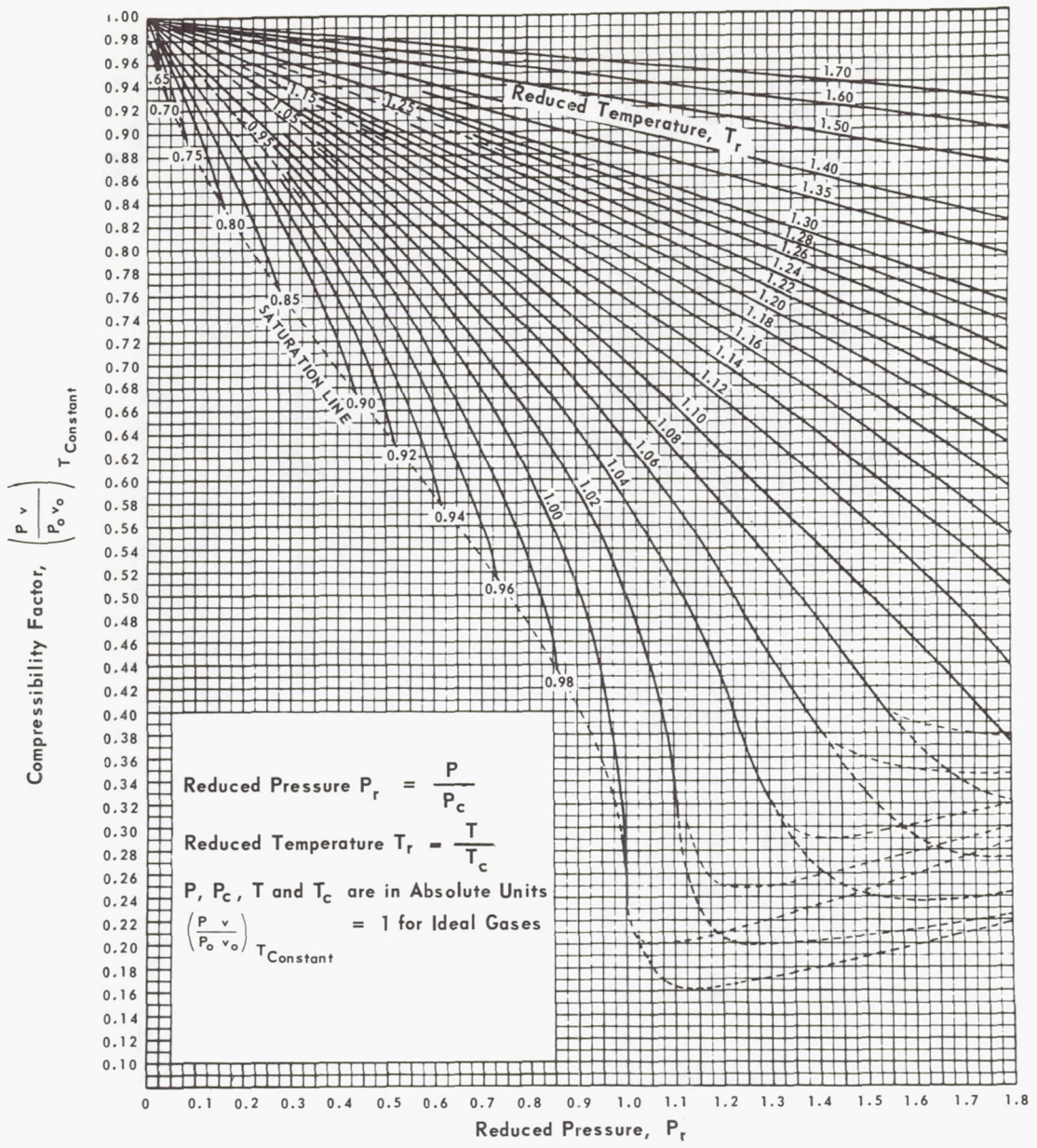


Figure 13.3. Compressibility factor for gases.—Continued. [*Courtesy of the American Society of Mechanical Engineers.*]

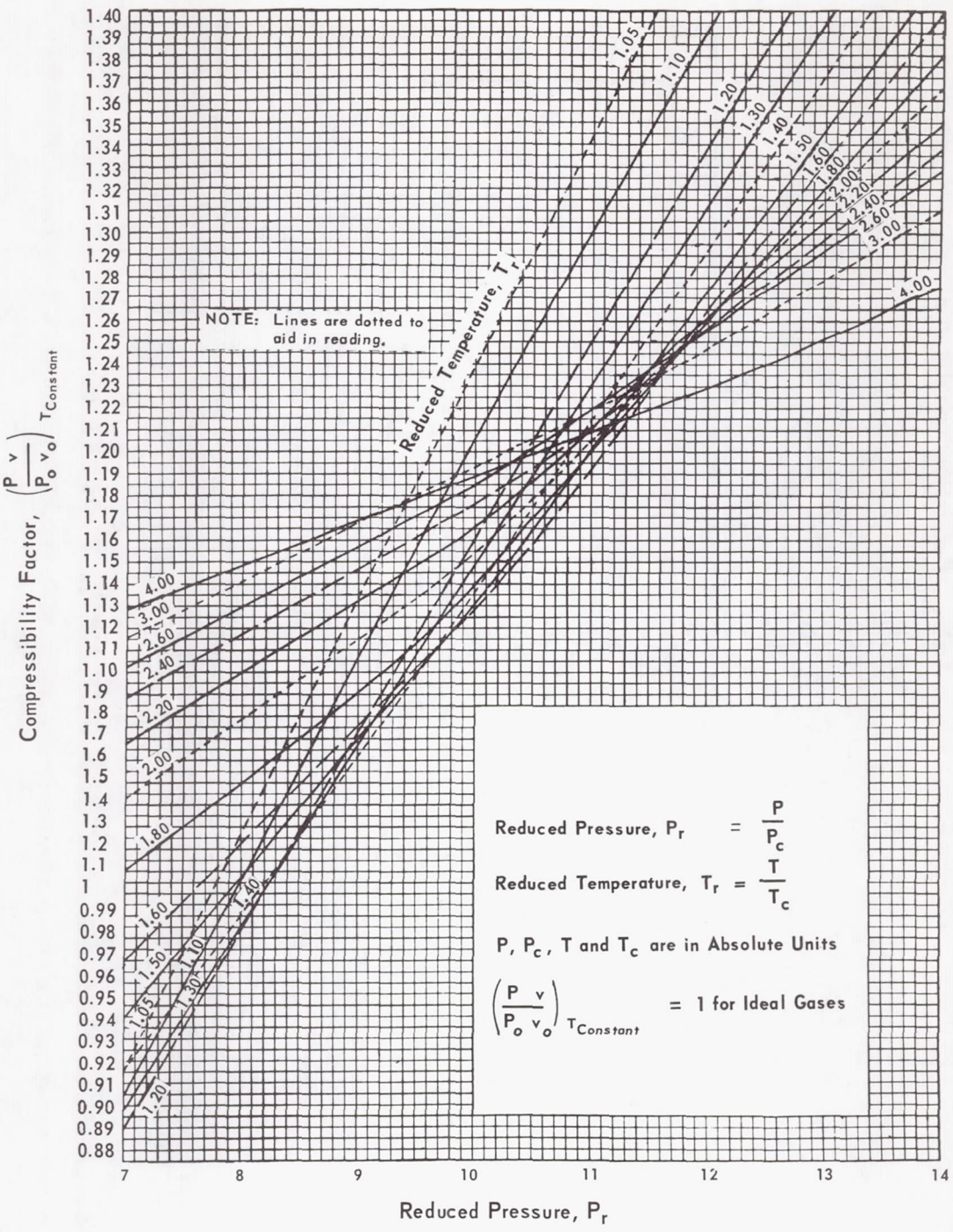


Figure 13.3. Compressibility factor for gases.—Continued. [*Courtesy of the American Society of Mechanical Engineers.*]

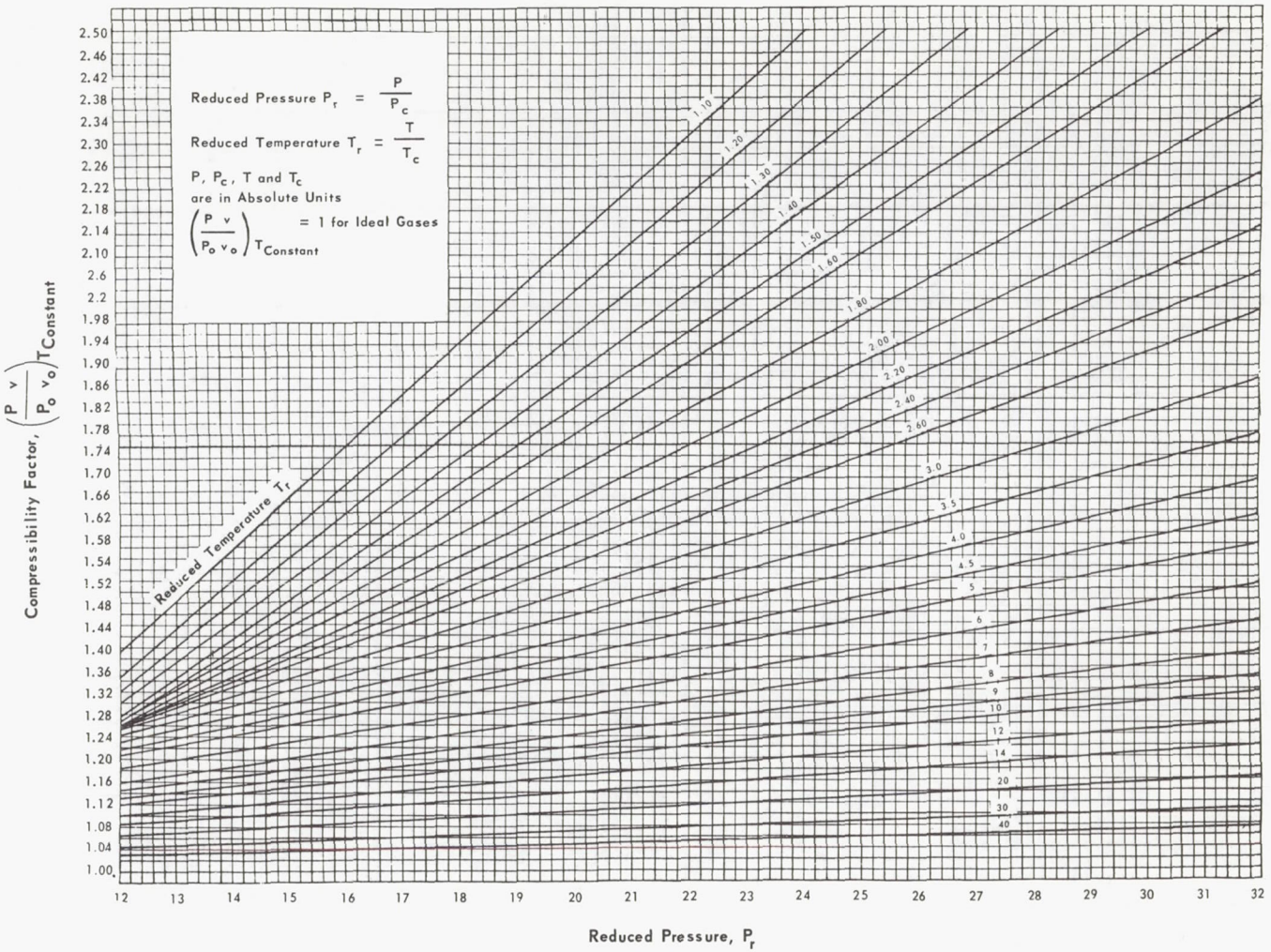


Figure 13.3. Compressibility factor for gases.—Continued. [*Courtesy of the American Society of Mechanical Engineers.*]

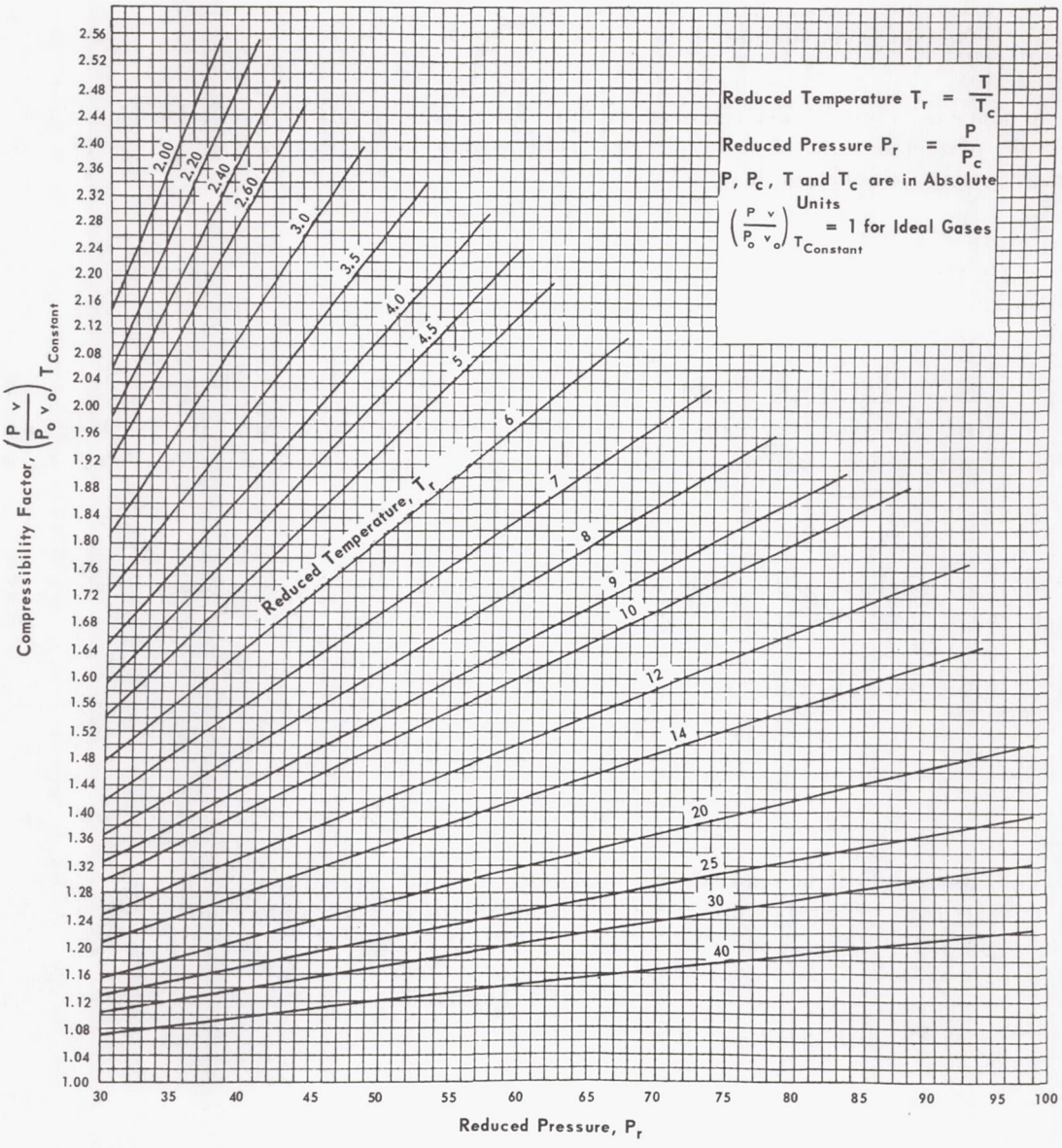


Figure 13.3. Compressibility factor for gases.—Concluded. [*Courtesy of the American Society of Mechanical Engineers.*]

EXAMPLE PROBLEM 13.2

Considering the same system as that described in example problem 13.1 and treating the gas as a real gas, determine the following:

(1) The final mass of gas in the tank

(2) The final temperature of the gas in the tank

SOLUTION

Since the equation derived in example problem 13.1 to relate w_1 and w_2 does not depend on the perfect-gas law for its validity, it may be used in the real-gas analysis. Repeating the contained mass equation then

$$W_2 = W_1 \left(\frac{h_{in} - u_1}{h_{in} - u_2} \right)$$

Also, the volume equation may be written as

$$\bar{V} = W_2 v_2$$

In the foregoing two equations, $\bar{V}$ is known from the statement of the problem, and w_1, h_{in}, and u_1 may be evaluated as follows. To evaluate W_1, the real-gas relation is used

$$p_1 \bar{V} = W_1 Z_1 R T_1$$

From the statement of the problem, $P_1 = 100$ psia and $T_1 = 70°$ F, as shown in figure C.2 (app. C) at the given temperature and pressure, Z_1 is read as

$$Z_1 = 1$$

Therefore

$$W_1 = \frac{(100)(144)(10.65)}{(1)(55.2)(460+70)}$$

$$= 5.24 \text{ lbm}$$

The enthalpy h_{in} can be read directly as $h_{in} = 160$ Btu/lbm from figure C.1 (app. C) by entering the chart at $P = 750$ psia and $T = 0°$ F. The internal energy u_1 can be found by reading the enthalpy at $P = 100$ psia and $T = 70°$ F,

$$h = 183.5 \text{ Btu/lbm}$$

then from the definition of enthalpy

$$u_1 = h_1 - \frac{P_1 v_1}{J}$$

or, since

$$Pv = ZRT$$

it follows that

$$u_1 = h_1 - \frac{Z_1 R T_1}{J}$$

Reading $Z = 1$ from figure C.2 (app. C), the following relations are obtained

$$u_1 = 183.5 - \frac{(1)(55.2)(530)}{788} = 146 \text{ Btu/lbm}$$

Substituting the values of $\bar{V}$, W_1, u_1, and h_{in} into the contained mass and volume equations yields

$$W_2 = 5.24\left(\frac{160-146}{160-u_2}\right) \qquad \text{or} \qquad u_2 = 160 - \frac{73.4}{W_2}$$

Also

$$v_2 = \frac{\bar{V}}{W_2} = \frac{10.65}{W_2}$$

Now there are two equations and three unknowns, and if there is no simple relation between any two of these properties for the real gas, a trial-and-error solution must be used.

A perfect-gas relationship is found to produce a very good approximation that yields a direct solution. Since

$$du = c_v\, dT$$

and since the data of figure C.4 (app. C) indicate a very nearly constant value of $c_v = 0.179$ Btu/lbm over the expected range of temperature and pressure, the following equation can be used with accuracy

$$\begin{aligned} u_2 &= u_1 + c_v(T_2 - T_1) \\ &= 146 + 0.179(T_2 - 530) \end{aligned}$$

The previous equation can be written in terms of T_2 also by substituting the perfect-gas law solved for W_2

$$u_2 = 160 - \frac{73.4}{\dfrac{(750)(144)(10.65)}{(1)(55.2)(T_2)}}$$

Equating this equation with the approximate equation for u_2 above permits a direct solution for T_2 yielding

$$\begin{aligned} T_2 &= 596^\circ \text{ R} \\ &= 136^\circ \text{ F} \end{aligned}$$

The final mass of gas in the tank is obtained by writing the perfect-gas law once again, including $Z = 1.0$,

$$\begin{aligned} W_2 &= \frac{(750)(144)(10.65)}{(1)(55.2)(596)} \\ &= 35.0 \text{ lbm} \end{aligned}$$

By comparison of these results with that of example problem 13.1, the real-gas effects in this problem caused a lower final temperature and a slightly greater final stored mass.

CHAPTER 14

APPLICATION OF FUNDAMENTALS OF INCOMPRESSIBLE FLOW

The term "fluid" is applied to substances which, by the nature of their internal structure, offer comparatively little resistance to a change in form. Incompressible fluids, however, offer great resistance to volume change.

No fluid is capable of any internal adjustment which will enable it to maintain equilibrium at rest while subjected to a shear stress. If a shearing force is applied to any fluid, the fluid will continue to deform as long as the force is applied. There will invariably be some movement in which the velocity is proportional to the applied shear stress. The relation between force and velocity depends on, among other things, that property of fluids known as viscosity.

An ideal or perfect fluid is merely one which, for purposes of developing theory or making a mathematical demonstration, is conveniently assumed to be nonviscous or incompressible, or both. Such fluids do not exist, and theory based on such assumption is subject in its application to correction for the effect of these physical properties that have been neglected.

In this chapter only incompressible fluids are considered. The effect of work and heat addition or removal are neglected. In an incompressible fluid an increase in pressure will not cause an increase in density. The assumption that liquids are incompressible does not usually introduce an appreciable error. The assumption that gases are incompressible, for flows below a mach number of 0.2, introduces only very slight error. Beyond this point gases should be treated as compressible fluids.

MASS DENSITY AND SPECIFIC WEIGHT

"Mass density" is defined as the mass of a substance per unit volume. Specific weight is the gravitational force per unit volume exerted by the mass subjected to a given acceleration as a result of gravity. In this chapter units for density are slugs per cubic foot or pounds mass per cubic foot, and specific weight has units of pounds force per cubic foot. The relation between these quantities is determined from Newton's first law written in terms of gravity.

$$F_{wt} = mg \qquad [3.1a]$$

or

$$F_{wt} = \left(\frac{W}{g_c}\right) g \qquad [3.1b]$$

If both sides of equations (3.1a) and (3.1b) are divided by the total volume $\bar{V}$, it follows that

Preceding Page Blank

$$\frac{F_{wt}}{\bar{V}} = \left(\frac{W}{\bar{V}}\right)\frac{g}{g_c} = \frac{mg}{\bar{V}} = \rho g \qquad [3.2]$$

In this system, the units of g_c must have the units of lbm/slug or lbm-ft/lbf-sec^2. Using equation (3.2), the following definitions can be made

$$\text{Mass density} = \rho = \frac{m}{\bar{V}} \qquad \text{slugs/ft}^3 \text{ or lbf-sec}^2/\text{ft}^4 \qquad [3.3a]$$

$$\text{Weight density} = \gamma = \frac{W}{\bar{V}} \qquad \text{lbm/ft}^3 \qquad [3.3b]$$

$$\text{Specific weight} = \gamma' = \frac{F_{wt}}{\bar{V}} \qquad \text{lbf/ft}^3 \qquad [3.3c]$$

Rewriting equation (3.2) in terms of the above three definitions, the following relationships are obtained

$$\gamma = \rho g_c \qquad [3.4a]$$

and

$$\gamma' = \rho g = \gamma\left(\frac{g}{g_c}\right) \qquad [3.4b]$$

VISCOSITY OF FLUIDS

Viscosity is the property of a substance by which it offers resistance to shearing stresses. In a Newtonian fluid the viscosity is in linear proportion to the ability of the fluid to resist such shearing stresses.

All fluids, both liquids and gases, have viscosity. The viscosity of a liquid decreases with an increase in temperature, whereas the viscosity of a gas increases with temperature.

A shearing force applied to a viscous material causes an unlimited and continuous deformation of the material. The rate of deformation or shear becomes a measure of the viscosity of a fluid.

In considering the effect of viscosity on fluid flow, it is necessary to introduce two fundamental assumptions which become the basis for the theory and application of viscosity. These assumptions are

(1) There is no relative motion between a solid boundary and the layer of fluid in contact with it.

(2) The shearing stress between layers of fluid, of infinitesimal thickness, is proportional to the rate of angular deformation of the fluid (Newtonian fluids).

For a Newtonian fluid, the shear stress is given by

$$\tau = \mu\left(\frac{dV}{dy}\right) \qquad [3.5]$$

where μ is a coefficient of proportionality called the absolute viscosity or coefficient of

viscosity. Also, y is the distance measurement from the bounding surface measured normal to the flow direction.

In the English system of units, equation (3.5) requires that the units of viscosity be lbf-sec/ft^2.

An alternate form of expressing viscosity of liquids is the kinematic viscosity which is defined by the equation

$$\nu = \frac{\mu}{\rho} = \frac{\mu g_c}{\gamma} = \frac{\mu'}{\gamma} \qquad [3.6]$$

From equation (3.6), it follows that the units for kinematic viscosity in the English system are ft^2/sec. Viscosity units for other systems of units are shown in table 14.1.

Plots of viscosity versus temperature are presented in the appendixes for several liquids and for gases at low pressures. In the high-pressure regions, pressure effects on viscosity

TABLE 14.1.—*Equivalents of Viscosity*

Equivalents of Absolute Viscosity

Absolute or dynamic viscosity Mult ↓ by→ to obtain ↑		Centipoise (μ)	Poise $\frac{\text{g}}{\text{cm sec}}$ or $\frac{\text{dyne sec}}{\text{cm}^2}$ (100 μ)	$\frac{\text{slugs}}{\text{ft sec}}$ or $\frac{\text{lbf sec}}{\text{ft}^2}$ (μ')	$\frac{\text{lbm}}{\text{ft sec}}$ or $\frac{\text{poundal sec}}{\text{ft}^2}$ (μ)
Centipoise	(μ)	1	0.01	$2.09(10^{-5})$	$6.72(10^{-4})$
Poise $\frac{\text{g}}{\text{cm sec}}$ or $\frac{\text{dyne sec}}{\text{cm}^2}$	(100 μ)	100	1	$2.09(10^{-3})$	0.0672
$\frac{\text{slugs}}{\text{ft sec}}$ or $\frac{\text{lbf sec}}{\text{ft}^2}$	(μ')	47 900	479	1	g or 32.2
$\frac{\text{lbm}}{\text{ft sec}}$ or $\frac{\text{poundal sec}}{\text{ft}^2}$	(μ)	1487	14.87	$\frac{1}{g}$ or 0.0311	1

TABLE 14.1.—*Equivalents of Viscosity*—Continued

Equivalents of Kinematic Viscosity

Kinematic viscosity: Mult ↓ / by → / to obtain ↑		Centistokes (ν)	Stokes $\frac{cm^2}{sec}$ (100 ν)	$\frac{ft^2}{sec}$ (ν')
Centistokes	(ν)	1	0.01	$1.076(10^{-5})$
Stokes $\frac{cm^2}{sec}$	(100 ν)	100	1	$1.076(10^{-3})$
$\frac{ft^2}{sec}$	(ν')	92 900	929	1

may be appreciable. Hence, viscosity based on temperature considerations only may lead to significant error. This subject, however, will be considered in chapter 15.

CONTINUITY EQUATION

Since, by definition, no fluid can enter or leave a stream tube across the walls, it is possible to write an equation expressing the continuity of flow along a stream tube. The volume of fluid passing the station having area A in figure 14.1 in the time interval dt is $A\ ds$. The mass of the fluid is $(\gamma A\ ds)$, so that the mass rate of flow is

$$\frac{\gamma A\ ds}{dt} = \gamma AV$$

since $ds/dt = V$, the nominal velocity of flow at A.

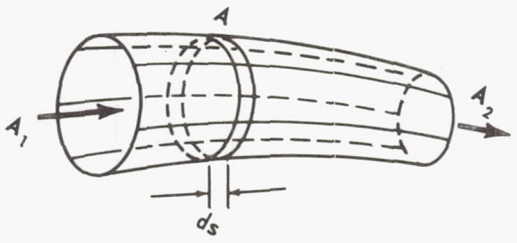


Figure 14.1. Stream tube.

If we let w represent mass flow per unit time, the law of conservation of mass requires that, for a steady flow, w in a stream tube is a constant, or

$$w = \gamma_1 A_1 V_1 = \gamma_2 A_2 V_2 = \gamma - aV \qquad [3.8]$$

since there can be no accumulation between stations in steady flow.

In incompressible fluid flow, where pressure changes do not cause changes in mass density, the continuity equation can be written simply as

$$\frac{w}{\gamma} = A_1 V_1 = A_2 V_2 = AV = \text{constant} \qquad [3.9]$$

BERNOULLI EQUATION

To obtain an equation for constant energy frictionless flow, consider the differential length of the stream tube shown in figure 14.2. Flow is caused in this stream tube by the difference in pressure acting along the stream tube axis.

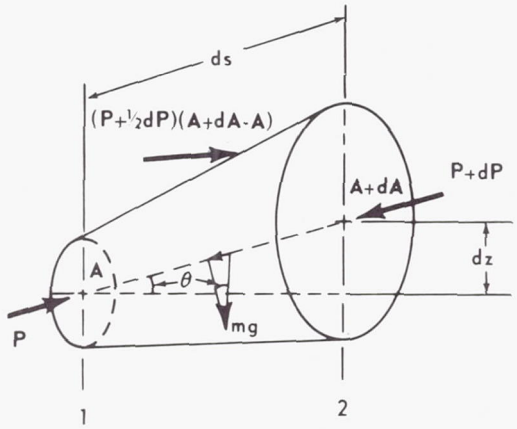


Figure 14.2. Forces acting on a stream-tube element in steady flow.

If the axial forces along the axis of the stream tube are summed, it follows from Newton's second law, $\Sigma F = m\alpha$, that

$$PA + \left(P + \frac{dP}{2}\right)(A + dA - A) - (A + dA)(P + dP) - mg \sin\theta = m\alpha$$

Neglecting all vanishingly small products of differentials and substituting

$$\alpha = \frac{dV}{dt} = \left(\frac{1}{2}\right)\frac{d(V^2)}{ds} \qquad \text{and} \qquad \sin\theta \approx \frac{dz}{ds}$$

yields

$$A\ dP\ ds + mg\ dz + \frac{m}{2}\ d(V)^2 = 0$$

This is an energy relation which states that, in a frictionless system work done by a force (in this case, the force due to the differing pressures acting on the stream tube elements) is balanced by equivalent changes in potential energy ($mg\ dz$) and kinetic energy [$m\ d(V^2)/2$] of the mass acted on.

By assuming the flow to be incompressible, there will be no expansion work, so that by substituting the continuity equation and converting the mass units to the gravitational system

$$V\left(\frac{g_c}{g}\right) dP + dz + \frac{d(V^2)}{2g} = 0 \qquad [3.10]$$

which integrates, at constant specific volume, to yield

$$\frac{P}{\gamma'} + z + \frac{V^2}{2g} = \text{constant} \qquad \text{ft} \qquad [3.11a]$$

and

$$\frac{P}{\gamma} + \left(\frac{g}{g_c}\right) z + \frac{V^2}{2g_c} = \text{constant} \qquad \text{ft-lbf/lbm} \qquad [3.11b]$$

This is the familiar Bernoulli equation for steady, frictionless, incompressible flow (in terms of fluid head) and energy per unit mass flowing, respectively.

MOMENTUM EQUATION

Newton's second law states that the resultant force applied to a free body can be equated to the rate of change of momentum of the body. Then in terms of the vector quantities

$$\Sigma \mathbf{F} = \frac{d}{dt}(\mathbf{mV}) \qquad [3.12a]$$

or in the impulse-momentum form

$$\Sigma \mathbf{F}\ dt = d(\mathbf{mV}) \qquad [3.12b]$$

The continuity equation can be substituted into equation (3.12a) and applied to two stations in a flow section where the velocity is constant, yielding

$$\begin{aligned} \Sigma \mathbf{F} &= \mathbf{m}_2\mathbf{V}_2 - \mathbf{m}_1\mathbf{V}_1 \\ &= (\rho_2\mathbf{A}_2\mathbf{V}_2^2) - (\rho_1\mathbf{A}_1\mathbf{V}_1^2) \end{aligned} \qquad [3.13a]$$

(The above equation is a modified version of that appearing in ch. 3.) Also, since continuity requires that the mass flow rate be the same at both stations (see eq. (3.13b))

$$\begin{aligned} \Sigma \mathbf{F} &= \mathbf{m}(\mathbf{V}_2 - \mathbf{V}_1) \\ &= \frac{\mathbf{w}}{\mathbf{g}_c}(\mathbf{V}_2 - \mathbf{V}_1) \end{aligned} \qquad [3.13b]$$

(The above equation is a modified version of that appearing in ch. 3.) This method of determining resultant forces on nozzles, piping systems, turbine blades, and so forth, offers the great advantage of evaluating only the inlet and outlet flow conditions and direction, rather

than a complicated investigation and integration of pressure distributions within the flow section of interest.

REYNOLDS NUMBER

The flow and heat-transfer behavior of fluids can often be conveniently described or categorized by dimensionless parameters. One of the more widely used of these parameters is the Reynolds number. The Reynolds number can be rationally derived from dimensional analysis and has as its defining equation

$$R_e = \frac{VL\rho}{\mu} \qquad [3.14a]$$

For the circular cross section, the length dimension is the diameter so that equation (3.14*a*) becomes

$$R_e = \frac{VD\rho}{\mu} \qquad [3.14b]$$

The physical significance of the Reynolds number is that it represents the relative magnitude of the inertial to viscous forces acting in the fluid stream. This ratio, in turn, has a definite effect on such factors as heat-transfer coefficients and the coefficient of viscous friction. It is also possible to describe types of flow in terms of the Reynolds number. For low Reynolds numbers, the viscous forces predominate and the flow is termed viscous flow, or laminar flow. The Reynolds number for laminar flow is generally 2000 or less. The upper limit for laminar flow, however, is subject to some extent to vibrational effects and perturbations in the flow stream. In laminar pipe flow, the velocity profile at a given section plots as a parabola with a velocity of zero at the pipe wall and a maximum velocity at the centerline. For Reynolds numbers of 4000 and above, the flow is governed by inertial forces, and the velocity profile is no longer parabolic. The velocity profile has a tendency to become blunt and almost a straight line across the entire pipe cross section.

Between Reynolds numbers of 2000 and 4000, the flow is termed transitional flow. In this region the flow can be either laminar or turbulent, or mixed. Above about 2100, if the system is disturbed or if there are any irregularities, the flow will change from laminar to turbulent. In general, when the Reynolds number is above 2000, the flow is considered turbulent to some degree.

HYDRAULIC RADIUS

The major part of all piping in flow systems is of round cross section, but in some instances this is not the case. Therefore, it is necessary to develop an equivalent diameter for these noncircular pipes. The equivalent diameter is used primarily for computing the Reynolds number and is known as the hydraulic diameter. This hydraulic diameter of any cross section is defined as four times the hydraulic radius, defined, in turn, as

$$R_h = \frac{\text{cross-sectional area}}{\text{wetted perimeter of cross section}} = \frac{D}{4} \qquad [3.15a]$$

Then, by definition, the hydraulic diameter can be expressed as

$$D = 4R_h = 4A\left(\frac{dL}{dA_w}\right) \qquad [3.15b]$$

FLOW OF FLUIDS IN PIPES

The axial velocity of fluid flowing in a pipe is dependent on the axial forces acting on the fluid, the predominant ones being that of differential pressure, viscous friction at the wall, and acceleration and gravity forces. Although the Bernoulli equation was developed for the idealized stream tube, it also applies to flow in pipes when an accounting for frictional pressure loss is included. The effects of friction are detected as reductions in the constant of equations (3.11*a*) and (3.11*b*) at successive downstream locations.

Multiplying equation (3.11*b*) through by the weight density γ yields the Bernoulli equation in terms of pressure, or

$$P + g\rho z + \left(\frac{1}{2}\right)\rho V^2 = P_t \qquad \text{lbf/ft}^2 \qquad [3.16]$$

Here, P_t is the constant, in terms of the total of all the pressure components. The effect of friction is an observed reduction in the total pressure of the stream as the fluid progresses down the pipe. In incompressible flow the terms of elevational pressure and dynamic pressure are independent of the frictional effects. More specifically, the effect of friction in any given pipe section is unaffected by its orientation and any resulting elevational pressure changes. Also, the dynamic pressure is an absolute quantity dependent only on the density and velocity as fixed by the continuity equation. Then the only term that can reflect a reduction in the total pressure is the static-pressure term P. The interchange of pressures and the loss in total pressure may be better understood by study of a pressure diagram such as figure 14.3, drawn for a typical section in a pipeline.

Certain features of the pressure diagram should be noted and reflected to the governing Bernoulli equation (eq. (3.16)).

(1) The elevational head pressure line becomes zero at the point where the pipe centerline intersects the horizontal elevational datum plane. This line is straight only because the pipe centerline was drawn straight.

(2) The dynamic pressure term is constant in the constant flow area sections, since continuity requires constant velocity for incompressible flow with constant area.

(3) The total pressure loss is a result of viscous friction alone in the constant area sections. In the variable area section, the loss is a result of additional turbulence and possibly boundary-layer separation, as well as friction. In such a diffuser section the total pressure loss and the static pressure recovery are greatly dependent on design.

(4) It should be especially noted that even though there may be a significant loss in total pressure across a diffuser section as shown, and also with a sudden expansion, there may be a net increase in static pressure due to the recovery of dynamic pressure.

An evaluation of the frictional pressure losses can be made by considering the flow in a horizontal constant area pipe. Since the dynamic and elevational terms are constant, the changes in total pressure between upstream and downstream points is just the change in static pressure, or

$$P_{t1} - P_{t2} = P_1 - P_2$$

In the absence of momentum change in incompressible flow, the static-pressure forces acting on a fluid element can be equated directly to the viscous shear forces at the pipe wall, resulting in

$$-dP = \left(\frac{f\rho V^2}{2D}\right) dL \qquad [3.17]$$

which can be integrated to produce

$$\Delta P_L = P_1 - P_2 = P_{t1} - P_{t2} = \left[f\left(\frac{L}{D}\right)\right]\left(\frac{1}{2}\right)\rho V^2 = \left[f\left(\frac{L}{D}\right)\right]\frac{\gamma V^2}{2g_c} \qquad [3.18]$$

(The above equation is a modified version of that appearing in ch. 3.) Equation (3.18) is the basis for computing pressure losses as a result of friction for turbulent incompressible flow in pipes and requires an evaluation of the friction factor which is discussed in detail in the next section.

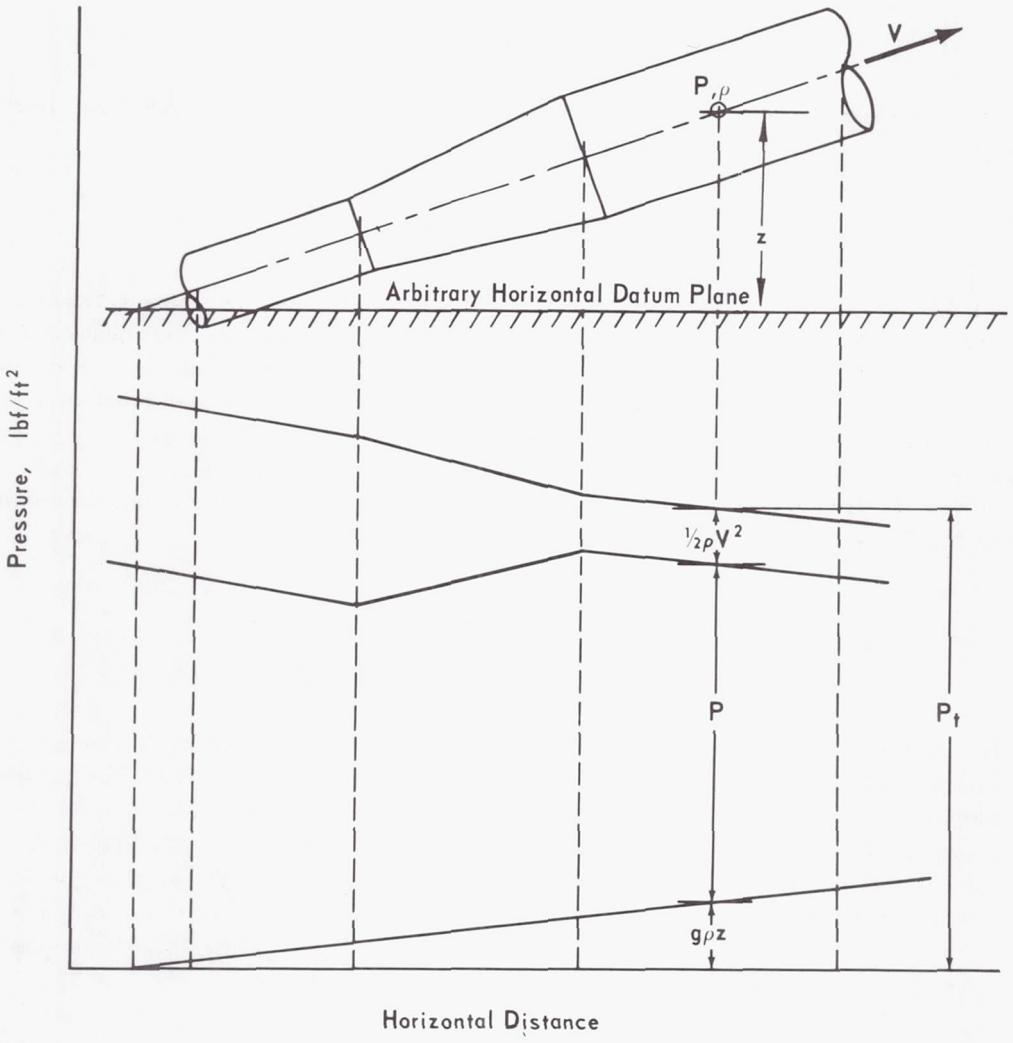


Figure 14.3. Pipeline section.

For the case of completely laminar flow ($R_e < 2000$), the exact expression for frictiona pressure loss is the Hagen-Poiseuille equation

$$\Delta P_L = \frac{32\mu LV}{D^2} \qquad [3.19]$$

where it is seen that the pressure loss is a linear function of velocity, rather than the usual square law. Substituting the definition of the Reynolds number yields

$$\Delta P_L = \left(\frac{64}{R_e}\right)\left[\left(\frac{L}{D}\right)\left(\frac{1}{2}\right)\rho V^2\right] = \left(\frac{64}{R_e}\right)\left(\frac{L}{D}\right)\frac{\gamma V^2}{2g_c} \qquad [3.20]$$

FRICTION FACTOR

Equation (3.20) represents the loss in pressure as a result of viscous friction. In this equation the value of the friction factor is given by

$$f = \frac{64}{R_e} \qquad R_e < 2000$$

which holds for viscous, or laminar, flow only. In turbulent flow, the above relation for f does not hold, and the friction factor must be determined in a manner so that equation (3.18) correctly yields the pressure loss. In turbulent flow, f is found to be defined by a more complex function of the Reynolds number and certain characteristics of the wall roughness.

L. F. Moody has constructed one of the most convenient charts for determining friction factors in clean, commercial pipe. This chart, presented in figure 14.4, is the basis for determining the friction factor for all ranges of R_e, both laminar and turbulent, accounting for wall roughness.

PRESSURE LOSSES IN PIPING SYSTEMS

Sudden Enlargement in Cross-Sectional Area

The pressure drop caused by a sudden area increase can be found by determining the forces acting on a system in the vicinity of the area change. In figure 14.5, the pressure upstream of the area change is P_1 and that downstream is P_2.

At section 1, just downstream of the area change, the pressure is still equal to P_1 due to insufficient distance for significant pressure drop to occur. At this section the force acting to the right is equal to P_1A_2. Farther downstream, the pressure has dropped to P_2, and at section 2 the force acting to the left is equal to P_2A_2. The total force acting on the section between 1 and 2 is equated to the momentum change to yield

$$(P_1 - P_2) = \frac{\dot{m}}{A_2}(V_2 - V_1) = \rho V_2(V_2 - V_1)$$

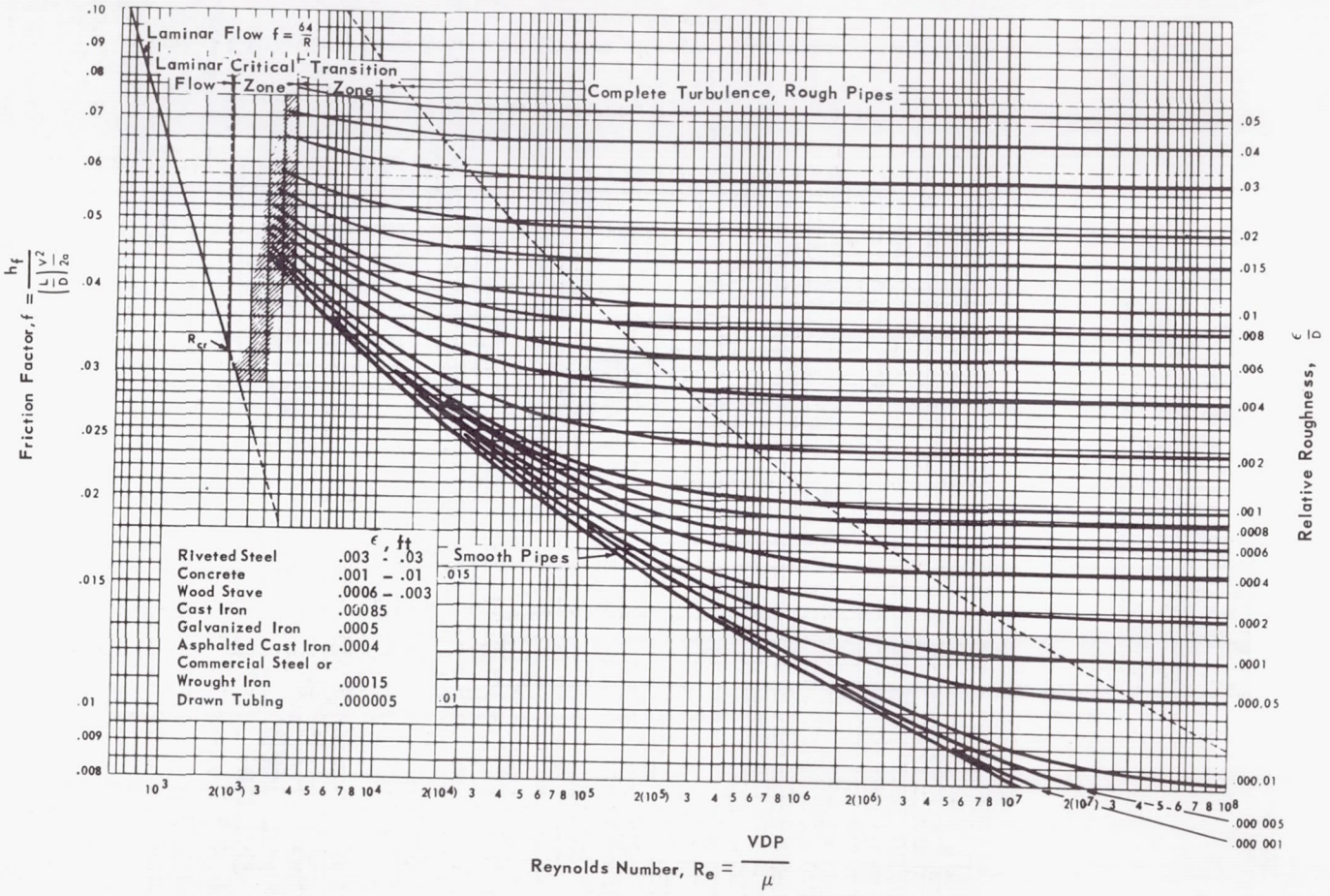


Figure 14.4. Friction factor diagram. [*Courtesy of the American Society of Mechanical Engineers.*]

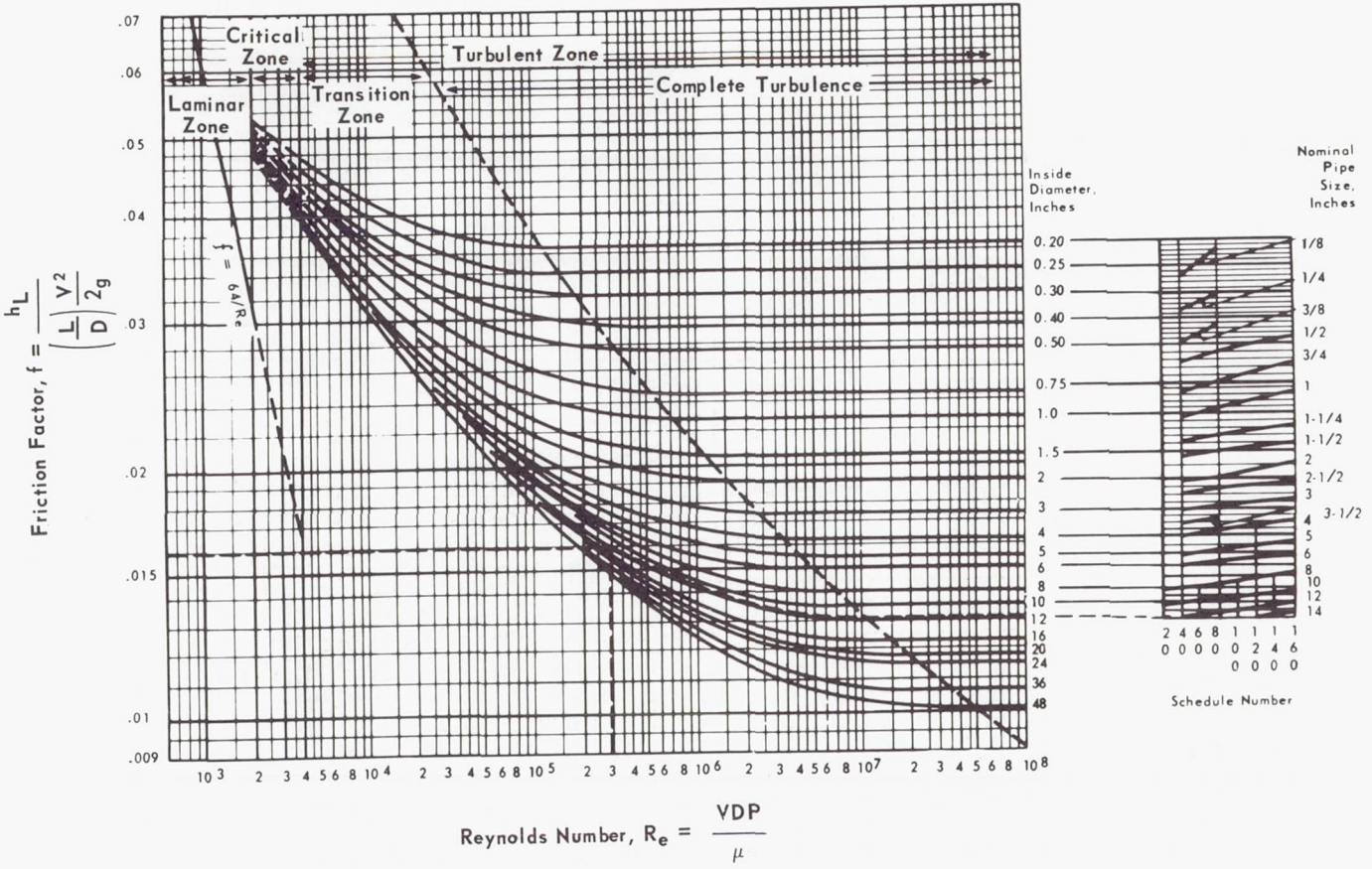


Figure 14.4. Friction factor diagram. — Continued. [*Courtesy of Crane Co., reproduced from Tech. Paper No. 410, Flow of Fluids.*]

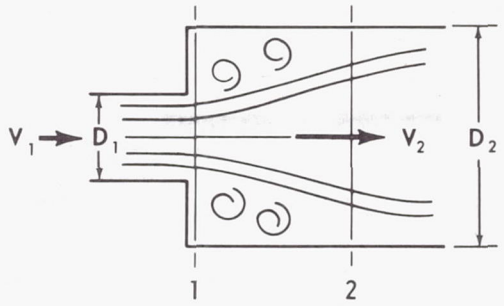


Figure 14.5. Sudden area increase.

Substituting this into the Bernoulli equation (3.16), writing between points 1 and 2 in terms of the total pressure loss, and clearing yield

$$\Delta P_{tL} = \left(1 - \frac{V_2}{V_1}\right)^2 \left(\frac{1}{2}\rho V_1^2\right) = K_t \left(\frac{1}{2}\rho V_1^2\right) \qquad [3.22]$$

(The above equation is a modified version of that appearing in ch. 3.) Then the total pressure loss factor for sudden expansion is

$$K_t = \left(1 - \frac{V_2}{V_1}\right)^2$$

For a steady incompressible flow there is no change in weight flow rate or density along the path. Hence, the velocities V_1 and V_2 are a function of flow area only, and the above relation may be written as

$$K_t = \left(1 - \frac{A_1}{A_2}\right)^2 = \left[1 - \left(\frac{D_1}{D_2}\right)^2\right]^2 \qquad [3.24]$$

(The above equation is a modified version of that appearing in ch. 3.) The K_t value for a sudden expansion as defined by equation (3.24) is plotted versus the ratio of upstream to downstream pipe diameter in figure 14.6. Also, shown in this figure is a plot for the sudden contraction in the flow stream. The second curve, however, cannot be determined by analytical means and is from experimental data. Note that the K_t factor plotted in figure 14.6 is based on the dynamic pressure in the smaller diameter pipe. This can be seen by observing that the defining equation for K_t (eq. (3.22)) is based on the velocity V_1. If it is desired to convert the published K_t factor so as to be used with the dynamic pressure in the larger diameter pipe, the new factor must be defined as

$$\Delta P_{tL} = K_t' \left(\tfrac{1}{2}\rho V_2^2\right) \qquad [3.25]$$

and the relation between the two factors is then, by an analysis similar to the foregoing,

$$K_t' = K_t \left(\frac{V_1}{V_2}\right)^2 = K_t \left(\frac{D_2}{D_1}\right)^4 \qquad [3.26]$$

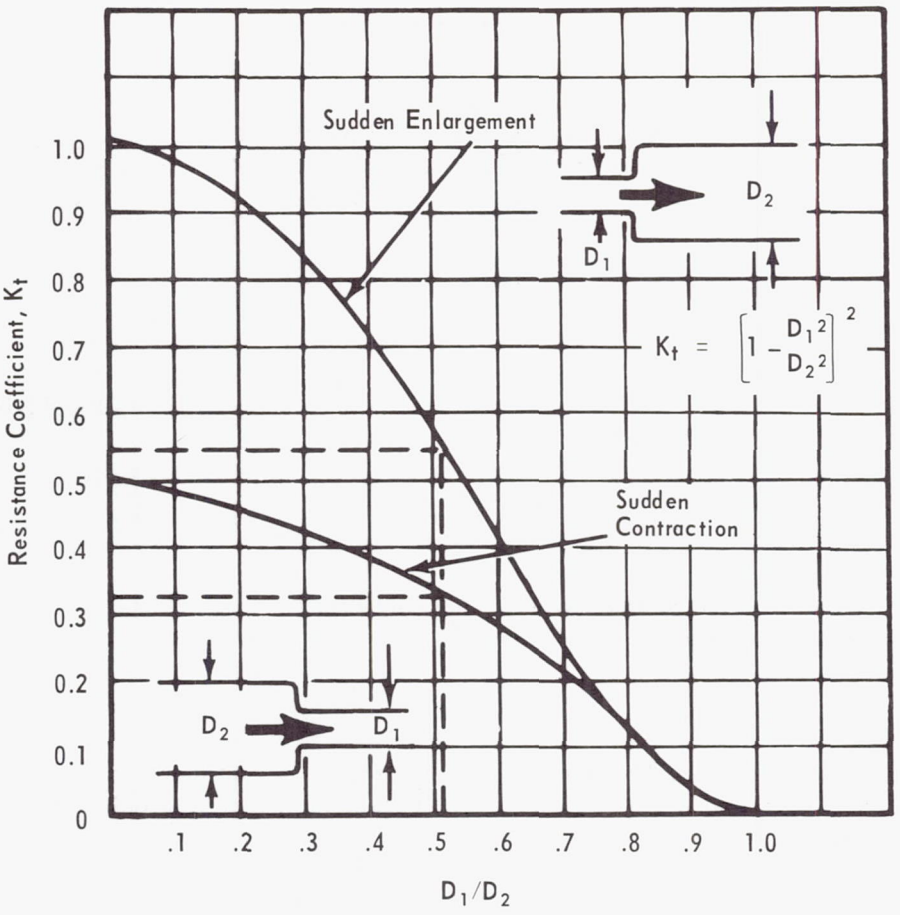


Figure 14.6. Loss factor for sudden area change. [*Courtesy of Crane Co., reproduced from Tech. Paper No. 410, Flow of Fluids.*]

Resistance of Bends

The resistance of bends to flow of an incompressible fluid can be attributed to viscous friction, secondary flow, and increased turbulence. The total pressure loss is found to vary in proportion to the local dynamic pressure, as with pipe friction. Then for bends

$$\Delta P_{tL} = K_{tb}\left(\frac{1}{2}\rho V^2\right) = \frac{K_{tb}}{2g_c\gamma}\left(\frac{w}{A}\right)^2$$

The bend loss coefficient is most accurately considered as that of equivalent lengths of straight pipe, having two parts as follows:

$$K_{tb} = \left[f\left(\frac{L}{D}\right)\right]_b = f\left(\frac{L_b}{D}\right) + f_{\text{tur}}\left(\frac{L_e}{D}\right)$$

The first term is that part of the loss factor resulting from viscous friction and should be computed as pipe friction loss for the centerline bend length L_b, as a function of R_e and ϵ/D using the Moody diagram. The second term is the result of the induced turbulence and secondary flow and is largely unaffected by changes in R_e. The equivalent length (L_e/D) is taken as bend resistance from the empirical data of figure 14.7 as a function of bend radius, and f_{tur} is taken from the Moody diagram in the highest range of R_e (fully turbulent flow) and the pertinent value of ϵ/D. Figure 14.8 presents similar approximate data for the total resistance equivalent length of miter bends, to which f_{tur} should be applied.

Although a 180° bend loss is not equal to that of two 90° bends, that assumption can be made to approximate conservatively pressure losses.

Entrance and Exit Losses

Since there is no pipe frictional length involved with entrances and exits, the total pressure loss factors are dependent solely on the configuration of the entrance or exit. Once again, the pressure loss is proportional to the local dynamic pressure in the pipe and a loss factor so that

$$\Delta P_{tL} = K_t(\tfrac{1}{2}\rho V^2) = \frac{K_t}{2g_c\gamma}\left(\frac{w}{A}\right)^2$$

Empirical values of K_t for various configurations are presented as figure 14.9. The reader is reminded that the static-pressure changes across an entrance or exit must be evaluated with a consideration of the changes in dynamic pressure per equation (3.16), written for the upstream and downstream points, and solved for $P_1 - P_2$. Then

$$\begin{aligned}\Delta P_L = P_1 - P_2 &= P_{t1} - P_{t2} - \tfrac{1}{2}\rho(V_1^2 - V_2^2)\\ &= K_t(\tfrac{1}{2}\rho V^2) - \tfrac{1}{2}\rho(V_1^2 - V_2^2)\end{aligned}$$

where V is either V_1 or V_2, whichever is the velocity in the adjacent pipe.

Then, for example, the equation predicts that for an entrance from a large reservoir, the static-pressure loss is the numerical sum of the total pressure loss and the dynamic pressure inside the pipe ($V = V_2$ and $V_1 = 0$).

Likewise, the static-pressure loss across an exit into a large reservoir is zero ($V = V_1$, $V_2 = 0$, and $K_t = 1$).

Valves and Fittings

The total pressure-loss coefficients for standard fittings and valves installed in pipelines are dependent on the internal configuration. Only insignificant variation occurs with changes in temperature and pressure of the component and the Reynolds number of flow when fully turbulent. Significant changes can occur in the pressure-loss coefficient for valves in the laminar flow condition, as in the case of frictional pipe flow. Typical values of K_t for turbulent flow through valves and fittings were taken from a number of sources, and are presented in tables 14.2 and 14.3. The wide variation in the tabulated values for a given component indicates the poor accuracy with which valve loss factors can be specified in a general manner. Greater accuracy requires testing of the individual component.

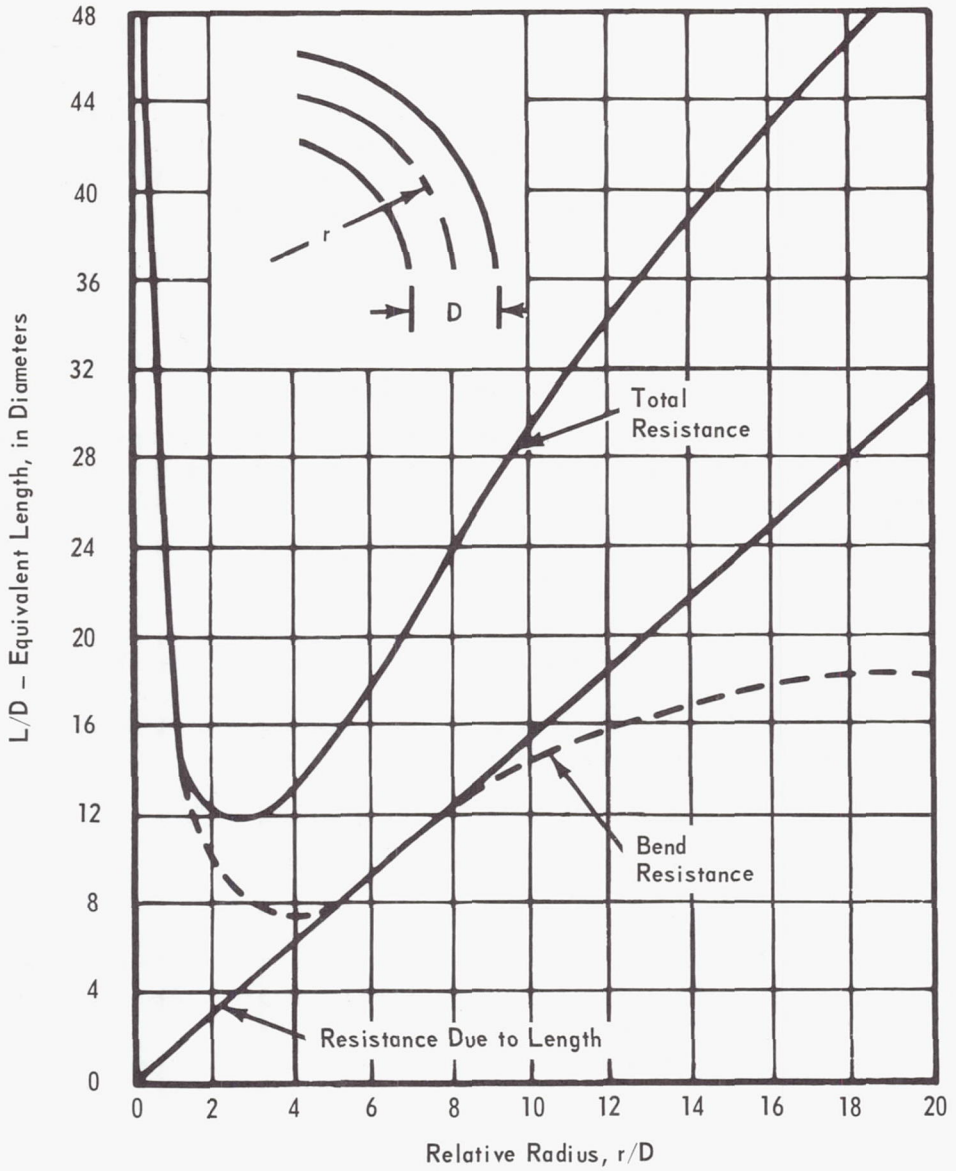


Figure 14.7. Resistance of bends. [*Courtesy of Crane Co., reproduced from Tech. Paper No. 410, Flow of Fluids.*]

The equivalent lengths shown in table 14.4 are based on the pipe size for which the component was designed. It has been shown by test that the pressure-drop variations as a result of mating the component to different schedules of the same nominal pipe size are small within reasonable limits. However, for calculation purposes, if the pipe size is altered, the value of L/D for the valve must also be altered. Since pressure drop varies as the

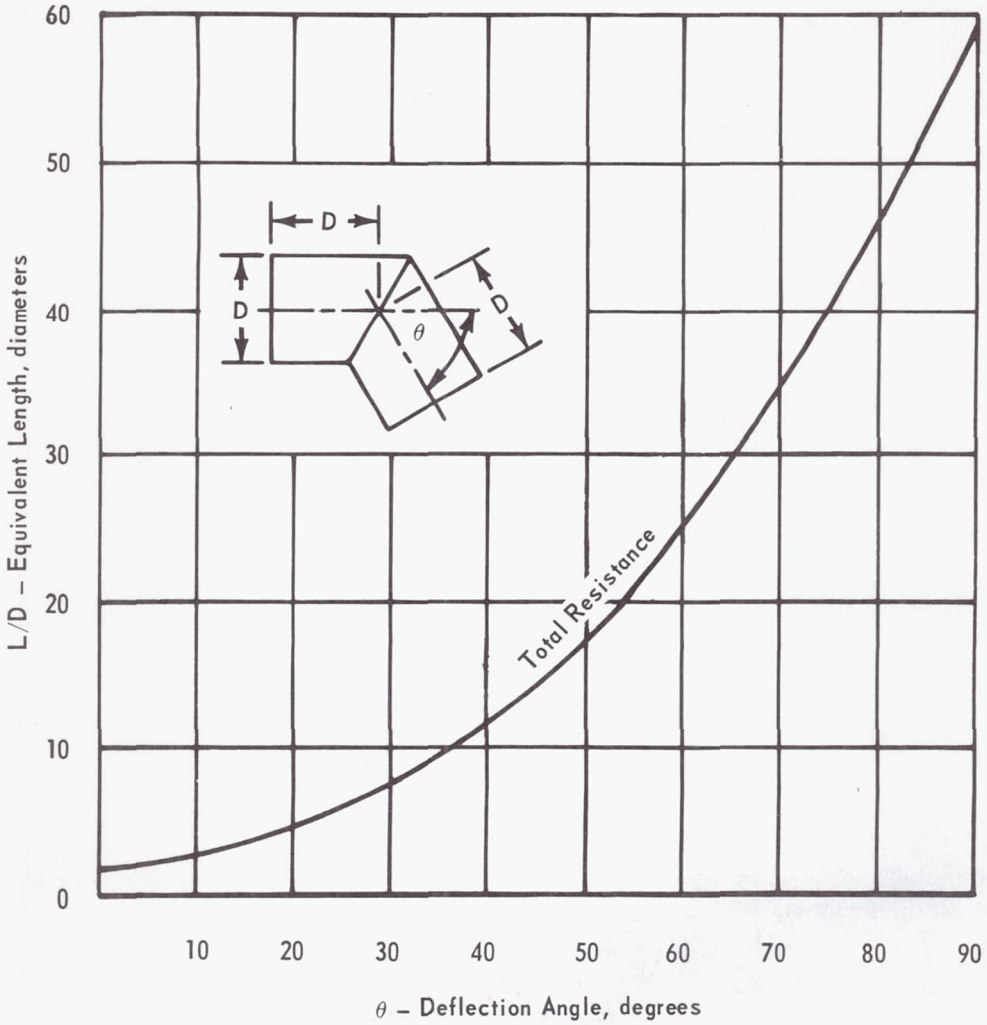


Figure 14.8. Resistance of miter bends. [*Courtesy of Crane Co., reproduced from Tech. Paper No. 410, Flow of Fluids.*]

second power of the velocity, which varies as the second power of the diameter, the relation between the two L/D values is

$$\frac{L}{D}=\left(\frac{L}{D}\right)_{\text{std}}\left(\frac{D}{D_{\text{std}}}\right)^4 \qquad [3.27]$$

Divergent Branches

The loss in pressure through divergent branches depends on the split in mass flow rate, the flow areas involved, and the branch angle. The empirical total pressure-loss factors for divergent branches are presented as figure 14.10. Using the nomenclature of the figure, the total pressure loss between locations 1 and 2 is

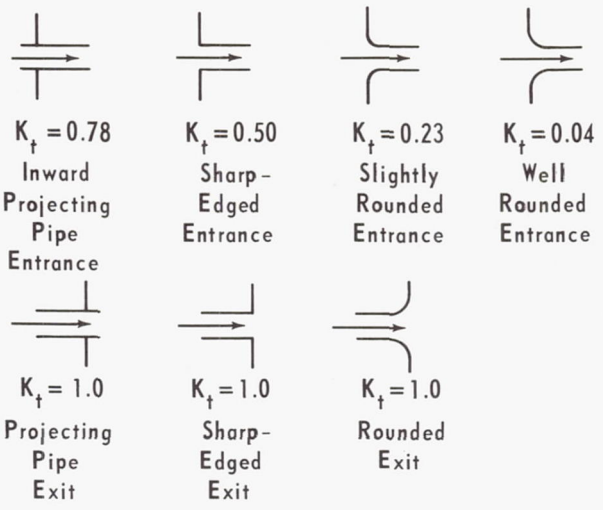


Figure 14.9. Loss because of sudden entrance and exit. [*Courtesy of Crane Co., reproduced from Tech. Paper No. 410, Flow of Fluids.*]

$$\Delta P_{tL} = {}_1K_{t2}\left(\frac{1}{2}\rho V_1^2\right) = \frac{{}_1K_{t2}}{2g_c\gamma}\left(\frac{w_1}{A_1}\right)^2 \qquad [3.28]$$

Convergent Branches

For the case of convergent branches, the pressure-loss factors must be computed by means of the equation

$${}_1K_{t3} = \lambda + \left(\frac{G_3}{G_1}\right)^2 - 2\left(\frac{A_1}{A_3}\right)\cos\beta' - \left(\frac{G_2}{G_1}\right)^2\left[2\left(\frac{A_2}{A_3}\right)\cos\delta'\right] \qquad [3.29]$$

Each of the variables and groups of variables can be read directly from figure 14.11 or can be computed directly, and once again, the total pressure loss between points 1 and 3 is

$$\Delta P_{tL} = {}_1K_{t3}\left(\frac{1}{2}\rho V_1^2\right) = \frac{{}_1K_{t3}}{2g_c\gamma}\left(\frac{w_1}{A_1}\right)^2 \qquad [3.30]$$

OVERALL LOSS FACTORS

Lines in Series

If pipes of different sizes are connected in series as shown in figure 14.12, an overall total pressure-loss coefficient for the system can be derived. Adding the total pressure losses due to both friction and area changes in the circuit yields

TABLE 14.2.—*Loss Factors for Valves and Fittings*

Type component	L/D [a]	L/D iron pipe [b]	L/D copper tubing [b]	K_t [c]	L/D [d]	K_t [e]	L/D [e]	K_t [f]
Angle valve conventional	145–200			2.1–3.1	165–204	3	170	
Angle poppet unobstructed with stem 45° from line of pipe								2.75
Angle poppet with stem 60° from line of pipe								3.4
Angle poppet in 90° pipe bend								6.5
Butterfly valve 6 in. and larger	20							
Butterfly valve 7 percent thick								.13
Butterfly valve 35 percent thick								.60
Check valve conventional swing	135							2.5
Check valve clear way swing	50							.95
Check valve in line ball	150							
Recessed swing check								
Gate valve conventional	13	12.5	17.5	0.05–0.19		.13	7	
Gate valve pulp stock	17							
Globe valve conventional	340–450	300.0	425.0	5.2–10.3	335–448	6.0	300	
Globe valve Y-pattern	145–175							
Bend 180° return close pattern	50			0.75–2.2		1.7	75	
Bend 180° medium return						1.2	50	
Bend flanged return composed of 2 90° elbows				0.38				
Bend flanged return long radius				0.26				
Cock 3-way flow straight through	44							
Cock 3-way flow through branch	140							
Coupling reducing		10.0	10.0					
45° elbow	16	17.8	17.8			.3	15	
45° long radius flange				0.14–0.23				
90° elbow standard radius	30	25.4	25.4		32	.74	32	
90° elbow medium radius	20	12.4	12.4			.60	26	
90° elbow long radius						.46	20	
90° elbow standard screw				0.56–0.90				
90° elbow long radius screw				0.22–0.60				
90° elbow standard flange				0.21–0.30				
Square-edged inlet				0.47–0.56				
Tee used as elbow entering run						1.3	60	
Tee used as elbow entering branch						1.9	90	
Standard tee flow through	20							
Standard tee flow through branch	60	45.0	30.0		65–96	1.3	60	
Standard screw tee flow through				40		1.9	90	
Standard screw tee flow through branch				0.85–1.30				
Long radius screw tee flow through branch				0.37–0.80				
Long radius screw tee flow through				0.50–0.52				
Reducer bell mouth				0.04–0.05				
Coupling and unions				0.02–0.07				

[a] Crane Corp., 1957.
[b] Jennings, 1958.
[c] Dahle, 1958.
[d] Kent, 1950.
[e] Perry, 1959.
[f] Society of Automotive Engineers, 1962.

TABLE 14.3.—*Equivalent Length of Fittings*

Fitting	Iron pipe, in.						Copper tube, in.				
	3/4	1	1¼	1½	2	3	3/4	1	1¼	1½	2
Elbows:											
90°	1.6	2.1	2.6	3.1	4.2	6.5	1.6	2.1	2.6	3.1	4.2
45°	1.1	1.5	1.8	2.2	2.9	4.5	1.1	1.5	1.8	2.2	2.9
90° long sweep	.8	1.0	1.3	1.6	2.1	3.0	.8	1.0	1.3	1.6	2.1
Tees:											
100% side diversion	2.8	3.8	4.7	5.6	7.5	13.0	1.9	2.5	3.1	3.7	5.0
50% side diversion	6.3	8.3	10.4	12.5	16.7	25.0	6.3	8.3	10.4	12.5	16.7
33% side diversion	14.3	18.7	23.4	28.1	37.5	56.0	18.7	23.5	29.4	35.2	46.9
25% side diversion	25.0	33.3	41.6	49.8	66.7	100.0	31.2	41.6	52.0	62.5	83.4
Valves:											
Globe fully open	18.7	25.0	33.8	36.8	50.0	66.0	26.6	35.4	44.2	53.0	70.8
Gate fully open	.8	1.0	1.3	1.6	2.1	3.0	1.1	1.5	1.8	2.2	2.9
Stopcock fully open	1.6	2.1	2.6	3.1	4.2	6.5	1.6	2.1	2.6	3.1	4.2
Angle fully open	3.6	4.2	5.2	6.2	8.3	12.5	4.7	6.3	7.8	9.4	12.5
Reducer coupling	.6	.8	1.0	1.3	1.7	2.5	.6	.8	1.0	1.3	1.7

$$\Delta P_{tL} = \left[f\left(\frac{L}{D}\right)\right]_1 \left(\frac{1}{2}\rho V_1^2\right) + K_{t1}\left(\frac{1}{2}\rho V_1^2\right) + \left[f\left(\frac{L}{D}\right)\right]_2 \left(\frac{1}{2}\rho V_2^2\right) + K_{t3}\left(\frac{1}{2}\rho V_3^2\right) + \left[f\left(\frac{L}{D}\right)\right]_3 \left(\frac{1}{2}\rho V_3^2\right) + \cdots$$

Then, in general terms, the overall coefficient for total pressure loss based on the dynamic pressure in section 1 of the pipe is

$$\frac{\Delta P_{tL}}{\frac{1}{2}\rho_1 V_1^2} = K_{to} = \sum \left(f\frac{L}{D}\right)_n \left(\frac{D_1}{D_n}\right)^4 + \sum K_{ts}\left(\frac{D_1}{D_s}\right)^4 \qquad [3.31]$$

Here, s indicates the smaller of the two pipes at the sudden area change, and K_{ts} is read from figure 14.12. Other types of fittings and valves can be included in the overall coefficient in the same manner, by including the diameter ratio factor when the device is of a different size than the reference size.

Lines in Parallel

In the case of series lines above, the loss in total pressure for the system was found to be the sum of the losses in the separate parts. In the case of parallel lines connected into common reservoirs on both ends, as in figure 14.13, the loss in total pressure is equal in all the lines:

TABLE 14.4.—*Equivalent Length of Valves and Fittings*

Pipe size, in.	Equivalent length, feet				
	Standard elbow	Side outlet tee	Gate valve fully open	Globe valve fully open	Angle valve fully open
1/2	1.3	3	0.3	14	7
3/4	1.8	4	.4	18	10
1	2.2	5	.5	23	12
1 1/4	3.0	6	.6	29	15
1 1/2	3.5	7	.8	34	18
2	4.3	8	1.0	46	22
2 1/2	5.0	11	1.1	54	27
3	6.5	13	1.4	66	34
3 1/2	8.0	15	1.6	80	40
4	9.0	18	1.9	92	45
5	11.0	22	2.2	112	56
6	13.0	27	2.8	136	67
8	17.0	35	3.7	180	92
10	21.0	45	4.6	230	112
12	27.0	53	5.5	270	132
14	30.0	63	6.4	310	152

then

$$\Delta P_{tL} = K_{t1}\left(\frac{1}{2}\rho V_1^2\right) = K_{t2}\left(\frac{1}{2}\rho V_2^2\right) = K_{tn}\left(\frac{1}{2}\rho V_n^2\right) = \cdots$$

Also, the total mass flow rate is the sum of the flow rates in each line so that

$$w_t = w_1 + w_2 + w_3 + \cdots + w_n + \cdots$$

It should be noted here that each of the parallel lines may be a complex series line having fittings, valves, and different size pipes as discussed in the previous section. If so, the

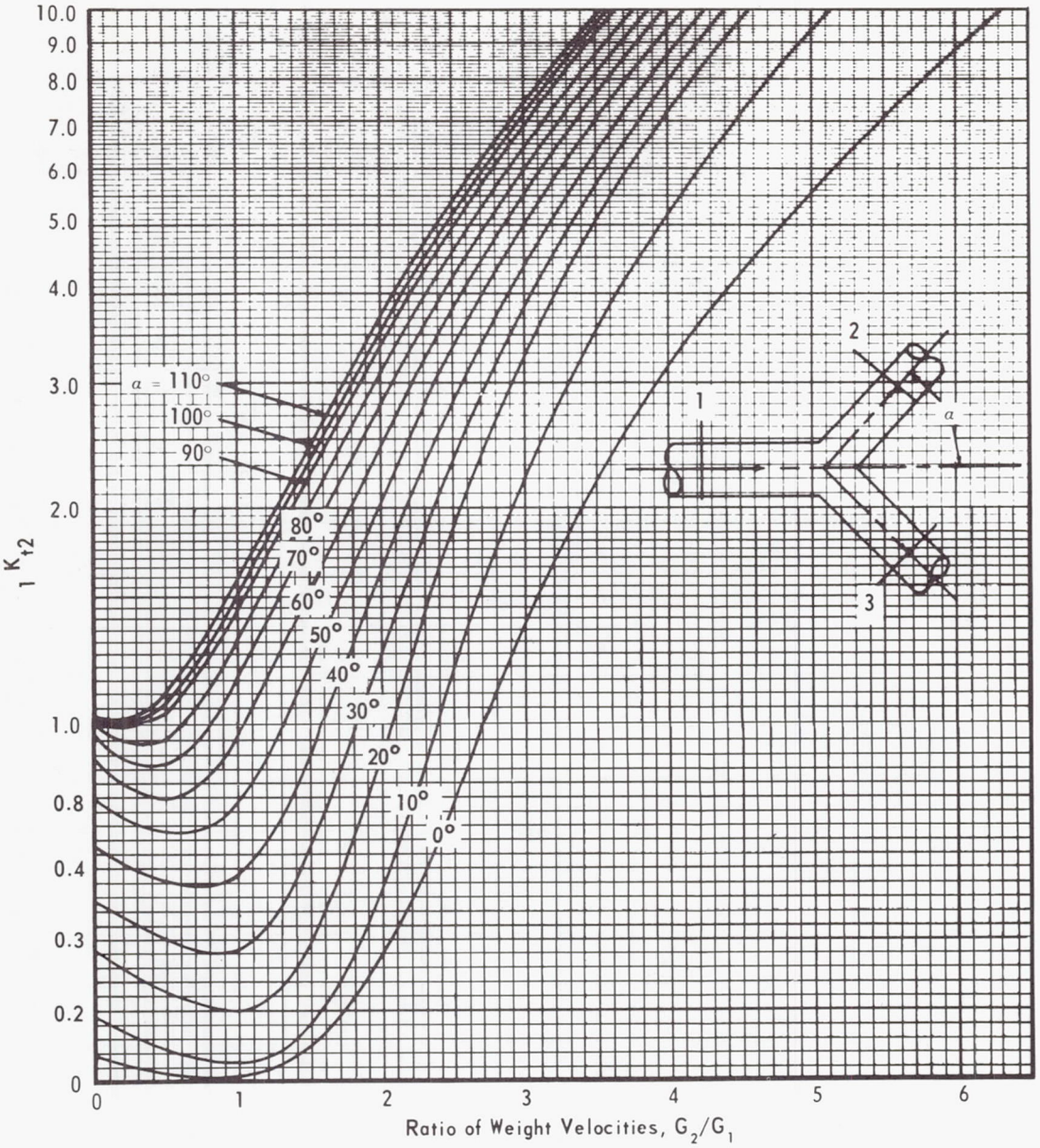


Figure 14.10. Divergent branch—loss coefficient. [*Courtesy of the Society of Automotive Engineers.*]

individual K_t factors mentioned here are the overall values for each series line K_{to}, as may be obtained by means of equation (3.31).

Proceeding, the individual mass flow rates can be expressed by means of the pressure-loss relationships above. Substituting and solving for mass flow rate in one line yield

$$w = A\sqrt{\frac{2g_c\gamma\ \Delta P_{tL}}{K_t}} \qquad [3.32]$$

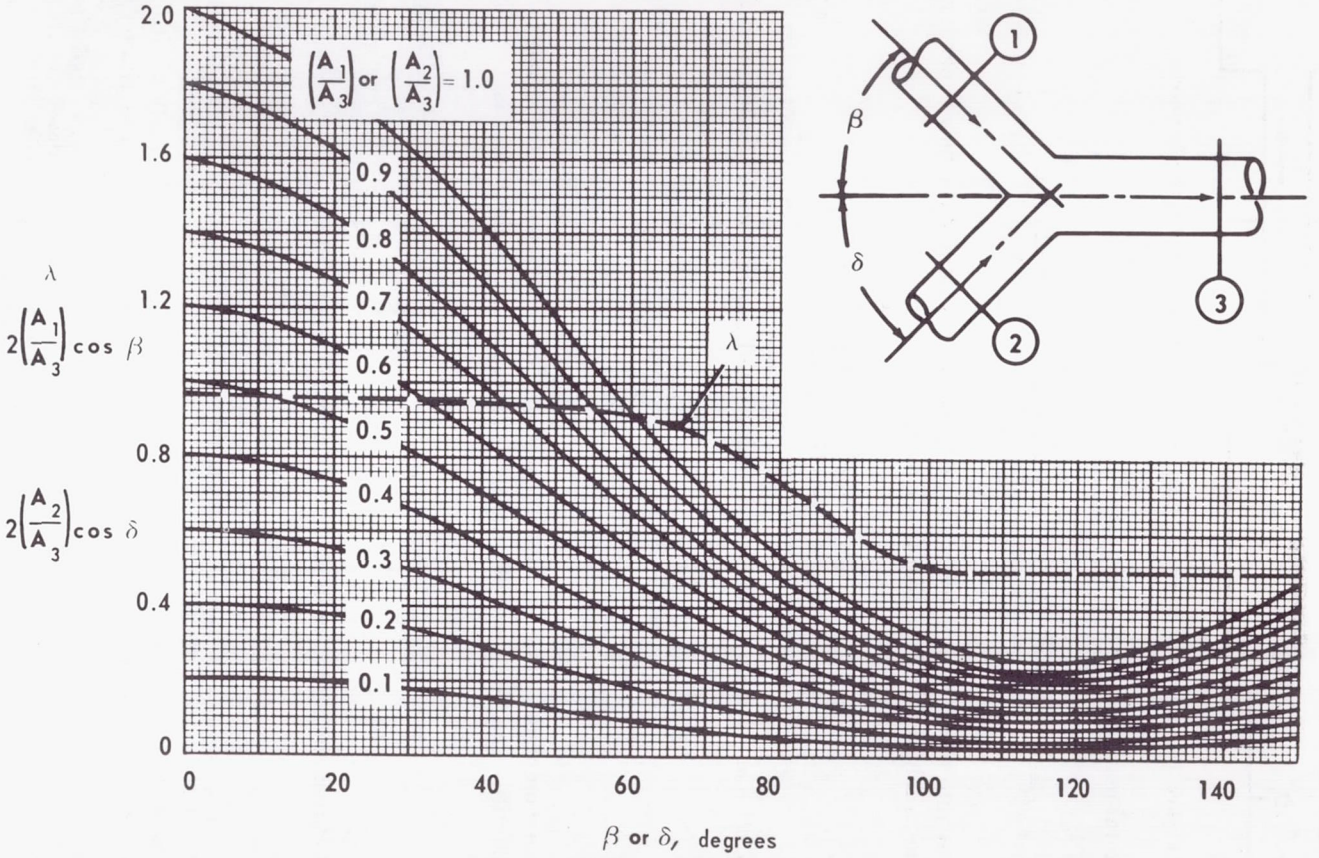


Figure 14.11. Convergent branch—loss coefficient. [*Courtesy of the Society of Automotive Engineers.*]

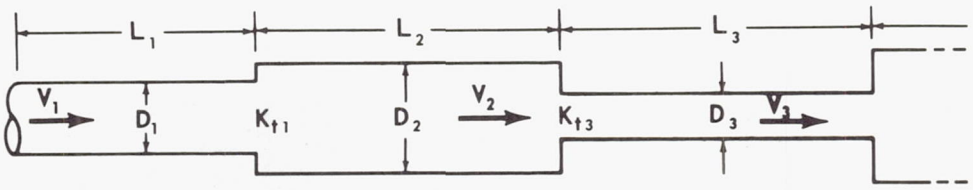


Figure 14.12. Lines in series. [*Courtesy of the Society of Automotive Engineers.*]

so that the total mass flow rate w_t is

$$w_t = \sqrt{2g_c\gamma\,\Delta P_{tL}}\left[\left(\frac{A}{\sqrt{K_t}}\right)_1 + \left(\frac{A}{\sqrt{K_t}}\right)_2 + \cdots + \left(\frac{A}{\sqrt{K_t}}\right)_n + \cdots\right]$$

The total flow rate can also be conveniently expressed as a ratio of the flow in some arbitrary reference line, such as line 1, so that for N pipes

$$\frac{w_t}{w_1} = \sum_1^N \left(\frac{D_n}{D_1}\right)^2 \sqrt{\frac{K_{t1}}{K_{tn}}} \qquad [3.33]$$

Equation (3.32) can be written for line 1, substituted into equation (3.33), and solved for ΔP_{tL} as

$$\Delta P_{tL} = \frac{K_{t1}}{2g_c\gamma}\left[\frac{w_t}{A_1 \sum_1^N \left(\frac{D_n}{D_1}\right)^2 \sqrt{\frac{K_{t1}}{K_{tn}}}}\right]^2 \qquad [3.34]$$

It is also convenient to define an overall, pressure-loss coefficient in the usual terms and involving quantities that are generally known. The most convenient form is

$$\Delta P_{tL} = K_{to}\,(\tfrac{1}{2}\rho V_t^2) = \frac{K_{to}}{2g_c\gamma}\left(\frac{w_t}{A_t}\right)^2 \qquad [3.35]$$

where the fictitious total or overall velocity is defined as

$$V_t = \frac{w_t}{\gamma A_t}$$

and A_t is the total flow area of all the lines. After combining and equating with equation (3.34), the overall loss factor is found in terms of only the piping system description as

$$K_{to} = K_{t1}\left[\frac{\sum_1^N \left(\frac{D_n}{D_1}\right)^2}{\sum_1^N \left(\frac{D_n}{D_1}\right)^2 \sqrt{\frac{K_{t1}}{K_{tn}}}}\right]^2 \qquad [3.36]$$

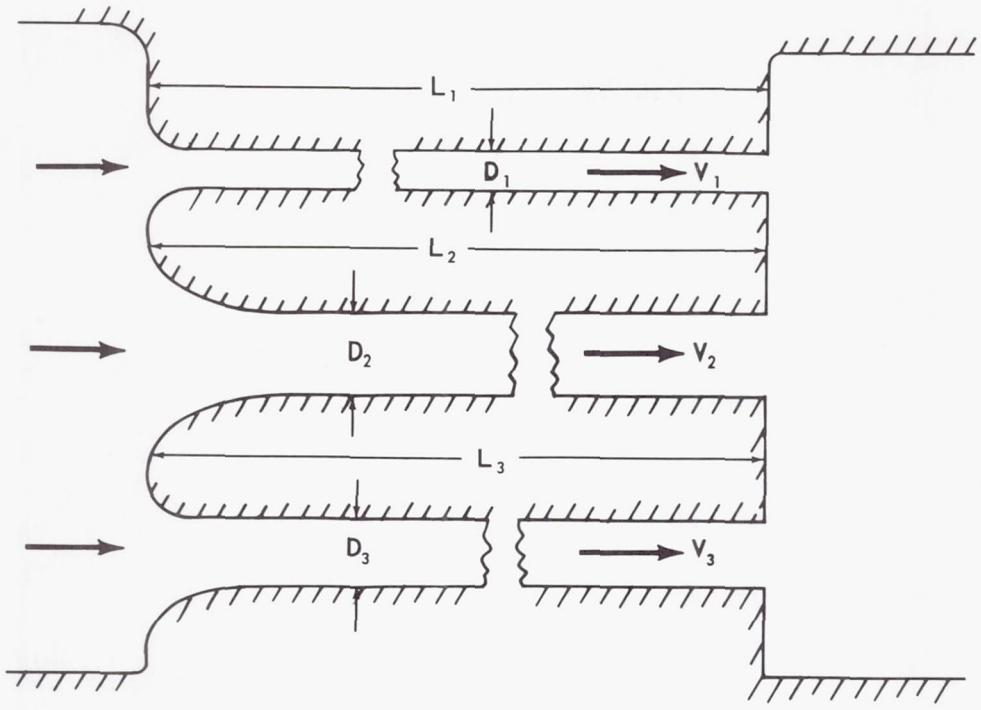


Figure 14.13. Parallel lines.

where

$$\sum_{1}^{N} \left(\frac{D_n}{D_1}\right)^2 = \frac{A_t}{A_1}$$

Then for a given total flow rate and the piping system description, the loss in total pressure (which is also the loss in static pressure between reservoirs in this case) can be computed using equations (3.35) and (3.36). Likewise, when the pressure loss is known, equation (3.35) can be solved explicitly for total mass flow rate.

It should be noted that when all the parallel lines have identical values of D and K_t, equation (3.36) predicts an overall loss factor equal to each of the individual loss factors.

CHAPTER 15

APPLICATION OF COMPRESSIBLE FLOW

Compressible flow is characterized by variation in fluid density along the flow path. In a compressible flow there are several parameters which are most convenient in relating fluid property changes along the flow path. These parameters are the speed of sound, the mach number, and the dimensionless flow parameter ϕ. In addition, the Reynolds number and viscosity are also used in compressible flows in characterizing flows and determining frictional lengths of piping systems.

Also involved in compressible flows are effects which are the results of high pressure. As will be illustrated herein, high pressure causes variation in viscosity and hence the Reynolds number, as well as significant variation in pressure-drop flow rate relations. In this chapter, the fundamental concepts of compressible flow are illustrated and also high-pressure effects on fluids are explained.

VELOCITY OF SOUND

The velocity of sound in a medium is simply the velocity of propagation of a pressure disturbance through the medium. For the perfect gas the velocity of sound may be expressed simply in terms of system properties as

$$c = \sqrt{kg_cRT} \qquad [4.5]$$

Equation (4.5) shows that the velocity of sound in a perfect gas is a function of temperature and the specific heat ratio only and is not affected by pressure.

For the real gas the simple expression (eq. (4.5)) does not hold and may lead to serious error in calculating velocity of sound.

In regions of temperature and pressure where a real-gas effect is appreciable, the more difficult P–v–T relations must be used to determine the velocity of sound.

Because of the complex nature of the P–v–T relations, a computer solution is necessary, and the data must be tabulated or plotted before computations can be made. Graphs of velocity of sound for various gases in the regions where real-gas equations of state must be used are given in the gas data appendixes (B through F).

If charts for velocity of sound in a real gas are not available, it is possible to determine approximate values from a Mollier diagram, or from other thermodynamic charts. The

Preceding Page Blank

method consists of determining an exponent k_s, which forces the relation

$$Pv^{k_s} = \text{constant} \qquad [4.6]$$

to hold along a constant entropy path. The value of k_s thus determined is then substituted into the equation

$$c_a = \sqrt{k_s g_c ZRT} \qquad [4.7]$$

The quantity k_s is termed the isentropic exponent and is simply a function which describes the P–v relation in real-gas regions during an isentropic expansion or compression. It is not a thermodynamic property and should not be associated with the specific heats, or the specific heat ratio for the real gas.

Useful expressions for k_s can be found by writing equation (4.6) in logarithmic form and differentiating to obtain

$$\frac{dP}{P} + k_s\left(\frac{dv}{v}\right) = 0$$

Rearranging yields

$$k_s = \frac{\gamma}{P}\left(\frac{\partial P}{\partial \gamma}\right)_s \qquad [4.9]$$

If k_s is assumed to be constant, which is valid over a short interval between points 1 and 2, equations (4.8) and (4.9) can be integrated to yield

$$k_s = \frac{\ln\left(\frac{P_2}{P_1}\right)}{\ln\left(\frac{\gamma_2}{\gamma_1}\right)} = \frac{\ln\left(\frac{P_2}{P_1}\right)}{\ln\left(\frac{v_1}{v_2}\right)} \qquad [4.10]$$

Good approximate values can be obtained from points read directly from accurate thermodynamic charts using equation (4.10) if the pressure change between points 1 and 2 is held small.

It must be pointed out that the accuracy of this method in predicting velocity of sound is greatly dependent on the accuracy of the thermodynamic chart used and the care with which data points are extracted.

EXAMPLE PROBLEM 4.1

Find the actual speed of sound in gaseous nitrogen at a temperature of 0° C and pressure of 6000 psi.

SOLUTION

To solve this problem, use the equation

$$c_a = \sqrt{k_s g_c ZRT}$$

where

$$k_s = \frac{\ln\left(\frac{P_2}{P_1}\right)}{\ln\left(\frac{\gamma_2}{\gamma_1}\right)}$$

To evaluate k_s, assume a small isentropic process where the pressure changes from 6000 psi to some smaller value, say 5500 psi. Then

$$\frac{P_2}{P_1} = \frac{5500}{6000} = 0.917$$

From appendix C, figure C.1, a constant entropy process from 0° C and 6000 psi (408 atm) to 5500 psi (374 atm) gives a temperature T_2 of $-9°$ C.

From figure C.3,

$$Z_1 = 1.270 \text{ (6000 psi and 273° K)}$$

$$Z_2 = 1.224 \text{ (5500 psi and 264° K)}$$

Since

$$\gamma_1 = \frac{P_1}{Z_1 RT_1} \qquad \gamma_2 = \frac{P_2}{Z_2 RT_2}$$

$$\frac{\gamma_2}{\gamma_1} = \frac{P_2 Z_1 RT_1}{P_1 Z_2 RT_2} = \frac{(5500)(1.270)(273)}{(6000)(1.224)(264)}$$

$$\frac{\gamma_2}{\gamma_1} = 0.983$$

Therefore,

$$k_s = \frac{\ln\left(\frac{P_2}{P_1}\right)}{\ln\left(\frac{\gamma_2}{\gamma_1}\right)} = \frac{\ln 0.917}{\ln 0.983} = \frac{-0.0866}{-0.0171} = 5.05$$

Solving for c_a,

$$c_a = \sqrt{k_s g_c ZRT} = \sqrt{(5.05)(32.2)(1.28)(55.2)(492)}$$

$$c_a = 2378 \text{ ft/sec}$$

The accuracy is dependent on the ability to read the charts and to round numbers.

MACH NUMBER

Flow characteristics in compressible flow have been found to vary as a function of the ratio of the stream-flow velocity to the velocity of sound. This ratio is termed the "mach number" and is defined by the equation

$$M = \frac{V}{c} \qquad [4.11]$$

where

M = mach number
V = flow velocity at a point in the flow stream
c = speed of sound in the media measured at the fluid conditions existing at the point where V is measured

By consideration of the continuity equation, other convenient forms of the mach number are

$$M=\left(\frac{w}{\gamma A}\right)\frac{1}{c} \qquad [4.12b]$$

and if the gas is perfect,

$$M=\left(\frac{w}{A}\right)\left(\frac{1}{P}\right)\sqrt{\frac{RT}{kg_c}} \qquad [4.12c]$$

Since for circular pipe

$$A=\frac{\pi D^2}{4}=\left(\frac{\pi}{4}\right)\frac{D^2}{144} \qquad \text{and} \qquad P=144p$$

equation (4.12b) may be written as

$$M=0.2245\left(\frac{w}{D^2}\right)\frac{1}{p}\sqrt{\frac{RT}{k}} \qquad [4.12d]$$

When the flow rate is known in terms of standard cubic feet per minute (scfm),

$$M=15.21\left(\frac{\text{SCFM}}{1000\,pD^2}\right)\sqrt{\frac{T}{kR}} \qquad [4.12e]$$

If flow is measured in cubic feet per second, the relation $V=q/A$ results, and the mach-number expression becomes

$$M=\frac{\frac{q}{A}}{c}=\frac{\frac{q}{A}}{\sqrt{kg_cRT}} \qquad [4.12f]$$

For real gases, the mach number is determined from

$$M=\frac{V}{c_a}=\frac{\frac{q}{A}}{c_a}=\frac{\frac{w}{A}}{\gamma c_a} \qquad [4.13a]$$

Using the real-gas equation of state, $P=\gamma ZRT$, the mach-number expression for a real gas becomes

$$M=\frac{w}{A}\left(\frac{ZRT}{P}\right)\frac{1}{c_a} \qquad [4.13b]$$

or when written for circular pipe and pressure in psia

$$M = 1.273 \left(\frac{w}{D^2}\right)\left(\frac{ZRT}{pc_a}\right) \qquad [4.13c]$$

If the flow units are in scfm, the mach-number expression becomes

$$M = 86.4 \left(\frac{\text{SCFM}}{1000}\right)\frac{ZT}{pD^2c_a} \qquad [4.13d]$$

In equation (4.13), the actual speed of sound can be found from charts of speed of sound for the gas, or in the absence of such charts, c_a may be determined from equation (4.7).

REYNOLDS NUMBER

The Reynolds number was defined for circular pipes in chapter 3 by the equation

$$R_e = \frac{VD\rho}{\mu} \qquad [3.14b]$$

or from continuity

$$R_e = \left(\frac{w}{\gamma A}\right)\frac{D\rho}{\mu}$$

and for circular pipe

$$R_e = \frac{w4(12)}{g_c\pi D}\left(\frac{1}{\mu}\right)$$

or from equation (4.14)

$$R_e = \left(\frac{48}{\pi}\right)\frac{w}{\mu' D} = 15.28\left(\frac{w}{\mu' D}\right) \qquad [4.14a]^*$$

Often, flow rates are given in terms of volumetric flow rate q and from the relation

$$w = \gamma q$$

The Reynolds number may be written as

$$R_e = 15.28\left(\frac{\gamma q}{\mu' D}\right) \qquad [4.14b]^*$$

For the perfect gas

$$\gamma = \frac{P}{RT} = \frac{P144}{RT}$$

*This equation is a variation of equation (4.14) and does not appear in chapter 4.

and the Reynolds number becomes

$$R_e = 15.28(144)\left(\frac{pq}{ZRT\mu' D}\right) \qquad (4.14c)^*$$

or for flow in scfm, equation (10.3) (SCFM = 14.75 $R\mathcal{W}$) can be substituted to yield

$$R_e = \left(\frac{15.28}{14.75}\right)\frac{\text{SCFM}}{R\mu' D} = 1.037\left(\frac{\text{SCFM}}{RD\mu'}\right) \qquad (4.14d)^*$$

VISCOSITY

Quantitative knowledge of viscosity is required in many engineering problems which involve heat-transfer, mass-transfer, or pressure-loss relationships. In analysis of high-pressure gas systems, experimental viscosity data are often not available for the gas in the region of pressure and temperature under investigation. To provide these data, a generalized method of estimating viscosity has been developed based on the critical viscosity of the gas.

TABLE 15.1.—*Critical Viscosities of Gases*

Gas	Critical viscosity, micropoise
Air	193
Ammonia	309
Argon	264
Ethane	210
Helium	25.4
Hydrogen	34.7
Methane	159
Neon	156
Nitrogen	180
Oxygen	250
Propane	228

At low pressure where the perfect-gas law is applicable, the viscosity of a gas is primarily dependent on temperature and is little affected by pressure. However, as the pressure greatly increases, the viscosity of the gas increases, though not nearly in proportion. If the viscosity of several gases is plotted in the low-pressure region versus reduced temperature, a family of curves results. If each curve is replotted as reduced viscosity (by dividing all data by the individual viscosities at the respective critical points of the gases), all data reduce to a single curve. From this curve, the low-pressure viscosity of any gas with known critical temperature may be determined if only the viscosity is known at the critical point. The same procedure can be repeated at a constant high value of reduced pressure, yielding a single curve that describes the reduced viscosity of all gases at that respective reduced pressure. By this means, it is possible to combine the low-pressure generalized viscosity curve with similar dimensionless correlations for high pressures, thereby expressing high-pressure effects for all gases on a single chart. Such a plot is shown in figure 15.1. All

*This equation is a variation of equation 4.14 and does not appear in chapter 4.

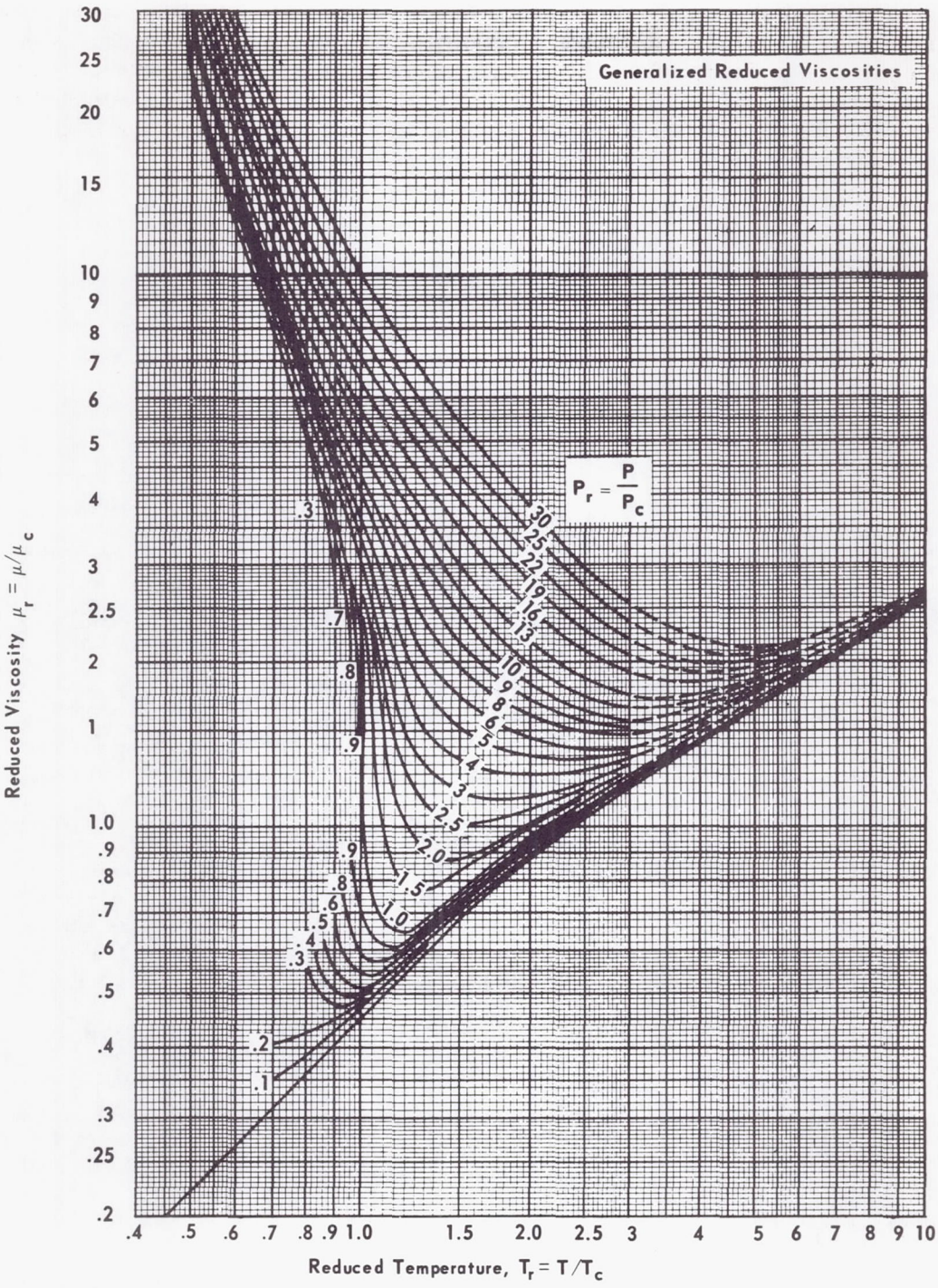


Figure 15.1. Reduced viscosities of gases. [*Reprinted from National Petroleum News, copyright McGraw-Hill, Inc., 1967.*]

that is required to determine the viscosity from this figure is a knowledge of the critical temperature, critical pressure, and the viscosity of the gas at the critical point. Critical-point pressures and temperatures for several gases are given in table 2.1, chapter 2. Critical-point viscosity values are listed in table 15.1. Also, viscosity data were extracted from figure 15.1 for the common gases (air, nitrogen, helium, hydrogen, and oxygen) and were plotted for the specific gases in the applicable sections of the appendixes.

CHAPTER 16

APPLICATION OF ADIABATIC AND ISENTROPIC FLOWS

GENERAL

Adiabatic flow can be assumed with accuracy when the flow transport time through the given flow process is very short and/or when the pipe-wall temperature is approximately that of the flowing fluid, as with a well-insulated pipe. With negligible heat transfer, there can be no change in stagnation enthalpy and, for a perfect gas, no change in stagnation temperature, regardless of any friction and turbulence that may exist.

Isentropic (reversible adiabatic) flow can be assumed with accuracy only when the requirements for adiabatic flow are fulfilled as described in the preceding paragraph and when there are none of the irreversible effects caused by turbulence, flow separation, fluid friction, and shock waves. In general, the physical changes that occur in isentropic flows are the result of smooth-flow area changes in relatively short distances. For isentropic flows of perfect gases, the stagnation values of pressure and density also remain constant, as does the stagnation temperature.

In all cases presented here, the flow is considered one dimensional, which implies that the velocity and fluid properties are constant across any cross section of the pipe. Therefore, the solutions cannot be expected to produce extreme accuracy in the analysis of rapidly expanding (overturned) nozzles, for example.

ADIABATIC FLOW

The steady-flow velocity of any fluid is related to its static and stagnation enthalpies by the energy equation (5.1) with a numerical value assigned to $2g_cJ$

$$V = [2g_cJ(h_0 - h)]^{1/2} = 223.8\sqrt{h_0 - h} \qquad [5.1]$$

Continuity requires the following relationship

$$w = \gamma AV = g_c \rho AV \qquad [5.3]$$

The mach number is defined by

$$M = \frac{V}{c} = \frac{V}{\left[\left(\frac{\partial P}{\partial \rho}\right)_s\right]^{1/2}} \qquad [5.5]$$

For a perfect gas, equations (5.1) and (5.5) can be simplified to the following

$$V = [2g_c J c_p (T_0 - T)]^{1/2} = \left[2g_c \left(\frac{kR}{k-1} \right) (T_0 - T) \right]^{1/2} \qquad [5.9]$$

(The above equation is a modified version of that appearing in ch. 5.)
and from equation (4.12*f*) where $V = q/A$

$$M = \frac{V}{c} = \frac{V}{(kg_c RT)^{1/2}}$$

The mach number of flow in pipes can be computed from weight flow rate and gas properties by

$$M = \left(\frac{w}{A}\right)\left(\frac{1}{P}\right)\sqrt{\frac{RT}{kg_c}} \qquad [5.22]$$

By converting the pressure term to units of psia, rather than psfa, and for the case of a circular pipe of diameter D, measured in inches, equation (5.22) becomes

$$M = 0.2245 \left(\frac{w}{D^2}\right)\left(\frac{1}{P}\right)\sqrt{\frac{RT}{k}} \qquad [5.22a]^*$$

Further conversion of the flow term to units of standard cubic feet per minute, rather than lbm/sec, yields

$$M = 15.21 \left(\frac{\text{SCFM}}{1000}\right)\frac{\sqrt{\frac{T}{kR}}}{pD^2} \qquad [5.22b]^*$$

Equation (5.22*a*) can be modified to produce an adiabatic weight flow parameter in terms of the stagnation temperature, the local static pressure, and mach number,

$$\left(\frac{w}{A}\right)\left(\frac{1}{P}\right)\sqrt{\frac{RT_0}{kg_c}} = M\left[1 + \left(\frac{k-1}{2}\right)M^2\right]^{1/2} \qquad [5.23]$$

The ratio of stagnation temperature to static temperature for a perfect gas in any adiabatic flow is defined as

$$\frac{T_0}{T} = 1 + \left(\frac{k-1}{2}\right)M^2 \qquad [5.10]$$

where T_0 remains constant throughout the adiabatic flow path. The stagnation temperature and stagnation enthalpy are the only two properties which remain constant in adiabatic flow.

*This equation is a variation of equation (5.22) and does not appear in chapter 5.

EXAMPLE PROBLEM 16.1

A storage bottle contains nitrogen at 1500 psia and 80° F. The gas is flowing from the bottle through a complex, insulated circuit to a point where the line pressure and temperature are measured as 10.3 psig and 0° F, and the pipe has a 1-inch internal diameter. Compute the velocity, weight flow rate, and stagnation pressure and temperature at the downstream location.

SOLUTION

The flow is assumed to be adiabatic, and the stagnation enthalpy is constant at the value existing in the bottle. At 1500 psia and 80° F, the Mollier chart for nitrogen (fig. C.1, app. C) yields $h_0 = 178.1$ Btu/lbm. Likewise, at 25 psia (10.3 psig) and 0° F, the chart yields $h = 166.6$. By equation (5.1)

$$V = 223.8\sqrt{178.1 - 166.6}$$

$$= 759 \text{ ft/sec}$$

The weight flow, by equation (5.2), is $w = \gamma AV$, where

$$\gamma = \frac{P}{ZRT}$$

The compressibility factor for nitrogen is found to be essentially unity at the downstream point of interest by reference to figure C.2, appendix C. Then, using the absolute units of pressure and temperature,

$$w = \frac{PAV}{ZRT} = \frac{[(144)(10.3 + 14.7)]\left[\frac{\pi (1)^2}{4(144)}\right](759)}{(1)(55.2)(460)}$$

$$= 0.588 \text{ lbm/sec}$$

Since the value of Z is found to be unity and the value of specific heat ratio is found to be the nominal 1.4, by figures C.3 and C.4 in appendix C, the nitrogen can be considered a perfect gas at the downstream location. Then the mach number is, by equation (5.22a)

$$M = 0.2245\left(\frac{0.588}{(1)^2}\right)\left(\frac{1}{25}\right)\sqrt{\frac{(55.2)(460)}{1.4}}$$

$$= 0.711$$

In figures 16.1 and 16.2, the pressure and temperature ratios are read at $M = 0.711$; thus

$$\frac{p}{p_0} = \frac{P}{P_0} = 0.713 \qquad \text{and} \qquad \frac{T}{T_0} = 0.910$$

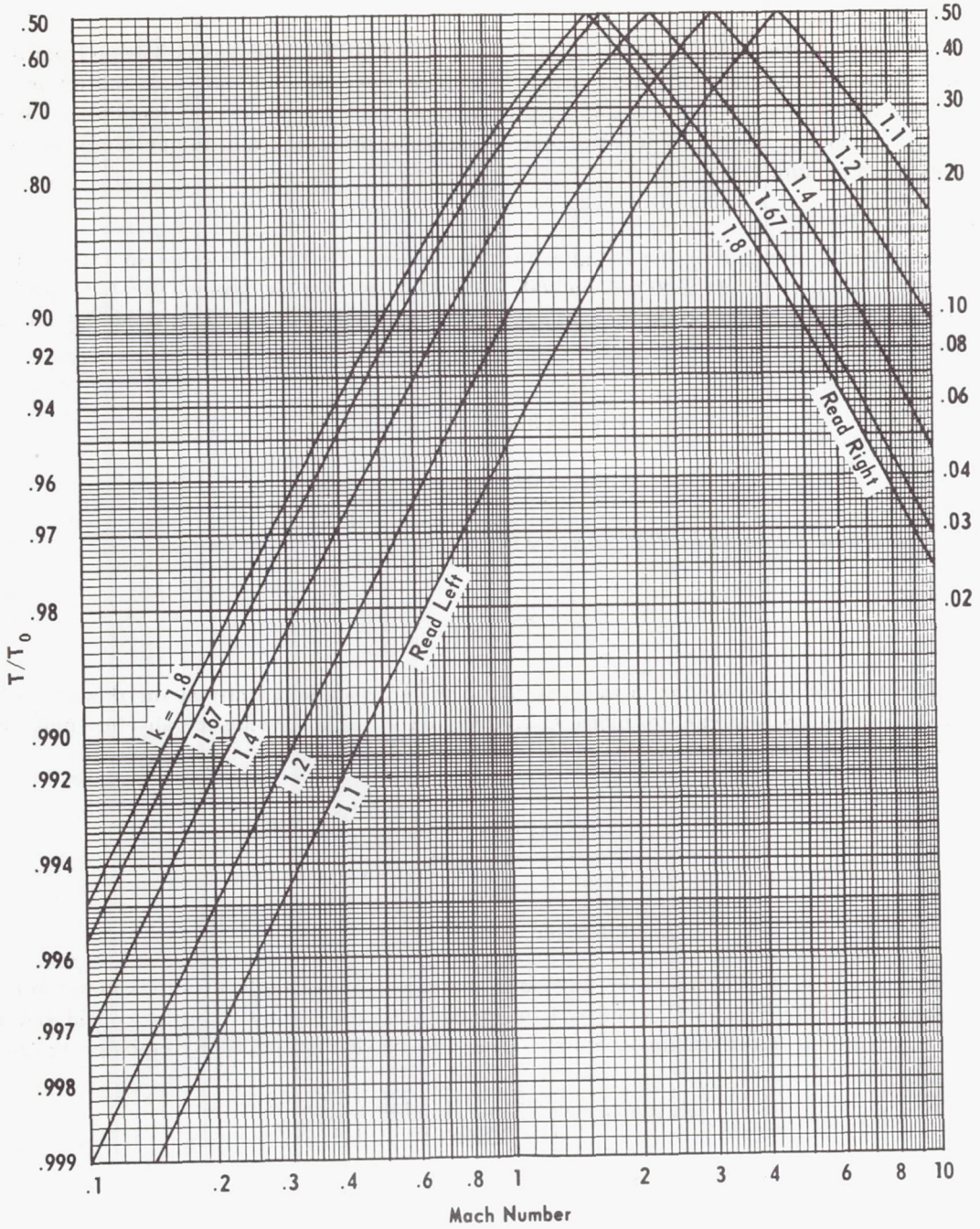


Figure 16.1. Isentropic temperature ratio.

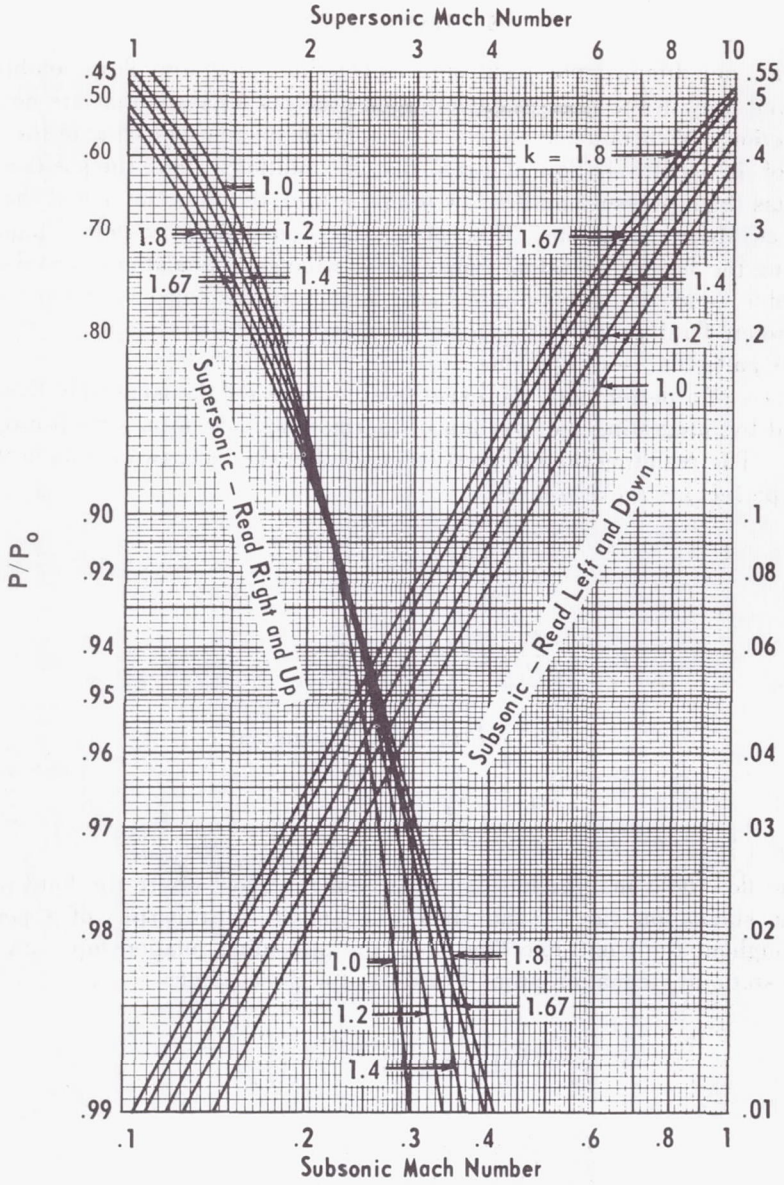


Figure 16.2. Isentropic pressure ratio.

Then the absolute static and stagnation pressures and temperatures are

$$p = 10.3 \text{ psig} = 25 \text{ psia} \qquad T = 0^\circ \text{F} = 460^\circ \text{R}$$

$$P_0 = \frac{25}{0.713} = 35.1 \text{ psia} \qquad T_0 = \frac{460}{0.910} = 505.5^\circ \text{R}$$

$$= 20.4 \text{ psig} \qquad = 45.5^\circ \text{F}$$

ISENTROPIC FLOW

In general, one-dimensional isentropic (reversible adiabatic) flow conditions can be closely achieved only in the case of smooth-area changes (changes that are not too abrupt), and where friction and turbulence effects are negligible compared to that of the area change. The analysis of the isentropic flow of a real gas, at conditions where the gas does not behave as a perfect gas (high pressure and/or low temperature), requires the use of thermodynamic charts, such as Mollier diagrams. The processes of real fluid property changes must be evaluated along the lines of constant entropy (for which the analytical formulations are not readily available) and the general adiabatic flow formulas (eqs. (5.1) and (5.2)). Other relations between fluid properties can be obtained graphically from the thermodynamic chart along the particular isentropic line.

For the case of a perfect gas, the exact relationships for the isentropic flow process can be established by integrating the first law of thermodynamics, after substituting perfect-gas relationships. The resulting fluid-property changes between any two points in the isentropic flow field of a perfect gas are as follows:

$$\frac{T_2}{T_1}=\left(\frac{\gamma_2}{\gamma_1}\right)^{k-1}=\left(\frac{v_1}{v_2}\right)^{k-1} \qquad [5.24]$$

$$\frac{P_2}{P_1}=\left(\frac{\gamma_2}{\gamma_1}\right)^{k}=\left(\frac{v_1}{v_2}\right)^{k} \qquad [5.25]$$

$$Pv^k=P_1v_1^k=P_2v_2^k=\text{constant} \qquad [5.26]$$

$$\frac{T_2}{T_1}=\left(\frac{P_2}{P_1}\right)^{\frac{k-1}{k}} \qquad [5.27]$$

Since the flow field may include an upstream reservoir where the fluid properties are the isentropic stagnation values, and since all stagnation properties of a perfect gas are constant throughout the isentropic flow field, the preceding relationships can also be used to obtain the static to stagnation property ratios at a given point.

$$\frac{T}{T_0}=\left(\frac{\gamma}{\gamma_0}\right)^{k-1}=\left(\frac{v}{v_0}\right)^{-(k-1)}=\left(\frac{P}{P_0}\right)^{\frac{k-1}{k}}. \qquad [5.28]$$

$$\frac{P}{P_0}=\left(\frac{\gamma}{\gamma_0}\right)^{k}=\left(\frac{v}{v_0}\right)^{-k}=\left(\frac{T}{T_0}\right)^{\frac{k}{k-1}} \qquad [5.29]$$

$$\frac{\gamma}{\gamma_0}=\left(\frac{v}{v_0}\right)^{-1}=\left(\frac{P}{P_0}\right)^{1/k}=\left(\frac{T}{T_0}\right)^{\frac{1}{k-1}} \qquad [5.30]$$

These isentropic stagnation ratios of pressure and weight density can be related to the local weight flow condition, specifically in terms of mach number, since it was shown previously by equation (5.10) that

$$\frac{T_0}{T}=1+\left(\frac{k-1}{2}\right)M^2$$

Then

$$\frac{P_0}{P}=\left[1+\left(\frac{k-1}{2}\right)M^2\right]^{\frac{k}{k-1}} \qquad [5.31]$$

and

$$\frac{\gamma_0}{\gamma}=\frac{v}{v_0}=\left[1+\left(\frac{k-1}{2}\right)M^2\right]^{\frac{1}{k-1}} \qquad [5.32]$$

When the flow becomes choked isentropically, as in the throat of a smooth nozzle, the choked throat static (*) to stagnation property ratios are obtained by substituting $M=1$ into the preceding equations, yielding

$$\frac{T^*}{T_0}=\frac{2}{k+1} \qquad [5.33]$$

$$\frac{P^*}{P_0}=\left(\frac{2}{k+1}\right)^{\frac{k}{k-1}} \qquad [5.34]$$

$$\frac{\gamma^*}{\gamma_0}=\left(\frac{2}{k+1}\right)^{\frac{1}{k+1}} \qquad [5.35]$$

where $\frac{\gamma^*}{\gamma_0}$ is also equal to $\frac{v_0}{v^*}$

An isentropic weight flow parameter can be obtained from equation (5.23) entirely in terms of stagnation properties (by substituting equations (5.10) and (5.31), since, in isentropic flow of a perfect gas, all stagnation properties are constant. Then the isentropic flow parameter is

$$\left(\frac{w}{A}\right)\left(\frac{1}{P_0}\right)\sqrt{\frac{RT_0}{kg_c}}=\frac{M}{M\left[1+\left(\frac{k-1}{2}\right)M^2\right]^{-\frac{k+1}{2(k-1)}}} \qquad [5.36]$$

although the local mach number is still defined by the local static properties and equation (5.22). The maximum flow rate is often of interest and can be established at the choked condition where $M=1$, so that

$$\left(\frac{w}{A}\right)_{\max}\left(\frac{1}{P_0}\right)\sqrt{\frac{RT_0}{kg_c}}=\left(\frac{w_{\max}}{A^*}\right)\left(\frac{1}{P_0}\right)\sqrt{\frac{RT_0}{kg_c}}=\left(\frac{2}{k+1}\right)^{\frac{k+1}{2(k-1)}} \qquad [5.37]$$

(The above equation is a modified version of that appearing in ch. 5.)

Since the case of a variable flow area is the most common application of isentropic flow in practice, the explicit effects of area change are useful. By combining equations (5.36)

and (5.37), the area at any point along the flow channel is related to that area which will cause choking as a function of the local mach number.

$$\frac{A}{A^*}=\frac{1}{M}\left\{\frac{2}{k+1}\left[1+\left(\frac{k-1}{2}\right)M^2\right]\right\}^{\frac{k+1}{2(k-1)}} \qquad [5.38]$$

(The above equation is a modified version of that appearing in ch. 5.)

The impulse function F_i is defined as the sum of the pressure and momentum forces that can be associated with a flow stream at a given location.

$$F_i=PA+\rho AV^2 \qquad [5.39]$$

The impulse function is especially useful in establishing the resultant forces on a containing channel within which a fluid is undergoing any steady-flow process. The resultant force acting on the fluid by the wall and in the direction of flow is

$$F_{wx}=F_{i_2}-F_{i_1} \qquad [5.39a]^*$$

The force of the fluid acting on the wall is equal to F_{wx} and opposite in direction. For a perfect gas

$$F_i=PA(1+kM^2) \qquad [5.40]$$

For a perfect gas and isentropic flow, the impulse function can be nondimensionalized once again as a ratio to the value, F_i^*, which the particular flow would exhibit at the point where $M=1$.

$$\frac{F_i}{F_i^*}=\frac{1+kM^2}{M\left\{2(k+1)\left[1+\left(\frac{k-1}{2}\right)M^2\right]\right\}^{1/2}} \qquad [5.41]$$

WORKING CHARTS AND TABLES

The several dimensionless ratios of fluid properties, flow area, and impulse function have been tabulated for the isentropic flow of perfect gases in numerous publications (Keenan and Kaye, 1948; Ames, 1953; and Pratt & Whitney Aircraft, 1963). For convenience, an abbreviated set of charts (figs. 16.1 through 16.8) is presented in this chapter to assist in problem solving. The functions are plotted versus the common independent variable, the mach number, which permits the evaluation of all the ratios once one of them has been determined.

The utility of the dimensionless form, always as a ratio to the stagnation (0) or sonic (*) values, stems from the fact that for any isentropic perfect-gas flow these reference values are constant throughout the flow field. Therefore, the change in properties, areas, and impulse functions between any two points in the flow can be obtained by finding the ratio of

*This equation is a variation of equation (5.39) and does not appear in chapter 5.

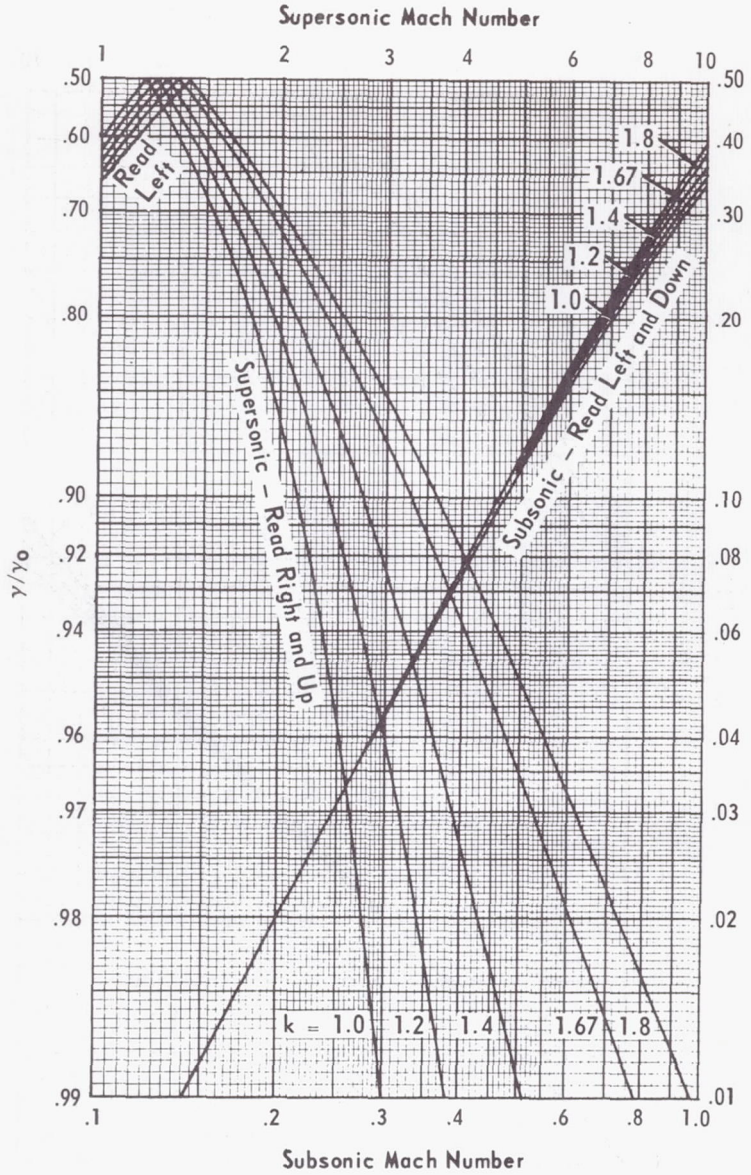


Figure 16.3. Isentropic density ratio.

the dimensionless ratios, each evaluated at their respective locations. For example,

$$\frac{T_2}{T_1}=\frac{\dfrac{T_2}{T_0}}{\dfrac{T_1}{T_0}} \qquad \text{and} \qquad \frac{A_2}{A_1}=\frac{\dfrac{A_2}{A^*}}{\dfrac{A_1}{A^*}}$$

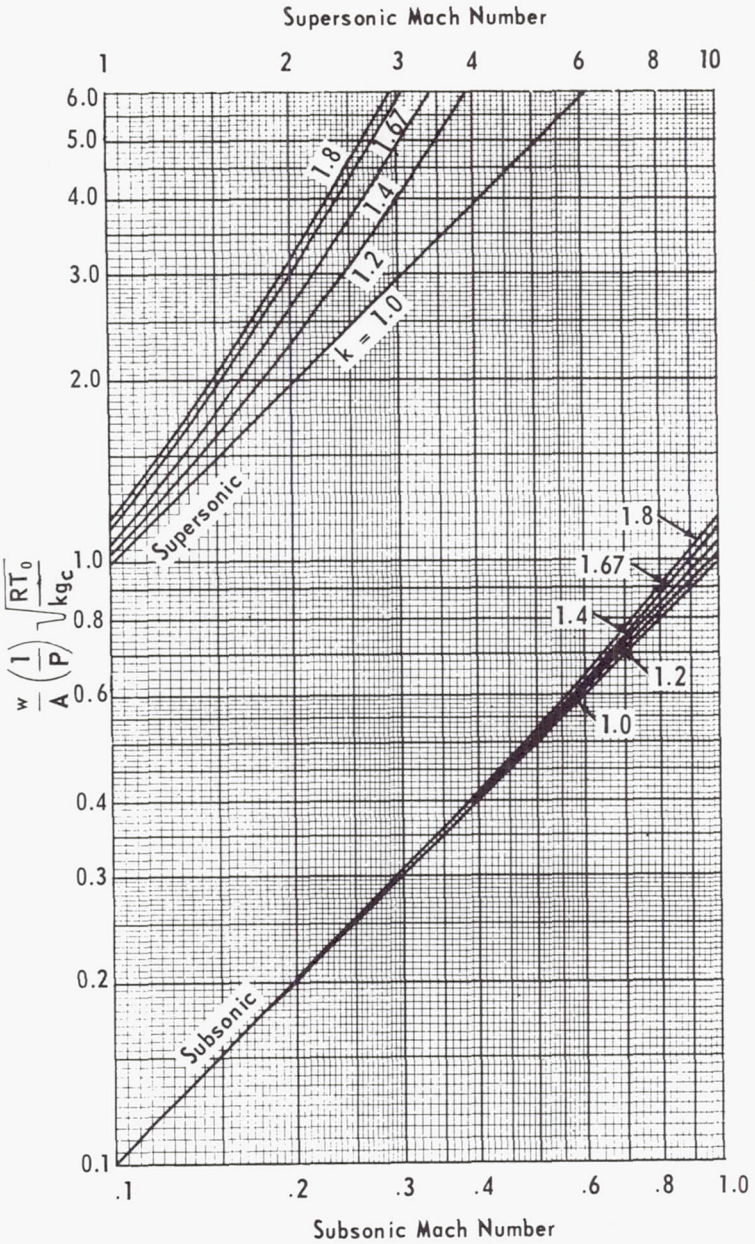


Figure 16.4. Adiabatic flow parameter.

Therefore, the first objective in solving an isentropic flow problem is usually to determine the mach number at the points of interest and/or some change in property or area by which the mach numbers can be obtained. Then, utilizing the plotted or tabulated isentropic flow functions (for the proper value of k) and remembering that all stagnation properties and sonic values are constant for all locations, the desired solution can be obtained.

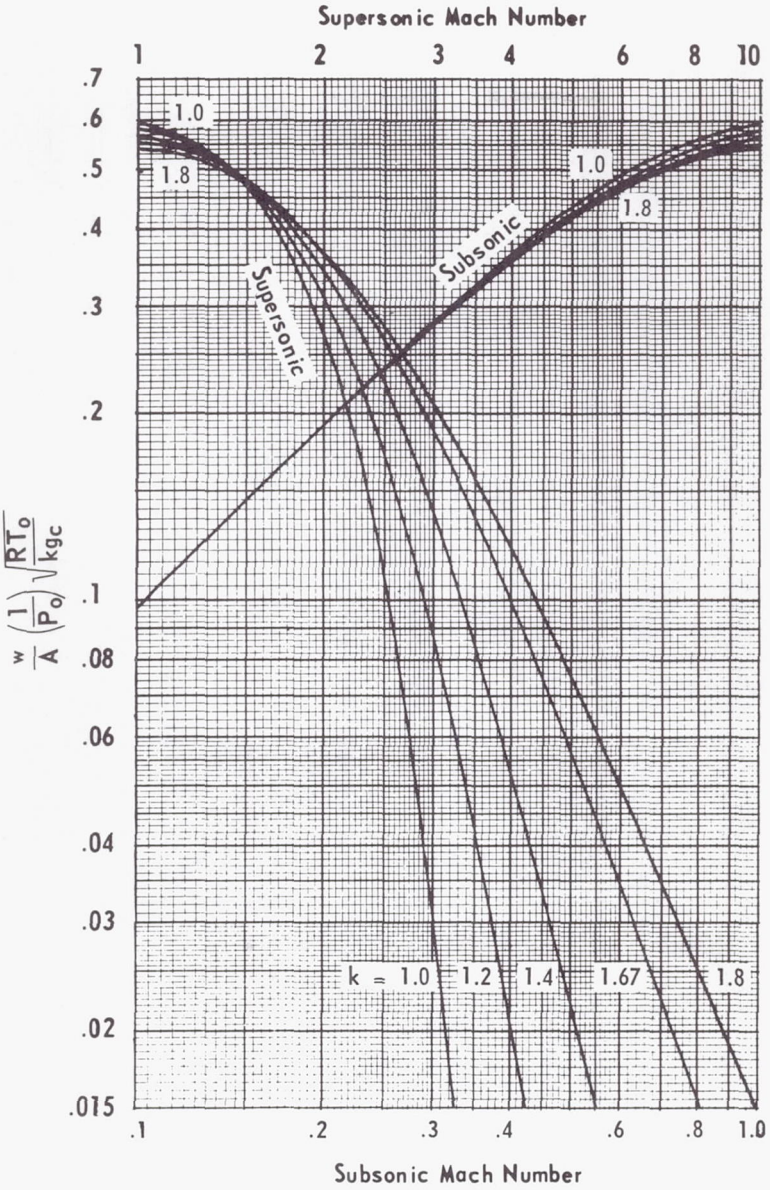


Figure 16.5. Isentropic flow parameter.

EXAMPLE PROBLEM 16.2

Nitrogen is to be supplied to a 2-inch (I.D.) pipe at 70° F and 1000 psia from a large manifold. A low-loss, nozzle-type entrance that incorporates a reduced throat size for the purposes of limiting the maximum flow to 15 000 scfm is to be used (fig. 16.9). The design flow rate is to be 10 000 scfm. Determine the required throat diameter D and the conditions at stations 1 and 2 at the design flow conditions. Also determine the resultant force of the fluid on the nozzle between the nozzle inlet (at the weld) and station 2.

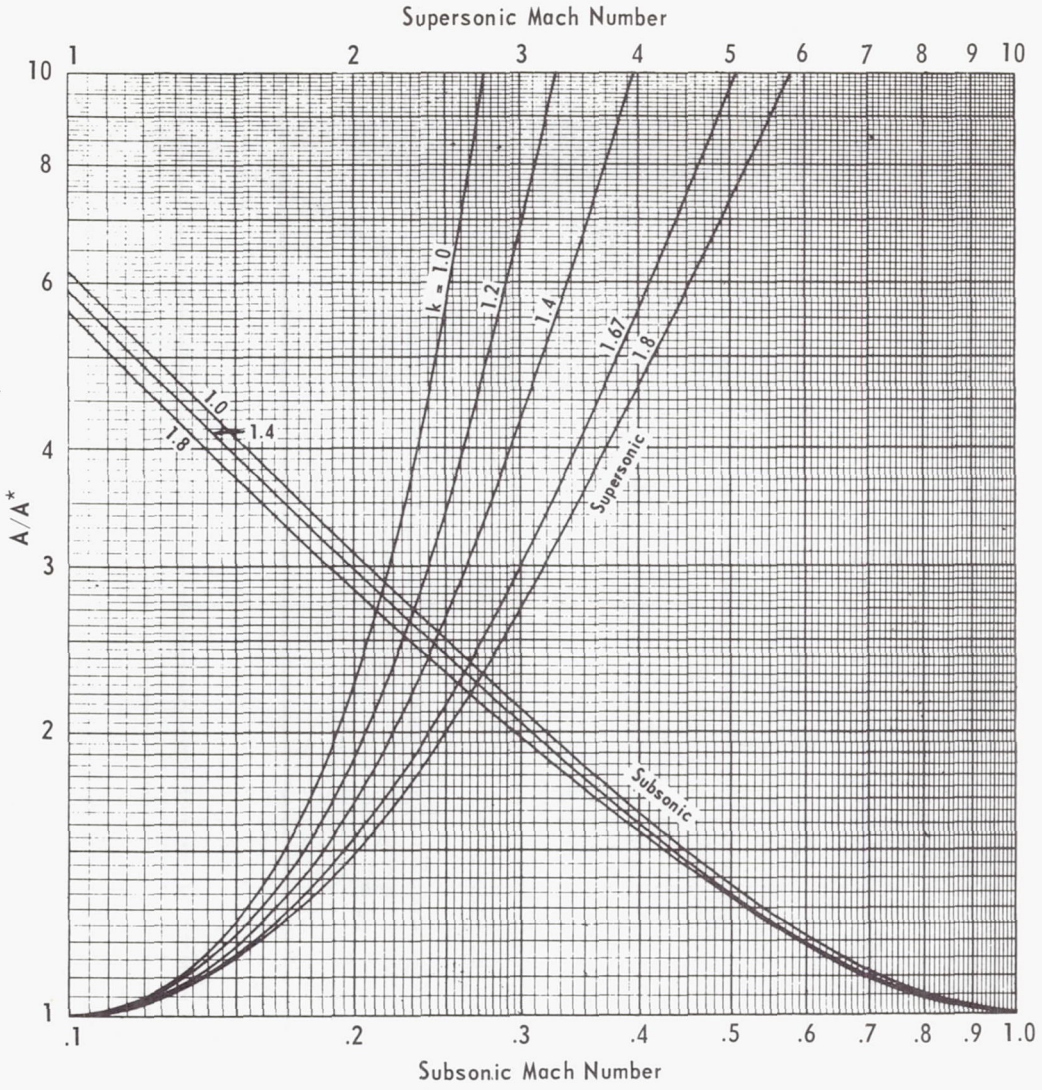


Figure 16.6. Isentropic area ratio.

SOLUTION

Assuming isentropic flow and the nitrogen to be essentially a perfect gas, with

$$k = 1.4 \qquad \text{and} \qquad R = 55.2 \qquad \text{ft-lbf/lbm-°R}$$

And since the limiting condition is choked flow, equation (5.37) and the unit conversions shown in equation (5.22) are used to find D,

$$15.21\left(\frac{15\,000}{1000}\right)\frac{\sqrt{\dfrac{460+70}{1.4(55.2)}}}{(1000)D^2} = \left(\frac{2}{1.4+1}\right)^{\frac{1.4+1}{2(1.4-1)}}$$

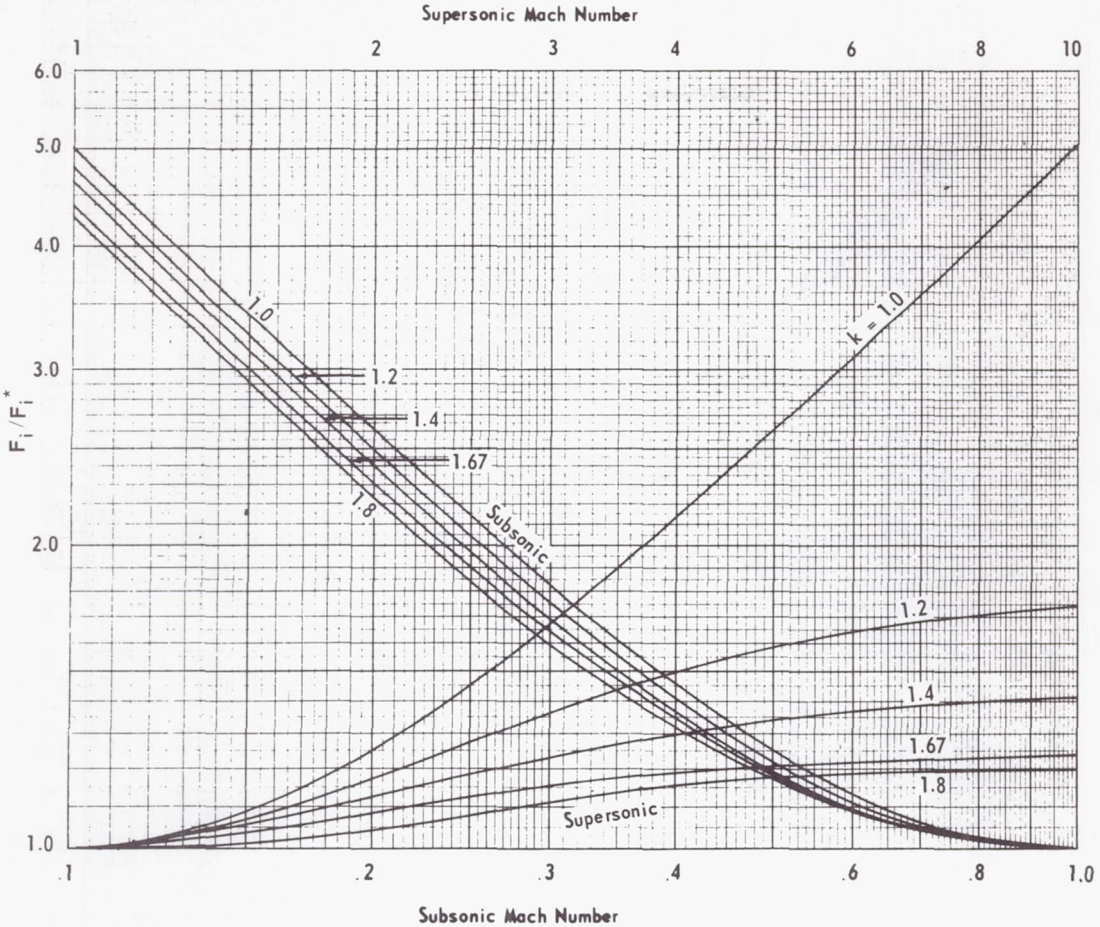


Figure 16.7. Isentropic impulse functions.

Solving for D yields

$$D = 1.016 \text{ in.}$$

For design flow conditions of 10 000 scfm, the isentropic flow parameter of equation (5.36) is evaluated with the unit conversions of equation (5.22).

$$\left(\frac{w}{A}\right)\left(\frac{1}{P_0}\right)\sqrt{\frac{RT_0}{kg_c}} = 15.21\left(\frac{10\,000}{1000}\right)\frac{\sqrt{\dfrac{460+70}{1.4(55.2)}}}{1000(1.016)^2}$$

$$= 0.386$$

Since equation (5.36) cannot be solved easily for the throat mach number, it is advantageous to use the plotted solution provided in figure 16.5 yielding

$$M_1 = 0.426$$

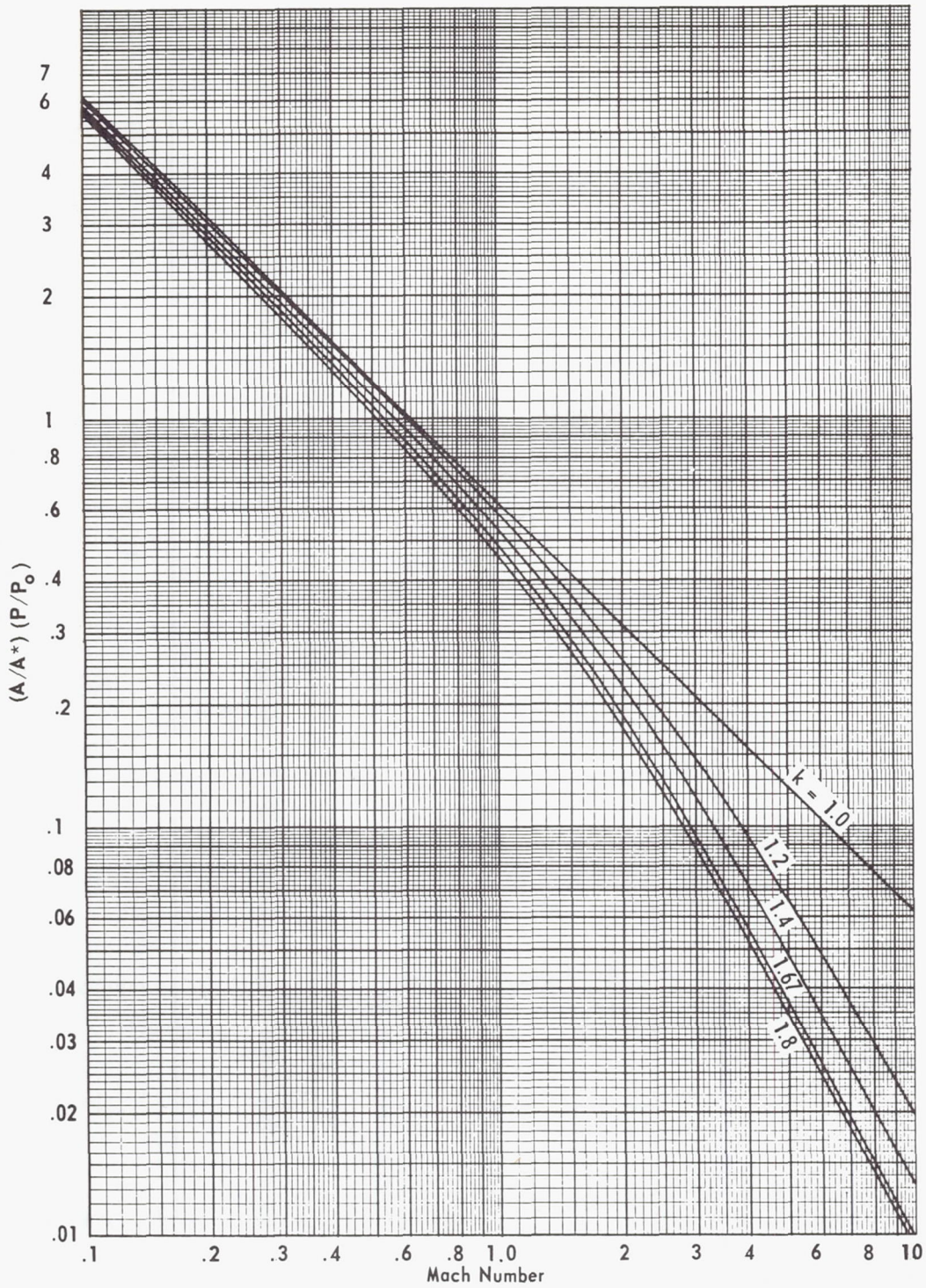


Figure 16.8. Product of area and pressure ratios.

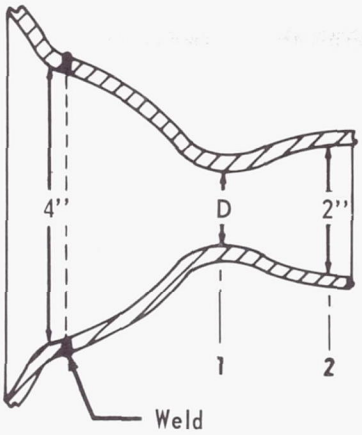


Figure 16.9. Low-loss, nozzle-type entrance.

The static fluid properties at the throat are from the isentropic ratios.

Figure 16.2 yields

$$\frac{p_1}{p_0}=0.881 \qquad \text{so that} \qquad p_1=1000(0.881)=881 \text{ psia}$$

Figure 16.1 yields

$$\frac{T}{T_0}=0.965 \qquad \text{so that} \qquad T_1=530(0.965)=512^\circ \text{R}$$

Figure 16.6 yields

$$\frac{A_1}{A^*}=1.5$$

Station 2 condition is easily found, using the known area ratio

$$\frac{A_2}{A_1}=\left(\frac{D_2}{D_1}\right)^2=\left(\frac{2}{1.016}\right)^2=3.87$$

and the value of (A_1/A^*) from the preceding, since

$$\frac{A_2}{A^*}=\left(\frac{A_2}{A_1}\right)\left(\frac{A_1}{A^*}\right)=(3.87)(1.5)=5.82$$

At this value of (A_2/A^*), the subsonic value of M_2 and the fluid property ratios at location 2 are obtained once again from figure 16.6. The subsonic value of M_2 is selected since, if M_1 is subsonic, flow is subsonic everywhere and

$$M_2=0.1$$

Then

$$\frac{p_2}{p_0}=0.993 \qquad \text{so that} \qquad p_2=1000(0.993)=993 \text{ psia}$$

and

$$\frac{T_2}{T_0}=0.998 \qquad \text{so that} \qquad T_2=530(0.998)=529^\circ \text{ R}$$

The resultant force on the nozzle is obtained best by equation (5.40) in this case, since the pressures and mach numbers are known at both locations. At the inlet, $M \approx 0$ because the area is approximately 16 times that of the throat, and the pressure is essentially the manifold pressure. At the outlet, station 2, the necessary quantities were evaluated as described. Then, by equations (5.39*a*) and (5.40)

$$F_{wx}=(993)\left(\frac{\pi}{4}\right)(2)^2\,[1+1.4\,(0.10)^2]-(1000)\left(\frac{\pi}{4}\right)(4)^2$$
$$=-9417 \text{ lbf}$$

Then the resultant force on the nozzle is 9417 lbf in the direction of the flow.

CHOKING IN ISENTROPIC FLOW

Choking in isentropic flow occurs only in a region of reduced flow area, whether the upstream flow is subsonic or supersonic. In the usual case of subsonic upstream flow, the pressure, temperature, and density decrease as the flow accelerates to the throat where the static properties, relative to the stagnation values, are represented by equations (5.33), (5.34), and (5.35). This occurs only when the back pressure is reduced sufficiently to cause choking. Beyond the throat, the flow can continue to accelerate to supersonic velocities in an expanding flow channel if the back pressures are very low or decelerate subsonically if the back pressures are relatively high. For intermediate back pressures, a normal shock will usually divide two isentropic flow regions within the downstream diverging section, with supersonic flow upstream and subsonic flow downstream of the shock. For any given reduced area and downstream configuration, there is a specific back pressure which will produce choking in the reduced area. Reduction in back pressure below this value will not increase the mass flow rate through the system. However, increases in flow rate can be achieved by increasing the upstream pressure. The isentropic flow relations presented earlier can be applied to choked flow in smooth-area change sections at least to the point of choking.

OPERATION OF NOZZLES

There are two basic types of nozzles: converging and converging-diverging. Converging nozzles, in the usual applications, generate flow velocities up to but no greater than sonic. Converging-diverging nozzles can generate supersonic velocities in the diverging section if the back pressure is maintained low enough. If the back pressure is lower than that required to choke the nozzle, but not low enough to produce the supersonic mach number associated with the area change of the divergent section, a normal shock will occur within the divergent section to slow the flow to a subsonic value ahead of the outlet.

A complete description of nozzle performance and computation methods can be found in "Operation of Nozzles" in chapter 6 and "Normal Shock Waves" in chapters 6 and 17.

PERFORMANCE OF REAL NOZZLES

Nozzle efficiency is a measure of the conversion from thermal energy to kinetic energy by the nozzle and is defined as the ratio of actual to isentropic static enthalpy changes between two pressures. Then

$$\eta=\frac{h_0-h_a}{h_0-h_s} \qquad \text{and} \qquad \eta=\frac{V_a^2}{V_s^2} \tag{5.42}$$

For a perfect gas,

$$\eta=\frac{\left(\frac{k-1}{2}\right)\left(\frac{V_a}{c_0}\right)^2}{1-\frac{T_s}{T_0}}=\left(\frac{k-1}{2}\right)\left(\frac{V_a}{c_0}\right)^2\left[1-\left(\frac{P_s}{P_0}\right)^{\frac{k-1}{k}}\right]^{-1} \tag{5.43}$$

The nozzle discharge coefficient is defined as

$$C_d=\frac{w_a}{w_s}$$

where w_s is the flow that would have occurred in a truly isentropic process with the given pressure drop and w_a is the flow that actually occurs.

An adiabatic relationship is found to be applicable to describe an irreversible process, although it consists of the product of two isentropic functions. This relationship is useful in establishing the conditions downstream of a choked nozzle, even though the flow immediately downstream of the nozzle is irreversible.

$$\left(\frac{1}{C_d}\right)\left(\frac{A_2}{A_t}\right)\left(\frac{P_2}{P_{01}}\right)=\left[\left(\frac{A}{A^*}\right)_2\left(\frac{P}{P_0}\right)_2\right]_{\text{isen}}=\frac{\left(\frac{2}{k+1}\right)^{\frac{k+1}{2(k-1)}}}{M_2\left[1+\left(\frac{k-1}{2}\right)M_2^2\right]^{1/2}} \tag{5.46}$$

This function is solved graphically in figure 16.8 and requires the knowledge of all the terms of the leftmost grouping. The station subscripts are based on the notation of figure 5.13 (ch. 5). Station 1 refers to the upstream location; t refers to the nozzle throat; and station 2 refers to the downstream location of interest. The very important requirements in applying this relationship are assurance of choked flow and knowledge of the downstream static pressure which must be obtained by other means.

Example Problem 16.3

When the nozzle of example problem 16.2 is operating as a flow limiter, the flow becomes choked at location 1, and supersonic flow exists in the divergent section. However, due to boundary-layer growth, the supersonic flow is shocked down by the complex system of shocks described in "Oblique Shock Waves" in chapter 6. At point 3 downstream of the nozzle in the constant area pipe, a static pressure gage measures 150 psig. Determine all the flow conditions at the downstream location 3.

SOLUTION

Assume $C_d = 1$ for the smooth nozzle. By equation (5.46), with proper subscripts for the problem,

$$\left[\left(\frac{A}{A^*}\right)_3\left(\frac{P}{P_0}\right)_3\right]_{\text{isen}} = \left(\frac{1}{1.0}\right)\left(\frac{2}{1.016}\right)^2\left(\frac{150+14.7}{1000}\right)$$

$$= 0.637$$

The graphic solution of equation (5.46) in figure 16.8 yields $M_3 = 0.85$, at which $P_3/P_{03} = 0.6235$ and $T_3/T_{03} = 0.8737$. Then

$$P_{03} = \frac{164.7}{0.6235}$$

$$= 264 \text{ psia}$$

Also, $T_{03} = T_0 = 530°$ R, so that

$$T_3 = 530\ (0.8737)$$

$$= 463° \text{ R}$$

CHAPTER 17

APPLICATION OF SHOCK-WAVE THEORIES

Shock waves are discontinuities in fluid properties which can occur in supersonic flow. Normal shock waves are discontinuities that lie in a plane normal to the flow and generally are the result of a straight-line deceleration under adiabatic conditions. Oblique shock waves are lesser discontinuities that are inclined to the flow direction at some angle less than 90°. Oblique shocks generally result from the turning of a supersonic flow under adiabatic conditions.

NORMAL SHOCK WAVES

A normal shock wave may be considered an extremely rapid change in fluid properties, occurring normal to the direction of flow of the fluid stream and taking place over an extremely short distance.

Changes in Properties

The downstream-to-upstream temperature ratio can be expressed in terms of the respective mach numbers, based on constant stagnation temperature for the adiabatic flow.

$$\frac{T_y}{T_x}=\frac{1+\left(\frac{k-1}{2}\right)M_x^2}{1+\left(\frac{k-1}{2}\right)M_y^2} \qquad [6.2]$$

Since the area is the same on both sides of the shock, the continuity equation yields

$$\frac{\dot{m}}{A}=\rho_x V_x=\rho_y V_y \qquad \text{or} \qquad \frac{w}{A}=\gamma_x V_x=\gamma_y V_y \qquad [6.3]$$

The static pressures are related by

$$\frac{P_y}{P_x}=\left(\frac{M_x}{M_y}\right)\sqrt{\frac{1+\left(\frac{k-1}{2}\right)M_x^2}{1+\left(\frac{k-1}{2}\right)M_y^2}} \qquad [6.5]$$

325-994 O-69—22

Equation (6.5) is also known as the equation of the Fanno line in terms of P and M and is obtained by combining the steady adiabatic flow-energy equation, continuity equation for constant area, and the perfect-gas law. The pressure ratio across the shock can be obtained differently by utilizing the momentum equation rather than the energy equation. The resulting equation defines the Rayleigh line in terms of P and M.

$$\frac{P_y}{P_x}=\frac{1+kM_x^2}{1+kM_y^2} \qquad [6.11]$$

The direct relation between upstream and downstream mach numbers is obtained by combining equations (6.5) and (6.11) to yield

$$M_y^2=\frac{M_x^2+\dfrac{2}{k-1}}{\left(\dfrac{2k}{k-1}\right)M_x^2-1} \qquad [6.14]$$

Substitution of equation (5.19) into equation (6.14) yields the useful relationship

$$M_x^* M_y^*=1 \qquad [6.15]$$

The substitution of equation (6.14) into (6.11) gives a ratio of downstream-to-upstream pressure ratio as function of upstream mach number only.

$$\frac{P_y}{P_x}=\left(\frac{2k}{k+1}\right)M_x^2-\frac{k-1}{k+1} \qquad [6.16]$$

The temperature ratio is obtained by substituting equation (6.14) into equation (6.2).

$$\frac{T_y}{T_x}=\frac{\left[1+\left(\dfrac{k-1}{2}\right)M_x^2\right]\left[\left(\dfrac{2k}{k-1}\right)M_x^2-1\right]}{\left[\dfrac{(k+1)^2}{2(k-1)}\right]M_x^2} \qquad [6.17]$$

The density ratio is expressed most simply as the ratio of equation (6.16) to equation (6.17).

$$\frac{\gamma_y}{\gamma_x}=\frac{\rho_y}{\rho_x}=\frac{\dfrac{P_y}{P_x}}{\dfrac{T_y}{T_x}} \qquad [6.18]$$

The combination of equation (6.18) with equation (6.3) gives the velocity ratio across the shock

$$\frac{V_y}{V_x}=\frac{\gamma_x}{\gamma_y}=\frac{\dfrac{T_y}{T_x}}{\dfrac{P_y}{P_x}} \qquad [6.19]$$

Similarly, using equations (6.14) and (6.16) and the isentropic flow relationships of chapter 5, the stagnation pressure change is found to be

$$\frac{P_{oy}}{P_{ox}}=\frac{\left[\frac{\left(\frac{k+1}{2}\right)M_x^2}{1+\left(\frac{k-1}{2}\right)M_x^2}\right]^{\frac{k}{k-1}}}{\left[\left(\frac{2k}{k+1}\right)M_x^2-\frac{k-1}{k+1}\right]^{\frac{1}{k-1}}} \qquad [6.20]$$

Equation (5.31) can be substituted into equation (6.20) to produce the downstream stagnation pressure in terms of upstream static pressure and mach number.

$$\frac{P_{oy}}{P_x}=\frac{\left[\left(\frac{k+1}{2}\right)M_x^2\right]^{\frac{k}{k-1}}}{\left[\left(\frac{2k}{k+1}\right)M_x^2-\frac{k-1}{k+1}\right]^{\frac{1}{k-1}}} \qquad [6.21]$$

Equations (6.14), (6.16), (6.17), (6.18), (6.20), and (6.21) are solved graphically and presented here as figures 17.1 through 17.6 to facilitate problem solving. Tabulated solutions can also be found in numerous other publications.

Convergent-Divergent Nozzles

Normal shock waves often occur in the divergent section of convergent-divergent nozzles. It is explained in chapter 5 that normal shock waves occur in overexpanded convergent-divergent nozzles when the nozzle back pressure P_b is:

(1) Less than a minimum (established for the particular nozzle) that will permit subsonic flow throughout the nozzle, except sonic at the throat; and

(2) Greater than a maximum value (established for the particular nozzle) that will permit supersonic isentropic flow throughout the divergent section to the nozzle exit.

Referring to the nomenclature of figure 6.2 (ch. 6), these back pressures causing a normal shock in the nozzle are in the range of $P_4 > P_b > P'_e$. As P_b is reduced from a value of P'_4, the normal shock moves downstream from the throat region toward the exit, until at $P_b = P'_e$, the normal shock stands in the nozzle exit.

The methods of establishing the flow conditions throughout the nozzle utilize the isentropic flow relationships upstream and downstream of the normal shock wave, and the normal shock functions establish the change in conditions across the shock. The isentropic equation (5.38) relates the local flow area of the nozzle to the local mach number, in both the supersonic and subsonic regions, as shown on the plotted solution in figure 5.6 (ch. 5). The procedure, outlined briefly in "Normal Shock Waves" (ch. 6), will be demonstrated in the following example.

EXAMPLE PROBLEM 17.1

A smooth convergent-divergent nozzle (fig. 17.7) is operating with air. The measured upstream pressures and temperatures are 500 psig and 80° F, respectively. The outlet

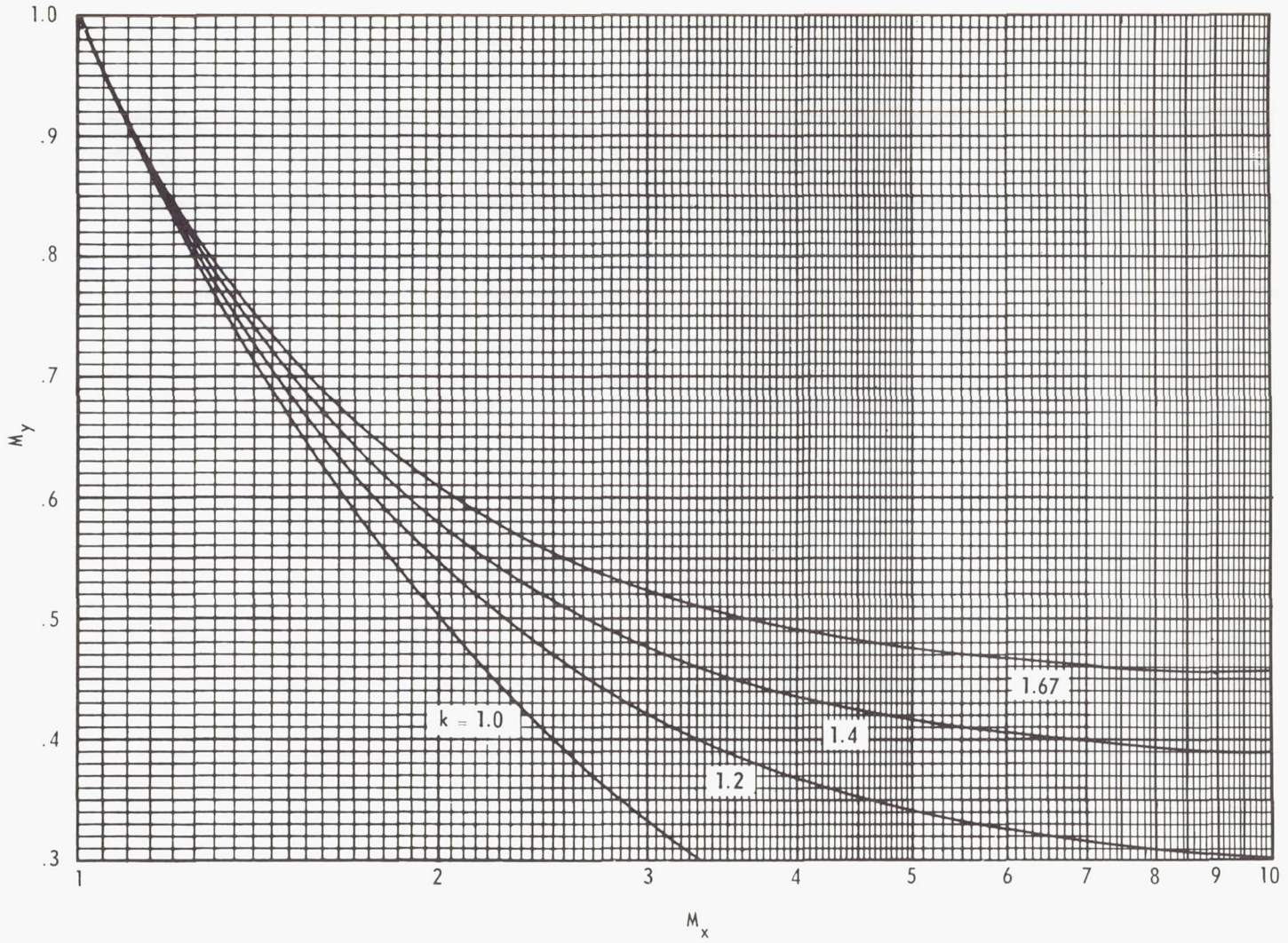


Figure 17.1. Mach-number changes across normal shocks.

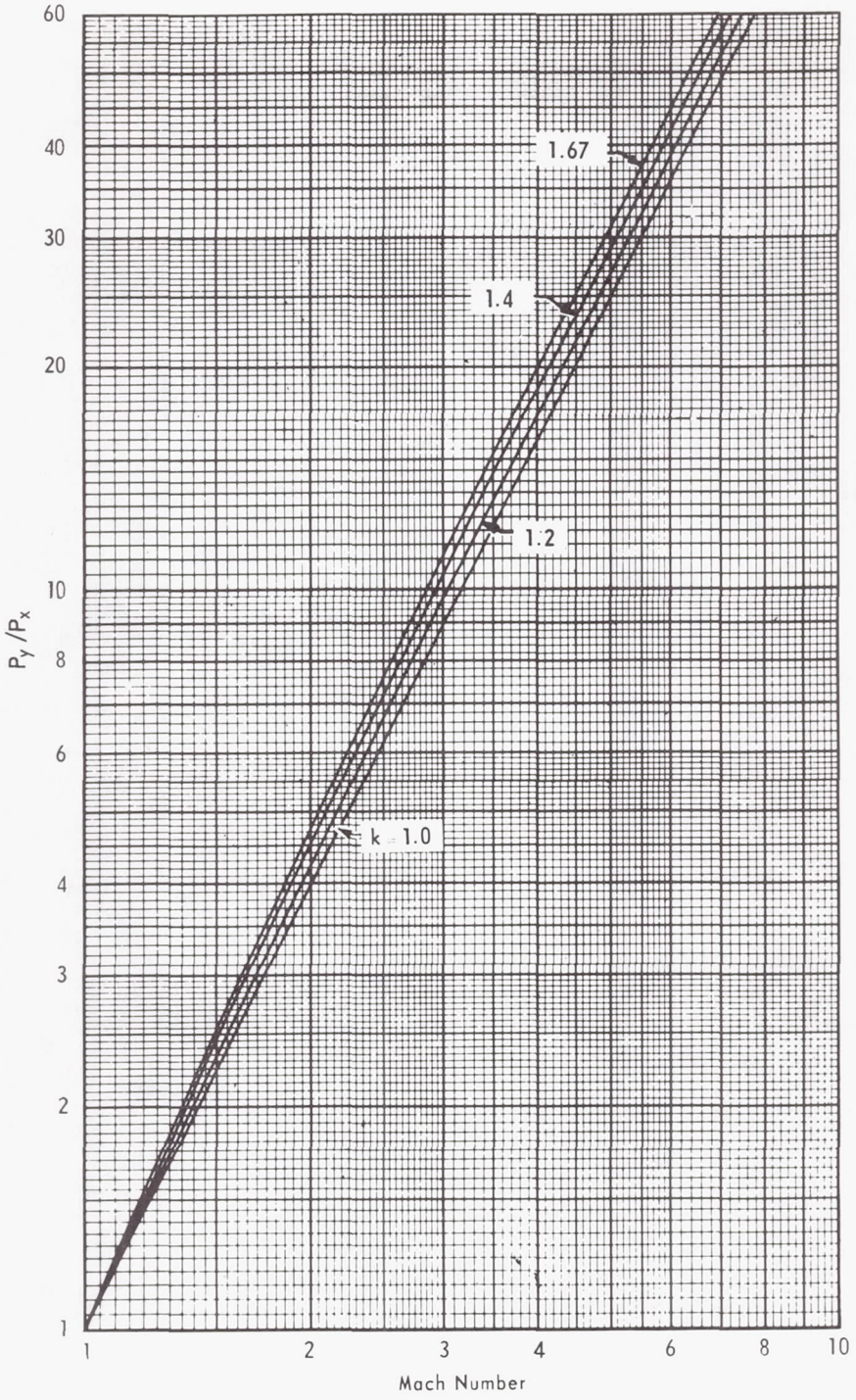


Figure 17.2. Static pressure changes across normal shocks.

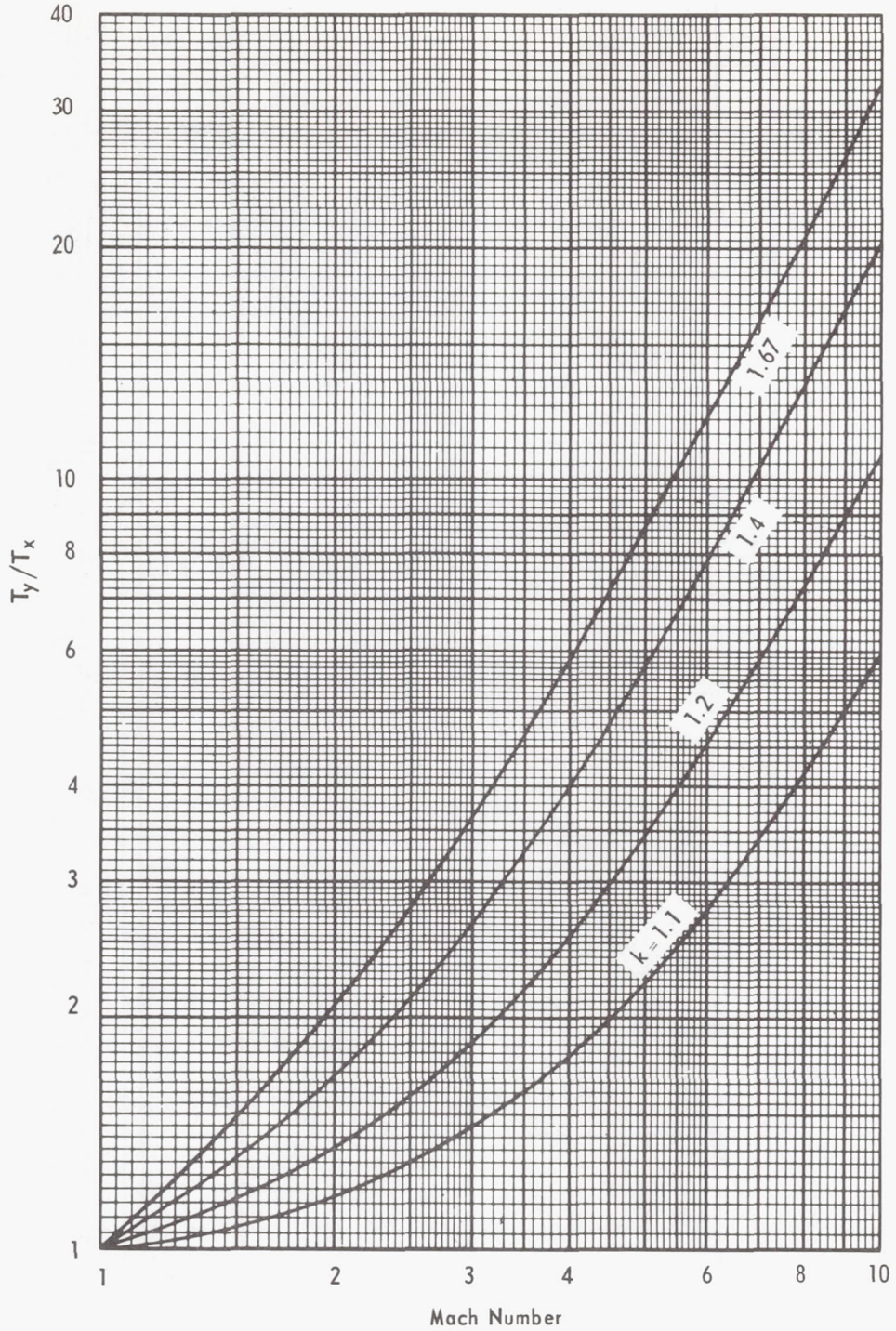


Figure 17.3. Static temperature changes across normal shocks.

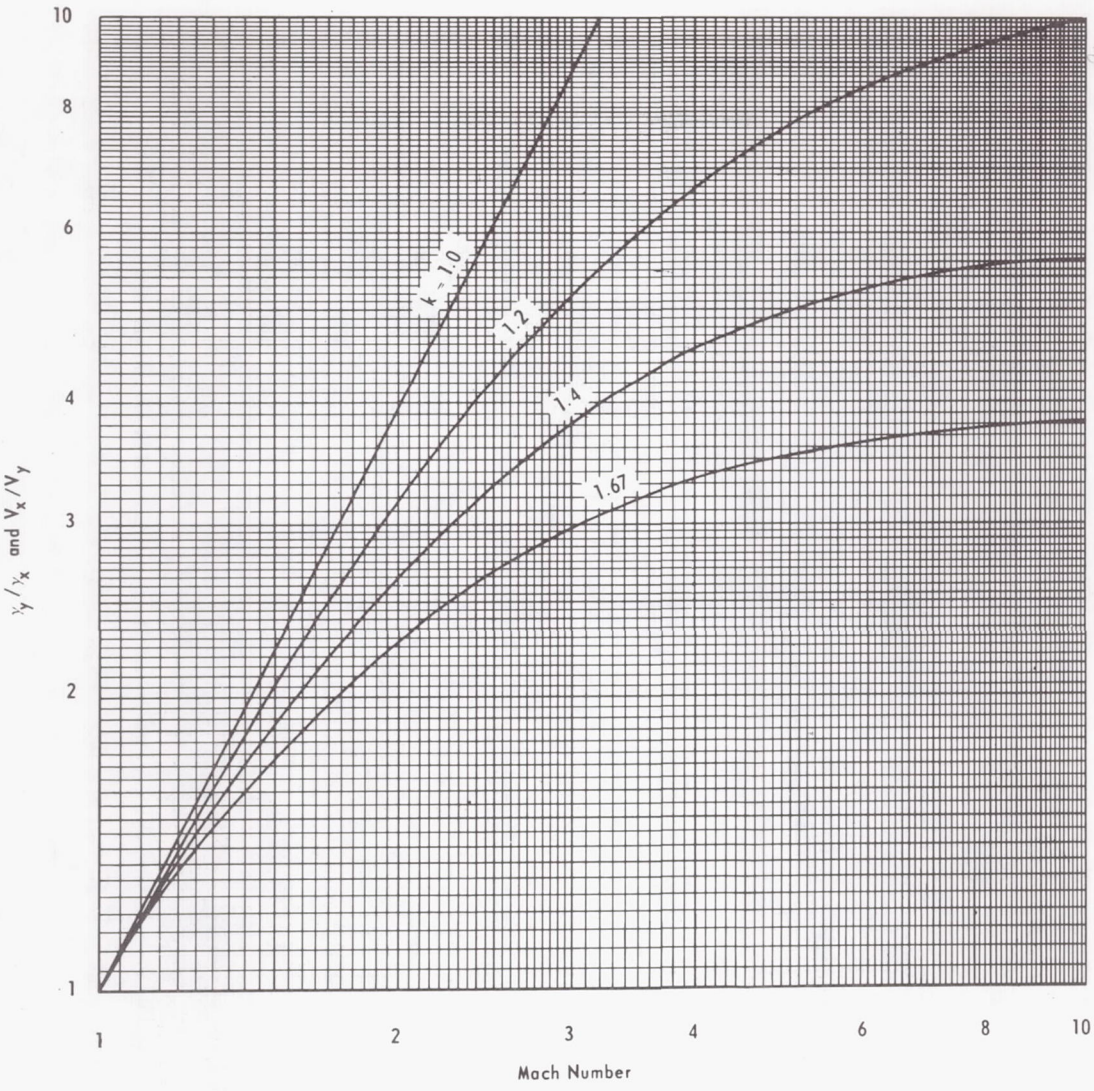


Figure 17.4. Density and velocity changes across normal shocks.

pressure is measured to be 165 psig. The upstream flow area is 0.3 square inch, the throat area is 0.1 square inch, and the nozzle exit area is 1 square inch. Determine:

(1) The weight flow rate;

(2) The location of normal shock, if one exists, in terms of the nozzle area at that point; and

(3) The flow conditions at the nozzle exit in terms of mach-number temperatures and pressures.

SOLUTION

(1) First, it must be established that the flow is choked in the nozzle throat. Proof of choked flow requires only that the exit pressure be shown less than the minimum all-subsonic-

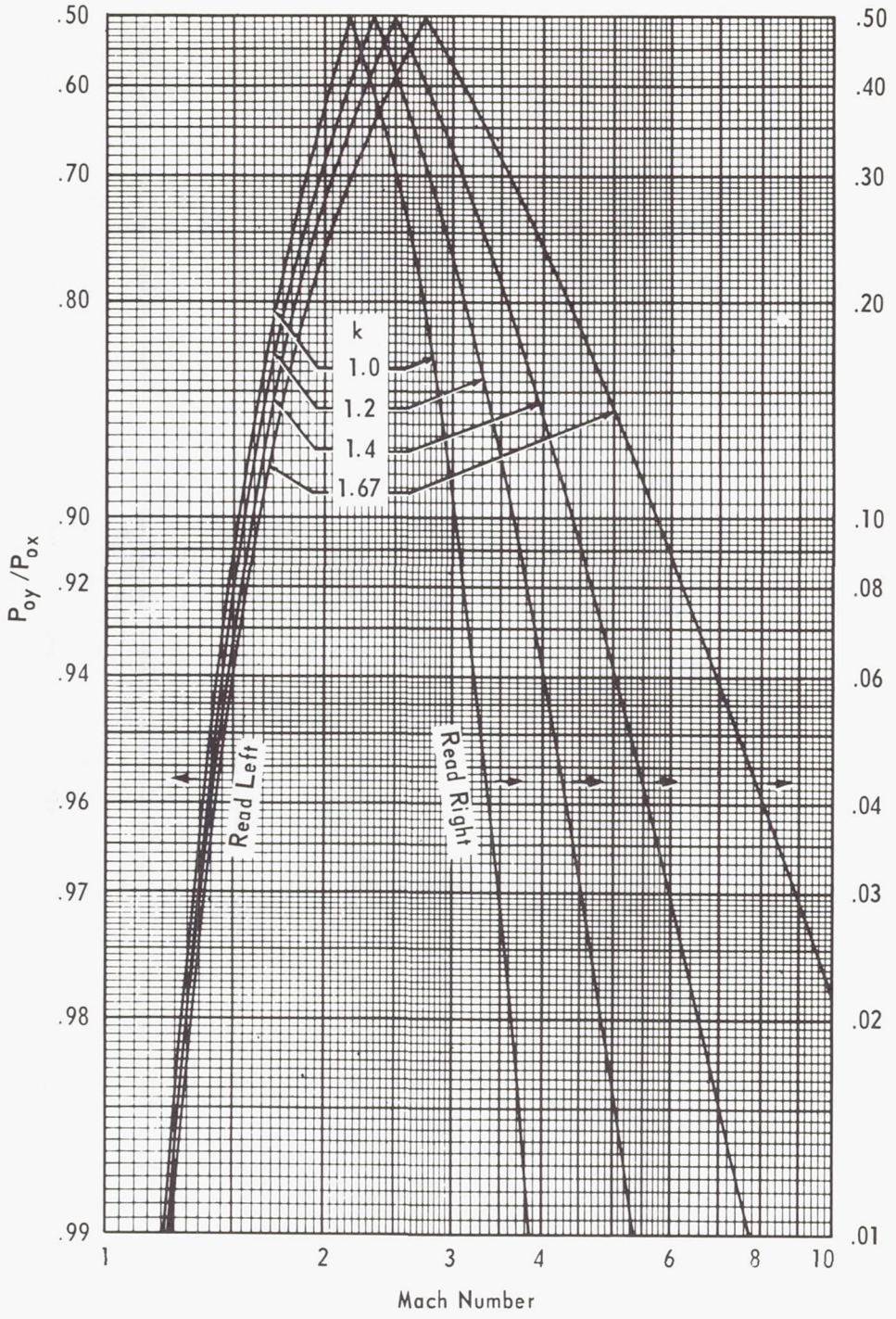


Figure 17.5. Stagnation pressure changes across normal shocks.

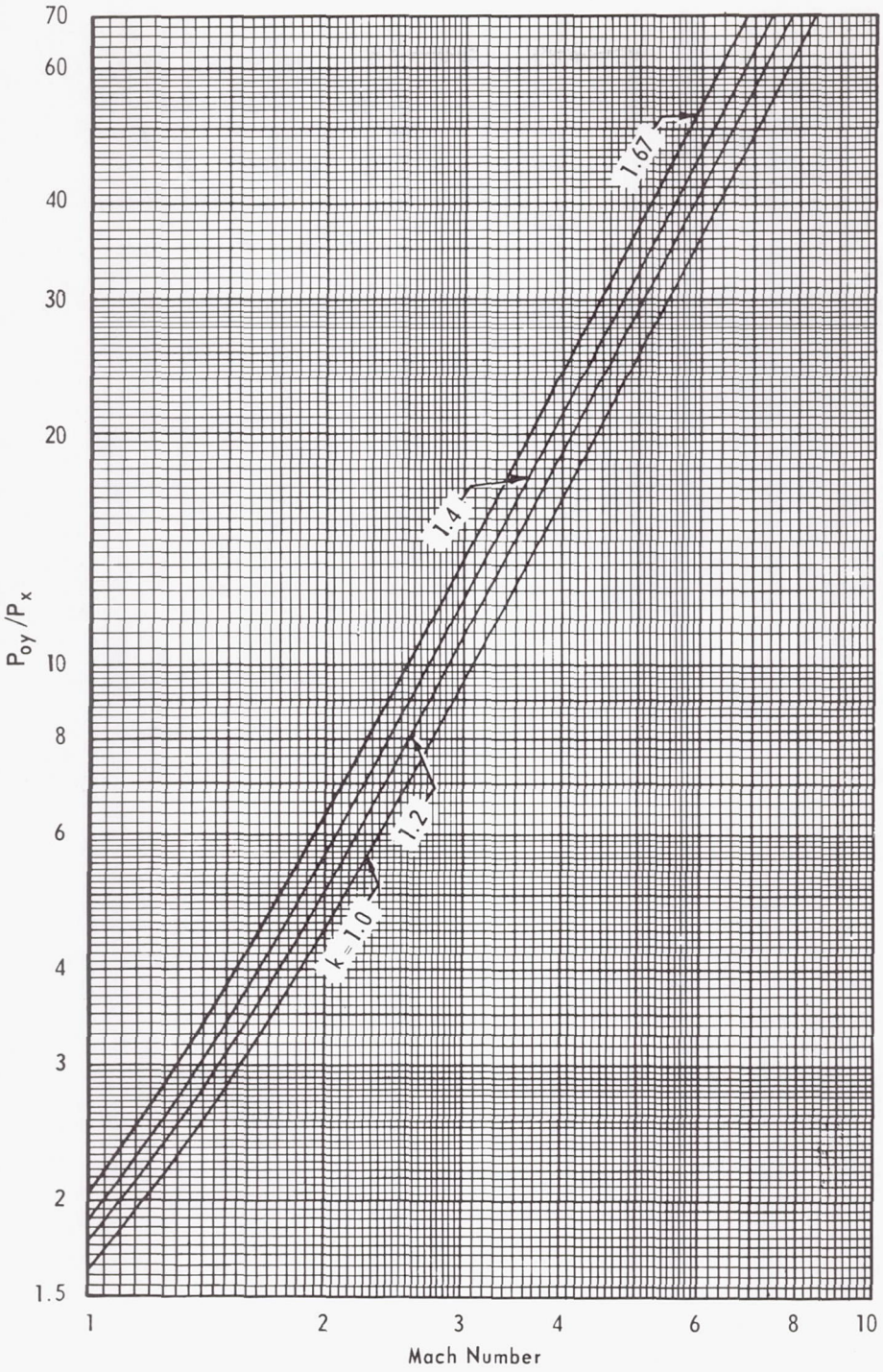


Figure 17.6. Ratio of downstream stagnation to upstream static pressure, normal shocks.

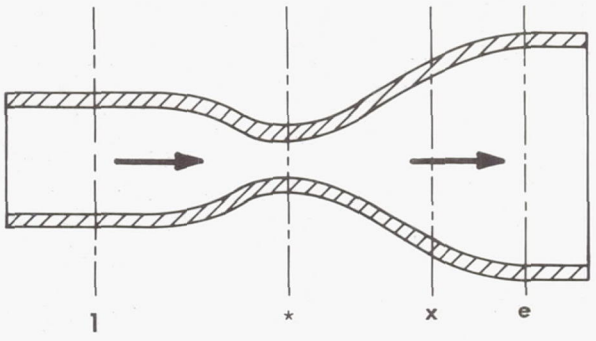


Figure 17.7. Smooth convergent-divergent nozzle.

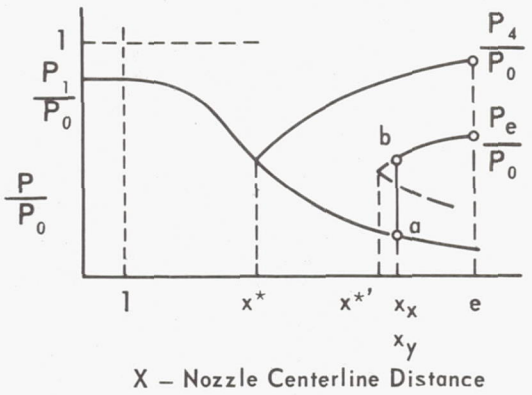


Figure 17.8. Pressure diagram.

flow exit pressure indicated as P_4 in figure 6.2 (ch. 6) and figure 17.8. The pressure diagram must be slightly modified to account for the upstream velocity which is significant in this case. Note that the upstream pressure P_1 is not the stagnation pressure and that, with isentropic subsonic flow throughout the nozzle, the outlet static pressure P_e must be greater than P_1 (nearer to stagnation) due to the larger area and lower velocity at the exit. Since the nozzle-exit pressure was measured to be much less than the inlet, it can be definitely concluded that the nozzle is choked, and the nozzle throat corresponds with the sonic (*) conditions. Then the mach number and stagnation conditions at station 1 can be established using the isentropic flow relations of figures 16.1, 16.2, and 16.6 (ch. 16) as follows. The area ratio for the upstream location is

$$\frac{A_1}{A^*}=\frac{0.3}{0.1}=3$$

For a value of $k=1.4$, and $A_1/A^*=3$, figure 16.6 (ch. 16) yields

$$M_1=0.198$$

Similarly, from figures 16.1 and 16.2 (ch. 16) at $M_1 = 0.198$

$$\frac{T_1}{T_0} = 0.9923 \qquad \text{so that} \qquad T_0 = \frac{460 + 80}{0.9923} = 544.2^\circ \text{ R}$$

and

$$\frac{P_1}{P_0} = 0.973 \qquad \text{so that} \qquad P_0 = \frac{500 + 14.7}{0.973} = 529 \text{ psia}$$

Equation (5.37) defines the choked flow rate as

$$w = w_{\max} = A^* P_0 \sqrt{\frac{kg_c}{RT_0}} \left(\frac{2}{k+1}\right)^{\frac{k+1}{2(k-1)}}$$

$$= \left(\frac{0.1}{144}\right) [(144)(529)] \sqrt{\frac{(1.4)(32.2)}{(53.3)(544)}} \left(\frac{2}{1.4+1}\right)^{\frac{1.4+1}{2(1.4-1)}}$$

$$= 1.206 \text{ lbm/sec}$$

(2) To determine the nozzle-flow conditions, a trial-and-error solution is required using the procedure outlined in "Normal Shock Waves" (ch. 6). This procedure requires that the nozzle area at the shock-wave location be assumed and computations repeated until the computed exit pressure agrees with the known pressure. Proceeding, assume arbitrarily that

$$\frac{A_x}{A^*} = 4.0$$

Entering figure 16.6 (ch. 16) for $k = 1.4$ and $A_x/A^* = 4$ in the supersonic region yields

$$M_x = 2.94$$

Obtain the mach number downstream of the shock, M_y, by entering figure 17.1 at $m_x = 2.94$ and $k = 1.4$.

$$M_y = 0.4788$$

Figure 17.5 yields the stagnation pressure change across the shock

$$\frac{P_{ob}}{P_{oa}} = \frac{P_{oy}}{P_{ox}} = 0.3457$$

The stagnation pressure is constant throughout each isentropic process upstream and downstream of the shock so that

$$\frac{P_{oe}}{P_{o1}} = 0.3457 \qquad \text{and} \qquad P_{oe} = 0.3457(529) = 182.9 \text{ psia}$$

The exit mach number M_e is found from the known area ratios involving the fictitious throat area $A^{*\prime}$ of the subsonic exit region. At $M_y = 0.4788$, figure 16.6 (ch. 16) yields

$$\frac{A_y}{A^*} = 1.383$$

The exit area ratio can now be calculated in terms of $A^{*\prime}$ as

$$\frac{A_e}{A^{*\prime}} = \left(\frac{A_e}{A_x}\right)\left(\frac{A_y}{A^{*\prime}}\right)$$

where $A_x = A_y$. The assumed value of $A_x/A^* = 4$ requires that

$$A_x = 4(0.1) = 0.4$$

Then

$$\frac{A_e}{A^{*\prime}} = \left(\frac{1.0}{0.4}\right)(1.383) = 3.46$$

The exit mach number from figure 16.6 (ch. 16) at $A_e/A^{*\prime} = 3.46$ and $k = 1.4$ in the subsonic region is

$$M_e = 0.170$$

Figure 16.2 (ch. 16) yields an outlet pressure ratio at M_2 of

$$\frac{P_e}{P_{oe}} = 0.980$$

which, when combined with the stagnation pressure obtained in the preceding equations, yields the outlet static pressure

$$\begin{aligned} P_e &= 0.980(182.9) \\ &= 179.2 \text{ psia} \\ &= 164.5 \text{ psig} \end{aligned}$$

This value of nozzle outlet pressure agrees sufficiently with the measured value of 165 psig. Therefore, the assumed location of the shock wave ($A_x/A^* = 4$) is correct, and the remaining flow parameters can now be evaluated based on that assumption. If the computed downstream pressure had not agreed with the known value, a new area ratio (A_x/A^*) would be assumed and the procedure repeated until agreement was reached. Increasing the area ratio reduces the computed outlet static pressure, and vice versa.

(3) The exit mach number M_e is 0.170 as computed, and the outlet temperature is obtained by noting that the stagnation temperature is constant throughout the adiabatic flow field, regardless of the irreversible shock wave. Then

$$T_e = T_o\left(\frac{T_e}{T_o}\right)$$

where T_e/T_o is evaluated in figure 16.1 (ch. 16) at $k=1.4$ and $M_e=0.170$. Finally

$$T_e=544.2(0.9942)$$
$$=541^\circ \text{ R}$$
$$=81^\circ \text{ F}$$

OBLIQUE SHOCK WAVES

Oblique shock waves are a general form of discontinuity in supersonic flow and, in the limit, they approach the normal shock wave. Oblique shocks are inclined to the flow direction, and they occur when a supersonic flow undergoes a change in direction requiring a compression.

Changes in Properties

A relation between pressure and density is obtained by combining the momentum and energy equations for the control volume with the velocity and geometrical considerations identified in figure 17.9. (The original equation (6.41a) from ch. 6 has been slightly modified.)

$$\frac{P_2}{P_1}=\frac{\left(\frac{k+1}{k-1}\right)\left(\frac{\gamma_2}{\gamma_1}\right)-1}{\frac{k+1}{k-1}-\frac{\gamma_2}{\gamma_1}} \qquad [6.41a]$$

Equation (6.41a) solved for density

$$\frac{\gamma_2}{\gamma_1}=\frac{\left(\frac{k+1}{k-1}\right)\left(\frac{P_2}{P_1}\right)+1}{\frac{k+1}{k-1}+\frac{P_2}{P_1}} \qquad [6.41b]$$

(The original equation (6.41b) from ch. 6 has been slightly modified.)

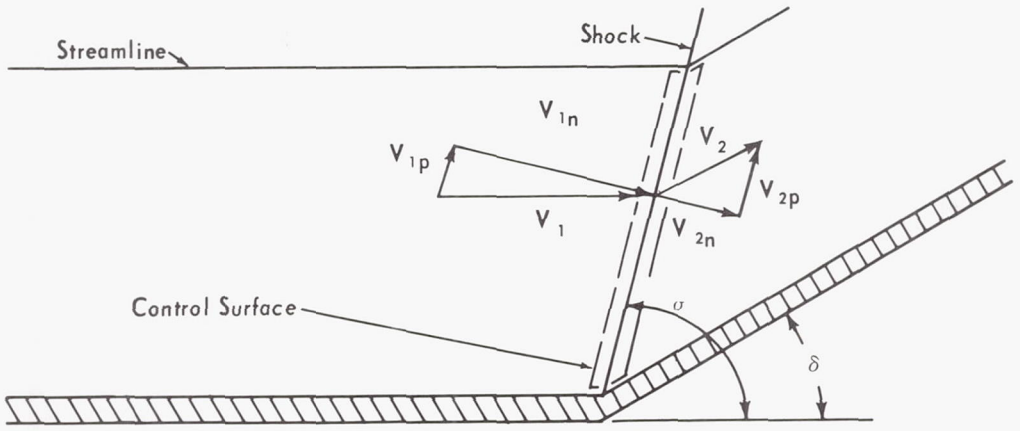


Figure 17.9. Schematic of oblique shock.

The velocity ratio across the shock can be expressed in terms of the two angles

$$\frac{V_2}{V_1}=\frac{\cos\sigma}{\cos(\sigma-\delta)} \qquad [6.42]$$

Combining this with the continuity equation yields a new expression for density ratio across the shock

$$\frac{\gamma_2}{\gamma_1}=\frac{\tan\sigma}{\tan(\sigma-\delta)} \qquad [6.44]$$

(The original equation (6.44) from ch. 6 has been slightly modified.)

Further combination of relationships for energy, momentum, continuity, and perfect-gas behavior yields two additional relationships for pressure change

$$\frac{P_2}{P_1}=1+k\left(1-\frac{\gamma_1}{\gamma_2}\right)M_1^2\sin^2\sigma \qquad [6.45]$$

and

$$\frac{P_1}{P_2}=1+k\left(1-\frac{\gamma_2}{\gamma_1}\right)M_2^2\sin^2(\sigma-\delta) \qquad [6.46]$$

Equations (6.41), (6.44), (6.45), and (6.46) have been solved simultaneously to produce the direct relations between the various parameters, and these relations are plotted as figures 17.10 through 17.13 to aid in problem solving. More detailed and exact graphs can be found in the NACA Technical Report 1135 (Ames, 1953).

The following temperature-change relationship is provided for completeness, as obtained from considerations of the change in kinetic energy to thermal energy.

$$\frac{T_2}{T_1}=1+\left(\frac{k-1}{2}\right)M_1^2\left[1-\frac{\cos^2\sigma}{\cos^2(\sigma-\delta)}\right] \qquad [6.47]$$

Analogy With Normal Shocks

It is often convenient to transform the coordinate system for oblique shocks so that the normal shock functions can be applied. This can be done by making the following analogies.

Normal Shocks	*Oblique Shocks*
M_x	$M_1\sin\sigma$
M_y	$M_2\sin(\sigma-\delta)$
P_y/P_x	P_2/P_1
P_{oy}/P_{ox}	P_{02}/P_{01}
T_y/T_x	T_2/T_1
γ_y/γ_x	γ_2/γ_1

Conical Shocks

The oblique-shock theory developed to this point corresponds with a two-dimensional surface such as a flat plate. A conical section will cause oblique shocks that are conical discontinuities rather than plane. For this case, the stream lines are not straight and parallel to the surface, as with the flat plate, but actually curve to approach asymptotically the direction of the conical surface. The initial flow deflection across the shock wave is the same as that described for the two-dimensional case, with the observed shock angle established for a cone. A more detailed description of oblique-shock theory for flat plates, wedges, and cones is beyond the scope of this book.

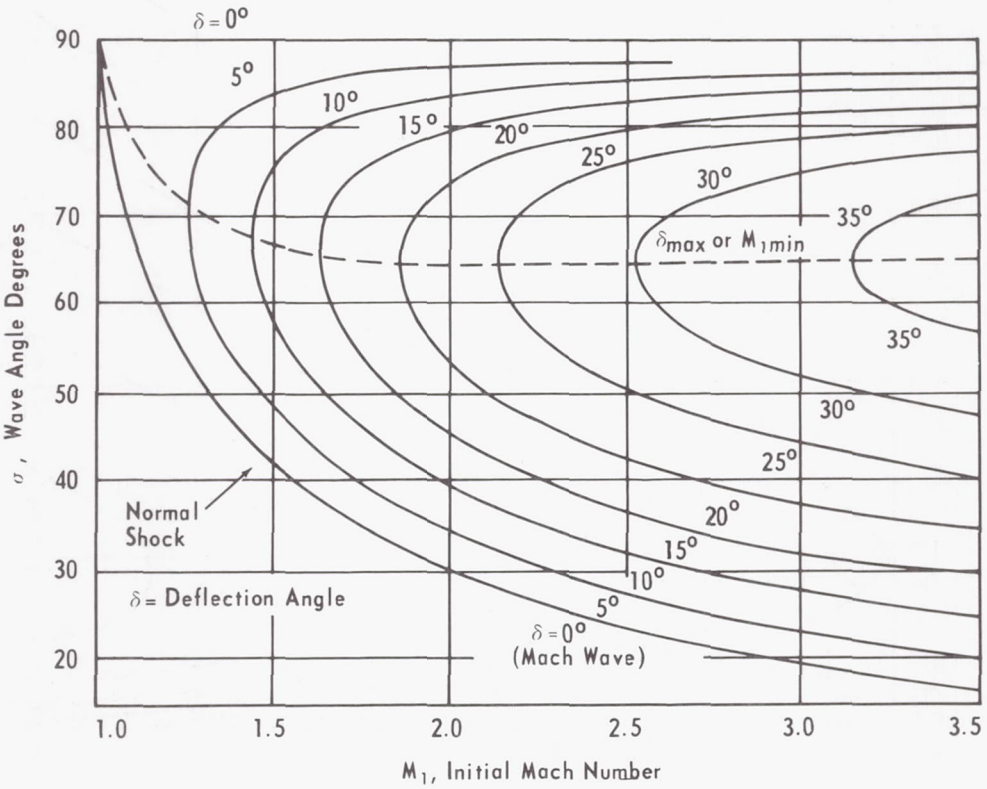


Figure 17.10. Wave-angle variances with initial mach number.

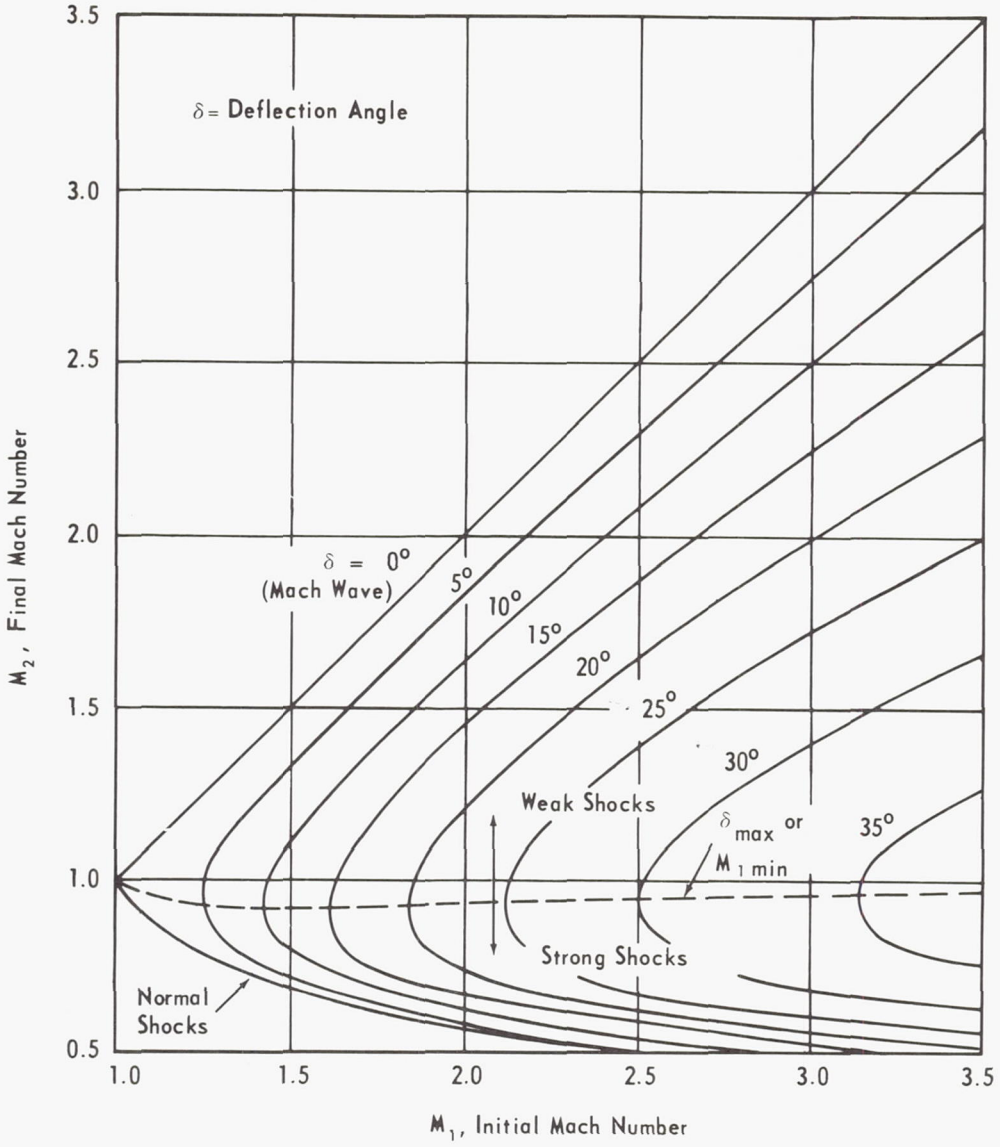


Figure 17.11. Final mach-number variances with initial mach number.

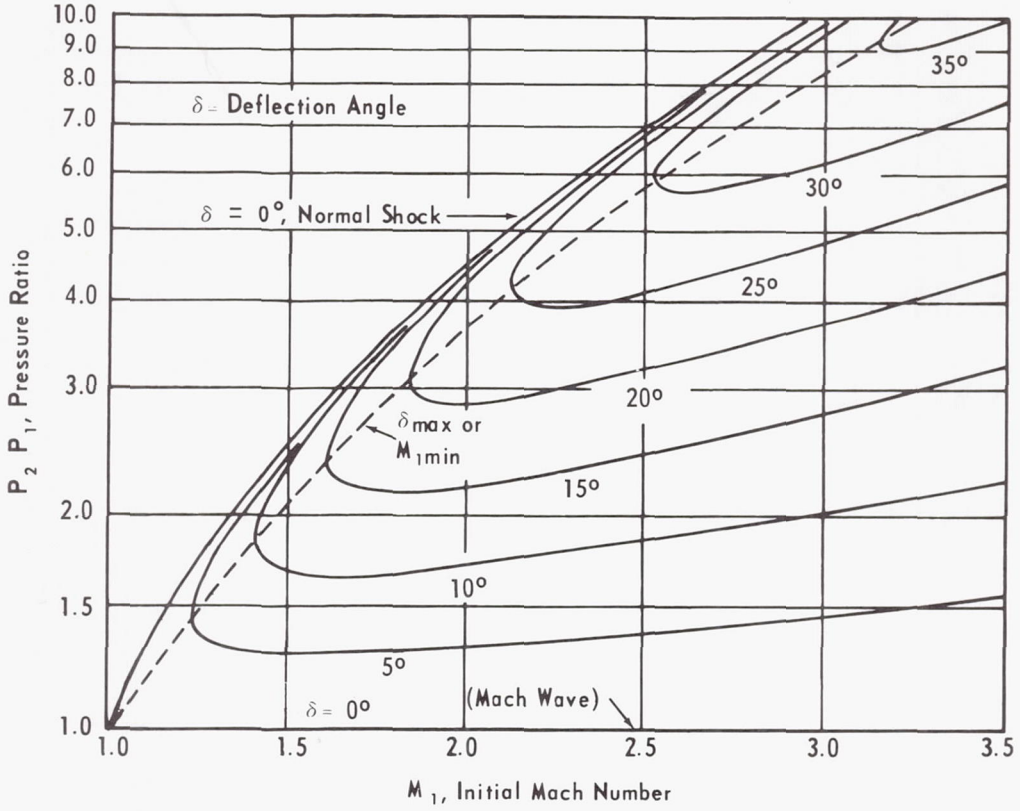


Figure 17.12. Pressure ratio variances with initial mach number.

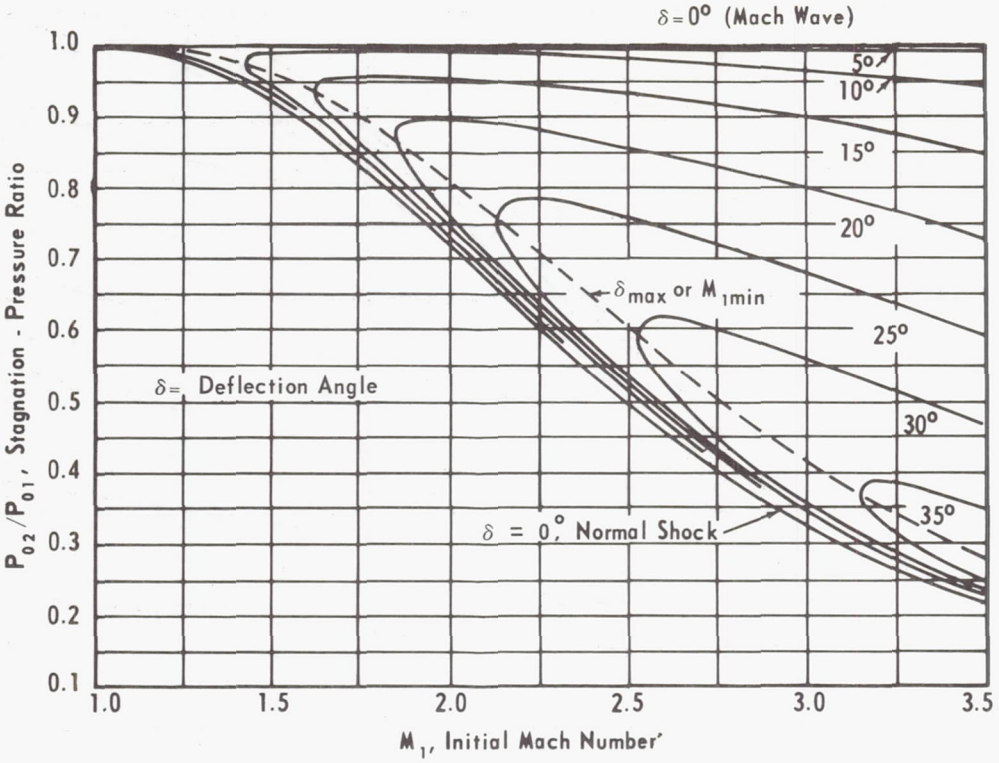


Figure 17.13. Stagnation pressure ratio variances with initial mach number.

CHAPTER 18

METHODS OF FLOW MEASUREMENT

The equations that predict the change in fluid properties caused by a restriction placed in the flow path are derived from the first law of thermodynamics when the flowing fluid is compressible, and Bernoulli's equation when the fluid is incompressible. These equations give the theoretical rate of flow, which must then be modified by flow coefficients to obtain the actual rate.

The value of the flow coefficient used with either of the above-mentioned equations depends, in part at least, on the geometry of the particular device being used for flow-measurement purposes. It will be found that the coefficient used in conjunction with the venturi tube is very near unity, which indicates that the theory employed to calculate venturi flow rate is extremely accurate. The flow coefficient used with the flow nozzle is also near unity, but not so near as the coefficient used with the venturi tube. The coefficient used with the orifice deviates considerably from unity, indicating that simple theory alone does not adequately describe the flow through an orifice.

THE HYDRAULIC EQUATION

The flow of an incompressible fluid through a constant-area passage into which a venturi tube, a nozzle, or an orifice has been inserted can be calculated by observation of Bernoulli's equation. The assumptions necessary are a steady, fully developed flow and no sensible heat transfer.

Writing Bernoulli's equation between an upstream section (1) and the throat section (2) yields

$$P_1 - P_2 = \frac{\gamma_2 V_2^2 - \gamma_1 V_1^2}{2g_c}$$

Since the flow is incompressible and steady, the preceding equation is rewritten, using the continuity equation

$$P_1 - P_2 = \frac{\gamma}{2g_c}\left[V_2^2 - \left(\frac{A_2}{A_1}\right)^2 V_2^2\right]$$

or, solving for the throat velocity,

$$V_2 = \left\{\frac{(P_1 - P_2)2g_c}{\left[1 - \left(\frac{A_2}{A_1}\right)^2\right]\gamma}\right\}^{1/2} \qquad [7.2]$$

Defining

$$\beta = \frac{D_2}{D_1} \qquad \beta^2 = \frac{A_2}{A_1}$$

Equation (7.2) becomes

$$V_2 = \left(\frac{2g_c}{\gamma}\right)^{1/2} \left(\frac{P_1 - P_2}{1-\beta^4}\right)^{1/2}$$

The weight flow may now be expressed in terms of the throat conditions as

$$w = A_2 \left[\frac{2g_c\gamma(P_1 - P_2)}{1-\beta^4}\right]^{1/2} \qquad [7.3]$$

Equation (7.3), known as the hydraulic equation, expresses the theoretical mass flow rate in terms of the three measurable variables: pressure, area, and mass density.

THE COMPRESSIBLE FLOW EQUATION

The equation for theoretical rate of flow of a compressible fluid through a venturi tube, a nozzle, or an orifice is found in a manner similar to that for incompressible flow. The assumptions necessary for this analysis are a perfect gas and steady, reversible adiabatic flow.

Writing the first law of thermodynamics between an upstream section (1) and the throat section (2) yields

$$\frac{V_2^2 - V_1^2}{2g_c J} = h_1 - h_2$$

Since the gas is perfect and the process is isentropic (reversible adiabatic), the foregoing relation may be written as

$$\frac{V_2^2 - V_1^2}{2g_c} = \frac{k}{(k-1)} (P_1 v_1 - P_2 v_2) \qquad [7.5]$$

For a steady flow, the continuity equation yields

$$V_1 = \left(\frac{\gamma_2 A_2}{\gamma_1 A_1}\right) V_2$$

Substituting for V_1 in equation (7.5) and solving for the throat velocity yields

$$V_2^2 = \frac{\left(\frac{k}{k-1}\right) 2g_c(P_1 v_1 - P_2 v_2)}{1 - \beta^4 \left(\frac{\gamma_2}{\gamma_1}\right)^2 \beta^4} \qquad [7.6]$$

where

$$\beta^4 = \left(\frac{A_2}{A_1}\right)^2$$

For an isentropic process

$$\frac{\gamma_2}{\gamma_1} = \left(\frac{P_2}{P_1}\right)^{1/k} = r^{1/k}$$

and it can be shown that

$$P_1 v_1 r^{(k-1/k)} = P_2 v_2 \qquad [7.8]$$

Substituting these two relations into equation (7.6),

$$V_2 = \left[\frac{\left(\frac{k}{k-1}\right) 2g_c (P_1 v_1)(1 - r^{(k-1)/k})}{1 - r^{2/k}\beta^4} \right]^{1/2} \qquad [7.9]$$

and the mass rate expression in terms of the throat conditions becomes

$$w = \gamma_2 A_2 \left[\frac{\left(\frac{k}{k-1}\right) 2g_c (P_1 v_1)(1 - r^{(k-1)/k})}{1 - r^{2/k}\beta^4} \right]^{1/2} \qquad [7.10]$$

Now, by employing the perfect-gas law and the isentropic property relation $Pv^k = \text{constant}$, the mass flow rate may be written as

$$w = A_2 \left[\frac{2g_c \gamma_1 (P_1 - P_2)}{1 - \beta^4} \right]^{1/2} \left[r^{2/k} \left(\frac{k}{k-1}\right) \left(\frac{1 - r^{(k-1)/k}}{1 - r}\right) \left(\frac{1 - \beta^4}{1 - r^{2/k}\beta^4}\right) \right]^{1/2} \qquad [7.13]$$

Note that equation (7.13) is simply the hydraulic equation modified by the factor Y_a where

$$Y_a = \left[r^{2/k} \left(\frac{k}{k-1}\right) \left(\frac{1 - r^{(k-1)/k}}{1 - r}\right) \left(\frac{1 - \beta^4}{1 - r^{2/k}\beta^4}\right) \right]^{1/2} \qquad [7.14]$$

The value of Y_a depends on the pressure ratio r, the diameter ratio β, and the specific heat ratio k. If the specific heat ratio is constant, it is possible to plot a family of curves to represent Y_a over the pressure ratio range from $r = 1$ to $r =$ pressure ratio at which sonic velocity occurs at the throat. Such a curve for k values between 1.0 and 1.8 is shown in figure 18.1. It is important to note at this point that the value Y_a just discussed applies to the measurements of a perfect gas using either the venturi tube or the flow nozzle. It does not apply to the thin-plate orifice. The value Y_1 used in the equation to calculate flow through a thin-plate orifice is empirically determined and cannot be found by theoretical considerations.

CORRECTIVE FLOW COEFFICIENTS

The theoretical weight rate of flow of a fluid through a venturi tube, nozzle, or an orifice, as given by equations (7.3) and (7.13), must be modified by an experimentally determined discharge coefficient, C_d, where

$$C_d = \frac{\text{actual weight rate of flow}}{\text{theoretical weight rate of flow}}$$

Applying this coefficient to equation (7.3) for an incompressible fluid, it follows that

$$w = C_d A_2 \left[\frac{2g_c \gamma (P_1 - P_2)}{1 - \beta^4} \right]^{1/2} \qquad [7.15]$$

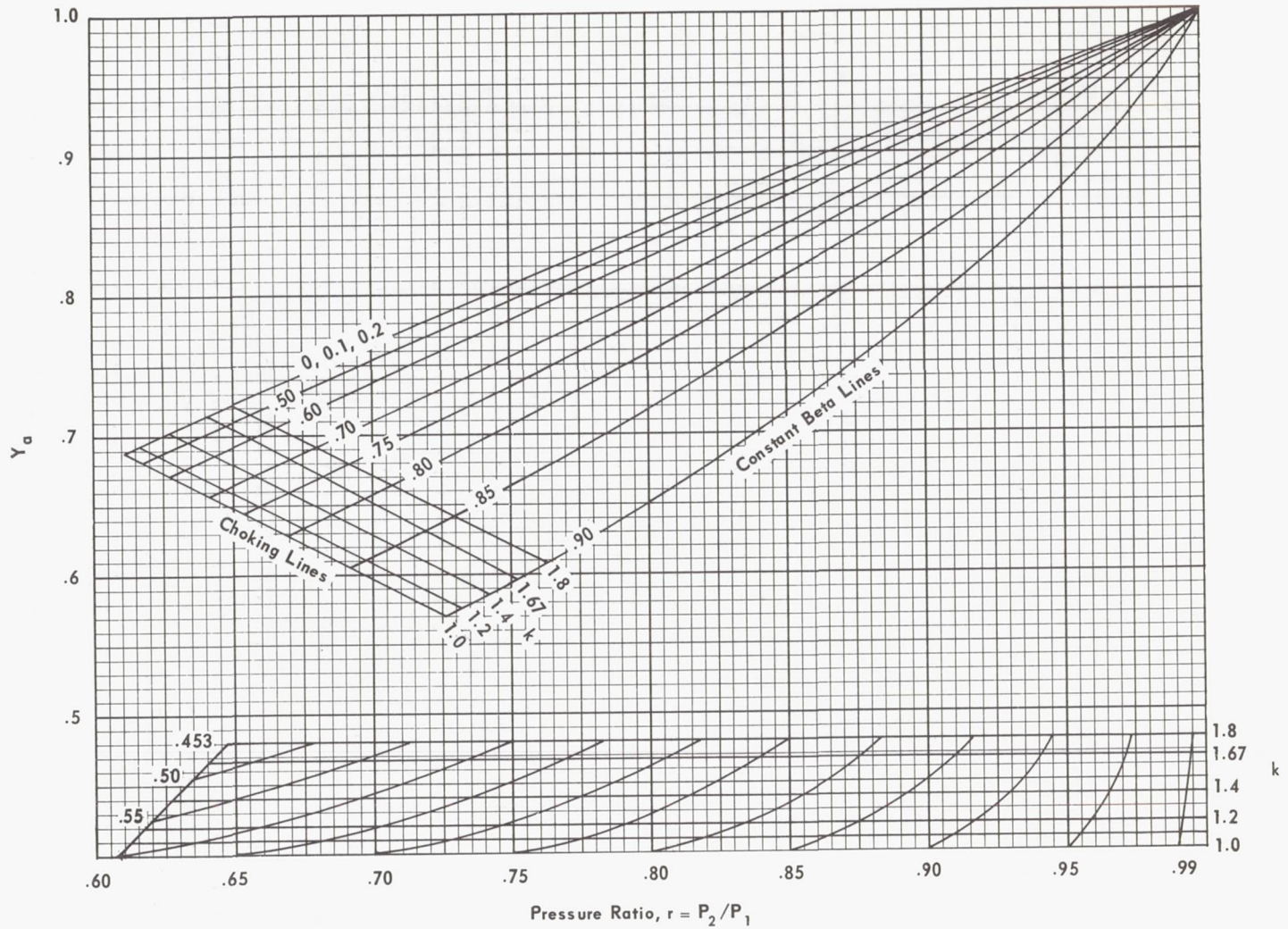


Figure 18.1. Expansion factors for nozzles and venturi tubes.

or

$$w = K_c A_2 \left[2 g_c \gamma (P_1 - P_2)\right]^{1/2} \qquad [7.15a]^*$$

where

$$K_c = \frac{C_d}{\sqrt{1-\beta^4}}$$

In terms of diameter in inches and pressure in psia, equation (7.15*a*) becomes

$$w = 0.525\, K_c D_2^2 \sqrt{\gamma (p_1 - p_2)} \qquad [7.15b]^*$$

Also, for flow in cfm

$$q = 31.5\, K_c D_2^2 \sqrt{\frac{p_1 - p_2}{\gamma}} \qquad [7.15c]^*$$

The quantity K_c is termed the flow coefficient, and $1/\sqrt{1-\beta^4}$ is termed the "velocity of approach factor."

The corrective flow coefficients just defined are illustrated graphically in figures 18.2 through 18.7. For the venturi tube, the discharge coefficient C_d is plotted versus Reynolds number R_e in figure 18.2. For the nozzle, C_d is plotted versus R_e in figure 18.3, and two plots of C_d-versus-β ratio are shown in figures 18.4 and 18.5. Figures 18.6 and 18.7 are plots of K_c versus R_e for the square-edged orifice.

The orifice flow coefficients K_c, plotted in figure 18.6, are taken from the ASME (1959) data for flange taps (taps are 1 inch upstream and downstream of the upstream face of the orifice plate) and 2-inch pipe (2.067-inch I.D.). These data agree within 1 percent (of the

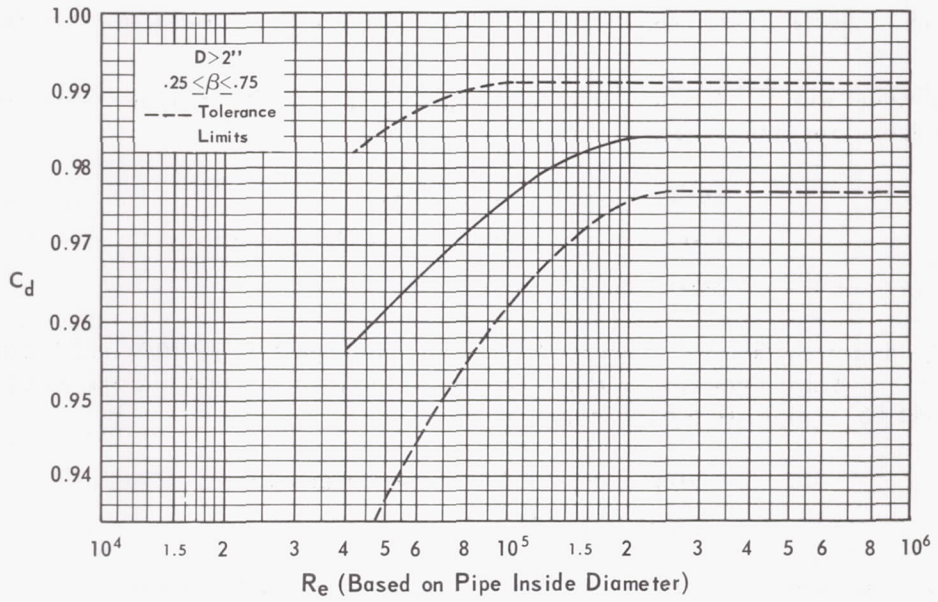


Figure 18.2. Discharge coefficients for Herschel-type venturi tube.

*This equation is a variation of equation (7.15) and does not appear in chapter 7.

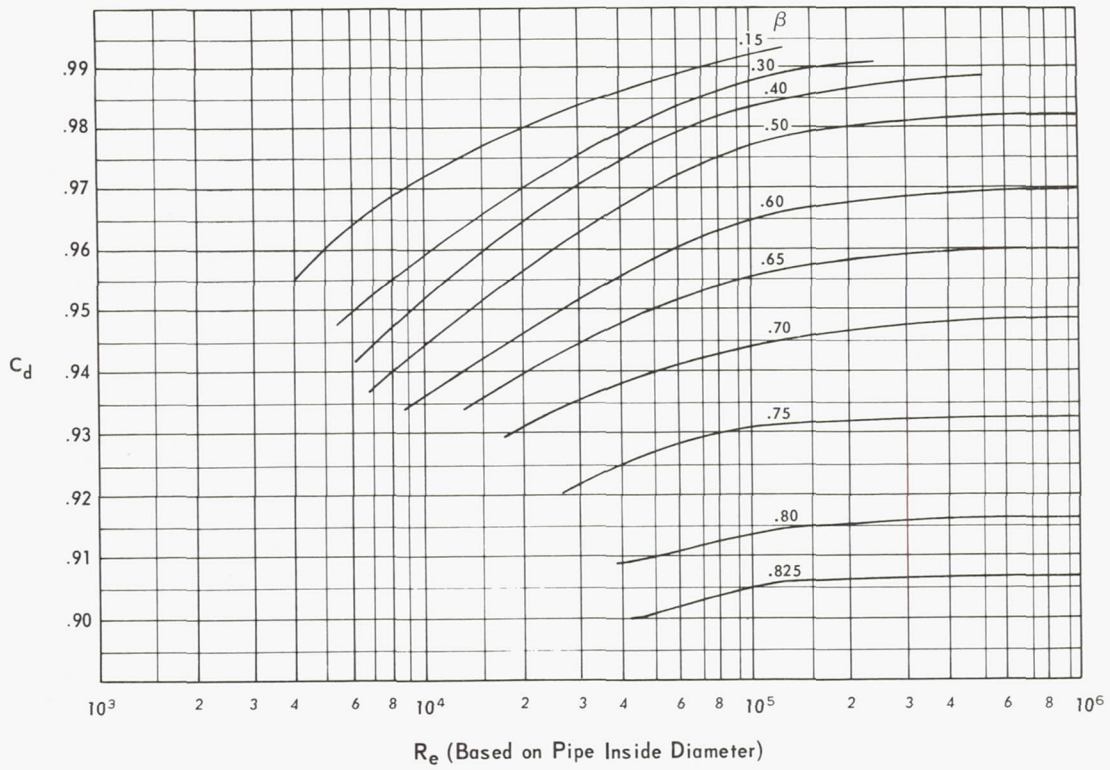


Figure 18.3. Discharge coefficients for flow nozzles. [*Courtesy of the American Society of Mechanical Engineers.*]

plotted value) with the data for $1D$ and $\frac{1}{2}D$ taps, vena contracta taps, and corner taps, as well as flange taps in the ranges:

$$1.610 \leq \text{pipe I.D.} \leq 4.026 \text{ inches}$$
$$50\,000 \leq R_e \leq 10^6 \quad \text{(based on pipe I.D.)}$$
$$0.20 \leq \beta \leq 0.60$$

The orifice coefficients of figure 18.7 are for pipe taps ($2D$ and $10D$) and 2-inch pipes (2.067 I.D.). These data agree within 1 percent (of the plotted value) with the data for pipe taps and $2.067 \leq$ pipe I.D. ≤ 6.065 inches in the ranges:

$$50\,000 \leq R_e \leq 10^6 \quad \text{(based on pipe I.D.)}$$
$$0.15 \leq \beta \leq 0.70$$

The data agree within 0.5 percent for $2.067 \leq$ pipe I.D. ≤ 4.026 in the ranges:

$$50\,000 \leq R_e \leq 10^6 \quad \text{(based on pipe I.D.)}$$
$$0.15 \leq \beta \leq 0.60$$

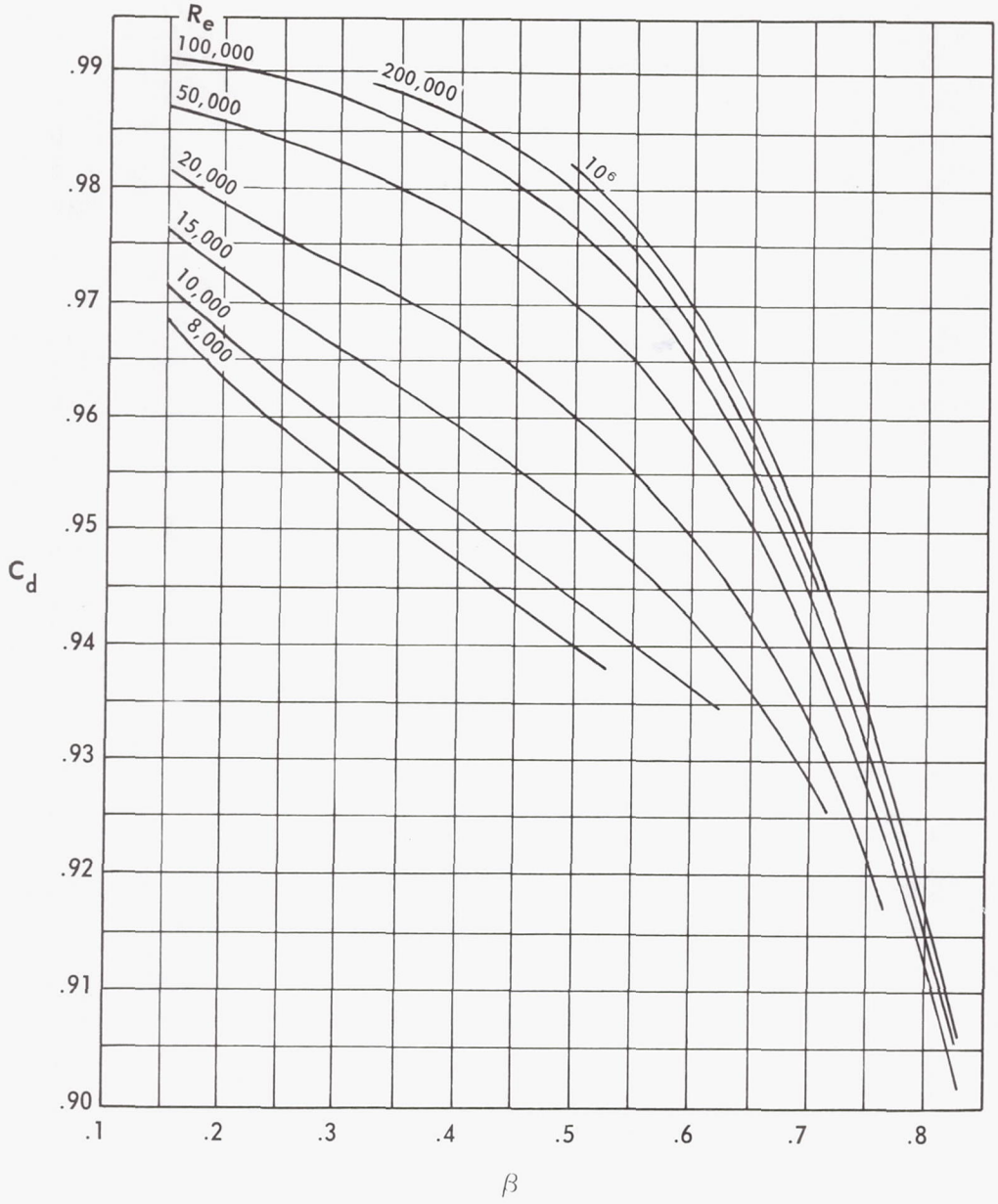


Figure 18.4. Discharge coefficients for flow nozzles. [*Courtesy of the American Society of Mechanical Engineers.*]

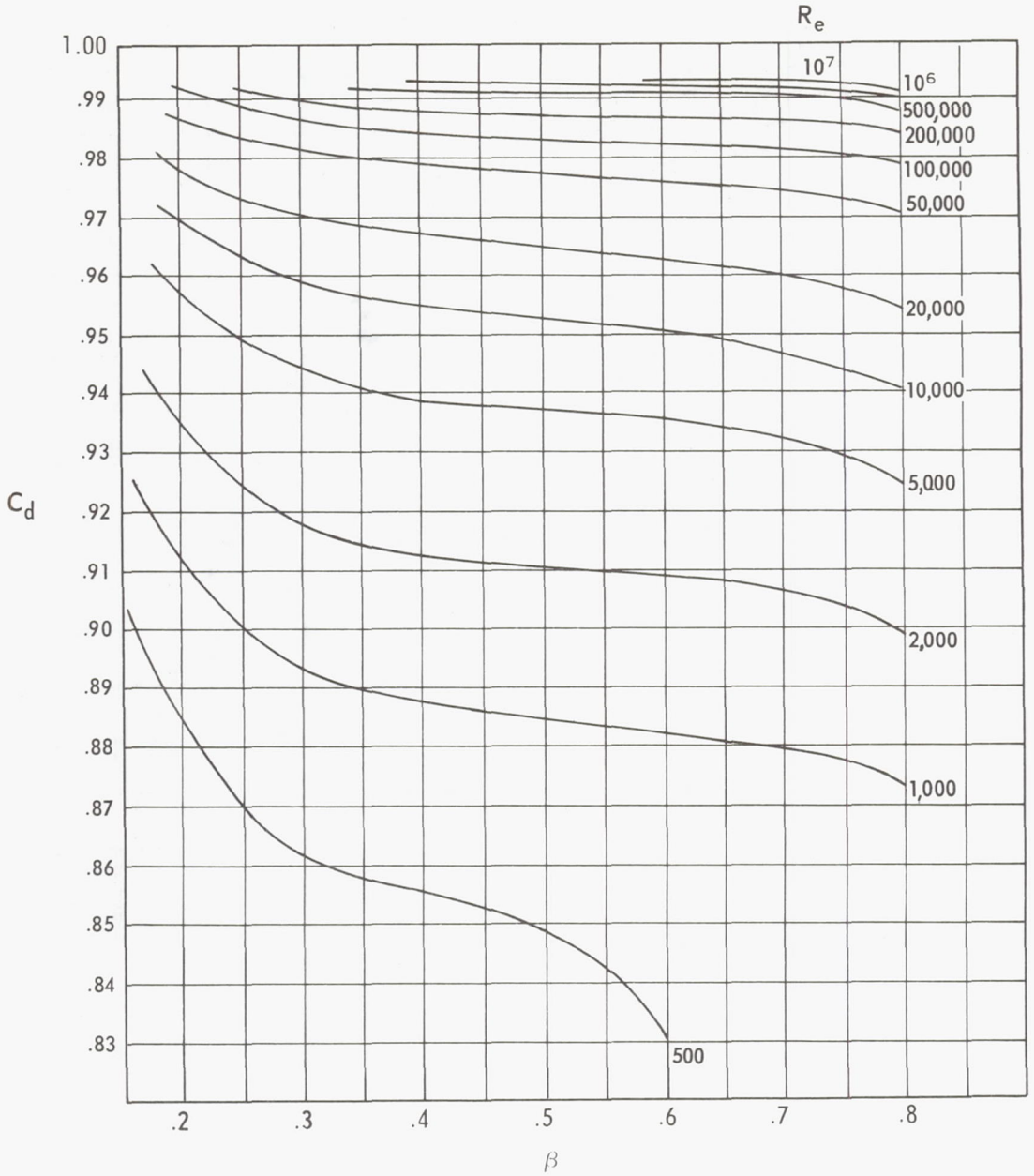


Figure 18.5. Discharge coefficients for ASME long-radius flow nozzles. [*Courtesy of the Society of Mechanical Engineers.*]

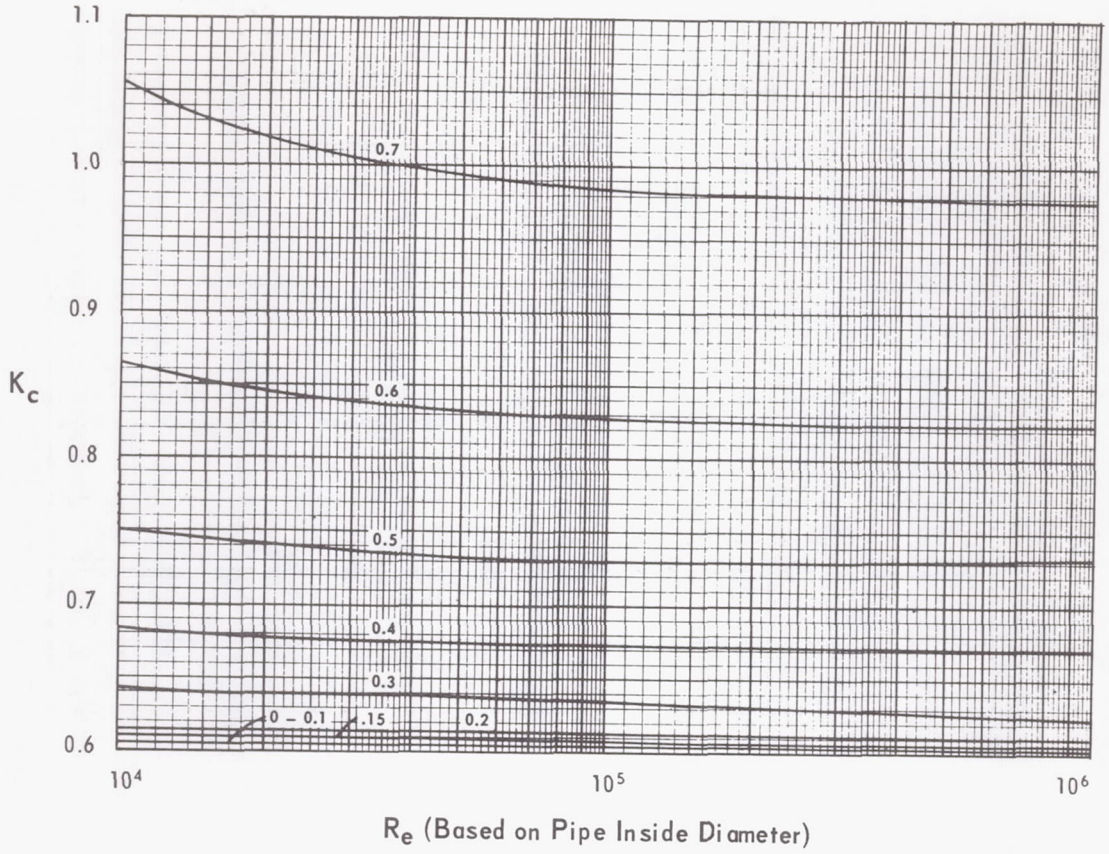


Figure 18.6. Flow factor for thin-plate orifices. [*Courtesy of the American Society of Mechanical Engineers.*]

Flange taps

Accuracy: ±1% when: $1.5 \leq$ pipe size ≤ 6
$50{,}000 \leq R_e \leq 10^6$
$0.15 \leq \beta \leq 0.70$

1D, 1/2D taps; vena contracta taps; and corner taps

Accuracy: ±1% when: $1.5 \leq$ pipe size ≤ 4
$50{,}000 \leq R_e \leq 10^6$
$0.20 \leq \beta \leq 0.60$

In using these charts for orifice coefficients, the tolerances tabulated by the ASME (1959) for the various types of pressure taps, ranges of R_e, β, and so forth, must be added to the previously quoted accuracies.

To meter compressible flows, all that is required is the addition of the expansion factor Y into equation (7.15). For a compressible fluid flowing through a venturi tube or a nozzle, the weight rate expression becomes

$$w = C_d Y_a A_2 \left[\frac{2g_c\gamma_1(P_1 - P_2)}{1-\beta^4}\right]^{1/2} \qquad [7.16]$$

where Y_a is given by figure 18.1. For the orifice

$$w = K_c A_2 Y_1 \left[2g_c\gamma_1(P_1 - P_2)\right]^{1/2} \qquad [7.16a]^*$$

*This equation is a variation of equation (7.16) and does not appear in chapter 7.

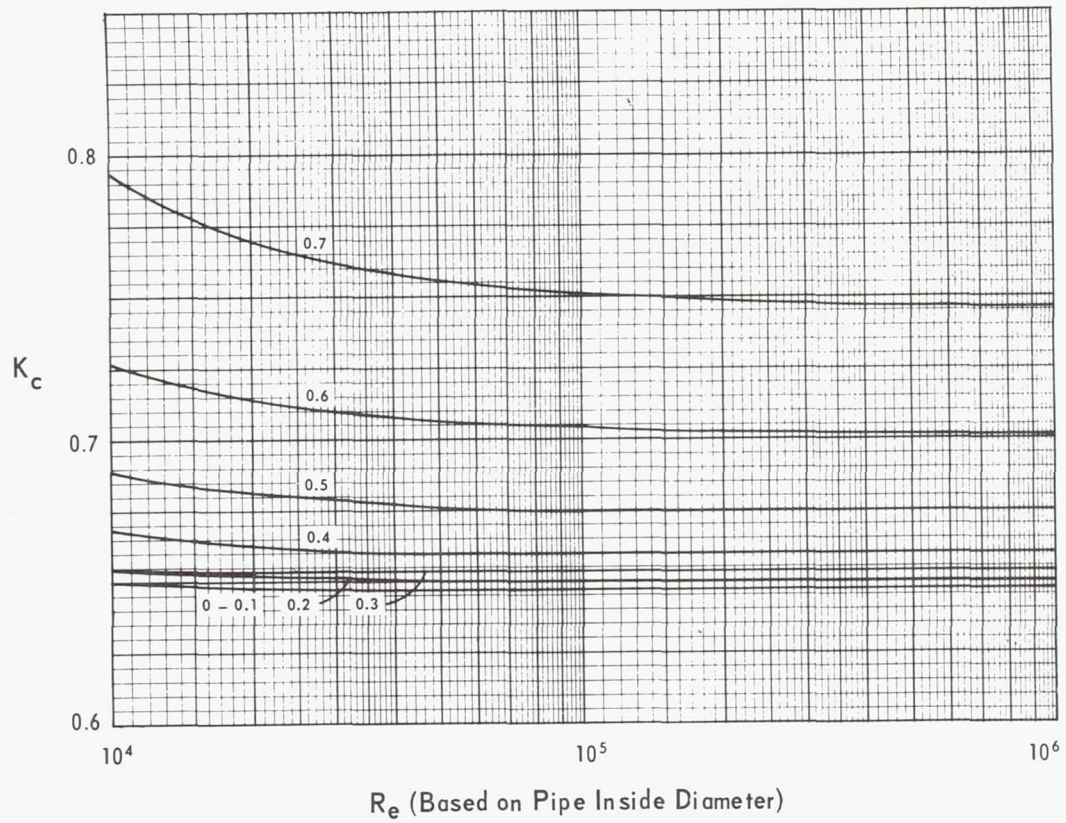


Figure 18.7. Flow factor for thin-plate orifices (pipe taps). [*Courtesy of the American Society of Mechanical Engineers.*]

Accuracy: ±1% when: $2 \leq$ pipe size ≤ 6; $50{,}000 \leq R_e \leq 10^6$; $0.15 \leq \beta \leq 0.70$

Accuracy: ±0.5% when: $2 \leq$ pipe size ≤ 4; $50{,}000 \leq R_e \leq 10^6$; $0.15 \leq \beta \leq 0.6$

where Y_1 is given by figures 18.8 through 18.11. Additional data can be obtained on these factors from the ASME (1959).

Equation (7.16) can be written in more convenient units of pipe I.D. (inches) and pressure (psia) as

$$w = 0.525\, K_c Y D_2^2 \sqrt{\gamma_1 (p_1 - p_2)} \qquad [7.16b]^*$$

or for flow in cfm

$$q = 31.5\, K_c Y D_2^2 \sqrt{\frac{p_1 - p_2}{\gamma_1}} \qquad [7.16c]^*$$

or in terms of scfm

$$\text{scfm} = 7.74\, R K_c Y D_2^2 \sqrt{\gamma_1 (p_1 - p_2)} \qquad [7.16d]^*$$

*This equation is a variation of equation (7.16) and does not appear in chapter 8.

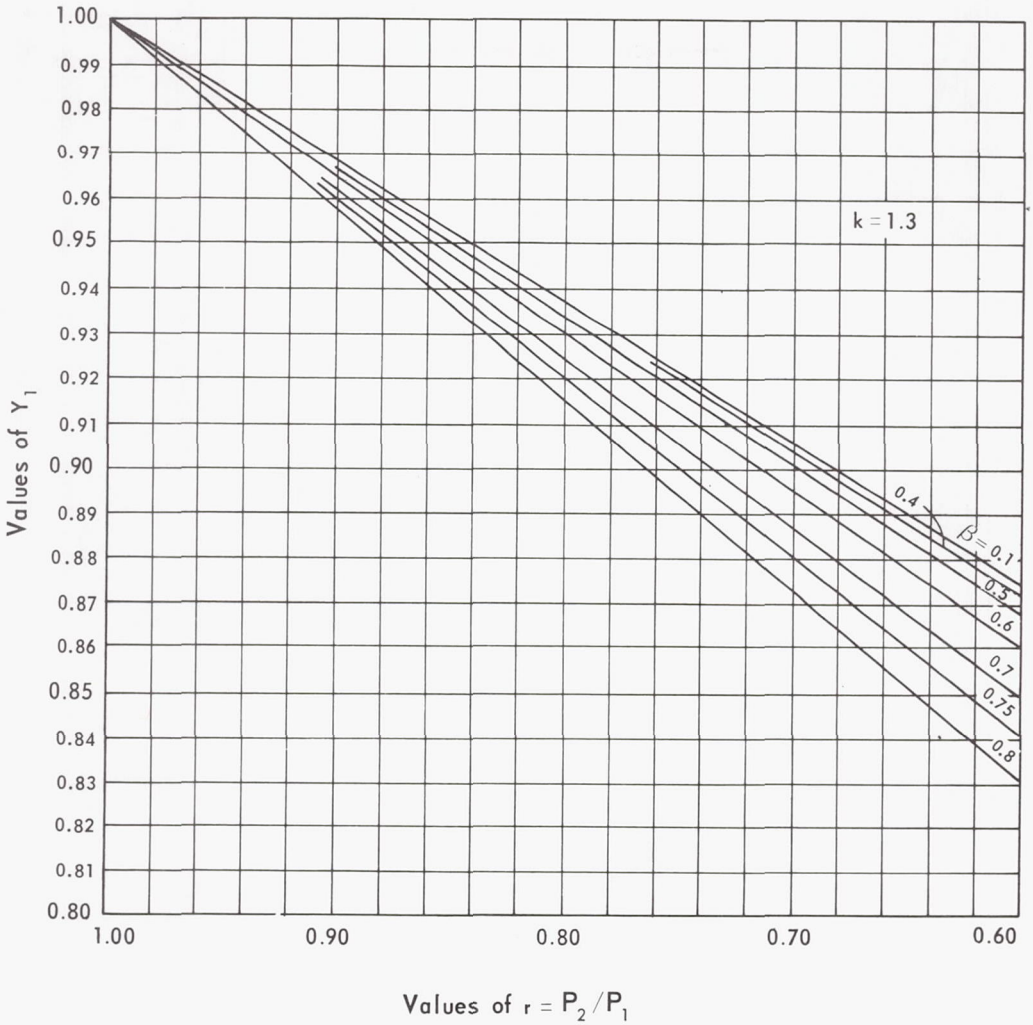


Figure 18.8. Expansion factor for square-edged orifice, $k = 1.3$. [*Courtesy of the American Society of Mechanical Engineers.*]

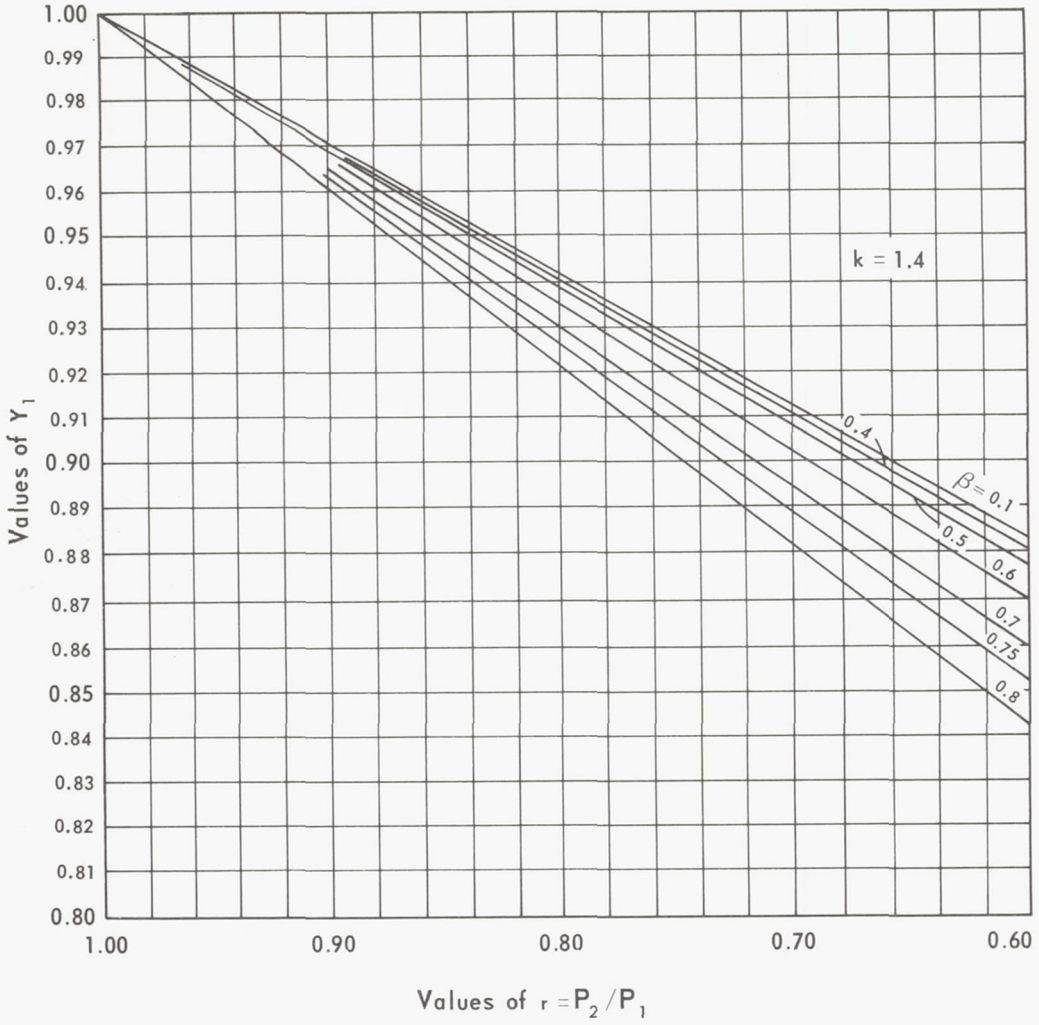


Figure 18.9. Expansion factor for square-edged orifice, $k = 1.4$. [*Courtesy of the American Society of Mechanical Engineers.*]

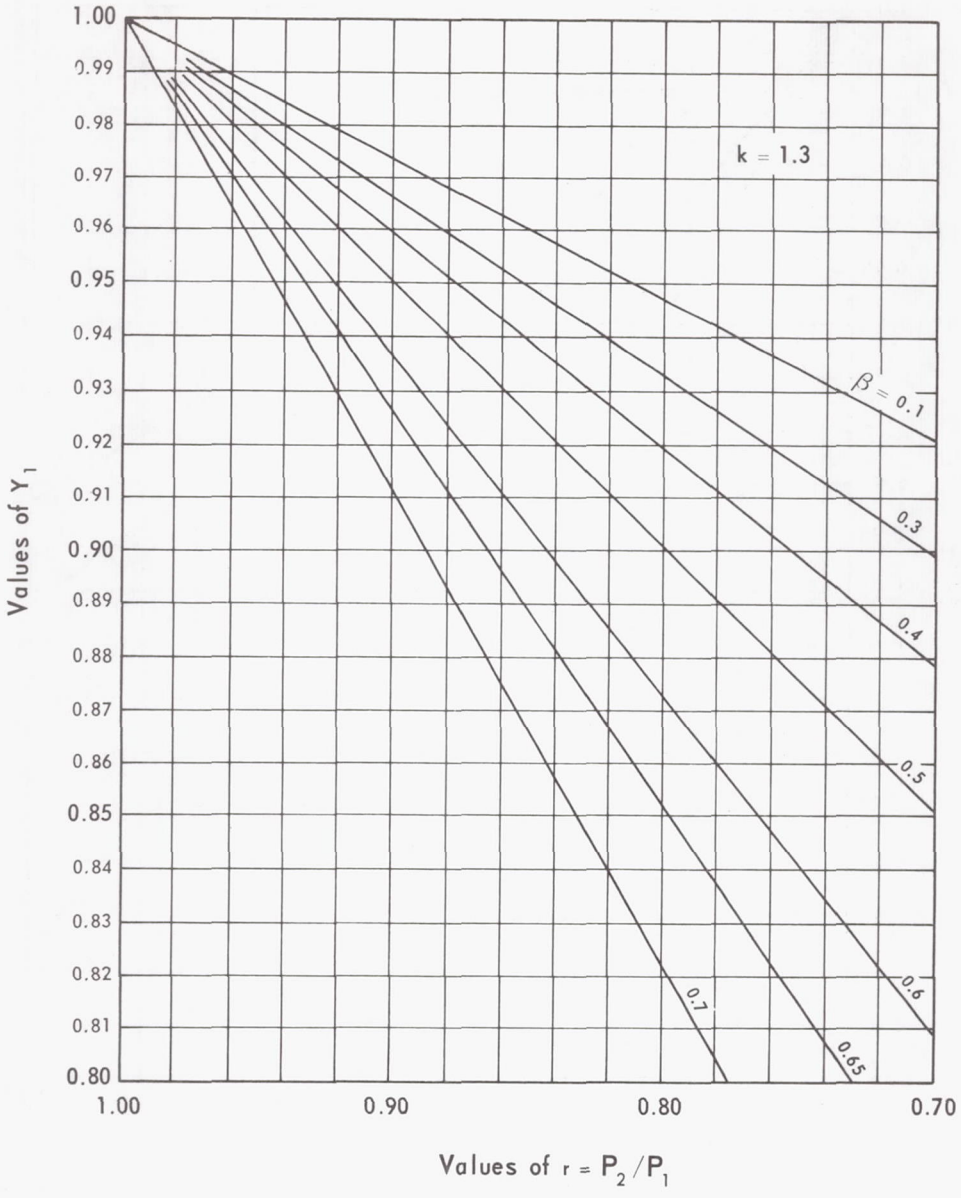


Figure 18.10. Expansion factor for square-edged orifice, $k = 1.3$ (pipe taps). [*Courtesy of the American Society of Mechanical Engineers.*]

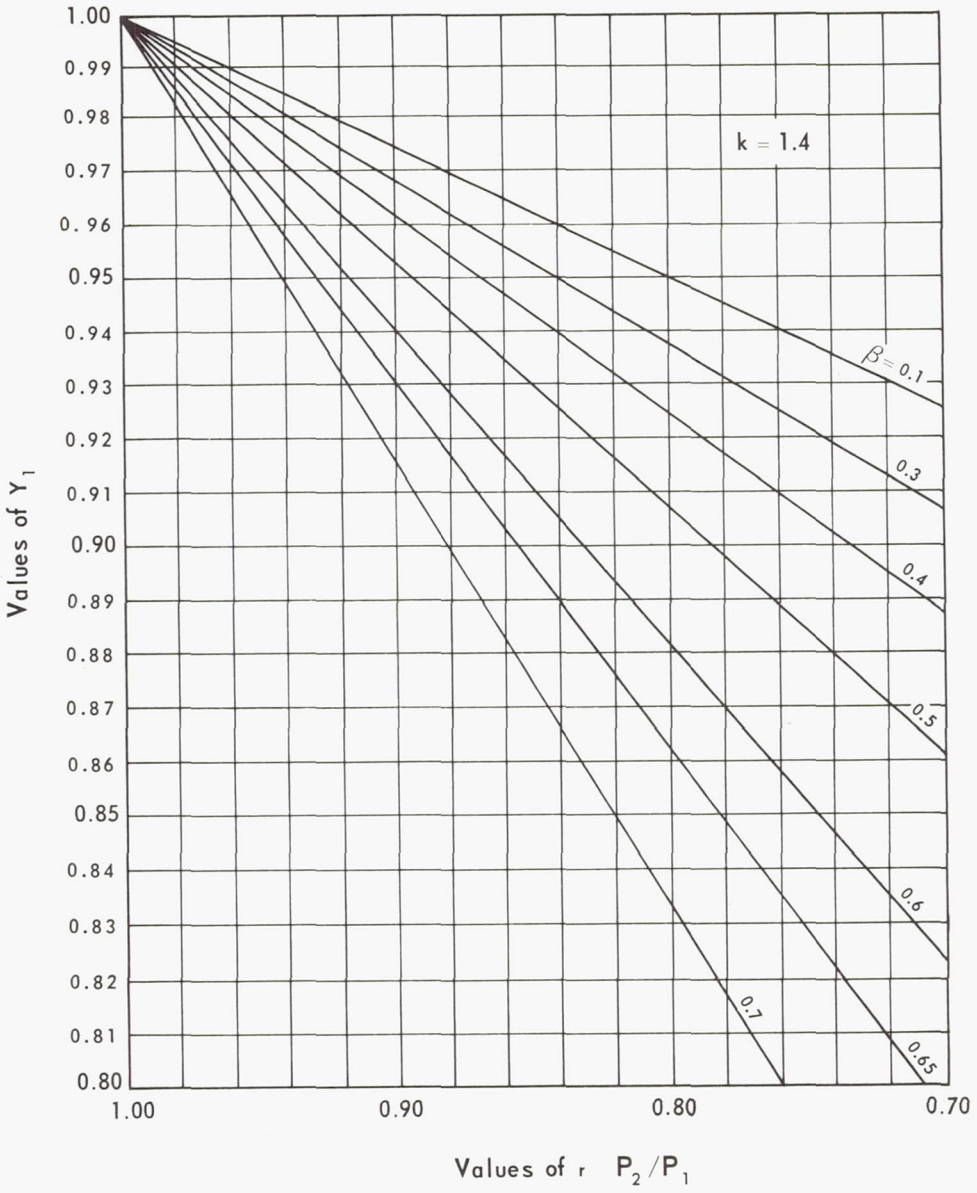


Figure 18.11. Expansion factor for square-edged orifice, $k = 1.4$ (pipe taps). [*Courtesy of the American Society of Mechanical Engineers.*]

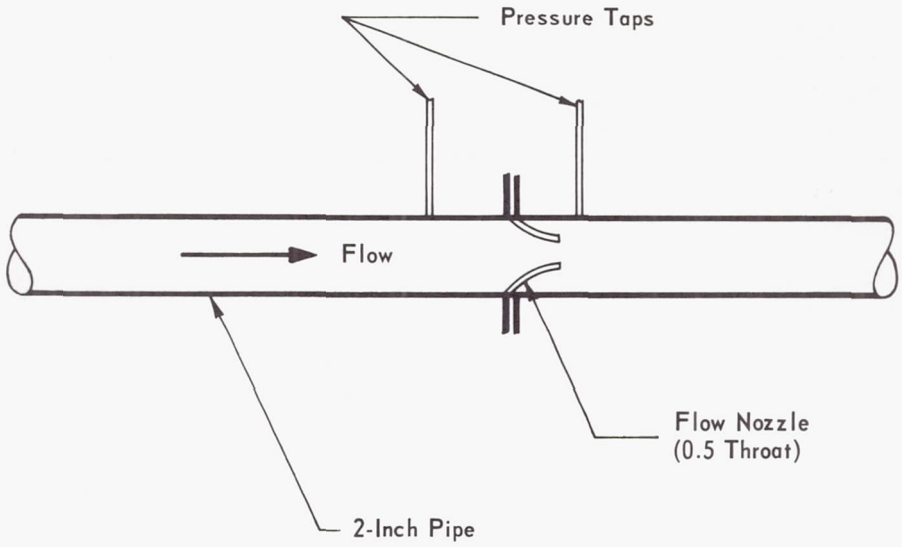


Figure 18.12. Nozzle flow.

EXAMPLE PROBLEM 18.1

Water at 60° F flows through a 2-inch-I.D. pipeline and through a nozzle with a 1/2-inch-diameter throat as shown in figure 18.12. If the pressure drop is 100 psi, measured with $1D$ and $\frac{1}{2}D$ taps, determine the mass flow rate.

SOLUTION

The weight rate of flow is calculated from equation (7.15*b*)

$$w = 0.525 \frac{C_d}{\sqrt{1-\beta^4}} D_2^2 \sqrt{\gamma(p_1 - p_2)}$$

The first step is to calculate C_d by assuming a Reynolds number and entering figure 18.5 at a β ratio of 0.25 and reading the coefficient C_d. Assume $R_e = 2(10^5)$; and, from figure 18.5, read $C_d = 0.992$.

Now, since $\gamma = 62.4$ and $p_1 - p_2 = 100$ psi, the weight flow rate is

$$w = 0.525 \left[\frac{0.992}{\sqrt{1-(0.25)^4}}\right] (0.5)^2 \sqrt{62.4(100)}$$

$$= 10.3 \text{ lbm/sec}$$

For this flow rate, R_e can be evaluated using equation (4.14). Viscosity of water at 60° F is $7.7(10^{-4})$ lbm/ft-sec.

$$R_e = 15.28 \left(\frac{w}{D_1 \mu'}\right)$$

$$= 15.28 \left\{\frac{10.3}{2.0[7.7(10^{-4})]}\right\}$$

$$= 1.02(10^5)$$

Since the value of C_d at the computed value of R_e is practically the same as at the assumed R_e, no iteration of the computation is warranted. When significant variation occurs, the calculation of flow rate should be repeated using a new value of C_d corresponding with the more accurate, computed value of R_e.

Compressible flow is computed in this same manner, except the appropriate Y expansion factor is included in the flow equation.

CHAPTER 19

APPLICATION OF ADIABATIC FRICTIONAL FLOW IN PIPES

GENERAL

The property changes that occur in a compressible fluid while flowing steadily through a constant-area pipeline are dependent on a variety of factors. The most important of these are:

(1) Characteristics of the gaseous fluid
(2) Mach number of the flow (a generalized mass flow parameter)
(3) Fluid friction acting on the pipe wall
(4) Existence of shock waves
(5) Elevational change
(6) Presence of pipe fittings, valves, and other components
(7) Heat transfer through the pipe wall

This chapter includes only the evaluation of the effects of items (1), (2), (3), and (4). The effects of changes in elevation are generally negligible in compressible flow problems as a result of the low gas densities and will be neglected here. When very high densities and great elevational changes occur, the effect on static pressure can be approximated by using an average density to compute the static pressure change. This is then added algebraically to the other losses.

The presence of pipe fittings, valves, and other components is not specifically considered in this chapter, since a complete discussion of the flow characteristics of components is found in chapter 10. However, it is general practice to assign equivalent nondimensional lengths (L/D) of straight pipe to fittings and simple components, based on empirical data, and treat them as extra pipe. This technique is considered acceptable in compressible flow problems only if the pressure loss across the component is a small percentage of the absolute pressure, and if the gas velocities are relatively low (corresponding to mach number of approximately 0.3 or less).

When heat is transferred between the fluid and the pipe wall, straightforward solutions can be obtained for special cases. These nonadiabatic flows are the subject of chapter 9.

The characteristics of the fluid are usually represented simply by the perfect-gas law and the knowledge of the specific heat ratio and molecular weight. This simple description of a real gas is satisfactory for conditions of high temperature and low pressure (relative to the critical values for the particular gas). In the region of low temperature and/or high

pressure, the deviation from the perfect-gas characteristics can be very significant. The deviations are discussed in detail in chapters 2 and 4, and methods of accounting for them in pipe-flow calculations are included in this chapter without further discussion. Otherwise, the analysis of the pipe flow phenomenon in this chapter will be based on the perfect-gas relationships.

The mach number is the general mass flow rate parameter in pipe flow analysis. The mach number also serves to factor into the analysis the molecular weight of the gas and the base levels of temperature and pressure.

When the effects of fluid friction on the pipe wall are considered in the analysis, the frictional pipe-length parameter $f(L/D)$ defines the frictional characteristics of the pipe. The friction factor f depends on the turbulent nature of the flow and also serves to factor into the analysis the effects of fluid viscosity and pipe internal-wall roughness. The friction factor is basically a function of the Reynolds number. The common case of frictional flow in an adiabatic pipe is the primary subject of this chapter.

The compressible flow functions developed in this chapter do not automatically account for choked flow conditions or shock waves. However, the solutions identify the choked conditions, and a discussion of choking and shock waves resulting from friction in constant area pipes is presented in "Choking Because of Friction " (ch. 8).

FANNO-LINE EQUATIONS

The flow of perfect gases through constant-area pipes, with friction and in the absence of heat transfer and elevational changes, is described fundamentally by the Fanno equation.

The combination of the first law total energy equation and the continuity equation yields the Fanno equation in terms of enthalpy and density.

$$h = h_0 - \frac{V^2}{2g_c J} \qquad \text{first law}$$

$$G = \frac{w}{A} = \gamma V = \frac{V}{v} \qquad \text{continuity equation}$$

$$h = h_0 - \frac{G^2 v^2}{2g_c J} \qquad \text{Fanno equation}$$

Figures 19.1 and 19.2 illustrate the general shape of the Fanno line on diagrams for h–v and h–s and are helpful in illustrating the effect of wall friction on fluid properties. Figure 19.2 is possible since, for a pure substance, entropy can be defined by the two properties h and v. When real-gas effects are significant, these plots can be made on the thermodynamic chart of the particular gas.

It was shown in "Normal Shock Waves" (ch. 6) that point A, the point of maximum entropy, represents the point where the mach number is unity. Also, it was shown that the lower portion of the curve (X to A) represents flow at supersonic velocity, and the upper portion (Y to A) represents subsonic velocity. Further, it can be shown that frictional effects are necessary to pass from point to point along the Fanno line to satisfy the momentum equation.

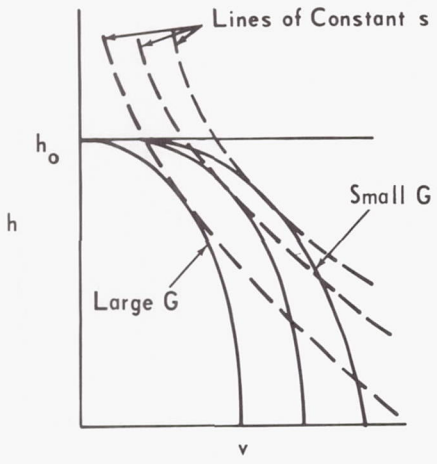


Figure 19.1. Fanno lines on h–v diagram.

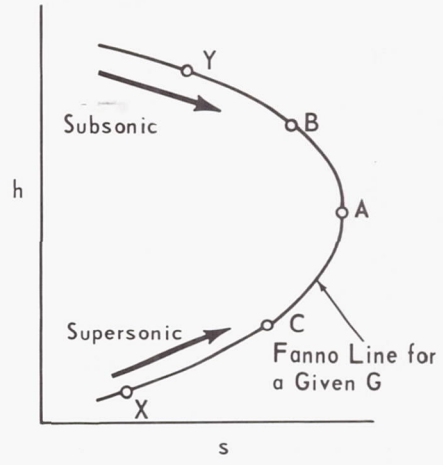


Figure 19.2. Fanno lines on h–s diagram.

The foregoing facts, used in conjunction with the second law of thermodynamics, lead to the following conclusions concerning adiabatic frictional flow through constant-area pipes. The second law requires that, in the absence of heat transfer, the change in entropy must be positive. Therefore, the flow processes described in the Fanno line must never be in the direction of decreasing entropy. Then, with reference to figure 19.2, for subsonic flow, the increasing entropy path occurs with decreasing static enthalpy and an associated decreasing pressure and increasing velocity. For supersonic flow, the increasing static enthalpy path requires an increasing pressure and decreasing velocity. Thus, the effects of friction on velocity, mach number, and pressure are seen to be opposite for subsonic and supersonic flows.

The Fanno-line equations establish quantitatively the changes in all the flow conditions that occur in the pipe as the fluid progresses down the pipe. These equations are derived from the perfect-gas law relationships, the definition of mach number, and the laws of conservation of energy, mass, and momentum. The result is five simultaneous differential equations that relate six differential variables. These include the fluid static properties, fluid velocity, mach number, and the frictional pipe length. These equations are then solved simultaneously and integrated to produce the desired relationships. Proceeding with reference to figure 19.3, the equation of state for a perfect gas in logarithmic form is

$$\ln P = \ln \gamma + \ln R + \ln T$$

which can be written in differential form as

$$\frac{dP}{P} = \frac{d\gamma}{\gamma} + \frac{dT}{T} \qquad [8.1]$$

The definition of mach number, written similarly in logarithmic differential form, is

$$\frac{dM^2}{M^2} = \frac{dV^2}{V^2} - \frac{dT}{T} \qquad [8.2]$$

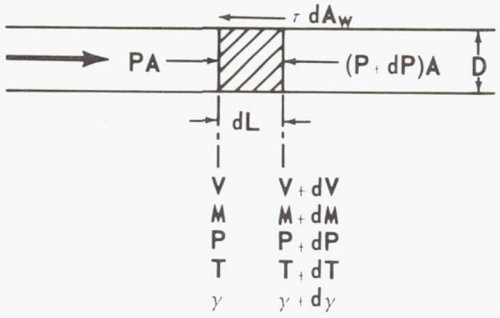


Figure 19.3. Pipe flow element.

For adiabatic flow (h_0 = constant) of a perfect gas and using the definitions of mach number and perfect-gas relationships, the total energy equation can be written as

$$\frac{dT}{T}+\left(\frac{k-1}{2}\right)M^2\left(\frac{dV^2}{V^2}\right)=0 \qquad [8.3]$$

The continuity equation can be written as

$$\frac{dV^2}{2V^2}+\frac{d\gamma}{\gamma}=0 \qquad [8.4]$$

Summing forces on the control volume of figure 19.3 yields the momentum equation for a perfect gas

$$\frac{dP}{P}+\frac{kM^2}{2}\left(\frac{4f_\tau}{D}\right)dL+\frac{kM^2}{2}\left(\frac{dV^2}{V^2}\right)=0 \qquad [8.5]$$

Equations (8.1) through (8.5) comprise the five necessary simultaneous differential equations in the six differential variables: dP/P, $d\gamma/\gamma$, dT/T, dM^2/M^2, dV^2/V^2, and $4f_\tau\, dL/D$. Although these equations are sufficient to yield the simultaneous solutions, it is desirable to include in the analysis the evaluation of the changes in stagnation pressure, impulse function, and entropy. The ratio of static pressure to stagnation pressure (eq. (5.31)) in logarithmic differential form is

$$\frac{dP_0}{P_0}=\frac{dP}{P}+\left[\frac{\frac{kM^2}{2}}{1+\left(\frac{k-1}{2}\right)M^2}\right]\frac{dM^2}{M^2} \qquad [8.6]$$

The definition of impulse function (eq. (5.40)) yields

$$\frac{dF_i}{F_i}=\frac{dP}{P}+\left(\frac{kM^2}{1+kM^2}\right)\frac{dM^2}{M^2} \qquad [8.7]$$

The entropy change is obtained from the first law of thermodynamics, and the perfect-gas relationship is

$$\frac{ds}{c_p}=\frac{dT}{T}-\left(\frac{k-1}{k}\right)\frac{dP}{P} \qquad [8.8]$$

By selecting the mach number as the independent variable, the remaining variables can be defined explicitly in terms of M by simultaneous solution of the eight equations.

The equations are then integrated with respect to mach number to produce the explicit relations between the fluid properties, frictional length, velocity, and impulse function by means of the common parameter, the mach number. It is first desirable to convert the coefficient of friction f_τ, since friction data are usually found in terms of f, such as in the Moody diagram. The conversion between these two coefficients can be derived from their definition, the definition of hydraulic diameter, and by equating the pressure and shear forces of an incompressible element, such as that of figure 19.3. Note that $dP_L = -dP$

$$f = 4f_\tau \qquad [8.17]$$

The lower limits of integration for the Fanno-line equations are selected at a point along the pipe where the mach number is M and where $L = 0$, the zero reference for pipe-length measurement. The upper limit is selected as the point where the mach number is unity and the distance corresponding to $M = 1$ is the maximum pipe length, L_{max}. Integrating and clearing the equation for the frictional length yield

$$\bar{f}\left(\frac{L_{max}}{D}\right) = \frac{1-M^2}{kM^2} + \left(\frac{k+1}{2k}\right) \ln \left\{ \frac{(k+1)M^2}{2\left[1+\left(\frac{k-1}{2}\right)M^2\right]} \right\} \qquad [8.18]$$

where $\bar{f}$ is the mean friction coefficient between 0 and L_{max}, defined by

$$\bar{f} = \frac{1}{L_{max}} \int_0^{L_{max}} f \, dL$$

The friction factor is usually found to vary only slightly over the length of the pipe. Hereafter, the average value will always be assumed, and the bar over the symbol will be omitted for simplicity. The variation should be checked using the Moody diagram of chapter 3. Integrating and clearing the remaining seven equations yield

$$\frac{P}{P^*} = \frac{1}{M} \sqrt{\frac{k+1}{2\left[1+\left(\frac{k-1}{2}\right)M^2\right]}} \qquad [8.19]$$

$$\frac{V}{V^*} = M \sqrt{\frac{k+1}{2\left[1+\left(\frac{k-1}{2}\right)M^2\right]}} \qquad [8.20]$$

$$\frac{T}{T^*} = \frac{c^2}{c^{*2}} = \frac{k+1}{2\left[1+\left(\frac{k-1}{2}\right)M^2\right]} \qquad [8.21]$$

$$\frac{\gamma}{\gamma^*}=\frac{V^*}{V}=\frac{1}{M}\sqrt{\frac{2\left[1+\left(\frac{k-1}{2}\right)M^2\right]}{k+1}} \qquad [8.22]$$

$$\frac{P_0}{P_0^*}=\frac{1}{M}\sqrt{\left\{\frac{2\left[1+\left(\frac{k-1}{2}\right)M^2\right]}{k+1}\right\}^{\frac{k+1}{k-1}}} \qquad [8.23]$$

$$\frac{F_i}{F_i^*}=\frac{1+kM^2}{M\sqrt{2(k+1)\left[1+\left(\frac{k-1}{2}\right)M^2\right]}} \qquad [8.24]$$

$$\frac{s-s^*}{c_p}=\ln\left(M^2\sqrt{\left\{\frac{k+1}{2M^2\left[1+\left(\frac{k-1}{2}\right)M^2\right]}\right\}^{\frac{k+1}{k}}}\right) \qquad [8.25]$$

Equations (8.18) through (8.25) are the Fanno-line equations, and accurate working charts of the most useful of these are plotted in figures 19.4 through 19.8. Solutions are also tabulated by Keenan and Kaye (1948), Ames (1953), and Pratt & Whitney Aircraft (1963).

The equations (8.19) through (8.25) relate the flow conditions at some upstream pipe location to the choked flow conditions (*) at the end of a pipe of length L_{max}. Then, for a given pipe system and a specified flow condition, there can be only one set of choked flow conditions, and these superscripted (*) quantities are the same, regardless of what upstream location is known and used to establish them. Conversely, the specification of flow conditions at any location fixes conditions throughout the pipe. The additional relationship of equation (8.18) establishes the frictional distance between the known upstream point and the location of choking. Then, with reference to figure 19.9,

$$L=(L_{max})_1-(L_{max})_2$$

so that

$$f\left(\frac{L}{D}\right)=\left[f\left(\frac{L_{max}}{D}\right)\right]_1-\left[f\left(\frac{L_{max}}{D}\right)\right]_2 \qquad [8.26]$$

Likewise, the entropy change from location 1 to 2 is found by

$$\frac{s_2-s_1}{c_p}=\left(\frac{s-s^*}{c_p}\right)_2-\left(\frac{s-s^*}{c_p}\right)_1 \qquad [8.27]$$

Since the other properties are related to the choked value as a ratio, a ratio form of equation is needed. The change in pressure, for example, between locations 1 and 2 is found by

$$\frac{P_2}{P_1}=\frac{\left(\frac{P}{P^*}\right)_2}{\left(\frac{P}{P^*}\right)_1} \qquad [8.28]$$

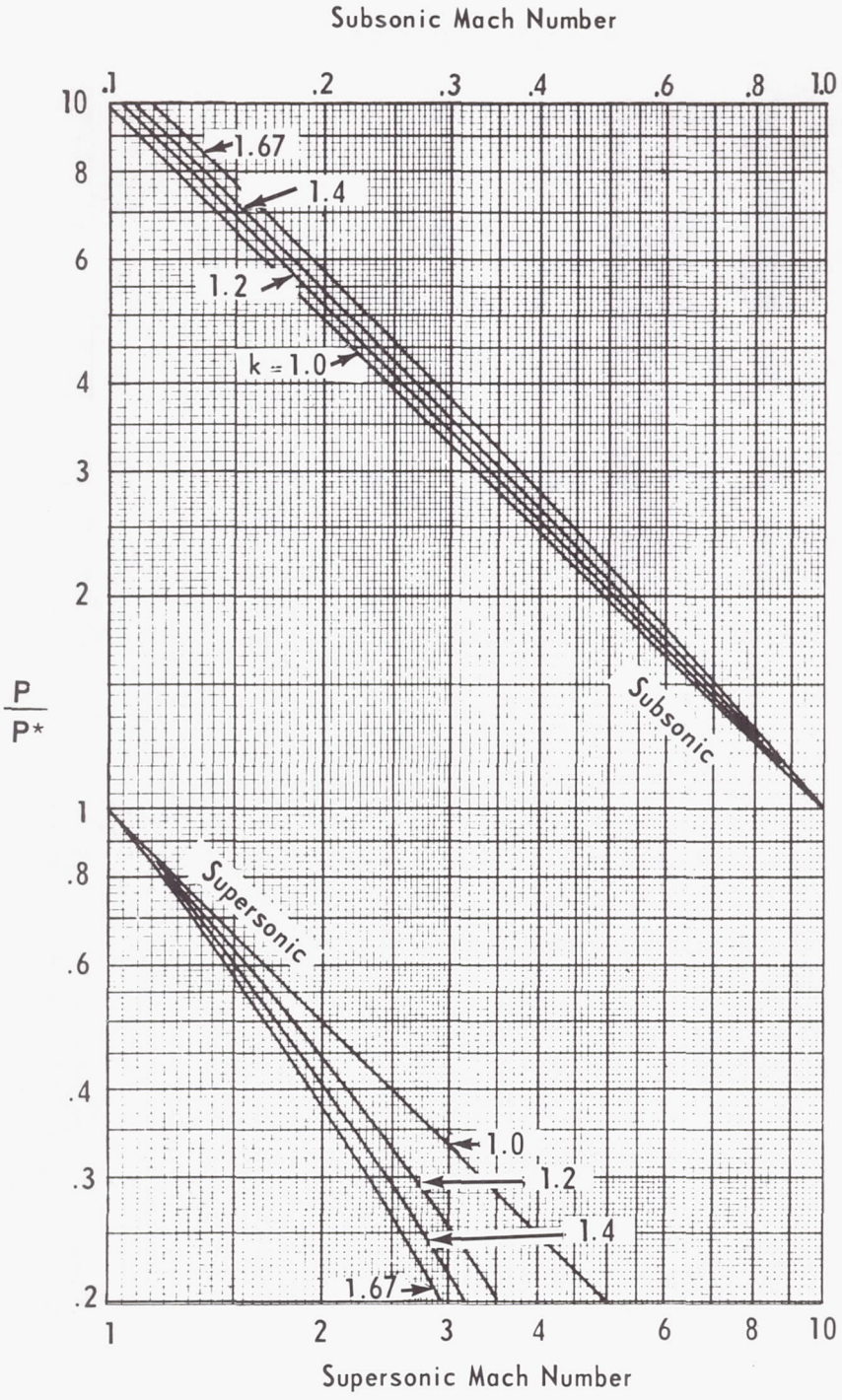


Figure 19.4. Fanno-line pressure ratio.

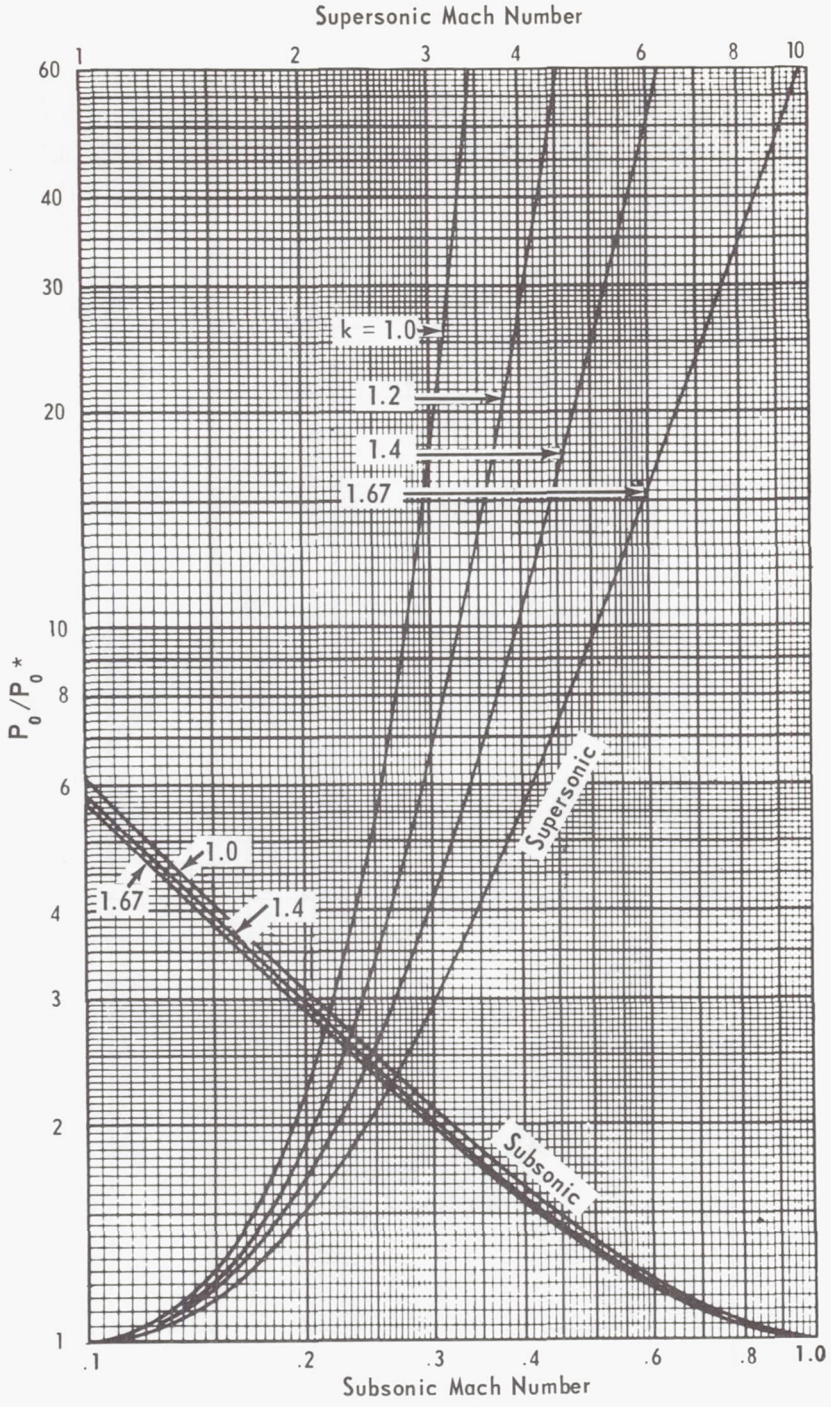


Figure 19.5. Fanno-line stagnation pressure ratio.

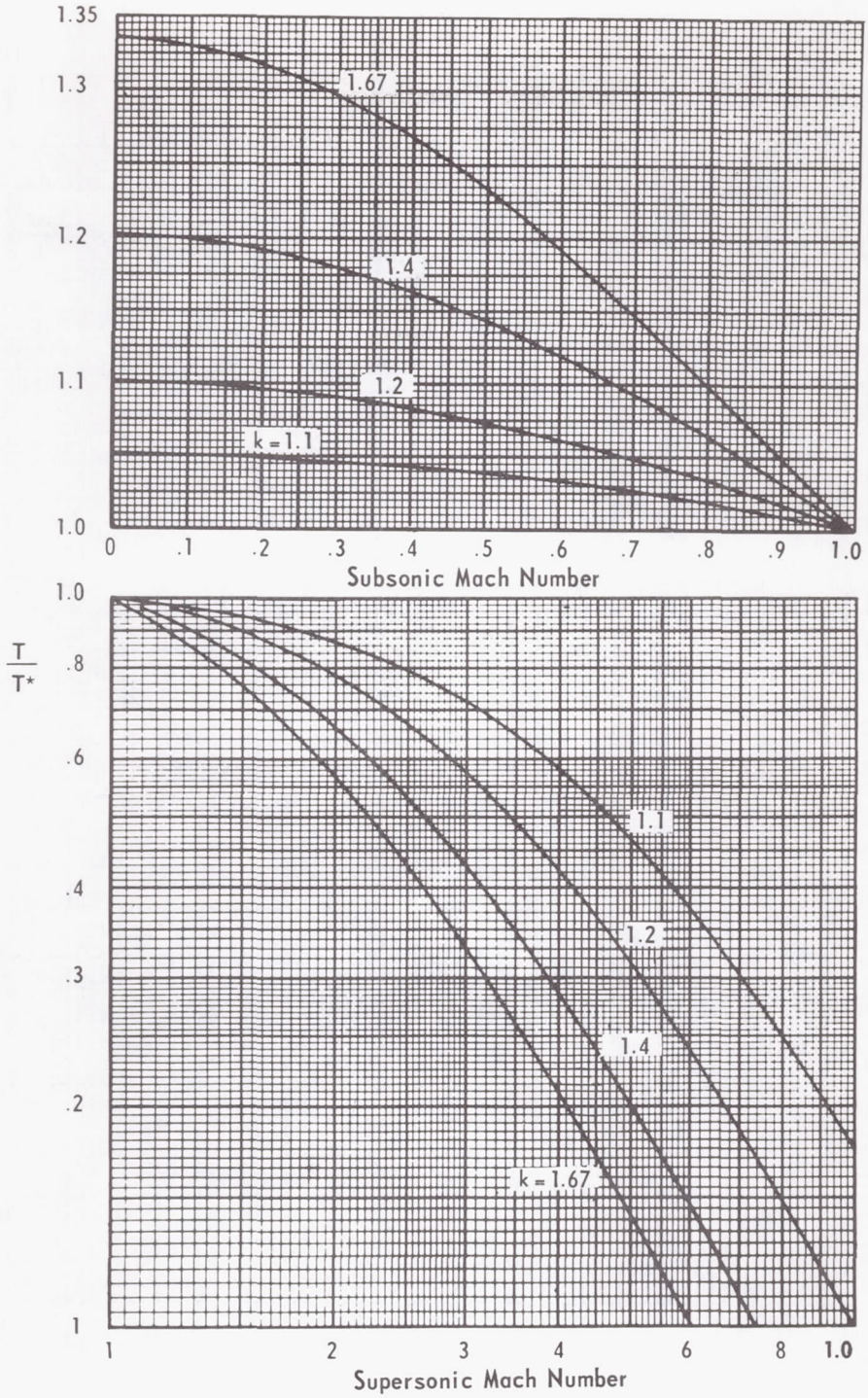


Figure 19.6. Fanno-line temperature ratio.

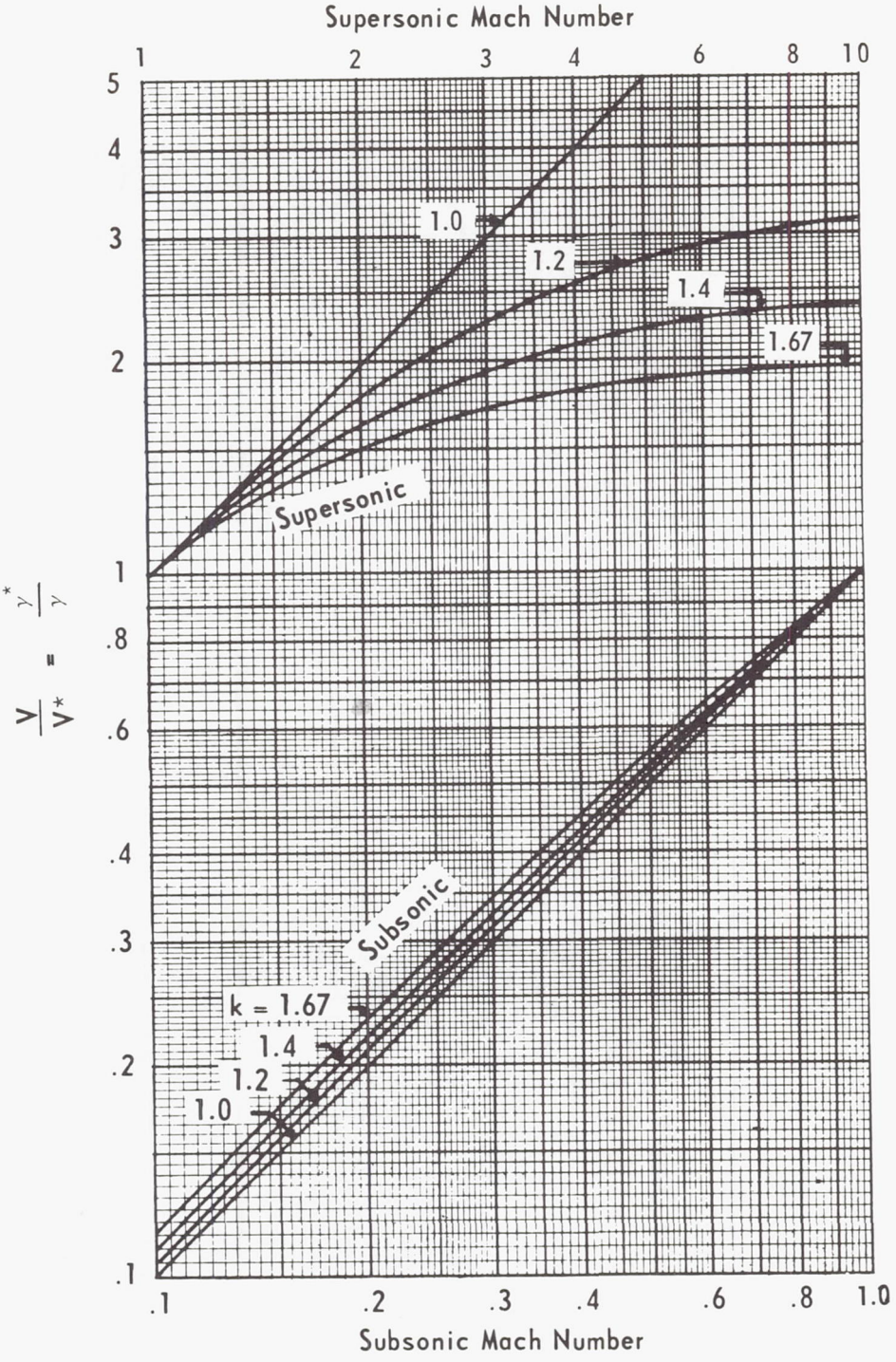


Figure 19.7. Fanno-line density and velocity ratios.

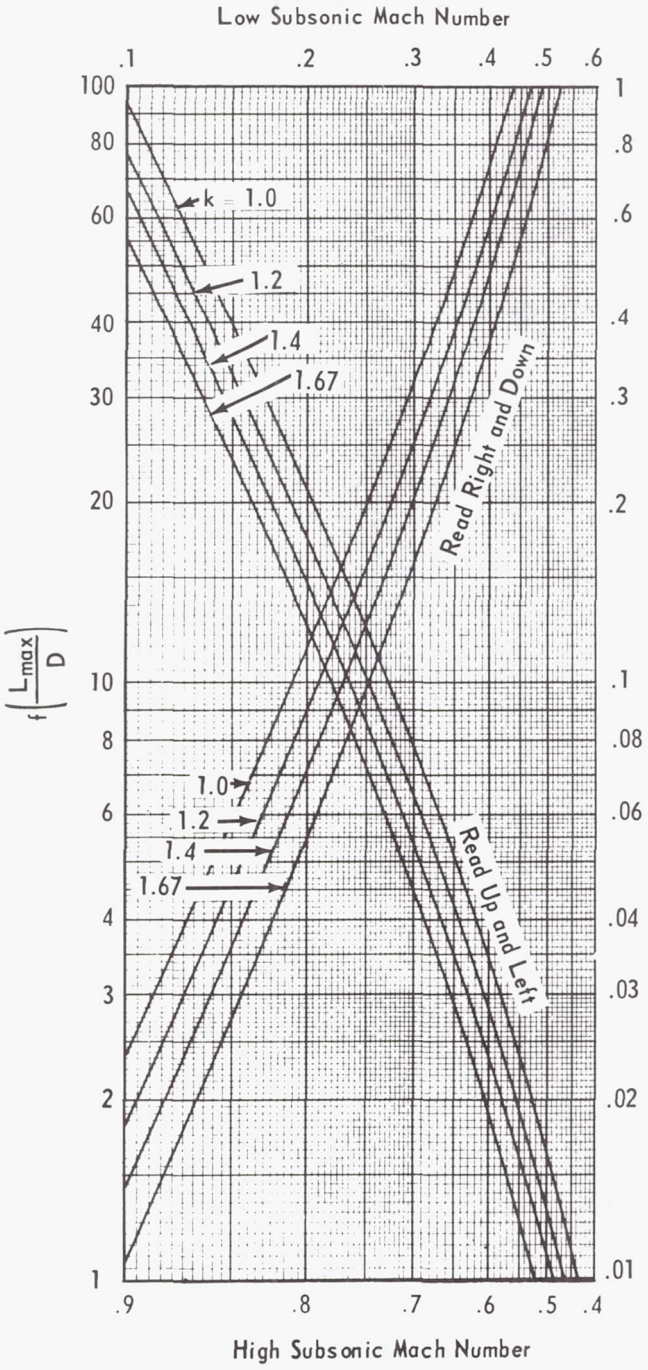


Figure 19.8. Frictional length parameter—subsonic and supersonic flow.

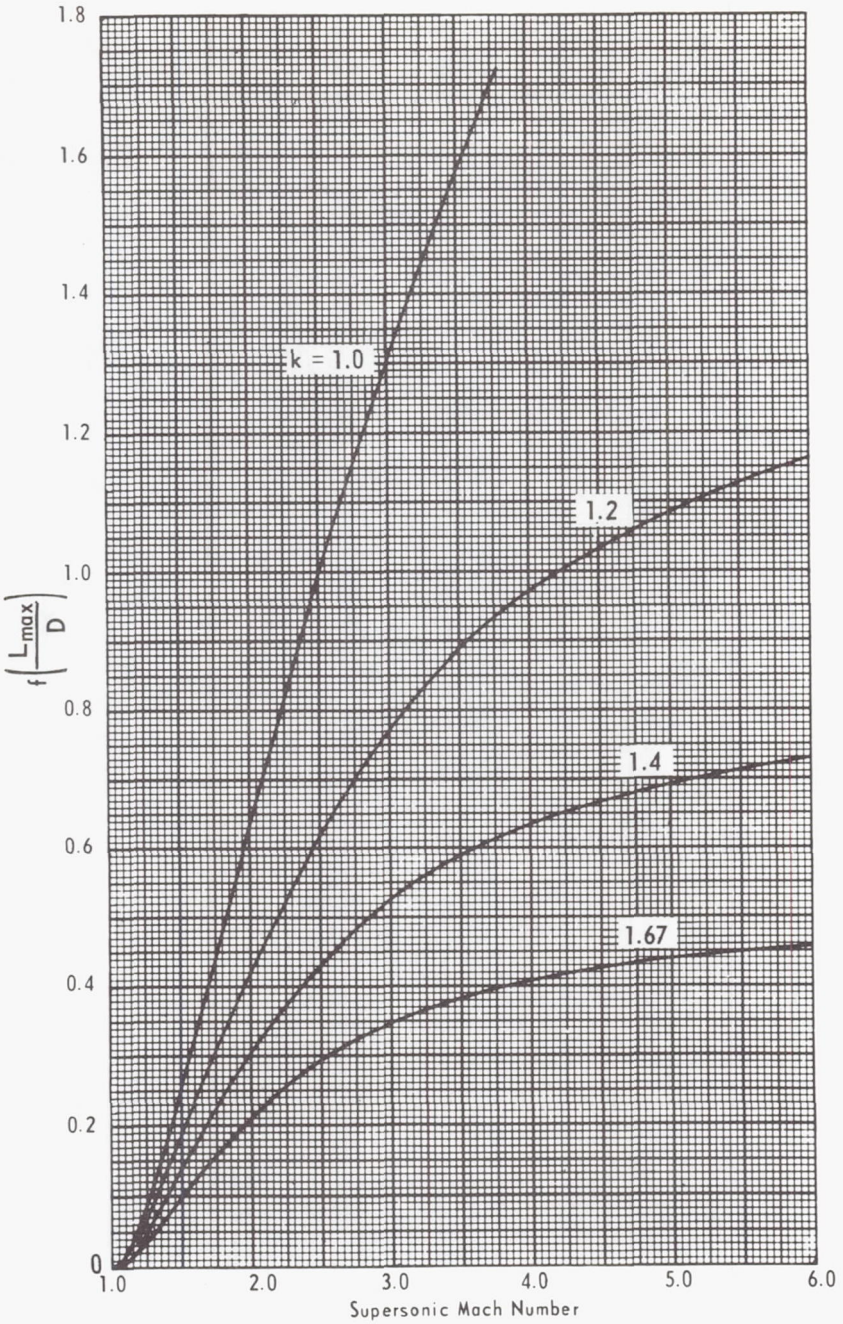


Figure 19.8. Frictional length parameter—subsonic and supersonic flow.—Concluded.

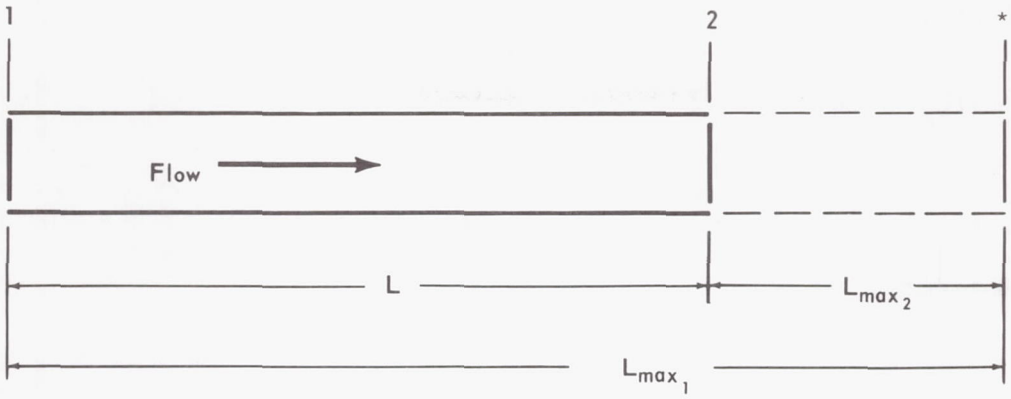


Figure 19.9. Pipe-length measurements.

All the other property changes are found by using the form of equation (8.28).

The usual procedure for computing the change in gas properties between two points in a pipe with the graphic or tabulated solution is as follows. The mach number is computed for the point in the pipe where the flow rate and fluid properties are known. Some convenient forms for perfect gases are as follows

$$M=\left(\frac{w}{A}\right)\left(\frac{1}{P}\right)\sqrt{\frac{RT}{kg_c}} \qquad [8.29]$$

Also, in more convenient terms for circular pipes and pressure in psia,

$$M=0.2245\left(\frac{w}{pD^2}\right)\sqrt{\frac{RT}{k}} \qquad [8.29a]^*$$

$$=15.21\left(\frac{\text{SCFM}}{1000\,pD^2}\right)\sqrt{\frac{T}{kR}} \qquad [8.29b]^*$$

$$=\frac{\frac{q}{A}}{c}=\frac{\frac{q}{A}}{\sqrt{kg_cRT}} \qquad [8.29c]^*$$

For imperfect gases (from ch. 4), using the actual sonic velocity (charted in appendixes) and the actual volume and weight flow rates

$$M=\frac{V}{c_a}=\frac{\frac{q}{A}}{c_a}=\frac{\frac{w}{A}}{\gamma c_a}=\left(\frac{w}{A}\right)\frac{ZRT}{Pc_a} \qquad [8.29d]^*$$

When written for circular pipes and pressure in psia

$$M=1.273\left(\frac{w}{D^2}\right)\frac{ZRT}{pc_a} \qquad [8.29e]^*$$

*This equation is a variation of equation (8.29) and does not appear in chapter 8.

and in terms of standard cubic feet per minute

$$M = 86.4 \left(\frac{\text{SCFM}}{1000}\right) \frac{ZT}{pD^2 c_a} \qquad [8.29f]^*$$

It must be remembered that the modification of M to the real-gas value is only a partial compensation for real-gas effects in a flow problem. The isentropic exponent k_s, as discussed in chapter 4, must be used in the calculations and charts in place of the specific heat ratio. The value of k_s can be obtained from the following equations, using the actual sonic velocity data or thermodynamic charts, as follows

$$k_s = \frac{c_a^2}{g_c ZRT} = 3.105 \left[\frac{\left(\frac{c_a}{1000}\right)^2}{Z\left(\frac{R}{100}\right)\frac{T}{100}} \right] = \frac{\ln\left(\frac{P_2}{P_1}\right)_s}{\ln\left(\frac{v_1}{v_2}\right)_s}$$

The point of known conditions may be either upstream, 1, or downstream, 2, as shown in figure 19.9. The frictional length parameters $f(L_{\max}/D)$ and the fluid property ratios of interest, such as P/P^*, are read from the graphs or tables at the computed mach number. The frictional length $f(L/D)$, between the points 1 and 2, is computed from the pipe description and combined with the value of $f(L_{\max}/D)$, as read from the tables, in accordance with equation (8.26). This computation establishes the value of $f(L_{\max}/D)$ for the other point in the pipe which, in turn, identifies the associated mach number and fluid property ratios for that location by means of the charts. The change in properties between the two points is then evaluated by means of equations (8.27) and (8.28), and others of that form.

EXAMPLE PROBLEM 19.1

A 30-foot run of straight 1-inch stainless-steel tubing (0.81-inch I.D.) is used to vent helium to the atmosphere. Because of a new system requirement, the quantity of helium that must be vented has increased to 15 000 scfm at an upstream temperature of 0° F, and at a pressure which may be as low as 1000 psig. Determine whether the tubing can vent the increased flow and the exit flow conditions.

SOLUTION

Because of the high flow rate requirement and the relatively short length of tubing, the flow is expected to closely approximate frictional adiabatic flow.

The charts of appendix D indicate that, for helium at 1015 psia (1000 psig) and 0° F, the compressibility factor Z and specific heat ratio (c_p/c_v) are practically the nominal values of 1.0 and 1.67, respectively, so that the helium can be considered a perfect gas. By equation (8.29*b*)

$$M = 15.21 \left[\frac{15\,000}{(1000)(0.81)^2(1015)} \right] \sqrt{\frac{460}{(1.66)(386)}}$$
$$= 0.2903$$

Entering figure 19.8 for $k = 1.67$

$$f\left(\frac{L_{\max}}{D}\right) = 4.72$$

*This equation is a variation of equation (8.29) and does not appear in chapter 8.

The evaluation of $f(L/D)$ for the actual tubing requires the evaluation of the coefficient of friction from the Reynolds number and the Moody diagram of figure 3.4 (ch. 3). The Reynolds number for circular pipes, by equation (4.14), is

$$R_e = \frac{DV\rho}{\mu} = 1.037\left(\frac{\text{SCFM}}{DR\mu'}\right)$$

From figure D.5 (app. D), $\mu_c = 0.0185$ centipoise at 1000 psig and 0° F, and since

$$\mu' = \mu g_c = (6.72)\,10^{-4}\,\mu_c$$

so that

$$R_e = 1.037\left[\frac{15000}{(0.81)(386)(0.0185)(6.72\times 10^{-4})}\right]$$
$$= 4.00\times 10^6$$

For drawn tubing and a Reynolds number of 4.0×10^6, figure 3.4 yields

$$f = 0.0096$$

Then

$$f\left(\frac{L}{D}\right) = 0.0096\left[\frac{30}{\frac{0.81}{12}}\right]$$
$$= 4.27$$

Since $f(L/D) < f(L_{\max}/D)$, the tubing will vent the increased flow. The exit conditions, 2, are obtained as follows. By equation (8.26)

$$\left[f\left(\frac{L_{\max}}{D}\right)\right]_2 = 4.72 - 4.27$$
$$= 0.45$$

Figure 19.8 for $k = 1.67$ and $[f(L_{\max}/D)]_2 = 0.45$ yields

$$M_2 = 0.582$$

The exit pressures are obtained from figure 19.4 at $M_1 = 0.2903$ and $M_2 = 0.582$.

$$\frac{P_1}{P^*} = 3.91 \qquad \text{and} \qquad \frac{P_2}{P^*} = 1.88$$

so that

$$P_2 = P_1\left(\frac{\frac{P_2}{P^*}}{\frac{P_1}{P^*}}\right) = 1015\left(\frac{1.88}{3.91}\right) = 488 \text{ psia}$$
$$= 473 \text{ psig}$$

Similarly, the exit temperature is obtained from figure 19.6

$$\frac{T_1}{T^*} = 1.300 \qquad \text{and} \qquad \frac{T_2}{T^*} = 1.202$$

Then

$$T_2 = T_1 \left(\frac{\frac{T_2}{T^*}}{\frac{T_1}{T^*}} \right) = 460 \left(\frac{1.202}{1.300} \right) = 425^\circ \text{ R}$$

$$= -35^\circ \text{ F}$$

DIRECT GRAPHIC METHODS—SUBSONIC FLOW

The adiabatic frictional flow equations can be derived and integrated in the subsonic range between two specific locations in the piping system to produce solutions that can be charted. These charts then provide a direct method for calculating the compressible fluid property changes between two locations in a piping system.

For example, if the mass flow rate and fluid properties are known at a point in the pipe, the mass flow parameter can be computed. And if the piping system is defined, the frictional length parameter $f(L/D)$ can be computed for the piping between the two points. Entering the proper chart with these values, the fluid property changes that occur between the two points can be read directly. These charts are graphic solutions of exact compressible flow equations which have the same theoretical basis and are subject to the same assumptions as the Fanno-line equations derived previously.

In solving practical problems, the known (reference) flow conditions will generally occur in one of three locations, relative to the location where the flow conditions are to be established.

Case 1: Conditions are known at an upstream point in the pipe.

Case 2: Conditions are known at a downstream point in the pipe.

Case 3: Conditions are known in an upstream reservoir.

The three locations where the flow conditions are known require three different sets of charts to prevent the need for trial-and-error solutions. In developing the necessary equations, the location designations will follow that of figure 19.10.

Conditions Known in an Upstream Pipe Location

The basic pipe flow equations are developed for the section from 1 to 2. By assuming various flow conditions, the fluid property changes between 1 and 2 can be computed for selected values of $f(L/D)$ to produce the chart for case 1. As discussed previously, for any assumed flow condition and piping system, the properties of the fluid are fixed throughout the pipe and the upstream reservoir, if one should exist, regardless of the location of the known flow conditions. Therefore, the data required to produce the charts for cases 2 and 3 are obtained by modifying the flow parameters and fluid property changes to reflect the change in the reference location from 1 to 2 or to 0, respectively. The assumed frictionless nozzle of case 3 also provides the relation between the downstream static conditions and the stagnation conditions at the upstream pipe location, 1. In a practical problem involving a real reservoir, a square-edged entrance would be accommodated by increasing the effective pipe length parameter, $f(L/D)$.

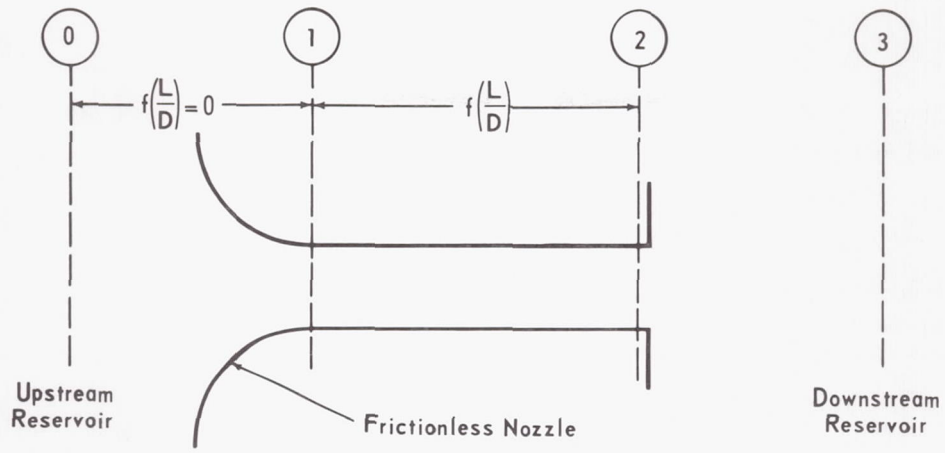


Figure 19.10. Location designation for piping systems.

Proceeding with case 1, the equation of state, which describes the state of the fluid as it progresses through the pipe, is established by noting that the total specific enthalpy of the fluid is constant if the flow is adiabatic. Then

$$\mathrm{d}\left(\frac{V^2}{2g_c}\right)+J\,\mathrm{d}h=\mathrm{d}\left(\frac{V^2}{2g_c}\right)+J\,\mathrm{d}u+\mathrm{d}\,(Pv)=0 \qquad [8.30]$$

Combining this with the perfect-gas relationships yields

$$\mathrm{d}(Pv)=-\left(\frac{k-1}{k}\right)\mathrm{d}\left(\frac{V^2}{2g_c}\right) \qquad [8.31]$$

Integrating equation (8.31) between points 1 and 2 in the pipe yields the equation of state,

$$Pv+\left(\frac{k-1}{2kg_c}\right)V^2=P_1v_1+\left(\frac{k-1}{2kg_c}\right)V_1^2=P_2v_2+\left(\frac{k-1}{2kg_c}\right)V_2^2 \qquad [8.32]$$

Substituting the continuity equation and definition of mach number into the equation of state yields the equation relating the fluid property changes to the upstream mach number.

$$\frac{P_2}{P_1}=\frac{v_1}{v_2}\left\{1-\left[\left(\frac{k-1}{2}\right)M_1^2\right]\left[\left(\frac{v_2}{v_1}\right)^2-1\right]\right\} \qquad [8.33]$$

Combining with the perfect-gas law yields

$$\frac{T_2}{T_1}=1-\left[\left(\frac{k-1}{2}\right)M_1^2\right]\left[\left(\frac{v_2}{v_1}\right)^2-1\right] \qquad [8.34]$$

An additional equation relates the fluid property changes to the frictional length of the pipe. This equation is the Bernoulli theorem, obtained from momentum considerations, and is written

$$d\left(\frac{V^2}{2g_c}\right)+v\,dP+f\left(\frac{V^2}{2g_c}\right)\frac{dL}{D}=0 \qquad [8.36]$$

A combination of equations (8.31), (8.32), and (8.36) and the continuity equation yields the following integrable equation

$$(k+1)\int_{V_1}^{V_2}\frac{dV}{V}-\left[2kg_cP_1v_1+(k-1)V_1^2\right]\int_{V_1}^{V_2}\frac{dV}{V^3}+\frac{kf}{D}\int_0^L dL=0$$

Carrying out the integration and substituting the definitions of sonic velocity and mach number yield the equation that relates the frictional length $f(L/D)$, measured between the two pipe locations, to the fluid properties and mach number.

$$f\left(\frac{L}{D}\right)=\frac{1}{k}\left[\frac{2+(k-1)M_1^2}{2M_1^2}\right]\left[1-\left(\frac{v_1}{v_2}\right)^2\right]-\left(\frac{k+1}{2k}\right)\ln\left(\frac{v_2}{v_1}\right)^2 \qquad [8.37]$$

Equations (8.33) and (8.37) can be solved simultaneously to produce the charts for case 1, which consist of separate charts for each value of k that is to be represented. Figures 19.11 through 19.16 represent the case 1 charts for perfect and real gases having k (or k_s) = 1.0, 1.4, 1.67, 1.8, 2.5, and 4.0. Note that the mass flow parameter ϕ_1 has been chosen as

$$\phi_1=\sqrt{k}\,(M_1)=\left(\frac{w}{A}\right)\left(\frac{1}{P_1}\right)\sqrt{\frac{RT_1}{g_c}} \qquad [8.38]$$

Comparing equations (8.38) and (8.39) shows that ϕ_1 is merely a slightly modified mach number, made independent of $k[\phi_1=\sqrt{k}\,(M_1)]$. This selection is made to provide easier interpolation between charts for uneven values of k and k_s. For example, for any value of k, ϕ_1 needs to be calculated only once and the charts drawn for all specific values of k can be entered, using the same value of ϕ_1. It can be shown by cross-plotting the data versus k that linear interpolation between the charts for any in-between values of k yields good accuracy.

Lines of constant static temperature are computed for the case 1 charts by the equation resulting from a combination of equations (8.34) and (8.38) and the perfect-gas law.

$$\frac{P_2}{P_1}=\frac{T_2}{T_1}\left[\frac{1-\dfrac{T_2}{T_1}}{\left(\dfrac{k-1}{2k}\right)\phi_1^2}+1\right]^{-1/2} \qquad [8.39]$$

where ϕ is substituted for M_1 of equation (8.39) in chapter 8. The sonic flow line identifies the maximum or choked flow conditions and is obtained from equation (8.19) rewritten as

$$\frac{P_2}{P_1}=\frac{P^*}{P_1}=\phi_1\sqrt{\frac{2+\left(\dfrac{k-1}{k}\right)\phi_1^2}{k(k+1)}} \qquad [8.40]$$

(The above equation is a simplified version of the original equation in ch. 8.)

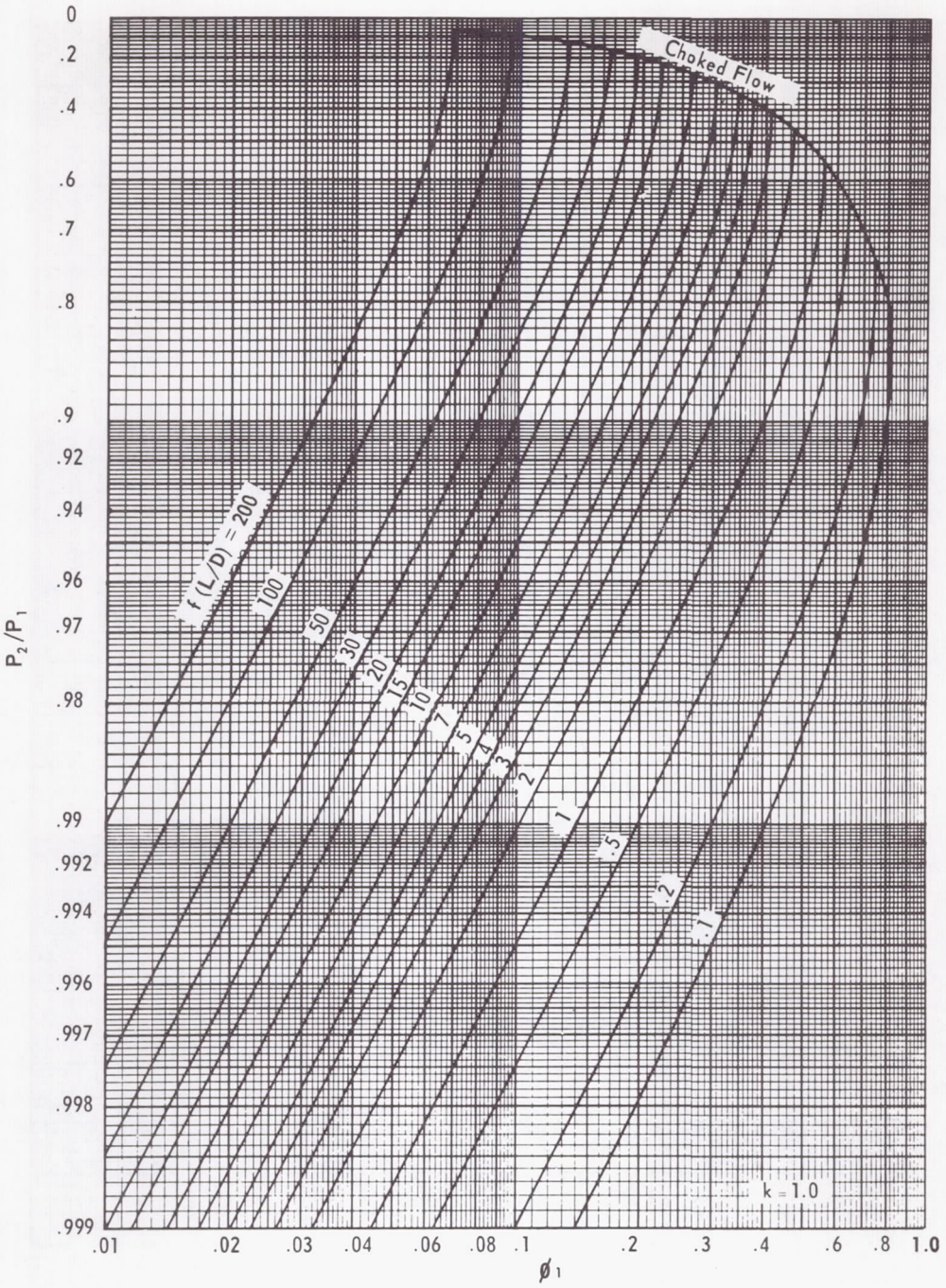


Figure 19.11. Compressible adiabatic flow with friction in constant-area pipes based on conditions in an upstream pipe location, $k = 1.0$.

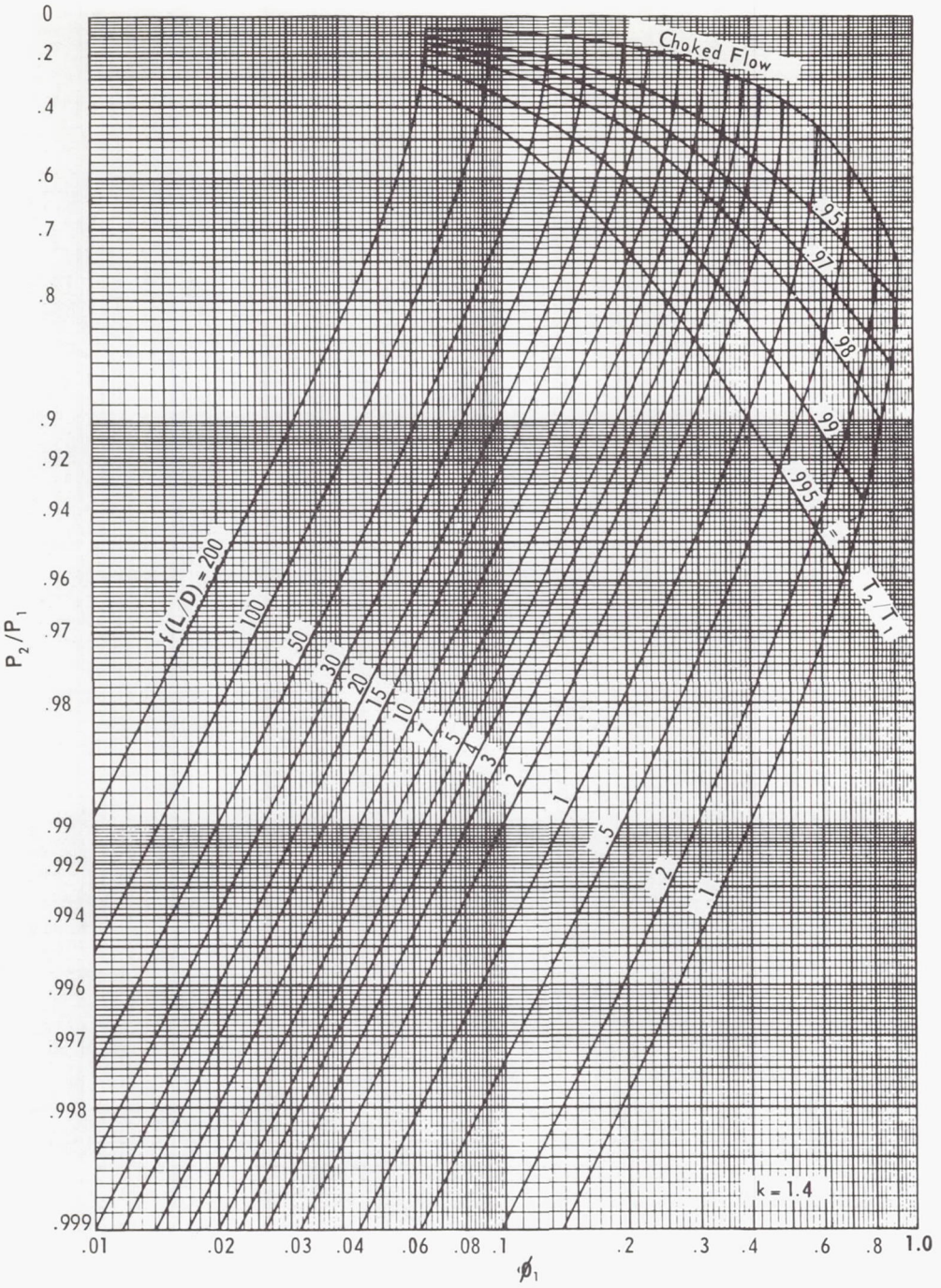


Figure 19.12. Compressible adiabatic flow with friction in constant-area pipes based on conditions in an upstream pipe location, $k = 1.4$.

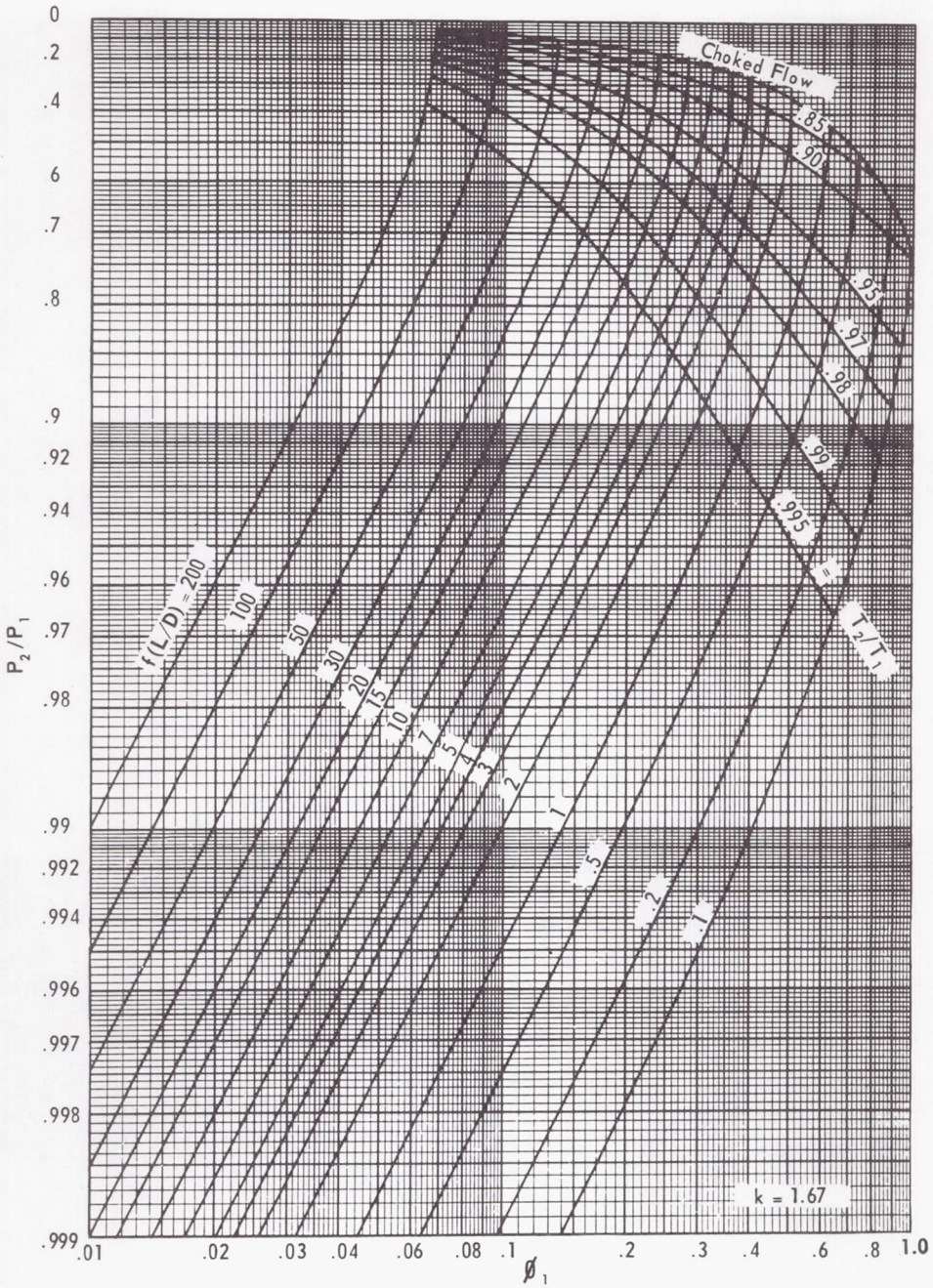


Figure 19.13. Compressible adiabatic flow with friction in constant-area pipes based on conditions in an upstream pipe location, $k = 1.67$.

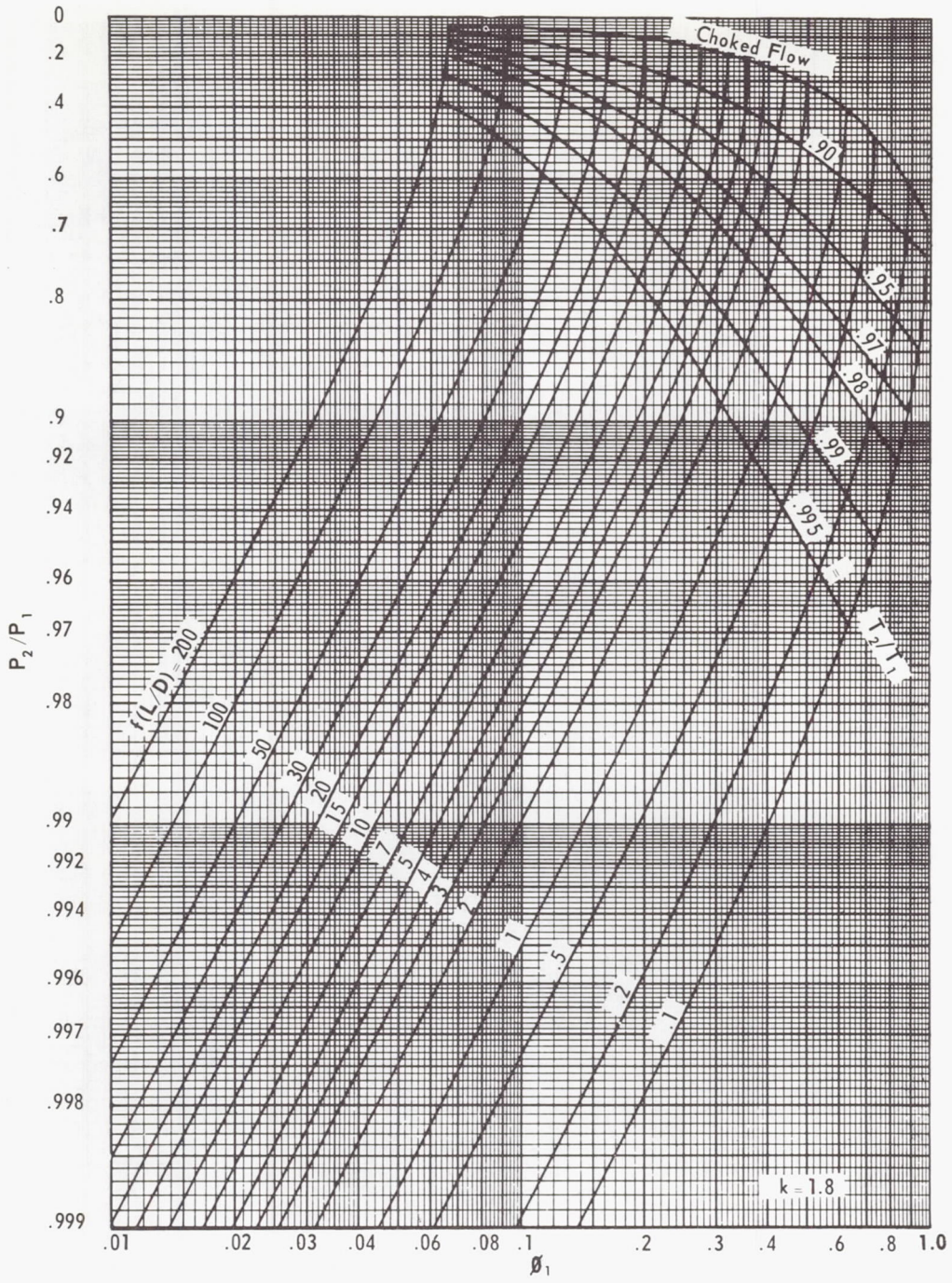


Figure 19.14. Compressible adiabatic flow with friction in constant-area pipes based on conditions in an upstream pipe location, $k = 1.8$.

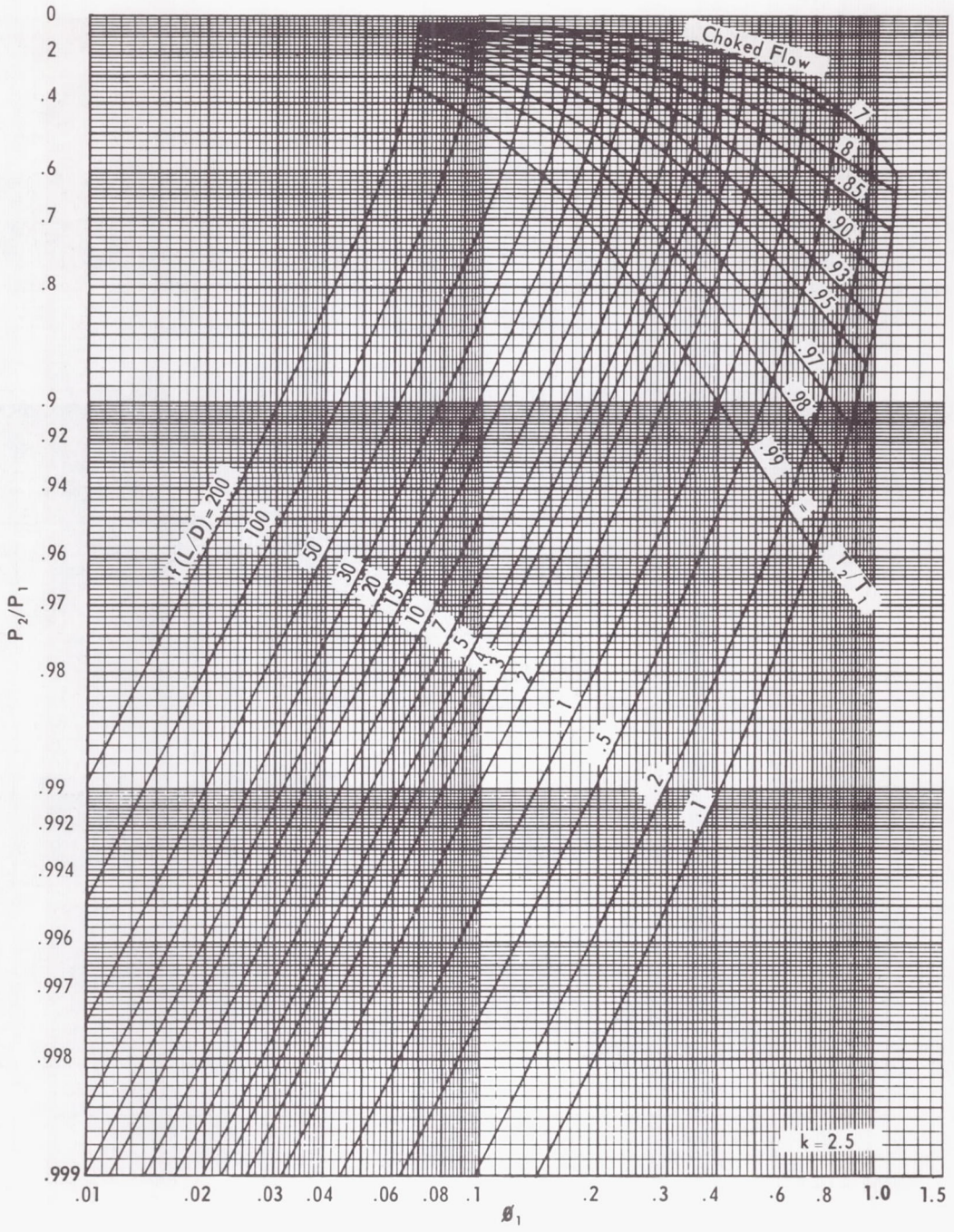


Figure 19.15. Compressible adiabatic flow with friction in constant-area pipes based on conditions in an upstream pipe location, $k = 2.5$.

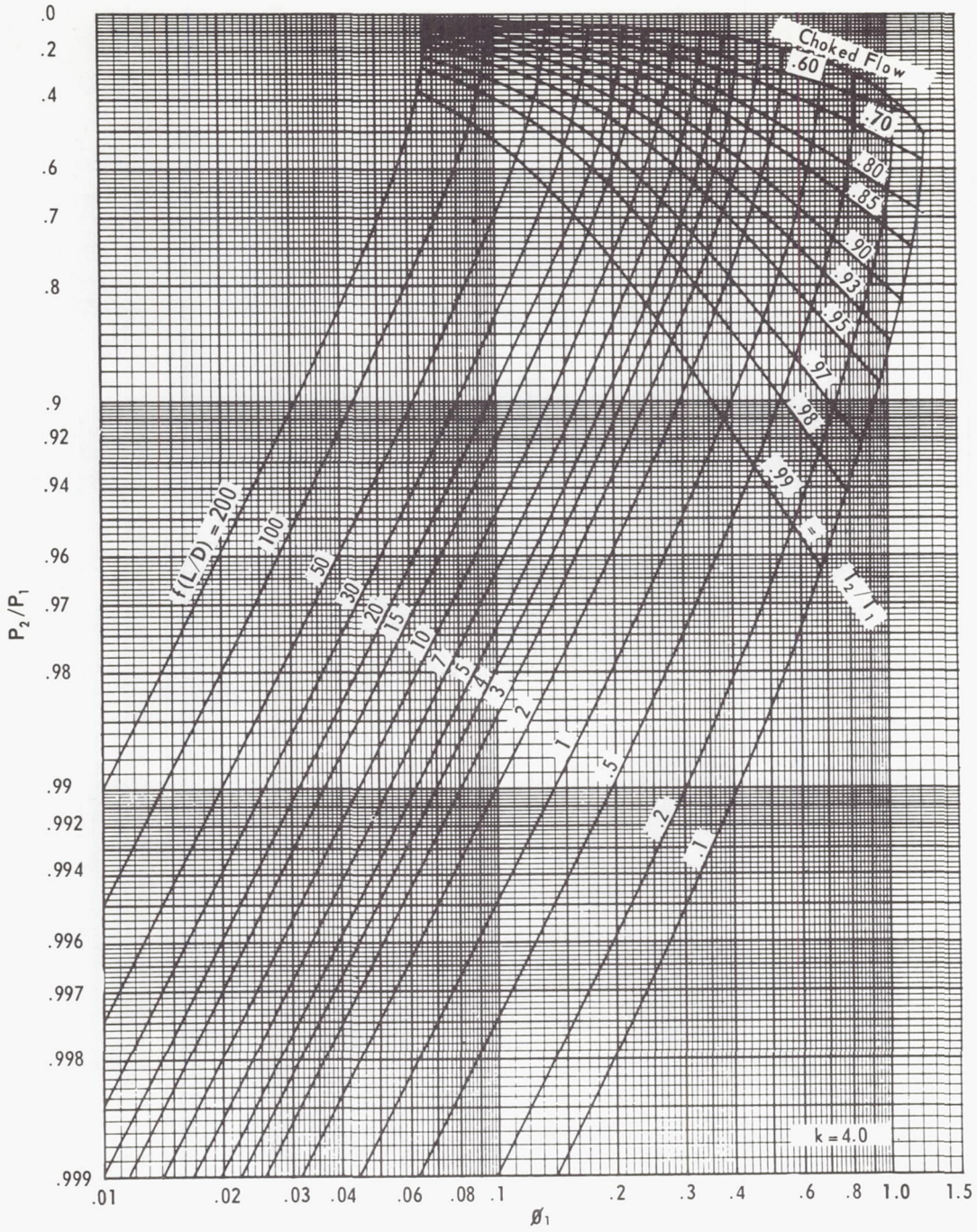


Figure 19.16. Compressible adiabatic flow with friction in constant-area pipes based on conditions in an upstream pipe location, $k = 4.0$.

Conditions Known in a Downstream Pipe Location

The charts of case 2 are plotted from the data computed for case 1, except that the flow parameter is redefined for the downstream location as

$$\phi_2 = \sqrt{k}(M_2) = \left(\frac{w}{A}\right)\left(\frac{1}{P_2}\right)\sqrt{\frac{RT_2}{g_c}} \qquad [8.41]$$

which is obtained directly from the values of ϕ_1 by

$$\phi_2 = \phi_1\left(\frac{\phi_2}{\phi_1}\right) = \phi_1\left(\frac{\sqrt{\frac{T_2}{T_1}}}{\frac{P_2}{P_1}}\right) \qquad [8.42]$$

The lines of constant-temperature ratio are obtained by combining equations (8.34), (8.38), (8.41), and (8.42) with the perfect-gas law and solving for (P_2/P_1) in terms of (T_2/T_1) and ϕ_2

$$\frac{P_2}{P_1} = \left(\frac{T_2}{T_1}\right)\left[1 - \frac{\frac{T_1}{T_2} - 1}{\left(\frac{k-1}{2k}\right)\phi_2^2}\right]^{1/2} \qquad [8.43]$$

The sonic flow line occurs as a vertical line on the charts of case 2. Since the choked condition occurs at the pipe exit where the flow parameter ϕ_2 is computed, and since M_2 is unity, the sonic flow line is described using equation (8.41) as

$$\phi_2 = \sqrt{k} \qquad [8.44]$$

The case 2 charts are plotted as figures 19.17 through 19.22 for perfect and real gases having k (or k_s) = 1.0, 1.4, 1.67, 1.8, 2.5, and 4.0.

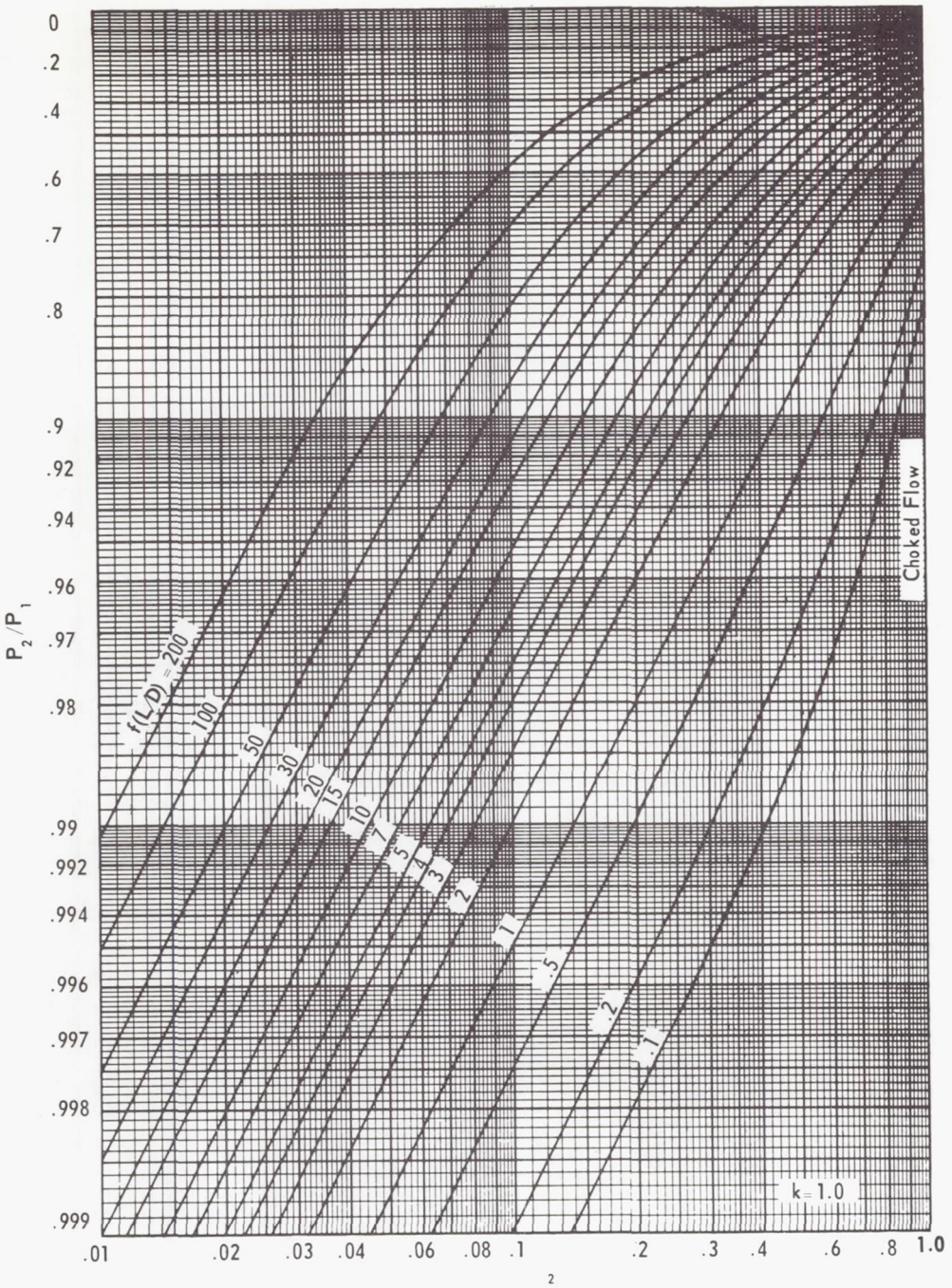


Figure 19.17. Compressible adiabatic flow with friction in constant-area pipes based on conditions in a downstream pipe location, $k = 1.0$.

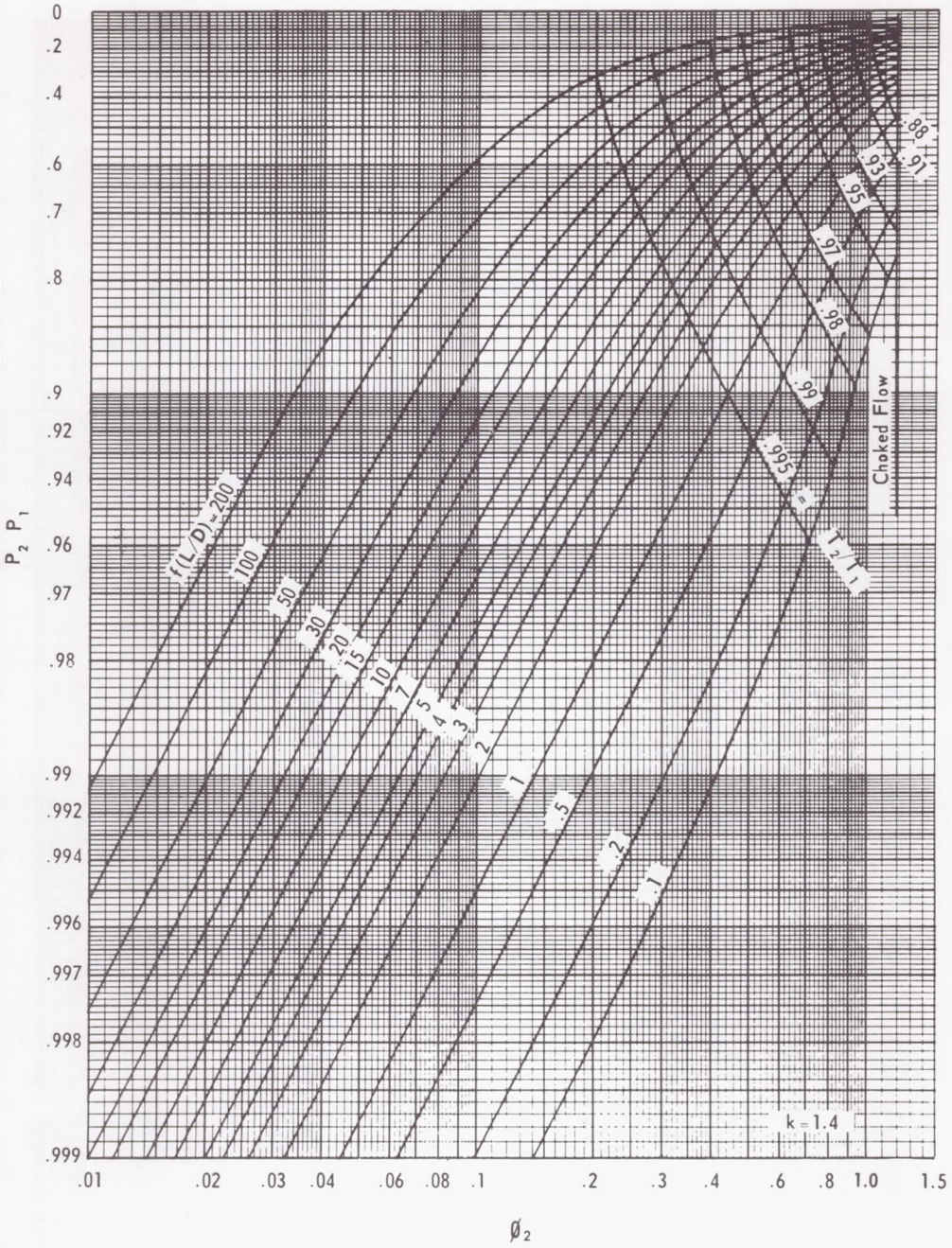


Figure 19.18. Compressible adiabatic flow with friction in constant-area pipes based on conditions in a downstream pipe location, $k = 1.4$.

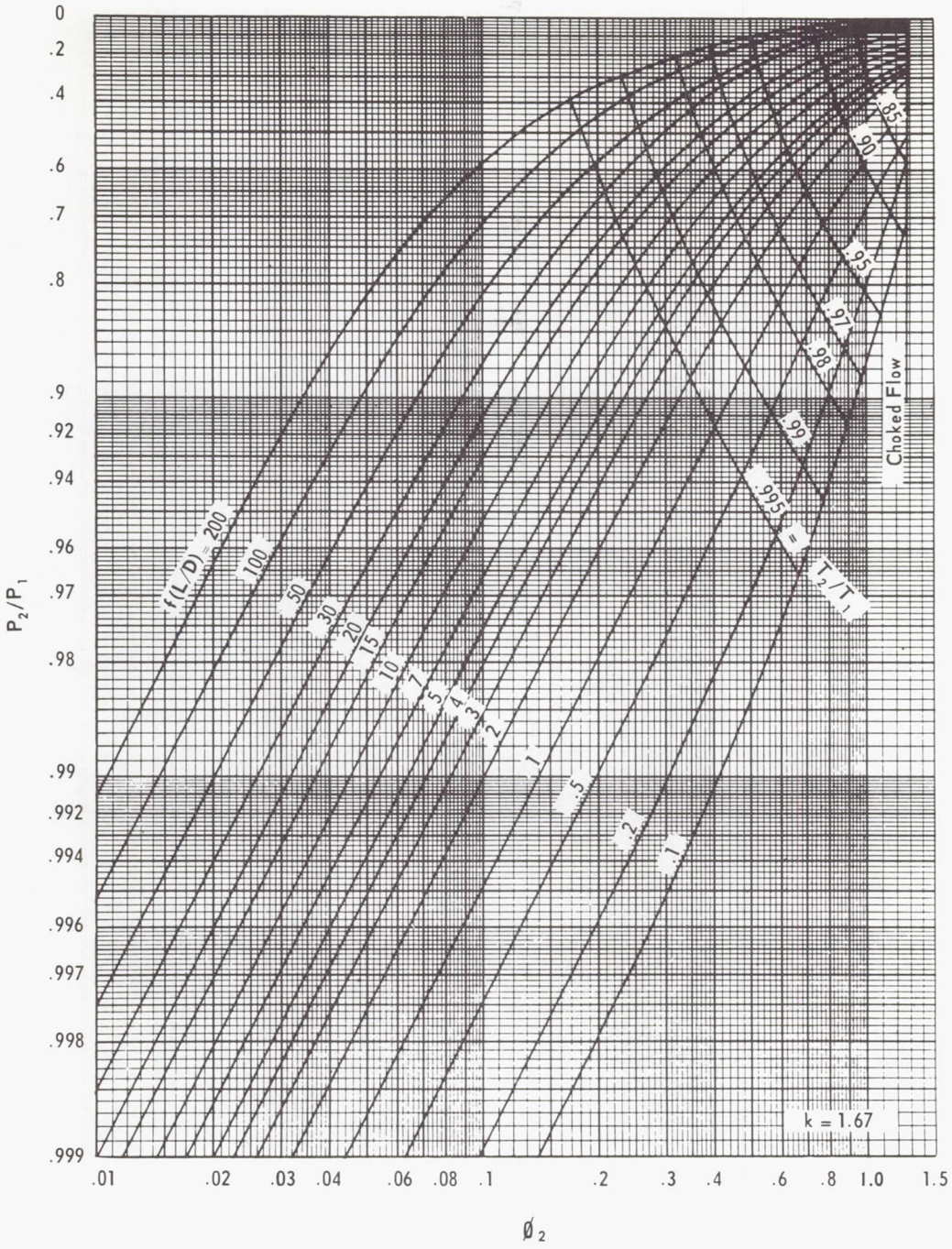


Figure 19.19. Compressible adiabatic flow with friction in constant-area pipes based on conditions in a downstream pipe location, $k = 1.67$.

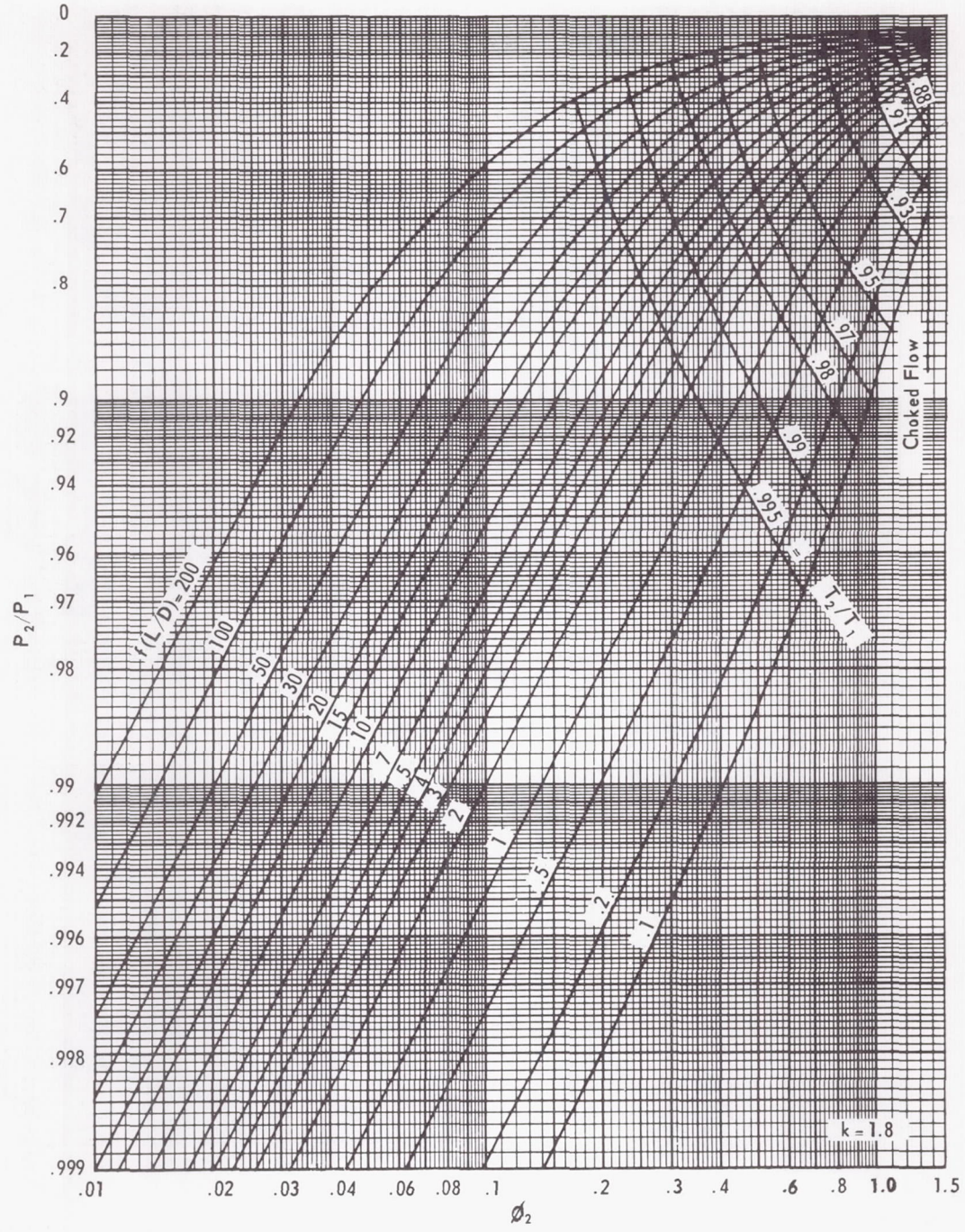


Figure 19.20. Compressible adiabatic flow with friction in constant-area pipes based on conditions in a downstream pipe location, $k = 1.8$.

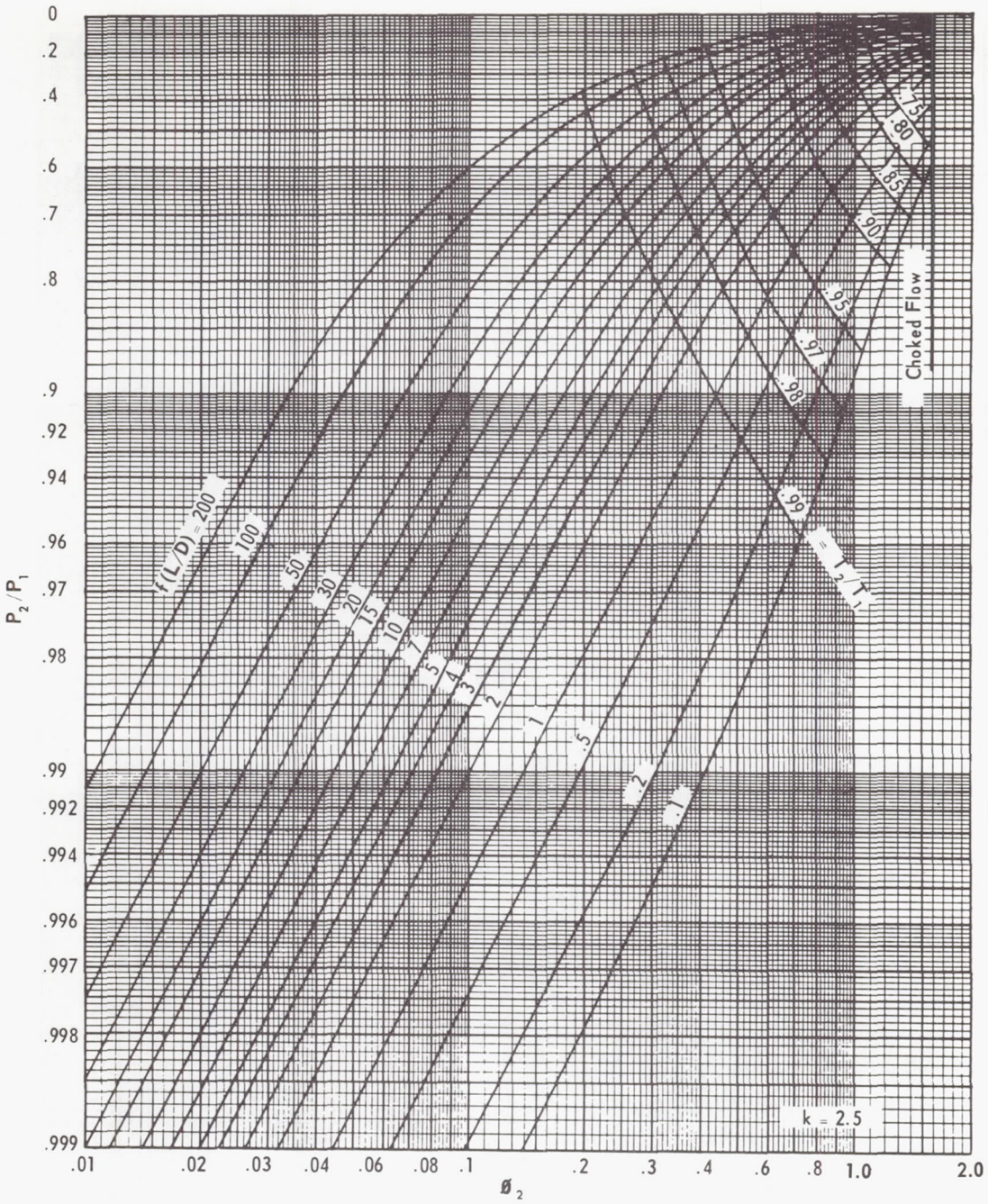


Figure 19.21. Compressible adiabatic flow with friction in constant-area pipes based on conditions in a downstream pipe location, $k = 2.5$.

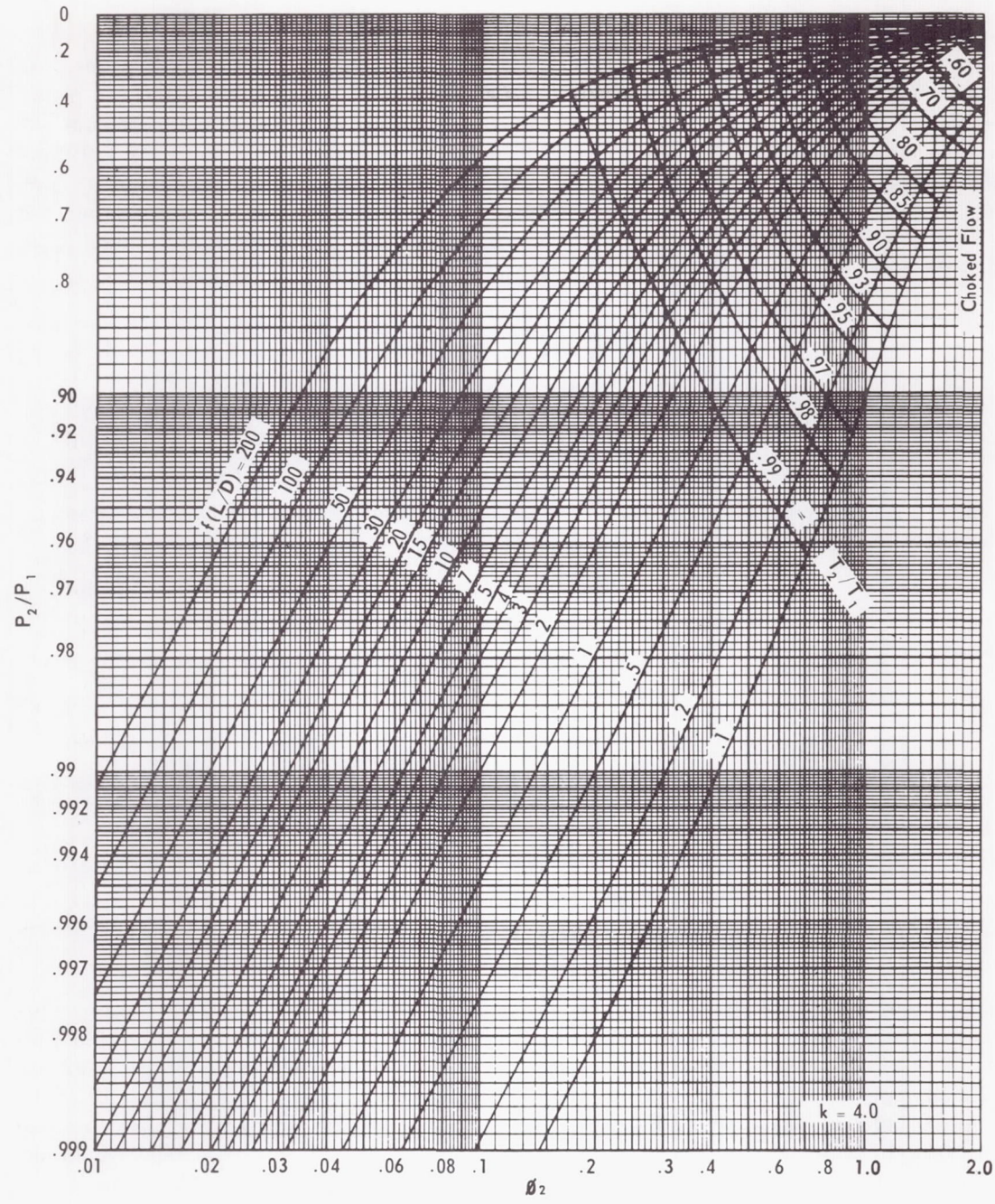


Figure 19.22. Compressible adiabatic flow with friction in constant-area pipes based on conditions in a downstream pipe location, $k=4.0$.

Conditions Known in an Upstream Reservoir

To extend the analysis to case 3, which accounts for a reservoir ahead of the pipe, it is convenient to assume a frictionless nozzle at the pipe inlet. This permits the use of the isentropic flow relationships to define the changes in properties between the upstream reservoir location 0 and the pipe inlet 1. These charts are also applicable, therefore, for computation between two pipe locations when the upstream stagnation properties in the pipe are known. The pipe inlet corresponds to the nozzle throat. Then for this section, the pressure and temperature ratios across the nozzle are obtained directly from equation (8.38) and the previously derived isentropic relationships of equations (5.31) and (5.10).

$$\frac{P_1}{P_0}=\left[1+\left(\frac{k-1}{2k}\right)\phi_1^2\right]^{\frac{-k}{k-1}} \qquad [8.45]$$

$$\frac{T_1}{T_0}=\left[1+\left(\frac{k-1}{2k}\right)\phi_1^2\right]^{-1} \qquad [8.46]$$

where ϕ is substituted for M_1 of equations (8.45) and (8.46) in chapter 8. The flow parameter for case 3 is defined as

$$\phi_0=\left(\frac{w}{A}\right)\left(\frac{1}{P_0}\right)\sqrt{\frac{RT_0}{g_c}} \qquad [8.49]$$

which is related to ϕ_1 for the isentropic process by

$$\phi_0=\phi_1\left(\frac{\frac{P_1}{P_0}}{\sqrt{\frac{T_1}{T_0}}}\right) \qquad [8.50]$$

(The above equation is a simplified version of the original equation appearing in ch. 8)

$$\phi_0=\phi_1\left(\frac{P_1}{P_0}\right)^{\frac{k+1}{2k}}=\sqrt{k}\,(M_1)\left(\frac{P_1}{P_0}\right)^{\frac{k+1}{2k}} \qquad [8.51]$$

Using equations (8.45), (8.46), (8.49), and (8.51), the case 3 charts of P_2/P_0 and T_2/T_0 versus ϕ_0 are plotted from case 1 data. Note that there is no real mach number associated with ϕ_0, which is based on upstream reservoir conditions or the stagnation conditions in an upstream pipe location 1. The case 3 charts are plotted as figures 19.23 through 19.28 for perfect and real gases having k (or k_s) = 1.0, 1.4, 1.67, 1.8, 2.5, and 4.0. The extra curve for $f(L/D)=0$ relates the upstream reservoir conditions to the upstream pipe conditions [$P_2/P_0=P_1/P_0$ for $f(L/D)=0$], which is also the relation between the stagnation and static conditions for the upstream pipe location 1. The $f(L/D)=0$ is derived separately from equation (8.51), where M_1 is obtained from the isentropic equation (5.31).

$$\phi_0\left[f\left(\frac{L}{D}\right)=0\right]=\sqrt{\frac{2k}{k-1}\left[\left(\frac{P_1}{P_0}\right)^{\frac{2}{k}}-\left(\frac{P_1}{P_0}\right)^{\frac{k+1}{k}}\right]} \qquad [8.52]$$

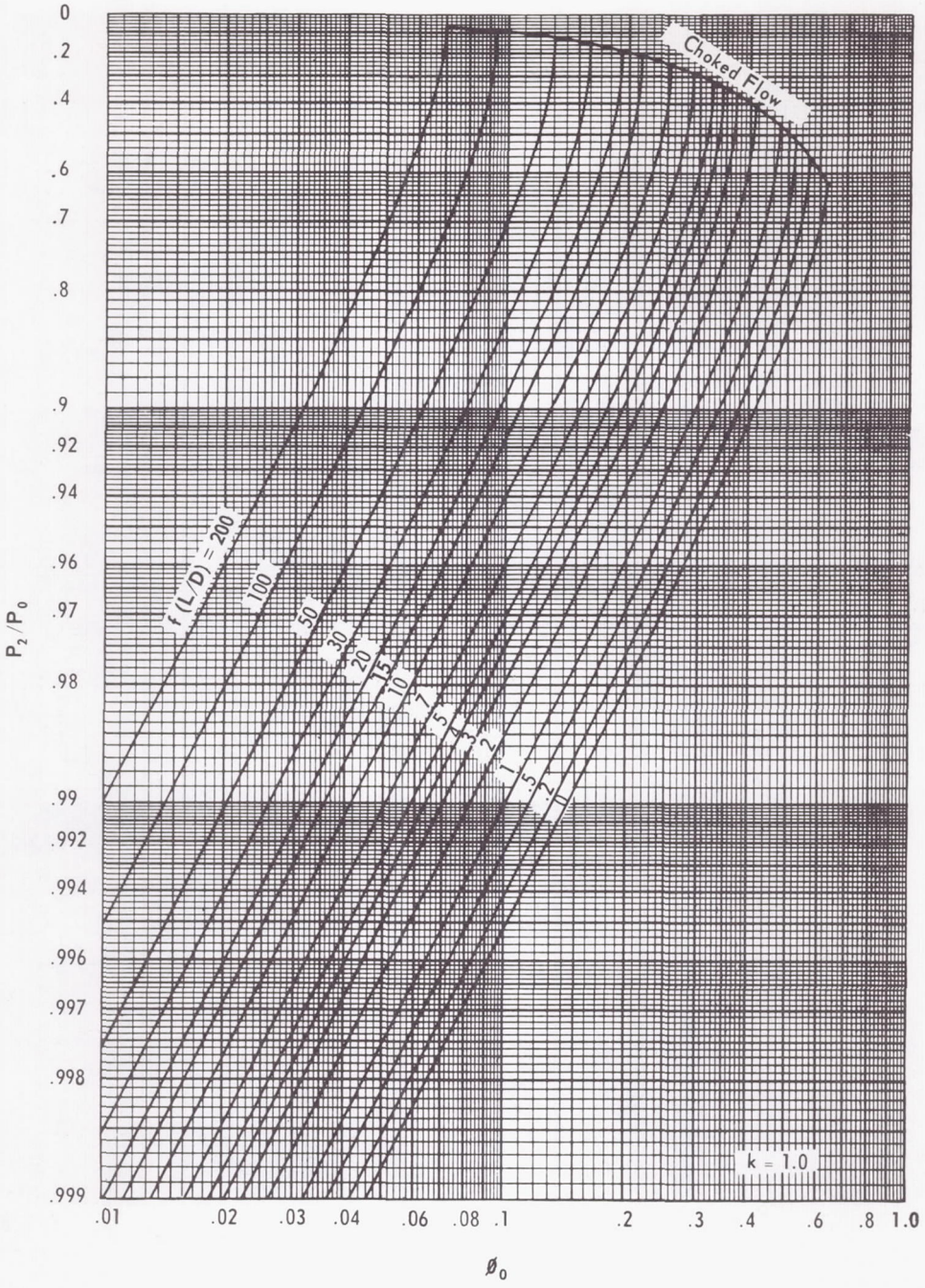


Figure 19.23. Compressible adiabatic flow with friction in constant-area pipes based on conditions in an upstream reservoir location, $k = 1.0$.

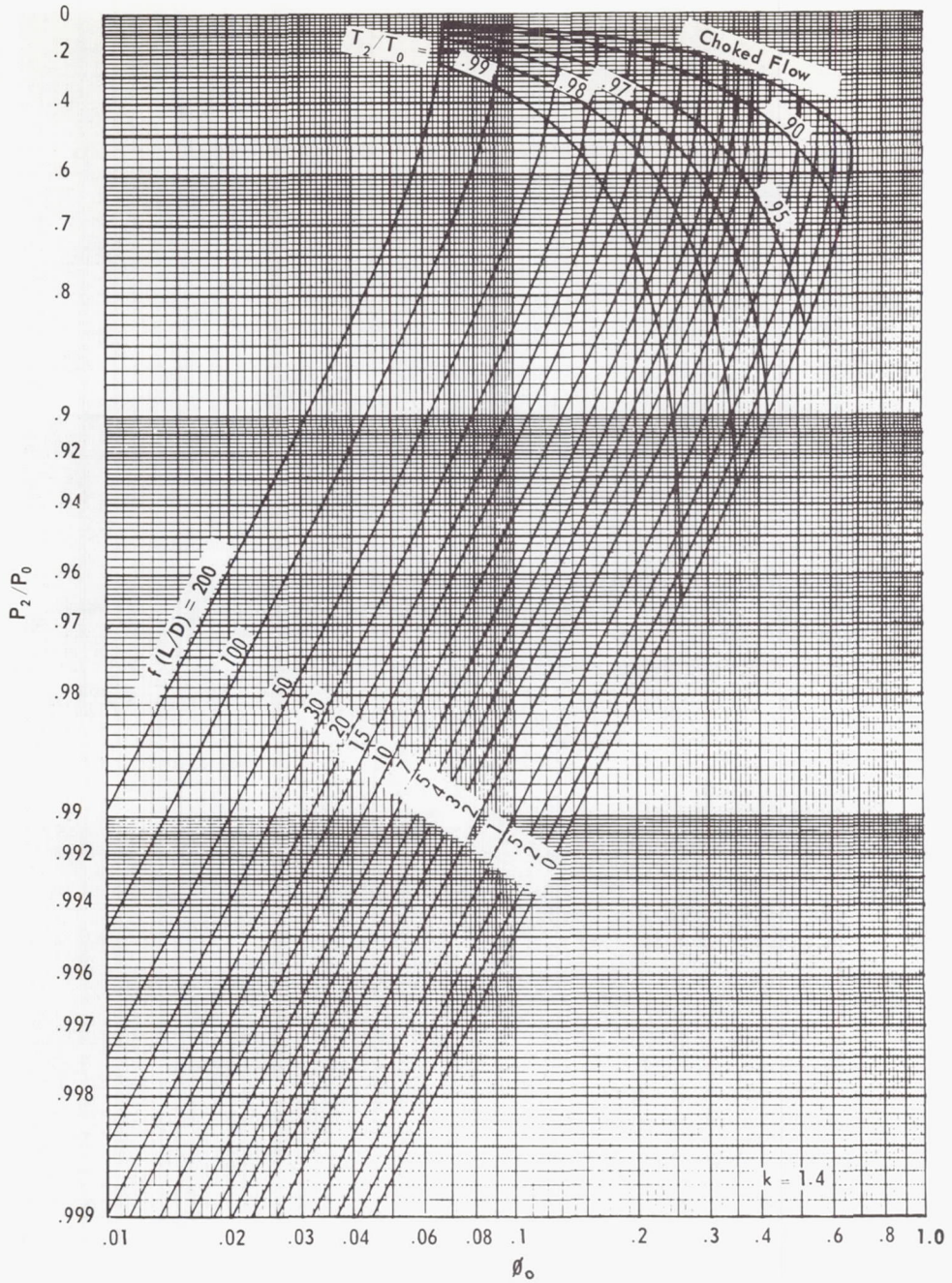


Figure 19.24. Compressible adiabatic flow with friction in constant-area pipes based on conditions in an upstream reservoir location, $k = 1.4$.

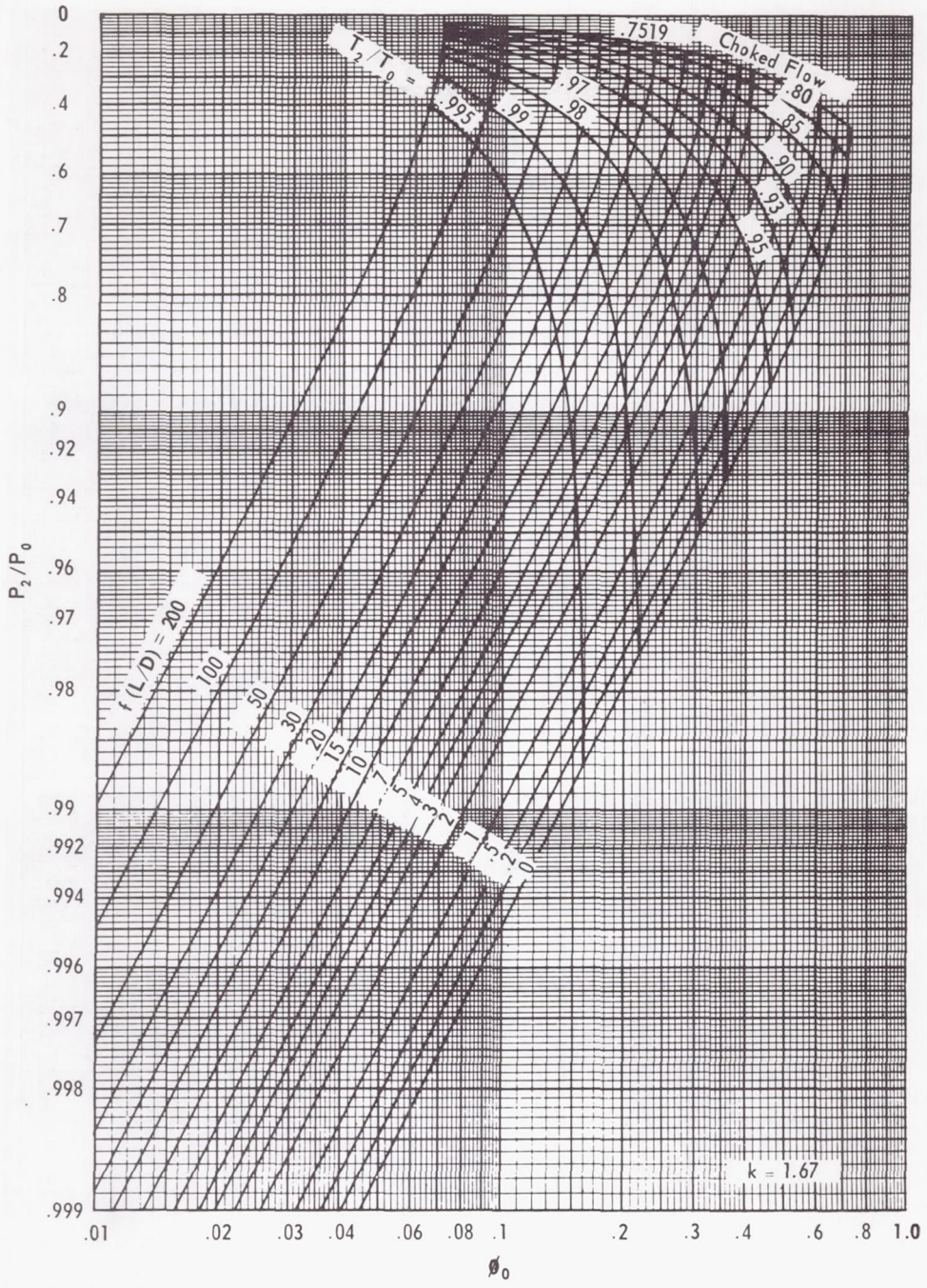


Figure 19.25. Compressible adiabatic flow with friction in constant-area pipes based on conditions in an upstream reservoir location, $k = 1.67$.

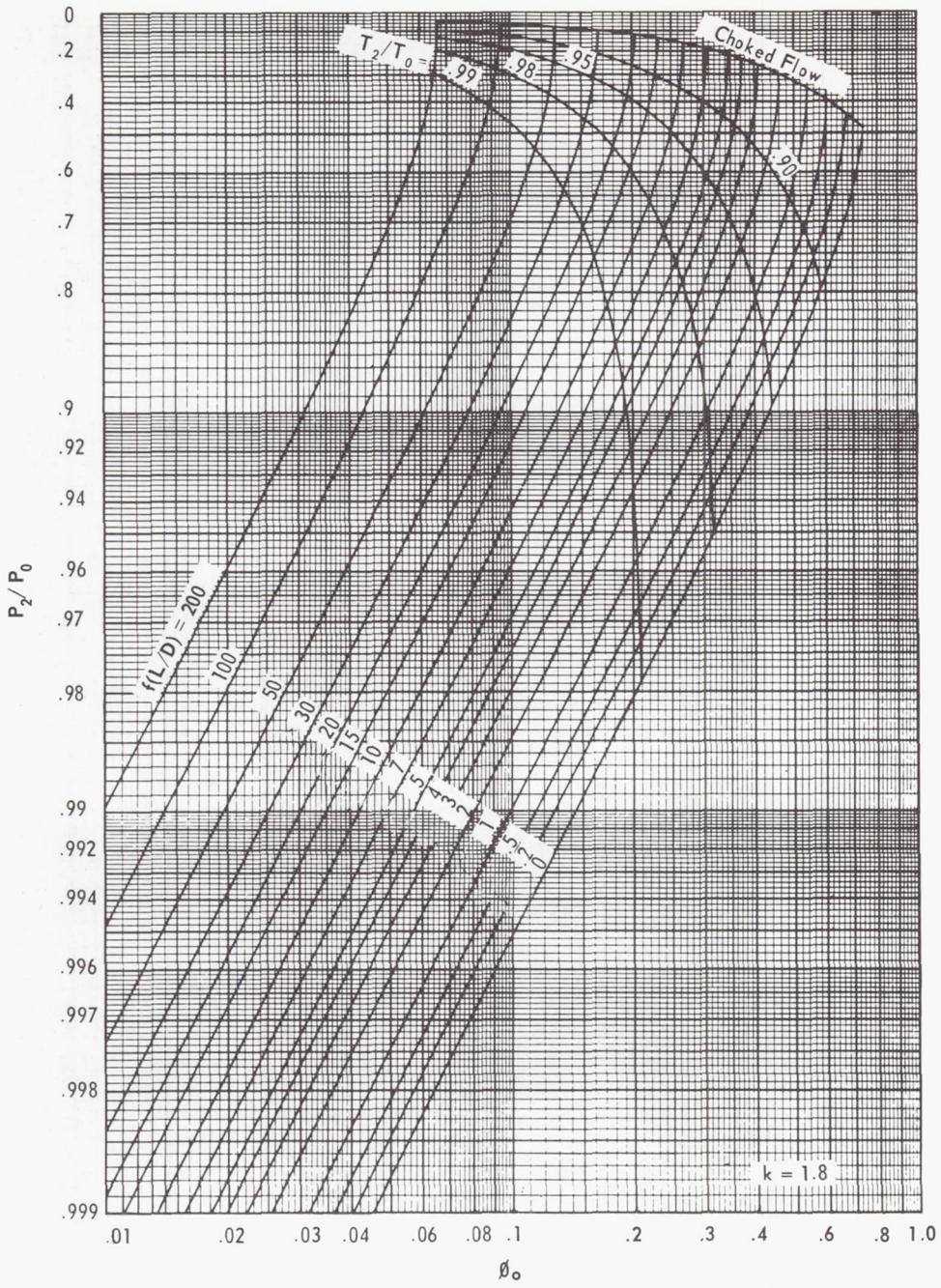


Figure 19.26. Compressible adiabatic flow with friction in constant-area pipes based on conditions in an upstream reservoir location, $k = 1.8$.

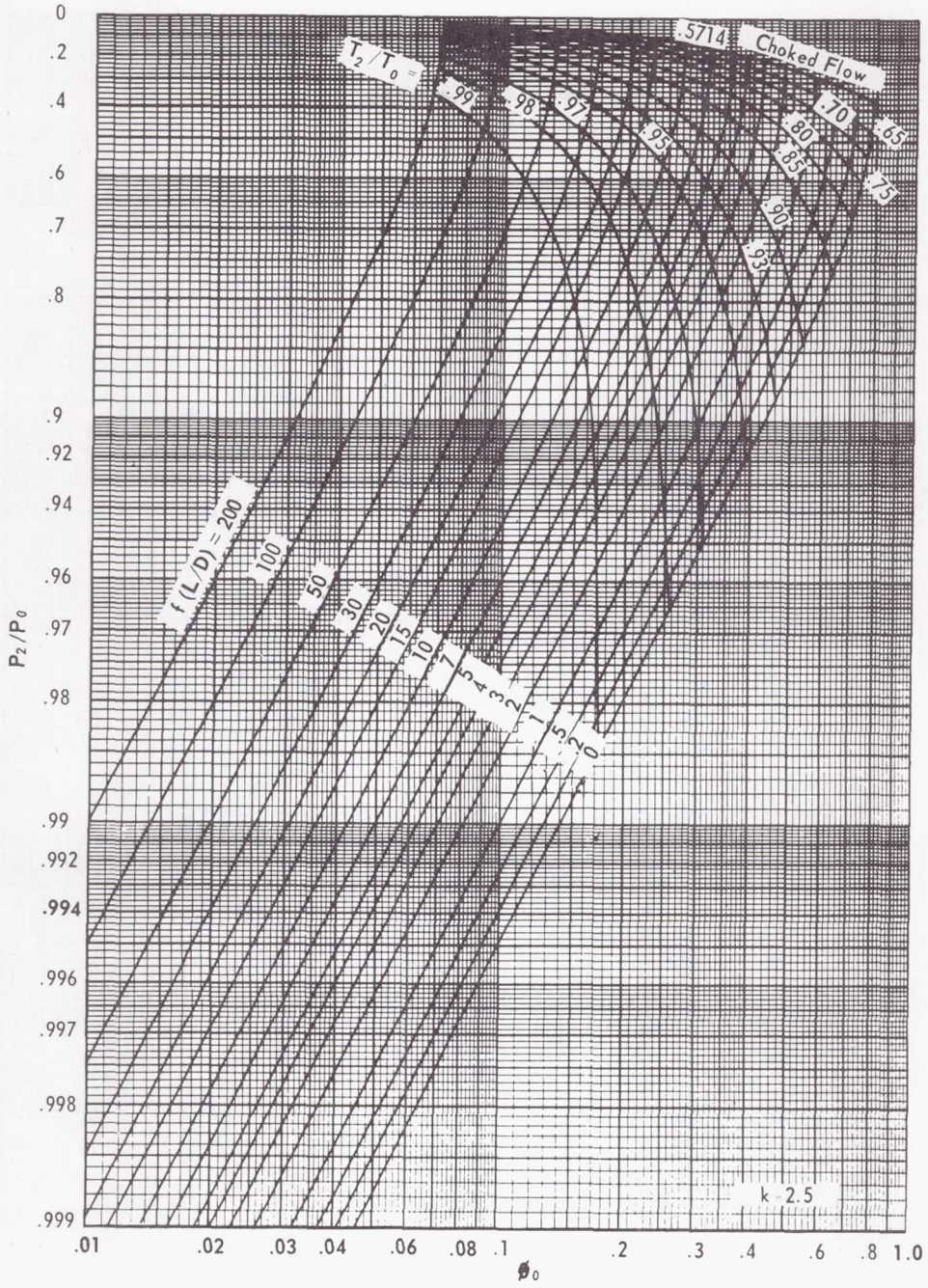


Figure 19.27. Compressible adiabatic flow with friction in constant-area pipes based on conditions in an upstream reservoir location, $k = 2.5$.

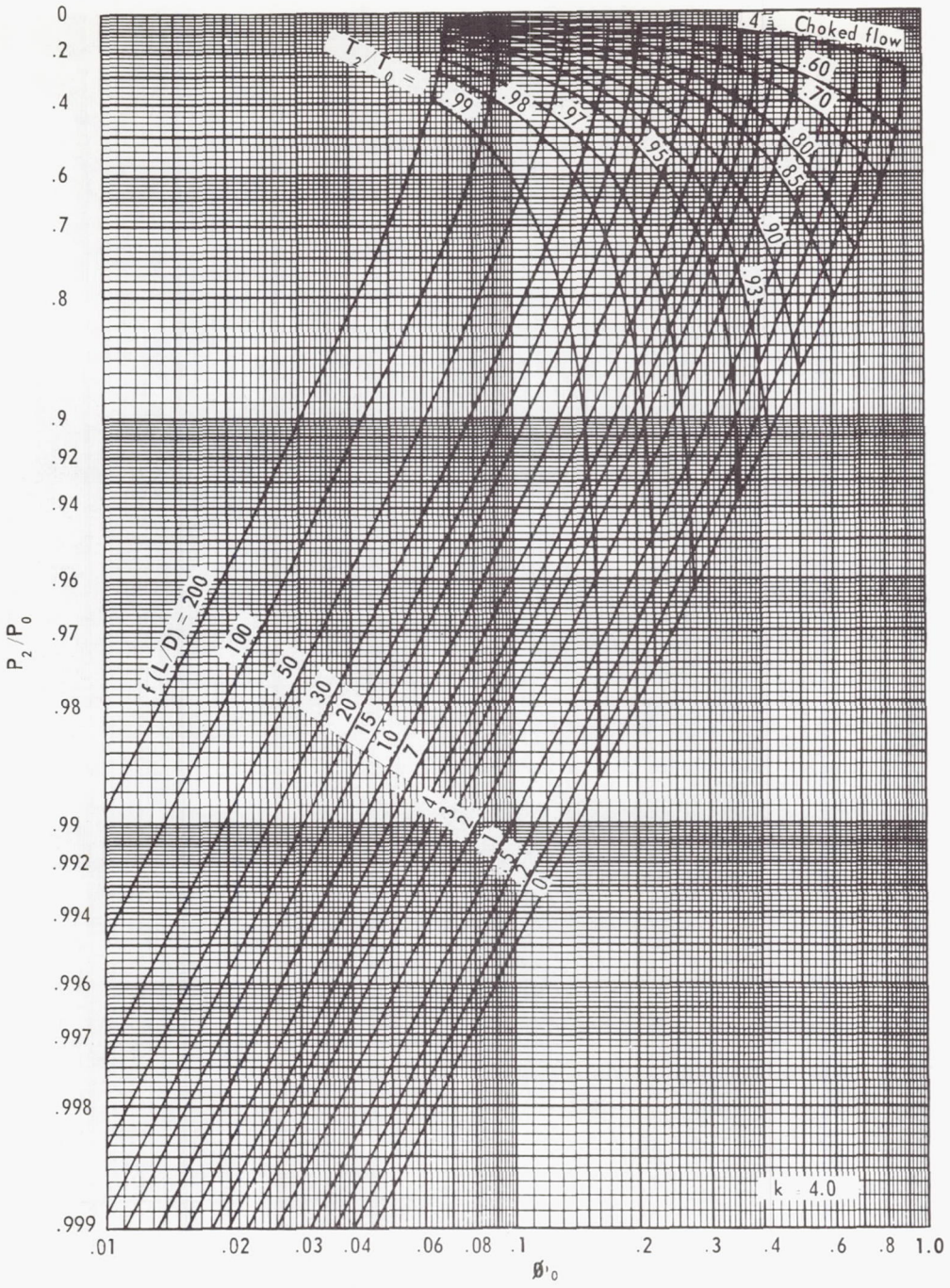


Figure 19.28. Compressible adiabatic flow with friction in constant-area pipes based on conditions in an upstream reservoir location, $k = 4.0$.

The constant-temperature ratio lines are obtained by combining equations (8.34), (8.46), and (8.50) and the perfect-gas law to obtain

$$\frac{P_2}{P_0}=\phi_0\left(\frac{T_2}{T_0}\right)\sqrt{\frac{\frac{k-1}{2k}}{1-\frac{T_2}{T_0}}} \qquad [8.53]$$

The sonic flow line can be derived by substituting into equation (8.19) the relationships

$$\frac{P^*}{P_1}=\left(\frac{\frac{P^*}{P_0}}{\frac{P_1}{P_0}}\right)$$

M_1 from equation (8.51), and p_1/p_0 from equation (8.45)

$$\frac{p^*}{p_0}=\phi_0\sqrt{\frac{2}{k(k+1)}} \qquad [8.54]$$

More convenient forms for computing ϕ_0, ϕ_1, and ϕ_2 can be obtained directly from equations (8.29) which are the convenient forms for computing M, since, in general, $\phi=\sqrt{k}(M)$. The only exception is that no real mach number can be associated with ϕ_0, which involves stagnation conditions. For example, if $\phi_0=\sqrt{k}(M_0)$, by necessity,

$$\phi_0=\sqrt{k}(M_0)=\sqrt{k}\left(\frac{V_0}{c_0}\right)=\sqrt{k}\left(\frac{\frac{w}{A\gamma_0}}{c_0}\right)$$

$$=\frac{w}{A}\left(\frac{1}{P_0}\right)\sqrt{\frac{RT_0}{g_c}}$$

Therefore, V_0 must be the velocity that would exist in the pipe if the fluid properties were that of stagnation, which they cannot physically be, and c_0 is the velocity of sound at the stagnation conditions.

For a perfect gas in circular pipes and pressure in psia,

$$\phi=0.2245\left(\frac{w}{pD^2}\right)\sqrt{RT} \qquad [8.55a]^*$$

$$\phi=15.21\left(\frac{\text{SCFM}}{1000\ pD^2}\right)\sqrt{\frac{T}{R}} \qquad [8.55b]^*$$

and, for ϕ_1 and ϕ_2 only

$$\phi=\frac{\frac{q}{A}}{c}=\frac{\frac{q}{A}}{\sqrt{kg_cRT}} \qquad [8.55c]^*$$

*This equation does not appear in chapter 8.

For imperfect gases, ϕ_1 and ϕ_2 can be obtained in terms of actual rates of volumetric flow using the actual sonic velocity of the gas c_a (charted in appendixes).

$$\phi = \sqrt{k_s}(M) = \sqrt{k_s}\left(\frac{V}{c_a}\right)$$

$$= \sqrt{k_s}\left(\frac{V}{\sqrt{k_s g_c ZRT}}\right) = \frac{\frac{q}{A}}{\sqrt{g_c ZRT}} \qquad [8.55d]^*$$

For ϕ_0, ϕ_1, and ϕ_2, in terms of weight flow rate

$$\phi = \frac{w}{AP}\left(\sqrt{\frac{ZRT}{g_c}}\right) = \frac{w}{AP}\left(\sqrt{\frac{Pv}{g_c}}\right) \qquad [8.55e]^*$$

and when written for circular pipes and for pressure in psia

$$\phi = 0.2245\left(\frac{w}{pD^2}\right)\sqrt{ZRT} \qquad [8.55f]^*$$

$$\phi = 15.21\left(\frac{\text{SCFM}}{1000\,pD^2}\right)\sqrt{\frac{ZT}{R}} \qquad [8.55g]^*$$

The properties in the preceding equations must be those existing at the location for which ϕ is being written. For example, writing equation (8.55f) specifically for ϕ_1 is

$$\phi_1 = 0.2245\left(\frac{w}{p_1 D^2}\right)\sqrt{Z_1 RT_1}$$

As with the real-gas mach number, the use of the real-gas value of ϕ obtained by the use of Z or c_a is only a partial compensation for the real-gas effects. The flow formulas and charts must be entered with the isentropic exponent k_s obtained from the following equations using the actual sonic velocity data or thermodynamic charts as described in chapter 4.

$$k_s = \frac{c_a^2}{g_c ZRT} = 3.105\left[\frac{\left(\frac{c_a}{1000}\right)^2}{Z\left(\frac{R}{100}\right)\frac{T}{100}}\right] = \frac{\ln\left(\frac{P_2}{P_1}\right)_s}{\ln\left(\frac{v_1}{v_2}\right)_s}$$

EXAMPLE PROBLEM 19.2

A high-pressure transmission line is to supply nitrogen to a pressure regulation station from a 4000-psig, 70° F, storage bottle at a design rate of 40 000 scfm. The total distance is 100 feet, and the line will contain ten 90° elbows and two Y-pattern globe valves. If the static-pressure loss in the entire line is not to exceed 10 percent of the upstream pressure at the design flow rate, determine the optimum line size.

*This equation does not appear in chapter 8.

SOLUTION

The chart for ϕ_0 will apply because of the upstream reservoir, and

$$\frac{P_2}{P_0} \geq 0.90$$

With the overall pressure loss as low as 10 percent, the elbows and valves can be accounted for with sufficient accuracy as equivalent lengths of pipe, or as K loss factors, added to the $f(L/D)$ computed for the straight lengths of pipe. Then from table 3.2 (ch. 3), the equivalent lengths are 30 diameters for standard elbows, up to 175 diameters for Y-pattern globe valves, and $f(L/D)$ is 0.5 for a square entrance.

Then the total equivalent length is

$$\frac{L}{D} = \frac{12(100)}{D} + 10(30) + 2(175) + \frac{0.5}{f}$$

which is seen to depend on the unknown pipe inside diameter, requiring that D be initially assumed here and checked later against the computed value. The friction factor is obtained from figure 3.4 (ch. 3) as a function of the Reynolds number, which is also dependent on the unknown diameter, and a value must be estimated. For commercial steel pipe, figure 3.4 (ch. 3) indicates a relative roughness of 0.00015, and if R_e is in the range of 10^6, $f \sim 0.014$. Then assuming f is 0.014 and that a pipe is to be used which has an inside diameter of 2 inches

$$f\left(\frac{L}{D}\right) \approx 0.014(1{,}250) + 0.5 = 18.0$$

Before the ϕ chart of the direct graphic solution can be entered, the isentropic exponent must be estimated for the real gas. At 70° F and 4,015 psia, figures C.2 and C.6 (app. C) yield $Z = 1.12$ and $c_a = 1{,}585$ ft/sec.

By equation (4.7)

$$k_s = 3.105\left[\frac{(1.585)^2}{(1.12)(0.552)(5.3)}\right]$$
$$= 2.38$$

Entering the ϕ_0 charts of figures 19.26 and 19.27 at

$$f\left(\frac{L}{D}\right) = 18$$

and at $P_2/P_0 = 0.90$, which allows 10 percent pressure loss, a value of $\phi_0 = 0.10$ is found to apply for any value of k_s between 1.8 and 2.5. Then the required pipe size D is obtained from equation (8.55g), solved for D^2

$$D^2 = 15.21\left[\frac{40\,000}{1000(4{,}015)(0.10)}\right]\sqrt{\frac{(1.12)(530)}{55.2}} = 4.97$$

so that $D = 2.23$ inches. The pipe-size data of appendix A specify internal diameters for 2½- and 3-inch, double extra-strong pipe as 1.771 and 2.30 inches, respectively, so that the 3-inch pipe is selected.

The pressure loss for the 3-inch pipe can now be computed directly. The value of ϕ_0 is computed from the previous value, since only D has changed

$$\phi_0 = 0.10\left(\frac{2.23}{2.30}\right)^2$$
$$= 0.094$$

The viscosity, from figure C.5 (app. C) at 4000 psig and 530° R, is 5.7×10^{-7} lbf-sec/ft². Then by equation (4.14)

$$R_e = \frac{(1.037)40\,000}{(2.30)(55.2)(5.7 \times 10^{-7})(32.2)}$$
$$= 1.78 \times 10^7$$

The friction factor, from figure 3.4 (ch. 3) at a relative roughness of 0.00015 and $R_e = 1.78 \times 10^{-7}$, is 0.0129. Then, as before, the frictional length is

$$f\left(\frac{L}{D}\right) = 0.0129\left[\frac{12(100)}{2.30} + 10(30) + 2(175)\right] + 0.5$$
$$= 15.62$$

Then from the ϕ_0 charts at $f(L/D) = 15.62$ and $\phi_0 = 0.094$

$$\frac{P_2}{P_0} = 0.922$$

for $k_s = 2.3$, interpolating between charts for $k_s = 1.8$ and 2.5. The temperature change is negligible as reflected by $(T_2/T_1) \approx 1.0$. The pressure loss will be 7.8 percent of the upstream pressure resulting in a downstream static pressure of

$$p_2 = 0.922(4015)$$
$$= 3700 \text{ psia} = 3685 \text{ psig}$$

Also, the static pressure loss is

$$\Delta p = p_1 - p_2 = 315 \text{ psid}$$

EXAMPLE PROBLEM 19.3

Determine the static pressure and temperature change that could be expected if the 2½-inch (nominal) pipe size had been selected in example problem 19.2. Also, determine the mach number and velocity at the upstream and downstream pipe locations.

SOLUTION

The inside diameter of the 2½-inch pipe was found to be 1.771 inches. Then, as before

$$\phi_0 = 15.21\left[\frac{40\,000}{1000(4015)(1.771)^2}\right]\sqrt{\frac{(1.12)(530)}{55.2}}$$
$$= 0.1587$$

$$R_e = 1.037\left[\frac{40000}{(1.771)(55.2)(5.7\times10^{-7})(32.2)}\right]$$
$$= 2.31\times10^{7}$$

At

$$R_e = 2.31\times10^{7} \qquad \text{and} \qquad \epsilon/D = 0.00015$$

figure 3.4 (ch. 3) yields $f = 0.0128$

$$f\left(\frac{L}{D}\right) = 0.0128\left[\frac{12(100)}{1.771} + 10(30) + 2(175)\right] + 0.5$$
$$= 17.5$$

Entering the ϕ_0 charts for $k_s = 1.8$ and 2.5, at $\phi_0 = 0.1587$ and $f(L/D) = 17.5$, yields by interpolation for $k_s = 2.38$

$$\frac{P_2}{P_0} = 0.720 \qquad \text{and} \qquad \frac{T_2}{T_0} = 0.986$$

Then

$$p_2 = 0.720(4015) = 2888 \text{ psia} = 2873 \text{ psig}$$

The pressure loss is

$$\Delta p = 4015 - 2888 = 1127 \text{ psid}$$

which is 28 percent of the upstream absolute pressure. Likewise, the downstream temperature is

$$T_2 = 0.986(530) = 522.5^\circ \text{ R} = 62.5^\circ \text{ F}$$

The temperature change is therefore -7.5° F.

The conditions at the pipe inlet 1, which in this case is just downstream of a square pipe entrance having an equivalent $f(L/D) = 0.5$, is read directly from the ϕ_0 chart at $f(L/D) = 0.5$ and $\phi_0 = 0.1587$. Note that in the low pressure-drop regions of the charts, the flow is essentially incompressible and the results are independent of k.

$$\left(\frac{P_2}{P_0}\right)_{\left[f\left(\frac{L}{D}\right)=0.5\right]} = \frac{P_1}{P_0} = 0.981$$

$$\left(\frac{T_2}{T_0}\right)_{\left[f\left(\frac{L}{D}\right)=0.5\right]} = \frac{T_1}{T_0} = 0.995$$

Then, by equation (8.51)

$$\phi_1 = \phi_0\left(\frac{\sqrt{\frac{T_1}{T_0}}}{\frac{P_1}{P_0}}\right) = 0.1587\left(\frac{\sqrt{0.995}}{0.981}\right)$$
$$= 0.1613$$

The value of ϕ_1 can also be obtained from ϕ_1 charts at P_2/P_1 and $f(L/D)$ evaluated between points 1 and 2

$$\frac{P_2}{P_1}=\frac{\frac{P_2}{P_0}}{\frac{P_1}{P_0}}=\frac{0.720}{0.981}=0.734$$

$$\left[f\left(\frac{L}{D}\right)\right]_{1-2}=17.5-0.5=17.0$$

Then, entering the ϕ_1 charts (interpolating for $k_s=2.38$) at $P_2/P_1=0.734$ and $f(L/D)=17.0$ yields the same value of ϕ_1 obtained in the preceding equation. Then, by definition,

$$M_1=\frac{\phi_1}{\sqrt{k_s}}=\frac{0.1613}{\sqrt{2.38}}$$
$$=0.1045$$

The velocity at location 1 is

$$V_1=M_1c_a=M_1\sqrt{k_sg_cZRT_0\left(\frac{T_1}{T_0}\right)}$$
$$=0.1045\sqrt{(2.38)(32.2)(1.12)(55.2)(530)(0.995)}$$
$$=165.1 \text{ ft/sec}$$

The downstream location 2 conditions are obtained directly from the ϕ_2 charts at the same value of $P_2/P_1=0.734$ and $[f(L/D)]_{1-2}=17.0$. For $k_s=2.38$, figures 19.17 and 19.18 yield

$$\phi_2=0.221$$

Then

$$M_2=\frac{\phi_2}{\sqrt{k_s}}=\frac{0.221}{\sqrt{2.38}}$$
$$=0.1432$$

The velocity at location 2 is

$$V_2=M_2c_a=M_2\sqrt{k_sg_cZRT_2}$$
$$=0.1432\sqrt{(2.38)(32.2)(1.12)(55.2)(522.5)}$$
$$=225.2 \text{ ft/sec}$$

It should be noted that the conditions computed for location 2 are approximate because of the changes in real-gas effects that are actually experienced over the wide pressure range encountered. For example, at the downstream conditions computed as $P_2=2888$ psia and $T_2=522.5°$ R, the values of Z, c_a, and k_s can be evaluated as 1.06, 1425 ft/sec, and 2.05, respectively. These changes from the upstream reservoir condition have not been accounted for in the analysis, since the upstream values were used as constants. The error can be reduced by applying the analysis to short segments of the pipeline, using recomputed real-gas constants for each segment. In this example, the error can be found to be almost negligible.

However, when higher pressures and higher mach numbers are encountered, the changes in real-gas constants can become much more significant, and the segmented solution should be used for greater accuracy.

CHOKING DUE TO FRICTION

The Fanno equations and direct graphic solutions developed in the previous paragraphs describe compressible pipe flow that does not exceed the maximum theoretical rates for a given piping system and that flow which is also shockless. Various choking processes prevent flow rates from exceeding some maximum rates in subsonic flow and cause shock waves to occur in supersonic flows. These complex processes are described in detail in chapter 8 and will not be repeated here. Some practical aspects are discussed in the following paragraphs with methods of evaluating flow problems that involve choking.

Subsonic Flow

In designing a piping system for subsonic flow of compressible fluids, it is possible to specify a pipe size and length and a flow rate that cannot be physically achieved. Such a situation is identified when the piping system frictional length $f(L/D)$ exceeds the $f(L_{max}/D)$, corresponding with the flow parameter (such as M or ϕ) computed for an upstream location. The maximum flow and/or maximum length can be identified using the chart of figure 19.8 or the choked flow lines of figures 19.11 through 19.28. If such a flow condition were physically attempted, with fixed upstream fluid conditions, the flow is said to become choked and reaches a maximum value less than originally specified or desired. The reduced flow rate and its associated reduced upstream flow parameters (M or ϕ) correspond with the computed value of $f(L/D)$ for the pipe, which is now $f(L_{max}/D)$, and the flow is choked (sonic) at the pipe exit. The reduced flow rate can be determined from the charts of $f(L_{max}/D)$, or the ϕ chart, and the definition of the flow parameter M (or ϕ), equations (8.29) and (8.55).

The preceding example presupposes that the back pressure at the pipe exit is sufficiently low to permit the flow to accelerate to sonic velocity. The required back pressure to produce choking, P^*, is also identified by the choked flow lines of the ϕ charts, or by figure 19.4 at the reduced mach number.

Choked flow can also be achieved by reducing the back pressure of a piping system until the choked condition is achieved at an increased flow rate. Such an increasing flow process can be directly identified as a constant $f(L/D)$ line on the ϕ charts of figures 19.11 through 19.28. Back-pressure reductions below the choked flow values occur outside the pipe and cause no further changes within the pipe.

Supersonic Flow

Supersonic flow in pipes is relatively uncommon, and the behavior can deviate considerably from the theoretical predictions. This is primarily due to the formation of viscous boundary layers as discussed in detail in chapter 6. However, it is important to note some of the characteristics of choking in supersonic flow.

Supersonic flow in pipes is generally produced by an upstream convergent-divergent nozzle, operating with a low back pressure. An important difference is that, in the supersonic case, the flow rate (w) is constant, as controlled by the upstream conditions and the size of the choked convergent-divergent nozzle upstream. Therefore, the flow conditions are defined by a single Fanno line, so long as the back pressure is maintained low enough to

choke the nozzle. Consequently, the concept of choking is slightly different in supersonic flow and is associated with the formation of normal shock waves within the pipe, rather than a limit on flow rate and/or pipe length. Shock waves can be caused by excessive back pressure or excessive pipe lengths, or both. An important similarity to subsonic flow is the existence of a maximum pipe length at which the flow will become sonic ($M = 1$) at the exit with shockless flow.

If the pipe length is less than L_{max}, as identified by some upstream flow conditions, and the back pressure P_g is less than that which will cause a normal shock at the pipe exit, the flow process will progress to the pipe exit along the supersonic part of the Fanno line. The back pressure can be equal to, less than, or slightly greater than the pipe-exit pressure. The higher back pressure P_g required to produce a normal shock at the exit can be identified from the normal shock functions of chapter 7, where the upstream conditions x are those described by the Fanno line at the pipe exit. Then, with $L < L_{max}$, and the back pressure less than P_g, the pipe flow is described by the Fanno line, and the flow leaves the pipe exit at a supersonic velocity. If the back pressure is P_g, or greater, a normal shock stands somewhere in the pipe dividing the pipe into regions of supersonic (upstream) and subsonic (downstream) flow. The pipe-exit pressure is now equal to the back pressure, since the exit velocities are subsonic. Increasing back pressure moves the normal shock upstream. The flow process can be analyzed by using the charted (or tabulated) Fanno-line equations for the subsonic and supersonic regions and the normal shock functions of chapter 7 that define the changes that occur across the shock wave.

If the pipe length is greater than L_{max}, a normal shock must exist at some upstream pipe location, regardless of the back pressure, so long as the convergent-divergent supply nozzle remains choked. The flow process is still defined by the Fanno-line equations (for a single Fanno line) and the normal shock functions. If the back pressure is greater than P^*, the pipe outlet flow will be subsonic, and the exit pressure will match the back pressure. If the back pressure is less than P^*, the downstream subsonic flow will become choked with sonic velocity existing at the exit. In this case, the expansion from the pipe-exit pressure of P^* to the back pressure occurs outside the pipe.

CHAPTER 20

APPLICATION OF NONADIABATIC FLOW IN PIPES

The three most important types of compressible flow through pipes with heat exchange are analyzed in this chapter. The least complex is that of isothermal flow, followed by a flow process with simple heating and negligible friction, and finally the most complex flow involving both friction and heat transfer.

ISOTHERMAL FRICTIONAL FLOW IN PIPES

Isothermal flow can be assumed for long pipelines and low mach-number flows. For such cases, the small amount of heat transfer required to maintain the flowing gas at the temperature of the surroundings can be assumed with accuracy. Although the low speed of such a flow causes a tendency toward incompressible flow, long frictional lengths cause large pressure losses and large associated density changes. The flow must therefore be treated as compressible, with essentially constant temperature.

Governing Equations

For isothermal flow (constant temperature), the perfect-gas law and definition of mach number can be written as

$$\frac{dP}{P}=\frac{d\gamma}{\gamma} \qquad [9.1]$$

and

$$\frac{dM^2}{M^2}=\frac{dV^2}{V^2}=2\left(\frac{dV}{V}\right) \qquad [9.2]$$

The continuity and momentum equations written for adiabatic flow in chapter 8 apply unchanged as

$$\frac{d\gamma}{\gamma}=-\left(\frac{1}{2}\right)\left(\frac{dV^2}{V^2}\right)=-\frac{dV}{V} \qquad [9.3]$$

and

$$\frac{dP}{P}+\left(\frac{kM^2}{2}\right)f\left(\frac{dL}{D}\right)+\left(\frac{kM^2}{2}\right)\left(\frac{dV^2}{V^2}\right)=0 \qquad [9.4]$$

325-994 O-69—27

Equations (9.1) through (9.4) can be combined to produce the following explicit relation between the frictional length and mach number, which can be integrated as follows in

$$\frac{dM^2}{M^2}=\left(\frac{kM^2}{1-kM^2}\right)f\left(\frac{dL}{D}\right) \qquad [9.5]$$

It should be noted before integrating that the factor $(1-kM^2)$ identifies the choked condition (where the factor becomes zero) at $M=1/\sqrt{k}$ in isothermal flow. This is in contrast to adiabatic flow where $M=1$ at the choked condition. Integrating equation (9.5) between the usual limits of a variable upstream mach number and pipe location where $L=0$, to the location of choking where $M=1/\sqrt{k}$ and $L=L_{max}$, yields

$$f\left(\frac{L_{max}}{D}\right)=\frac{1-kM^2}{kM^2}+\ln kM^2 \qquad [9.6]$$

Equation (9.5) can also be integrated between two arbitrary pipe locations separated by a frictional length $f(L/D)$ yielding

$$f\left(\frac{L}{D}\right)=\frac{1-kM_1^2}{kM_1^2}-\frac{1-kM_2^2}{kM_2^2}+\ln\left(\frac{M_1^2}{M_2^2}\right) \qquad [9.7]$$

By combination of the definition of mach number with the perfect-gas law and continuity, the following relation between pressure and mach number can be obtained for isothermal flow

$$\frac{P_1}{P_2}=\frac{M_2}{M_1} \qquad [9.9]$$

Equation (9.9) and the definition of the flow parameter $\phi[\phi_1=\sqrt{k}(M_1)]$ can be substituted into equation (9.7) to produce a closed-form equation relating the flow parameter and frictional length to the static pressure change with isothermal flow.

$$\phi_1=\frac{w}{A}\left(\frac{1}{P_1}\right)\sqrt{\frac{RT_1}{g_c}}=\left[\frac{1-\left(\frac{P_2}{P_1}\right)^2}{f\left(\frac{L}{D}\right)-\ln\left(\frac{P_2}{P_1}\right)^2}\right]^{1/2} \qquad [9.11]$$

Equation (9.11) can be used to predict pressure loss with isothermal flow of any perfect gas, regardless of k. The solution is found to coincide exactly with the direct graphic solutions for adiabatic flow of gases having a specific heat ratio of unity. Therefore, the ϕ_1 chart of chapter 19 plotted for $k=1.0$ can be used without approximation to analyze isothermal flow of any perfect gas when the upstream pipe conditions are known.

Equation (9.9) can also be substituted into equation (9.7) in such a way as to eliminate M_1. The resulting equation relates the pressure change and frictional length to the flow parameter written at the downstream location.

$$\phi_2 = \frac{w}{A}\left(\frac{1}{P_2}\right)\sqrt{\frac{RT_2}{g_c}} = \left[\frac{\left(\frac{P_2}{P_1}\right)^{-2} - 1}{f\left(\frac{L}{D}\right) - \ln\left(\frac{P_2}{P_1}\right)^2}\right]^{1/2} \qquad [9.12]$$

As with equation (9.11), this equation is found to coincide exactly with the direct graphic solutions for adiabatic flow for gases having $k = 1.0$. Therefore, the ϕ_2 chart of chapter 19 plotted for $k = 1.0$ can be used without approximation to analyze isothermal flow of any perfect gas when the downstream pipe conditions are known. A number of more practical forms useful in computing ϕ for perfect and real gases are presented as equations (8.55) in chapter 19.

Although the compressible flow from a reservoir to within a pipe entrance cannot usually be treated as isothermal, in the low mach numbers generally required of an isothermal assumption, the temperature change in the entrance is negligible. Therefore, it follows that the adiabatic ϕ_0 chart of chapter 19 plotted for $k = 1.0$ can also be applied to low mach number, isothermal flow of any perfect gas.

Additional equations can be written in logarithmic differential form to describe the changes in stagnation pressure and temperature. These can be combined with equations (9.1) through (9.4) and integrated to produce the following relationships that refer the changes to the conditions of choking (superscripted ** in isothermal flow where $M = M^{**} = 1/\sqrt{k}$).

$$\frac{P_0}{P_0^{**}} = \left[\frac{1}{(\sqrt{k})M}\right]\left\{\left(\frac{2k}{3k-1}\right)\left[1 + \left(\frac{k-1}{2}\right)M^2\right]\right\}^{\frac{k}{k-1}} \qquad [9.18]$$

$$\frac{T_0}{T_0^{**}} = \left(\frac{2k}{3k-1}\right)\left[1 + \left(\frac{k-1}{2}\right)M^2\right] \qquad [9.19]$$

Since the choked flow conditions are fixed in a given flow problem, the change that occurs between any two locations can be obtained by taking ratios of the parameter evaluated at the two locations such as

$$\frac{P_{02}}{P_{01}} = \frac{\left(\frac{P_0}{P_0^{**}}\right)_2}{\left(\frac{P_0}{P_0^{**}}\right)_1}$$

Required Heat Transfer

The heat that must be added between any two points to maintain the isothermal condition is computed from the change in stagnation temperature.

$$Q'_{1-2} = c_p(T_{02} - T_{01}) \qquad [9.20]$$

Substituting the stagnation temperature change (obtained by the method described above) and equation (9.9) (to eliminate the mach number), the heat transfer required is

$$\frac{Q'_{1-2}}{c_p T_{01}} = \frac{\frac{k-1}{2}\left[\left(\frac{P_2}{P_1}\right)^{-2} = 1\right]}{\frac{k}{\phi_1^2} + \frac{k-1}{2}} \qquad [9.22]$$

and

$$\frac{Q'_{1-2}}{c_p T_{02}} = \frac{\frac{k-1}{2}\left[1 - \left(\frac{P_2}{P_1}\right)^{2}\right]}{\frac{k}{\phi_2^2} + \frac{k-1}{2}} \qquad [9.23]$$

where ϕ is substituted for M of equations (9.22) and (9.23) in chapter 9. Equations (9.22) and (9.23) apply when the upstream and downstream pipe conditions, respectively, are known, and the necessary pressure data can be obtained from the ϕ charts of chapter 19 plotted for $k = 1.0$.

FRICTIONLESS FLOW IN PIPES WITH HEAT EXCHANGE

A simple, compressible flow process with heat transfer and no friction is seldom attained. However, the condition can be approached when the heat-transfer rate is high and the pipe length is relatively short so that the frictional effects are negligible relative to that of heat transfer.

The Rayleigh Line

Just as the Fanno line describes the adiabatic frictional flow of compressible fluids in pipes, the Rayleigh line describes the flow with heat transfer in the absence of friction (simple T_0 change). The impulse function (eq. (5.39)) is a constant in constant-area, frictionless flow. Combining this function with the continuity equation yields the Rayleigh-line equation

$$P + \frac{G^2}{g_c \gamma} = P + \left(\frac{G^2}{g_c}\right) v = \frac{Fi}{A} = \text{constant} \qquad [9.24]$$

The Rayleigh line can be plotted on an h–s diagram in the same manner as the Fanno line. Once again, the point of maximum entropy identifies the point of choking where $M = 1.0$. The upper portion of the curve describes the subsonic flow process, and the lower portion describes the supersonic flow. Heating processes follow the lines to the right (increasing entropy) and cooling processes toward the left (decreasing entropy). (See fig. 9.1, ch. 9.)

Governing Equations

As in previous derivations, the relationships defining a perfect-gas, mach-number, and the stagnation properties are combined with the conservation laws of mass, momentum, and energy, written in accordance with the boundary conditions of the problem. Thus, it is possible to write the equations in integrated form at the two pipe locations of interest. Simultaneous solution yields the following relations between the fluid properties and the mach number at the two locations.

$$\frac{P_2}{P_1}=\frac{1+kM_1^2}{1+kM_2^2} \qquad [9.26]$$

$$\frac{T_2}{T_1}=\left[\frac{M_2(1+kM_1^2)}{M_1(1+kM_2^2)}\right]^2 \qquad [9.29]$$

$$\frac{\gamma_2}{\gamma_1}=\frac{V_1}{V_2}=\left(\frac{M_1}{M_2}\right)^2\left(\frac{1+kM_2^2}{1+kM_1^2}\right) \qquad [9.30]$$

$$\frac{s_2-s_1}{c_p}=\ln\left[\left(\frac{M_2}{M_1}\right)^2\left(\frac{1+kM_1^2}{1+kM_2^2}\right)^{\frac{k+1}{k}}\right] \qquad [9.31]$$

$$\frac{P_{02}}{P_{01}}=\left(\frac{1+kM_1^2}{1+kM_2^2}\right)\left[\frac{1+\left(\frac{k-1}{2}\right)M_2^2}{1+\left(\frac{k-1}{2}\right)M_1^2}\right]^{\frac{k}{k-1}} \qquad [9.32]$$

$$\frac{T_{02}}{T_{01}}=\left[\frac{M_2\,(1+kM_1^2)}{M_1\,(1+kM_2^2)}\right]^2\left[\frac{1+\left(\frac{k-1}{2}\right)M_2^2}{1+\left(\frac{k-1}{2}\right)M_1^2}\right] \qquad [9.33]$$

Equations (9.26) through (9.33) yield the changes in fluid properties and velocity only if the mach number for each of the two locations is known independently of the heat transfer. The heat transfer causes a change in stagnation temperature, which is then used to establish the mach number by equation (9.33). The necessary key relation between heat transfer and stagnation temperature can be obtained from the steady-flow energy equation which yields, in the absence of work and elevational change,

$$Q'=c_p\,(T_{02}-T_{01})$$

and

$$\frac{T_{02}}{T_{01}}=1+\frac{Q'}{c_pT_{01}} \qquad [9.34]$$

The equation can also be written in terms of rates of heat transfer and mass flow as

$$\frac{T_{02}}{T_{01}}=1+\frac{\dot{Q}}{wc_pT_{01}} \qquad [9.35]$$

When this expression for stagnation temperature is substituted into equation (9.33), the unknown mach number can theoretically be computed. However, because of the complexity of the function, a charted or tabulated solution is required to establish the unknown mach number at the given stagnation temperature ratio. In addition, the existence of both M_1 and M_2 in the equation imposes a plotting problem which makes it necessary, once again, to normalize the equation. This is done by normalizing the variable properties and mach num-

ber to the choked conditions, where $M=1$, and the properties are superscripted with an *. The Rayleigh-line equations then become

$$\frac{P}{P^*}=\frac{k+1}{1+kM^2} \qquad [9.36]$$

$$\frac{T}{T^*}=\left[\frac{(k+1)M}{1+kM^2}\right]^2 \qquad [9.37]$$

$$\frac{V}{V^*}=\frac{\gamma^*}{\gamma}=\frac{(k+1)M^2}{1+kM^2} \qquad [9.38]$$

$$\frac{s-s^*}{c_p}=\ln\left[M^2\left(\frac{k+1}{1+kM^2}\right)^{\frac{k+1}{k}}\right] \qquad [9.39]$$

$$\frac{P_0}{P_0^*}=\left(\frac{k+1}{1+kM^2}\right)\left\{\frac{2\left[1+\left(\frac{k-1}{2}\right)M^2\right]}{k+1}\right\}^{\frac{k}{k-1}} \qquad [9.40]$$

$$\frac{T_0}{T_0^*}=\frac{2(k+1)M^2\left[1+\left(\frac{k-1}{2}\right)M^2\right]}{(1+kM^2)^2} \qquad [9.41]$$

Equations (9.36) through (9.41) are plotted in figure 20.1 for $k=1.4$ and $k=1.67$. The use of this working chart is demonstrated in the following example problem.

EXAMPLE PROBLEM 20.1

Air at 100 psia is being heated in a once-through heat-exchanger tube. The airflow is 0.40 lbm/sec, the tube inside diameter is 0.81 in., and the inlet air temperature is 70° F. The heat input is 7.5 Btu/sec. Determine the static pressure and temperature at the tube exit.

SOLUTION

The inlet mach number is determined most easily by the practical form of equation (8.29*a*) in chapter 19.

$$M_1=0.2245\left[\frac{0.40}{(100)(0.81)^2}\right]\sqrt{\frac{(53.3)(530)}{1.4}}=0.1947$$

At $M_1=0.1947$, figure 20.1 yields $(T_0/T_0^*)_1=0.1654$. Also $(P/P^*)_1=2.279$ and $(T/T^*)_1=0.1970$.

By equation (9.35), the downstream-to-upstream stagnation temperature is computed in terms of the heat transfer and flow rates and the initial stagnation temperature. The value of T_{01} is evaluated at $M_1=0.1947$, using the isentropic functions of chapter 16, figure 16.1, yields

$$\frac{T_1}{T_{01}}=0.9922$$

so that

$$T_{01} = \frac{530}{0.9922}$$

$$= 534.0^\circ \text{ R}$$

Then, by equation (9.35)

$$\frac{T_{02}}{T_{01}} = 1 + \frac{7.5}{(0.40)(0.24)(534)}$$

$$= 1.1462$$

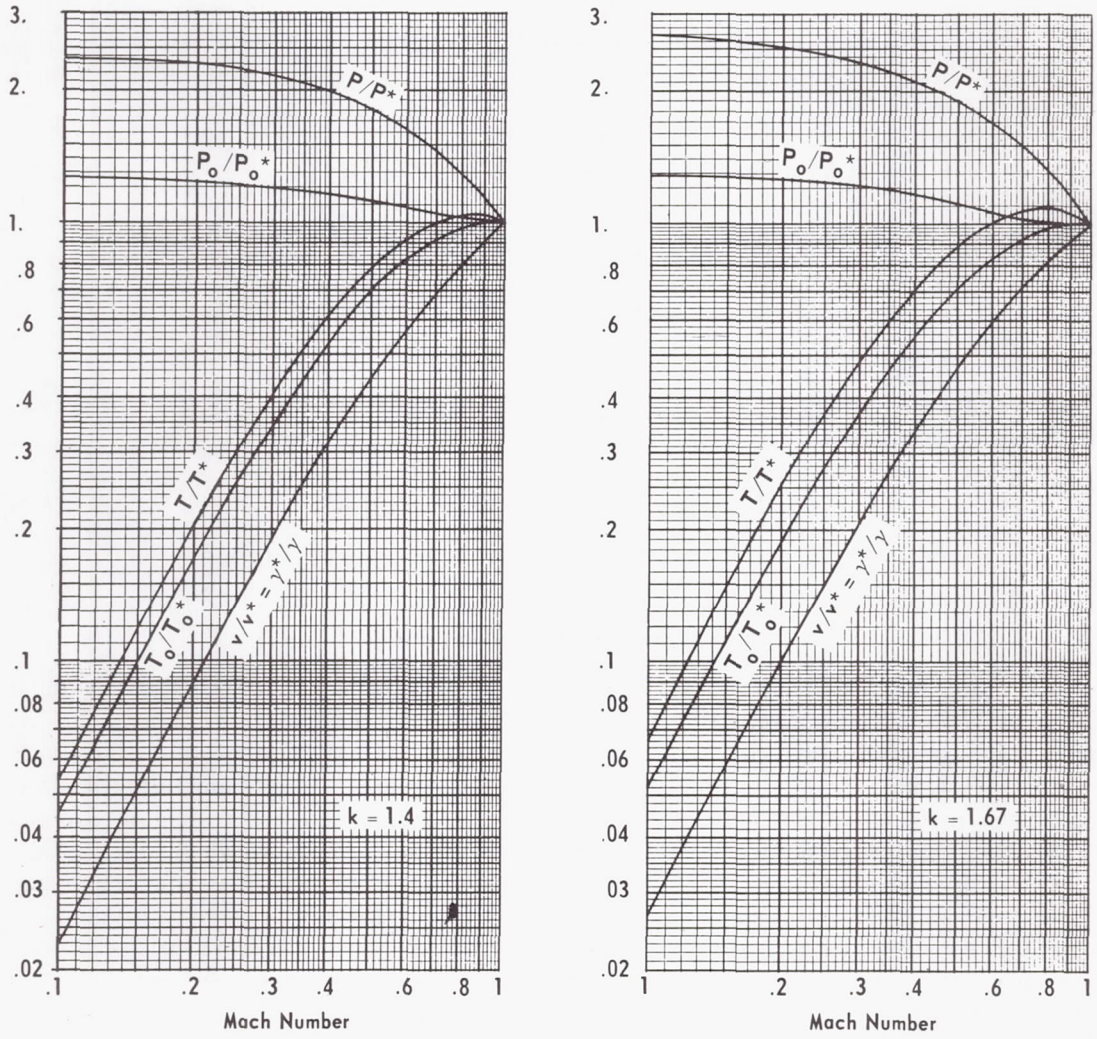


Figure 20.1. Frictionless pipe flow with heat exchange (simple T_0 change).

and since

$$\frac{T_{02}}{T_0^*}=\left(\frac{T_0}{T_0^*}\right)_2=\left(\frac{T_{02}}{T_{01}}\right)\left(\frac{T_0}{T_0^*}\right)_1$$

$$\frac{T_{02}}{T_0^*}=(1.1462)(0.1654)$$
$$=0.1898$$

The exit mach number is now read at $(T_0/T_0^*)_2=0.1898$ in figure 20.1 as $M_2=0.2102$. At the same exit mach number, the exit pressure and temperature ratios are read as $(P/P^*)_2=2.2601$ and $(T/T^*)_2=0.2257$. Then the outlet static pressure is computed from

$$\frac{P_2}{P_1}=\frac{\left(\frac{P}{P^*}\right)_2}{\left(\frac{P}{P^*}\right)_1}=\frac{2.2601}{2.2790}=0.9917$$

so that

$$P_2=P_1\left(\frac{P_2}{P_1}\right)=(100)(0.9917)=99.17 \text{ psia}$$

Similarly, the outlet static temperature is computed from

$$\frac{T_2}{T_1}=\frac{\left(\frac{T}{T^*}\right)_2}{\left(\frac{T}{T^*}\right)_1}=\frac{0.2257}{0.1970}=1.1457$$

so that

$$T_2=T_1\left(\frac{T_2}{T_1}\right)=530(1.1457)=607.2^\circ \text{ R}$$
$$=147.2^\circ \text{ F}$$

Choking Effects of Heating

The previous discussion of the Rayleigh-line characteristics pointed out that heating of subsonic and supersonic flows causes the flow process to proceed toward the point of choking at $M=1.0$, with the corresponding increase in entropy. If sufficient heat is added to a subsonic flow, the flow will become choked in the constant-area pipe and any further heating will cause a reduction in flow rate. In general, the effects of friction in such a case can seldom be neglected, since the frictional effects at high subsonic flow are usually very significant. The effects of friction can be expected to rush the process to the point of choking. In the case of supersonic flow, if more heat is added than that necessary to cause choking, a normal shock will exist in the divergent section of the convergent-divergent nozzle generating the supersonic pipe flow. Therefore, the upstream mach number will be reduced as in choked subsonic flow, but now as a result of changes in fluid properties rather than a reduced flow rate. A more detailed description of choking with simple T_0 change can be found in Shapirc (1953).

PIPE FLOW WITH COMBINED FRICTION AND HEAT TRANSFER

Reynolds analogy, which relates the coefficients of heat transfer and friction, is indicative of the close ties that exist between the processes of heat transfer and friction. In fact, the analogy identifies the direct proportion relation between the two coefficients, with other quantities being constant. Therefore, it can be said that the heat transfer between the pipe wall and the flowing stream is not only proportional to the temperature difference but also directly proportional to the coefficient of friction. Therefore, if a significant temperature difference exists between the pipe and the flowing gas and if the pipe has a significant frictional length, then the effects of both friction and heat transfer must be considered simultaneously in the analysis.

General Analysis

The heat transferred to the flowing gas is reflected as a change in stagnation enthalpy and for a perfect gas as a change in stagnation temperature. The heat transferred is also described in terms of the heat-transfer coefficient and temperature difference. Then

$$w\,\mathrm{d}Q' = \gamma A V c_p\,\mathrm{d}T_0 = h_q\,\mathrm{d}A_w(T_w - T_{\mathrm{aw}}) \qquad [9.43]$$

Substituting the definition of hydraulic diameter, $\mathrm{d}A_w = 4A(\mathrm{d}L/D)$ yields

$$\frac{\mathrm{d}T_0}{T_w - T_{\mathrm{aw}}} = \left(\frac{4h_q}{Vc_p\gamma}\right)\frac{\mathrm{d}L}{D}$$

Assuming the adiabatic wall temperature T_{aw} to be T_0 (only a slight inaccuracy), the heat-transfer equation becomes

$$\frac{\mathrm{d}T_0}{T_w - T_0} = \left(\frac{4h_q}{Vc_p\gamma}\right)\frac{\mathrm{d}L}{D} \qquad [9.44]$$

By further assuming Reynolds analogy to be accurate (proven generally accurate to within a few percent with fully developed gas flow in pipes)

$$\frac{hq}{Vc_p\gamma} = \frac{f}{8}$$

Equation (9.44) reduces to

$$\frac{\mathrm{d}T_0}{T_w - T_0} = \left(\frac{f}{2D}\right)\mathrm{d}L \qquad [9.45]$$

Equation (9.45) provides the direct integrable relation between the change in stagnation temperature and frictional length. The determination of the changes in other fluid properties requires a more thorough analysis of the flow process. Equations (8.1), (8.2), (8.4), and (8.5) (ch. 8) are found to be valid in this problem on inspection. Also, the steady-flow energy equation can be applied and, in the absence of work and elevational change, yields

$$\frac{\mathrm{d}Q}{c_pT} = \frac{\mathrm{d}T}{T} + \left(\frac{k-1}{2}\right)M^2\left(\frac{\mathrm{d}V^2}{V^2}\right) \qquad [9.46]$$

The isentropic stagnation temperature change can be written in logarithmic differential form as

$$\frac{dT_0}{T_0}=\frac{dT}{T}+\left[\frac{\left(\frac{k-1}{2}\right)M^2}{1+\left(\frac{k-1}{2}\right)M^2}\right]\frac{dM^2}{M^2} \qquad [9.47]$$

The four equations from chapter 8 and equations (9.45), (9.46), and (9.47) comprise seven equations in eight variables. These can be solved simultaneously to produce equation (9.49).

$$\frac{dM^2}{M^2}=\left\{\frac{(1+kM^2)\left[1+\left(\frac{k-1}{2}\right)M^2\right]}{1-M^2}+\left(\frac{kM^2\left[1+\left(\frac{k-1}{2}\right)M^2\right]}{1-M^2}\right)\left(\frac{2T_0}{T_w-T_0}\right)\right\}\frac{dT_0}{T_0} \qquad [9.49]$$

Equations (9.45) and (9.49) provide the means for solving the compressible pipe flow problems involving combined heat transfer and friction. Because of mathematical complexity, equation (9.49) cannot be integrated to produce a closed solution. Therefore, a numerical or graphical integration is required, along with a more detailed specification of the manner in which T_0 changes. The cases of constant wall temperature and constant heat flux will be developed below, including approximate closed solutions for low mach numbers. After the changes in M and T_0 are obtained by the numerical integration, or approximate methods, the other fluid property changes can be determined directly by the following equations developed strictly from continuity and definitions

$$\frac{P_2}{P_1}=\left(\frac{M_1}{M_2}\right)\sqrt{\frac{T_2}{T_1}} \qquad [9.50]$$

$$\frac{\gamma_2}{\gamma_2}=\left(\frac{M_1}{M_2}\right)\sqrt{\frac{T_1}{T_2}} \qquad [9.51]$$

$$\frac{V_2}{V_1}=\frac{\gamma_1}{\gamma_2} \qquad [9.52]$$

$$\frac{T_2}{T_1}=\left(\frac{T_{02}}{T_{01}}\right)\left[\frac{1+\left(\frac{k-1}{2}\right)M_1^2}{1+\left(\frac{k-1}{2}\right)M_2^2}\right] \qquad [9.53]$$

$$\frac{P_{02}}{P_{01}}=\left(\frac{P_2}{P_1}\right)\left[\frac{1+\left(\frac{k-1}{2}\right)M_2^2}{1+\left(\frac{k-1}{2}\right)M_1^2}\right]^{\frac{k}{k-1}} \qquad [9.54]$$

Constant Wall Temperature

In some cases the pipe-wall temperature can be assumed to be constant, such as when the pipe is surrounded by a boiling or condensing liquid. Then equation (9.45) can be integrated to produce the following direct relation between stagnation temperature and pipe-length. (The following equation is a simplified version of the equation in ch. 9.)

$$f\left(\frac{L_2}{D}\right)=2\ln\left[\frac{\frac{T_w}{T_{01}}-1}{\frac{T_u}{T_{01}}-\frac{T_{02}}{T_{01}}}\right] \qquad [9.55a]$$

and rearranged,

$$\frac{T_{02}}{T_{01}}=\frac{T_w}{T_{01}}-\left(\frac{T_w}{T_{01}}-1\right)e^{-\lambda fL_2/2D} \qquad [9.55b]$$

As stated previously, the evaluation of the other fluid property changes in the pipe requires a difficult numerical or graphical integration of equation (9.49). Except for low mach numbers, a digital-computer solution is recommended. For $M \lesssim 0.3$, the approximate solution outlined in the remaining part of this chapter yields accurate results.

As pointed out previously, equations (8.1), (8.2), (8.4), and (8.5) (ch. 8) apply. These equations can be combined with the definitions of stagnation temperature and pressure and equation (9.45) to produce

$$\frac{dP_0}{P_0}=\frac{d\left(\frac{P_0}{P_{01}}\right)}{\left(\frac{P_0}{P_{01}}\right)}=-kM^2\left(\frac{f}{2D}\right)\left(\frac{T_w-T_0}{2T_0}+1\right)dL \qquad [9.56]$$

By generalizing the downstream location and conditions, equations (9.50), (9.53), and (9.54) can be combined to yield

$$M^2=\left(\frac{P_{01}}{P_0}\right)^2\left(\frac{T_0}{T_{01}}\right)\left[\frac{1+\left(\frac{k-1}{2}\right)M^2}{1+\left(\frac{k-1}{2}\right)M_1^2}\right]^{\frac{k+1}{k-1}}M_1^2 \qquad [9.57]$$

This expression for M^2 can be substituted into equation (9.56). Now, for low mach numbers, the change in the bracketed term will be very small so that the term can be assumed to be a constant at the average value of the expression

$$\frac{1}{2}\left[1+\left(\frac{P_{02}}{P_{01}}\right)^2\left(\frac{T_{01}}{T_{02}}\right)\quad\left(\frac{M_2}{M_1}\right)^2\right]$$

as obtained from averaging equation (9.57). On this basis, equation (9.56) can be integrated to produce

$$\left(\frac{P_{02}}{P_{01}}\right)^2=1-\left(\frac{k}{2}\right)M_1^2\left[1+\left(\frac{P_{02}}{P_{01}}\right)^2\left(\frac{T_{01}}{T_{02}}\right)\left(\frac{M_2}{M_1}\right)^2\right]\frac{f}{2D}\int_0^{L_2}\left(\frac{T_w}{T_{01}}+\frac{T_0}{T_{01}}\right)dL \qquad [9.60]$$

Finally, by generalizing the downstream location in equation (9.55*b*), substituting into equation (9.60), and integrating, the following equation for stagnation pressure change is obtained

$$\left(\frac{P_{02}}{P_{01}}\right)^2 = 1 - \left(\frac{k}{2}\right) M_1^2 \left[1 + \left(\frac{P_{02}}{P_{01}}\right)^2 \left(\frac{T_{01}}{T_{02}}\right) \left(\frac{M_2}{M_1}\right)^2\right] \left\{\left[f\left(\frac{L_2}{D}\right)\right] \left(\frac{T_w}{T_{01}}\right) + \left(\frac{T_w}{T_{01}} - 1\right) \left(e^{-fL_2/2D} - 1\right)\right\} \qquad [9.61]$$

The existence of unknown terms in the equation requires a trial-and-error solution. A first trial can be made by assuming the entire bracketed term in which the unknown terms P_{02} and M_2 exist to have a value of 2. With the computed value of P_{02}/P_{01}, a second trial can be made in combination with a value of T_{02}/T_{01}, from equation (9.55*b*). The value of M_2 can be obtained most easily from the isentropic area ratio function plotted in figure 16.6 (ch. 16). Because of a coincidental similarity in the mach-number functions of equation (9.57) and that of (A/A^*), M_2 in figure 16.6 (ch. 16) can be read at a value of

$$\left(\frac{A}{A^*}\right)_{M_2} = \frac{\left(\frac{A}{A^*}\right)_{M_1} \left(\frac{P_{02}}{P_{01}}\right)}{\sqrt{\frac{T_{02}}{T_{01}}}} \qquad [9.62]$$

The ratio $(A/A^*)_{M_1}$ is read at M_1, and (P_{02}/P_{01}) is the approximate value computed in the previous trial. The solution should be iterated until sufficient agreement is reached between the assumed and computed values of P_{02}/P_{01}. The procedure also establishes the value of M_2/M_1, which is then used to compute the other fluid property changes using equations (9.50) through (9.53).

The heat transfer per unit mass is computed from the change in stagnation temperature as

$$Q' = c_p(T_{02} - T_{01}) = c_p T_{01} \left(\frac{T_{02}}{T_{01}} - 1\right) \qquad \text{Btu/lbm}$$

Also, the rate of heat transfer for the entire pipe is

$$\dot{Q} = wQ' \qquad \text{Btu/sec}$$

Constant Heat Flux

When the heat transfer from the pipe wall to the flowing gas is known to be relatively independent of location in the pipe, such as when the pipe is electrically heated, the constant heat flux requires that the temperature difference be constant (if h_q can be assumed constant). Then $(T_w - T_0) = (T_{w1} - T_{01})$, and equation (9.45) integrates simply to

$$\frac{T_{02} - T_{01}}{T_{w1} - T_{01}} = \frac{fL_2}{2D}$$

Just as in the case of constant wall temperature, an evaluation of the other fluid property changes requires a numerical or graphical integration of equation (9.49) but now incorporating

equation (9.65). An alternate approximate method for low mach-number flow ($M \lesssim 0.3$) can also be developed for the constant heat flux case. The resulting equation, which is equivalent to equation (9.61) developed for constant wall temperature, is found to be

$$\left(\frac{P_{02}}{P_{01}}\right)^2 = 1 - \left(\frac{k}{2}\right) M_1^2 \left[1 + \left(\frac{P_{02}}{P_{01}}\right)^2 \left(\frac{T_{01}}{T_{02}}\right) \left(\frac{M_2}{M_1}\right)^2\right] \left(\frac{fL_2}{2D}\right) \left[\frac{T_{w1}}{T_{01}} + \left(\frac{fL_2}{4D}\right) \left(\frac{T_{w1}}{T_{01}} - 1\right)\right] \qquad [9.66]$$

The trial-and-error solution is identical to that described for equation (9.61), including the use of the isentropic area ratio solutions.

CHAPTER 21

APPLICATION OF COMPRESSIBLE FLOW THROUGH COMPONENTS

In this chapter the flow characteristics of pneumatic components are described with special emphasis on passive restrictive elements such as fully open valves. The flow characteristics of partially open simple valves and the operating characteristics of pressure regulators are also described briefly.

COMPONENT PRESSURE LOSS AND FLOW CAPACITY

Because of the wide variety of complex internal geometric shapes encountered in pneumatic components, no purely analytical description of the flow process can be made, as has been done with nozzles and pipes. Consequently, a variety of empirical relationships and flow coefficients have come into general use for approximating flow characteristics and capacities of valves and similar components. Lack of standardization of these methods and coefficients stimulated personnel of the National Bureau of Standards (NBS) to establish a standardized method.

The NBS Flow Factor for Air

A study of the flow-test data from a large variety of pneumatic components has shown that the mass flow rate (which can be written in terms of standard volumetric flow rate) of standard temperature air flowing through a component can be related approximately to the static pressure ratio, by the following empirical expression.

$$\frac{(\text{SCFM})_A}{F_q p_1} = \sqrt{\frac{4}{3}(1-r^2)} \qquad [10.2]$$

The term F_q is defined as the "NBS flow factor" and is simply the value of airflow rate per unit upstream absolute pressure when the static pressure ratio, $p_2/p_1 = r = 1/2$. Equation (10.2) identifies the observed fact that for perfect gases the flow rate is directly proportional to the upstream absolute pressure, at any given pressure ratio, which is consistent with other dimensionless flow parameters such as mach number M, and also ϕ of chapter 19. The existence of the pressure function in terms of the pressure ratio, rather than pressure difference, is consistent with the form of all the other compressible flow formulations. By its definition, the NBS flow factor is not dimensionless but can be specified in any units. To convert from the above units of scfm/psia to lbm/sec-psia, the perfect-gas law can be solved to yield

$$\text{SCFM} = 14.75Rw \quad \text{scfm} \qquad [10.3]$$

Preceding Page Blank

where standard temperature is taken as 60° F. Note that the conversion from standard volumetric flow units to the usual mass flow units is dependent on the gas constant R. Then for air, $R=53.36$ so that $(\text{SCFM})_A=786w_A$, and $F_q=786F_w$. Substituting these values into equation (10.2) yields the general form of the empirical component flow correlation

$$\frac{(\text{SCFM})_A}{F_q p_1}=\frac{w_A}{F_w p_1}=\sqrt{\left(\frac{4}{3}\right)(1-r^2)} \qquad [10.4]$$

Three other empirical equations have been written consistent with the definitions of F_q and F_w.

$$\frac{(\text{SCFM})_A}{F_q p_1}=2\sqrt{r(1-r)} \qquad [10.5]$$

$$\frac{(\text{SCFM})_A}{F_q p_1}=\sqrt{\frac{8}{5}r(1-r)(3-r)} \qquad [10.6]$$

$$\frac{(\text{SCFM})_A}{F_q p_1}=\sqrt{15.3(r^{1.43}-r^{1.71})} \qquad [10.7]$$

Equation (10.5) describes a minimum expected pressure drop, and equation (10.6) defines an average function that best describes the bulk of the data. Equations (10.4) through (10.7) are plotted in figure 21.1.

An obvious deficiency of the NBS flow factor equations is the lack of a means of accounting for temperatures other than standard, or gases other than air. The flow parameters (the left side of the equations) can be generalized by applying the same terms that occur in the rigorously established flow parameters for compressible adiabatic flow in nozzles and pipes. The parameter generally used is the mach number, which can always be simplified to ϕ by including the specific heat ratio k with the remainder of the particular function. Then since

$$\phi_1=(\sqrt{k})M_1=\frac{w}{AP_1}\sqrt{\frac{RT_1}{g_c}}=\frac{\text{SCFM}}{14.75AP_1}\sqrt{\frac{T_1}{g_c R}}$$

the NBS component flow equations can be generalized to the following, while maintaining the NBS flow factor as defined, which can now be applied to any perfect gas and temperature. The following equation is a combination of equations (10.8) and (10.9).

$$\frac{w}{F_w p_1}\sqrt{\left(\frac{R}{53.36}\right)\left(\frac{T_1}{520}\right)}=\frac{\text{SCFM}}{F_q p_1}\sqrt{\left(\frac{53.36}{R}\right)\left(\frac{T_1}{520}\right)}=f(r)$$

The function $f(r)$ can be either of those described by equations (10.4) through (10.7). When the real-gas effects are factored into the flow parameter, the equations become

$$\frac{w}{F_w p_1}\sqrt{\left(\frac{Z_1 R}{53.36}\right)\left(\frac{T_1}{520}\right)}=\frac{\text{SCFM}}{F_q p_1}\sqrt{\left(\frac{53.36}{R}\right)\left(\frac{Z_1 T_1}{520}\right)}=f(r)$$

which is a combination of equations (10.11) and (10.12). The effects of the variation of the specific heat ratio k for perfect gases, and isentropic exponent k_s for real gases, cannot be

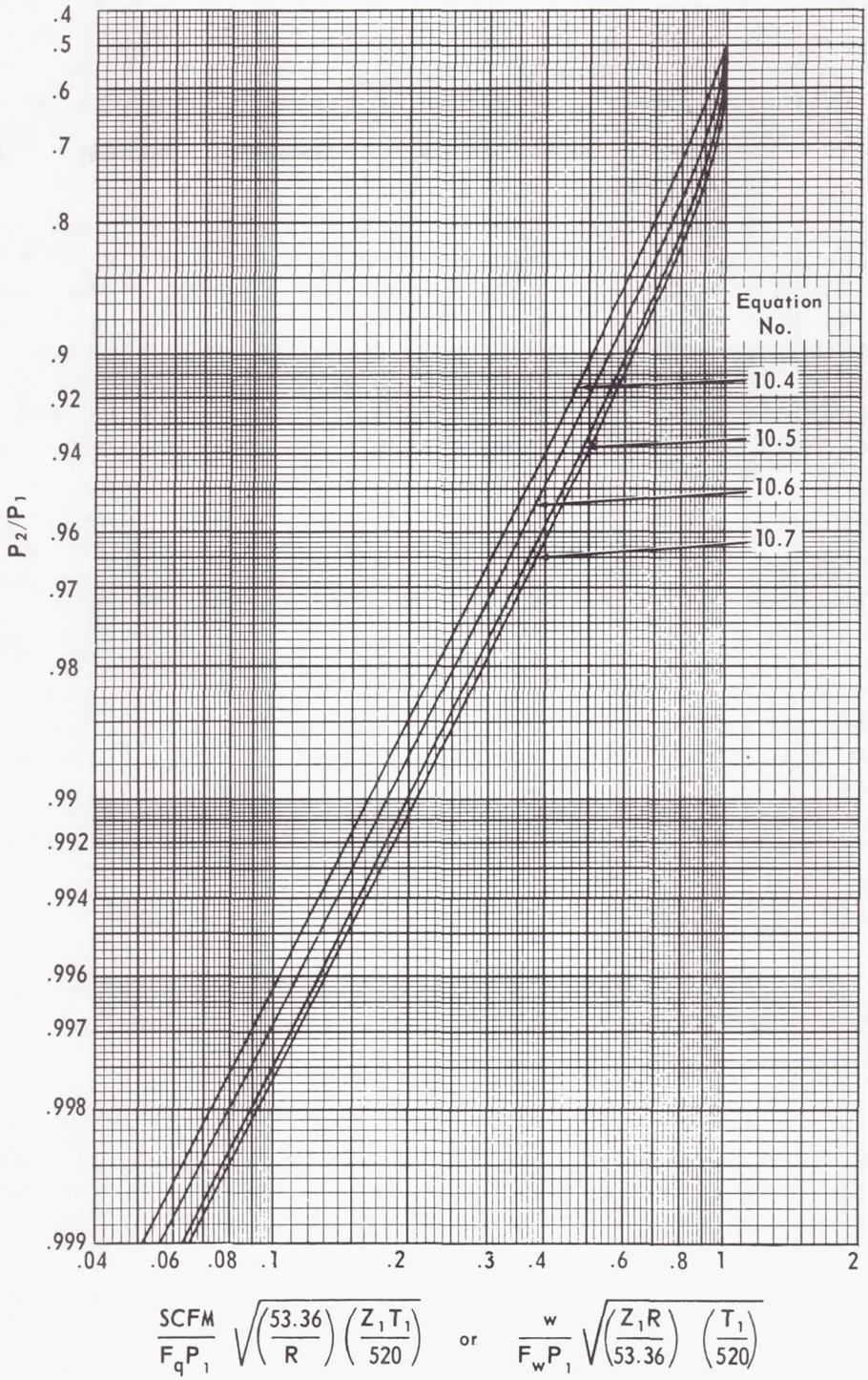


Figure 21.1. NBS component flow characteristics.

325-994 O-69—28

accounted for in the NBS equations. In the theoretical description of nozzle flow and pipe flow of perfect gases, k is part of the analytical function. The absence of k in the empirical functions of equations (10.4) through (10.7) is not considered serious; however, since in the exact solutions for nozzle and pipe flow, the effect of k is found to be significant only at nearly choked flow conditions.

Conversion Factors Relating Flow Coefficients

There are several other widely used flow coefficients to describe the flow capacity of components such as valves. The most common are C_v, d_0, and K (or $f(L/D)$), which are all based on incompressible flow. The conversion of these coefficients to any compressible flow factor can be made only by drawing the equivalence in the low flow rate, low pressure-drop (pressure ratio near unity) regime of the compressible flow which is also incompressible in nature.

The factor C_v is based on the water flow test and is equal to the flow rate of 60° F water, in gpm, that will flow through the component with 1-psid differential pressure across the component. More specifically, C_v is based on the formula

$$(\mathrm{GPM})_{(60^\circ \mathrm{F},\, w)} = C_v\sqrt{p_1 - p_2} \qquad [10.13]$$

By writing the general formula for incompressible flow of any fluid (from eq. (7.15)),

$$q = AV = AK_c\sqrt{\frac{2g_c(144)\,(p_1 - p_2)}{\gamma}}$$

and combining with the necessary unit conversions between the various flow quantities, the water flow formula can be written for standard temperature air as

$$(\mathrm{SCFM})_A = 0.997C_vp_1\sqrt{1 - r} \qquad [10.14]$$

And since the NBS component flow equation is

$$(\mathrm{SCFM})_A = F_qp_1f(r)$$

the conversion between C_v and F_q is

$$\frac{F_q}{C_v} = 0.997\left(\frac{\sqrt{1 - r}}{f(r)}\right) \qquad [10.15]$$

which is seen to be dependent on the NBS function selected. Inserting each of the three functions into the conversion equation, and evaluating in the incompressible flow regime where $r = 1$ yields (for eqs. (10.4), (10.5), (10.6), and (10.7), respectively):

$$\left(\frac{F_q}{C_v}\right) = 0.6105 \qquad [10.16a]$$

$$\left(\frac{F_q}{C_v}\right) = 0.4985 \qquad [10.16b]$$

$$\left(\frac{F_q}{C_v}\right)=0.5580 \qquad [10.16c]$$

$$\left(\frac{F_q}{C_v}\right)=0.482 \qquad [10.16d]$$

The conversions of d_o and K can most easily be obtained by first relating them to C_v, and then to F_q by means of equations (10.16). The general flow formula for incompressible flow can be written once again, but now in terms of the equivalent orifice of diameter d_0 and a discharge coefficient. The equivalent orifice is defined as one having a discharge coefficient of 0.60. The equation reduces to

$$(\text{GPM})_{(60^\circ \text{F},\, W)}=17.9d_o^2\sqrt{p_1-p_2}$$

so that

$$C_v=17.9d_o^2 \qquad [10.17]$$

Then the conversion from d_0 to F_q is obtained by substituting equation (10.17) into equations (10.16).

The head loss factor, K or $f(L/D)$, is obtained from the incompressible-flow equation

$$144(p_1-p_2)=K\left(\frac{\gamma V^2}{2g_c}\right)=\left[f\left(\frac{L}{D}\right)\right]\left(\frac{\gamma V^2}{2g_c}\right)$$

Substituting the continuity equation to eliminate V, and also changing to volumetric units of water flow yields

$$(\text{GPM})_{(60^\circ \text{F},\, W)}=5472\left(\frac{A}{\sqrt{K}}\right)\sqrt{p_1-p_2}$$

Then the conversion from K to C_v is given by

$$C_v=5472\left(\frac{A}{\sqrt{K}}\right)$$

or in terms of the inside diameter of the circular connecting pipe,

$$C_v=29.8\,\frac{D^2}{\sqrt{K}}=29.8\left[\frac{D^2}{\sqrt{f\left(\frac{L}{D}\right)}}\right] \qquad [10.18]$$

Note that in the case of K, the conversion to C_v is dependent on the flow area, or inside diameter, of the pipe into which the component is connected. The conversion of K and $f(L/D)$ to F_q is accomplished by substituting equation (10.18) into equations (10.16).

A final conversion from d_o to K is obtained by combining equations (10.17) and (10.18) to yield

$$d_o=17.48\left[\frac{\sqrt{A}}{(K)^{1/4}}\right]=1.29\left[\frac{D}{(K)^{1/4}}\right] \qquad [10.19]$$

Nominal flow coefficients (taken from a variety of sources) for typical components can be found in table 3.1 (ch. 3). To be included, coefficients in terms of equivalent length (L/D) require the full turbulent flow friction factor f (taken from the Moody diagram of fig. 3.4 (ch. 3)). The wide variations found in the data of table 3.1 (ch. 3) are indicative of the uncertainty involved with a general treatment of components. Accurate flow characteristics can be obtained only by tests run at conditions closely duplicating the service conditions in all respects. Otherwise, good engineering judgment must be exercised in selecting a flow coefficient so that a conservative, yet accurate, evaluation results. Flow coefficients should be obtained from the manufacturer, whenever possible, along with an exact definition of any quoted flow coefficient.

Component Equivalence With Frictional Pipes

In the analysis of incompressible flow through components, fittings, and so forth, the empirical expression used to compute pressure loss is the same as that used for frictional pipes

$$\Delta P_L = K\left[\rho\left(\frac{V^2}{2}\right)\right] = \left[f\left(\frac{L}{D}\right)\right]\left[\rho\left(\frac{V^2}{2}\right)\right]$$

Therefore, the treatment of components and fittings as equivalent lengths of straight pipe in incompressible flow is as accurate as the empirical method itself.

In the more difficult compressible flow case, the exact solutions for adiabatic frictional pipe flow are obtained by the Fanno equations or, more conveniently, by the direct graphic methods, both of which are presented in chapter 8. The possibility of treating components as equivalent lengths of frictional pipe should not be overlooked as a means for correlating component flow characteristics in pneumatic systems. This is especially true, since the methods using the NBS flow factors and equations, as well as all other general approaches to compressible flow through components, are themselves only good approximations, at best.

Exact equivalence between the compressible flow solutions of chapter 8 and the incompressible flow equations above can be proven in the low pressure-drop (pressure ratio near unity) flow regimes. By eliminating the velocity term in the equation above, using the continuity equation, and rearranging, the incompressible flow equation can be written precisely in terms of the compressible pipe flow parameter, ϕ_1.

$$\phi_1 = \left(\frac{w}{AP_1}\right)\sqrt{\frac{P_1 v}{g_c}} = \frac{w}{A}\sqrt{\frac{1}{g_c P_1 \gamma}} = \sqrt{\frac{2\left(1-\frac{P_2}{P_1}\right)}{f\left(\frac{L}{D}\right)}} = \sqrt{\frac{2\Delta P_L}{P_1\left[f\left(\frac{L}{D}\right)\right]}} \qquad [10.20]$$

Equation (10.20) plots as a straight line with a slope of 2 on the ϕ_1 charts of chapter 19 and the lines coincide exactly with the more complex compressible flow curves in the low pressure-drop (incompressible) range. It should be noted that the empirical flow equations have also been made equivalent to the incompressible flow in the low pressure-drop range by the flow coefficient conversions performed at $P_2/P_1 = 1$. Then the incompressible equation, the NBS method, and the ϕ_1 chart method all produce identical results in the low pressure-drop range. The use of the ϕ_1 charts merely substitutes the plotted exact pipe flow functions in place of the four empirical pressure ratio functions. The use of the ϕ_1 charts offers the added means of accounting for variations in specific heat ratio, and the established methods of accounting for real-gas effects.

A high degree of accuracy should be expected well into the compressible flow range of the ϕ_1 charts. However, the equivalent-length method cannot be expected to yield accurate results at flow conditions approaching that of choked pipe flow. Components usually have reduced flow areas that cause the choked conditions to be reached at lower values of ϕ_1 than the equivalent constant area pipe. Flow characteristics in the regions just below and above the point of choking are probably more dependent on the minimum area ratio, the orifice-type flow contraction, and the pressure recovery afforded by the flow-path geometry downstream of the point of choking.

The equivalent-length method using the ϕ_1 charts of chapter 19 requires the calculation of the general flow parameter ϕ_1 from the usual expression of equation (8.55) of chapter 19. Repeating

$$\phi_1 = (\sqrt{k})M_1 = \left(\frac{w}{AP_1}\right)\sqrt{\frac{Z_1RT_1}{gc}} = 0.2245\left(\frac{w}{p_1D^2}\right)\sqrt{Z_1RT_1} \qquad [10.21a]$$

and in terms of standard cubic feet per minute

$$\phi_1 = 15.21\left(\frac{\text{SCFM}}{1000p_1D^2}\right)\sqrt{\frac{Z_1T_1}{R}} \qquad [10.21b]$$

where A and D correspond with the connecting piping. The equivalent $f(L/D)$ can be added to that of the piping of a system being analyzed, or treated separately. The value of $f(L/D)$ can be computed in terms of the flow coefficients already mentioned by the following relationships, obtained from equations (10.16a), (10.17), (10.18), and (10.19).

$$f\left(\frac{L}{D}\right) = K = 332\left(\frac{D^4}{F_q^2}\right) = 890\left(\frac{D^4}{C_v^2}\right) = 2.77\left(\frac{D}{d_o}\right)^4 \qquad [10.22]$$

Then at the computed values of ϕ_1 and $f(L/D)$, the static-pressure ratio across the component is read directly on the ϕ_1 chart of the appropriate value of k or k_s.

When very accurate component flow characteristics are required, the component should be subjected to flow tests that closely duplicate the expected flow conditions. Test data reduction should be of the general form of the ϕ_1 charts to identify any equivalence with straight frictional pipe, and so that the data can be applied to any other gases and flow conditions.

Example Problem 21.1

A hand valve, having the general configuration of a Y-pattern globe valve, is placed in a 2-inch, double-extra-strong nitrogen line. The design flow rate through the valve is 50 000 scfm with an upstream pressure of 4000 psig and temperature of 70° F. Compute the pressure drop across the valve at the design conditions.

Solution

In the absence of better data, the flow coefficient is estimated from the data of table 3.1 (ch. 3). A range of values of $145 \leq L/D \leq 175$ is specified. Assuming a value of 170 and

reading the fully turbulent friction factor from figure 3.4 (ch. 3) yields

$$f\left(\frac{L}{D}\right) = 0.0129(170)$$
$$= 2.19$$

Using the NBS flow equation (10.4), the conversion of the equivalent-length factor to the NBS flow factor is obtained from equations (10.16*a*) and (10.18). Pipe-size data of appendix *A* yield the diameter $D = 1.771$ inches. Then

$$C_v = 29.8\left[\frac{(1.771)^2}{\sqrt{2.19}}\right] = 63.2 \qquad \text{and} \qquad F_q = 0.6105(63.2) = 38.6$$

The more general NBS mass flow parameter is defined by equation (10.12). The value of Z_1 is read on figure C.2 of appendix C as 1.12. Then the NBS mass flow parameter is

$$\frac{50\,000}{(38.6)(4015)}\left[\sqrt{\left(\frac{53.36}{55.2}\right)\frac{(1.12)(530)}{520}}\right] = 0.339$$

Equation (10.4) plotted on figure 21.1 yields

$$\frac{P_2}{P_1} = 0.9563$$

so that

$$\Delta p_L = p_1 - p_2 = p_1\left(1 - \frac{P_2}{P_1}\right)$$
$$= 4015(1 - 0.9563)$$
$$= 175.3 \text{ psid}$$

Similarly, equations (10.5) and (10.6) predict pressure losses of 183.7 and 177.8 psid, respectively.

The pressure loss can also be computed by the equivalent-length method using the charts of chapter 19. The flow parameter ϕ_1 is computed using equation (8.55*g*) of chapter 19 as

$$\phi_1 = 15.21\left[\frac{50\,000}{1000(4015)(1.771)^2}\right]\sqrt{\frac{(1.12)(530)}{55.2}}$$
$$= 0.1982$$

Inspection of the ϕ_1 charts (figs. 19.18 through 19.21) indicates that in the range of $\phi_1 = 0.1982$ and $f(L/D) = 2.19$, the value of P_2/P_1 is essentially independent of k (or k_s), and $P_2/P_1 = 0.955$. Then, as before,

$$p_2 = p_1\left(1 - \frac{P_2}{P_1}\right)$$
$$= 4015(1 - 0.955)$$
$$= 181 \text{ psid}$$

This pressure-loss prediction compares favorably with the three NBS method predictions of 175.3, 183.7, and 177.8 psid.

VALVE OPENING FLOW CHARACTERISTICS

Valves are often designed to provide special characteristics of flow-versus-valve-stem position. The three most common types are those with linear relations between flow and valve position, equal-percentage relations, and quick opening. The characteristics are produced by a shaped plug extension which controls the size of the annular flow area throughout the partially open range. The three types are shown in figure 21.2, along with the typical flow characteristic curves.

The linear and quick-opening valves are well described by their definition. The quick-opening valve is also linear in the initial stages of opening. The equal-percentage characteristic is more complicated, especially with respect to the mathematical description of the characteristic curve. The important difference distinguishing the equal percentage from the linear is that the percent change is based on the initial value of flow capacity (before the change, which is a variable) rather than the fully open flow capacity (which is a constant, C_v). Mathematically, this can be described by

$$\frac{dC}{C} = K' \, dx \qquad [10.23]$$

where C is the flow capacity measured as a fraction of the total flow capacity C_v, and x is the plug displacement measured as a fraction of the maximum displacement. K' is a constant of proportionality dependent on some initial point on the curve. Such a valve will never close completely, so that practical designs usually incorporate a shoulder on the plug to provide quick opening and closing near the fully closed position. The point of interruption of the curve is useful in evaluating K', and is described here by (C_0, x_0). Integrating equation (10.23) and eliminating K' in terms of C_0 and x_0 yield

$$C = C_0^{(1-x)/(1-x_0)} \qquad [10.24]$$

(The above equation is a simplified version of that appearing in ch. 10.). The position-dependent valve coefficient, $C_v(x)$, is then written as

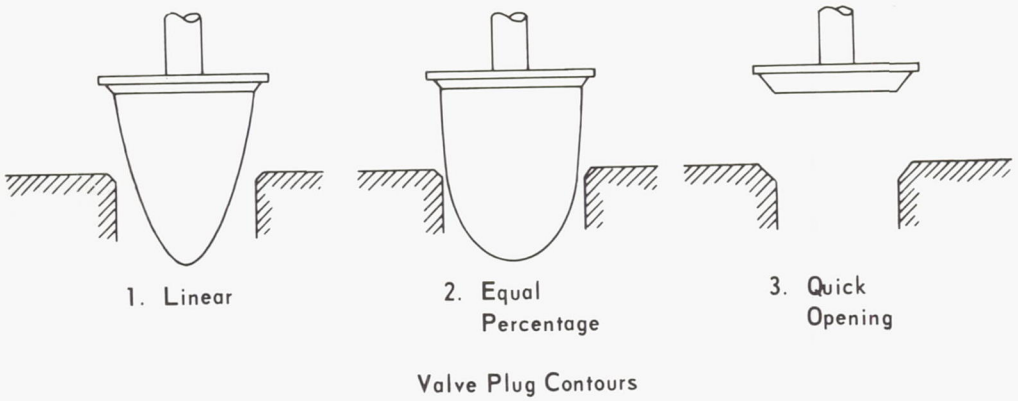
$$C_v(x) = CC_v = C_v C_0^{(1-x)/(1-x_0)} \qquad [10.25]$$

Equal-percentage characteristics are desirable for precise flow control and in applications where large and fast changes in valve flow rate must be avoided. Plug extensions can be shaped to provide a variety of characteristics depending on the application. The displacement dependent $C_v(x)$, which like C_v is based on the incompressible water flow test, must be subjected to the considerations outlined in the first section of this chapter when applied to compressible pneumatic systems.

PRESSURE REGULATORS

Description

Pressure regulators are active, valve-type devices that automatically provide a controlled pressure source of gas from a higher, variable pressure source. Regulators generally



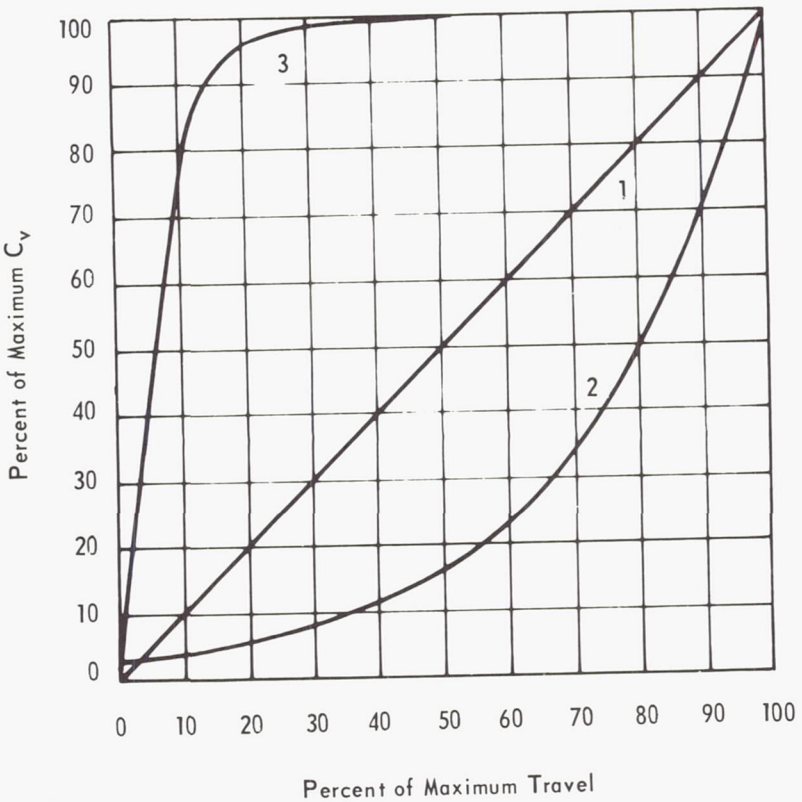


Figure 21.2. Valve opening flow characteristics.

consist of three functional elements. The restricting element restricts the flow and is often of the same basic configuration as a globe valve. The measuring element produces a valve-

closing force on the restricting element proportional to the outlet pressure, usually by applying the outlet pressure to a stem-connected diaphragm or piston. The loading element produces a valve-opening force on the restricting element that opposes the force of the measuring element, usually by means of an adjustable spring or by a diaphragm or piston pressurized from a separate source. For steady-flow operation and a motionless restricting element (plug and stem), the forces of the measuring and loading elements must balance. In a given application, the loading force is held constant at a value dependent on the desired outlet pressure. A change in outlet pressure unbalances the forces thereby causing valve-stem motion. The stem motion is always in the direction that will cause corrective changes in the flow restriction as required to return the outlet pressure to the force-balancing set pressure.

Flow Characteristics

The fully open flow characteristics of pressure regulators are very similar to that of other fully open valves, such as shown in figure 21.3 in terms of a general compressible flow parameter and the pressure ratio. With fixed upstream conditions, the operating line is ideally vertical as shown, depicting the full range of mass flow rates possible with the constant, regulated downstream pressure. When the upstream pressure changes, and/or when the outlet set pressure is changed, the vertical operating line is shifted to the left or right accordingly.

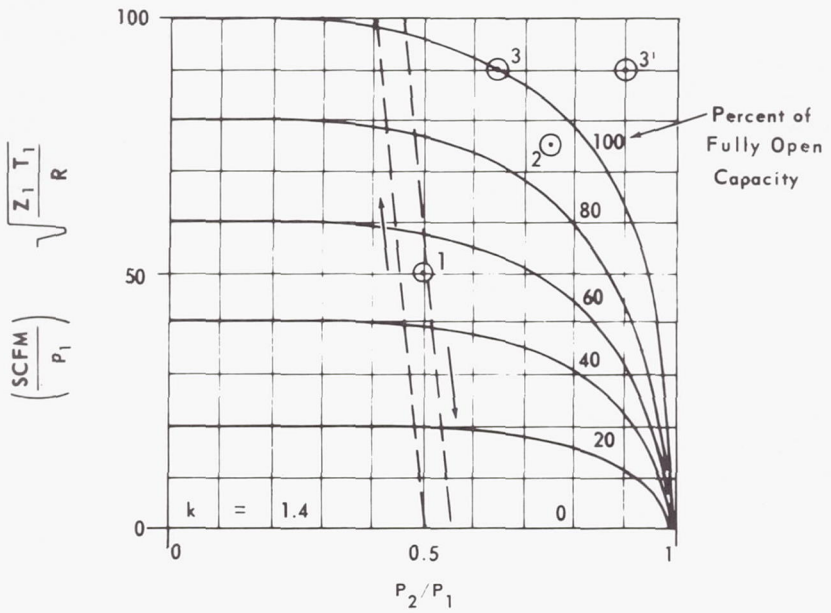


Figure 21.3. Pressure regulator flow characteristics.

Changes in upstream pressure can have a very drastic effect on the flow capacity of a regulator, especially if the outlet pressure requirement is held constant. For example, if the upstream pressure is reduced while all other quantities are held constant, both the generalized flow parameter and the pressure ratio are increased because of the included

P_1 terms. Therefore, the operating point moves up and to the right from the initial operating point, and both changes are in the direction of increasing percentage of fully open capacity. To illustrate, at the initial operating point (1) of the hypothetical regulator of figure 21.3, $p_1 = 6000$ psia, set pressure $p_2 = 3000$ psia, and the flow rate corresponding with a value of the flow parameter of 50. Then, if p_1 is reduced to 4000 psia with unchanged flow and other upstream conditions, the new operating point occurs at a flow parameter value of 75 and $P_2/P_1 = 0.75$. The change in upstream pressure has caused a change in flow conditions from 52 percent of capacity to 90 percent of capacity, although the mass flow rate is unchanged. Further reduction in P_1 to 3333 psia results in an impossible operating point (3′), which is beyond the regulator capacity. Consequently, if the mass flow rate is still maintained at the original value, the real operating point (3) will occur on the fully open line, and the unregulated value of $P_2/P_1 = 0.65$ will result in the deficient outlet pressure of

$$p_2 = p_1 \left(\frac{P_2}{P_1}\right) = 3333\ (0.65)$$

$$= 2167 \text{ psia}$$

The vertical operating line might be tilted for practical designs, as shown by the dashed lines in figure 21.3, especially when the loading element consists of a spring. The spring force will decrease as the valve opens at a rate dependent on the spring constant. This will cause the outlet pressure to decrease with increasing flow, and the operating lines will slope slightly to the left.

Regulators of practical design often experience a significant amount of friction in the moving elements which causes the operating line to exist as a deadband of possible pressure ratios, as depicted by the two dashed lines in figure 21.3, due to the hysteresis-type action.

Regulators of practical design are often unstable at very low flow rate conditions because the valve plug chatters against the seat. The action is caused by self-generated pressure pulses resulting from inadvertent complete closure of the valve, followed by excessive rebound, and so forth, while the regulator hunts the desired, practically shut position.

Flow Capacity and Sizing

Determining the flow capacity and the sizing pressure regulators is best accomplished using the various manufacturers' sizing charts, since designs vary widely, and the quoted flow coefficients are not standardized, nor defined adequately. The charts can be entered at the highest flow capacity expected (highest flow rate and downstream pressure, and lowest upstream pressure combination) to identify the model and orifice size required for the particular application.

CHAPTER 22

APPLICATION OF THERMODYNAMICS OF PRESSURE VESSELS

The analysis of the thermodynamic behavior of a container of gas undergoing a charging or discharging process is usually based on an assumption of no heat transfer. This simplified procedure yields accurate results only when the process is relatively fast, since the thermodynamic processes always cause temperature changes and, therefore, temperature differences and heat transfer. Because of the short time interval of fast processes, the heat transfer occurs mainly after the process is complete, and the adiabatic analysis of the process itself is valid.

Analysis made to include heat transfer between the containing vessel and the enclosed gas is considerably more complicated, and closed analytical solutions can be obtained only for specific simplified cases. Numerical solutions are possible, of course, for the nonlinear differential equations involving variable flow rates, wall temperatures, external heat transfer from ambient temperature, and so forth. In general, the analysis will be based on the perfect-gas theory.

The basic theory describing the processes of pneumatic-pressure vessels is the first law of thermodynamics as applied to open systems. The analytical developments of equation (1.5) (ch. 1) can be applied to produce the following energy equation

$$d(Wu) = \delta Q + h_{0\,\text{in}}\, dW_{\text{in}} - h_{0\,\text{out}}\, dW_{\text{out}} \qquad [11.1]$$

ADIABATIC CHARGING

Adiabatic charging can be assumed only when the process occurs over a short time interval so that the integrated heat transfer will be insignificant in spite of the temperature differences.

Evacuated Receivers

For adiabatic charging of receivers, initially evacuated, with a source of gas having constant $h_{0\,\text{in}}$, equation (11.1) can be simplified and integrated to produce

$$u_2 = h_{0\,\text{in}} \qquad [11.2]$$

so that for calorically perfect gases,

$$T_2 = kT_{0\,\text{in}} \qquad [11.3a]$$

and

$$P_2\left(\frac{W_{\text{in}}}{\bar{V}}\right)kRT_{0\text{ in}} \qquad [11.3b]$$

It is noteworthy that the contained gas temperature is greater than the entering stagnation temperature by the constant factor k.

Partially Filled Receivers

If the receiver contains an amount of gas at the beginning of the charging process, equation (11.1) reduces and integrates to produce

$$\frac{W_2}{W_1}=1+\frac{W_{\text{in}}}{W_1}=\frac{h_{0\text{ in}}-u_1}{h_{0\text{ in}}-u_2} \qquad [11.5]$$

and for perfect gases,

$$\frac{T_2}{T_1}=\frac{kT_{0\text{ in}}}{T_1}-\frac{\left(k\dfrac{T_{0\text{ in}}}{T_1}\right)-1}{\dfrac{W_2}{W_1}} \qquad [11.6b]$$

and

$$\frac{P_2}{P_1}=\frac{\left(\dfrac{T_2}{T_1}\right)\left(\dfrac{T_1}{kT_{0\text{ in}}}-1\right)}{\left(\dfrac{T_1}{kT_{0\text{ in}}}\right)\left(\dfrac{T_2}{T_1}\right)-1} \qquad [11.7b]$$

Equations (11.6) and (11.7) are plotted for various values of k in figures 22.1 through 22.4.

For the special case where the entering gas temperature equals the initial temperature of the stored gas

$$\frac{T_2}{T_1}=\frac{k\left(\dfrac{P_2}{P_1}\right)}{\left(\dfrac{P_2}{P_1}\right)+k-1} \qquad [11.8a]$$

Equation (11.8a) is plotted in figure 22.5 for various values of k. The associated relationship with stored mass is taken from figures 22.1 through 22.4 using the curves for $(T_{0\text{ in}}/T_1)=1$.

NONADIABATIC CHARGING

When the charging process occurs over a significant time interval, the heat exchange should not be neglected, and equation (11.1) must be written in terms of a time-rate differential equation. This equation is then combined with an energy balance equation that describes the containing vessel, and standard heat-transfer equations. This produces the following two simultaneous differential equations written in dimensionless form

$$w_*W_*\left(\frac{\mathrm{d}T_*}{\mathrm{d}W_*}\right)+B_i(T_*-T_{w*})+w_*(T_*-kT_{0\text{ in}*})=0 \qquad [11.15]$$

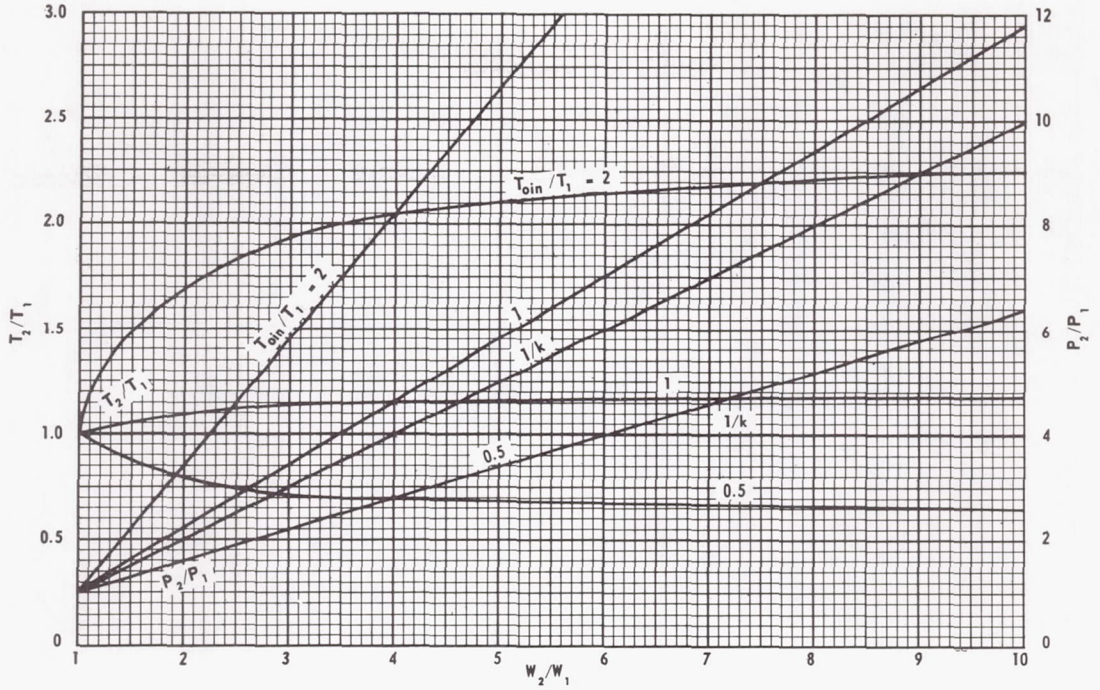


Figure 22.1. Adiabatic charging of a partially filled vessel, $k = 1.2$.

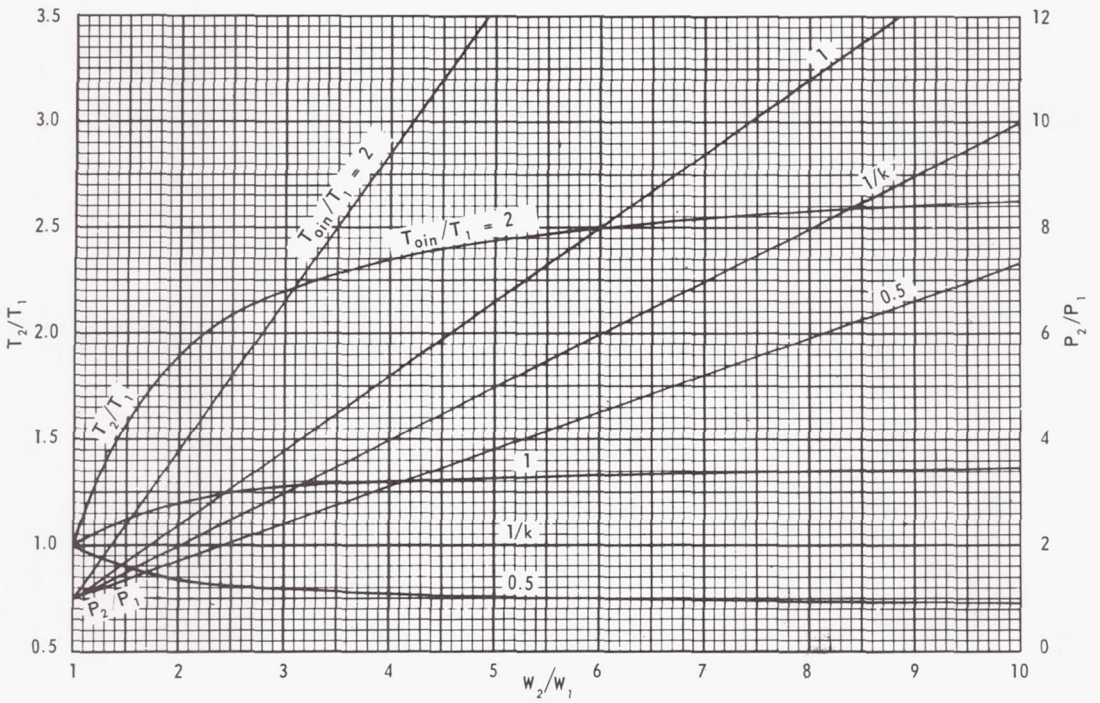


Figure 22.2. Adiabatic charging of a partially filled vessel, $k = 1.4$.

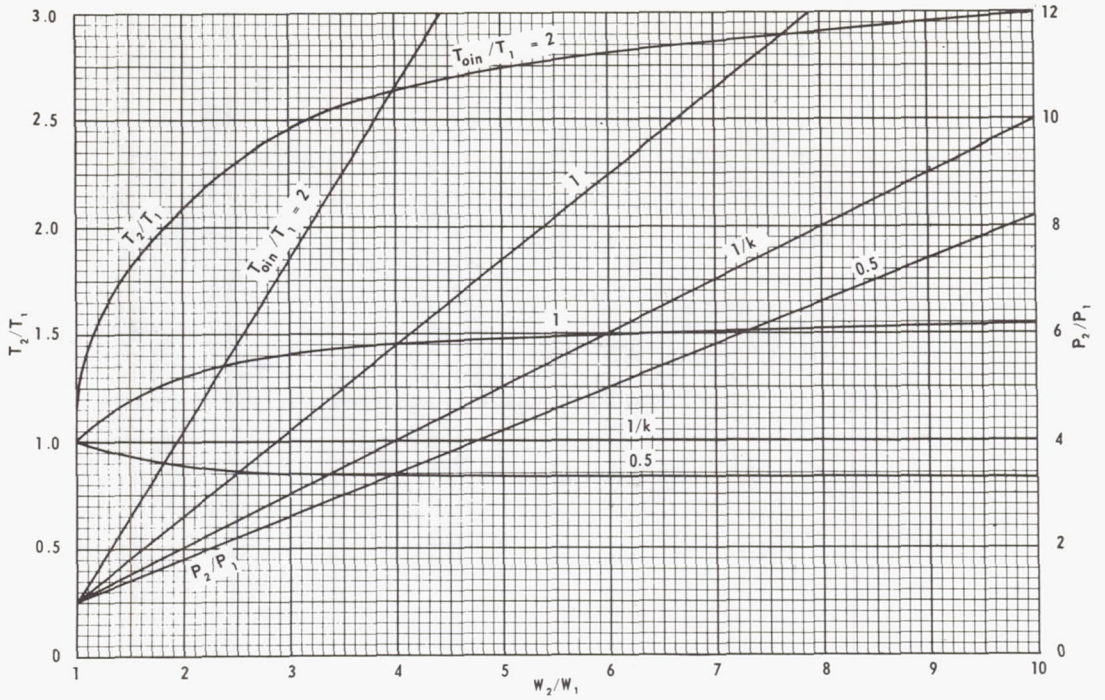


Figure 22.3. Adiabatic charging of a partially filled vessel, $k = 1.6$.

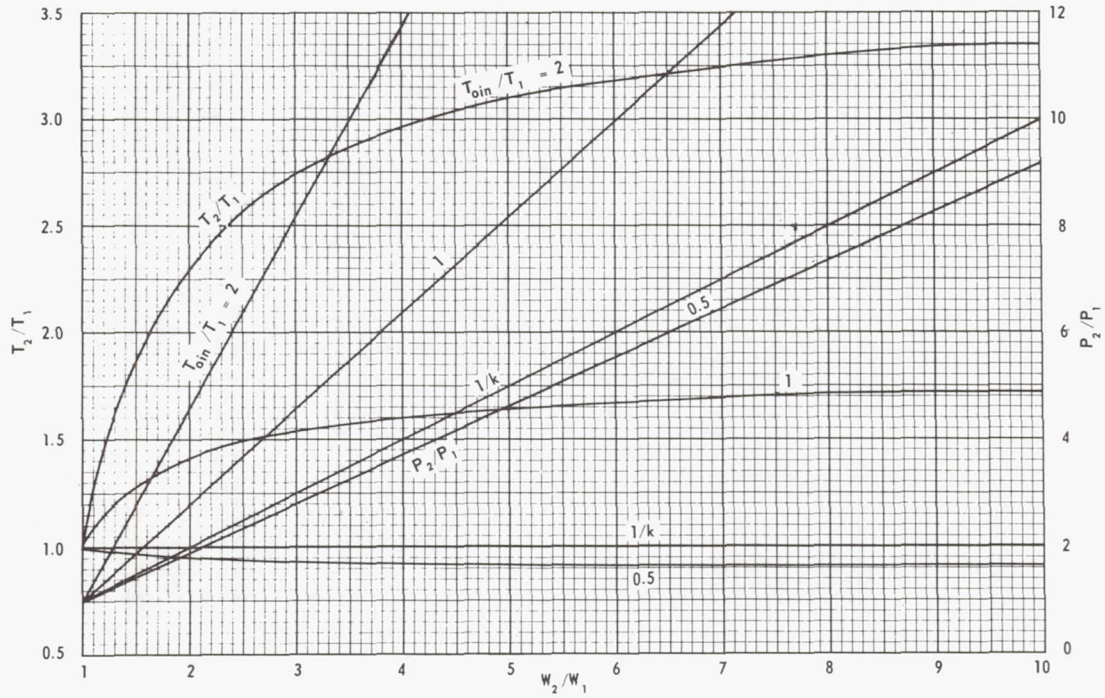


Figure 22.4. Adiabatic charging of a partially filled receiver, $k = 1.8$.

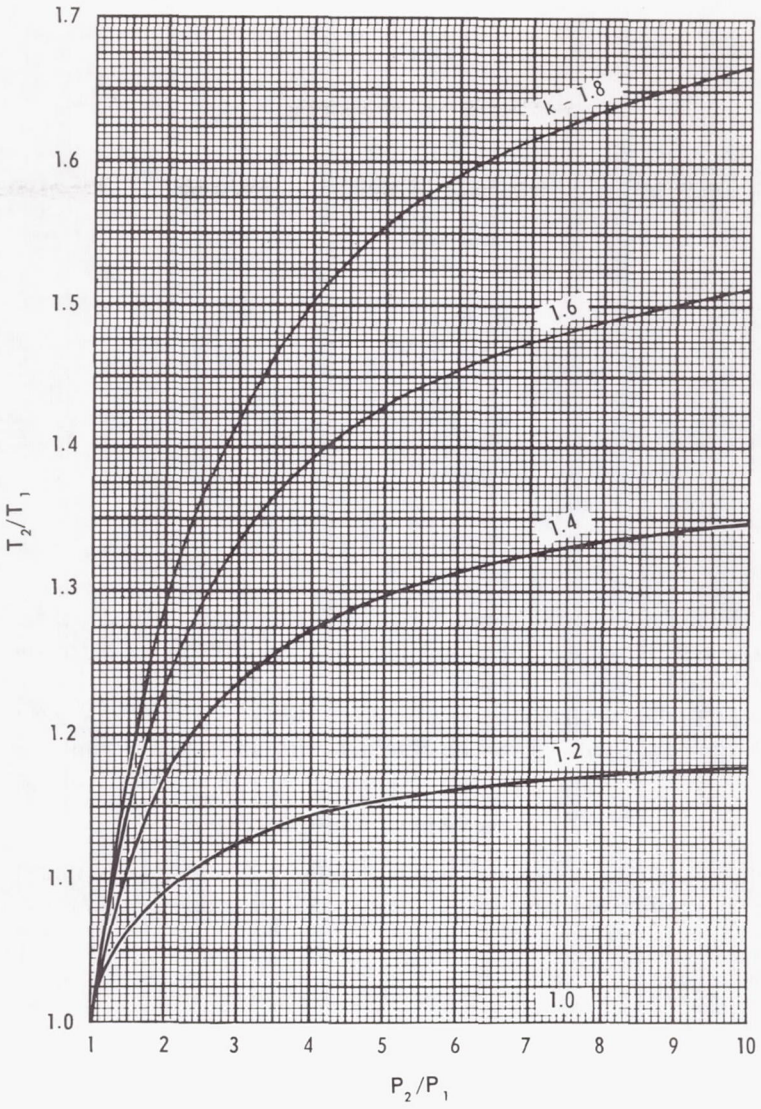


Figure 22.5. Adiabatic charging of a partially filled vessel, $T_{0\,\text{in}} = T_1$.

$$w_* \left(\frac{dT_{w*}}{dW_*}\right) + \left(\frac{B_i + B_\infty}{C_{0*}}\right) T_{w*} - \left(\frac{B_i}{C_{0*}}\right) T_* - \left(\frac{B_\infty}{C_{0*}}\right) T_{\infty*} = 0 \qquad [11.16]$$

The dimensionless terms are defined as follows:

$$B = \frac{(h_q A_w)}{(w_1 c_v)}$$

$$C_{0*} = \frac{(Wc)_w}{W_1 c_v}$$

$$T_* = \frac{T}{T_1} \quad \text{or} \quad \frac{T_2}{T_1}$$

$$T_{w*} = \frac{T_w}{T_1}$$

$$T_{0\,\text{in}*} = \frac{T_{0\,\text{in}}}{T_1}$$

$$T_{\infty *} = \frac{T_\infty}{T_1}$$

$$w_* = \frac{w}{w_1} \quad \text{or} \quad \frac{w_2}{w_1}$$

$$W_* = \frac{W}{W_1} \quad \text{or} \quad \frac{W_2}{W_1}$$

The subscript i refers to the inner surface of the vessel and the subscript ∞ refers to the outer surface and the ambient conditions. The quantity $(Wc)_w$ is the total (or effective) heat capacitance of the container walls.

Equations (11.15) and (11.16) are linear and solvable only if the mass flow rate is constant, and $w_* = 1$. Numerical solutions can be obtained with all complications included, however.

Isothermal Charging

Isothermal charging can be approached with receivers having large thermal capacitance, high heat-transfer coefficients, and low flow rates. In this case, $T_2 = T_1$, so that

$$\frac{P_2}{P_1} = \frac{W_2}{W_1} \qquad [11.17a]$$

and for real gases,

$$\frac{P_2}{P_1} = \left(\frac{Z_2}{Z_1}\right)\frac{W_2}{W_1} \qquad [11.17b]$$

Charging at Constant Mass Flow Rate With Heat Transfer to a Constant Temperature Container

When the thermal capacitance of the container walls is much greater than that of the gas, the wall temperature remains essentially constant. For this case, equation (11.15) integrates to

$$T_* = \frac{kT_{0\,\text{in}*} + B_i T_{w*} - (kT_{0\,\text{in}*} - 1 - B_i + B_i T_{w*})\, W_*^{-B_i+1}}{B_i + 1} \qquad [11.18]$$

Equation (11.18) is plotted in figures 22.6 through 22.9 for the case of $T_{0\,\text{in}*} = 1$, $T_{w*} = 1$, and various values of k.

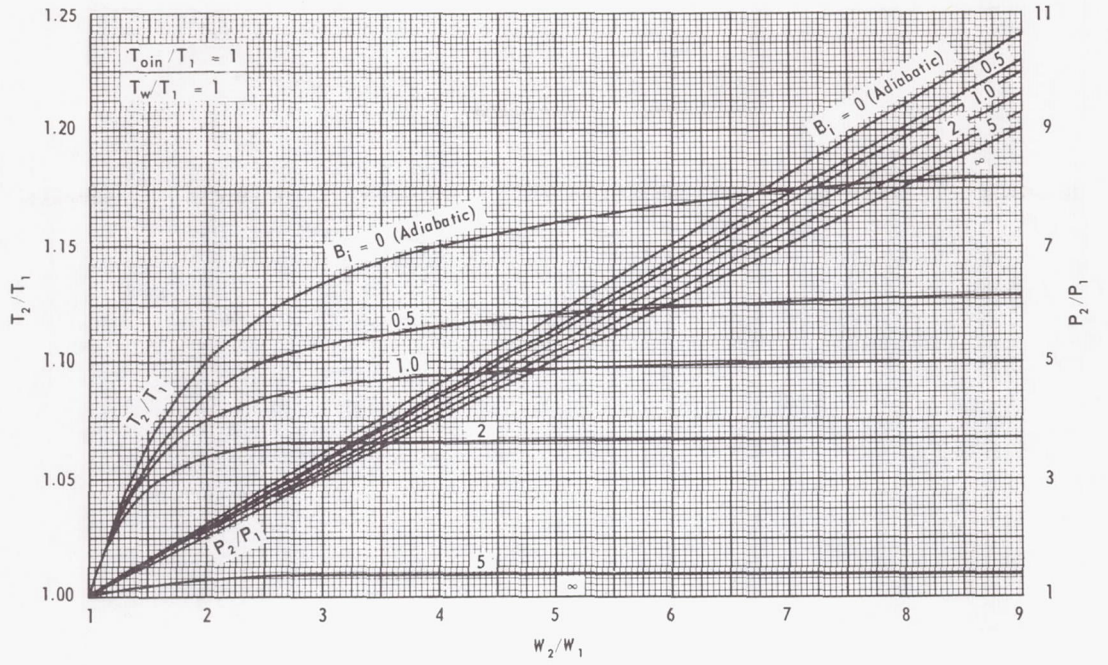


Figure 22.6. Charging at constant mass flow with heat transfer to an isothermal sink, $k=1.2$.

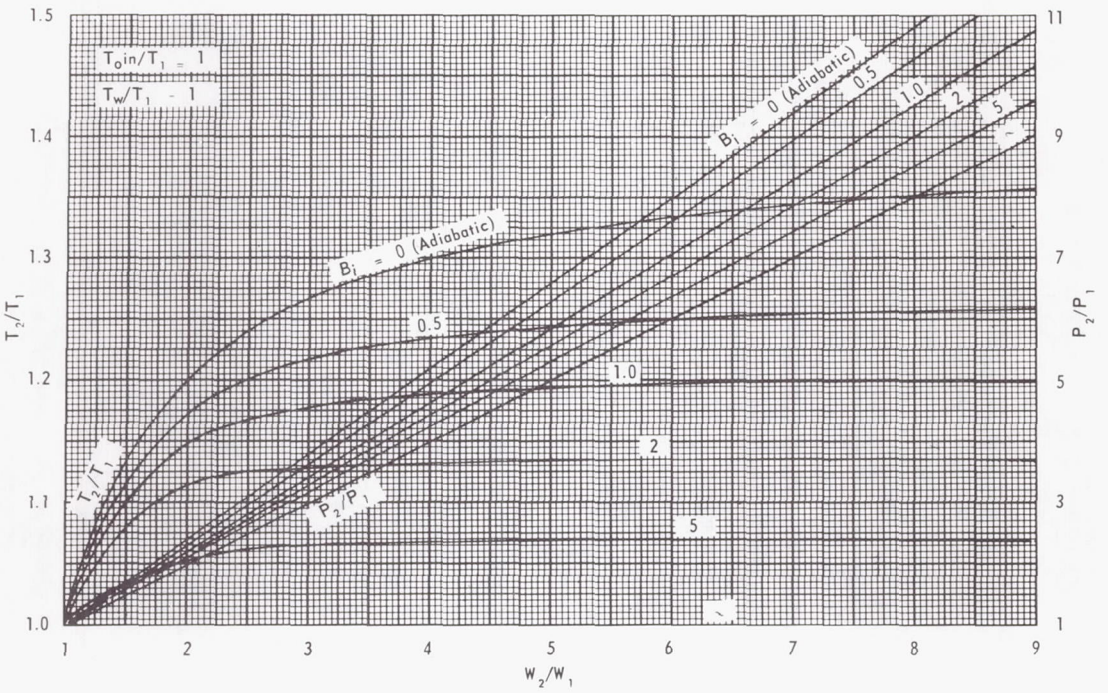


Figure 22.7. Charging at constant mass flow with heat transfer to an isothermal sink, $k=1.4$.

325-994 O-69—29

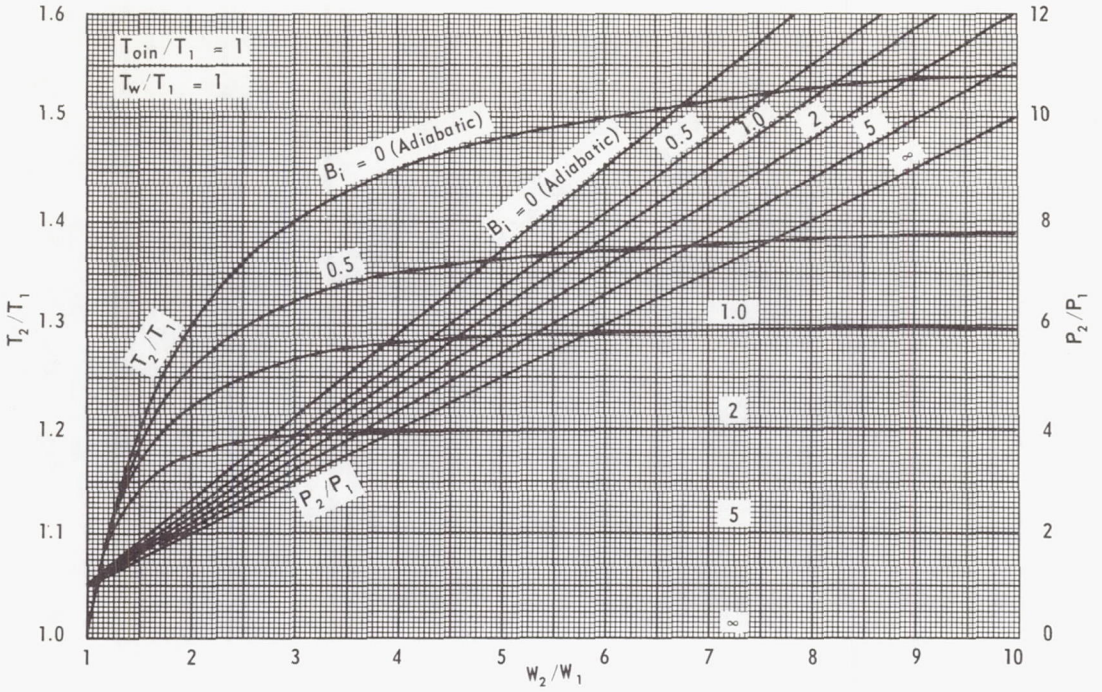


Figure 22.8. Charging at constant mass flow with heat transfer to an isothermal sink, $k = 1.6$.

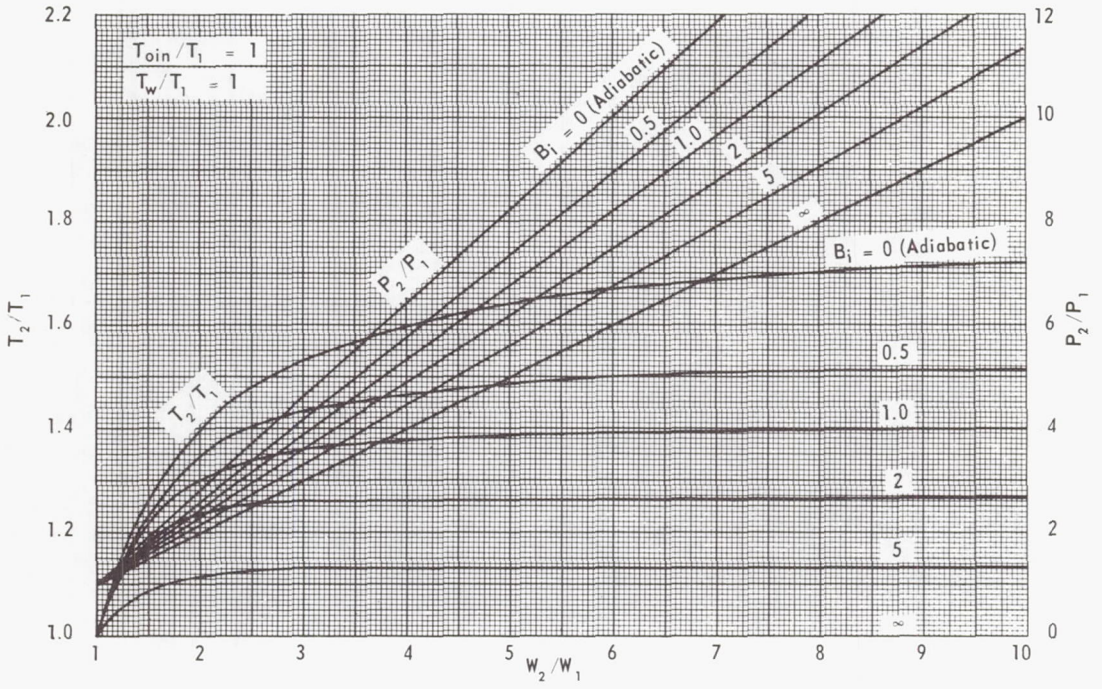


Figure 22.9. Charging at constant mass flow with heat transfer to an isothermal sink, $k = 1.8$.

Charging at Constant Mass Flow Rate With Perfect Heat Transfer to the Container

Very high values of B_i result when the mass flow rate is low, and the inside heat conductance is high and the area is large. In the limit when B_i approaches infinity, equation (11.15) reduces to $T_* = T_{w*}$. Equations (11.15) and (11.16) yield the following integrated equation after simultaneous solution to eliminate B_i.

$$T_* = T_{w*} = \left(\frac{1}{1+B_\infty}\right)\left[(1+B_\infty - kT_{0\,\mathrm{in}*} - B_\infty T_{\infty *})\left(\frac{C_{0*}+1}{C_{0*}+W_*}\right)^{1+B_\infty} + kT_{0\,\mathrm{in}*} + B_\infty T_{\infty *}\right] \qquad [11.20]$$

Equation (11.20) is plotted in figures 22.10 through 22.13 along with the pressure ratio for the case of negligible external heat transfer ($B_\infty = 0$), $T_{0\,\mathrm{in}*} = 1$, and various values of k.

ADIABATIC DISCHARGING

When the rate of flow from a receiver is sufficiently rapid so that the total heat transfer is negligible during blowdown, the expansion process occurring in the receiver is essentially isentropic. Therefore, the following isentropic relationships from chapter 5 apply directly to constant volume receivers.

$$\frac{T_2}{T_1} = \left(\frac{\gamma_2}{\gamma_1}\right)^{k-1} = \left(\frac{W_2}{W_1}\right)^{k-1} = \left(\frac{v_1}{v_2}\right)^{k-1} = \left(\frac{P_2}{P_1}\right)^{(k-1)/k} \qquad [11.21]$$

$$\frac{P_2}{P_1} = \left(\frac{\gamma_2}{\gamma_1}\right)^{k} = \left(\frac{W_2}{W_1}\right)^{k} = \left(\frac{v_1}{v_2}\right)^{k} = \left(\frac{T_2}{T_1}\right)^{k/(k-1)} \qquad [11.22]$$

$$\frac{W_2}{W_1} = \frac{\gamma_2}{\gamma_1} = \frac{v_1}{v_2} = \left(\frac{P_2}{P_1}\right)^{1/k} = \left(\frac{T_2}{T_1}\right)^{1/(k-1)} \qquad [11.23]$$

Figure 22.14 is the representation of these relations between temperature, pressure, and contained mass for various values of k.

NONADIABATIC DISCHARGING

The general analysis of the thermodynamics of gas vessels discharging nonadiabatically can be made by reapplying equation (11.1), except that now $w = -\mathrm{d}W/\mathrm{d}t$. Also, the positive heat transfer is inward, which is the expected direction. The two resulting dimensionless equations describing the internal gas and the containing vessel, as coupled by the heat-transfer equations, are

$$w_* W_* \left(\frac{\mathrm{d}T_*}{\mathrm{d}W_*}\right) - [(k-1)w_* + B_i]T_* + B_i T_{w*} = 0 \qquad [11.31]$$

and

$$w_* \left(\frac{\mathrm{d}T_{w*}}{\mathrm{d}W_*}\right) - \left(\frac{B_i + B_\infty}{C_{0*}}\right) T_{w*} + \left(\frac{B_i}{C_{0*}}\right) T_* + \left(\frac{B_\infty}{C_{0*}}\right) T_{\infty *} = 0 \qquad [11.32]$$

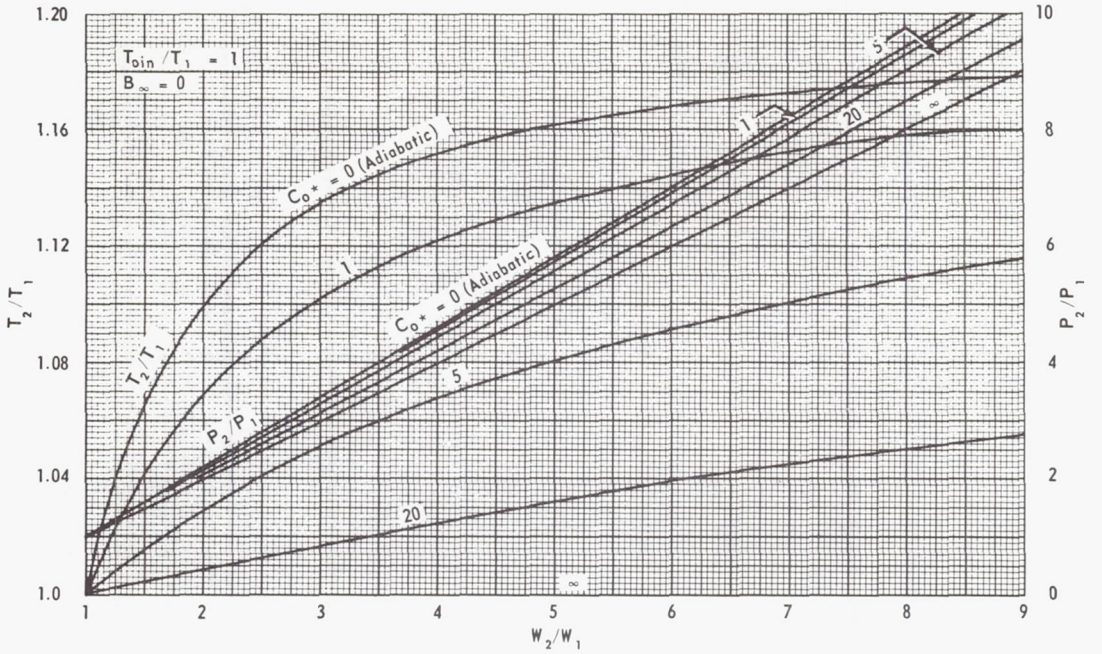


Figure 22.10. Charging at constant mass flow with inside resistance negligible, $k = 1.2$.

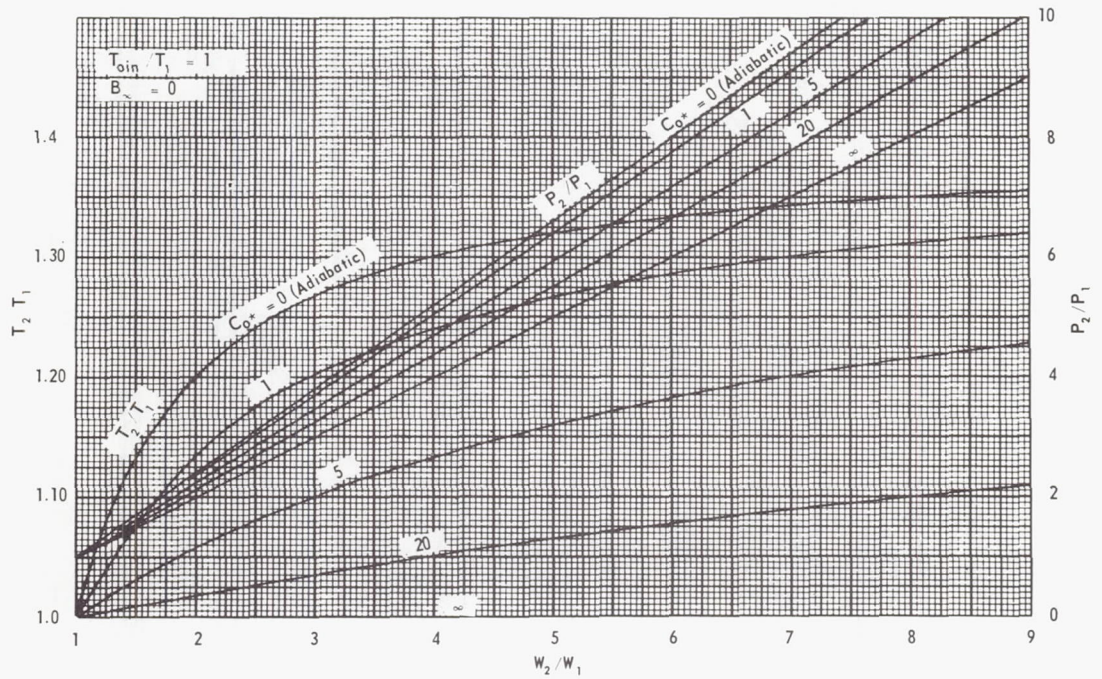


Figure 22.11. Charging at constant mass flow with inside resistance negligible, $k = 1.4$.

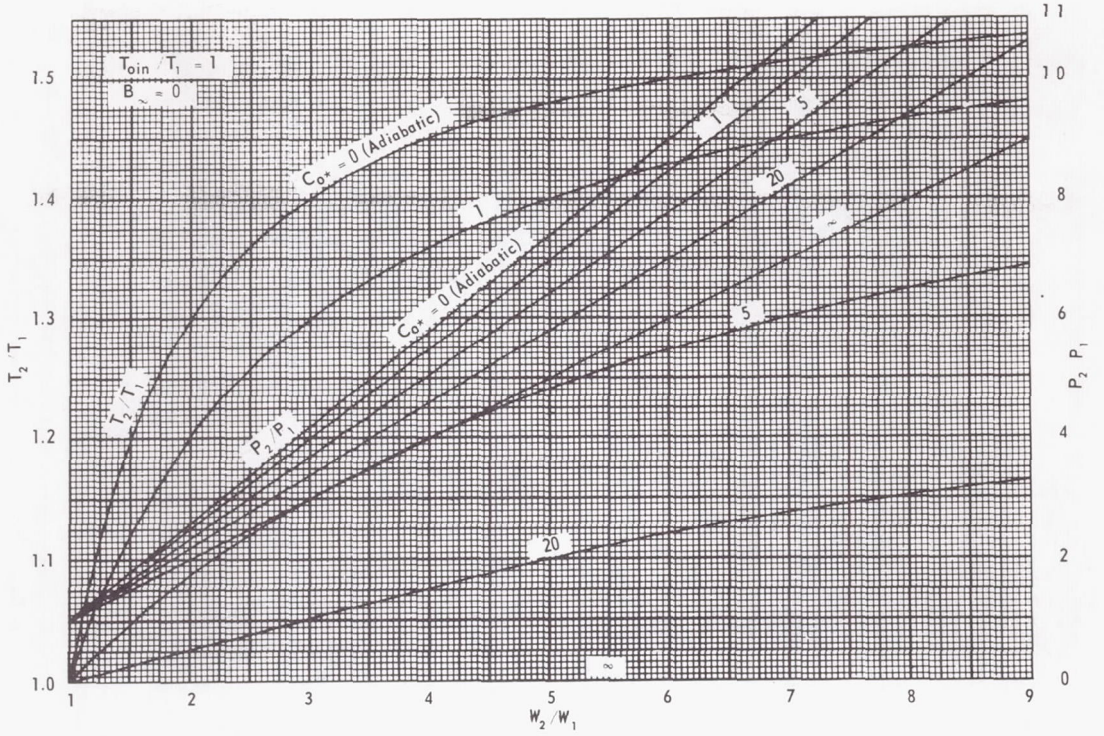


Figure 22.12. Charging at constant mass flow with inside resistance negligible, $k = 1.6$.

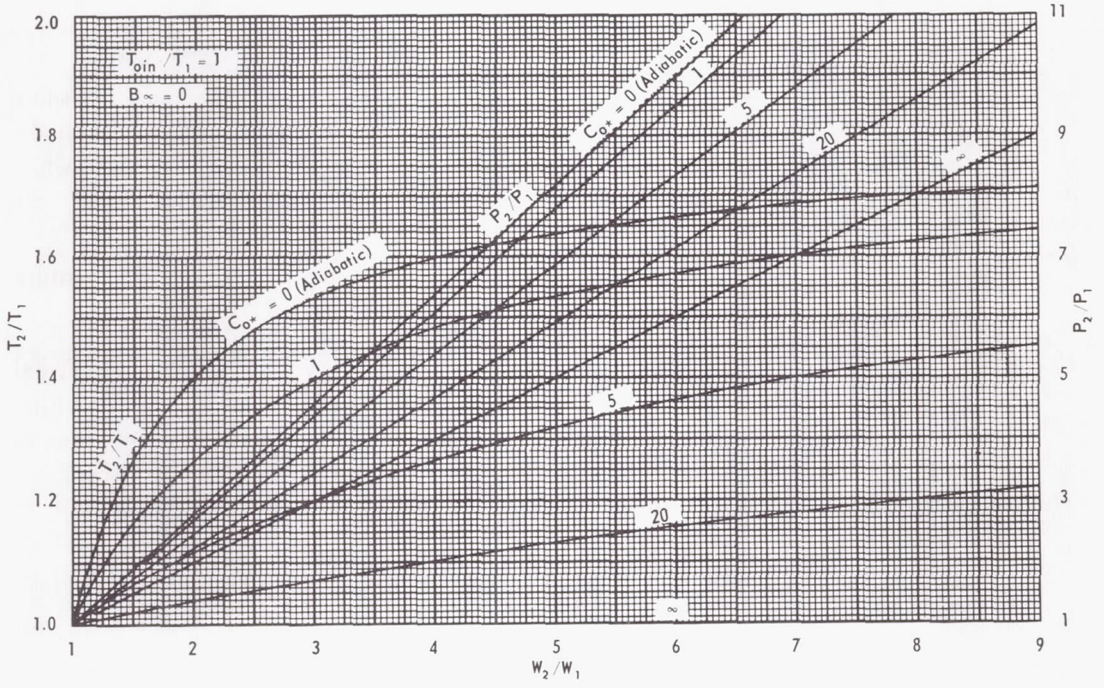


Figure 22.13. Charging at constant mass flow with inside resistance negligible, $k = 1.8$.

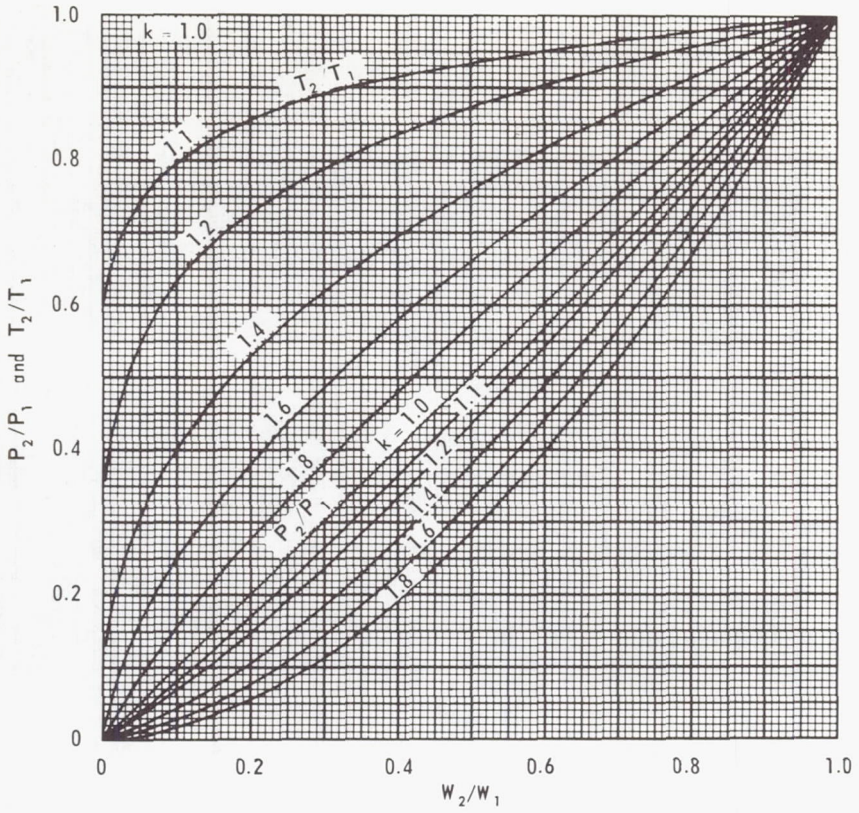


Figure 22.14. Adiabatic discharging (isentropic).

These equations are equivalent to equations (11.15) and (11.16) written for the charging process. Once again, the equations can be solved generally only by numerical methods. Closed analytical solutions can be obtained only when mass flow rate is constant and when the problem is further specified.

Discharging at Constant Mass Flow Rate With Heat Transfer From a Constant Temperature Container

When the total thermal capacitance of the receiver walls is large relative to the thermal capacitance of the enclosed gas, the wall-temperature change will be slight. In the limiting case, C_{0*} is infinite, and when the mass flow rate is constant, equation (11.31) integrates to

$$T_* = \frac{(k-1+B_i-B_iT_{w*})W_*^{(k-1+B_i)}+B_iT_{w*}}{k-1+B_i} \qquad [11.33]$$

Equation (11.33) is plotted in figures 22.15 through 22.18 with the associated pressure changes, for the special case of $T_{w*}=1$ and for various values of k.

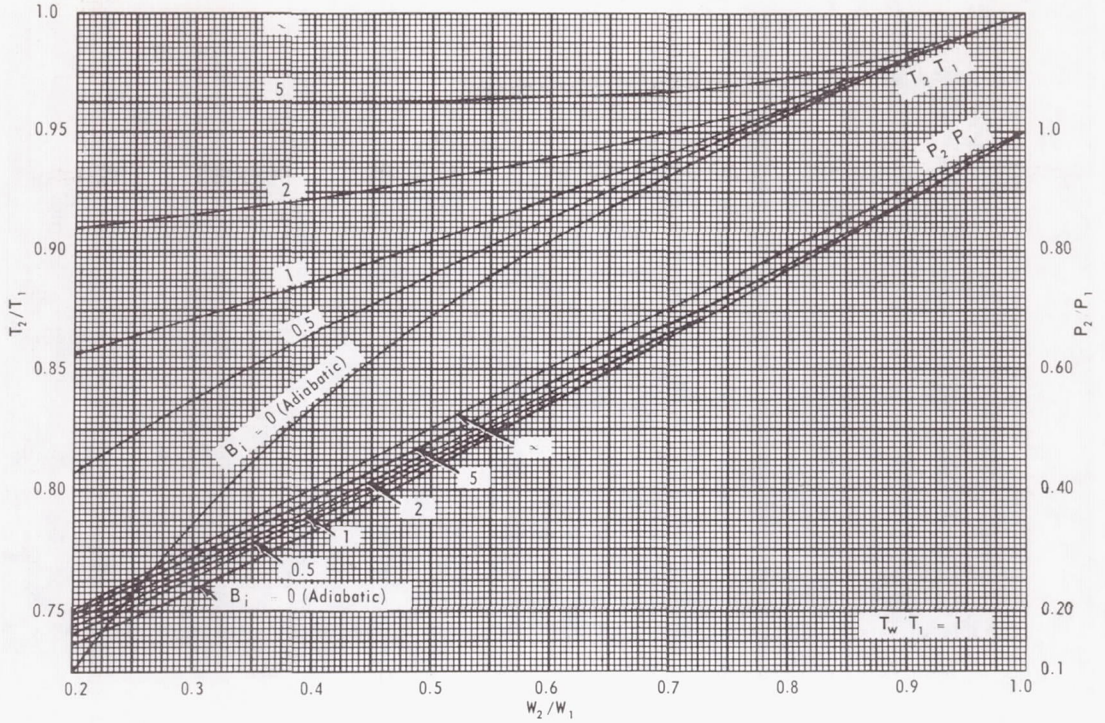


Figure 22.15. Discharge at constant mass flow with heat transfer from an isothermal source, $k = 1.2$.

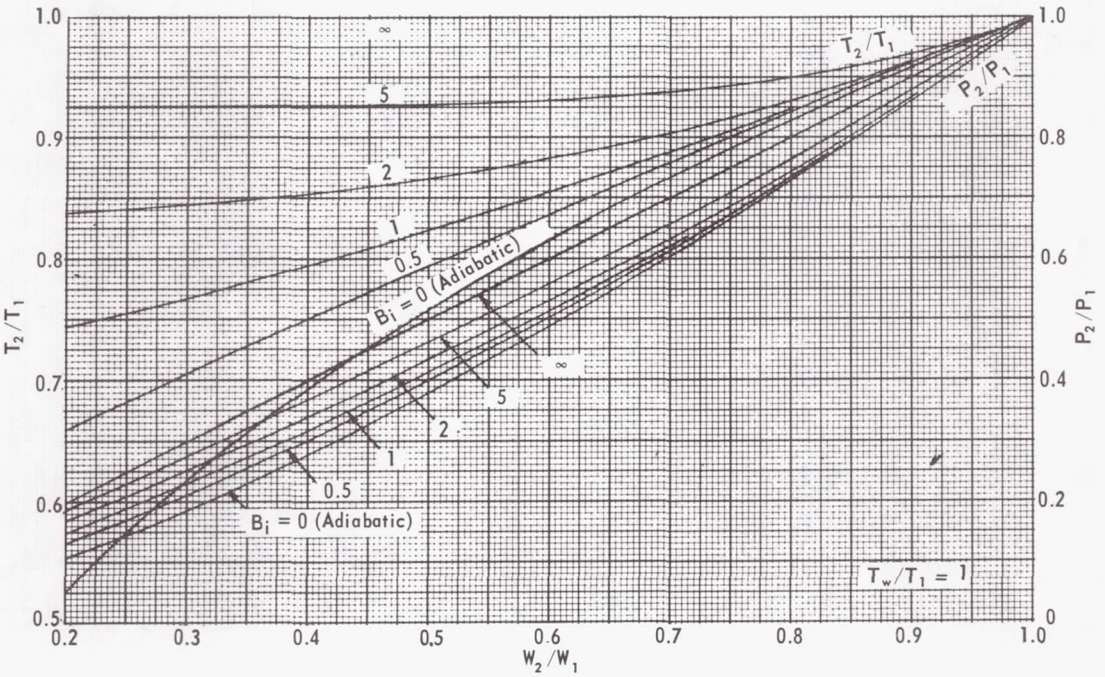


Figure 22.16. Discharge at constant mass flow with heat transfer from an isothermal source, $k = 1.4$.

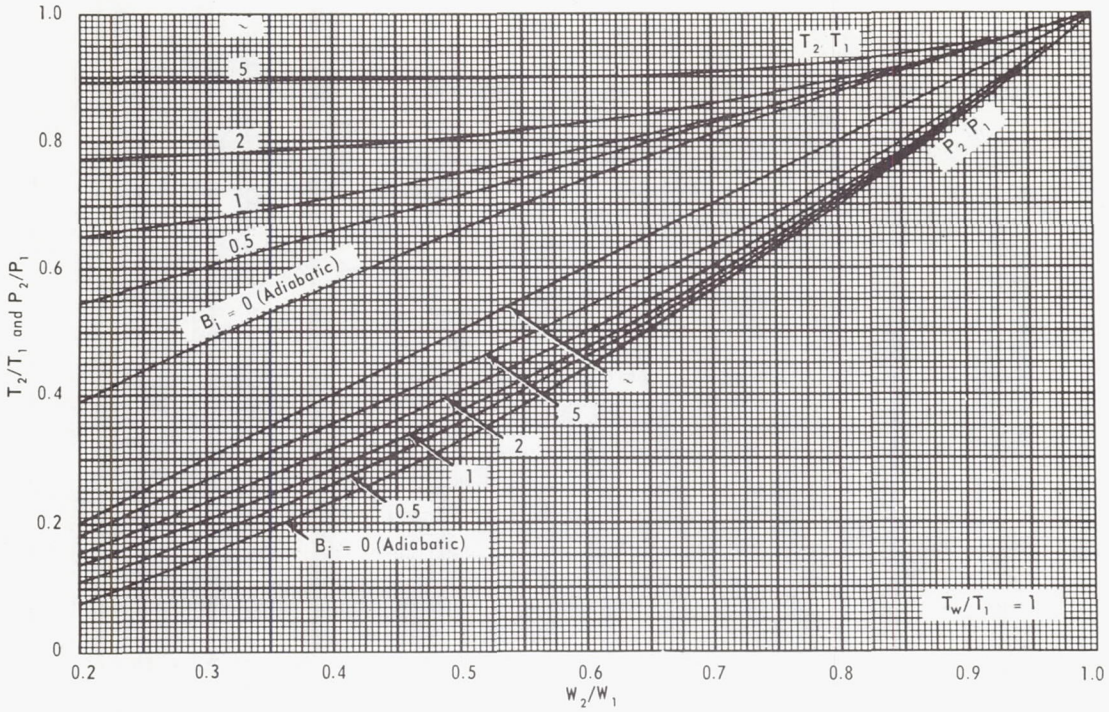


Figure 22.17. Discharge at constant mass flow with heat transfer from an isothermal source, $k = 1.6$.

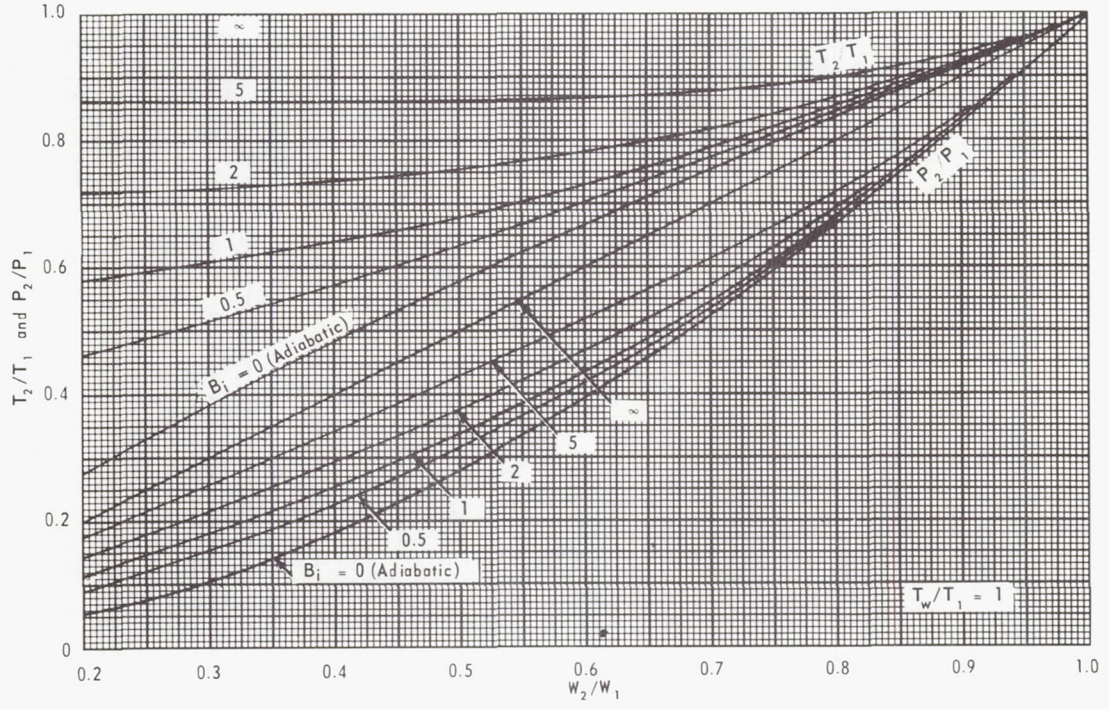


Figure 22.18. Discharge at constant mass flow with heat transfer from an isothermal source, $k = 1.8$.

Discharging Through a Critical Flow Nozzle With Heat Transfer From a Constant Temperature Container

When the discharging mass flow rate is governed by a choked nozzle, the flow rate can be described in terms of the dimensionless quantities as

$$w_* = W_* \sqrt{T_*}$$

Combining this with equation (11.31), and assuming constant wall temperature, yields

$$W_* \left(\frac{dT_*}{dW_*}\right) - (k-1)T_* + \frac{B_i(T_{w*} - T_*)}{W_* \sqrt{T_*}} = 0 \qquad [11.35]$$

Equation (11.35) is nonlinear and must be solved numerically. A typical solution is plotted in figure 11.10 (ch. 11) for $T_{w*} = 1$ and $k = 1.4$.

Discharging at Constant Mass Flow Rate With Perfect Heat Transfer From Container

As in the case of charging, if the mass flow rate is constant and at a low value, and if the inside-wall heat conductance is high and the area is large, the value of B_i becomes very high. In the limit when B_i is infinite, the wall and internal gas temperatures vary together ($T_* = T_{w*}$). Equations (11.31) and (11.32) yield the following integrated equation after simultaneous solution to eliminate B_i.

$$T_* = T_{w*} = \left(\frac{1}{k-1+B_\infty}\right)\left[(k-1+B_\infty - B_\infty T_{\infty *})\left(\frac{W_* + C_{0*}}{1+C_{0*}}\right)^{(k-1+B_\infty)} + B_\infty T_{\infty *}\right] \qquad [11.37]$$

Equation (11.37) with the associated pressure ratio is plotted in figures 22.19 through 22.22 for the special case of $B_\infty = 0$ and various values of k.

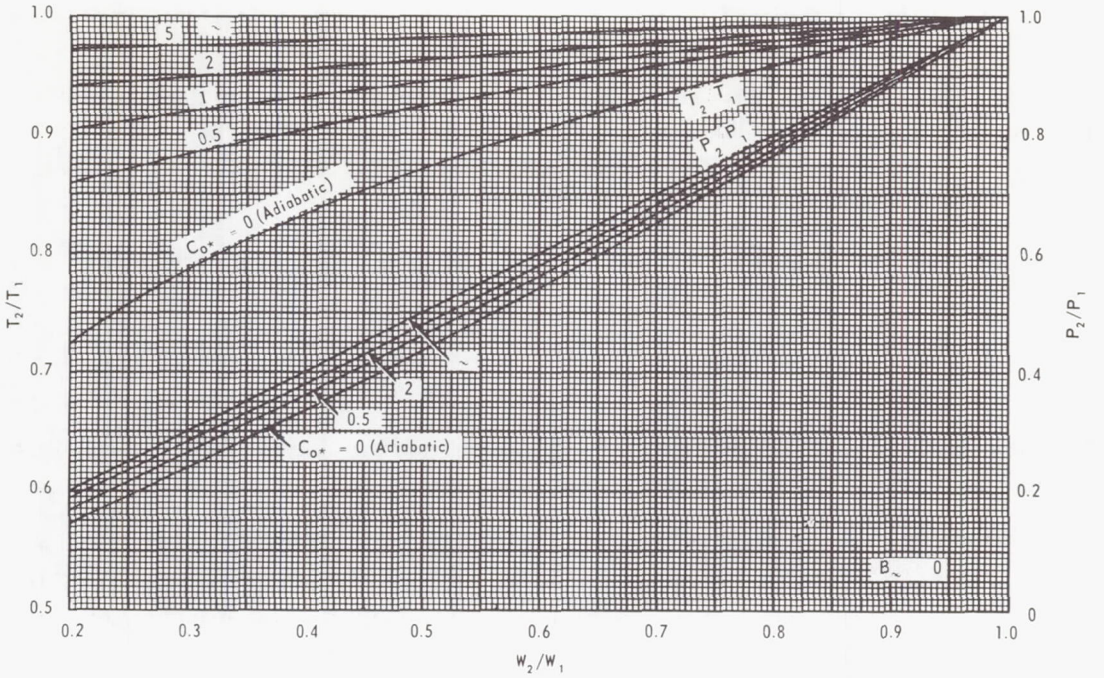


Figure 22.19. Discharge at constant mass flow with inside resistance negligible, $k = 1.2$.

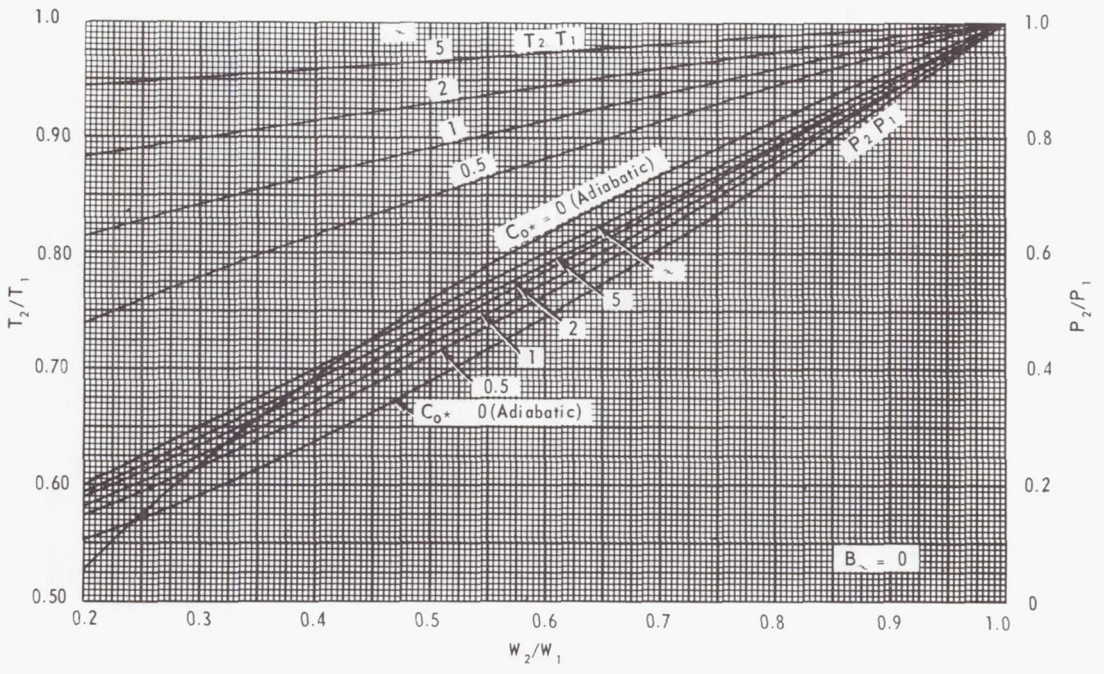


Figure 22.20. Discharge at constant mass flow with inside resistance negligible, $k = 1.4$.

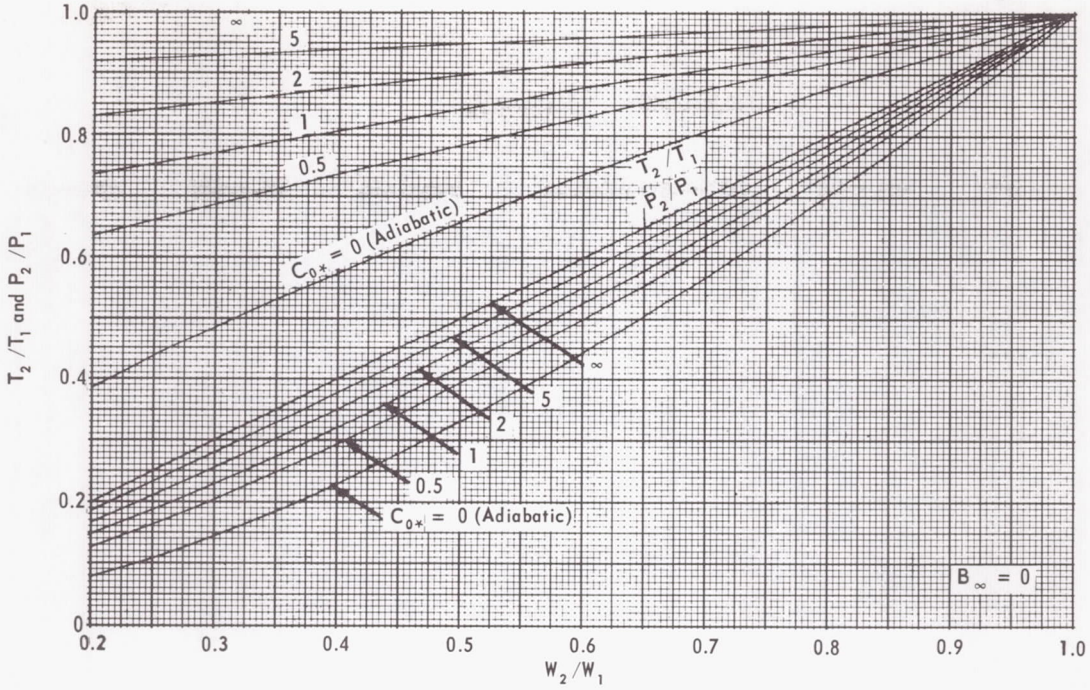


Figure 22.21. Discharge at constant mass flow with inside resistance negligible, $k = 1.6$.

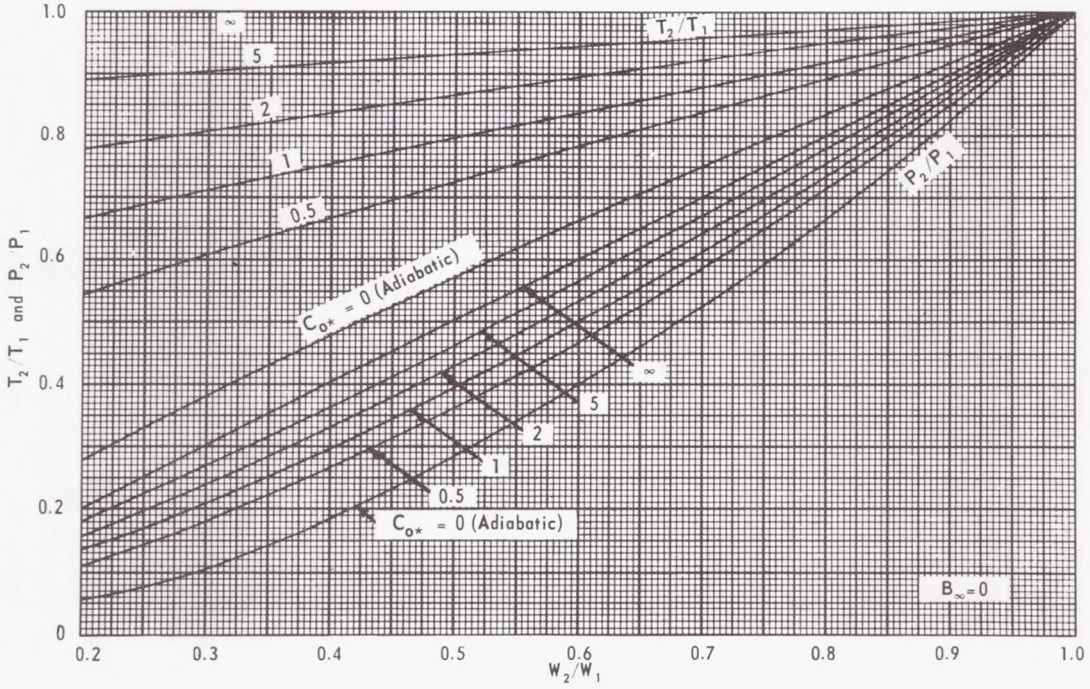


Figure 22.22. Discharge at constant mass flow with inside resistance negligible, $k = 1.8$.

APPENDIX A

GENERAL ENGINEERING DATA

Preceding Page Blank

TABLE A.1.—*Tube Data*

Tube size, in.	Wall thickness, in.	Inside diameter		Inside diameter functions, in.				Transverse internal area	
		D, in.	D, ft	D^2	D^3	D^4	D^5	a, in.^{2}	A, ft^2
1/4	0.035	0.180	0.01499	0.0324	0.00583	0.00105	0.000187	0.02544	0.00017
3/8	.035	.305	.02541	.0930	.02837	.00865	.00263	.07304	.00050
	.049	.277	.02308	.0767	.02125	.00589	.00162	.16024	.00041
	.065	.245	.02041	.0600	.01471	.00360	.00088	.4712	.00032
1/2	.049	.402	.03349	.1616	.06496	.02611	.01049	.12692	.00088
	.065	.370	.03083	.1369	.05065	.01874	.00693	.10752	.00074
3/4	.049	.652	.05433	.4251	.27717	.18071	.11781	.33387	.00231
	.065	.620	.05166	.3844	.23833	.14776	.09160	.30190	.00209
	.095	.560	.04666	.3136	.17562	.09834	.05507	.24630	.00170
1	.095	.810	.06749	.6561	.53144	.43047	.34867	.51530	.00357

TABLE A.2.—*Commercial Wrought Steel Pipe Data*

[Schedule wall thickness—per ASA B36.10—1950]

Nominal pipe size, in.	Outside diameter, in.	Thickness, in.		Inside diameter		Inside diameter functions, in.				Transverse internal area	
		Nominal	Minimum	D, in.	D, ft	D^2	D^3	D^4	D^5	a, in.^{2}	A, ft^2
Schedule 10:											
14	14	0.250	0.21875	13.5	1.125	182.25	2460.4	33215	448400	143.14	0.994
16	16	.250	.21875	15.5	1.291	240.25	3723.9	57720	894660	188.69	1.310
18	18	.250	.21875	17.5	1.4583	306.25	5359.4	93789	1641309	240.53	1.670
20	20	.250	.21875	19.5	1.625	380.25	7414.9	144590	2819500	298.65	2.074
24	24	.250	.21875	23.5	1.958	552.25	12977	304980	7167030	433.74	3.012
30	30	.312	.27300	29.376	2.448	862.95	25350	744288	21864218	677.76	4.707
Schedule 20:											
8	8.625	.250	.21875	8.125	.6771	66.02	536.38	4359.3	35409	51.85	.3601
10	10.75	.250	.21875	10.25	.8542	105.06	1076.9	11038	113141	82.52	.5731
12	12.75	.250	.21875	12.25	1.021	150.06	1838.3	22518	275855	117.86	.8185
14	14	.312	.27300	13.376	1.111	178.92	2393.2	32012	428185	140.52	.9758
16	16	.312	.27300	15.376	1.281	236.42	3635.2	55894	859442	185.69	1.290
18	18	.312	.27300	17.376	1.448	301.92	5246.3	91156	1583978	237.13	1.647

20	20	.375	.32812	19.250	1.604	370.56	7133.3	137317	2643352	291.04	2.021
24	24	.375	.32812	23.25	1.937	540.56	12568	292205	6793832	424.56	2.948
30	30	.500	.43750	29.00	2.417	841.0	24389	707281	20511149	660.52	4.587
Schedule 30:											
8	8.625	.277	.24237	8.071	.6726	65.14	525.75	4243.2	34248	51.16	.3553
10	10.75	.307	.26862	10.136	.8447	102.74	1041.4	10555	106987	80.69	.5603
12	12.75	.330	.28875	12.09	1.0075	146.17	1767.2	21366	258304	114.80	.7972
14	14	.375	.32812	13.25	1.1042	175.56	2326.2	30821	408394	137.88	.9575
16	16	.375	.32812	15.25	1.2708	232.56	3546.6	54084	824801	182.65	1.268
18	18	.438	.38325	17.124	1.4270	293.23	5021.3	85984	1472397	230.30	1.599
20	20	.500	.43750	19.00	1.5833	361.00	6859.0	130321	2476099	283.53	1.969
24	24	.562	.49175	22.876	1.9063	523.31	11971	273853	6264703	411.00	2.854
30	30	.625	.54687	28.75	2.3958	826.56	23764	683201	19642160	649.18	4.508
Schedule 40:											
1/8	.405	.068	.05950	.269	.0224	.0724	.0195	.005242	.00141	.057	.00040
1/4	.540	.088	.07700	.364	.0303	.1325	.0482	.01756	.00639	.104	.00072
3/8	.675	.091	.07962	.493	.0411	.2430	.1198	.05905	.02912	.191	.00133
1/2	.840	.109	.09537	.622	.0518	.3869	.2406	.1497	.09310	.304	.00211
3/4	1.050	.113	.09887	.824	.0687	.679	.5595	.4610	.3799	.533	.00371
1	1.315	.133	.11637	1.049	.0874	1.100	1.154	1.210	1.270	.864	.00600
1 1/4	1.660	.140	.12250	1.380	.1150	1.904	2.628	3.625	5.005	1.495	.01040
1 1/2	1.900	.145	.12687	1.610	.1342	2.592	4.173	6.718	10.82	2.036	.01414
2	2.375	.154	.13475	2.067	.1722	4.272	8.831	18.250	37.72	3.355	.02330
2 1/2	2.875	.203	.17762	2.469	.2057	6.096	15.051	37.161	91.75	4.788	.03322
3	3.500	.216	.18900	3.068	.2557	9.413	28.878	88.605	271.8	7.393	.05130
3 1/2	4.000	.226	.19775	3.548	.2957	12.59	44.663	158.51	562.2	9.886	.06870
4	4.500	.237	.20737	4.026	.3355	16.21	65.256	262.76	1058	12.730	.08840
5	5.563	.258	.22575	5.047	.4206	25.47	128.56	648.72	3275	20.006	.1390
6	6.625	.280	.24500	6.065	.5054	36.78	223.10	1352.8	8206	28.891	.2006
8	8.625	.322	.28175	7.981	.6651	63.70	508.36	4057.7	32380	50.027	.3474
10	10.75	.365	.31937	10.02	.8350	100.4	1006.0	10080	101000	78.855	.5475
12	12.75	.375	.32812	11.938	.9965	142.5	1701.3	20306	242470	111.93	.7773
Schedule 60:											
8	8.625	0.406	0.35525	7.813	0.6511	61.04	476.93	3725.9	29113	47.94	0.3329
10	10.75	.500	.43750	9.750	.8125	95.06	926.86	9036.4	88110	74.66	.5185
12	12.75	.562	.49175	11.626	.9688	135.16	1571.4	18268	212399	106.16	.7372
14	14.0	.593	.51887	12.814	1.0678	164.20	2104.0	26962	345480	128.96	.8956
16	16.0	.656	.57400	14.688	1.2240	215.74	3168.8	46544	683618	169 44	1.1766
18	18.0	.750	.65625	16.500	1.3750	272.25	4492.1	74120	1222982	213.83	1.4849
20	20.0	.812	.71050	18.376	1.5313	337.68	6205.2	114028	2095342	265.21	1.8417
24	24.0	.968	.84700	22.064	1.8387	486.82	10741	236994	5229036	382.35	2.6552

TABLE A.2.—*Commercial Wrought Steel Pipe Data*—Continued

[Schedule wall thickness—per ASA B36.10—1950]

Nominal pipe size, in.	Outside diameter, in.	Thickness, in.		Inside diameter		Inside diameter functions, in.				Transverse internal area	
		Nominal	Minimum	D, in.	D, ft	D^2	D^3	D^4	D^5	a, in.^{2}	A, ft^2
Schedule 80:											
1/8	0.405	0.095	0.08312	0.215	0.0179	0.0462	0.00994	0.002134	0.000459	0.036	0.00025
1/4	.540	.119	.10412	.302	.0252	.0912	.0275	.008317	.002513	.072	.00050
3/8	.675	.126	.11025	.423	.0353	.1789	.0757	.03200	.01354	.141	.00098
1/2	.840	.147	.12862	.546	.0455	.2981	.1628	.08886	.04852	.234	.00163
3/4	1.050	.154	.13475	.742	.0618	.5506	.4085	.3032	.2249	.433	.00300
1	1.315	.179	.15662	.957	.0797	.9158	.8765	.8387	.8027	.719	.00499
1 1/4	1.660	.191	.16712	1.278	.1065	1.633	2.087	2.6667	3.409	1.283	.00891
1 1/2	1.900	.200	.17500	1.500	.1250	2.250	3.375	5.062	7.594	1.767	.01225
2	2.375	.218	.19075	1.939	.1616	3.760	7.290	14.136	27.41	2.953	.02050
2 1/2	2.875	.276	.24150	2.323	.1936	5.396	12.536	29.117	67.64	4.238	.02942
3	3.5	.300	.26250	2.900	.2417	8.410	24.389	70.728	205.1	6.605	.04587
3 1/2	4.0	.318	.27825	3.364	.2803	11.32	38.069	128.14	430.8	8.888	.06170
4	4.5	.337	.29487	3.826	.3188	14.64	56.006	214.33	819.8	11.497	.07986
5	5.563	.375	.32812	4.813	.4011	23.16	111.49	536.38	2583	18.194	.1263
6	6.625	.432	.37800	5.761	.4801	33.19	191.20	1101.6	6346	26.067	.1810
8	8.625	.500	.43750	7.625	.6354	58.14	443.32	3380.3	25775	45.663	.3171
10	10.75	.500	.43750	9.564	.7970	91.47	874.82	8366.8	80020	71.84	.4989
12	12.75	.500	.43750	11.376	.9480	129.41	1472.2	16747	190523	101.64	.7058
Schedule 160:											
1/2	.840	.187	.16362	.466	.0388	.2172	.1012	.04716	.02197	.1706	.00118
3/4	1.050	.218	.19075	.614	.0512	.3770	.2315	.1421	.08726	.2961	.00206
1	1.315	.250	.21875	.815	.0679	.6642	.5413	.4412	.3596	.5217	.00362
1 1/4	1.660	.250	.21875	1.160	.0966	1.346	1.561	1.811	2.100	1.057	.00734
1 1/2	1.900	.281	.24587	1.338	.1115	1.790	2.395	3.205	4.288	1.406	.00976
2	2.375	.343	.30012	1.689	.1407	2.853	4.818	8.138	13.74	2.241	.01556
2 1/2	2.875	.375	.32812	2.125	.1771	4.516	9.596	20.39	43.33	3.546	.02463
3	3.50	.438	.38325	2.624	.2187	6.885	18.067	47.41	124.4	5.408	.03755
4	4.50	.531	.46462	3.438	.2865	11.82	40.637	139.7	480.3	9.283	.06447
5	5.563	.625	.54687	4.313	.3594	18.60	80.230	346.0	1492	14.61	.1015
6	6.625	.718	.62825	5.189	.4324	26.93	139.72	725.0	3762	21.15	.1469
8	8.625	.906	.79275	6.813	.5677	46.42	316.24	2155	14679	36.46	.2532
10	10.75	1.125	.98437	8.500	.7083	72.25	614.12	5220	44371	56.75	.3941

12	12.75	1.312	1.14800	10.126	.8438	102.54	1038.3	10514.	106461.	80.53	.5592
14	14.0	1.406	1.23025	11.188	.9323	125.17	1400.4	15668.	175292.	98.31	.6827
16	16.0	1.593	1.39387	12.814	1.0678	164.20	2104.0	26961.	345482.	128.96	.8956
18	18.0	1.781	1.55837	14.438	1.2032	208.45	3009.7	43454.	627387.	163.72	1.1369
20	20.0	1.968	1.72200	16.064	1.3387	258.05	4145.3	66590.	1069715.	202.67	1.4074
24	24.0	2.343	2.05012	19.314	1.6095	373.03	7204.7	139152.	2687582.	292.98	2.0346
Double-extra-strong pipe:											
1/2	.840	.294	.21787	.252	.0210	.0635	.0160	.004032	.00102	.050	.00035
3/4	1.050	.308	.26950	.434	.0362	.1884	.0817	.03549	.01540	.148	.00103
1	1.315	.358	.31325	.599	.0499	.3588	.2149	.1287	.07711	.282	.00196
1 1/4	1.660	.382	.33425	.896	.0747	.8028	.7193	.6445	.5775	.630	.00438
1 1/2	1.900	.400	.35000	1.100	.0917	1.210	1.331	1.4641	1.611	.950	.00660
2	2.375	.436	.38150	1.503	.1252	2.259	3.395	5.1031	7.670	1.774	.01232
2 1/2	2.875	.552	.48300	1.771	.1476	3.136	5.554	9.8345	17.42	2.464	.01710
3	3.500	.600	.52500	2.300	.1917	5.290	12.167	27.984	64.36	4.155	.02885
3 1/2	4.000	.636	.55650	2.728	.2273	7.442	20.302	55.383	151.1	5.845	.04059
4	4.500	.674	.58975	3.152	.2627	9.935	31.315	98.704	311.1	7.803	.05419
5	5.563	.750	.65625	4.063	.3386	16.51	67.072	272.58	1107	12.966	.09006
6	6.625	.864	.75600	4.897	.4081	23.98	117.43	575.04	2816	18.835	.1308
8	8.625	.875	.76562	6.875	.5729	47.27	324.95	2234.4	15360	37.122	.2578

TABLE A.3.—*Conversion Factors*

Multiply—	By—	To obtain—
Atmospheres:	76.00	Centimeters of mercury
	29.92	Inches of mercury
	33.90	Feet of water
	10 332	Kilograms per square meter
	14.70	Pounds per square inch
	1.058	Tons per square foot
Bars:	0.9869	Atmospheres
	1.0000	Dynes per square centimeter
	1.020×10^4	Kilograms per square meter
	2089	Pounds per square foot
	14.50	Pounds per square inch
British thermal units:	778.2	Foot-pounds
	3.930×10^{-4}	Horsepower-hours
	1055	Joules
	0.2520	Kilogram-calories
	107.6	Kilogram-meters
	2.930×10^{-4}	Kilowatt hours
British thermal units per minute:	12.97	Foot-pounds per second
	0.02358	Horsepower
	0.01758	Kilowatts
	17.58	Watts
Centimeters:	3.281×10^{-2}	Feet
	0.3937	Inches
	0.01	Meters
	6.214×10^{-6}	Miles
	10	Millimeters
	393.70	Mils
	1.094×10^{-2}	Yards
Centimeters of mercury:	0.01316	Atmospheres
	0.4461	Feet of water
	136.0	Kilograms per square meter
	27.85	Pounds per square foot
	0.1934	Pounds per square inch
Cubic meters:	10^{-6}	Cubic centimeters
	35.31	Cubic feet
	61 023	Cubic inches
	1.308	Cubic yards
	264.2	Gallons
	10^3	Liters
	2113	Pints (liquid)
	1057	Quarts (liquid)
Cubic yards:	7.646×10^5	Cubic centimeters
	27	Cubic feet
	46 656	Cubic inches
	0.7646	Cubic meters
	202.0	Gallons
	764.6	Liters
	1616	Pints (liquid)
	807.9	Quarts (liquid)
Cubic yards per minute:	0.45	Cubic feet per second
	3.367	Gallons per second
	12.74	Liters per second
Dynes:	1.020×10^{-3}	Grams
	7.233×10^{-5}	Poundals
	2.248×10^{-6}	Pounds
Dynes per square centimeter:	1	Bars
Feet:	30.48	Centimeters
	12.00	Inches
	0.3048	Meters
	1.894×10^{-4}	Miles
	1/3	Yards
Feet of water:	0.02950	Atmospheres
	0.8826	Inches of mercury
	304.8	Kilograms per square meter
	62.43	Pounds per square foot
	0.4335	Pounds per square inch

Centimeters per second:	1.968	Feet per minute
	0.03281	Feet per second
	0.036	Kilometers per hour
	0.6	Meters per minute
	0.02237	Miles per hour
	3.728×10^{-4}	Miles per minute
Centimeters per second per second:	0.03281	Feet per second per second
	0.036	Kilometers per hour per second
	0.02237	Miles per hour per second
Cubic centimeters:	3.531×10^{-5}	Cubic feet
	6.102×10^{-2}	Cubic inches
	10^{-6}	Cubic meters
	1.308×10^{-6}	Cubic yards
	2.642×10^{-4}	Gallons
	10^{-3}	Liters
	2.113×10^{-3}	Pints (liquid)
	1.057×10^{-3}	Quarts (liquid)
Cubic feet:	2.832×10^{4}	Cubic centimeters
	1728	Cubic inches
	0.02832	Cubic meters
	0.03704	Cubic yards
	7.481	Gallons
	28.32	Liters
	59.84	Pints (liquid)
	29.92	Quarts (liquid)
Cubic feet per minute:	472.0	Cubic centimeters per second
	0.1247	Gallons per second
	0.4720	Liters per second
	62.4	Pounds of water per minute
Cubic inches:	16.39	Cubic centimeters
	5.787×10^{-4}	Cubic feet
	1.639×10^{-5}	Cubic meters
	2.143×10^{-5}	Cubic yards
	4.329×10^{-3}	Gallons
	1.639×10^{-2}	Liters
	1.061×10^{5}	Mil-feet
	0.03463	Pints (liquid)
	0.01732	Quarts (liquid)

Feet per minute:	0.5080	Centimeters per second
	0.01667	Feet per second
	0.01829	Kilometers per hour
	0.3048	Meters per minute
	0.01136	Miles per hour
Feet per second:	30.48	Centimeters per second
	1.097	Kilometers per hour
	0.5921	Knots
	18.29	Meters per minute
	0.6818	Miles per hour
	0.01136	Miles per minute
Feet per second per second:	30.48	Centimeters per second per second
	1.097	Kilometers per hour per second
	0.3048	Meters per second per second
	0.6818	Miles per hour per second
Foot-pounds:	1.285×10^{-3}	British thermal units
	1.356×10^{7}	Ergs
	5.050×10^{-7}	Horsepower-hours
	1.356	Joules
	3.238×10^{-4}	Kilogram-calories
	0.1383	Kilogram-meters
	3.766×10^{-7}	Kilowatt-hours
Foot-pounds per minute:	1.285×10^{-3}	British thermal units per minute
	0.01667	Foot-pounds per second
	3.030×10^{-5}	Horsepower
	3.238×10^{-4}	Kilogram-calories per minute
	2.260×10^{-5}	Kilowatts
Foot-pounds per second:	7.712×10^{-2}	British thermal units per minute
	1.818×10^{-3}	Horsepower
	1.943×10^{-2}	Kilogram-calories per minute
	1.356×10^{-3}	Kilowatts
Gallons:	3785	Cubic centimeters
	0.1337	Cubic feet
	231	Cubic inches
	3.785×10^{-3}	Cubic meters
	4.951×10^{-3}	Cubic yards

TABLE A.3.—*Conversion Factors*—Continued

Multiply—	By—	To obtain—
Gallons (Continued):	3.785	Liters
	8	Pints (liquid)
	4	Quarts (liquid)
Gallons per minute:	2.228×10^{-3}	Cubic feet per second
	0.06308	Liters per second
Grams:	980.7	Dynes
	15.43	Grains
	10^{-3}	Kilograms
	10^{3}	Milligrams
	0.03527	Ounces
	0.03215	Ounces (troy)
	0.07093	Poundals
	2.205×10^{-3}	Pounds
Gram-centimeters:	9.297×10^{-8}	British thermal units
	980.7	Ergs
	7.235×10^{-5}	Foot-pounds
	9.807×10^{-5}	Joules
	2.343×10^{-8}	Kilogram-calories
	10^{-5}	Kilogram-meters
Grams per centimeter:	5.600×10^{-3}	Pounds per inch
Grams per cubic centimeter:	62.43	Pounds per cubic foot
	0.03613	Pounds per cubic inch
	3.405×10^{-7}	Pounds per mil-foot
Horsepower:	42.40	British thermal units per minute
	33 000	Foot-pounds per minute
	550	Foot-pounds per second
	1.014	Horsepower (metric)
	10.68	Kilogram-calories per minute
	0.7457	Kilowatts
	745.7	Watts
Horsepower-hours:	2544	British thermal units
	1.98×10^{6}	Foot-pounds
Meters per minute (Continued):	0.06	Kilometers per hour
	0.03728	Miles per hour
Meters per second:	196.8	Feet per minute
	3.281	Feet per second
	3.6	Kilometers per hour
	0.06	Kilometers per minute
	2.237	Miles per hour
	0.03728	Miles per minute
Meters per second per per second:	3.281	Feet per second per second
	3.6	Kilometers per hour per second
	2.237	Miles per hour per second
Miles per minute:	2682	Centimeters per second
	88	Feet per second
	1.609	Kilometers per minute
	52.10	Knots
	60	Miles per hour
Poundals:	13 826	Dynes
	14.10	Grams
	0.03108	Pounds
Pounds:	444 823	Dynes
	7000	Grains
	453.6	Grams
	16	Ounces
	32.17	Poundals
Pounds of water:	0.01602	Cubic feet
	27.68	Cubic inches
	0.1198	Gallons
Pounds of water per minute:	2.669×10^{-4}	Cubic feet per second
Pounds per cubic foot:	0.01602	Grams per cubic centimeters
	16.02	Kilograms per cubic meter

	2.684×10^6	Joules
	641.1	Kilogram-calories
	2.737×10^5	Kilogram-meters
	0.7455	Kilowatt-hours
Hours:	4.167×10^{-2}	Days
	60	Minutes
	3600	Seconds
	5.952×10^{-3}	Weeks
Inches:	2.540	Centimeters
	8.333×10^{-2}	Feet
	1.578×10^{-5}	Miles
	10^3	Mils
	2.778×10^{-2}	Yards
Inches of mercury:	0.03342	Atmospheres
	1.133	Feet of water
	345.3	Kilograms per square meter
	70.73	Pounds per square foot
	0.4912	Pounds per square inch
Inches of water:	0.002458	Atmospheres
	0.07355	Inches of mercury
	25.40	Kilograms per square meter
	0.5781	Ounces per square inch
	5.204	Pounds per square foot
	0.03613	Pounds per square inch
Log_{10} N:	2.303	Log N or ln N
Log N or ln N:	0.4343	Log_{10} N
Meters:	100	Centimeters
	3.281	Feet
	39.37	Inches
	10^{-3}	Kilometers
	6.214×10^{-4}	Miles
	10^3	Millimeters
	1.094	Yards
Meters per minute:	1.667	Centimeters per second
	3.281	Feet per minute
	0.05468	Feet per second
	5.787×10^{-4}	Pounds per cubic inch
	5.456×10^{-9}	Pounds per mil-foot
Pounds per cubic inch:	27.68	Grams per cubic centimeter
	2.768×10^4	Kilograms per cubic meter
	1728	Pounds per cubic foot
	9.425×10^{-6}	Pounds per mil-foot
Pounds per square foot:	4.725×10^{-4}	Atmospheres
	0.01602	Feet of water
	1.414×10^{-2}	Inches of mercury
	4.882	Kilograms per square meter
	6.944×10^{-3}	Pounds per square inch
Pounds per square inch:	0.06804	Atmospheres
	2.307	Feet of water
	2.036	Inches of mercury
	703.1	Kilograms per square meter
	144	Pounds per square foot
Square centimeters:	1.973×10^5	Circular mils
	1.076×10^{-3}	Square feet
	0.1550	Square inches
	10^{-4}	Square meters
	3.861×10^{-11}	Square miles
	100	Square millimeters
	1.196×10^{-4}	Square yards
Square feet:	2.296×10^{-5}	Acres
	1.833×10^8	Circular mils
	929.0	Square centimeters
	144	Square inches
	0.09290	Square meters
	3.587×10^{-8}	Square miles
	1/9	Square yards
Temperature (degrees centigrade) + 273:	1	Absolute temperature (degrees centigrade)
Temperature (degrees centigrade) + 17.8:	1.8	Temperature (degrees Fahrenheit)

TABLE A.3.—*Conversion Factors*—Continued

Multiply—	By—	To obtain—	Multiply—	By—	To obtain—
Temperature (degrees Fahrenheit)+460:	1	Absolute temperature (degrees Fahrenheit)	Temperature (degrees Fahrenheit)−32:	5/9	Temperature (degrees centigrade)

TABLE A.4—*Prefixes*

pico	10^{-12}
nano	10^{-9}
micro	10^{-6}
milli	10^{-3}
centi	10^{-2}
deci	10^{-1}
uni	10^{0}
deka	10^{1}
hecto	10^{2}
kilo	10^{3}
mega	10^{6}
giga	10^{9}
tera	10^{12}

TABLE A.5—*Low-Temperature Physical Properties of Gases*

[Courtesy of Air Products and Chemicals, Inc.]

Name	Formula	Molecular weight	Normal boiling point			Critical point		Triple point or melting point		Specific heat, c_p at {70° F, 14.7 psia} Btu/lb-mole °F	Gas density at 70° F, 14.7 psia
			Temp, °F	Liquid density, lb/ft³	Latent heat, Btu/lb-mole	Temp, °F	Pressure, psia	Temp, °F	Pressure, psia		
Acetylene	C_2H_2	26.04	[c] −119.20	[c] 38.700	[c] 9 180.0	96.0	906	−114.6	17.40	10.60	0.068000
Air [a]	[b]	28.96	−317.90	54.560	2 556.0					7.00	.074930
Ammonia	NH_3	17.03	−28.10	42.600	10 037.0	270.3	1639	−108.0	8.8×10^{-1}	8.60	.044500

Argon [a]	A	39.95	−302.60	86.980	2 804.0	−187.6	705	−308.9	9.99	4.98	.103400
Carbon dioxide	CO_2	44.01	[c] 109.30	[c] 97.500	[c] 10 854.0	87.9	1071	−69.9	75.10	8.95	.114400
Carbon monoxide	CO	28.01	−311.90	49.300	2 597.0	−220.4	508	−337.1	2.23	6.97	.072500
Carbonyl sulfide	COS	60.07	−58.30	73.000	7 961.0	221.0	89€	−271.8	.....	9.92	.152100
Chlorine	Cl_2	70.91	−29.30	97.400	8 780.0	291.2	1118	−149.8	2.02×10^{-1}	8.20	.185300
Deuterium	D_2	4.03	−417.30	10.700	540.0	−390.8	239	−426.0	2.48	6.97	.010400
Ethane	C_2H_6	30.07	−127.60	33.800	6 315.0	90.1	708	−297.9	1.20×10^{-4}	12.60	.078300
Ethylene	C_2H_4	28.05	−154.80	35.200	5 826.0	49.1	735	−272.5	1.70×10^{-2}	10.40	.072900
Fluorine	F_2	38.00	−306.60	93.800	2 815.0	−200.2	808	−363.3	.....	7.49	.098300
Freon-12	CCl_2F_2	120.92	−21.60	92.900	8 592.0	233.6	597	−252.4	.....	17.66	.318000
Freon-13	$CClF_3$	104.46	−114.60	95.000	6 670.0	83.9	561	−294.0	.....	16.09	.273000
Freon-14	CF_4	88.01	−198.40	122.400	5 160.0	−49.9	542	−299.2	1.70×10^{-2}	14.60	.228000
Freon-22	$CHClF_2$	86.47	−41.40	88.200	8 704.0	204.8	716	−256.0	.....	13.35	.229000
Helium [a]	He	4.00	−452.13	7.798	39.6	−450.2	33	[d] 455.8	[d] 7.35×10^{-1}	4.98	.010340
Hydrochloric acid	HCl	36.46	−120.90	74.300	6 948.0	124.5	1199	−173.0	.....	6.90	.095000
Hydrogen [a]	H_2	2.02	−422.99	4.418	389.0	−399.8	188	−434.5	1.0440	6.89	.005209
Hydrogen sulfide	H_2S	34.08	−75.40	60.000	8 033.0	212.7	1307	−122.0	3.3600	8.20	.089200
Krypton [a]	Kr	83.80	−244.00	150.600	3 884.0	−82.8	796	−250.9	10.6200	4.98	.217200
Methane	CH_4	16.04	−258.60	26.500	3 519.0	−116.6	670	−296.5	1.6900	8.60	.041600
Methyl chloride	CH_3Cl	50.49	−11.50	62.200	9 293.0	289.6	967	−144.0	1.2700	9.97	.133000
Neon [a]	Ne	20.18	−410.70	75.350	748.0	−379.7	395	−415.4	6.2700	4.98	.052150
Nitric oxide	NO	30.01	−241.00	79.300	5 953.0	−137.2	945	−263.6	3.1600	7.10	.077700
Nitrogen [a]	N_2	28.01	−320.40	50.460	2 405.0	−232.5	491	−345.9	1.8200	6.98	.072450
Nitrogen trifluoride	NF_3	71.01	−199.20	96.000	4 984.0	−38.7	657	−343.3	1.77×10^{-3}	.....	.186400
Nitrous oxide	N_2O	44.01	−127.20	76.800	7 110.0	97.7	1054	−131.6	12.7400	9.20	.114600
Oxygen [a]	O_2	32.00	−297.30	71.270	2 932.0	−181.1	737	−361.8	2.10×10^{-2}	7.02	.082810
Ozone	O_3	48.00	−169.40	101.800	6 174.0	10.2	791	−314.5	.....	.....	.124000
Propane	C_3H_8	44.10	−43.70	36.200	8 076.0	206.2	617	−305.8	8.39×10^{-11}	17.40	.115400
Propylene	C_3H_6	42.08	−53.80	37.500	7 925.0	197.4	667	−301.0	2.44×10^{-8}	15.30	.107000
Sulfur dioxide	SO_2	64.06	13.90	89.300	10 728.0	315.0	1142	−103.8	2.43×10^{-1}	9.60	.168700
Xenon [a]	Xe	131.30	−163.00	190.800	5 436.0	61.9	847	−169.2	11.82	4.98	.341600

[a] Based on data from the National Bureau of Standards—Compressed Gas Association Meeting, June 19, 1962.

[b] Proximate composition of dry air (mole percent): 78.09 N_2, 20.95 O_2, 0.93 Ar, 0.03 CO_2.

[c] Denotes sublimation and solid density.

[d] λ (lambda) point.

TABLE A.6—*Weight and Volume Equivalents*

Liquid and gaseous oxygen and nitrogen

Oxygen								Nitrogen							
Weight of liquid or gas		Volume of liquid at normal boiling point				Volume of gas at 70° F		Weight of liquid or gas		Volume of liquid at normal boiling point				Volume of gas at 70° F	
Pounds	Kilograms	Cubic feet	Liters	Quarts	Gallons	Cubic feet	Cubic meters	Pounds	Kilograms	Cubic feet	Liters	Quarts	Gallons	Cubic feet	Cubic meters
1.000	0.454	0.0140	0.397	0.420	0.105	12.08	0.342	1.000	0.454	0.0198	0.561	0.593	0.148	13.80	0.391
2.205	1.000	.0309	.876	.926	.231	26.62	.754	2.205	1.000	.0437	1.237	1.307	.327	30.43	.862
71.270	32.327	1.0000	28.316	29.922	7.481	860.60	24.370	50.460	22.888	1.0000	28.316	29.922	7.481	696.50	19.723
2.517	1.142	.0353	1.000	1.057	.264	30.39	.861	1.782	.808	.0353	1.000	1.057	.264	24.60	.697
2.382	1.080	.0334	0.946	1.000	.250	28.76	.814	1.686	.765	.0334	.946	1.000	.250	23.28	.659
9.527	4.321	.1337	3.785	4.000	1.000	115.05	3.258	6.746	3.060	.1337	3.785	4.000	1.000	93.11	2.637
8.281	3.756	.1162	3.290	3.477	.869	100.00	2.832	7.245	3.286	.1436	4.065	4.296	1.074	100.00	2.832
2.924	1.327	.0410	1.162	1.228	.307	35.31	1.000	2.558	1.160	.0507	1.436	1.517	0.379	35.31	1.000

Liquid and gaseous air and helium

Air								Helium							
Weight of liquid or gas		Volume of liquid at normal boiling point				Volume of gas at 70° F		Weight of liquid or gas		Volume of liquid at normal boiling point				Volume of gas at 70° F	
Pounds	Kilograms	Cubic feet	Liters	Quarts	Gallons	Cubic feet	Cubic meters	Pounds	Kilograms	Cubic feet	Liters	Quarts	Gallons	Cubic feet	Cubic meters
1.000	0.454	0.0183	0.519	0.548	0.137	13.34	0.378	1.000	0.454	0.1282	3.631	3.837	0.959	96.72	2.739
2.205	1.000	.0404	1.144	1.209	.302	29.42	.833	2.205	1.000	.2827	8.006	8.460	2.115	213.23	6.038
54.560	24.748	1.0000	28.316	29.922	7.481	728.10	20.618	7.793	3.537	1.0000	28.316	29.922	7.481	754.20	21.357
1.927	.874	.0353	1.000	1.057	.264	25.71	.728	.275	.125	.0353	1.000	1.057	.264	26.63	.754

1.823	.828	.0334	.946	1.000	.250	24.33	.689	.261	.118	.0334	.946	1.000	.250	25.21	.714
7.294	3.308	.1337	3.785	4.000	1.000	97.33	2.756	1.042	.473	.1337	3.785	4.000	1.000	100.82	2.855
7.493	3.399	.1373	3.889	4.110	1.027	100.00	2.832	1.034	.469	.1326	3.754	3.967	.992	100.00	2.832
2.646	1.200	.0485	1.373	1.451	.363	35.31	1.000	.365	.166	.0468	1.326	1.401	.350	35.31	1.000

Liquid and gaseous argon and hydrogen

Argon								Hydrogen							
Weight of liquid or gas		Volume of liquid at normal boiling point				Volume of gas at 70° F		Weight of liquid or gas		Volume of liquid at normal boiling point				Volume of gas at 70° F	
Pounds	Kilograms	Cubic feet	Liters	Quarts	Gallons	Cubic feet	Cubic meters	Pounds	Kilograms	Cubic feet	Liters	Quarts	Gallons	Cubic feet	Cubic meters
1.000	0.454	0.0115	0.326	0.344	0.086	9.67	0.274	1.000	0.454	0.2263	6.409	6.773	1.693	191.96	5.436
2.205	1.000	.0253	.718	.758	.190	21.32	.604	2.205	1.000	.4990	14.130	14.931	3.733	423.20	11.984
86.98	39.453	1.0000	28.316	29.922	7.481	841.20	23.820	4.418	2.004	1.0000	28.316	29.922	7.481	848.10	24.016
3.072	1.393	.0353	1.000	1.057	.264	29.71	.841	.155	.071	.0353	1.000	1.057	.264	29.95	.848
2.907	1.319	.0334	.946	1.000	.250	28.11	.796	.148	.067	.0334	.946	1.000	.250	28.34	.803
11.628	5.274	.1337	3.785	4.000	1.000	112.45	3.184	.591	.268	.1337	3.785	4.000	1.000	113.37	3.210
10.340	4.690	.1139	3.366	3.557	.889	100.00	2.832	.521	.236	.1179	3.339	3.528	.882	100.00	2.832
3.652	1.656	.0420	1.189	1.256	.314	35.31	1.000	.184	.083	.0416	1.179	1.246	.311	35.31	1.000

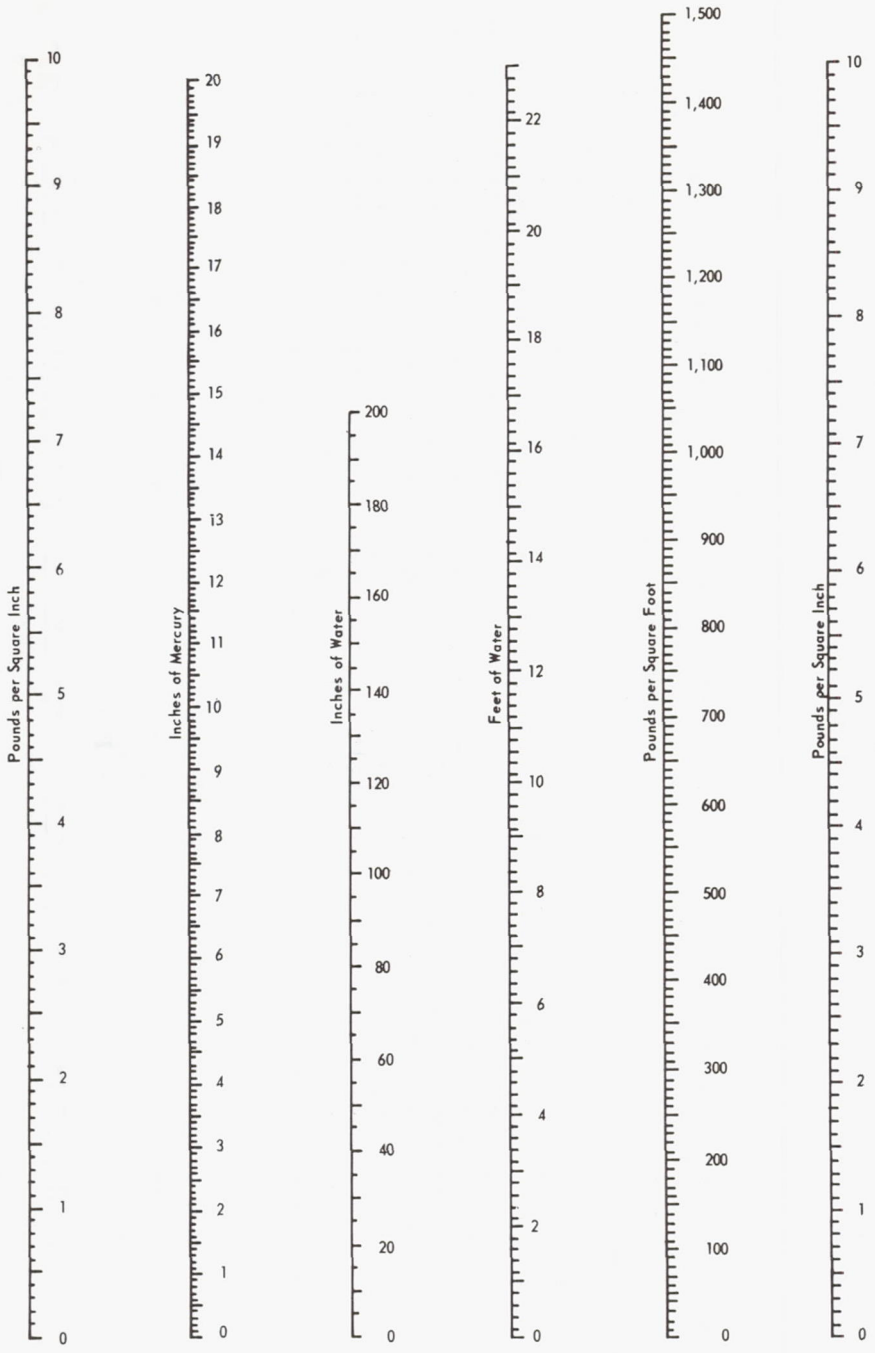


Figure A.1. Pressure conversion chart.

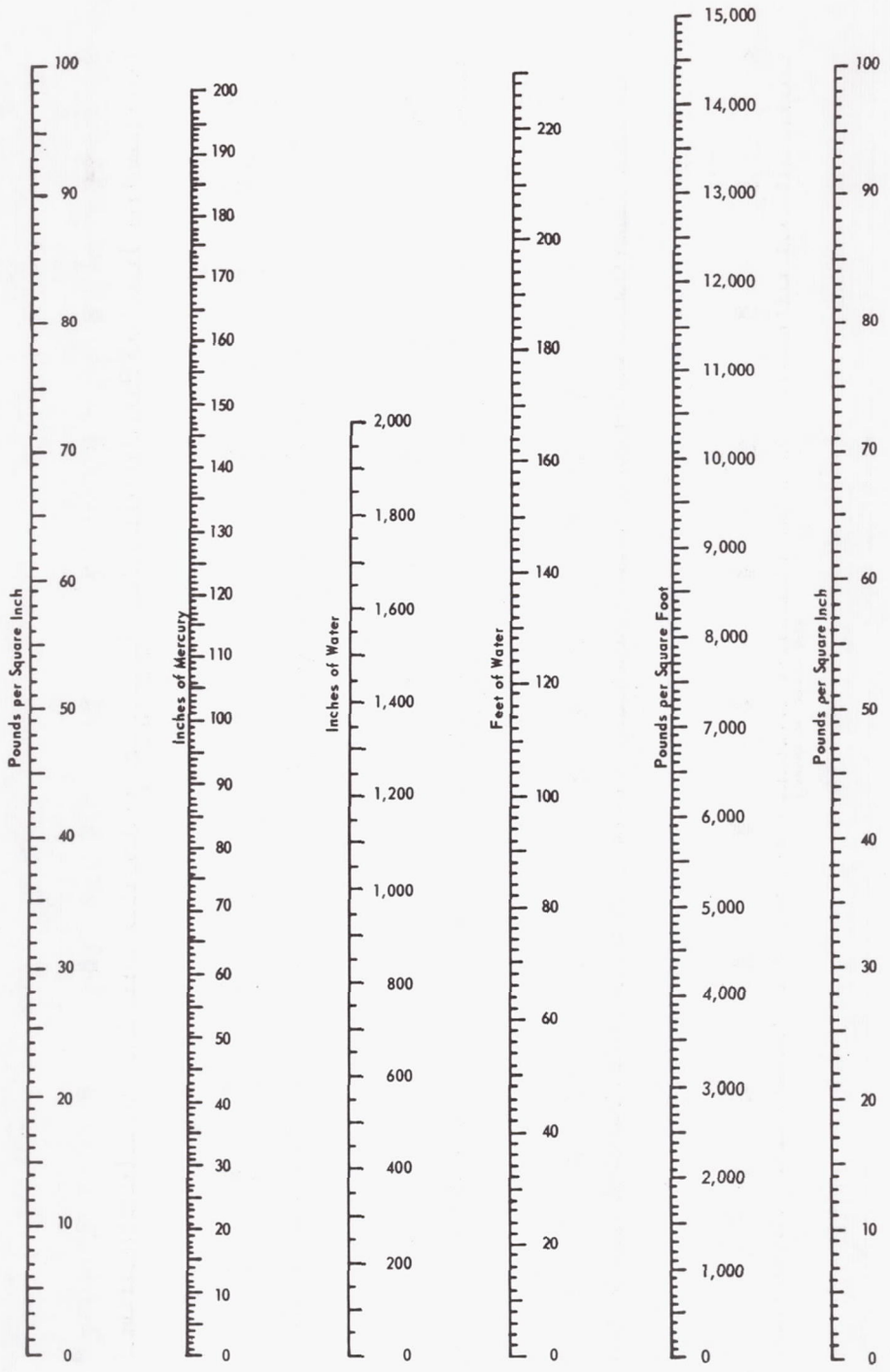


Figure A.1. Pressure conversion chart.—Continued.

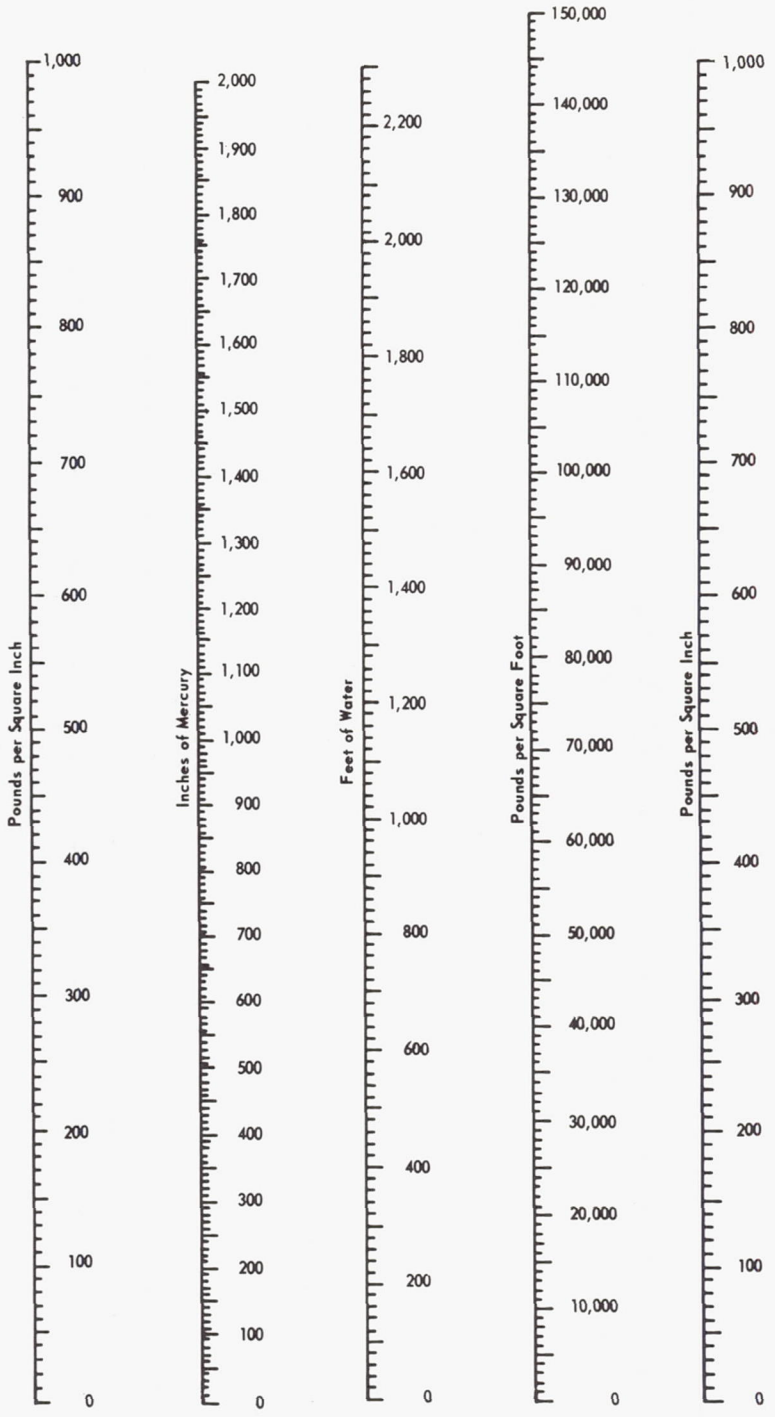


Figure A.1. Pressure conversion chart.—Continued.

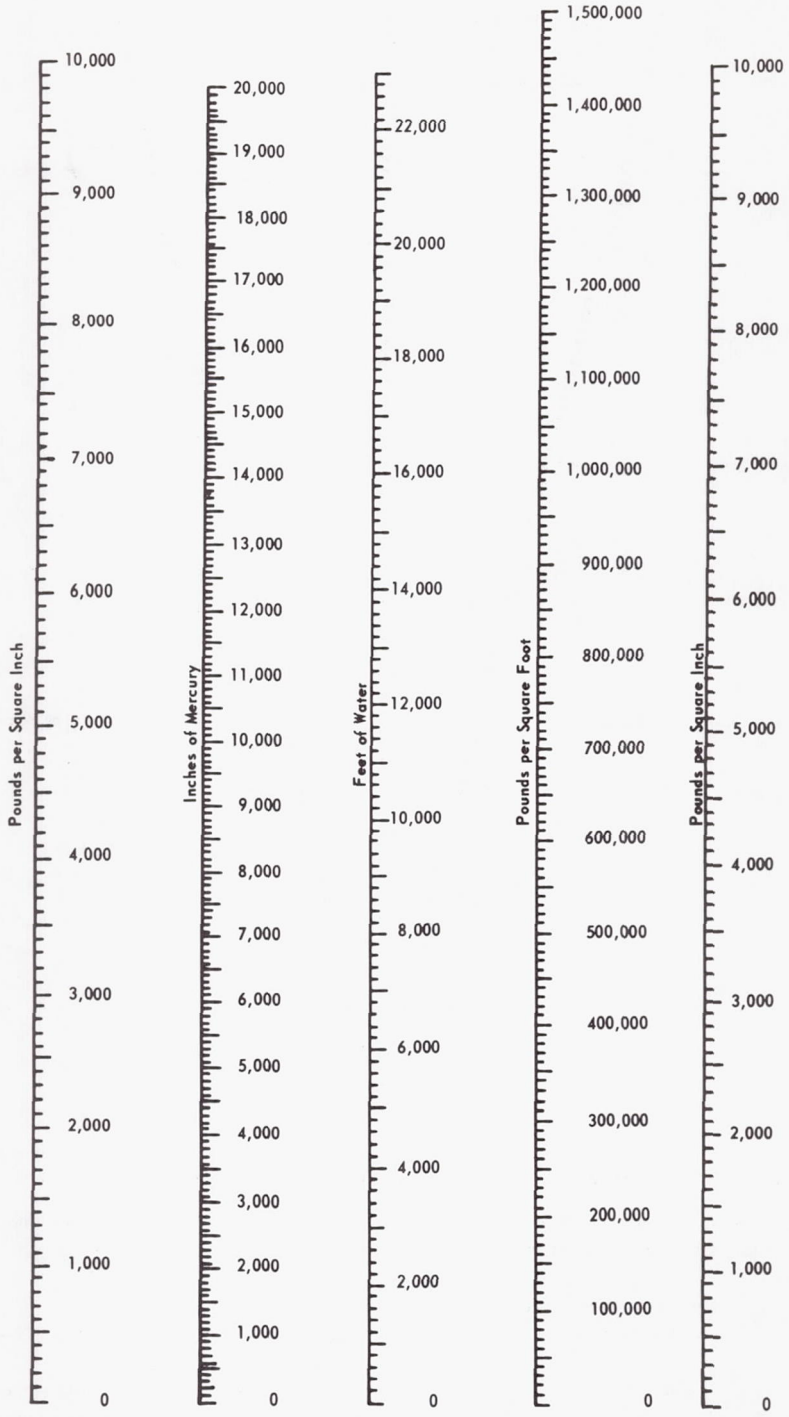


Figure A.1. Pressure conversion chart.—Continued.

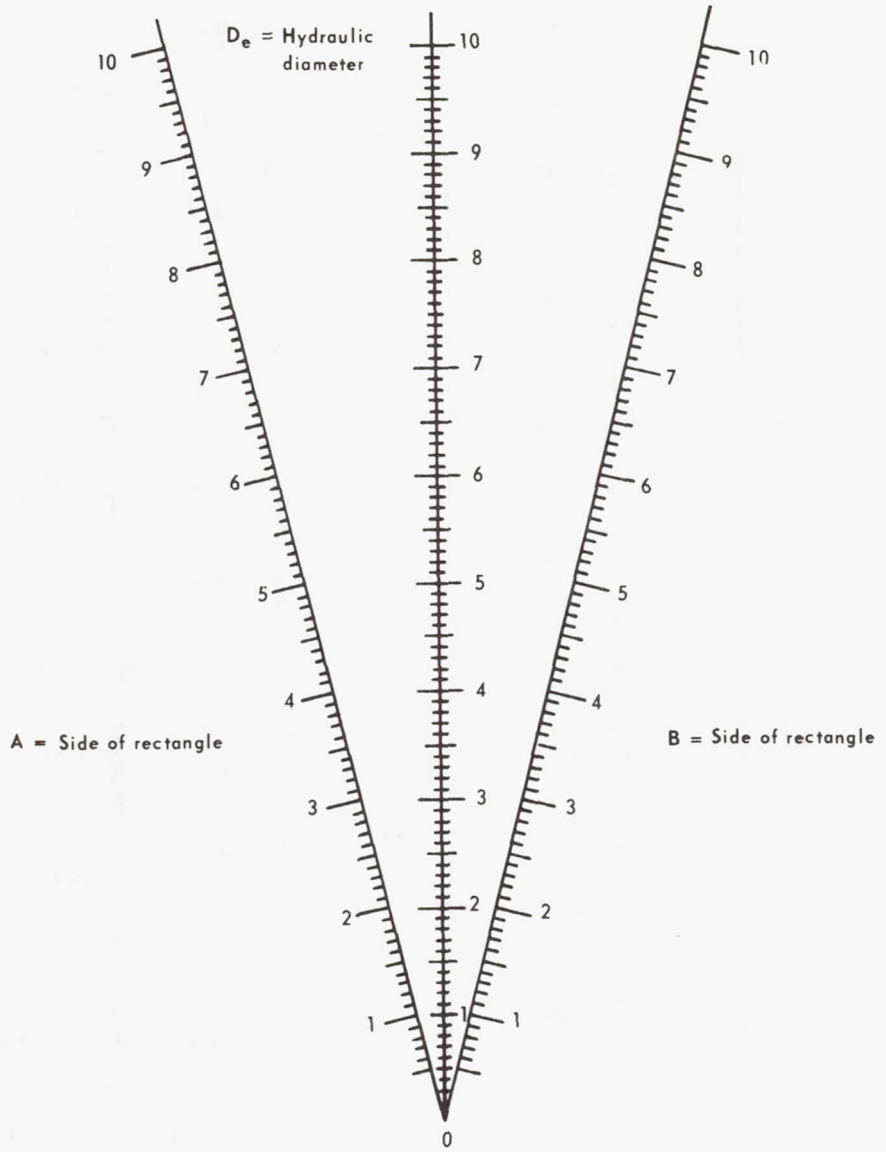


Figure A.2. Hydraulic diameter of rectangular pipes. [*Courtesy of Design News.*]

A rectangular pipe's equivalent hydraulic diameter, D_e, is 4 times the hydraulic radius:

$$D_e = 4\left(\frac{\text{cross-sectional area}}{\text{wetted perimeter}}\right)$$

$$= 4\left(\frac{AB}{2(A+B)}\right)$$

where A and B are the two dimensions.

The nomogram solves the equation:

$$D_e = \frac{2AB}{A+B}$$

If both A and B are multiplied by N, then D_e must also be multiplied by N.

Example: What is the equivalent hydraulic diameter of a pipe having sides of 60 and 30?

Solution: Aline (10)(6) with (10)(3) and read $D_e = (10)(4) = 40$.

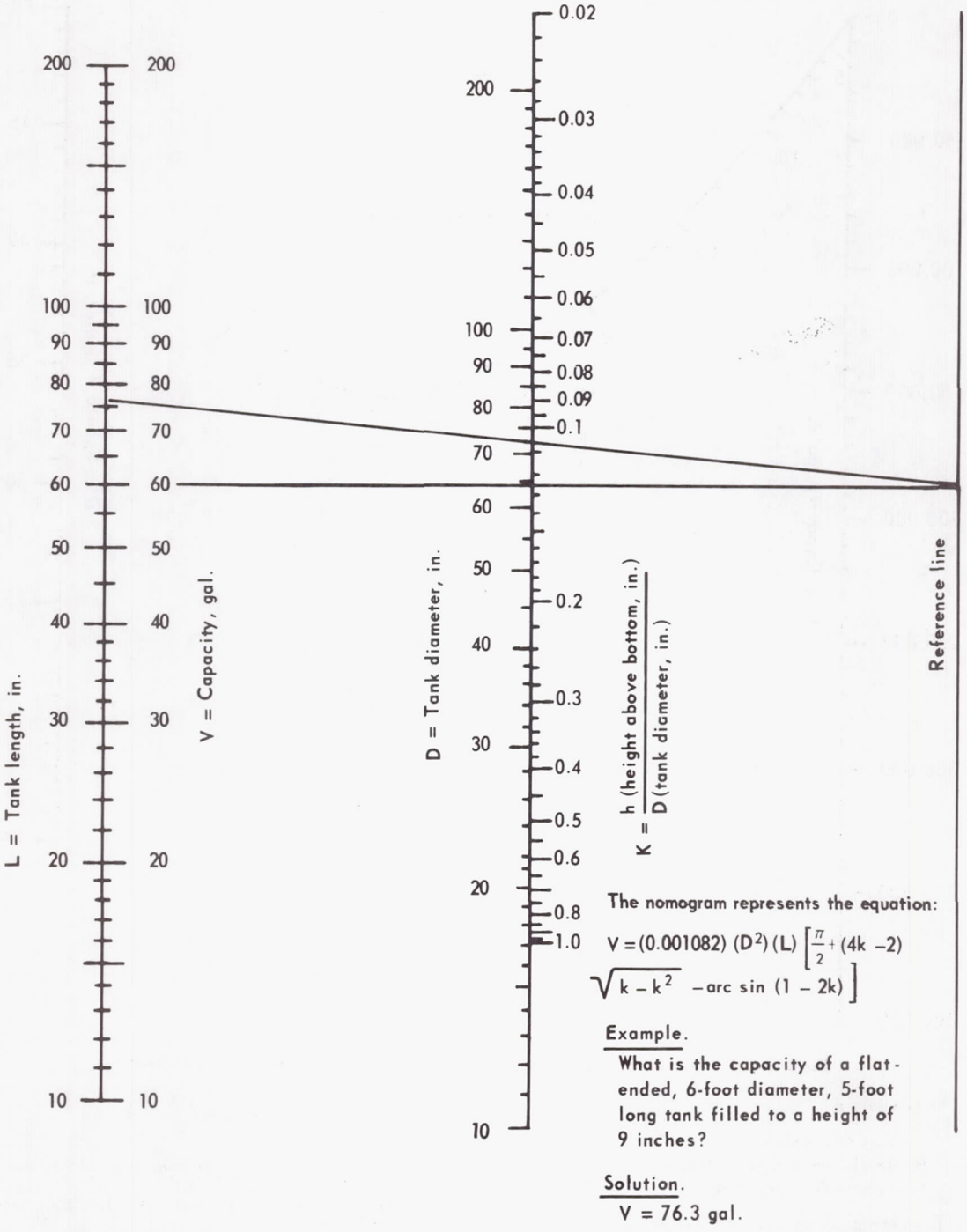


Figure A.3. Capacities and partially filled volumes of horizontal round tanks and pipes. [*Courtesy of Design News.*]

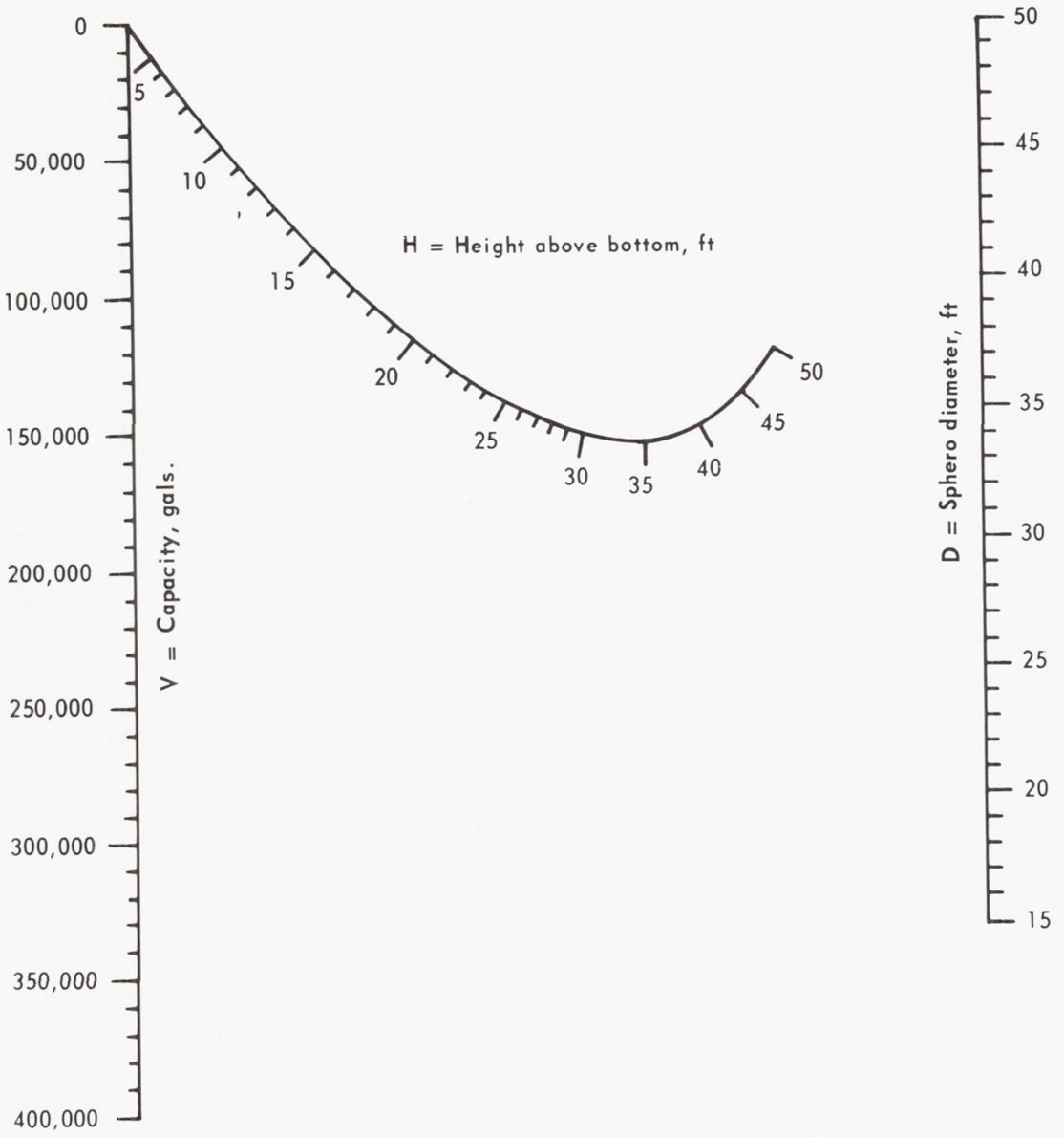


Figure A.4. Nomogram for partial volumes of spheres. [*Courtesy of Design News.*]

Nomenclature:

V = capacity, gallons
H = height above bottom, feet
D = sphere diameter, feet

The nomogram represents the equation:

$$V = 7.48\pi(H^2)\left(\frac{D}{2} - \frac{H}{3}\right)$$

Example: What is the volume in a 50-foot-diameter sphere filled to a height of 15 feet?

Solution: Aline $D = 50$ with $H = 15$ and read $V = 106{,}000$ gallons.

APPENDIX B

DATA ON AIR

325-994 O-69—31

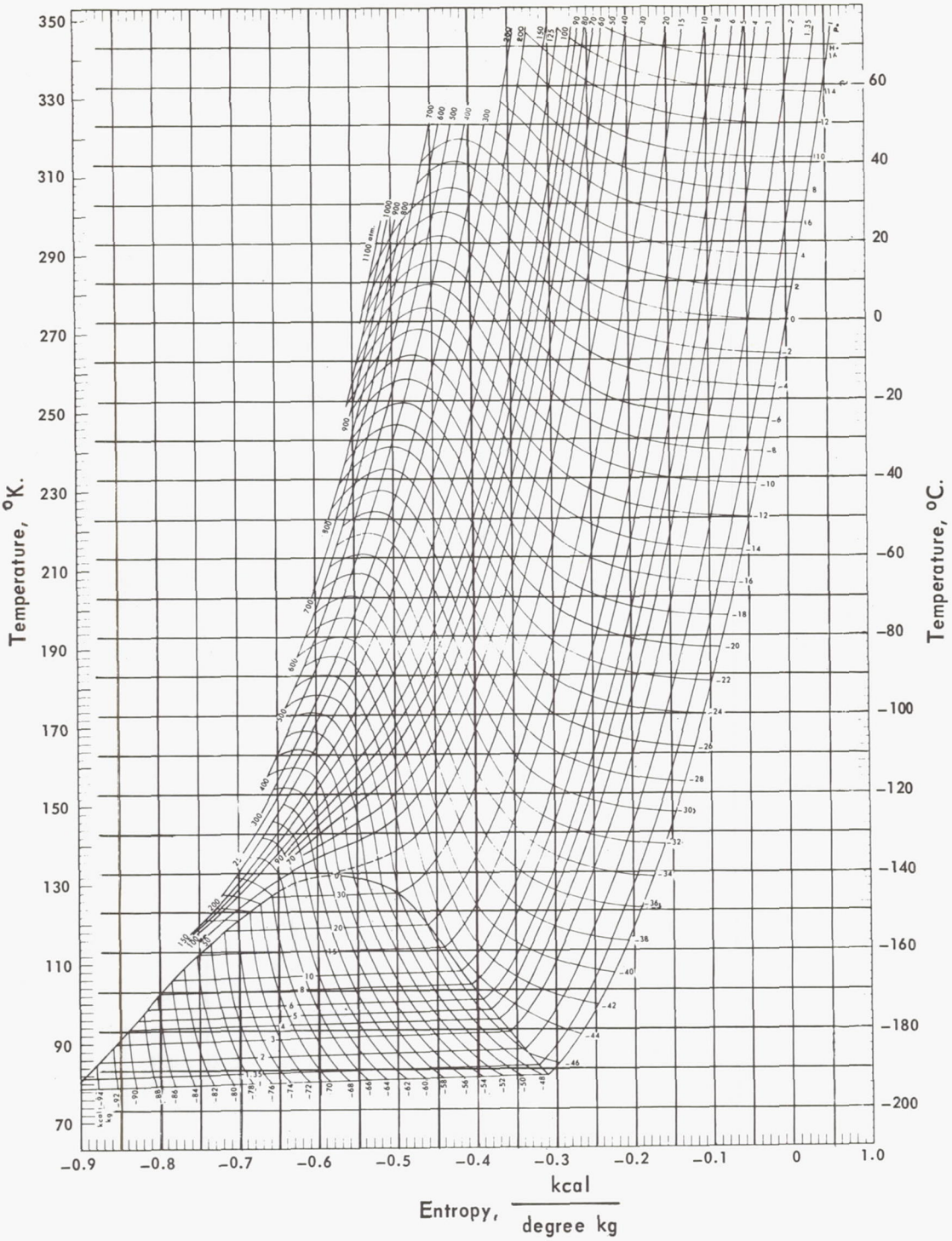


Figure B.1. Thermodynamic diagram, temperature versus entropy.

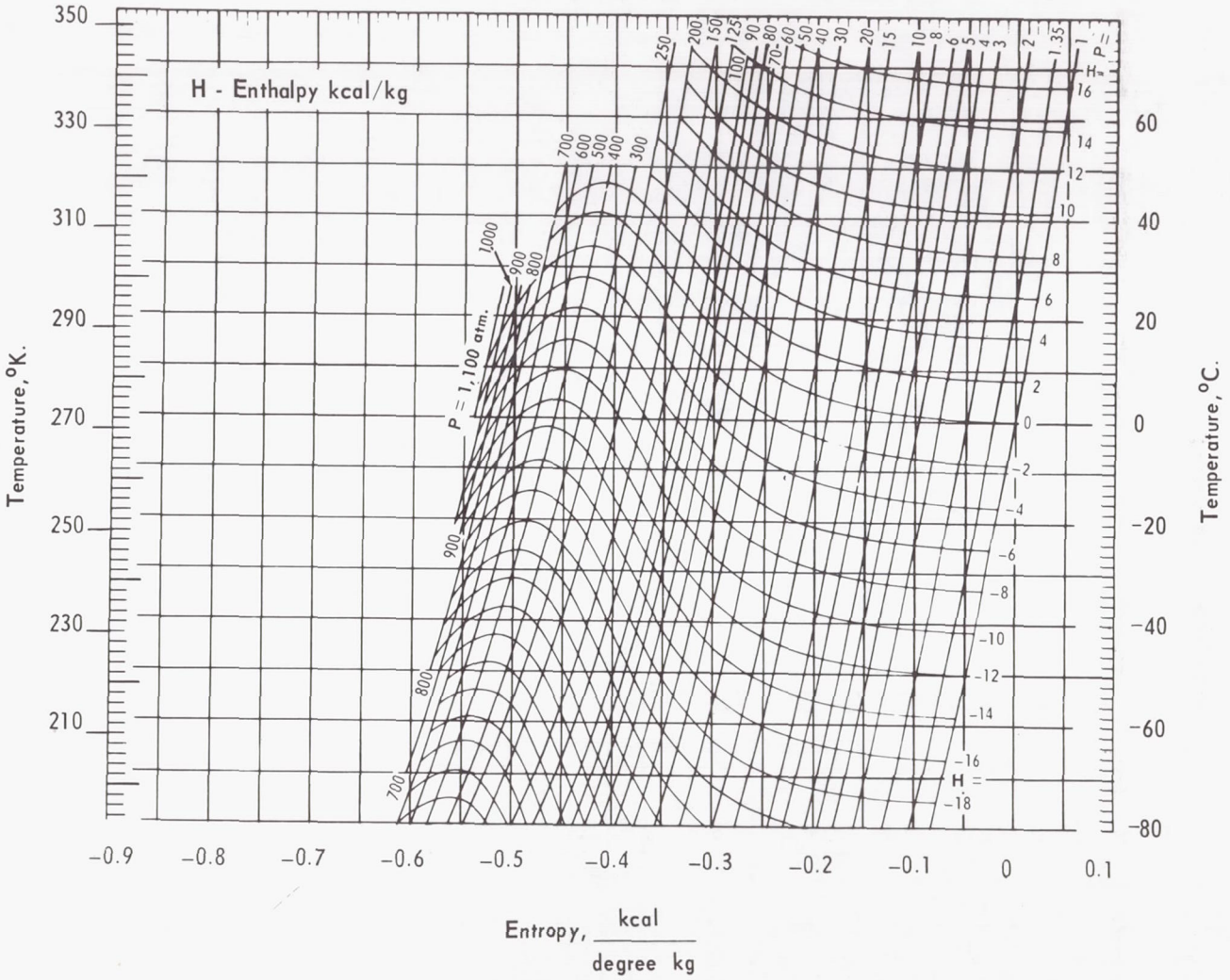


Figure B.1. Thermodynamic diagram, temperature versus entropy.—Continued. [*Reference NBS Chart D–8.*]

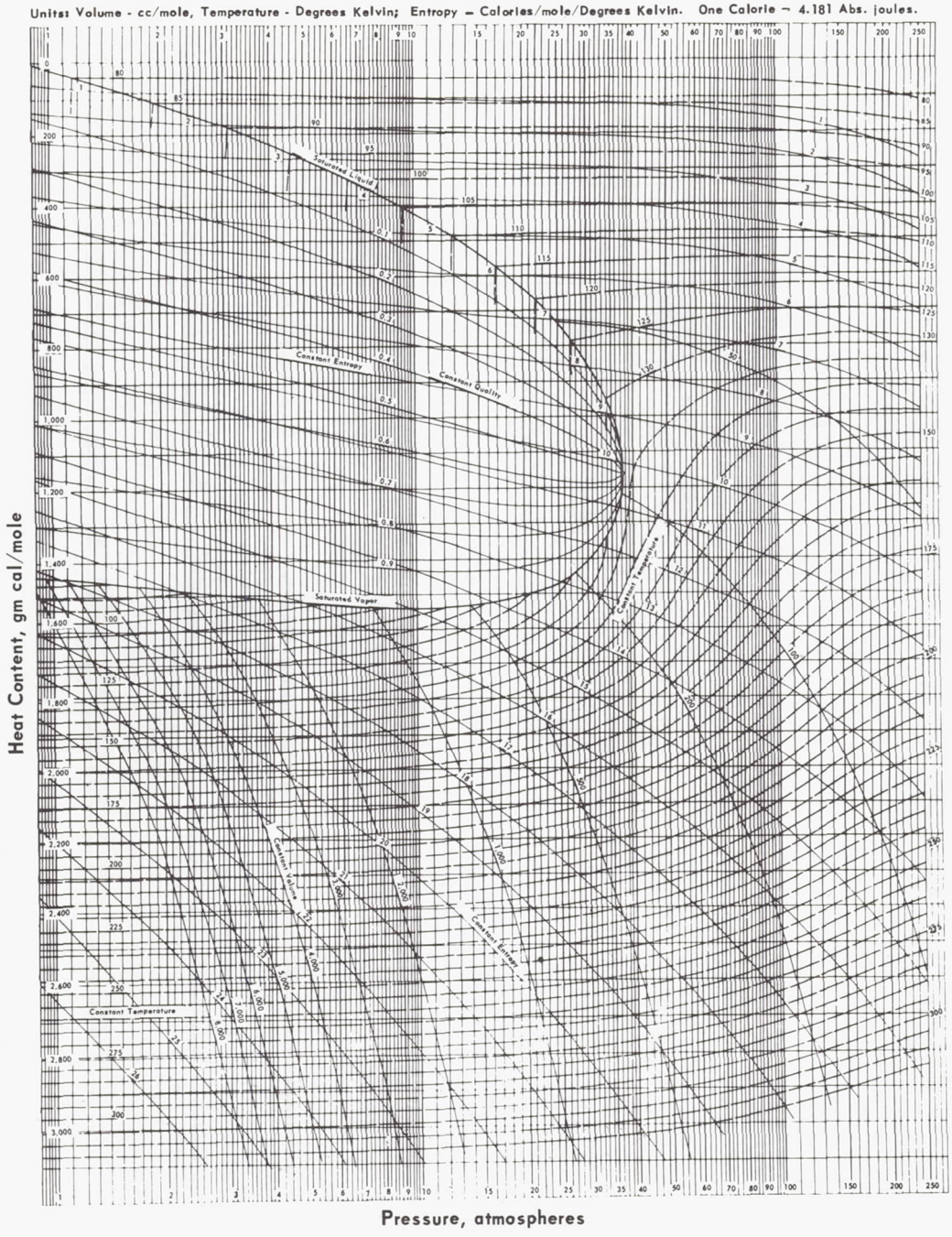


Figure B.2. Thermodynamic diagram, heat content versus pressure. [*Reference NBS Chart D–8.*]

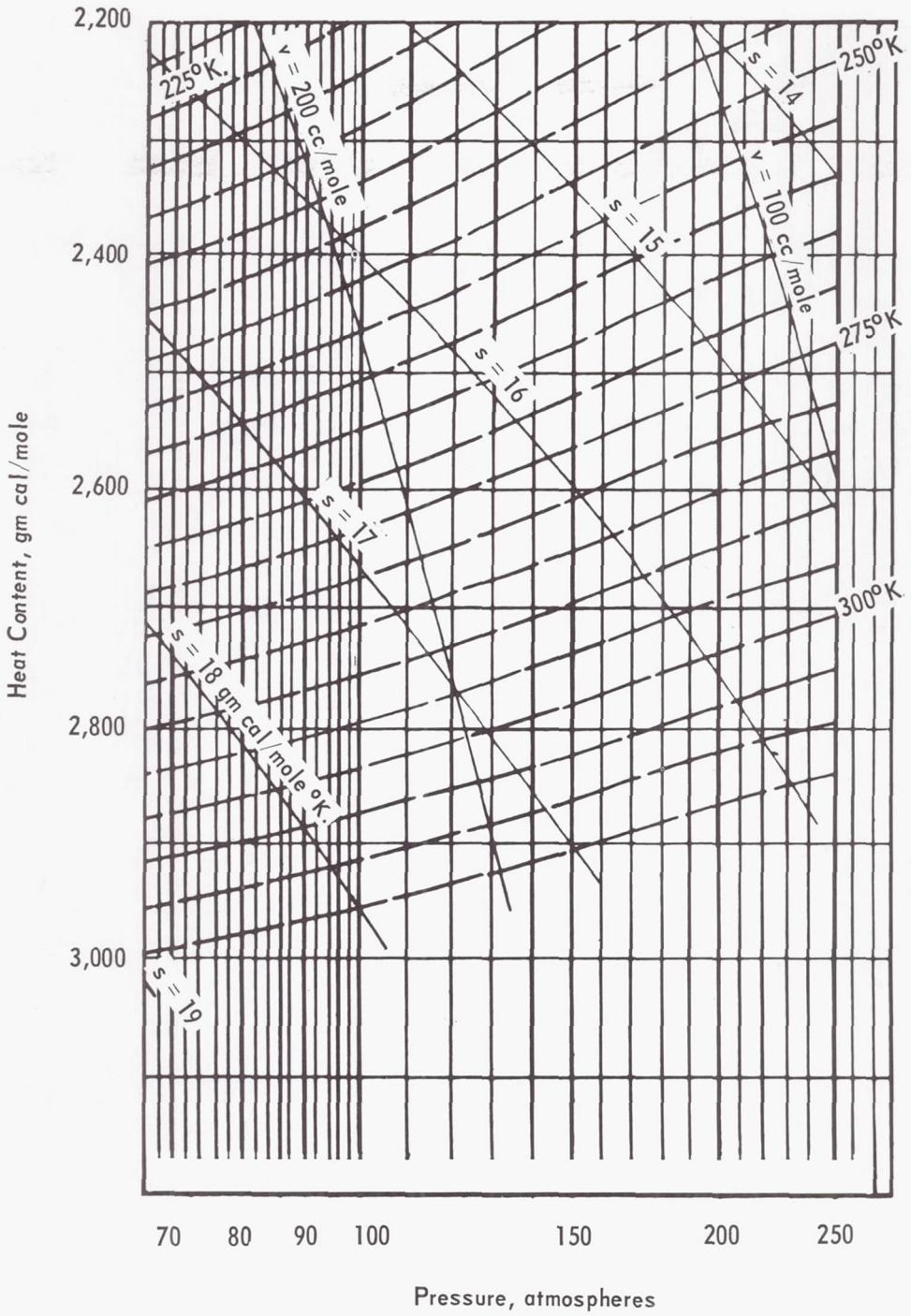


Figure B.2. Thermodynamic diagram, heat content versus pressure.—Continued. [*Reference NBS Chart D–11.*]

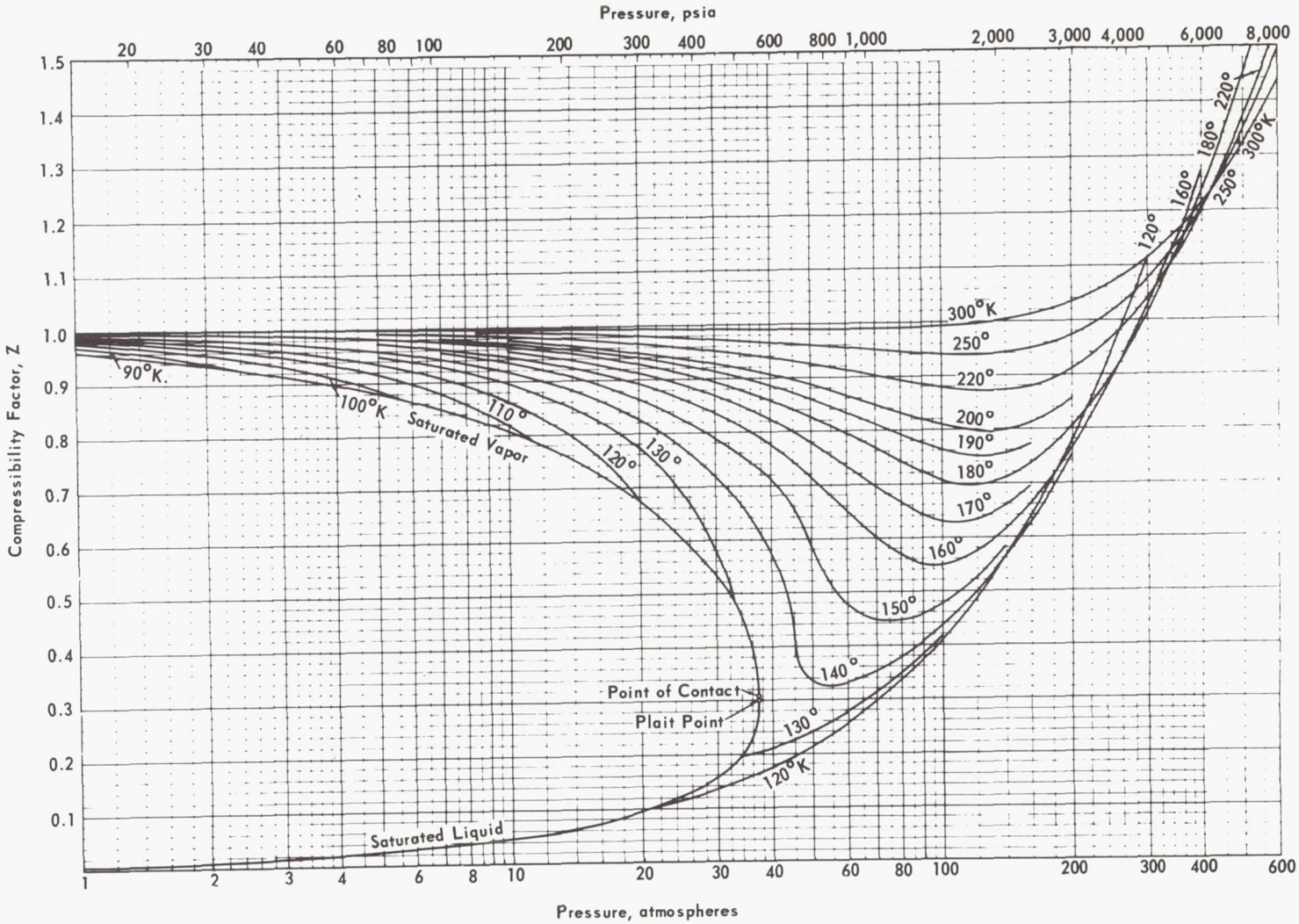


Figure B.3. Compressibility factor versus pressure. [*Reference NBS Chart D–11.*]

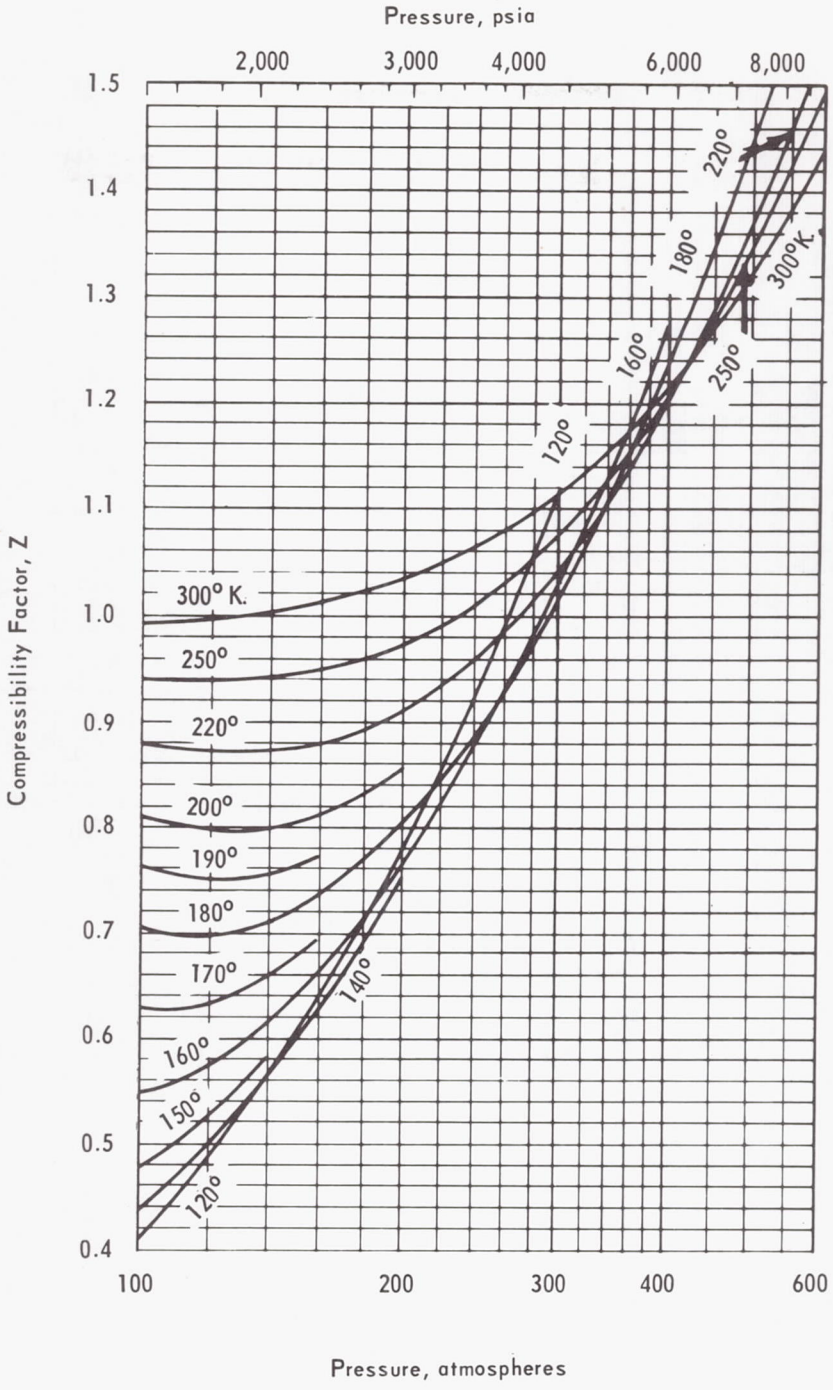


Figure B.3. Compressibility factor versus pressure.—Continued. [*Reference NBS Chart D–18A.*]

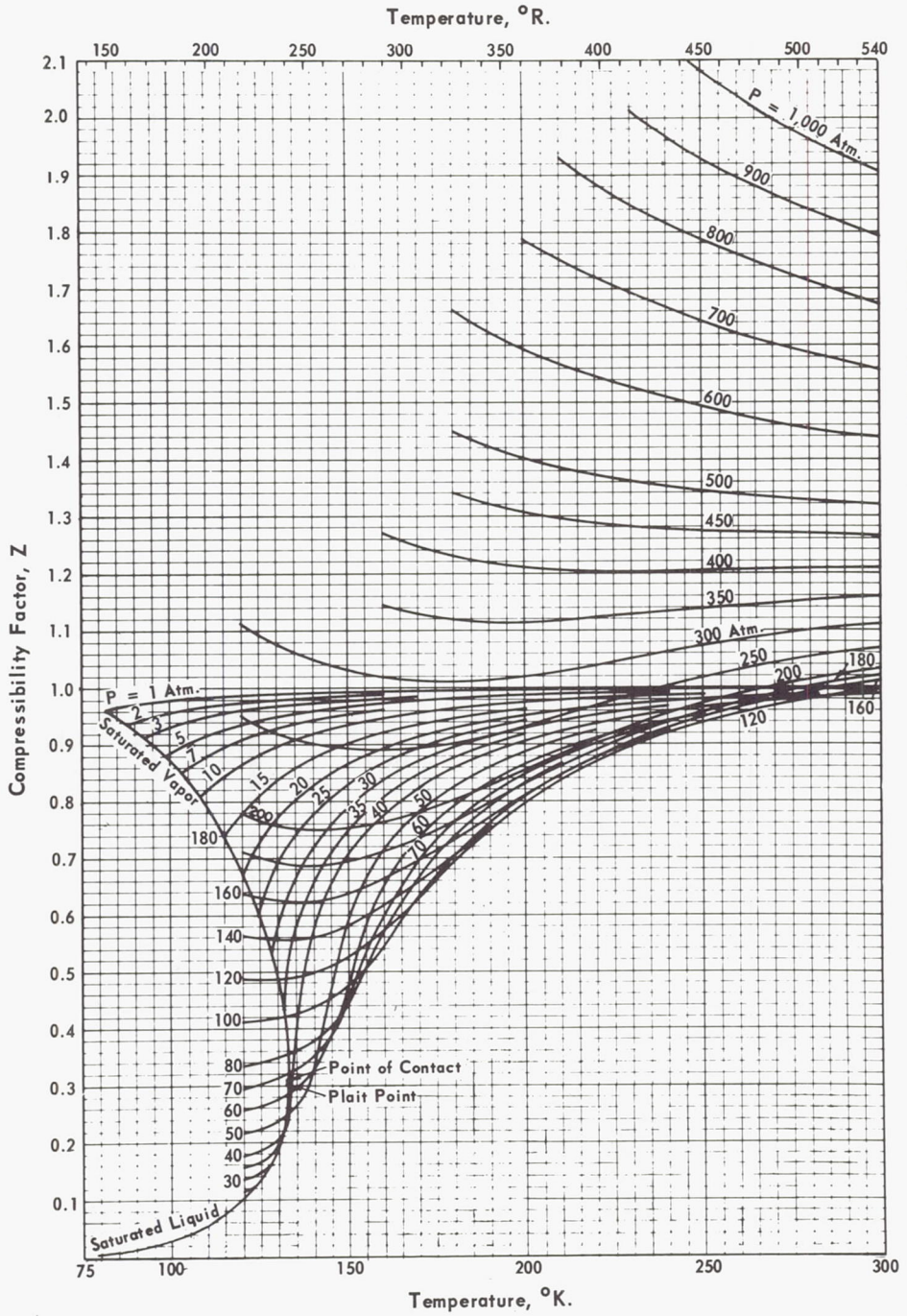


Figure B.4. Compressibility factor versus temperature. [*Reference NBS Chart D–18B.*]

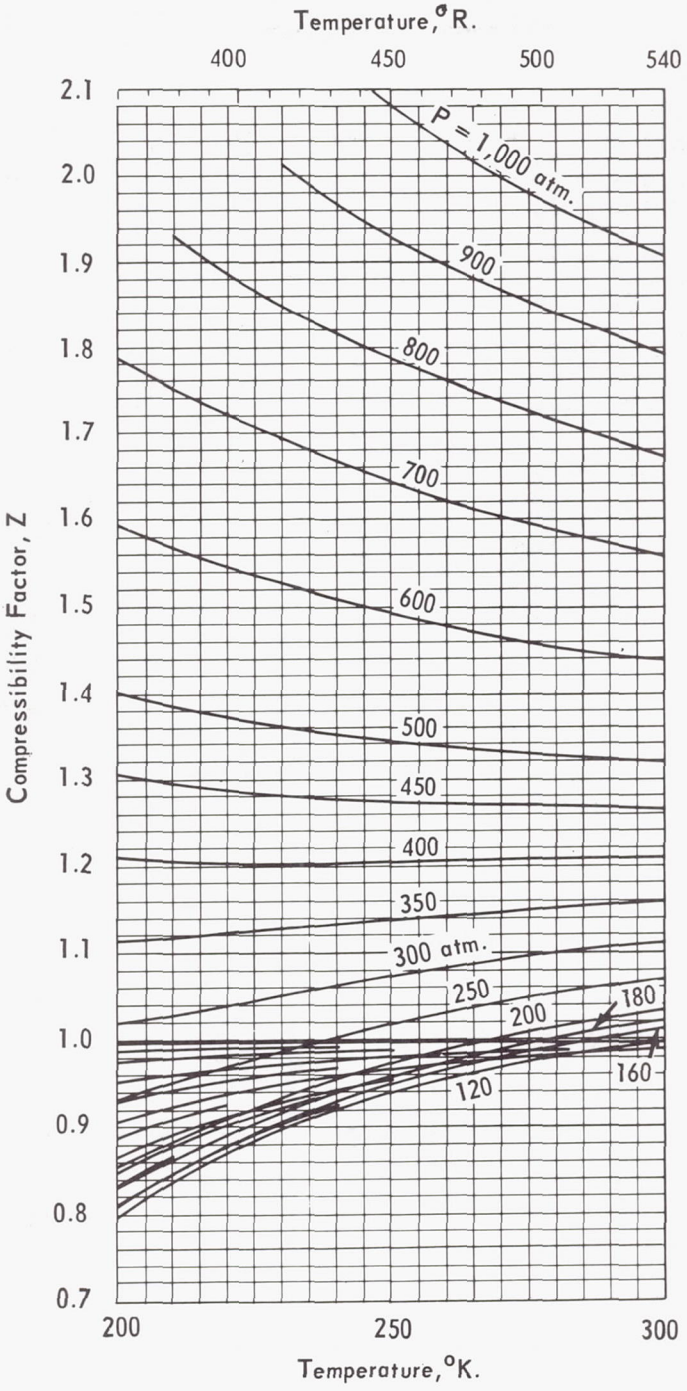


Figure B.4. Compressibility factor versus temperature.—Continued. [*Reference NBS Chart D–18B.*]

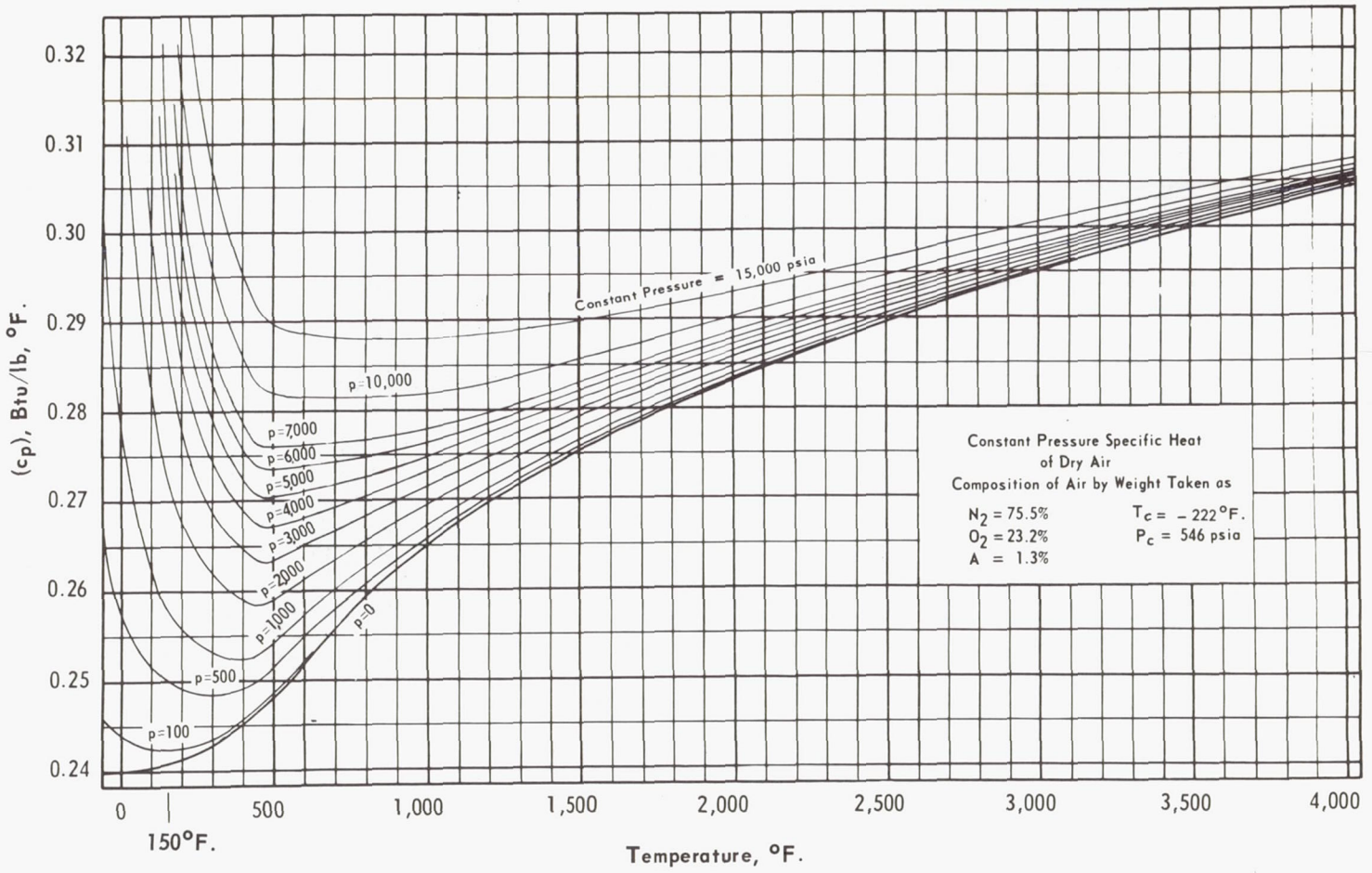


Figure B.5. Specific heat, c_p, versus temperature. [*Courtesy of Cornell University, Engineering Experiment Station Bulletin No. 30.*]

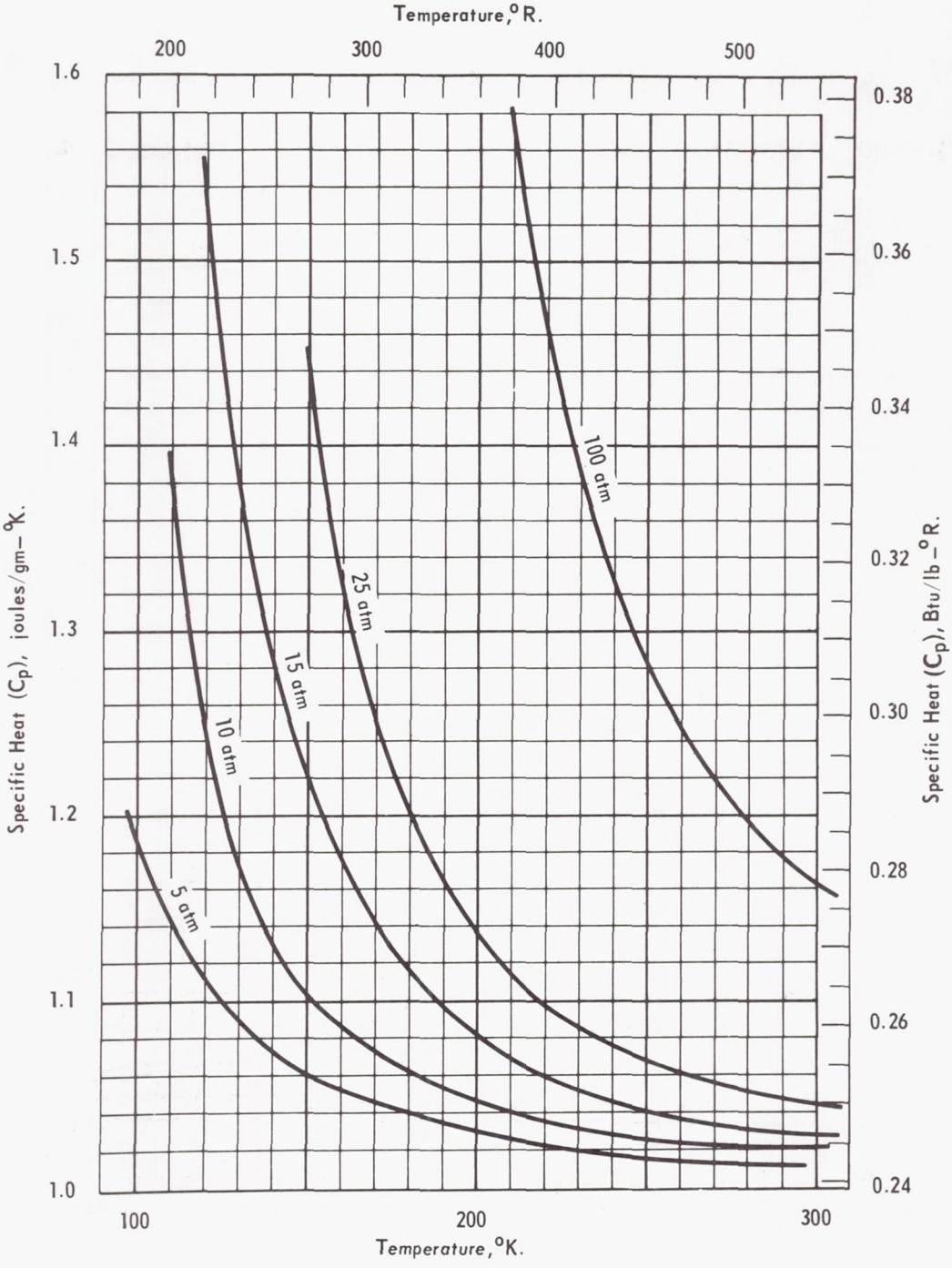


Figure B.5. Specific heat, c_p, versus temperature.—Continued. [*Reference WADD TR 60–56, Part I.*]

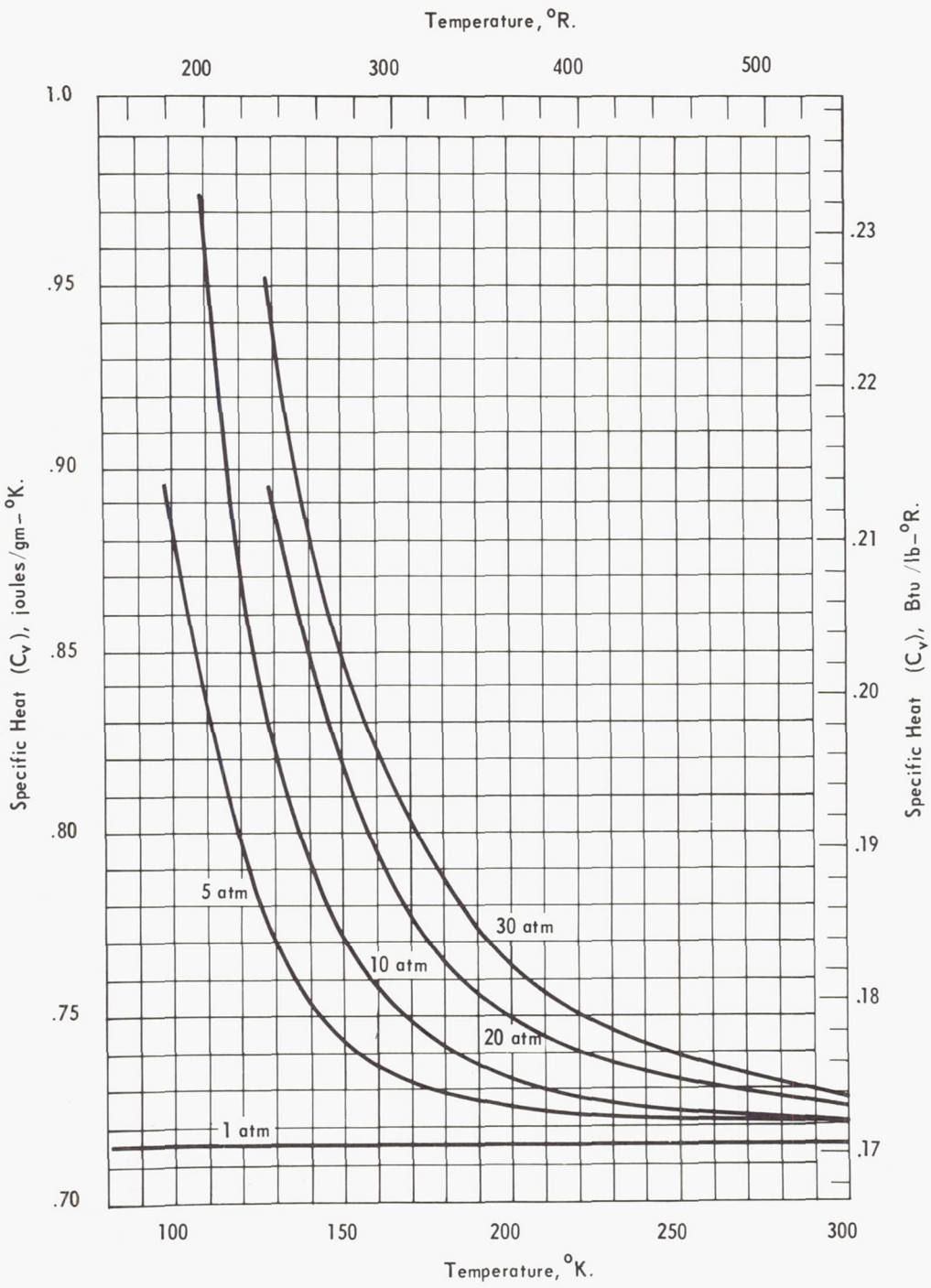


Figure B.6. Specific heat, c, versus temperature. [*Reference WADD TR 60–56, Part I.*]

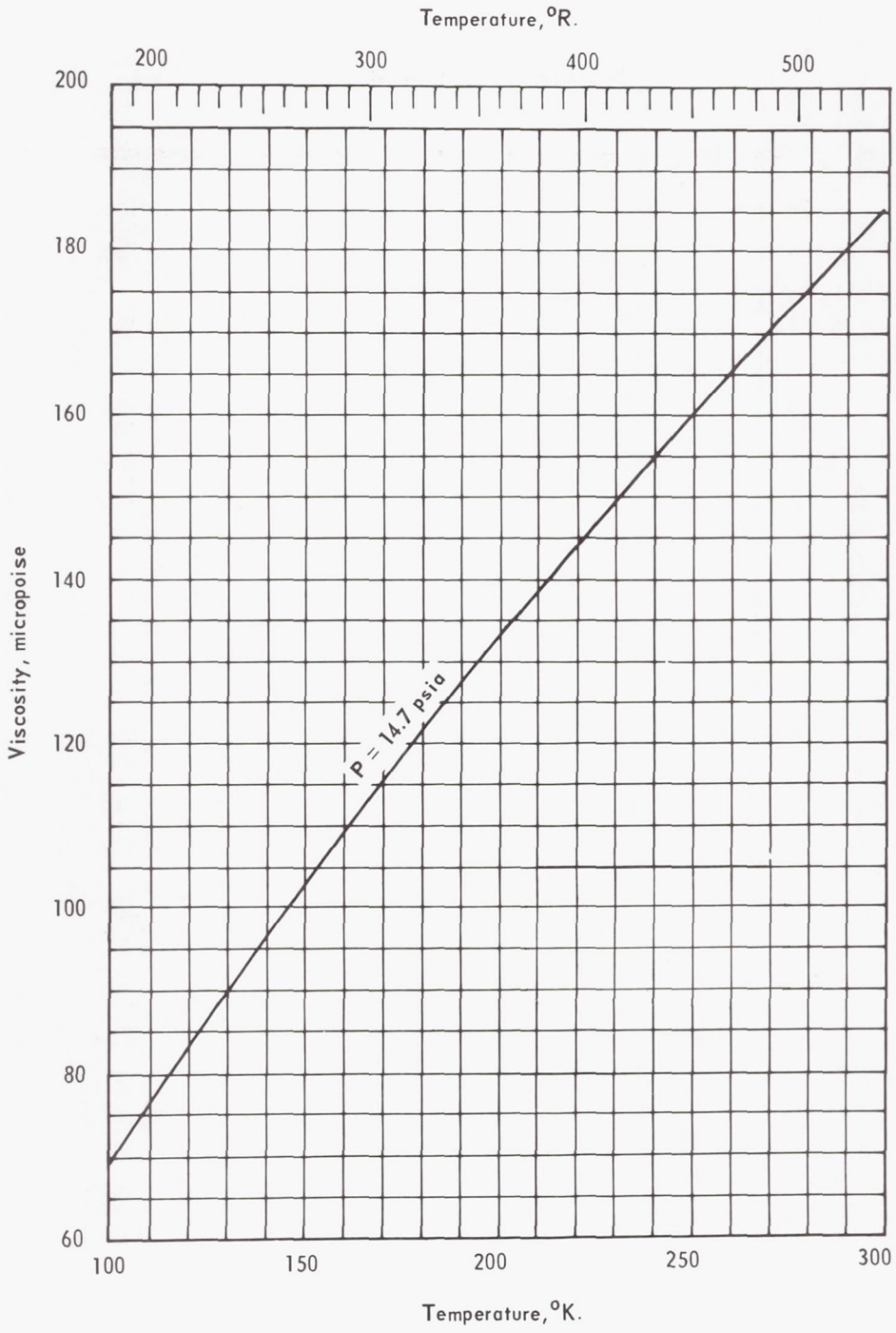


Figure B.7. Viscosity versus temperature. [*Reference WADD TR 60–56, Part I.*]

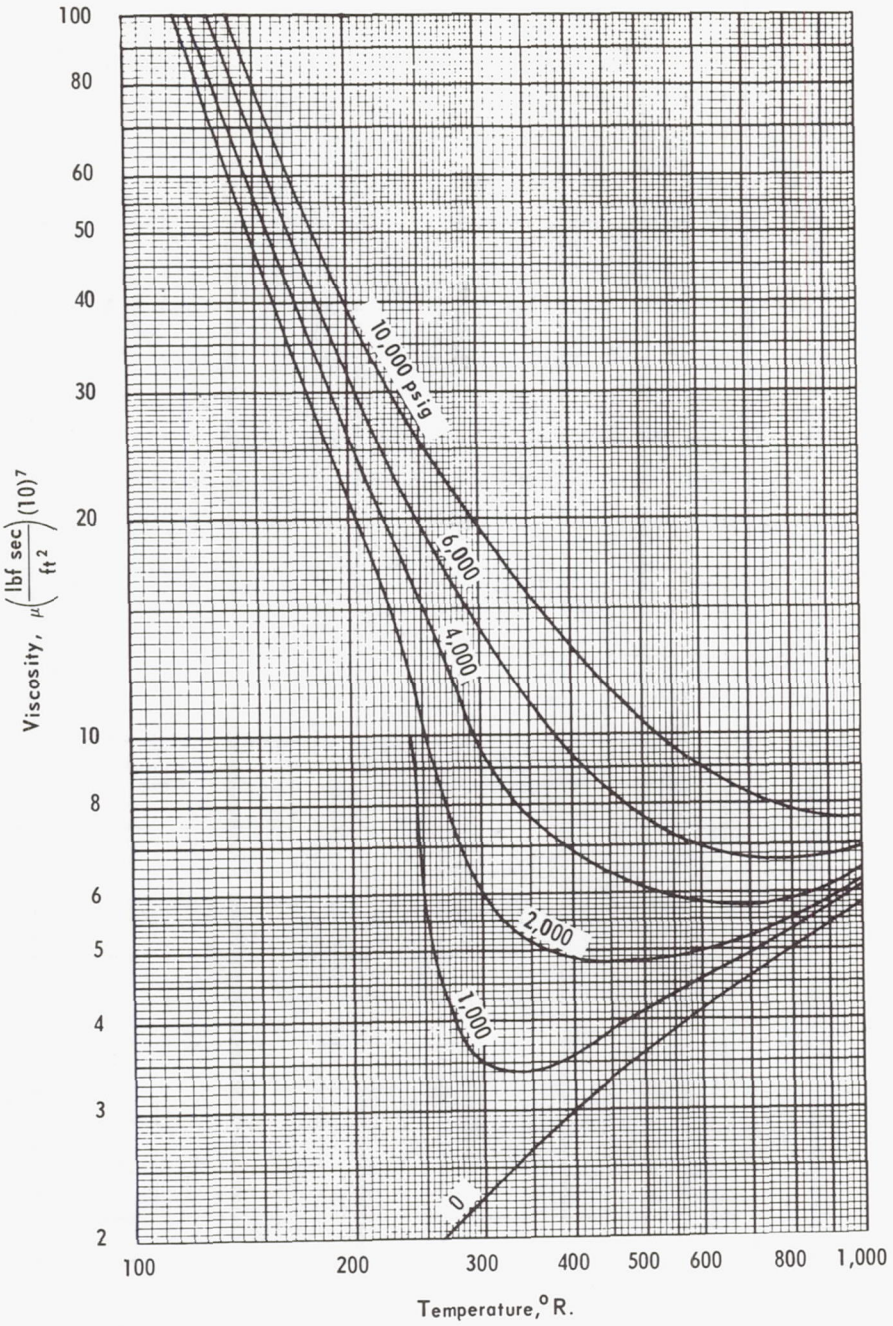


Figure B.7. Viscosity versus temperature. — Continued.

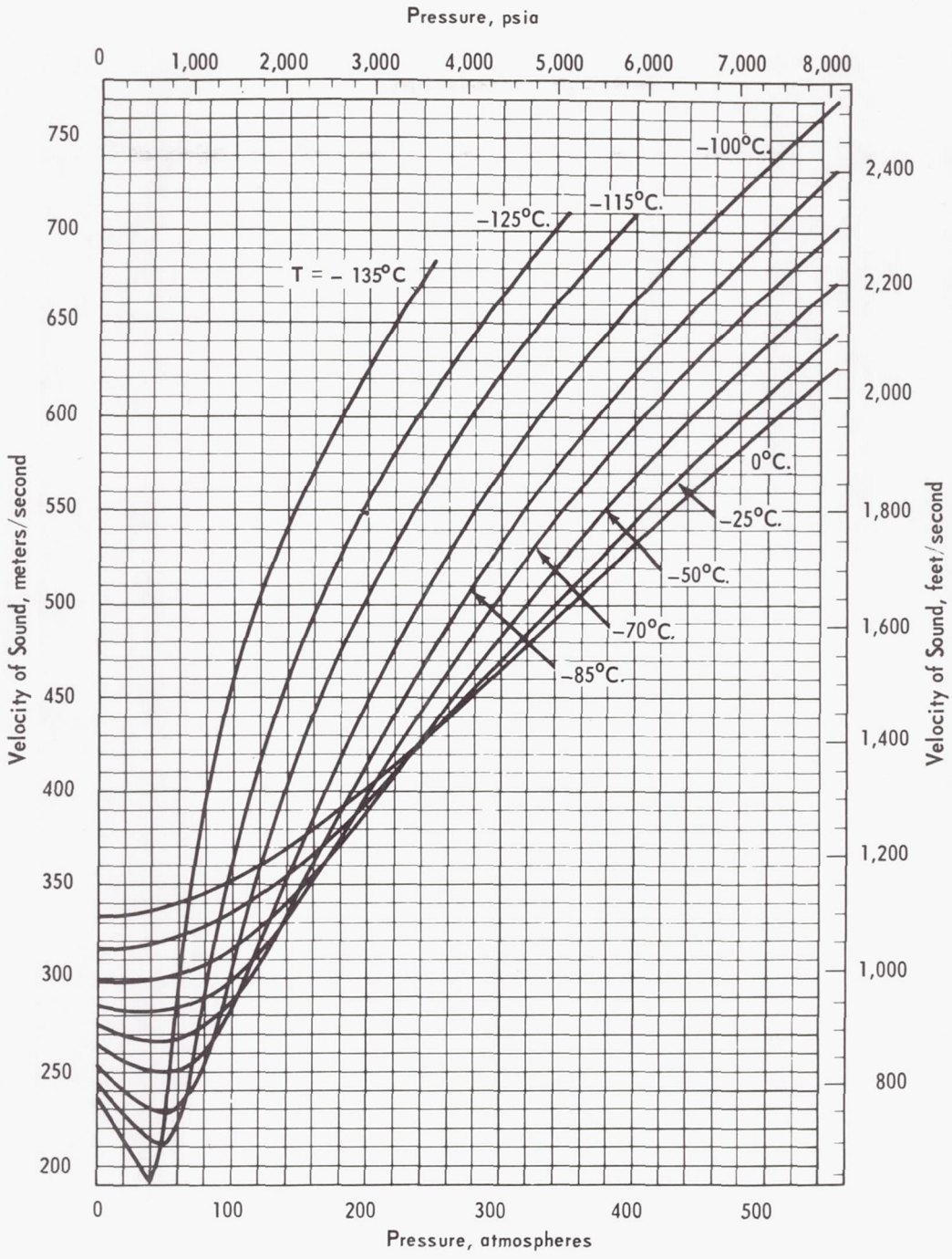


Figure B.8. Velocity of sound versus pressure. [*Reference WADD TR 60–56, Part IV.*]

APPENDIX C

DATA ON NITROGEN

325-994 O-69—32

Preceding Page Blank

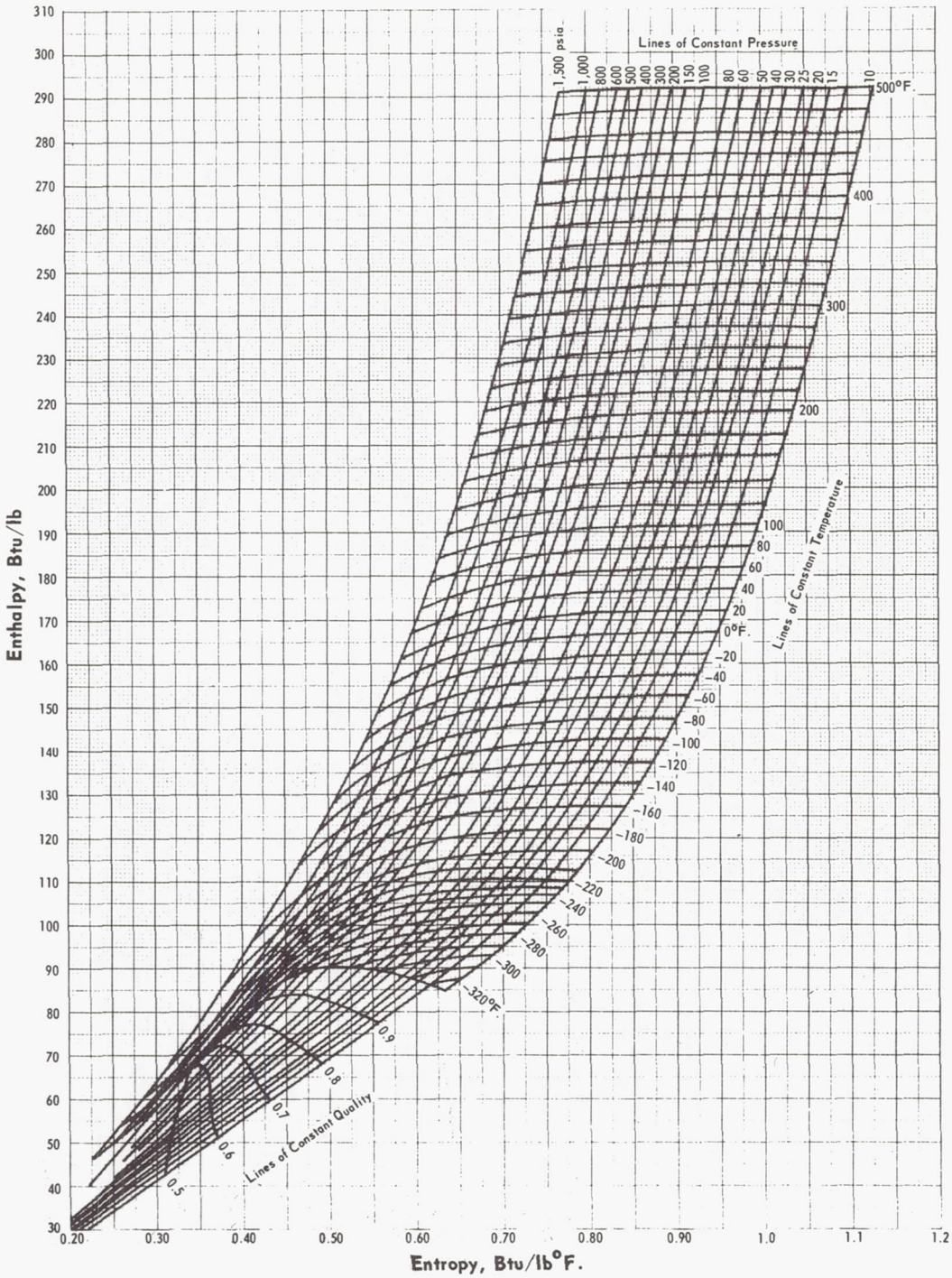


Figure C.1. Thermodynamic diagram, enthalpy versus entropy. [*Courtesy of the Institute of Gas Technology, Gas Technology Bulletin No. 18.*]

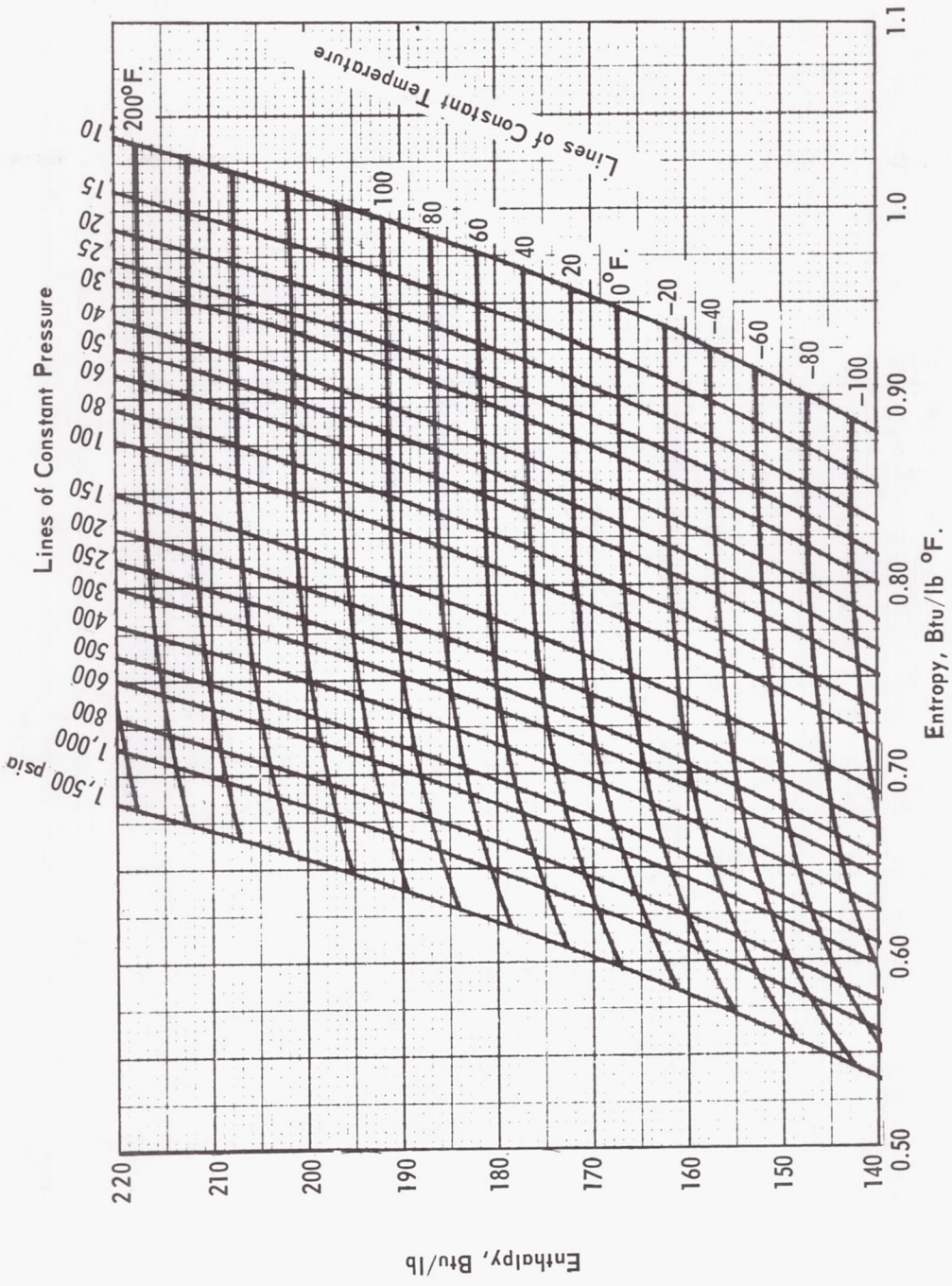


Figure C.1. Thermodynamic diagram, enthalpy versus entropy.—Continued. [*Courtesy of the Institute of Gas Technology, Gas Technology Bulletin No. 18.*]

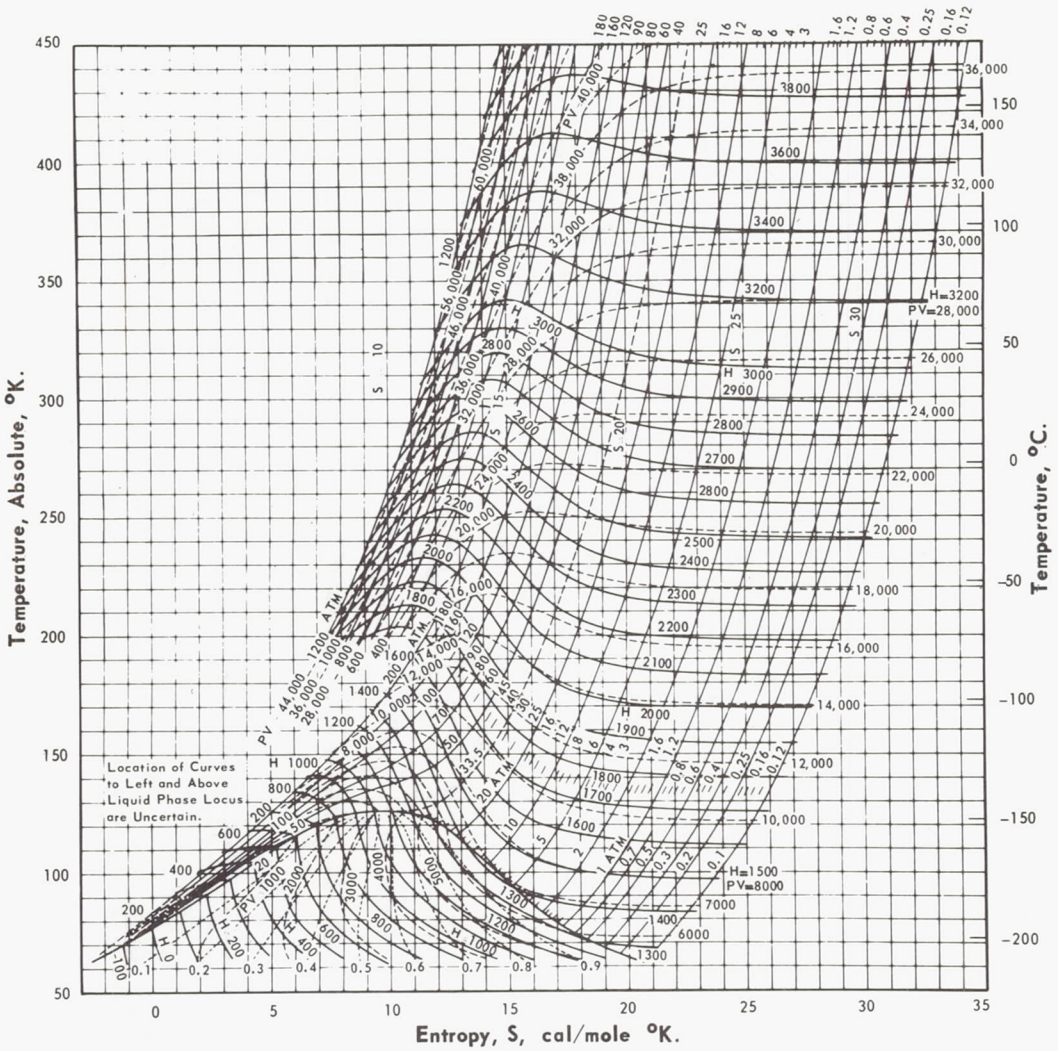


Figure C.2. Thermodynamic diagram, temperature versus entropy. [*Reference NBS Chart D–7.*]

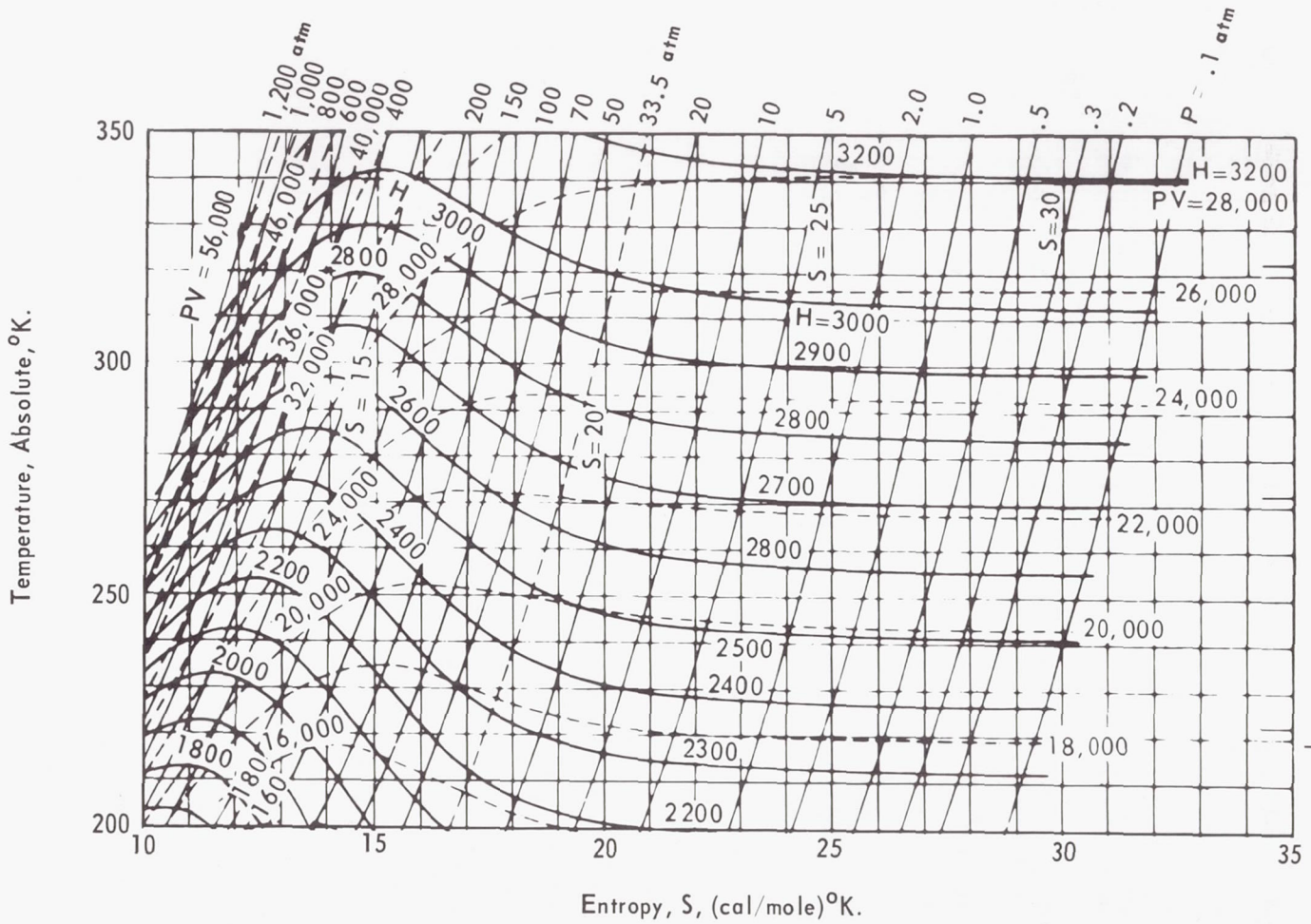


Figure C.2. Thermodynamic diagram, temperature versus entropy.—Continued. [*Reference NBS Chart D–7.*]

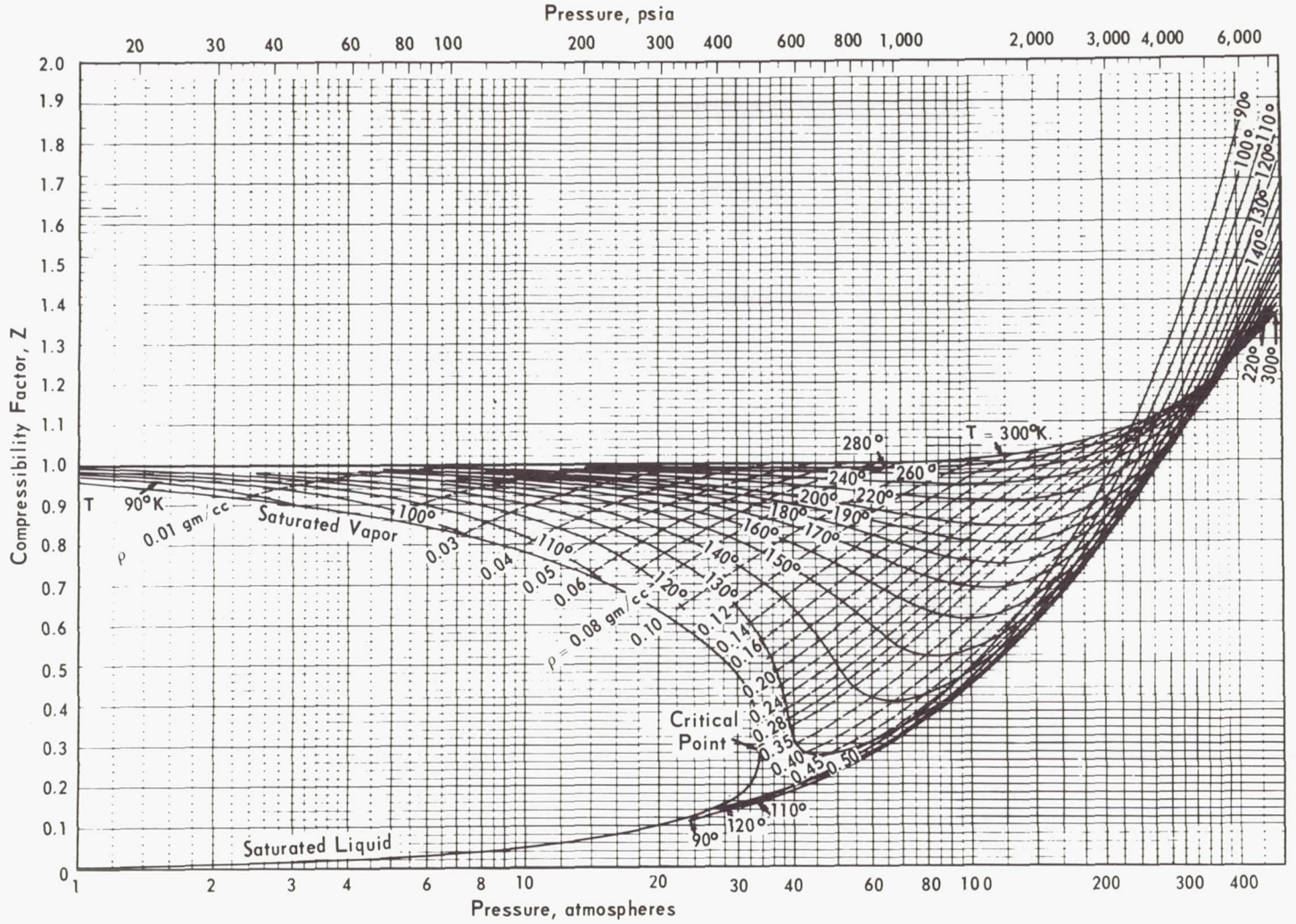


Figure C.3. Compressibility factor versus pressure. [*Reference NBS Chart D–16.*]

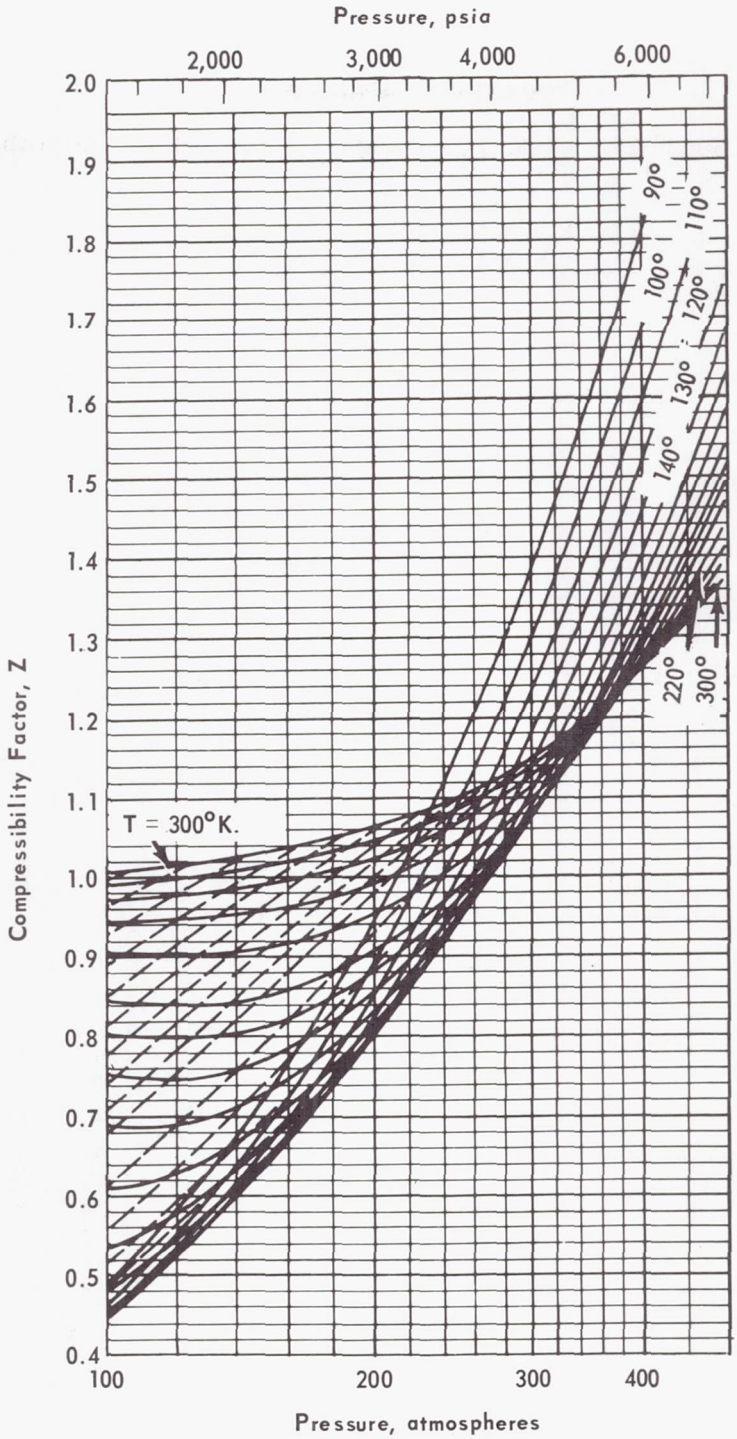


Figure C.3. Compressibility factor versus pressure.—Continued. [*Reference NBS Charts D–16 and –17.*]

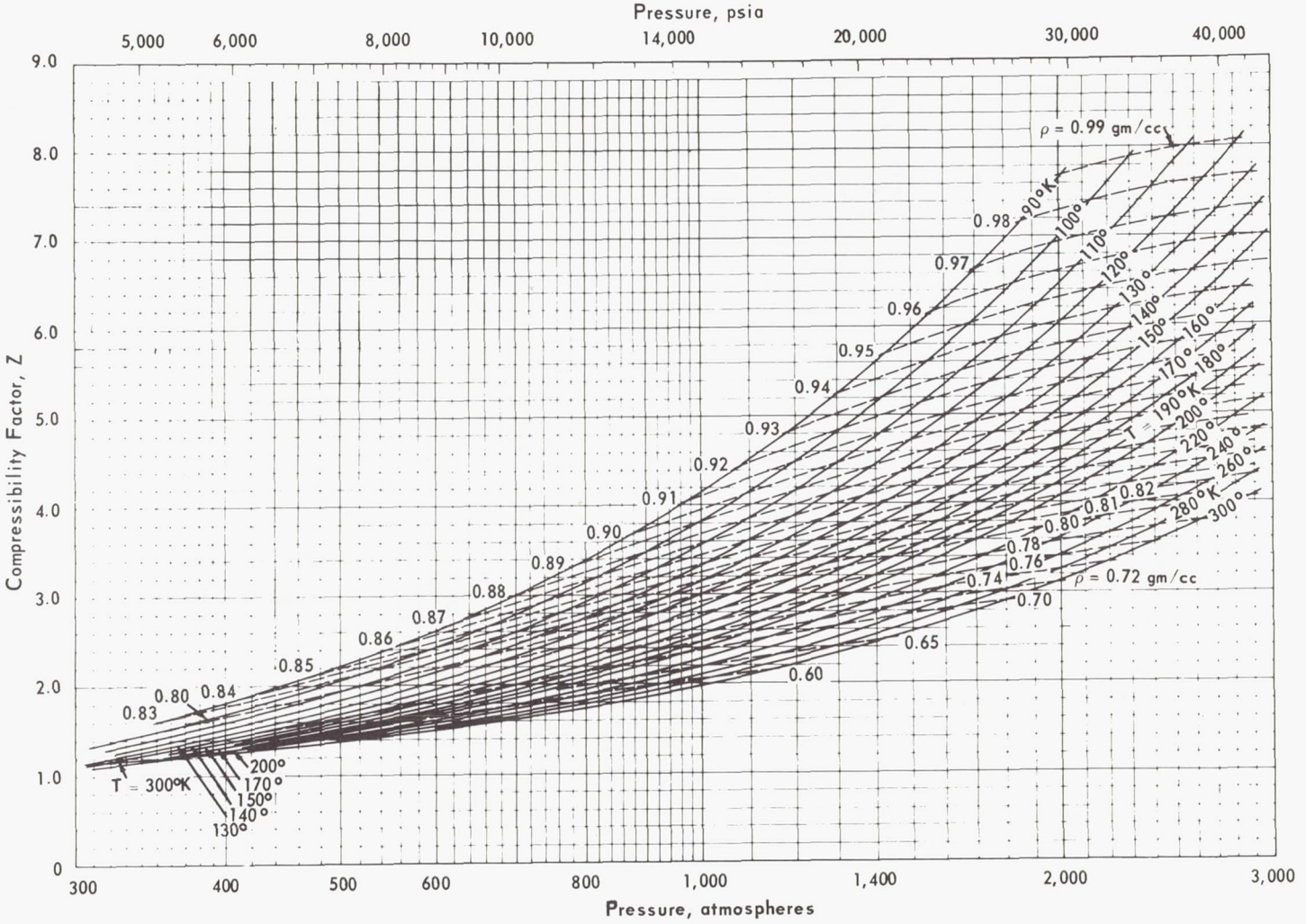


Figure C.3. Compressibility factor versus pressure.—Continued. [*Reference NBS Charts D–16 and –17.*]

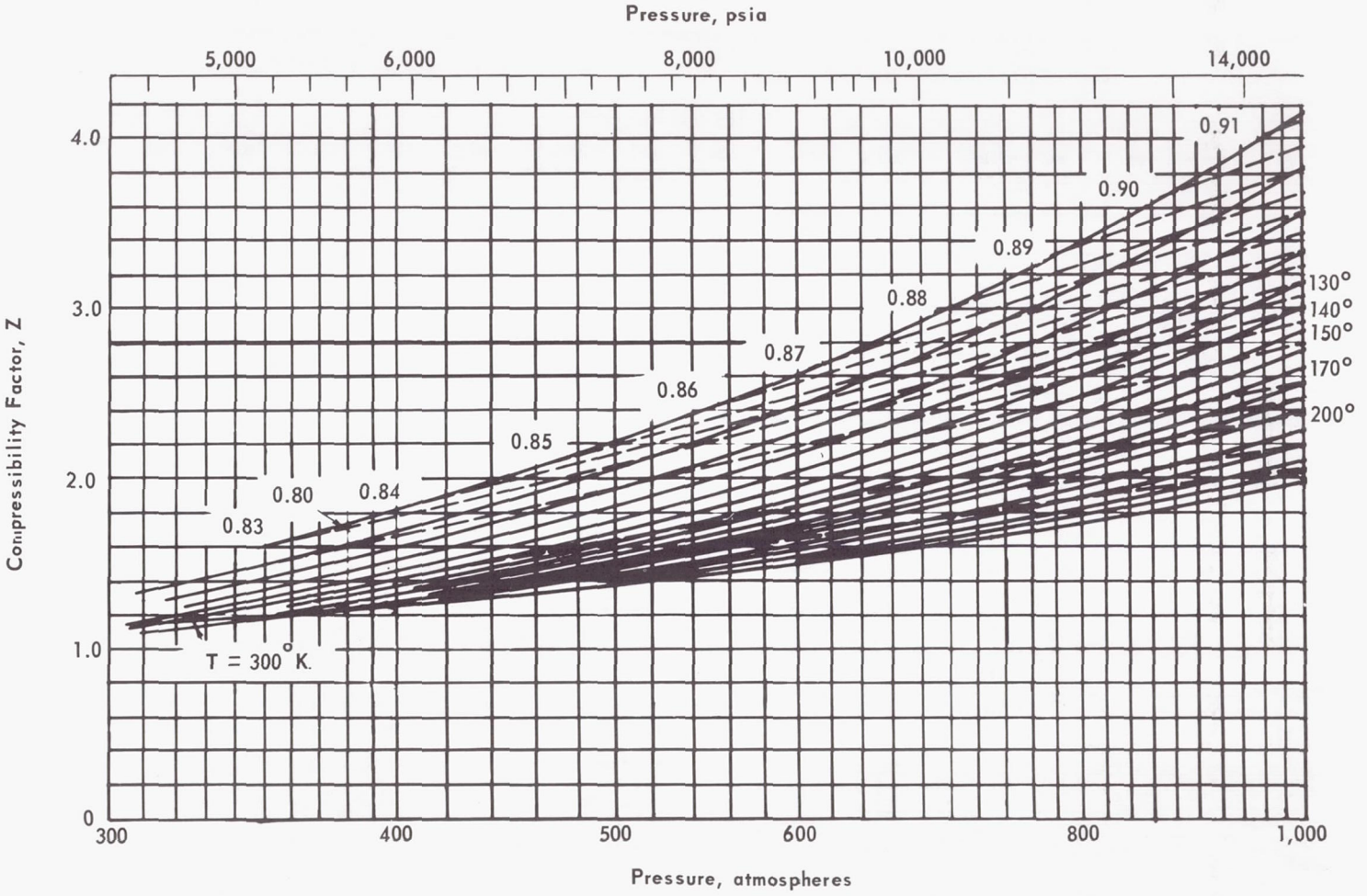


Figure C.3. Compressibility factor versus pressure. – Continued. [*Reference NBS Charts D–16 and –17.*]

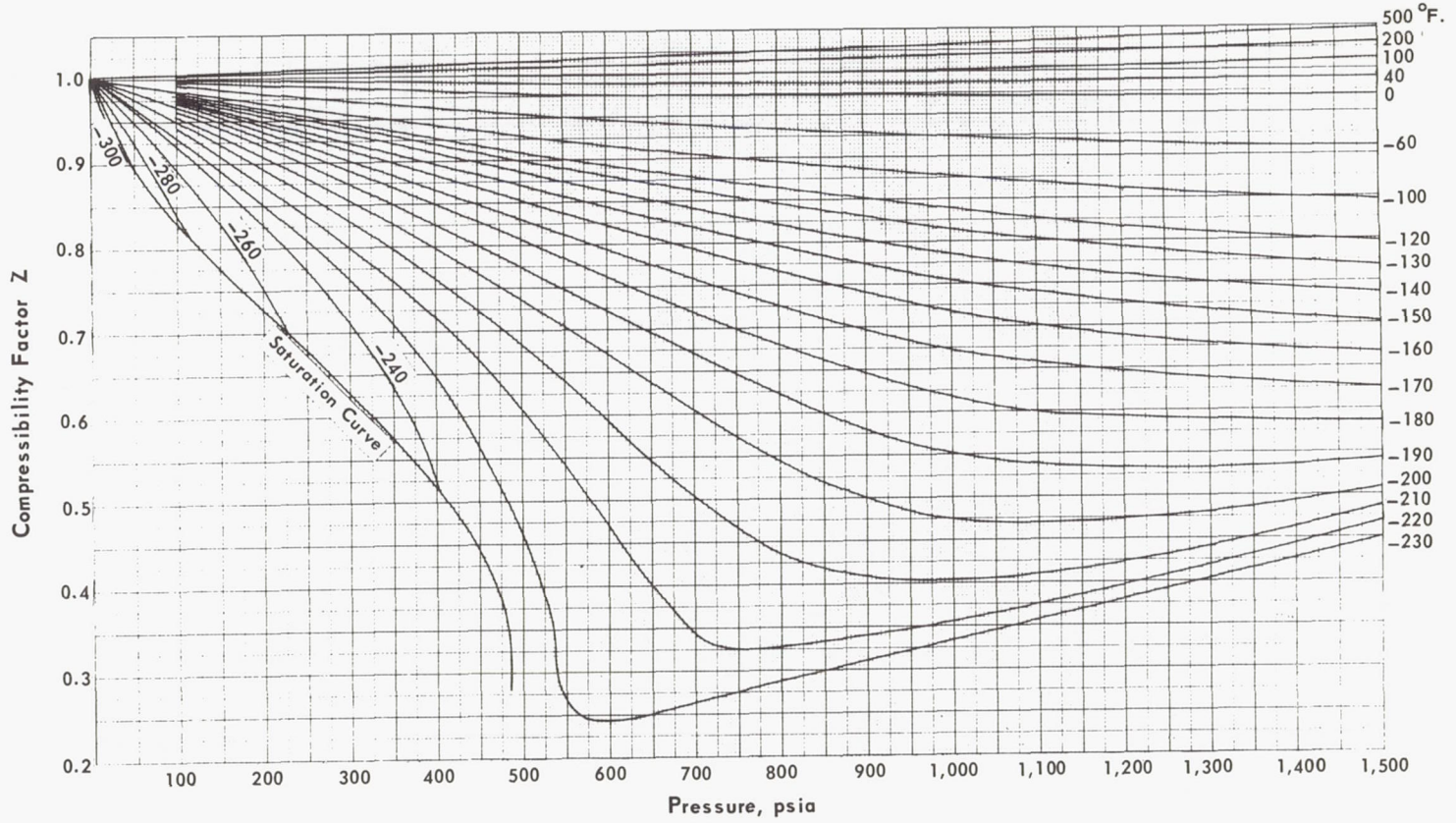


Figure C.3. Compressibility factor versus pressure.—Concluded. [*Reference NBS Chart D–18.*]

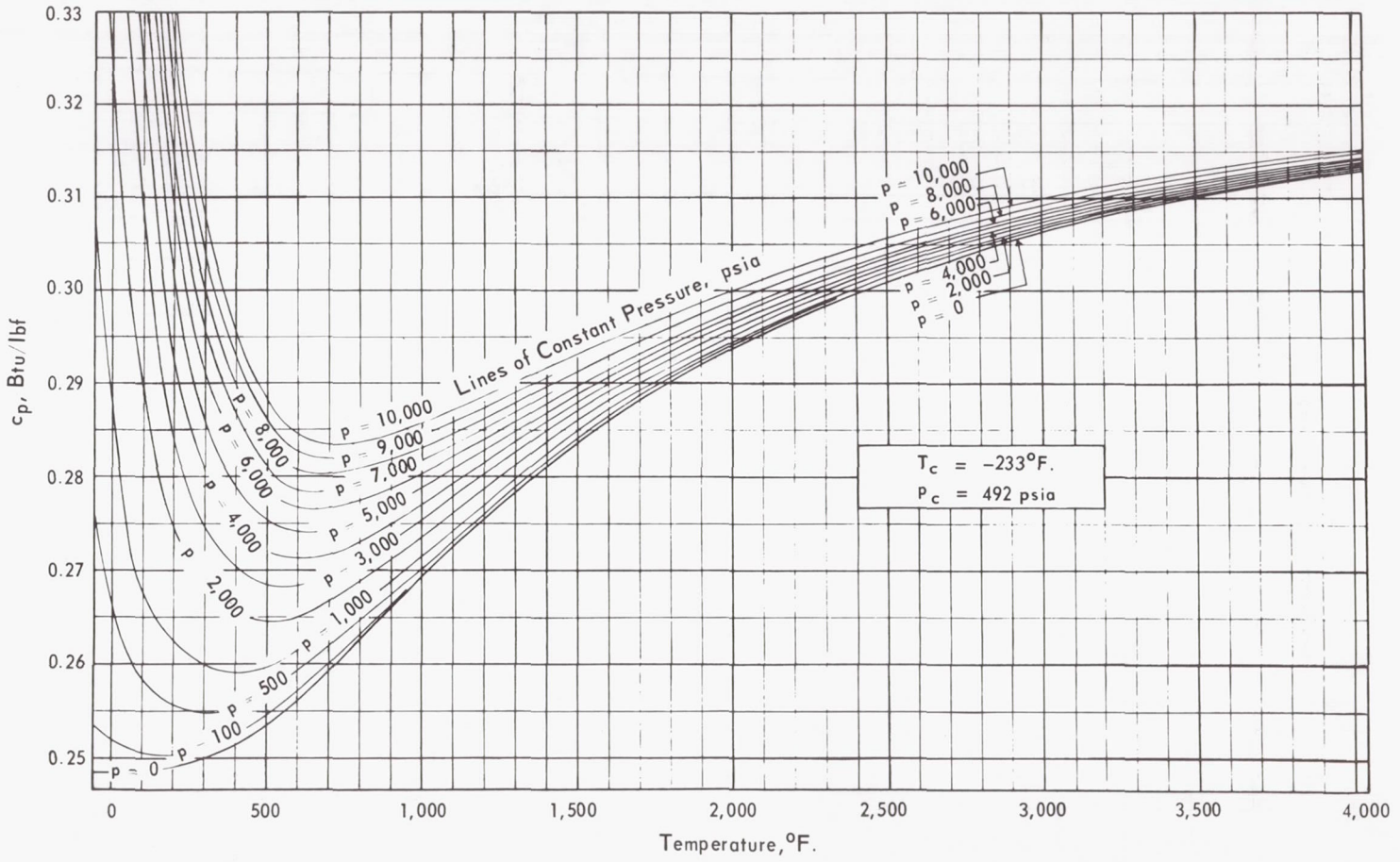


Figure C.4. Specific heat, c_p, versus temperature. [*Courtesy of the Cornell University, Engineering Experiment Station Bulletin No. 30.*]

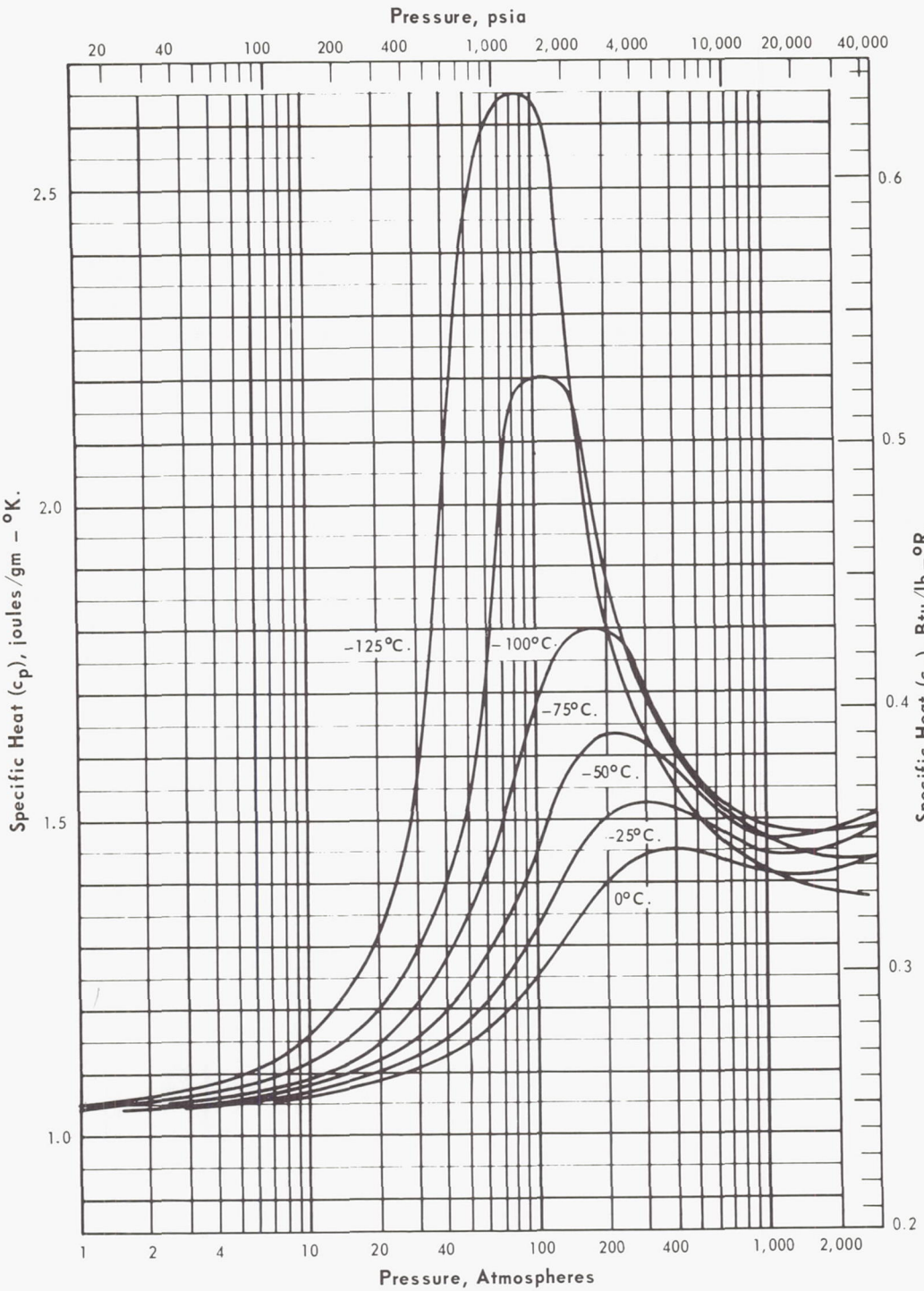


Figure C.5. Specific heat, c_p, versus pressure. [*Reference WADD TR 60–56, Part I.*]

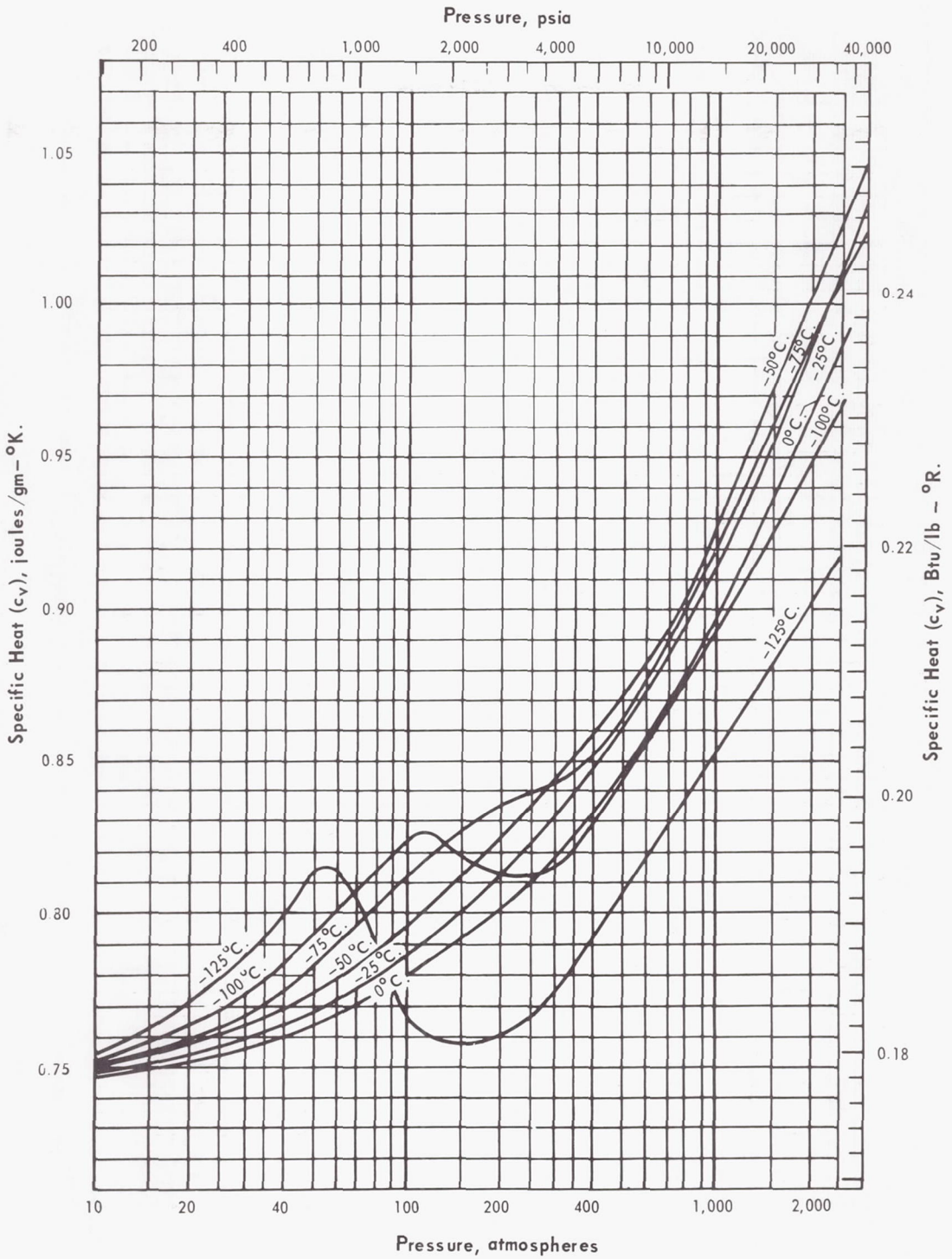


Figure C.6. Specific heat, c_v, versus pressure. [*Reference WADD TR 60–56, Part I.*]

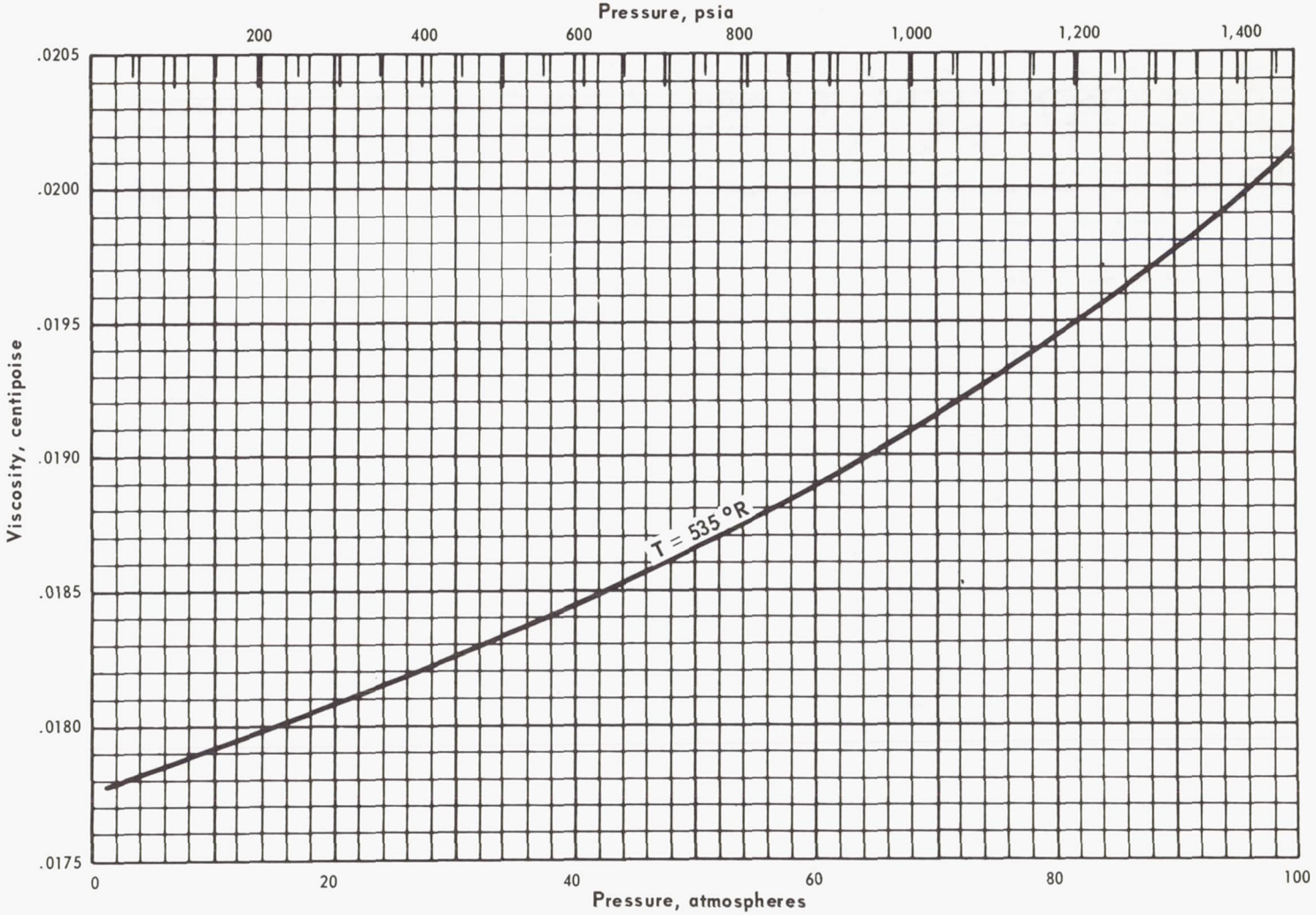


Figure C.7. Viscosity versus pressure. [*Reference WADD TR 60–56, Part I.*]

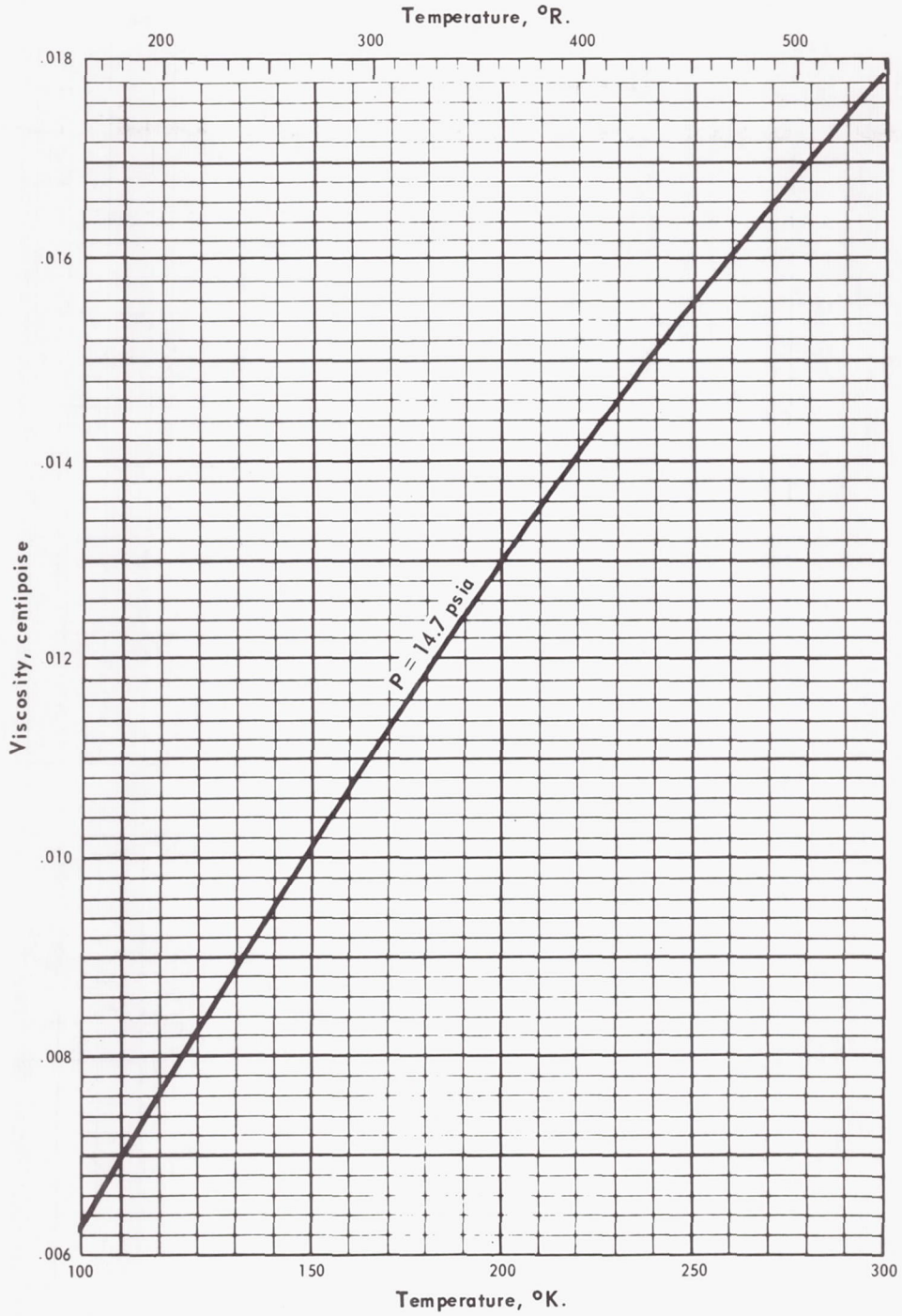


Figure C.8. Viscosity versus temperature.

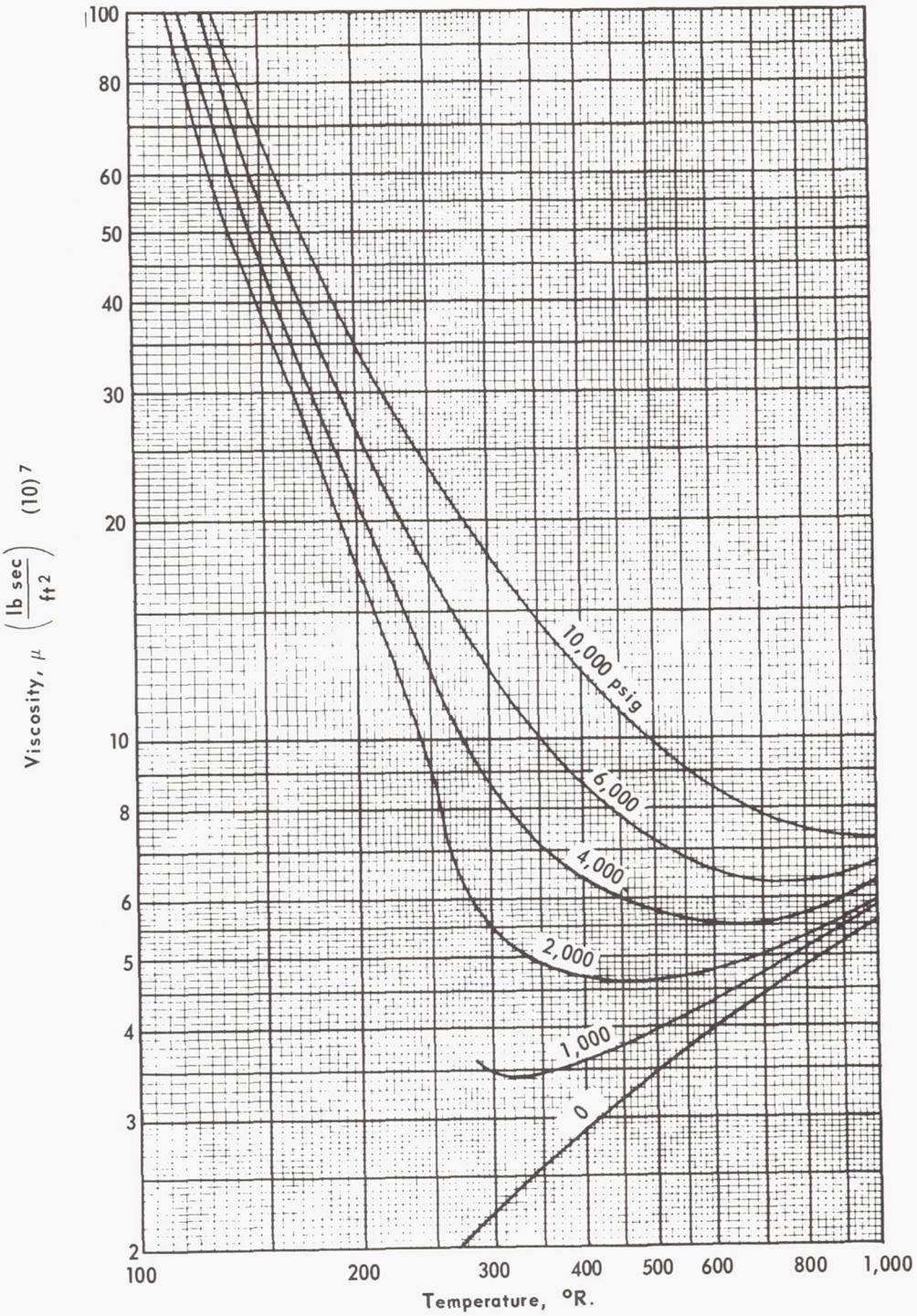


Figure C.8. Viscosity versus temperature.—Continued. [*Reference WADD TR 60–56, Part I.*]

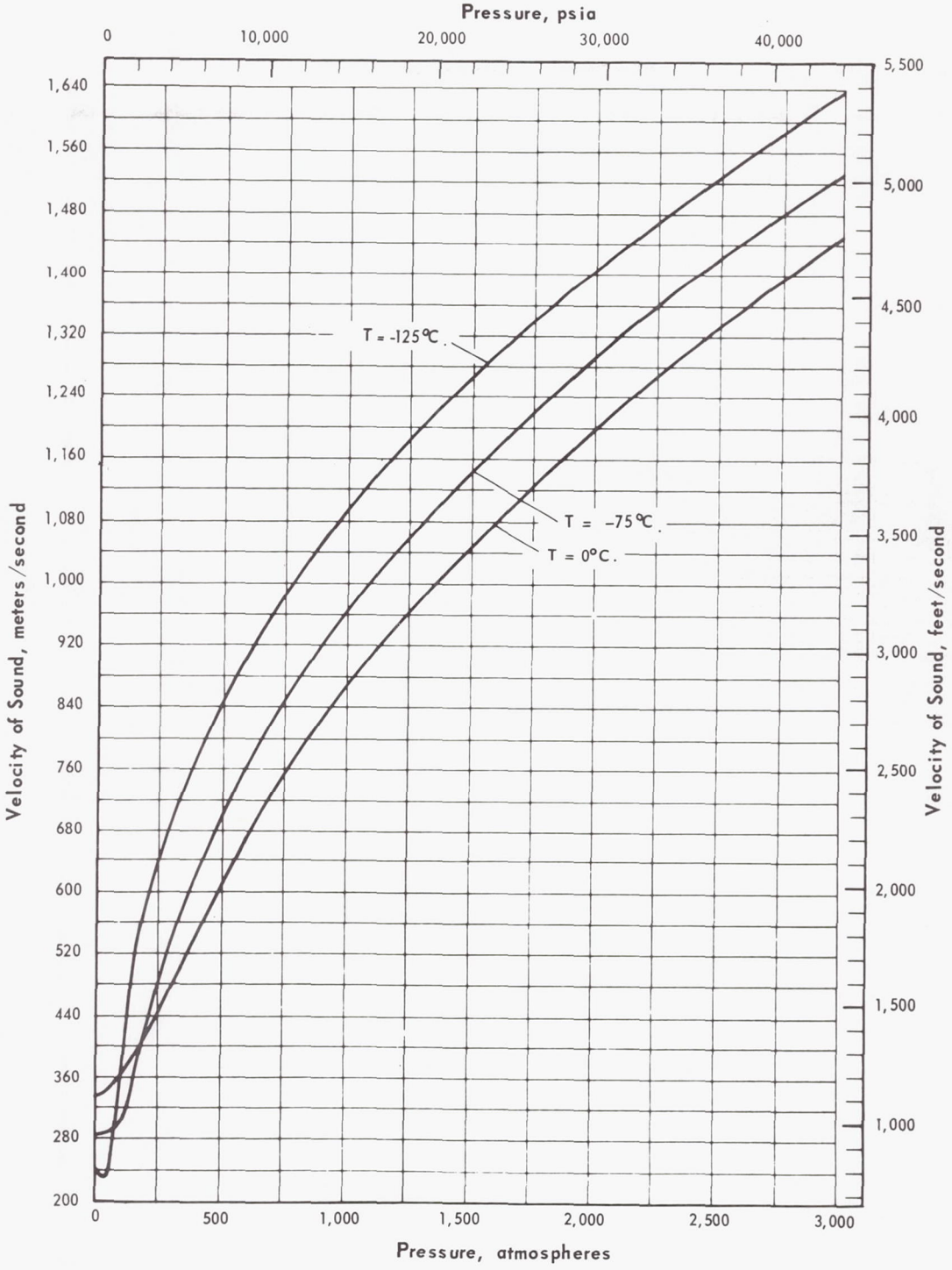


Figure C.9. Velocity of sound versus pressure. [*Reference WADD TR 60–56, Part IV.*]

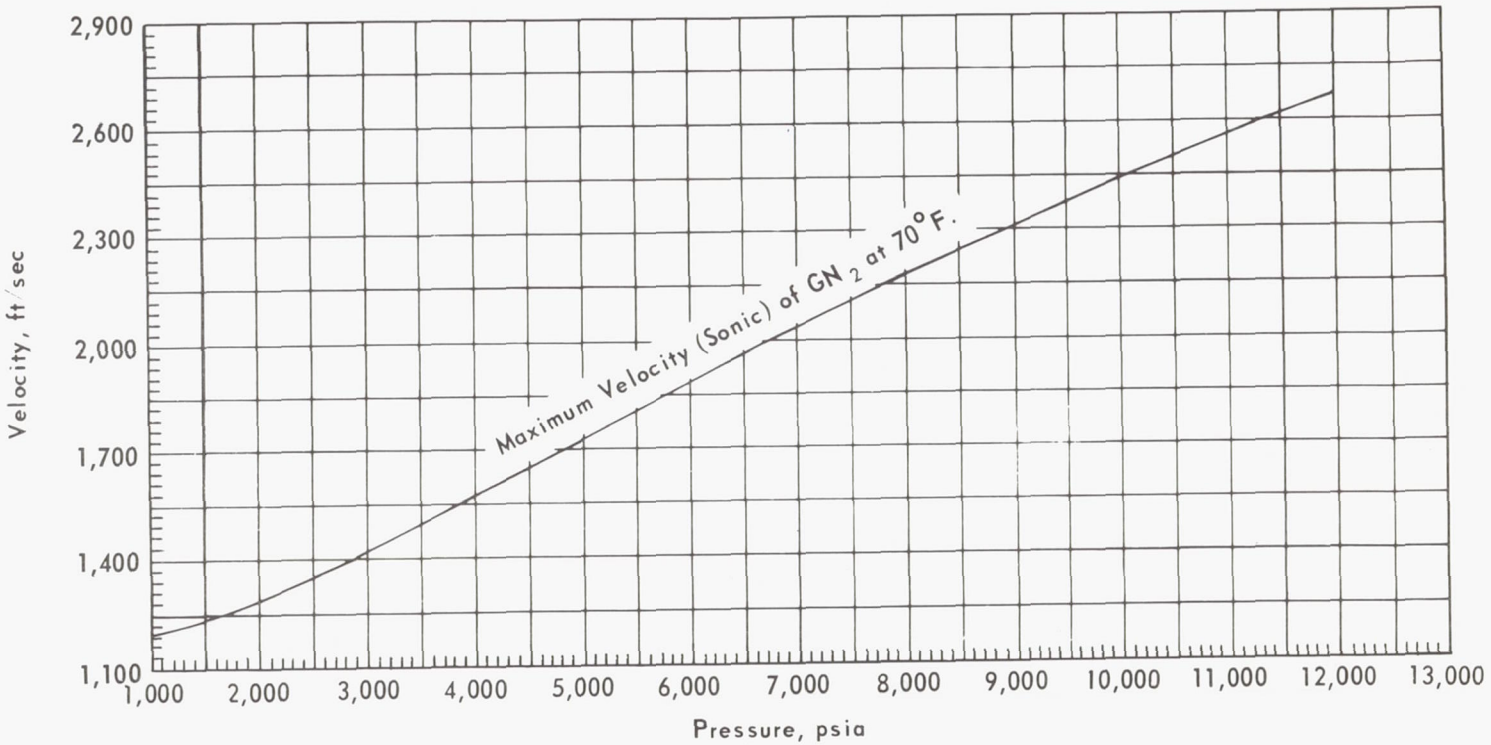


Figure C.9. Velocity of sound versus pressure.—Continued.

APPENDIX D

DATA ON ~~OXYGEN~~ Helium

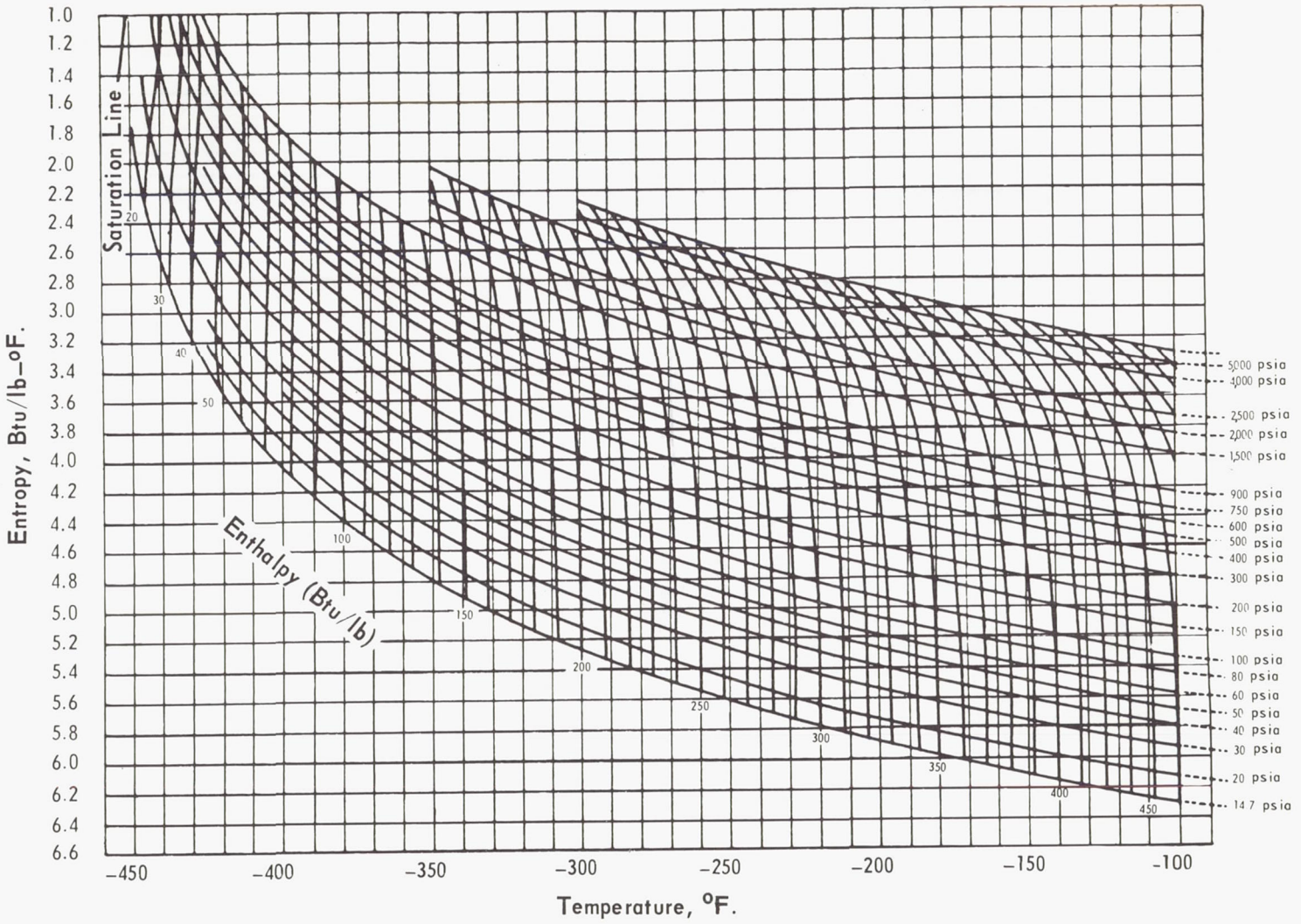


Figure D.1. Thermodynamic diagram, entropy versus temperature. [*Courtesy of the Whittaker Corp.*]

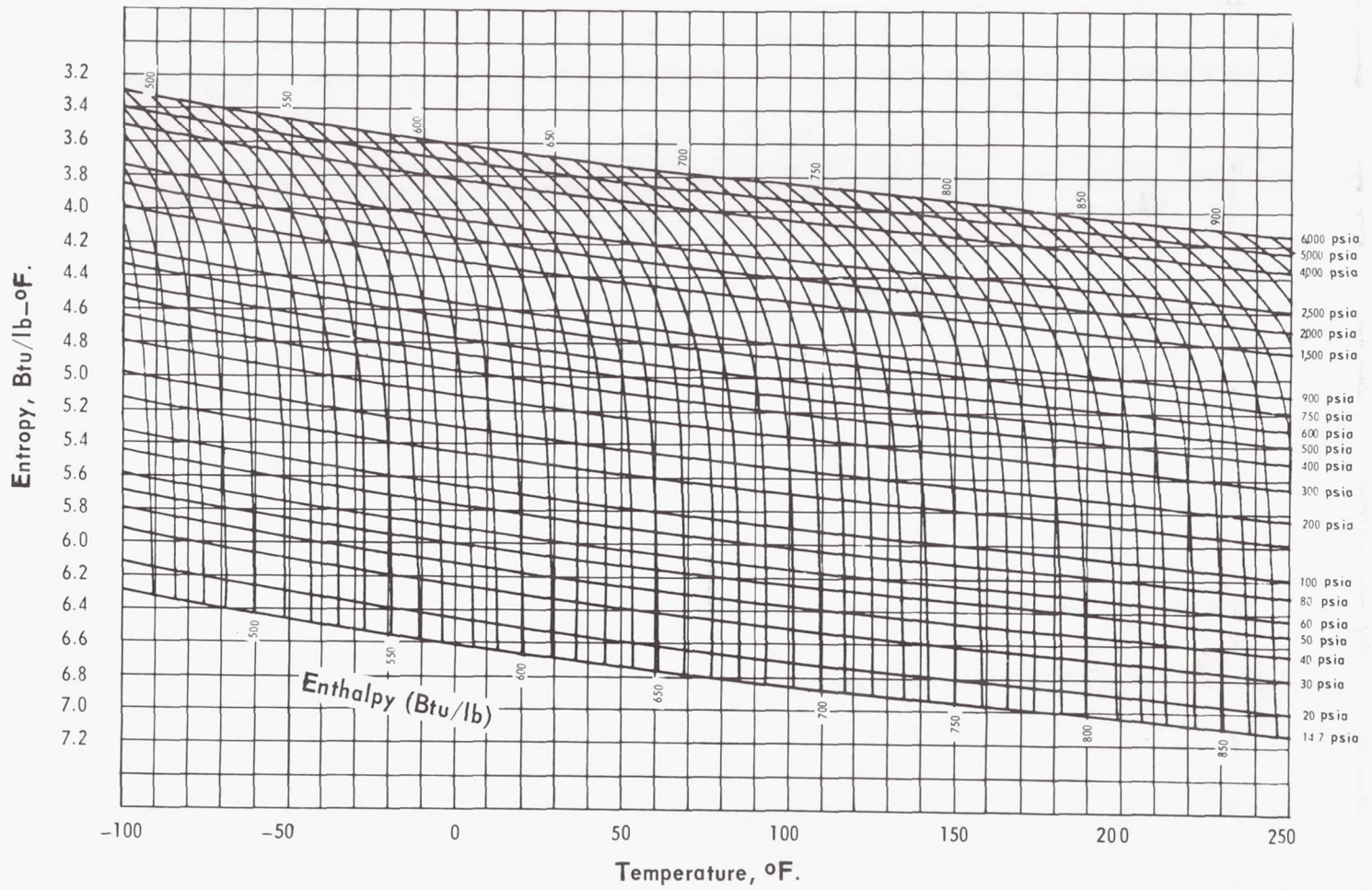


Figure D.1. Thermodynamic diagram, entropy versus temperature.—Continued. [*Courtesy of the Whittaker Corp.*]

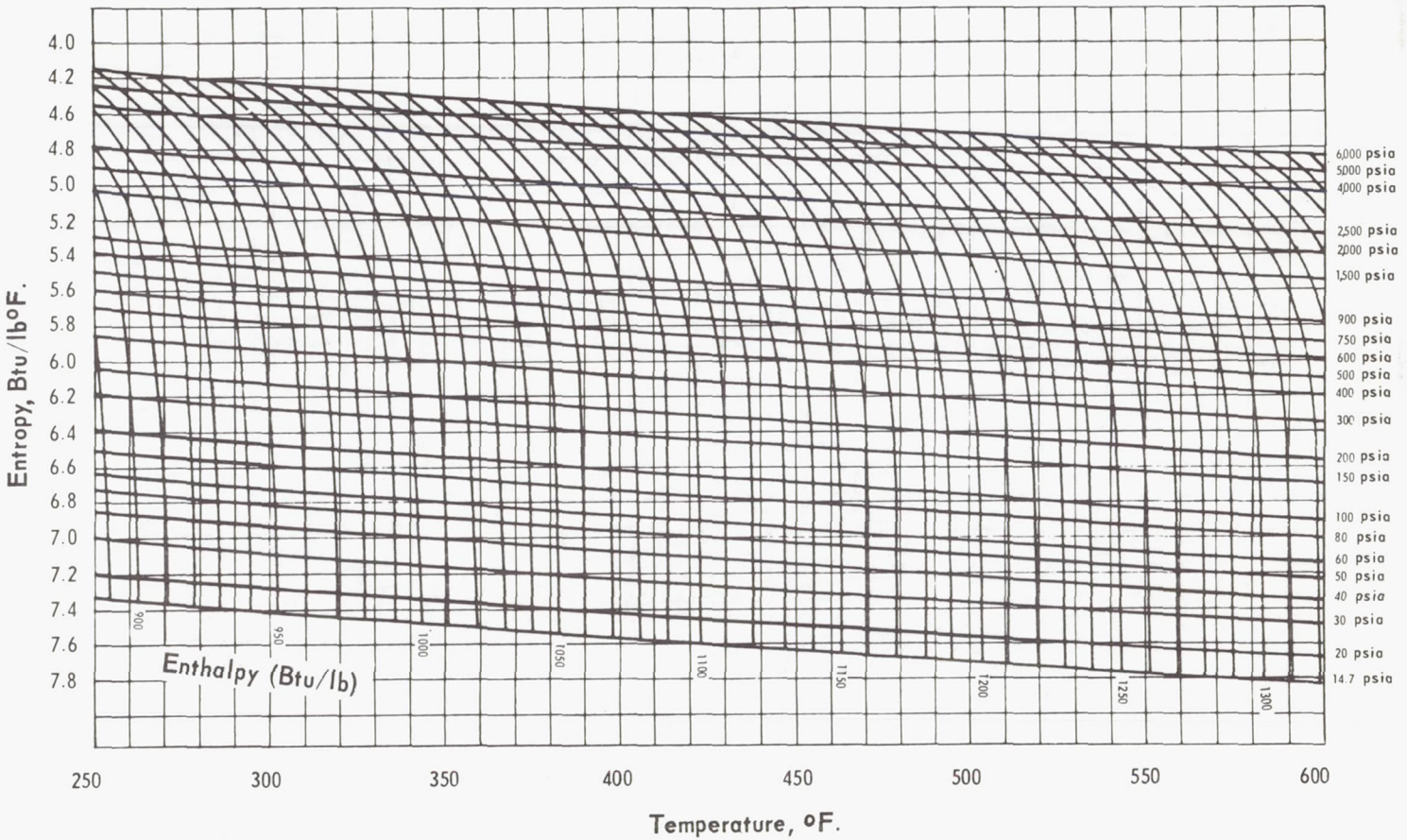


Figure D.1. Thermodynamic diagram, entropy versus temperature.—Concluded. [*Courtesy of the Whittaker Corp.*]

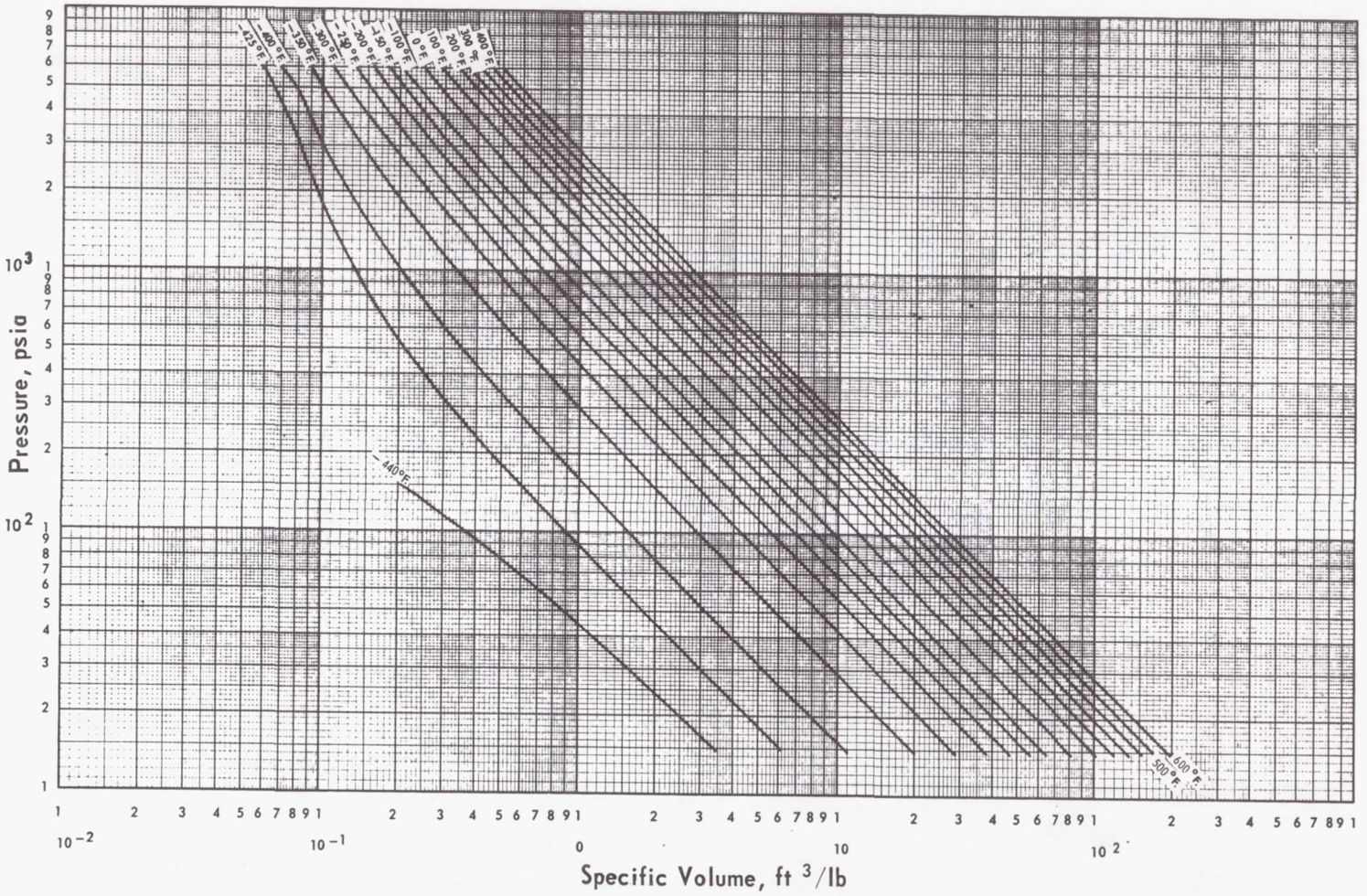


Figure D.2. Thermodynamic diagram, pressure versus specific volume. [*Courtesy of the Whittaker Corp.*]

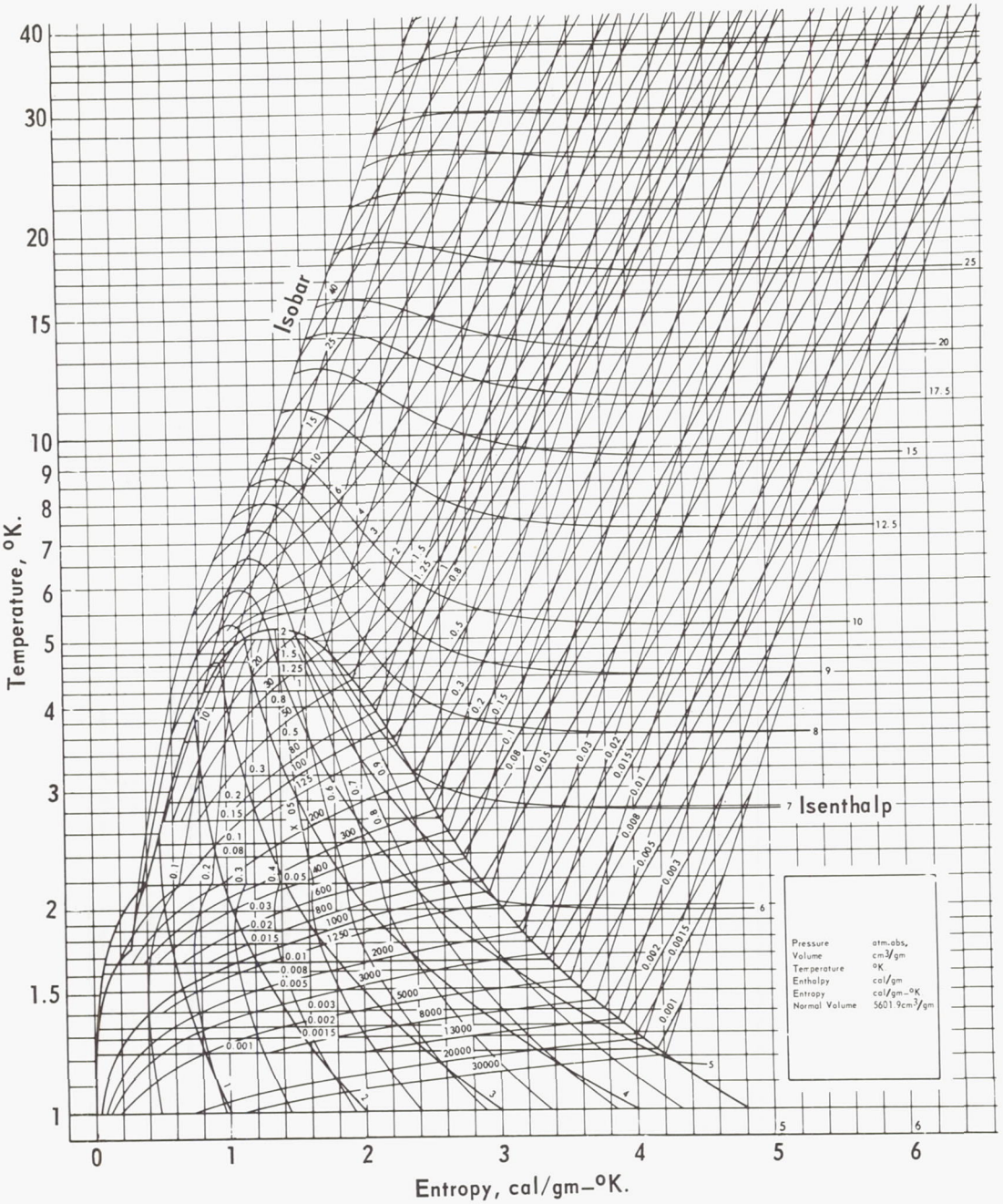


Figure D.3. Thermodynamic diagram, temperature versus entropy.

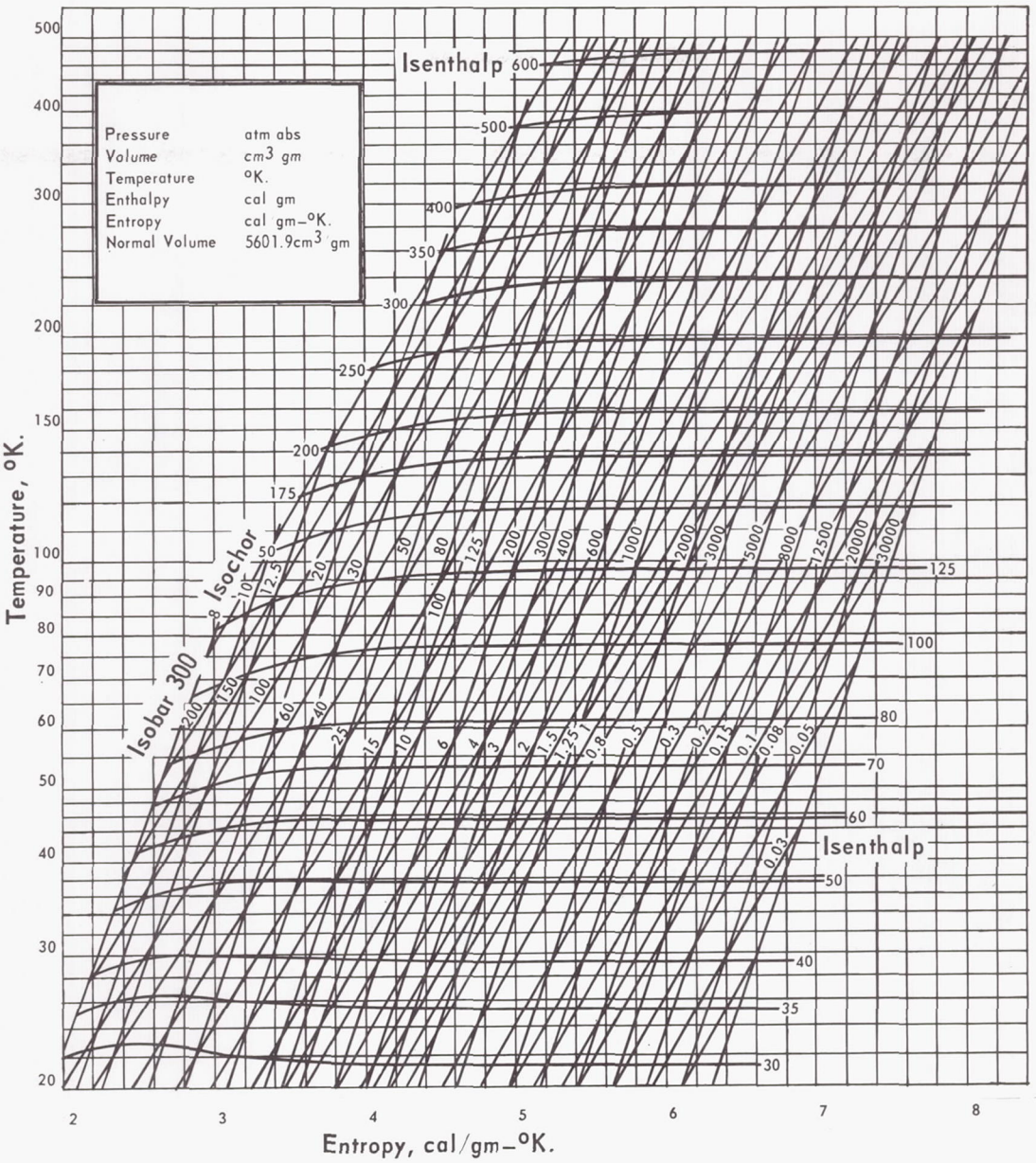


Figure D.3. Thermodynamic diagram, temperature versus entropy.—Continued.

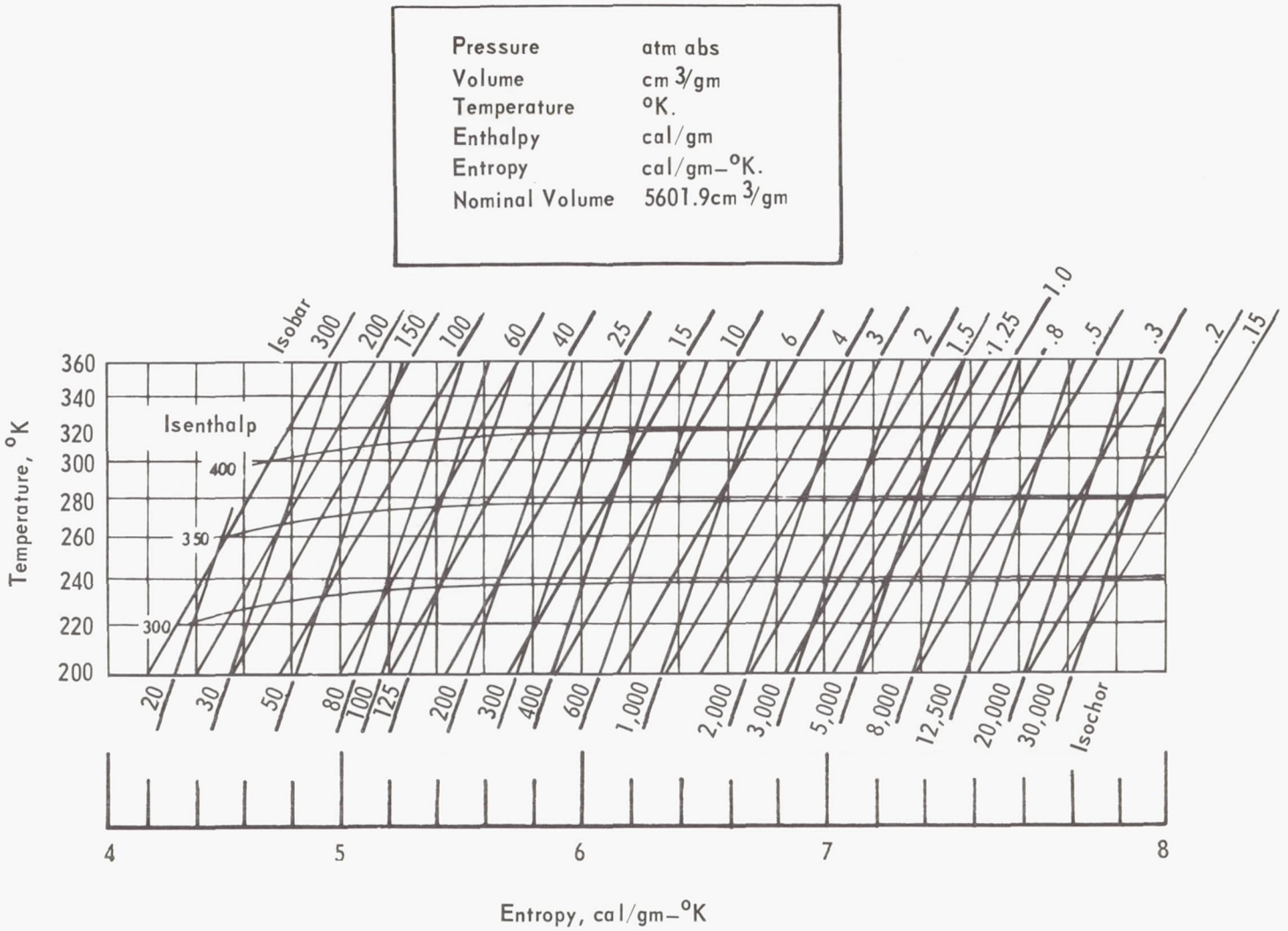


Figure D.3. Thermodynamic diagram, temperature versus entropy.—Continued.

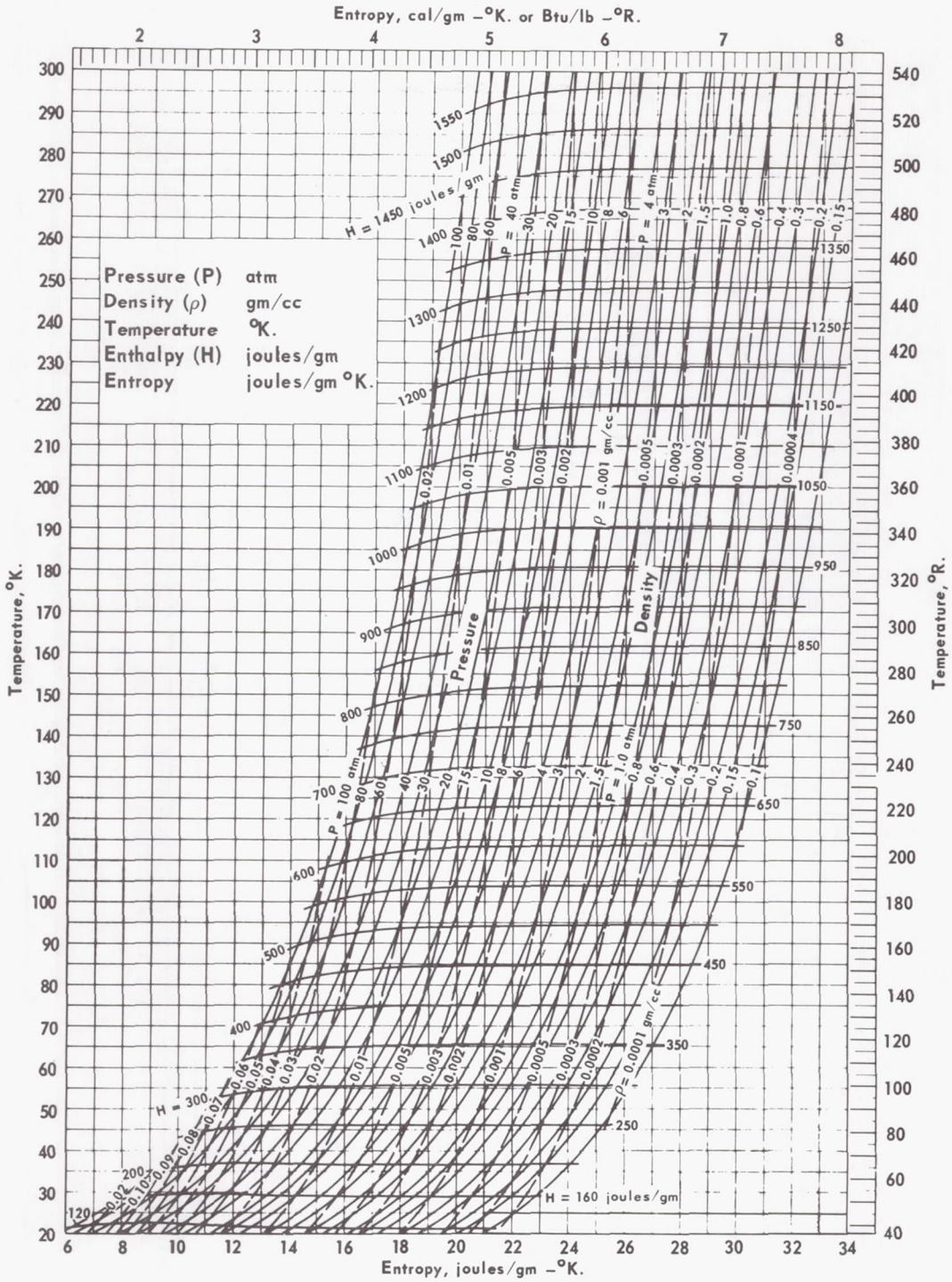


Figure D.3. Thermodynamic diagram, temperature versus entropy.—Continued.

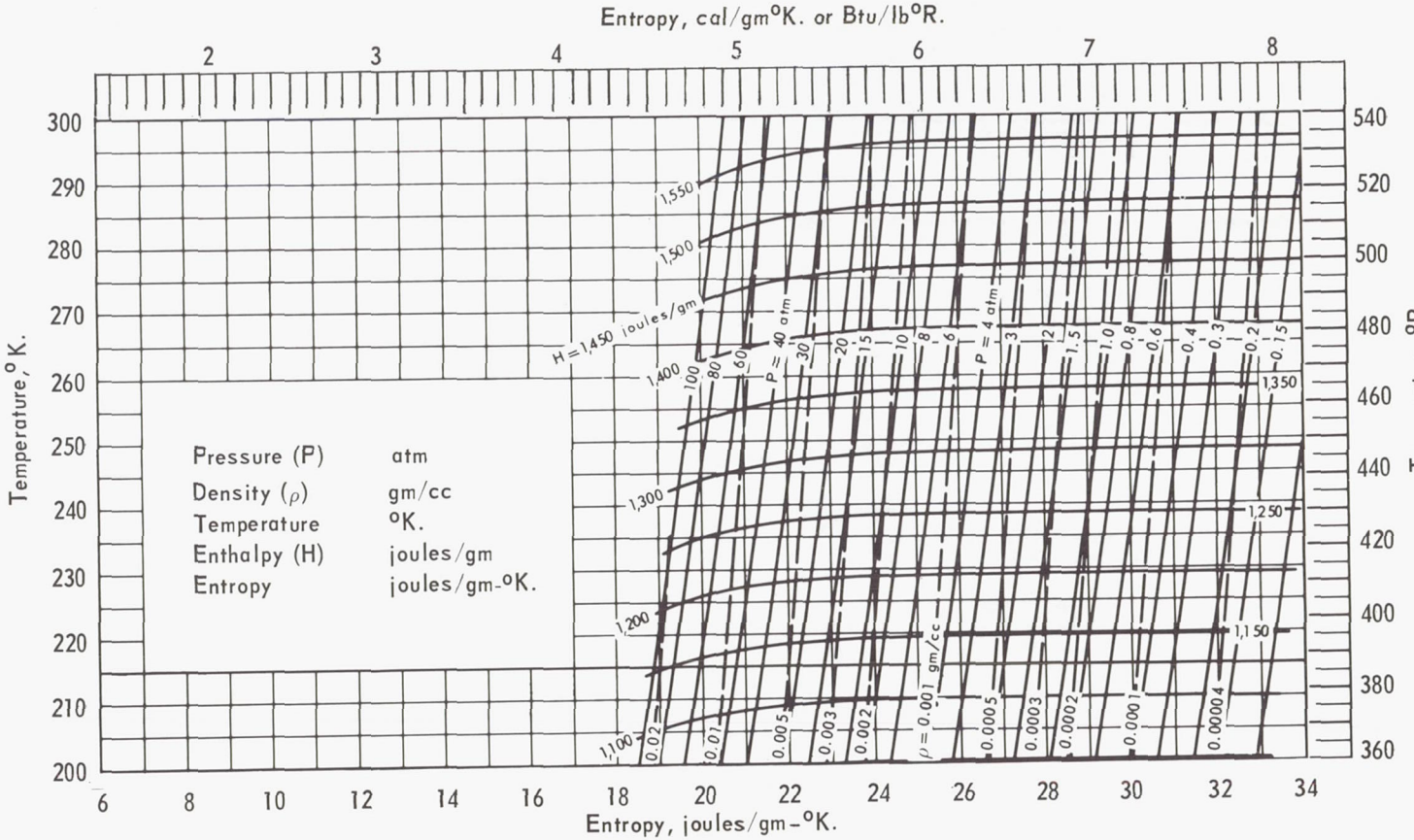


Figure D.3. Thermodynamic diagram, temperature versus entropy. — *Concluded.*

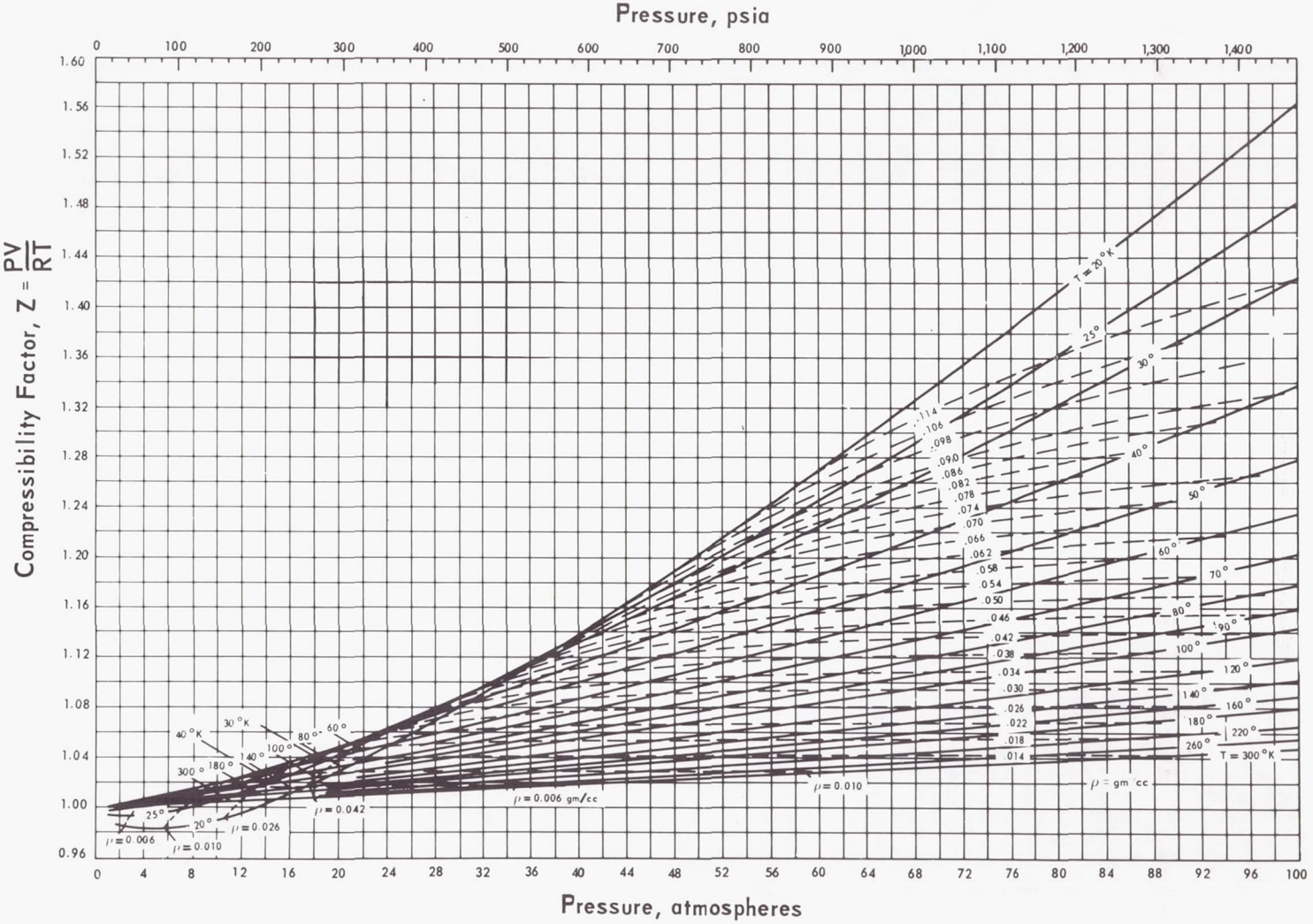


Figure D.4. Compressibility factor versus pressure.

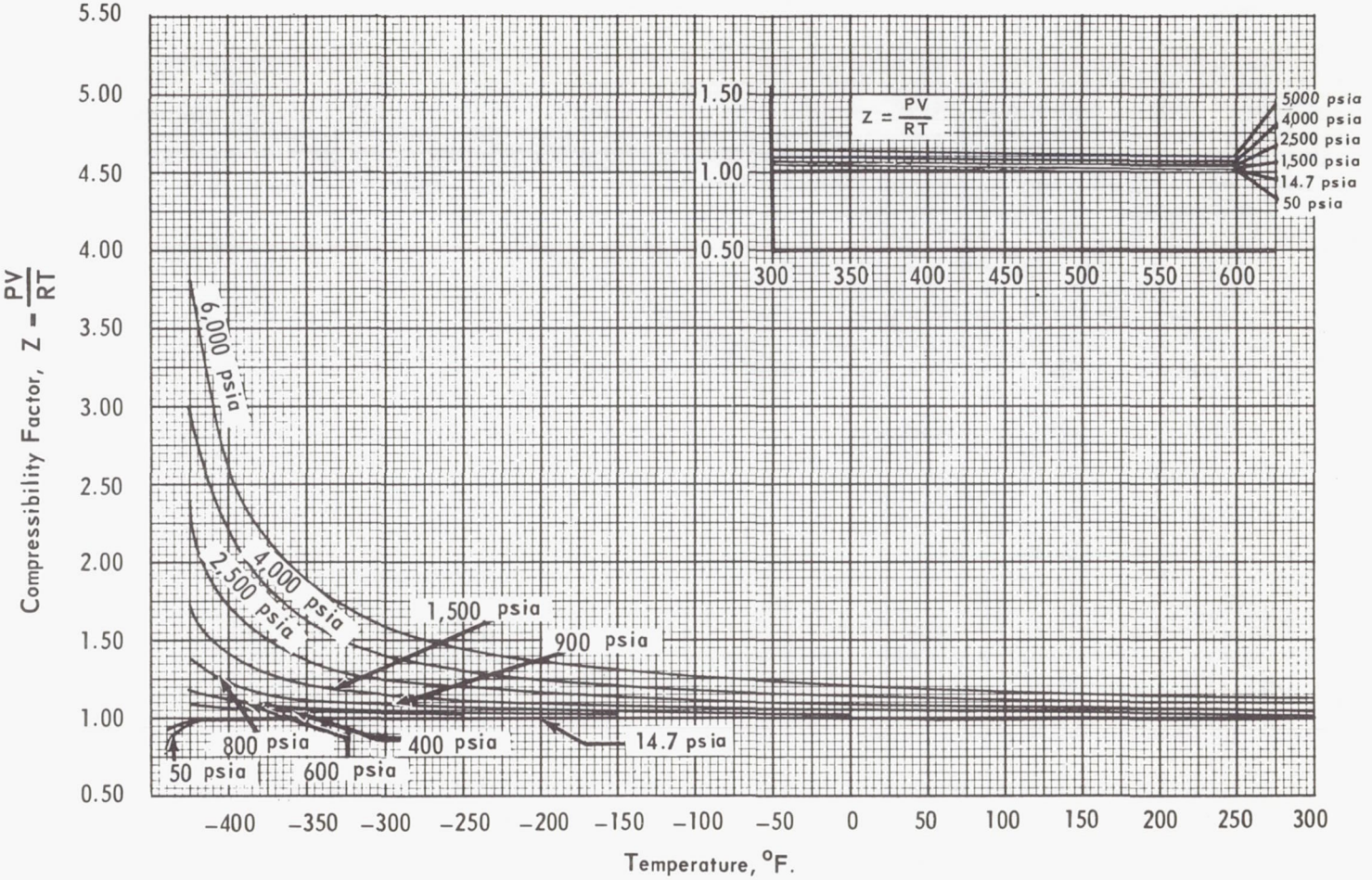


Figure D.5. Compressibility factor versus temperature. [*Courtesy of the Whittaker Corp.*]

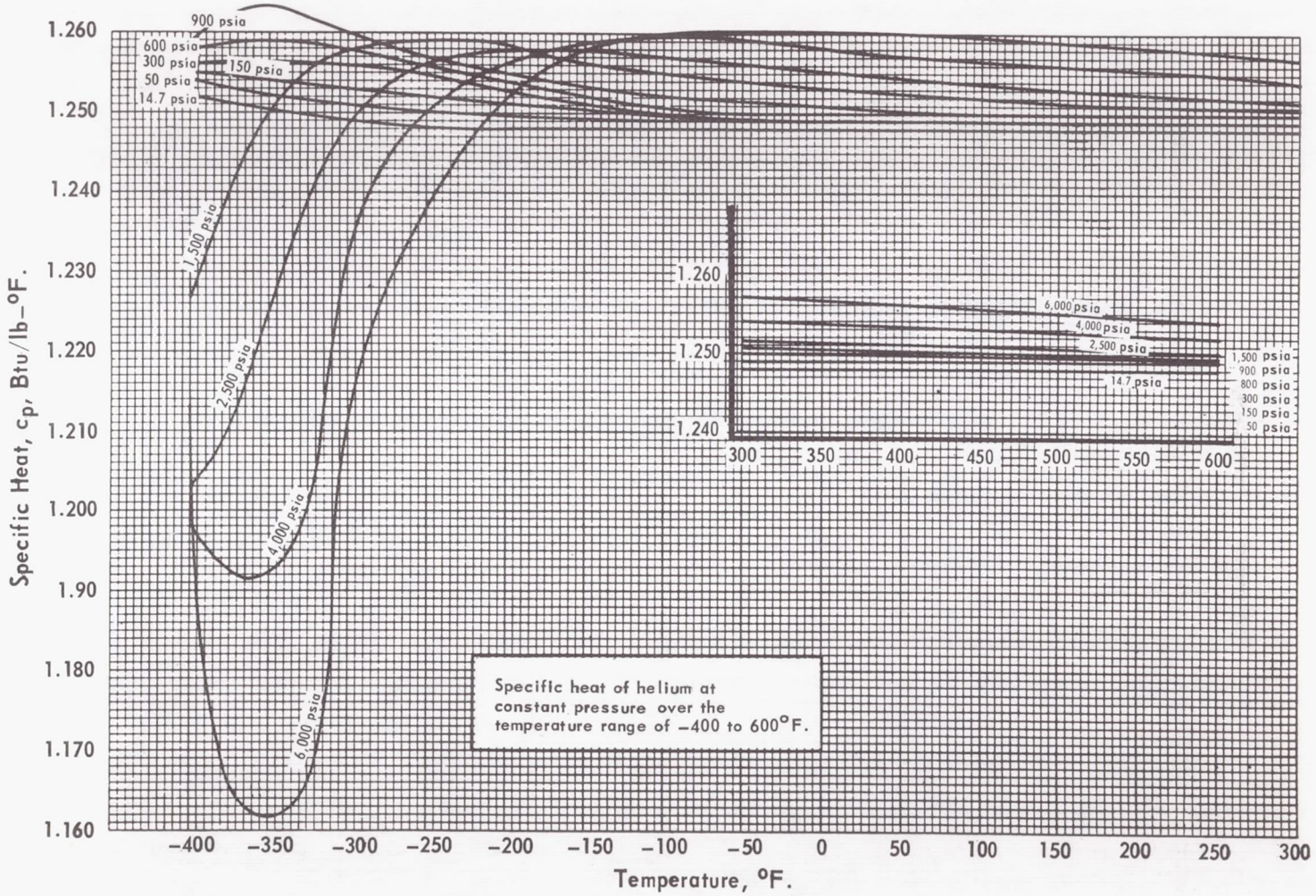


Figure D.6. Specific heat, c_p, versus temperature. [*Courtesy of the Whittaker Corp.*]

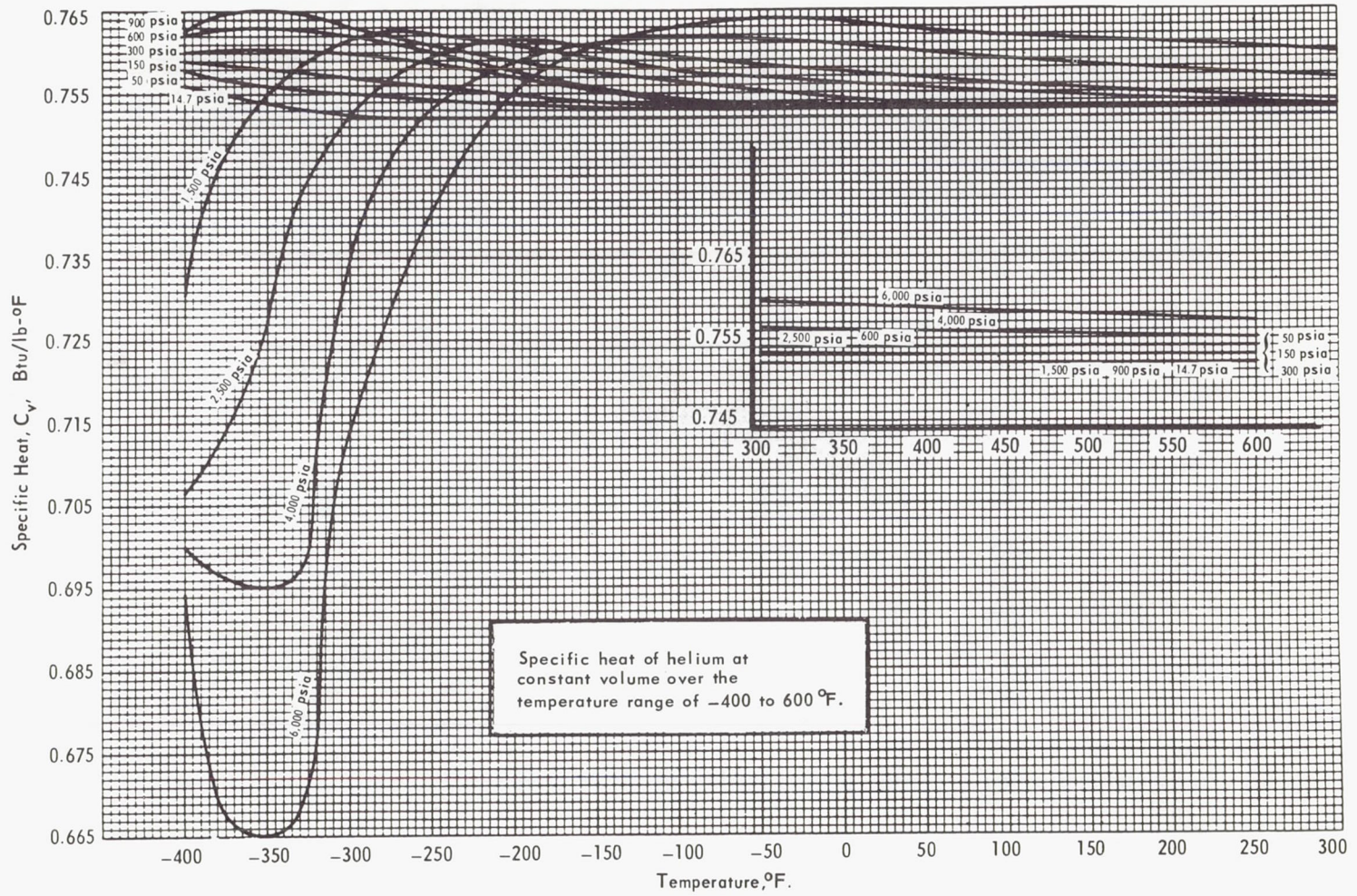


Figure D.7. Specific heat, c_v, versus temperature. [*Courtesy of the Whittaker Corp.*]

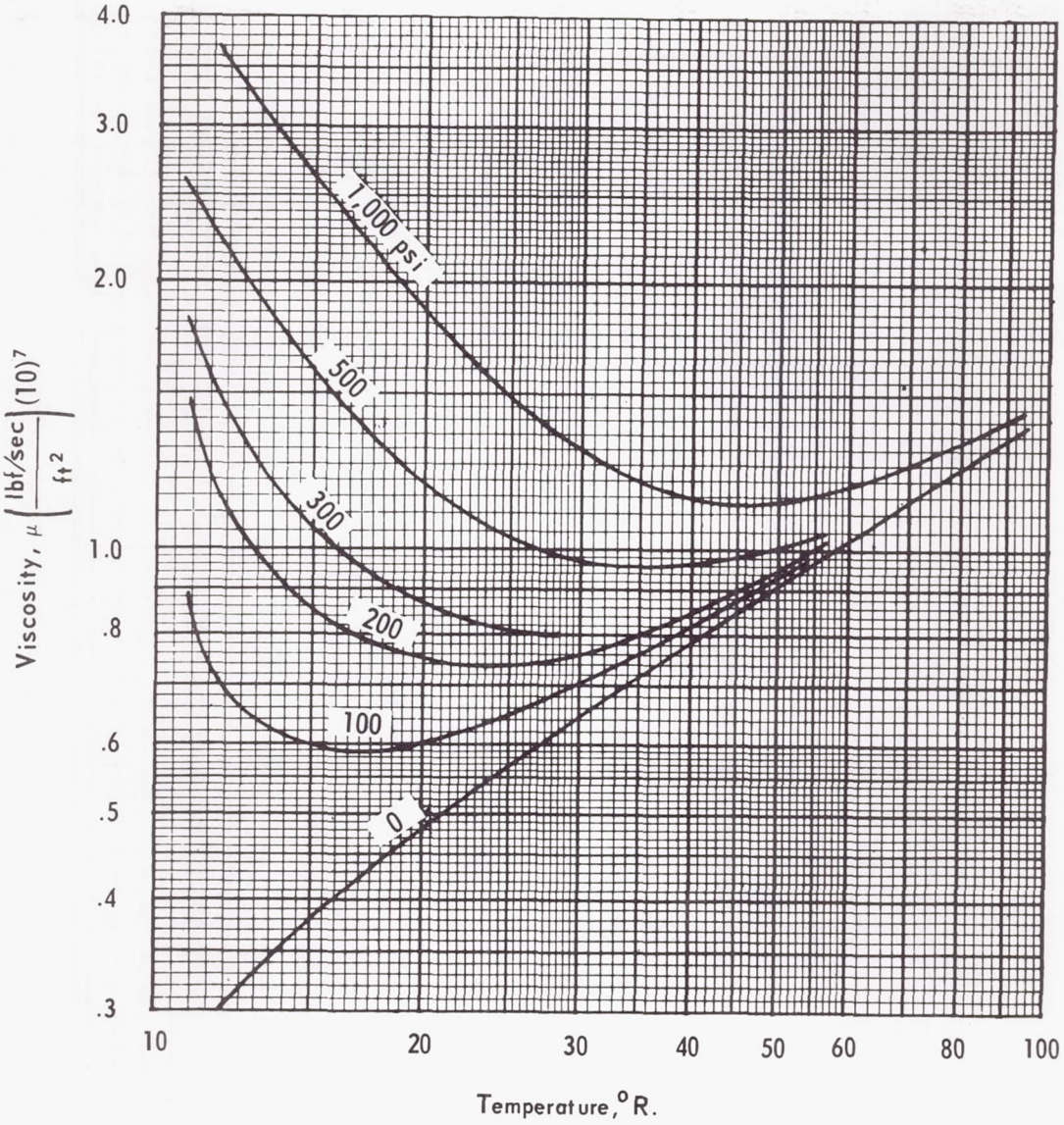


Figure D.8. Viscosity versus temperature.

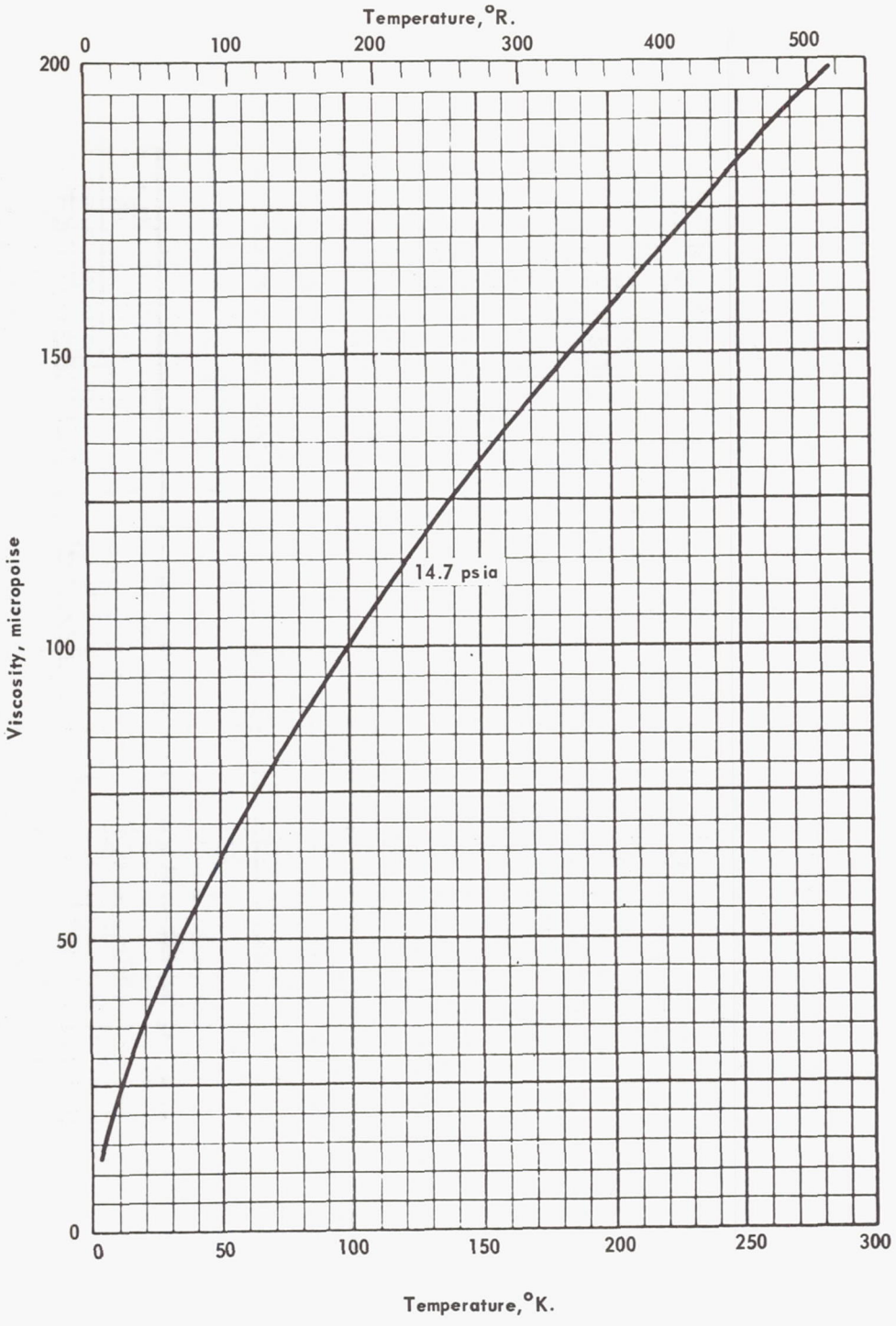


Figure D.8. Viscosity versus temperature. — Continued.

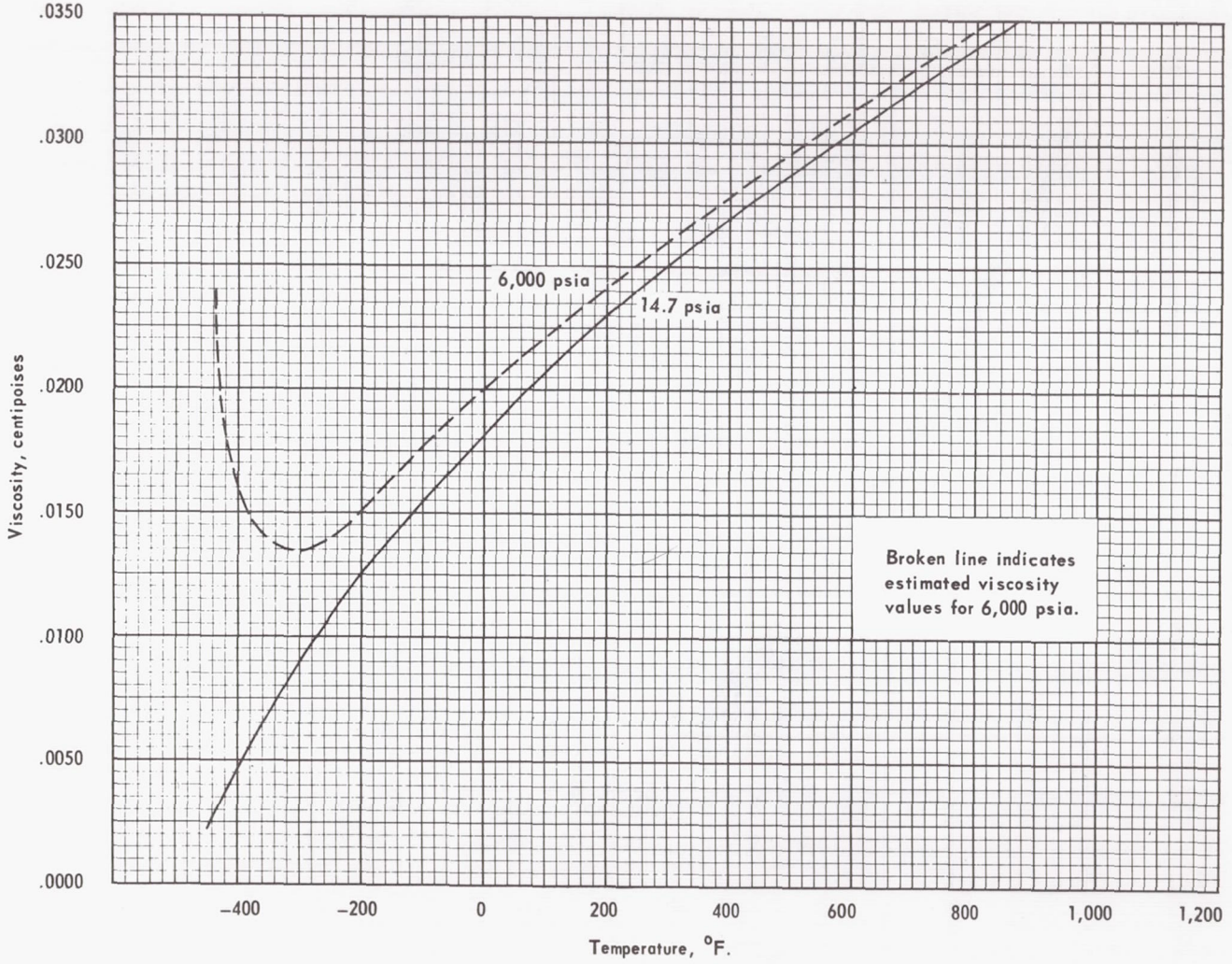


Figure D.8. Viscosity versus temperature.—Concluded. [*Courtesy of the Whittaker Corp.*]

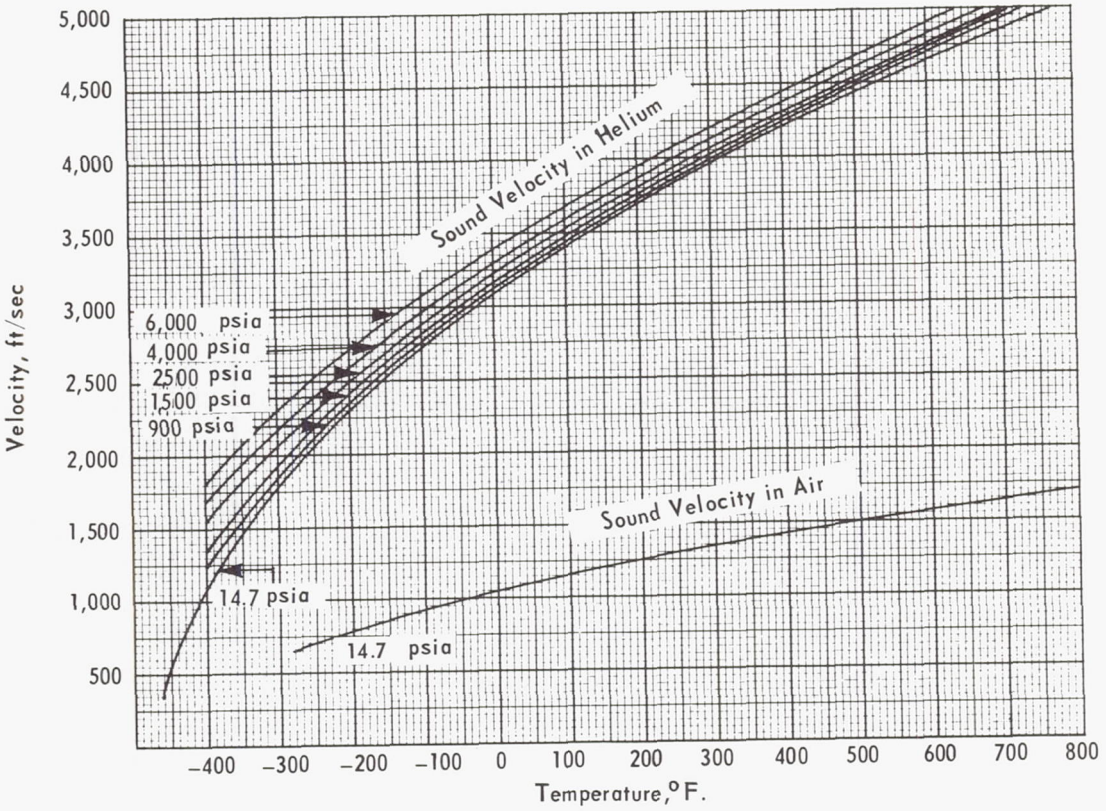


Figure D.9. Velocity of sound versus temperature. [*Courtesy of the Whittaker Corp.*]

APPENDIX E

DATA ON ~~HELIUM~~ Hydrogen

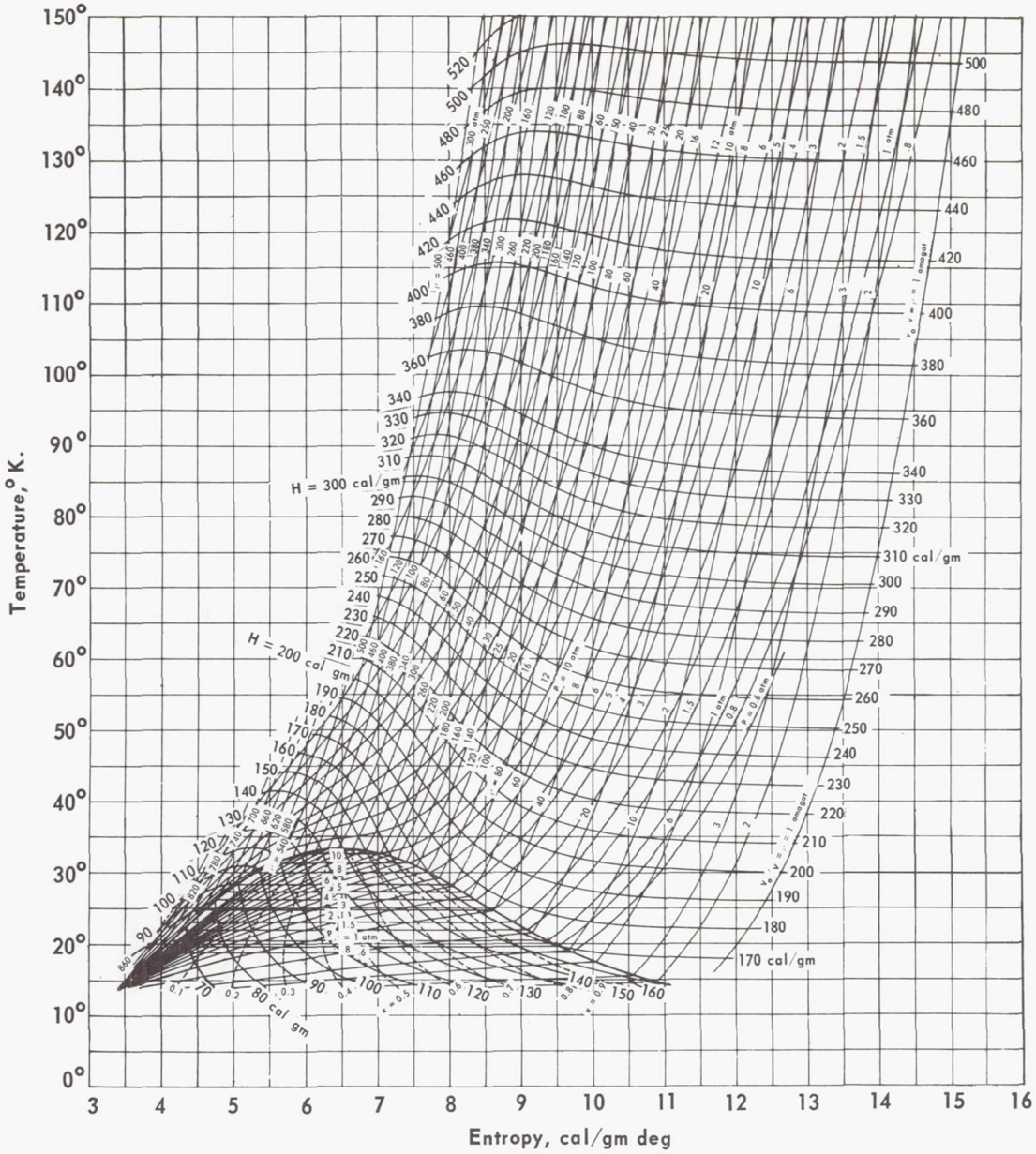


Figure E.1. Thermodynamic diagram, temperature versus entropy. [*Reference NBS Chart D–4.*]

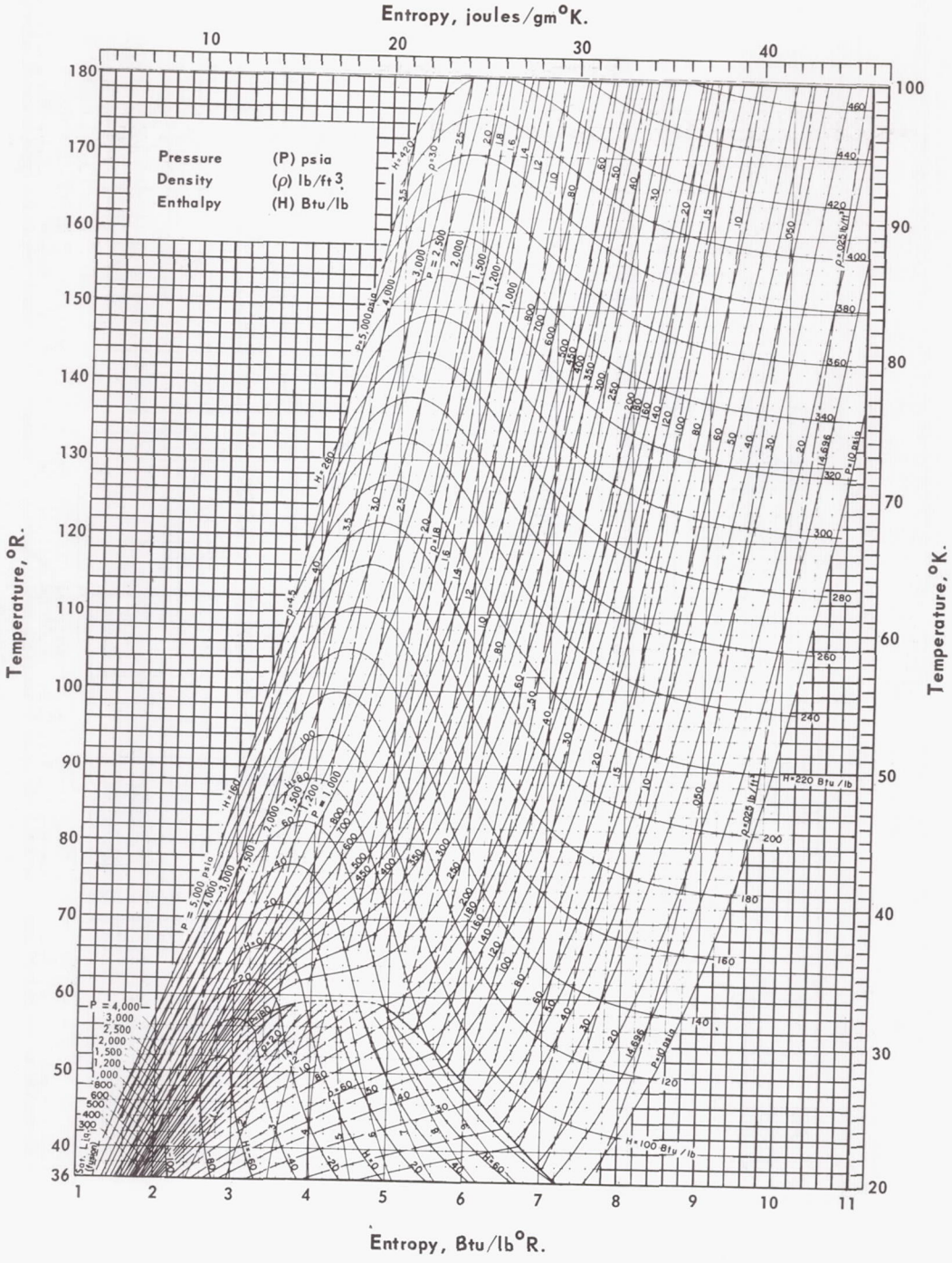


Figure E.1. Thermodynamic diagram, temperature versus entropy.—Continued. [*Reference NBS Chart D–4.*]

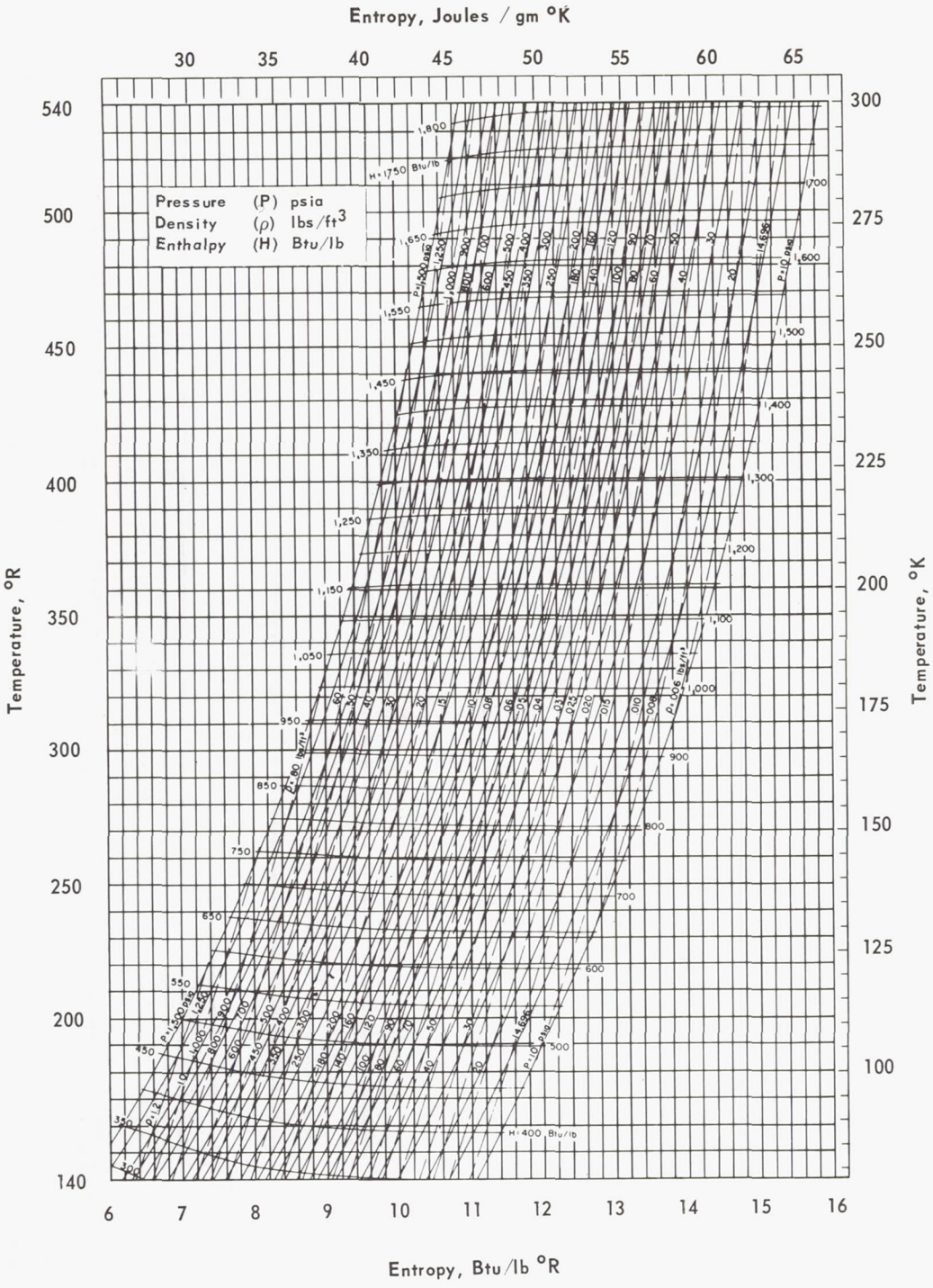


Figure E.1. Thermodynamic diagram, temperature versus entropy.—Continued. [*Reference NBS Chart D–4.*]

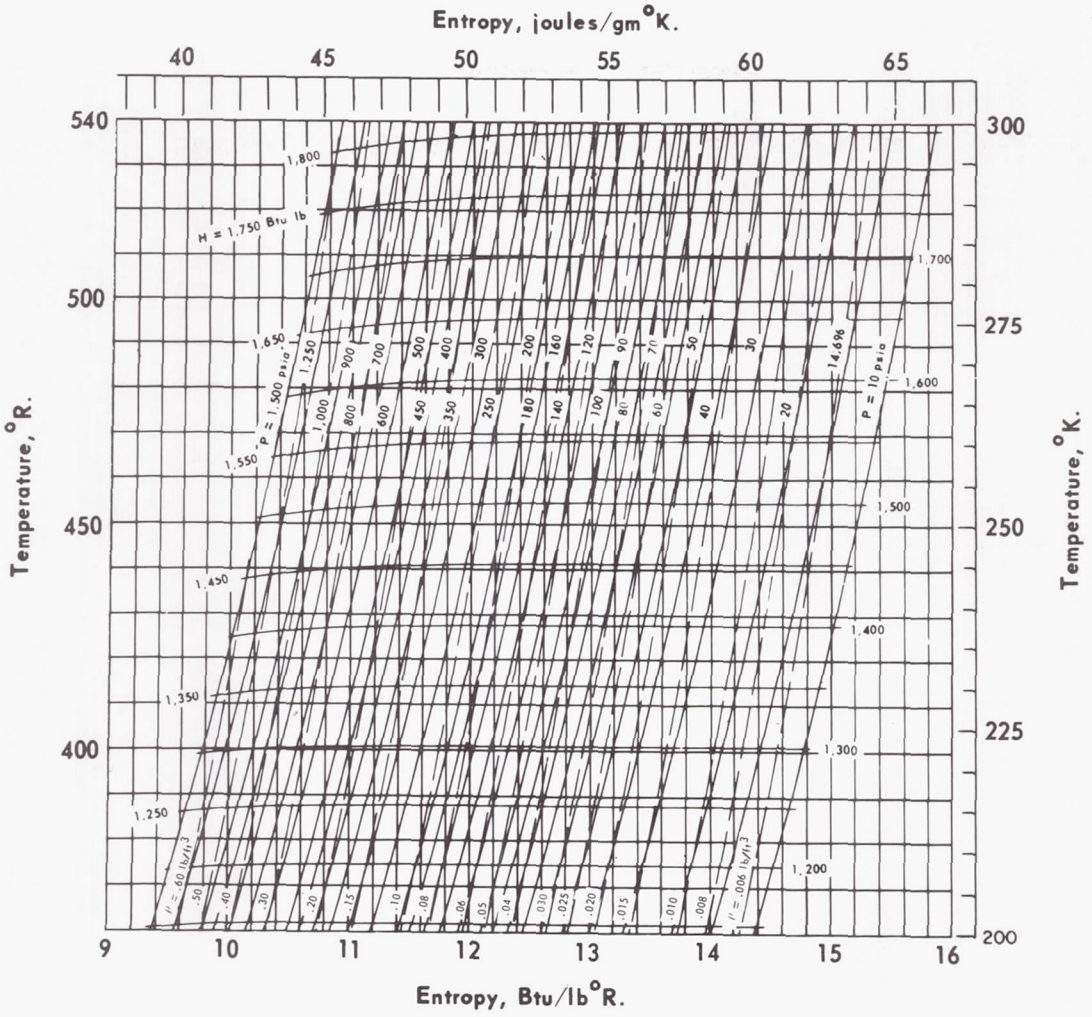


Figure E.1. Thermodynamic diagram, temperature versus entropy.—Continued. Pressure (p) psia, density (ρ) lbs/ft^3, enthalpy (H) Btu/lb.

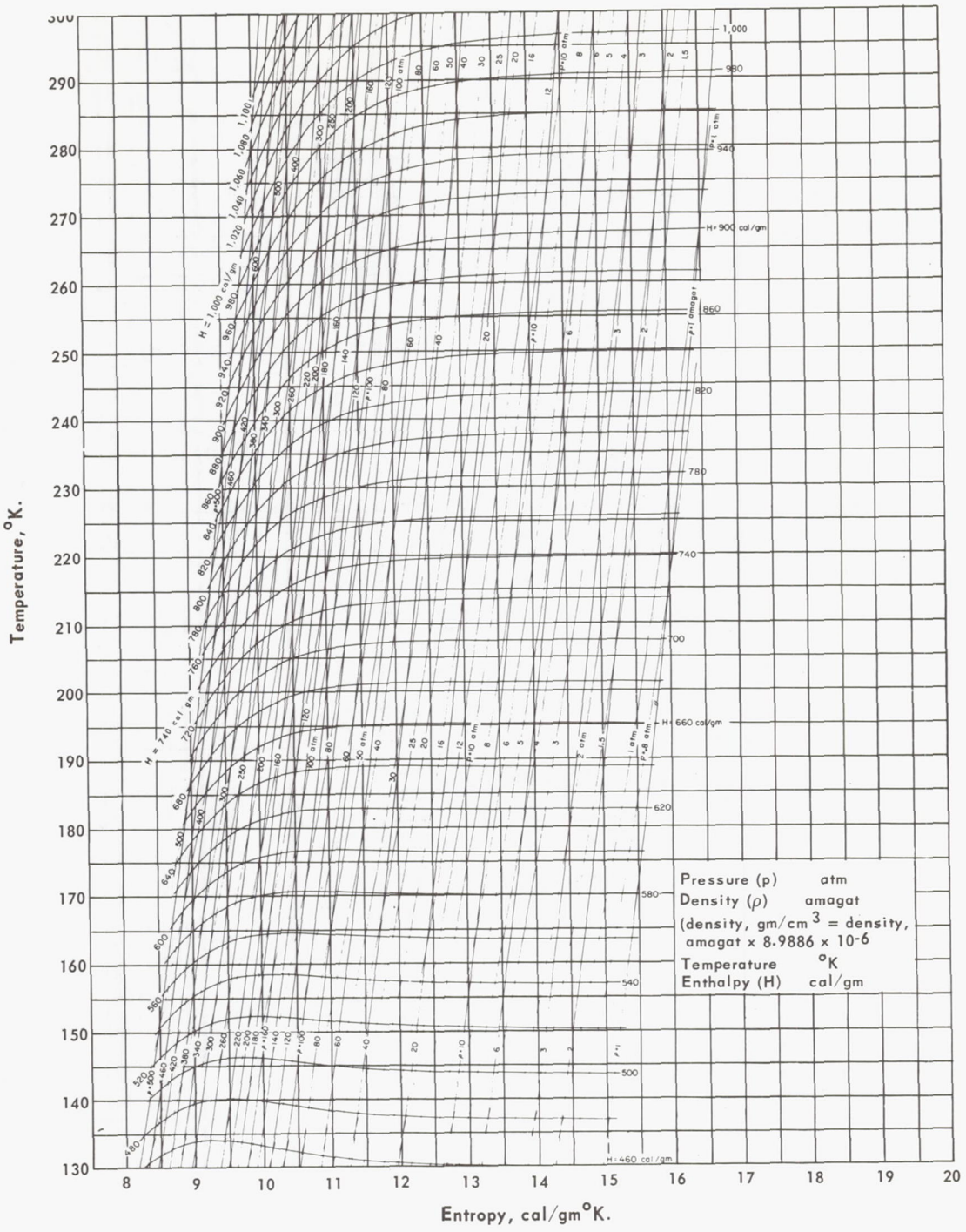


Figure E.1. Thermodynamic diagram, temperature versus entropy.—Continued. [*Reference NBS Charts D–20B, –21B, D–5.*]

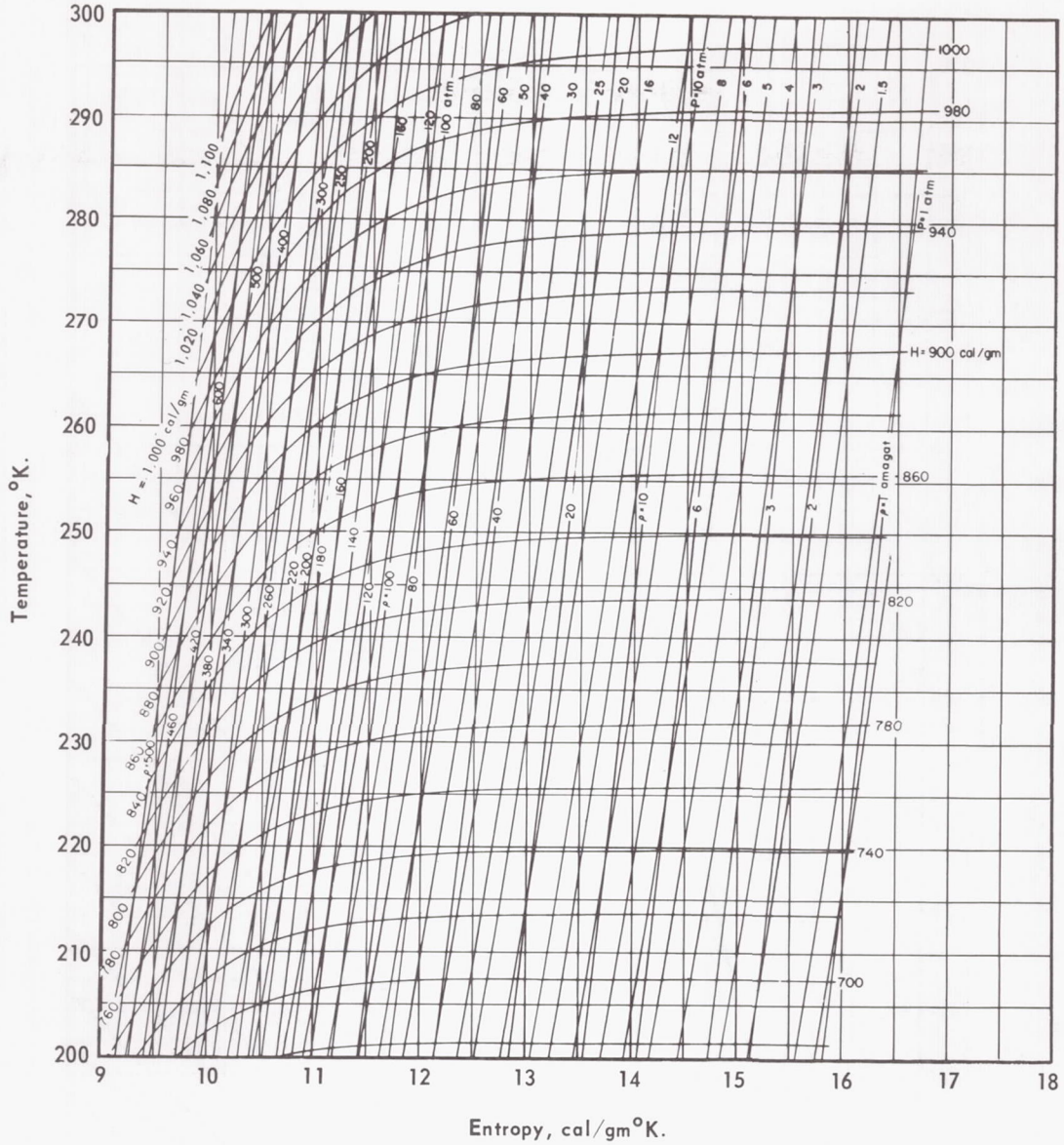


Figure E.1. Thermodynamic diagram, temperature versus entropy.—Concluded. Pressure (p): atm; density (p): amagat (density, g/cm^3 = density, amagat $\times$ 8.9886 $\times$ 10^{-6}); temperature: °K; enthalpy (H): cal/g. [*Reference NBS Chart D–5.*]

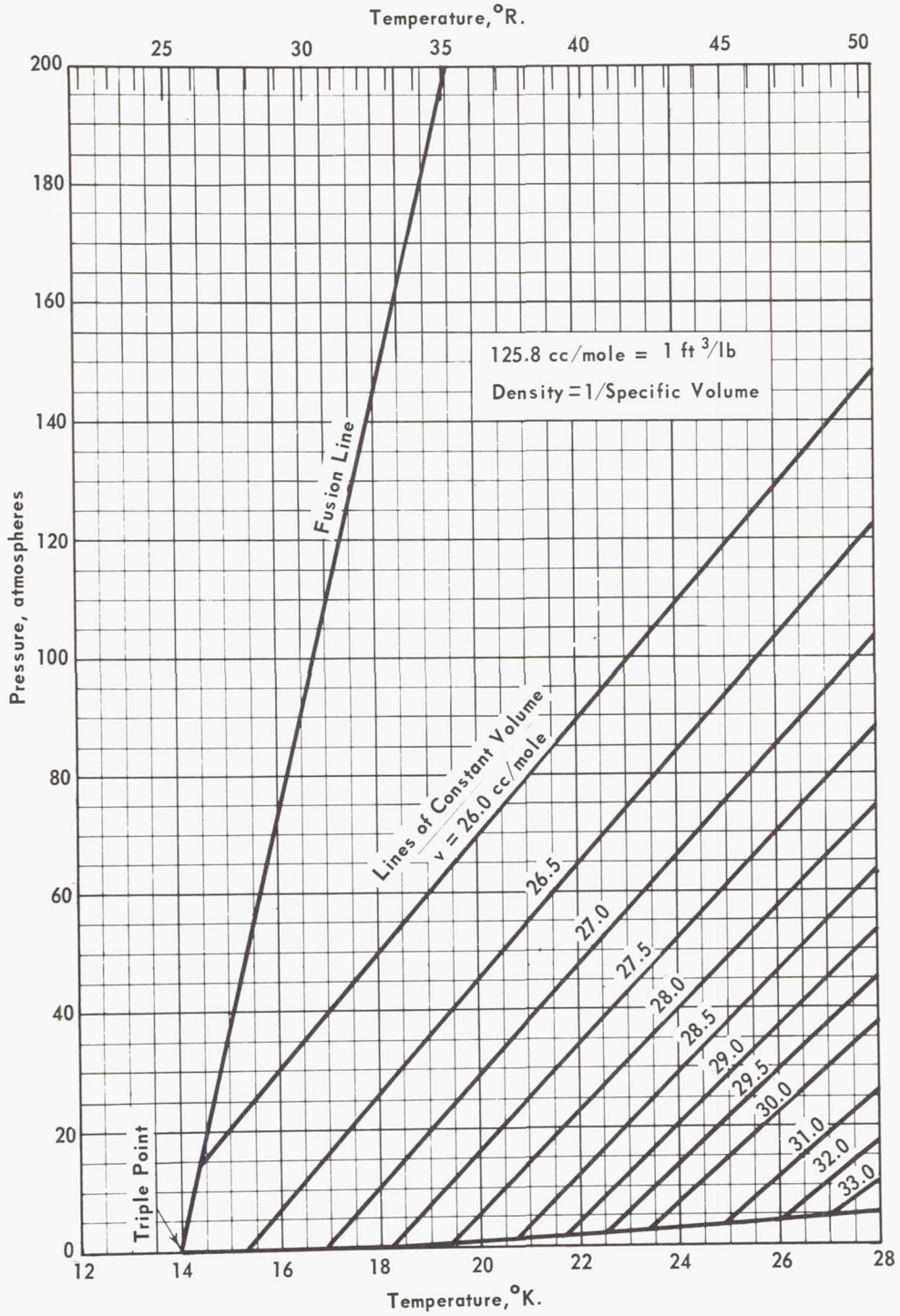


Figure E.2. Thermodynamic diagram, pressure versus temperature. [*Reference WADD TR 60–56, Part I.*]

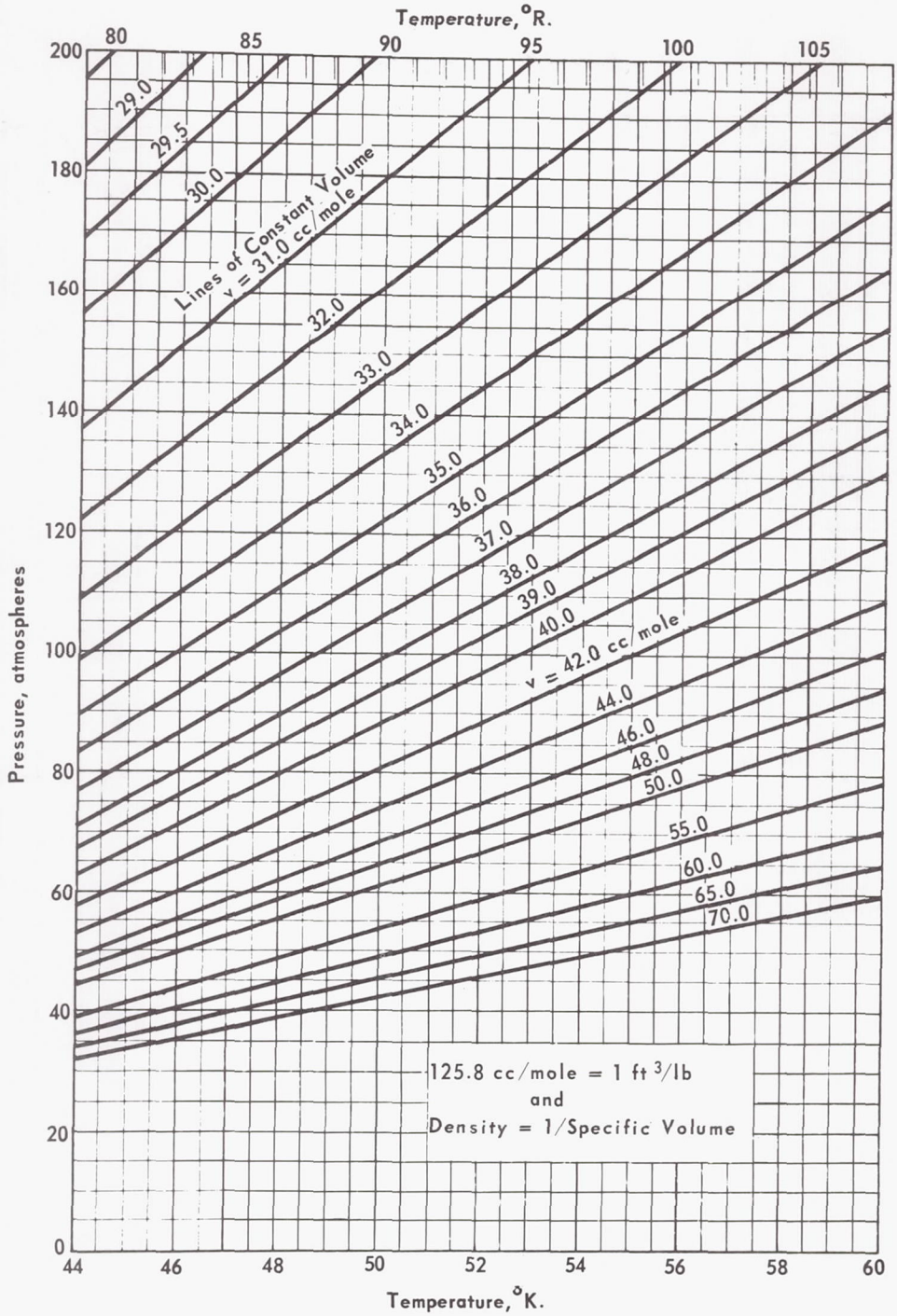


Figure E.2. Thermodynamic diagram, pressure versus temperature.—Concluded. [*Reference WADD TR 60–56, Part I.*]

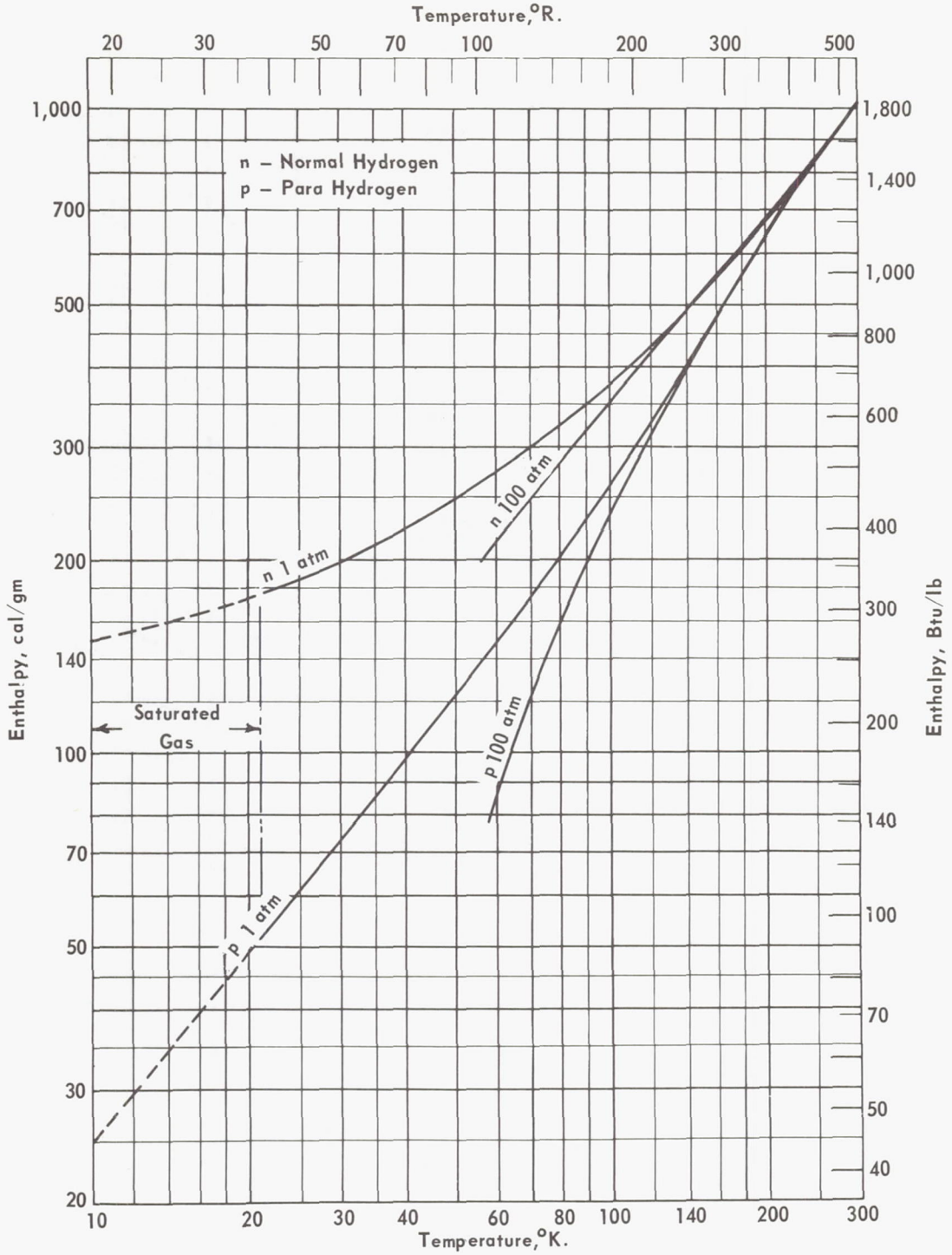


Figure E.3. Thermodynamic diagram, enthalpy versus temperature. [*Reference WADD TR 60–56, Part I.*]

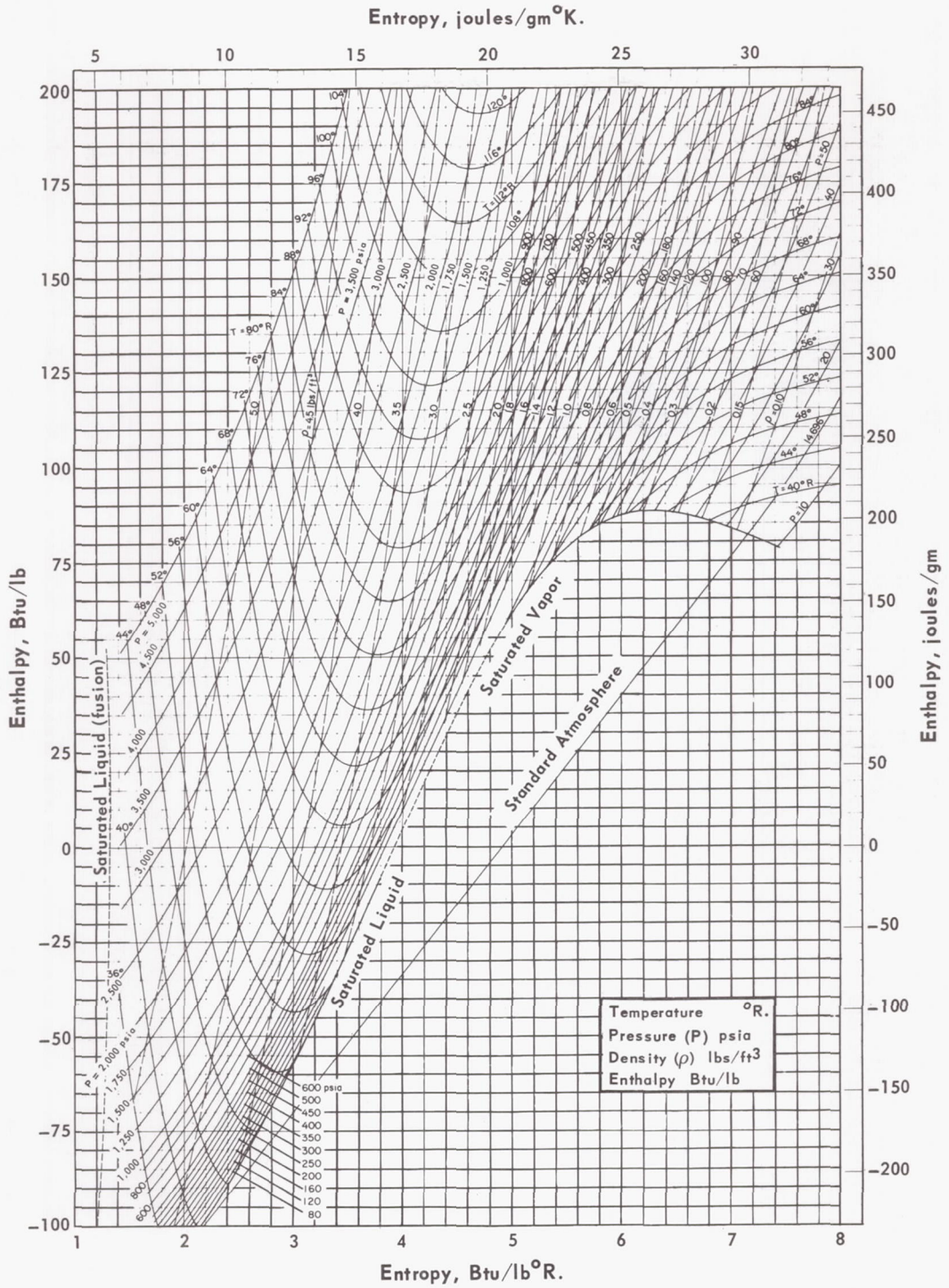
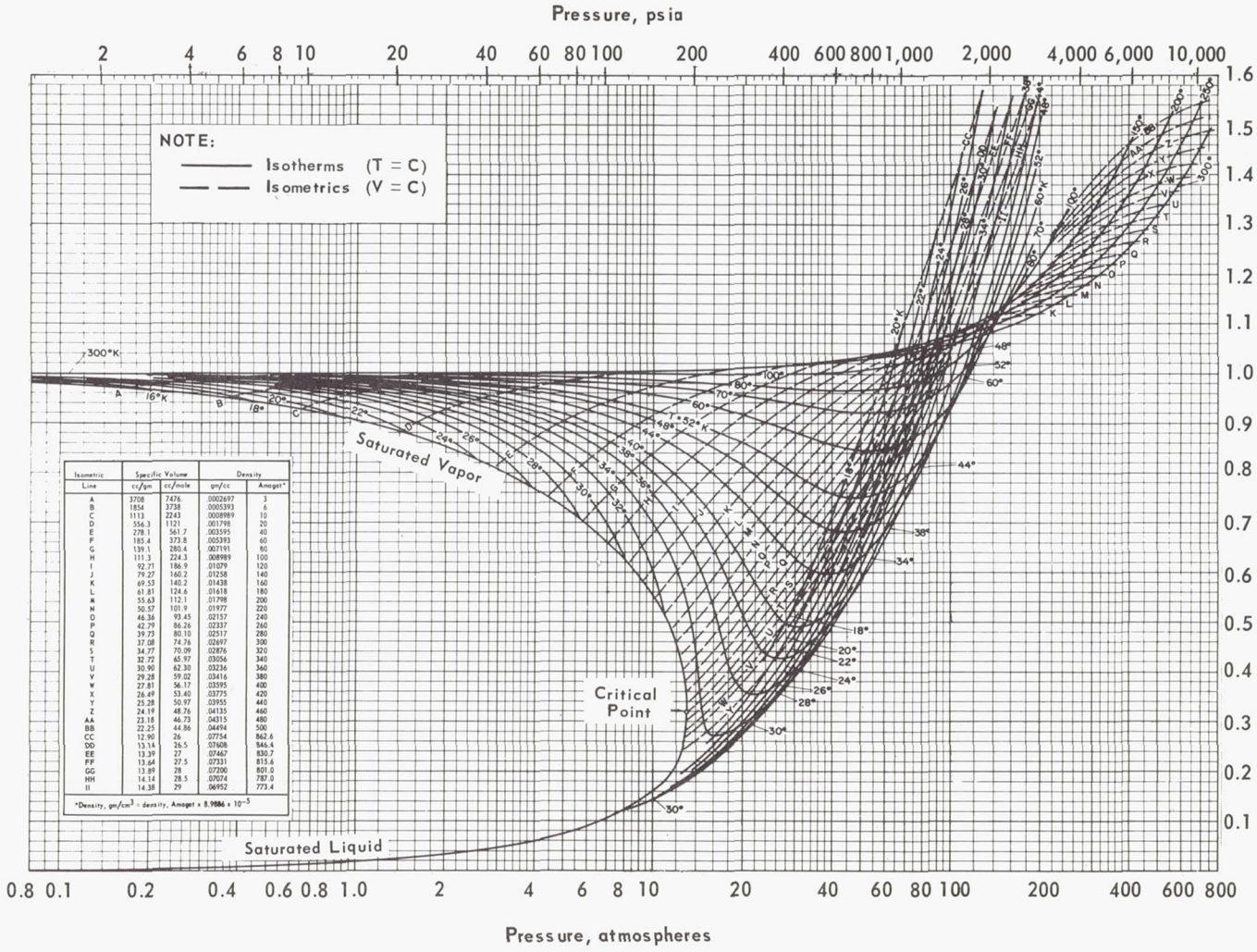


Figure E.4. Thermodynamic diagram, enthalpy versus entropy. [*Reference NBS Chart D–22B.*]



Isometric Line	Specific Volume cc/gm	Specific Volume cc/mole	Density gm/cc	Density Amagat*
A	3708	7476	.0002697	3
B	1854	3738	.0005393	6
C	1113	2243	.0008989	10
D	556.3	1121	.001798	20
E	278.1	561.7	.003595	40
F	185.4	373.8	.005393	60
G	139.1	280.4	.007191	80
H	111.3	224.3	.008989	100
I	92.71	186.9	.01079	120
J	79.27	160.2	.01258	140
K	69.53	140.2	.01438	160
L	61.81	124.6	.01618	180
M	55.63	112.1	.01798	200
N	50.57	101.9	.01977	220
O	46.36	93.45	.02157	240
P	42.79	86.26	.02337	260
Q	39.73	80.10	.02517	280
R	37.08	74.76	.02697	300
S	34.77	70.09	.02876	320
T	32.72	65.97	.03056	340
U	30.90	62.30	.03236	360
V	29.28	59.02	.03416	380
W	27.81	56.17	.03595	400
X	26.49	53.40	.03775	420
Y	25.28	50.97	.03955	440
Z	24.19	48.76	.04135	460
AA	23.18	46.73	.04315	480
BB	22.25	44.86	.04494	500
CC	12.90	26	.07754	862.6
DD	13.14	26.5	.07608	946.4
EE	13.39	27	.07467	830.7
FF	13.64	27.5	.07331	815.6
GG	13.89	28	.07200	801.0
HH	14.14	28.5	.07074	787.0
II	14.38	29	.06952	773.4

*Density, gm/cm^3 = density, Amagat x 8.9886×10^{-5}

Figure E.5. Compressibility factor versus pressure. [*Reference NBS Chart D–14.*]

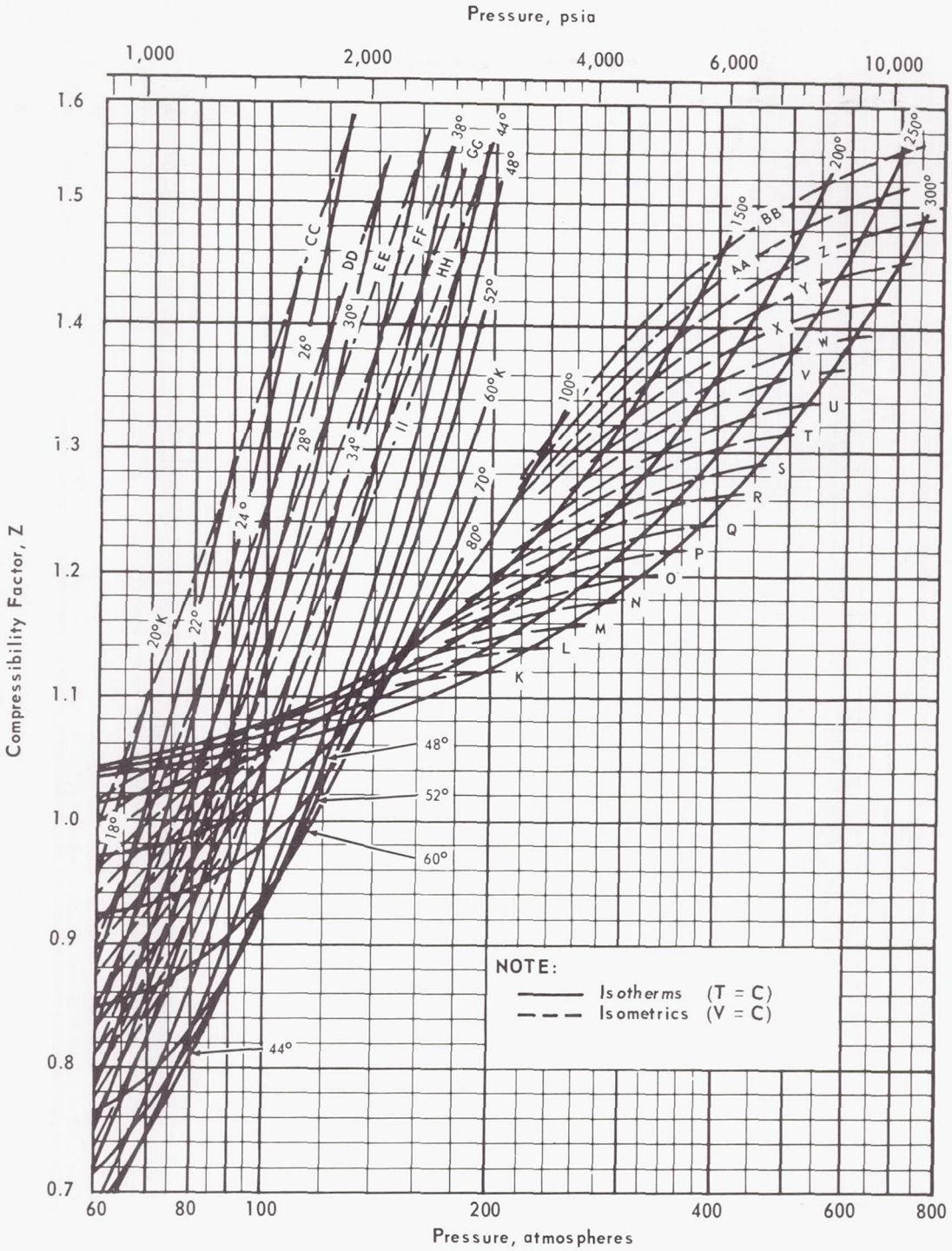


Figure E.5. Compressibility factor versus pressure.—Concluded. [*Reference NBS Chart D–14.*]

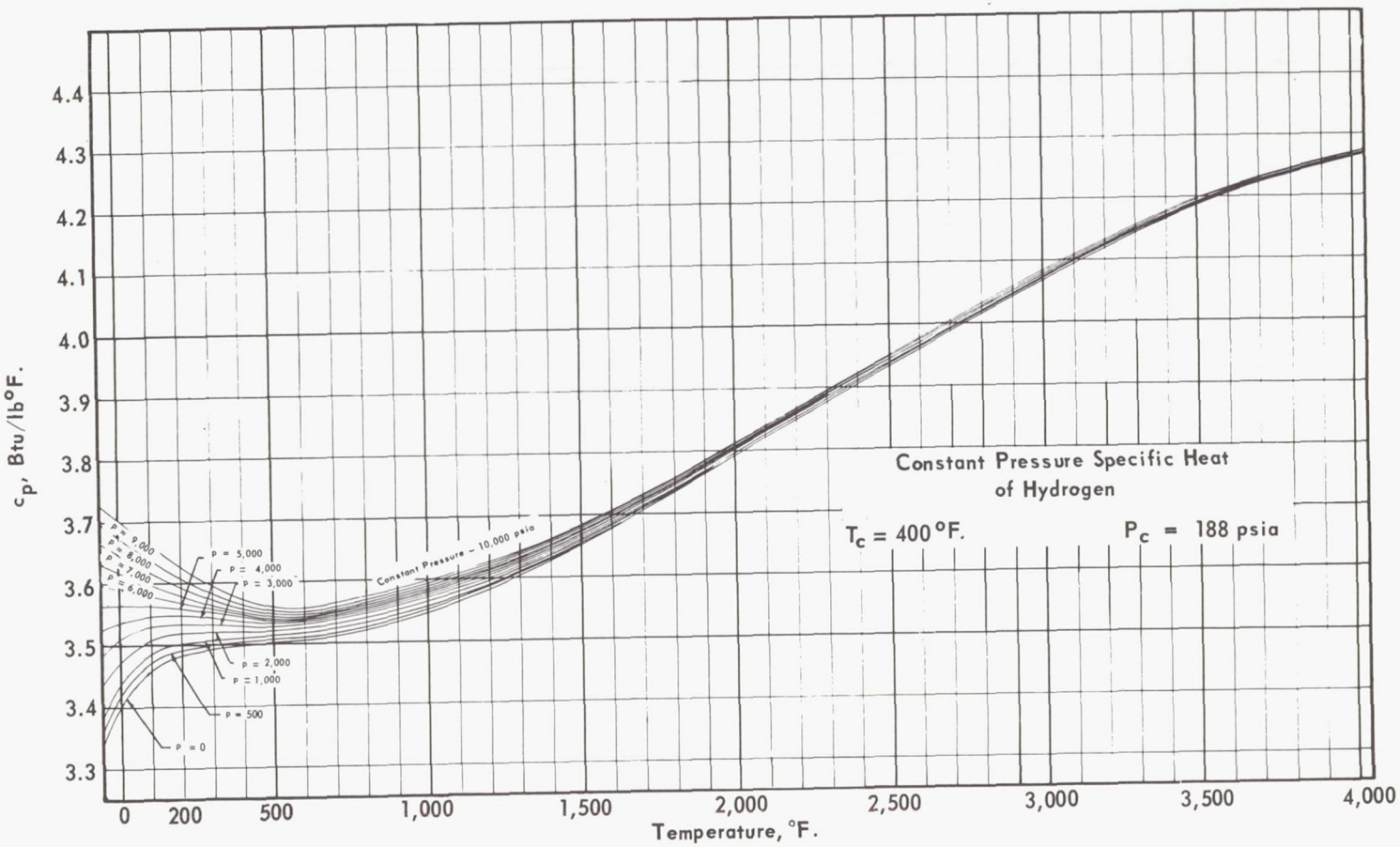


Figure E.6. Specific heat, c_p, versus temperature. [*Courtesy of the Cornell University, Engineering Experiment Station Bulletin No. 30.*]

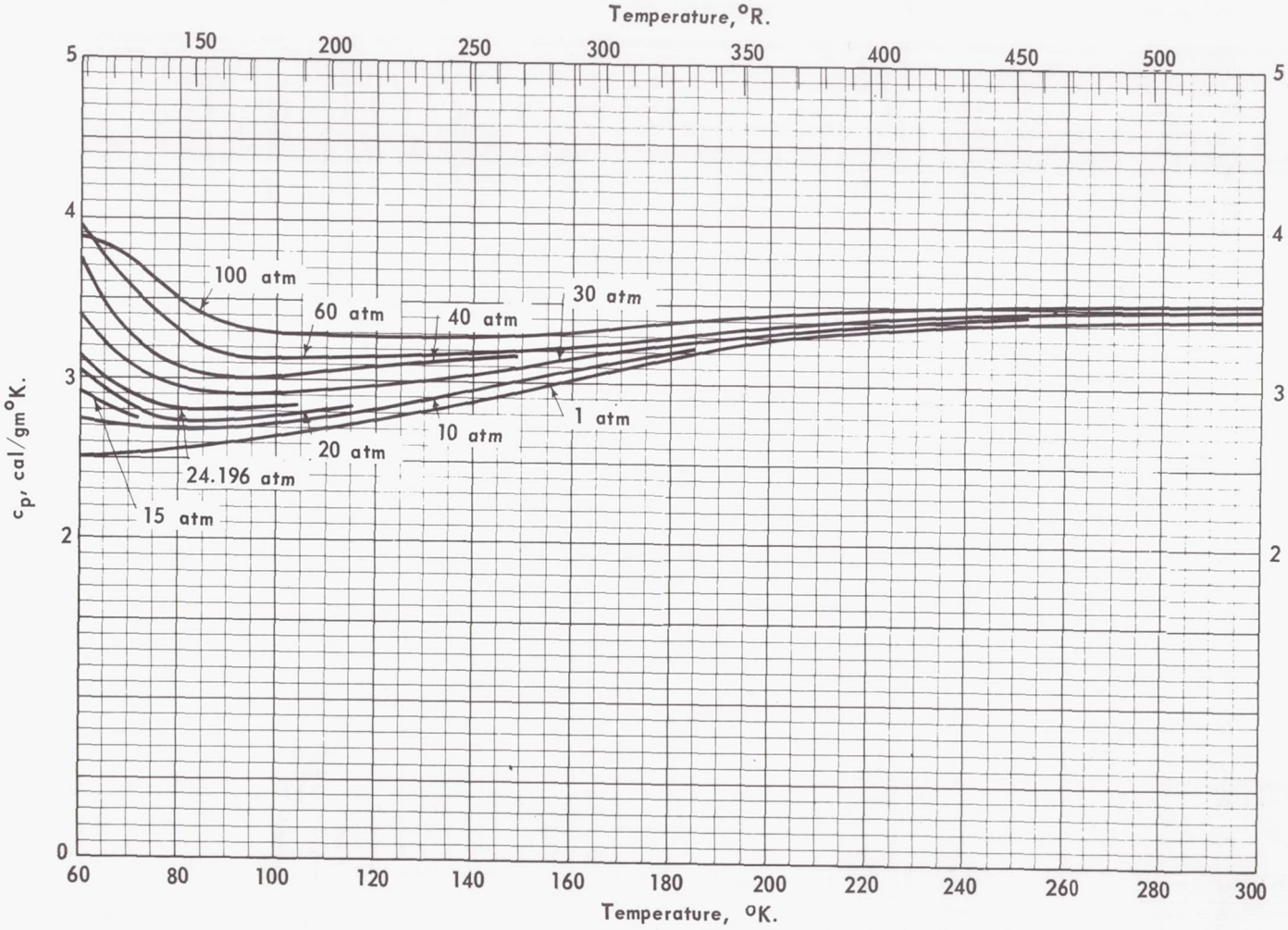


Figure E.6. Specific heat, c_p, versus temperature.—Continued. [*Reference WADD TR 60–56, Part I.*]

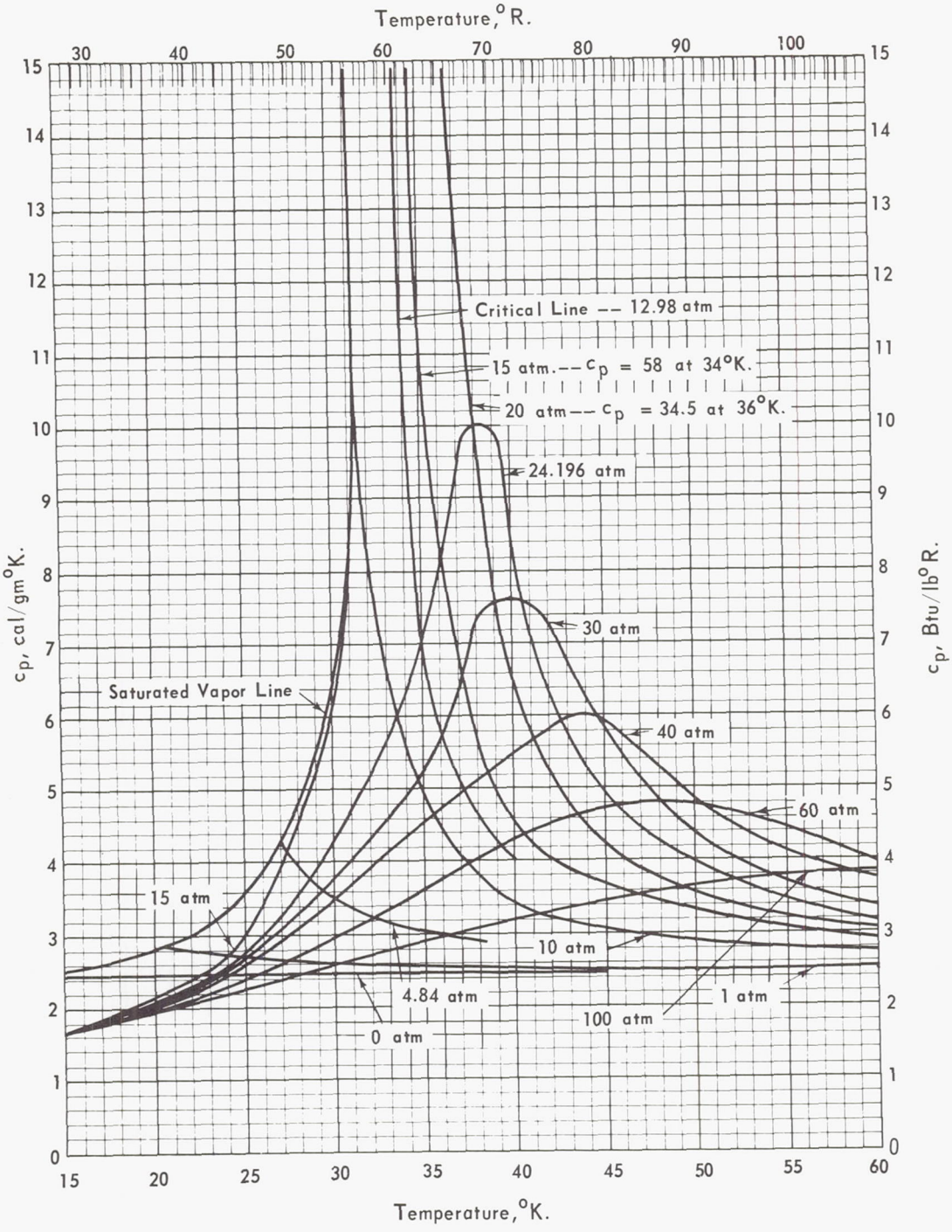


Figure E.6. Specific heat, c_p, versus temperature.—Concluded. [*Reference WADD TR 60–56, Part I.*]

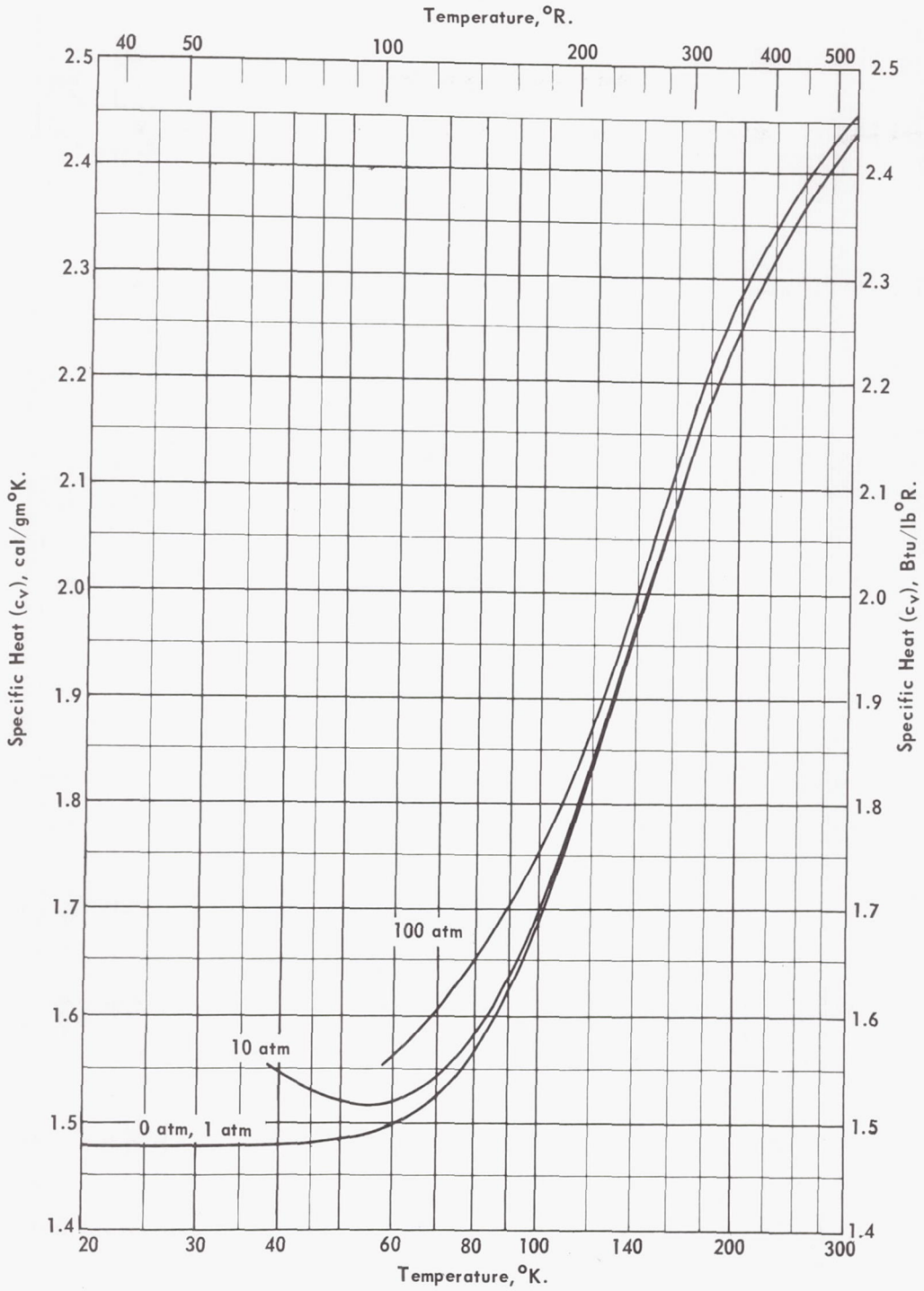


Figure E.7. Specific heat, c_v, versus temperature. [*Reference WADD TR 60–56, Part I.*]

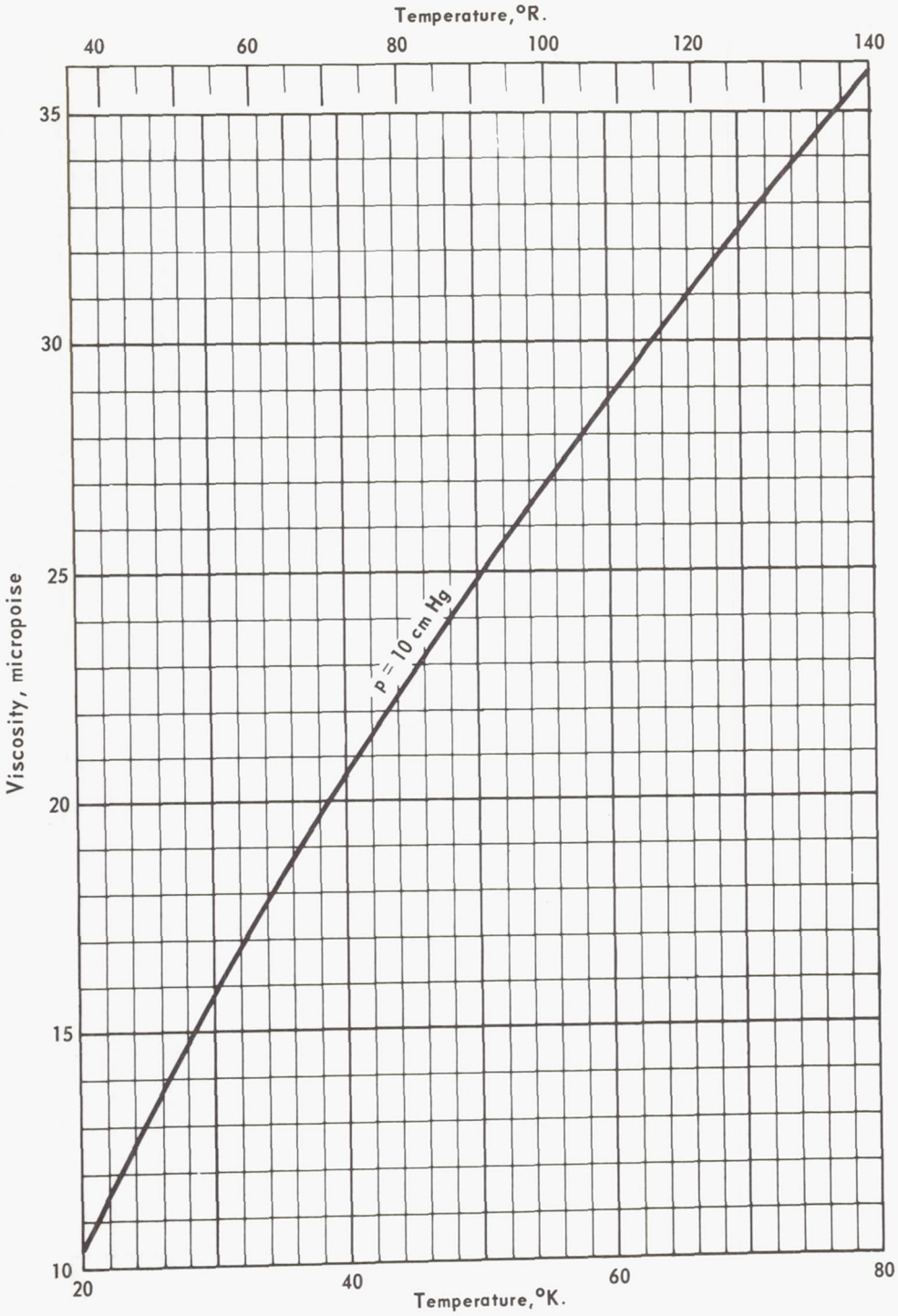


Figure E.8. Viscosity versus temperature.

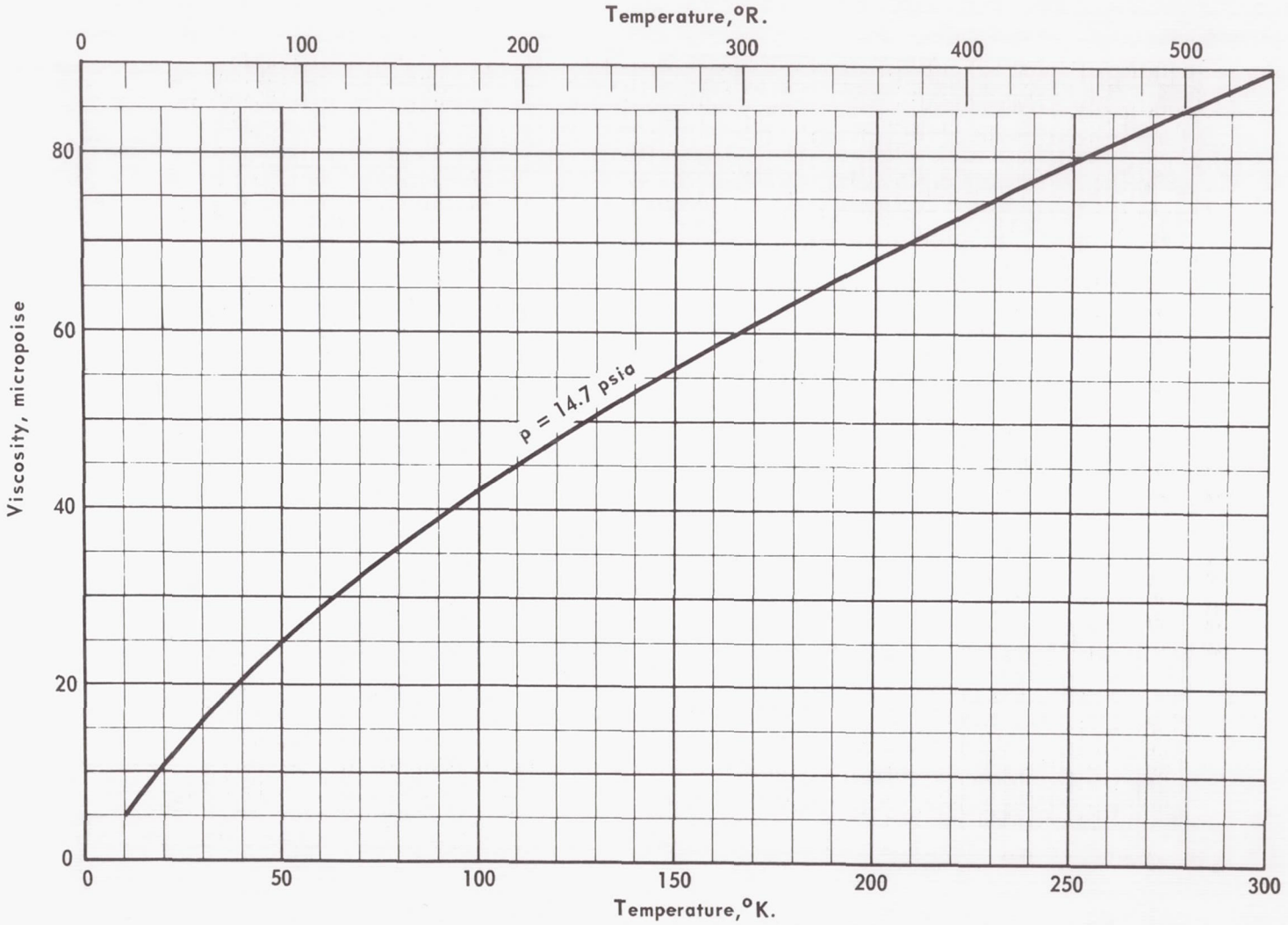


Figure E.8. Viscosity versus temperature.—Continued. [*Reference WADD TR 60–56, Part I.*]

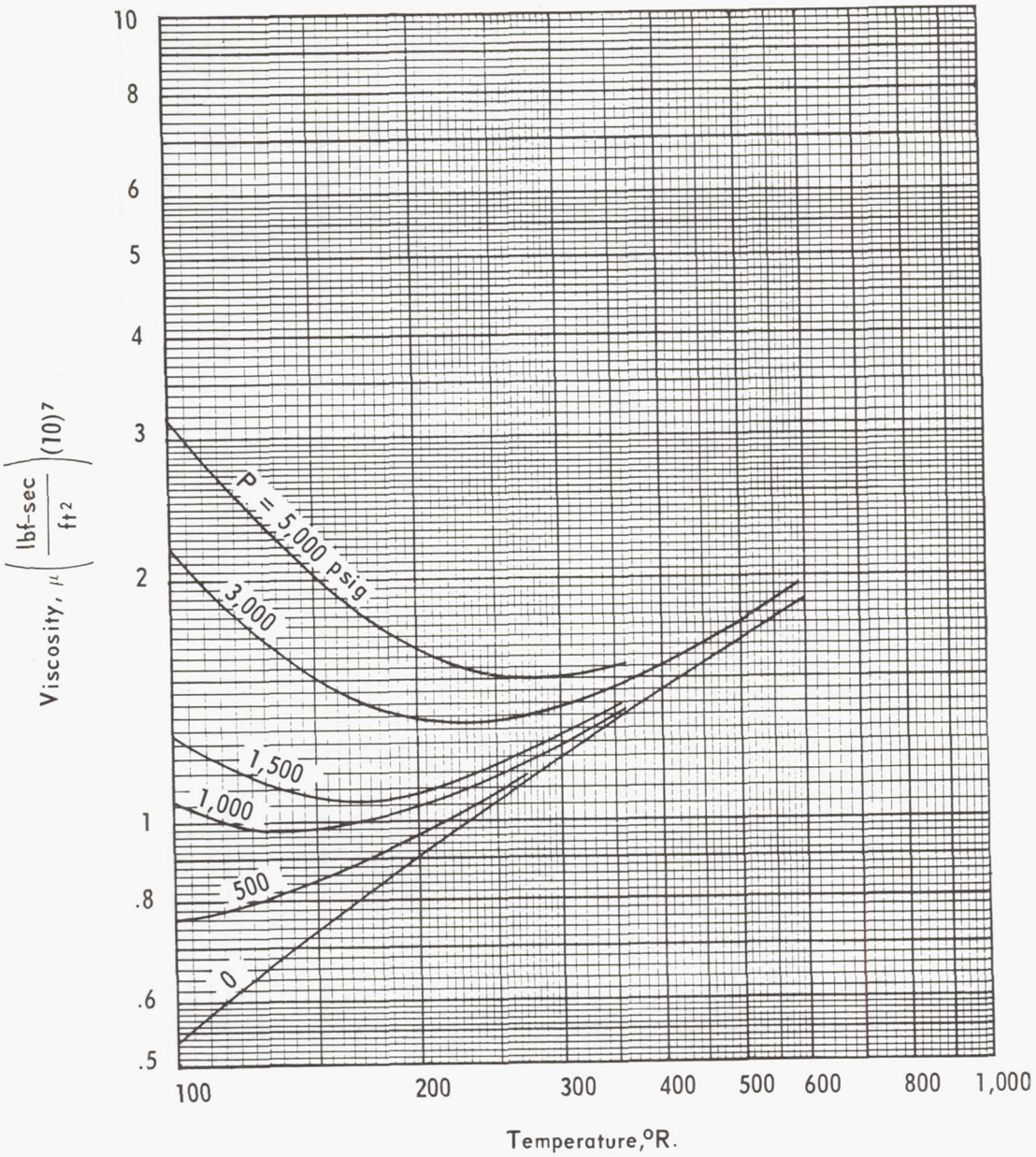


Figure E.8. Viscosity versus temperature. — Concluded. [*Reference WADD TR 60–56, Part I.*]

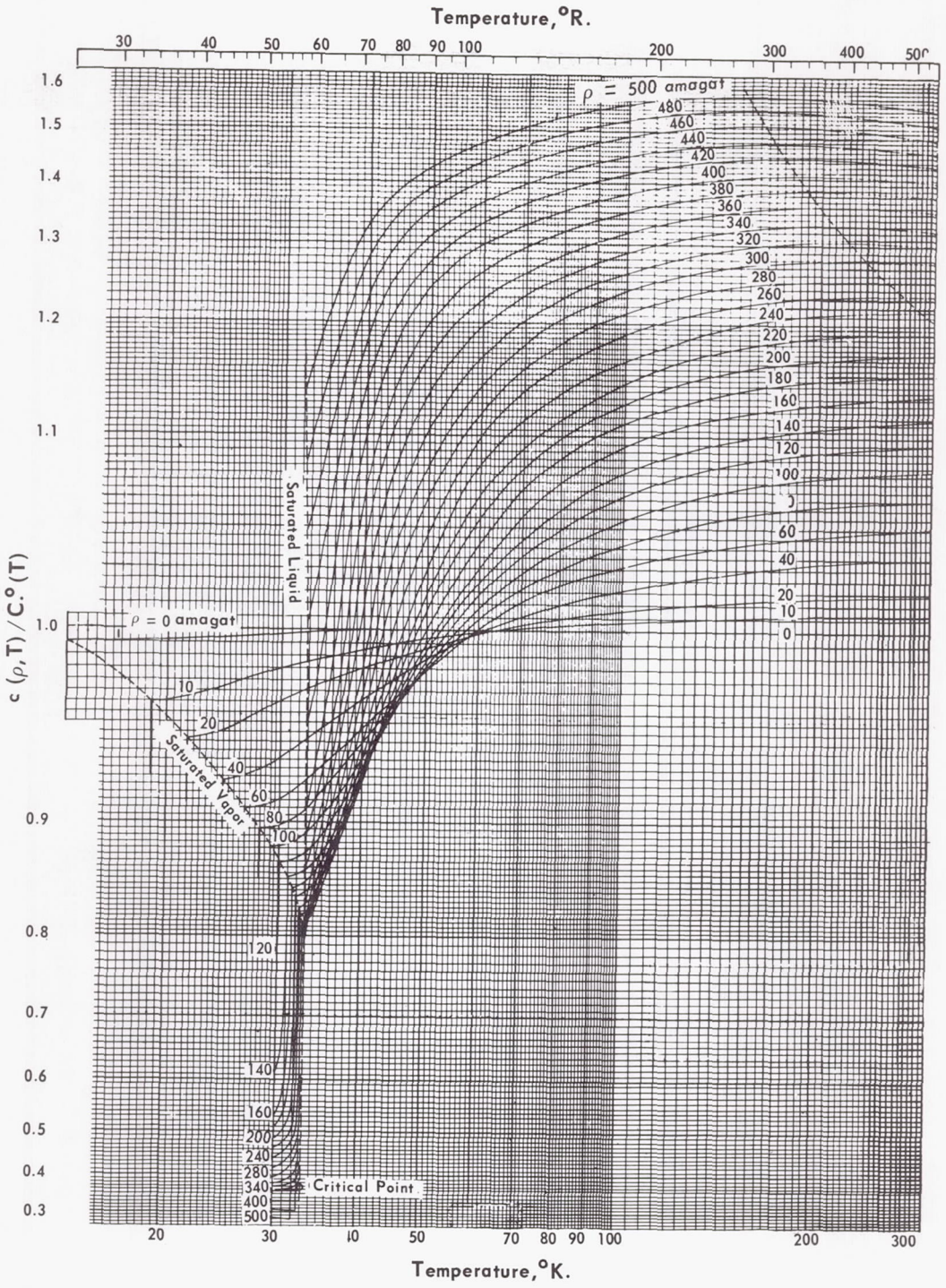


Figure E.9. Velocity of sound versus temperature. [*Reference WADD TR 60–56, Part IV.*]

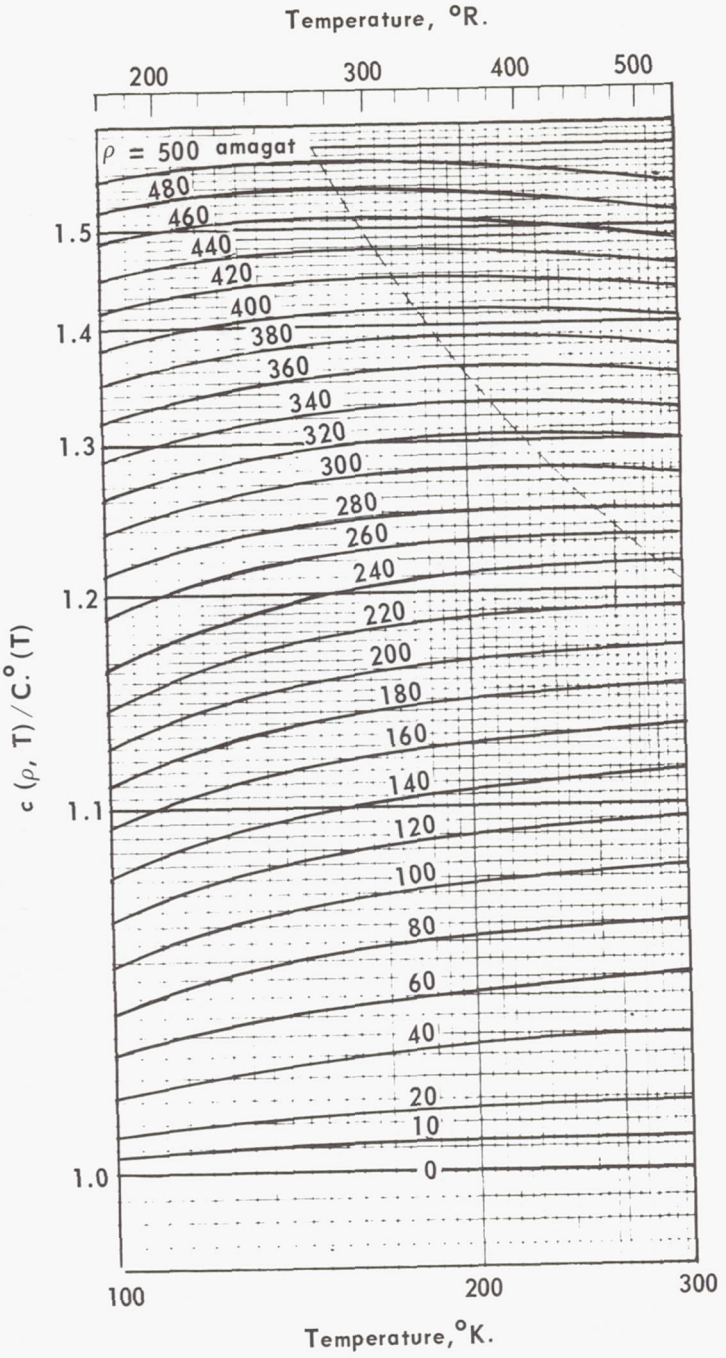


Figure E.9. Velocity of sound versus temperature.—Concluded. [*Reference WADD TR 60–56, Part IV.*]

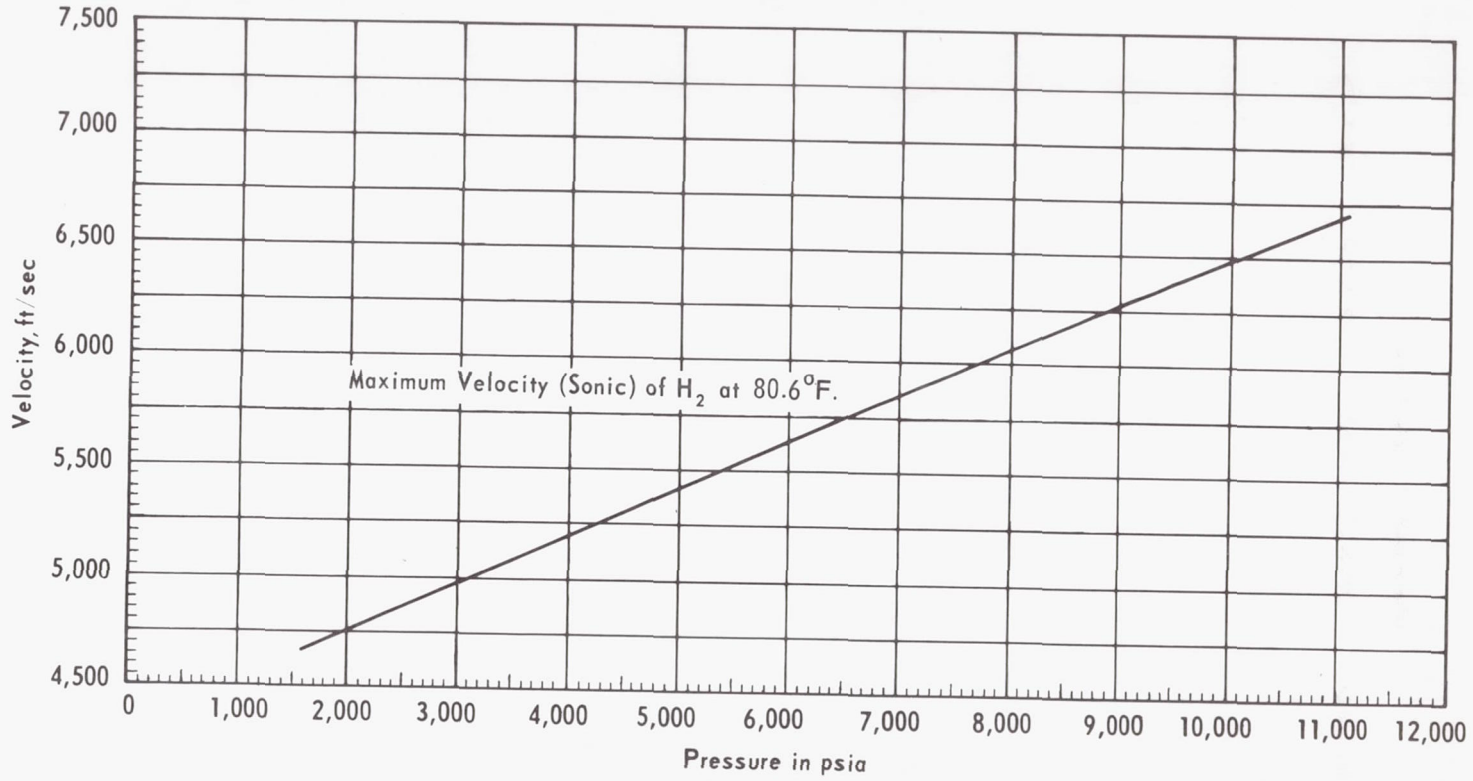


Figure E.10. Velocity of sound versus pressure. [*Reference NBS Chart D–10.*]

APPENDIX F

DATA ON ~~HYDROGEN~~ Oxygen

Preceding Page Blank

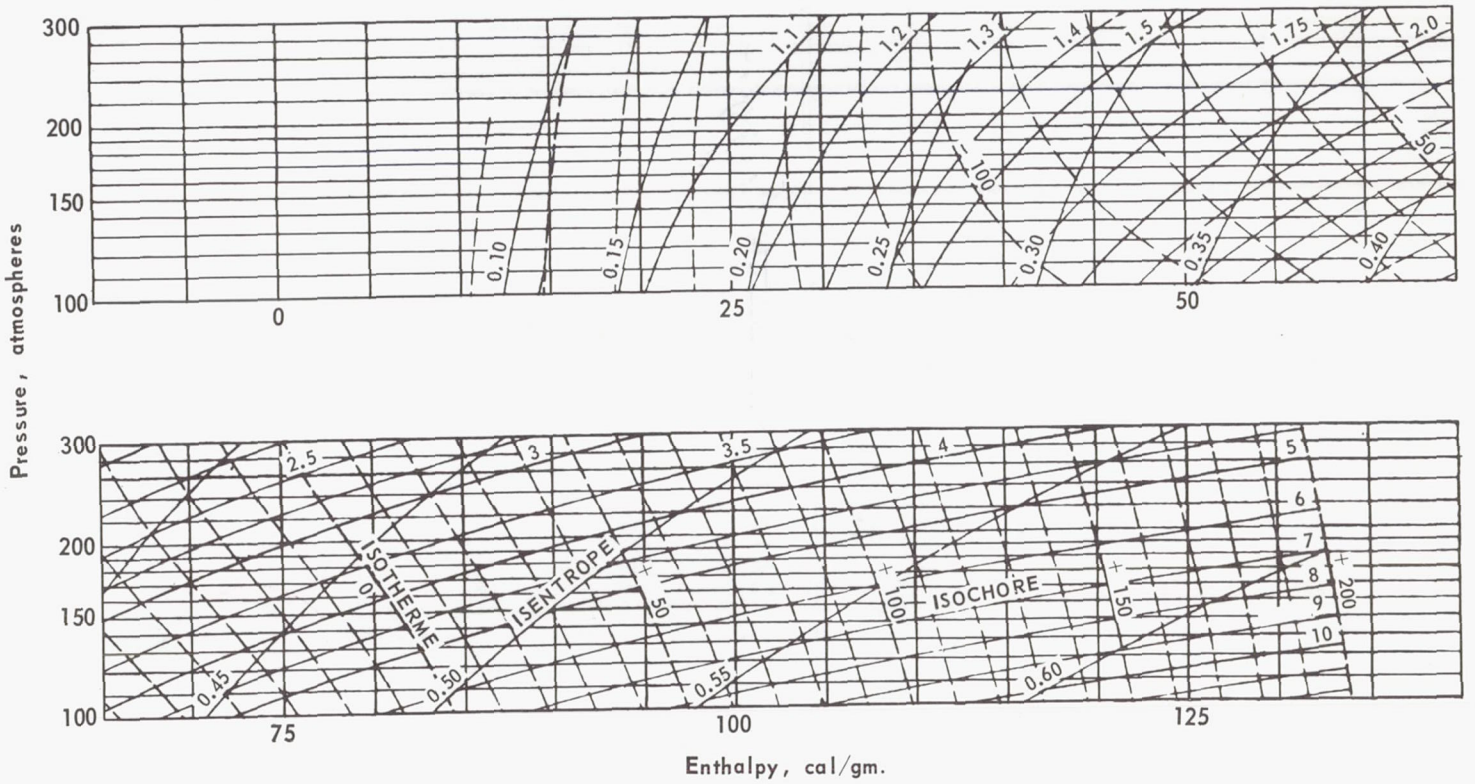


Figure F.1. Thermodynamic diagram, enthalpy versus pressure. [*Reference NBS Chart D–10.*]

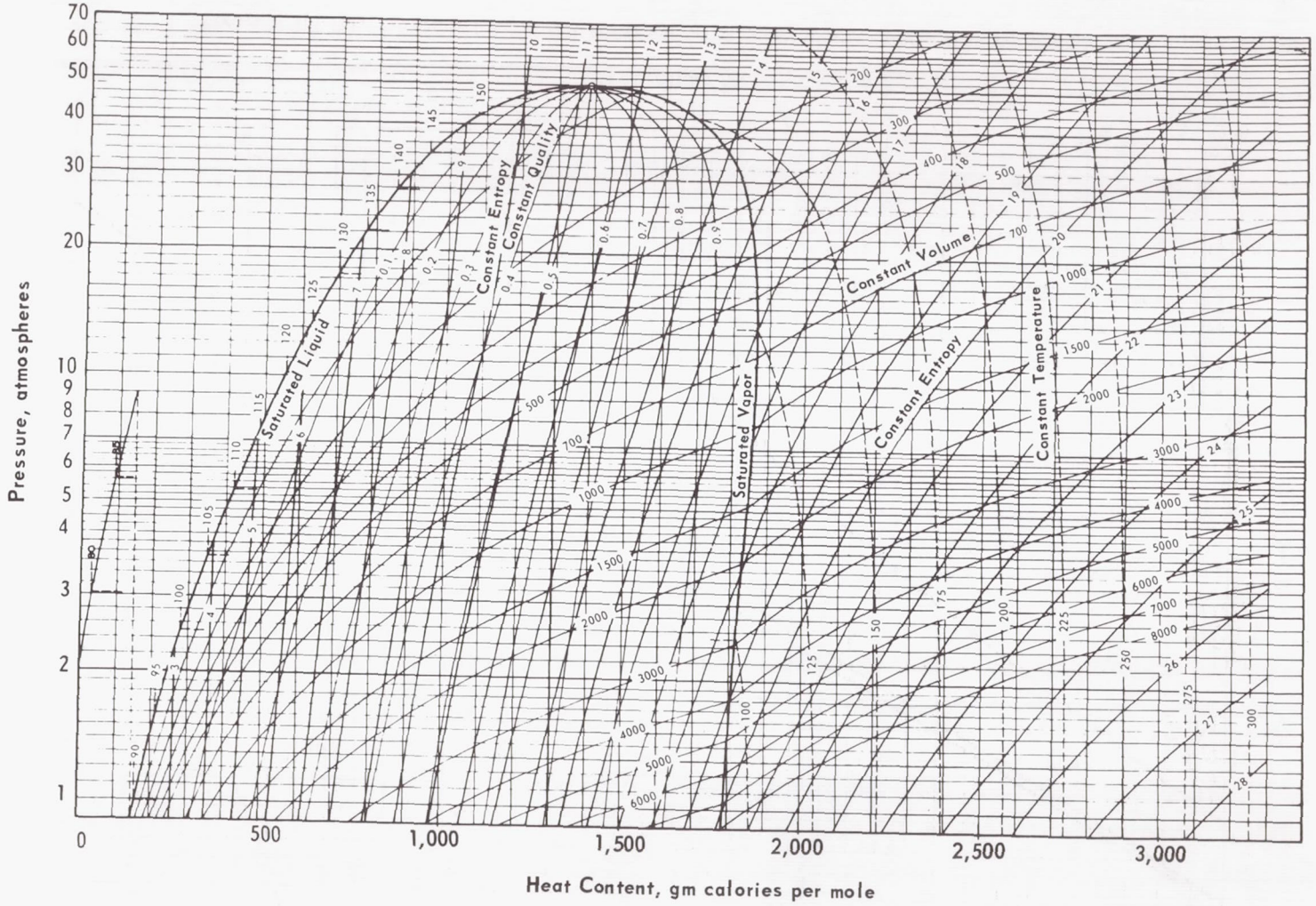


Figure F.2. Thermodynamic diagram, pressure versus heat content. [*Reference NBS Chart D–9.*]

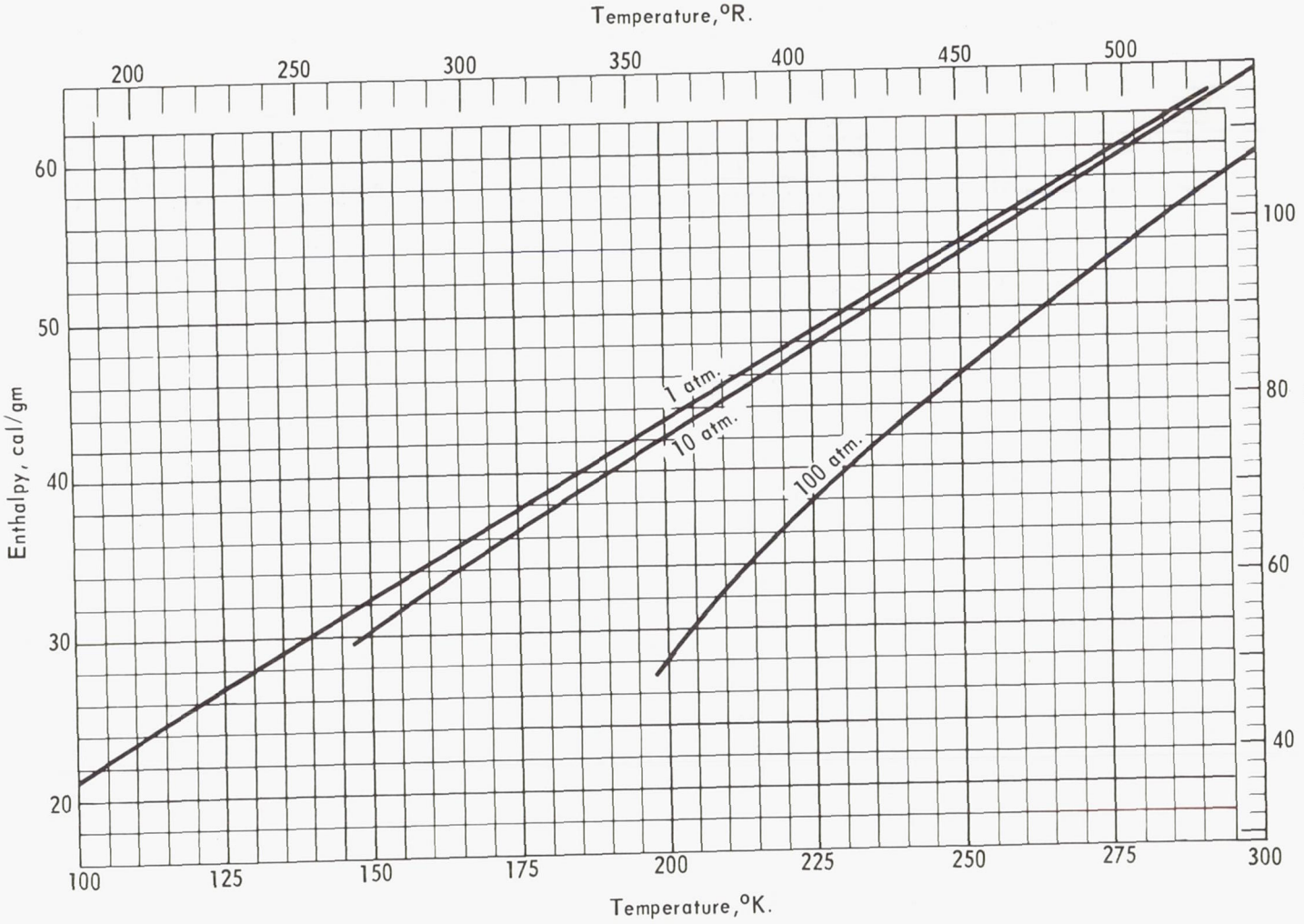


Figure F.3. Thermodynamic diagram, enthalpy versus temperature. [*Reference WADD TR 60–56, Part I.*]

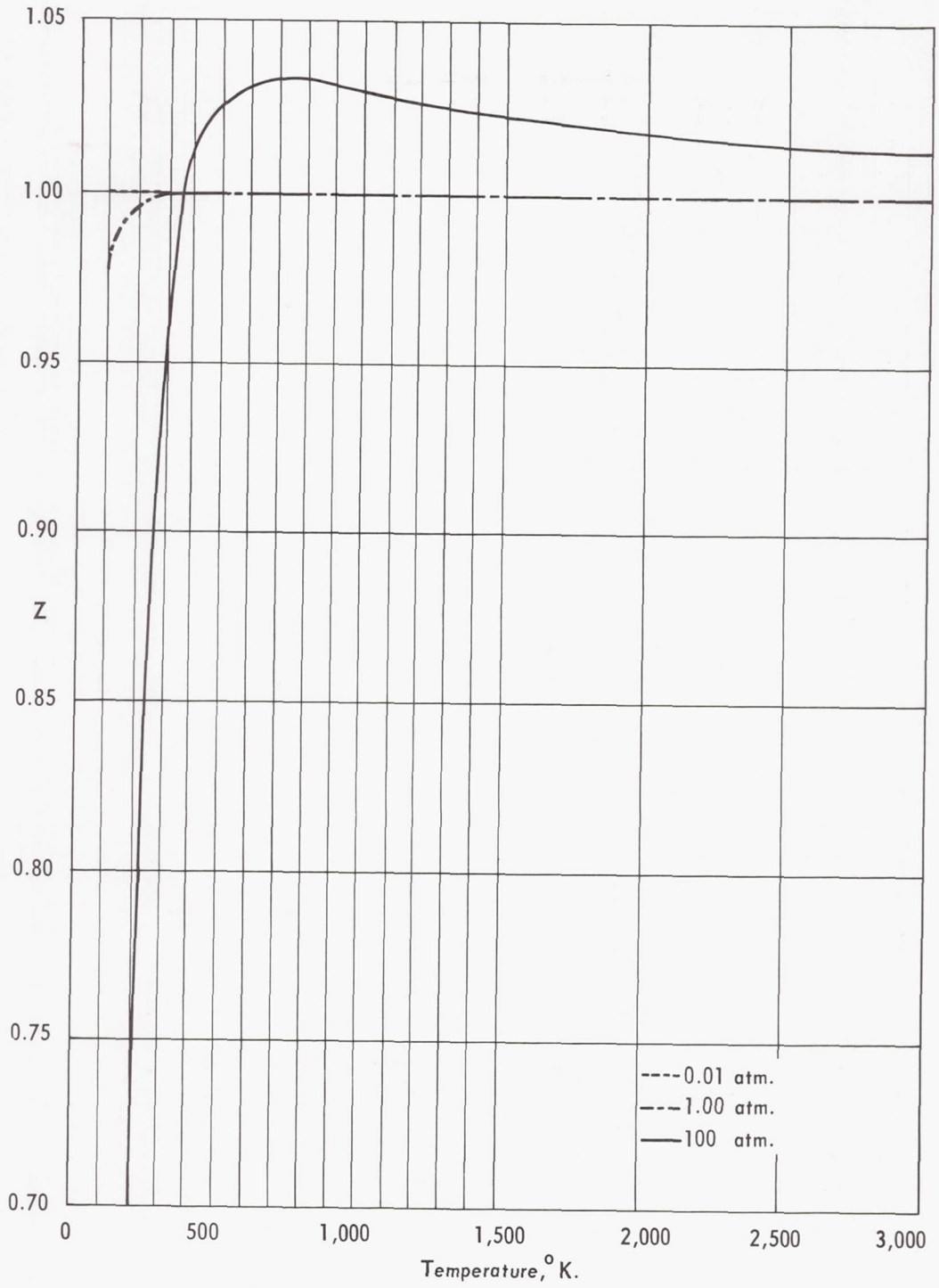


Figure F.4. Compressibility factor versus temperature.

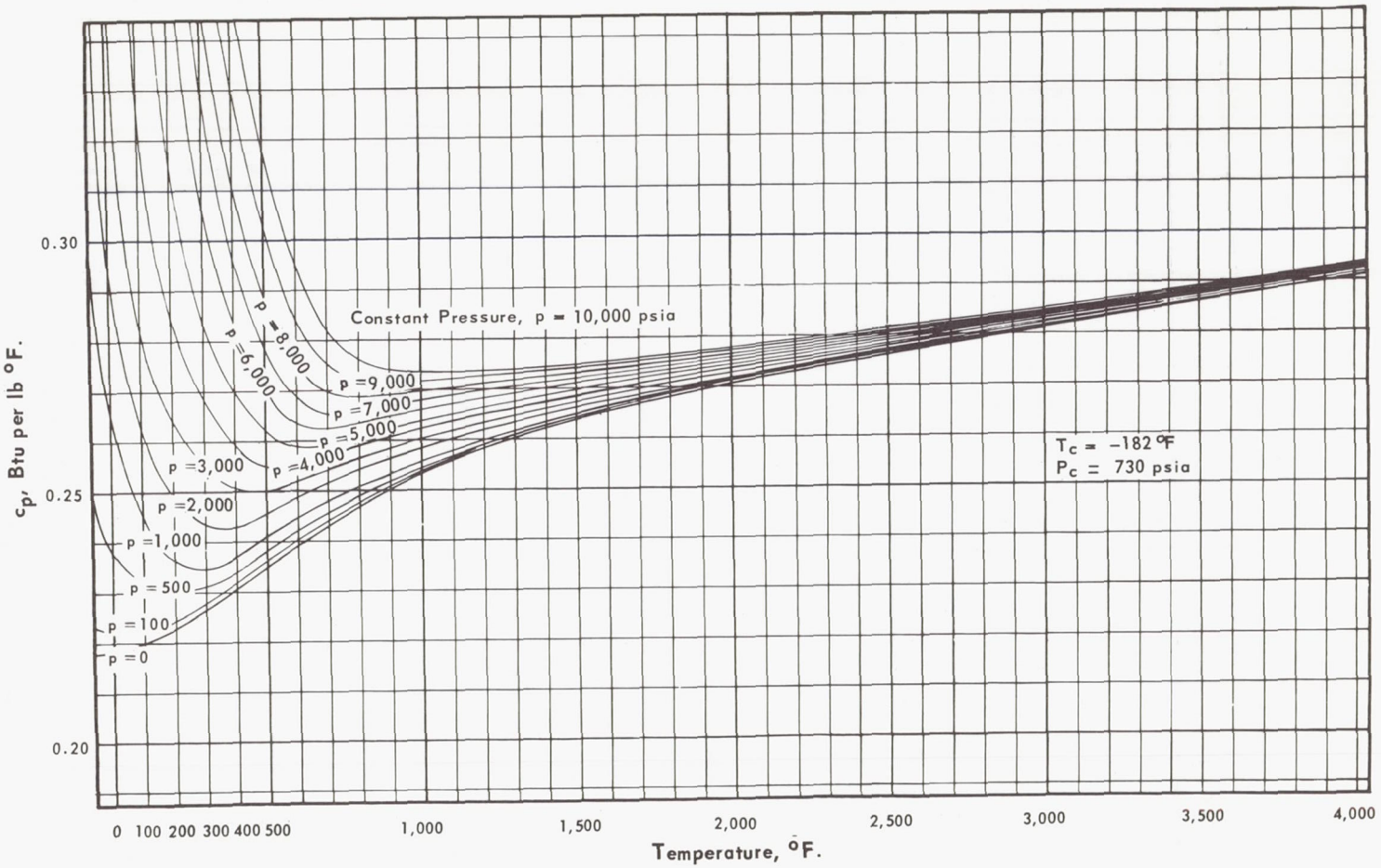


Figure F.5. Specific heat, c_p, versus temperature for gaseous oxygen. [*Courtesy of the Cornell University, Engineering Experiment Station Bulletin No. 30.*]

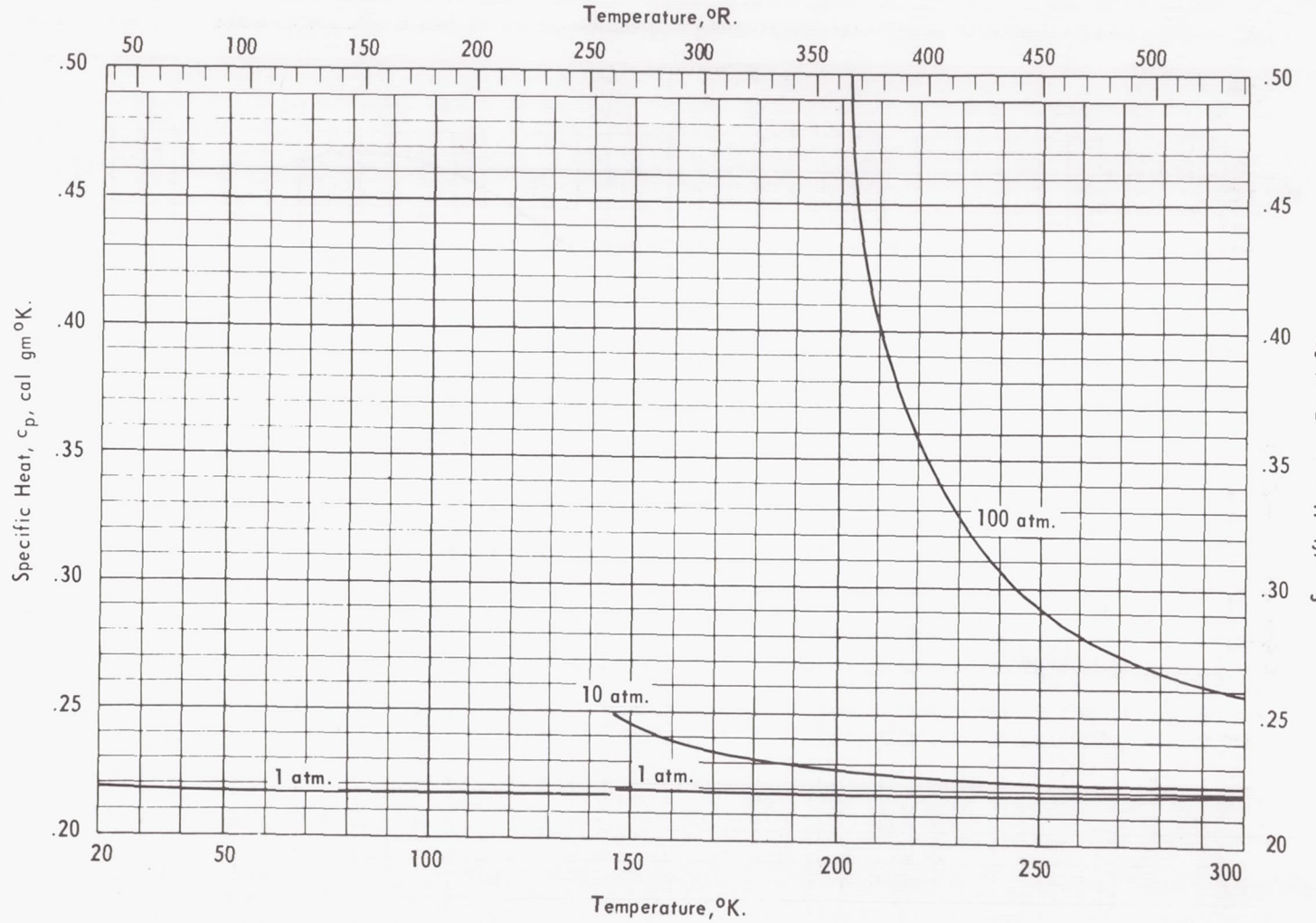


Figure F.5. Specific heat, c_p, versus temperature for gaseous oxygen. – Concluded. [*Reference WADD TR 60–56, Part I.*]

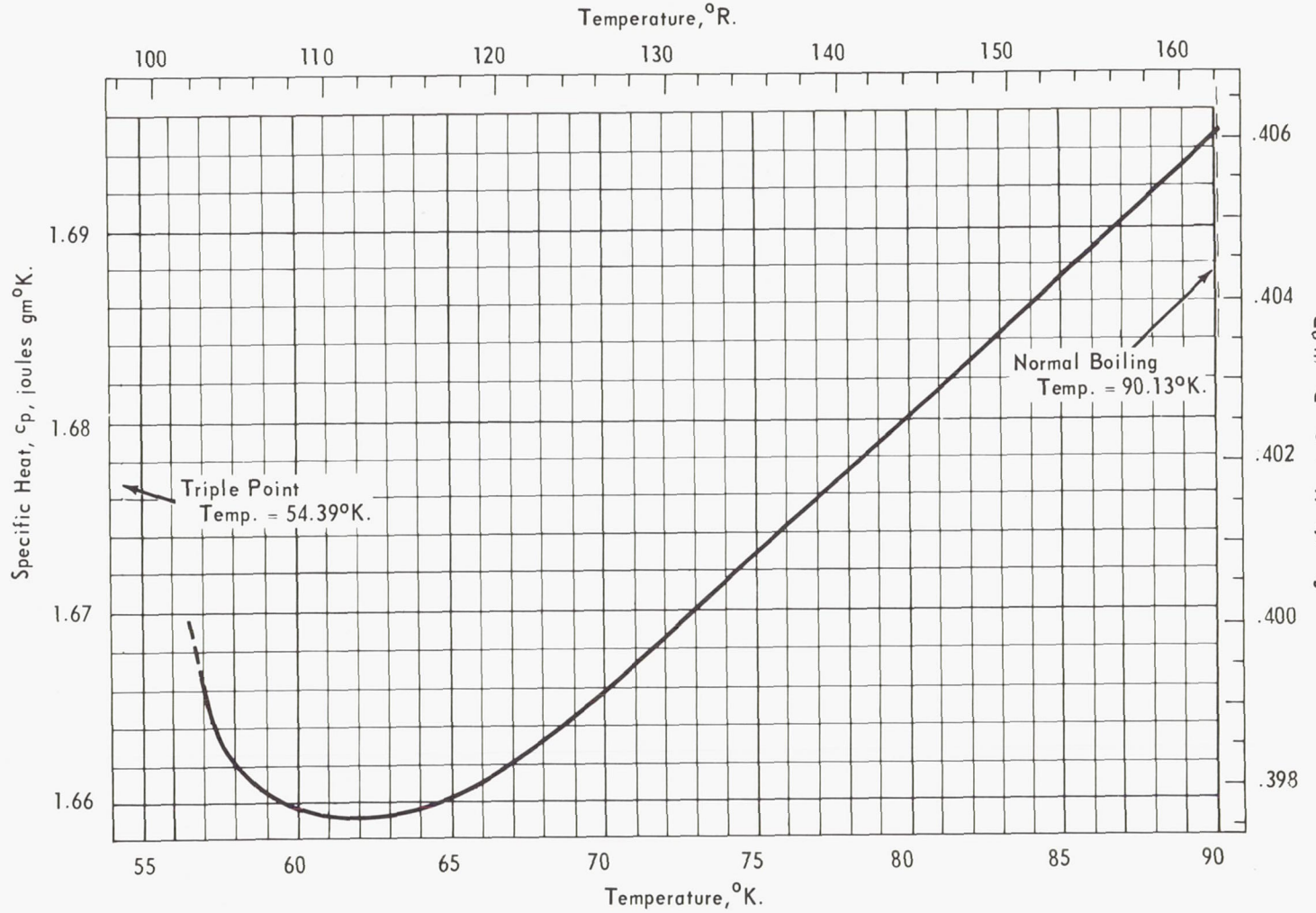


Figure F.6. Specific heat, c_p, versus temperature for liquid oxygen. [*Reference WADD TR 60–56, Part I.*]

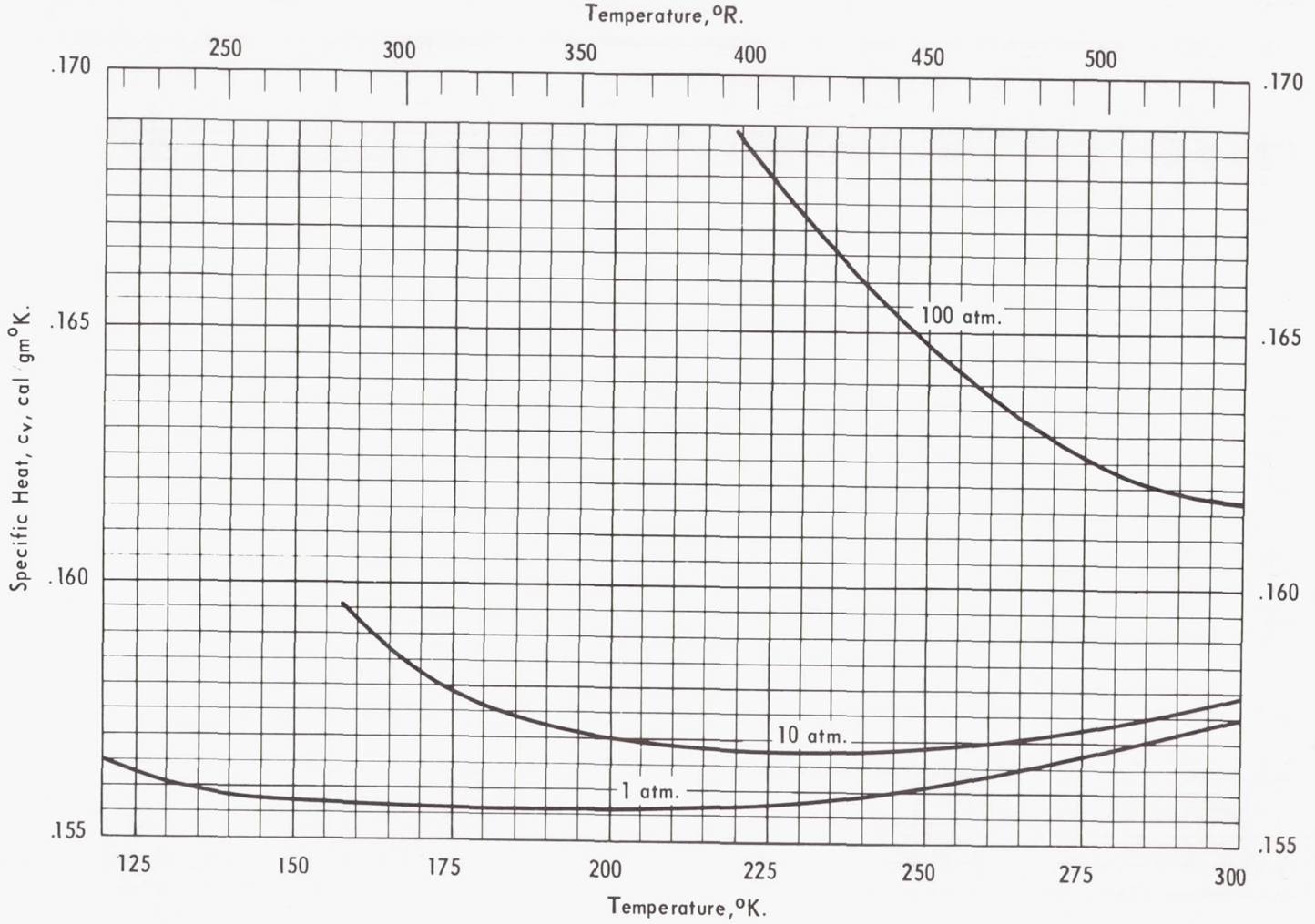


Figure F.7. Specific heat, c_v, versus temperature. [*Reference WADD TR 60–56, Part I.*]

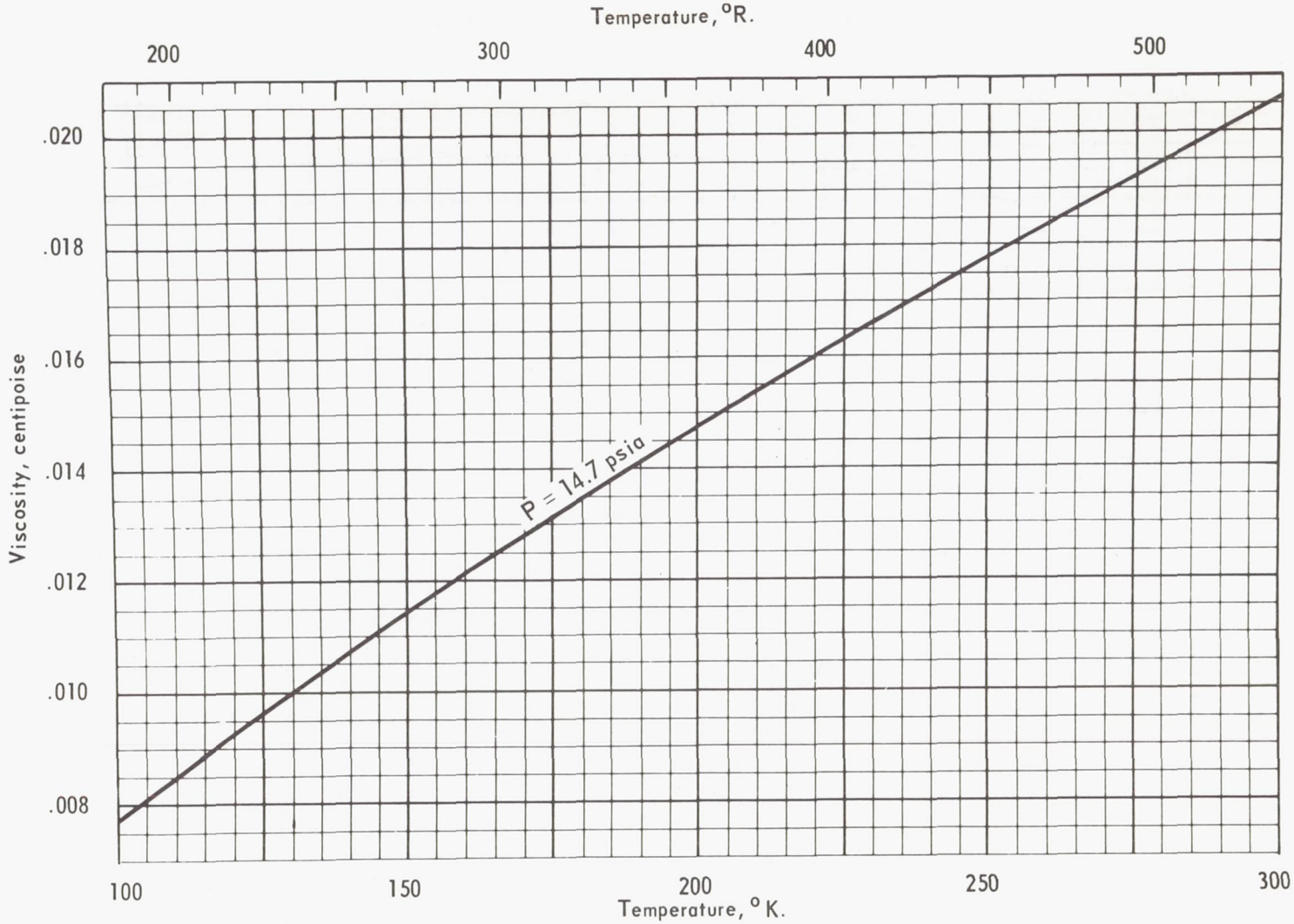


Figure F.8. Viscosity versus temperature for gaseous oxygen. [*Reference WADD TR 60–56, Part I.*]

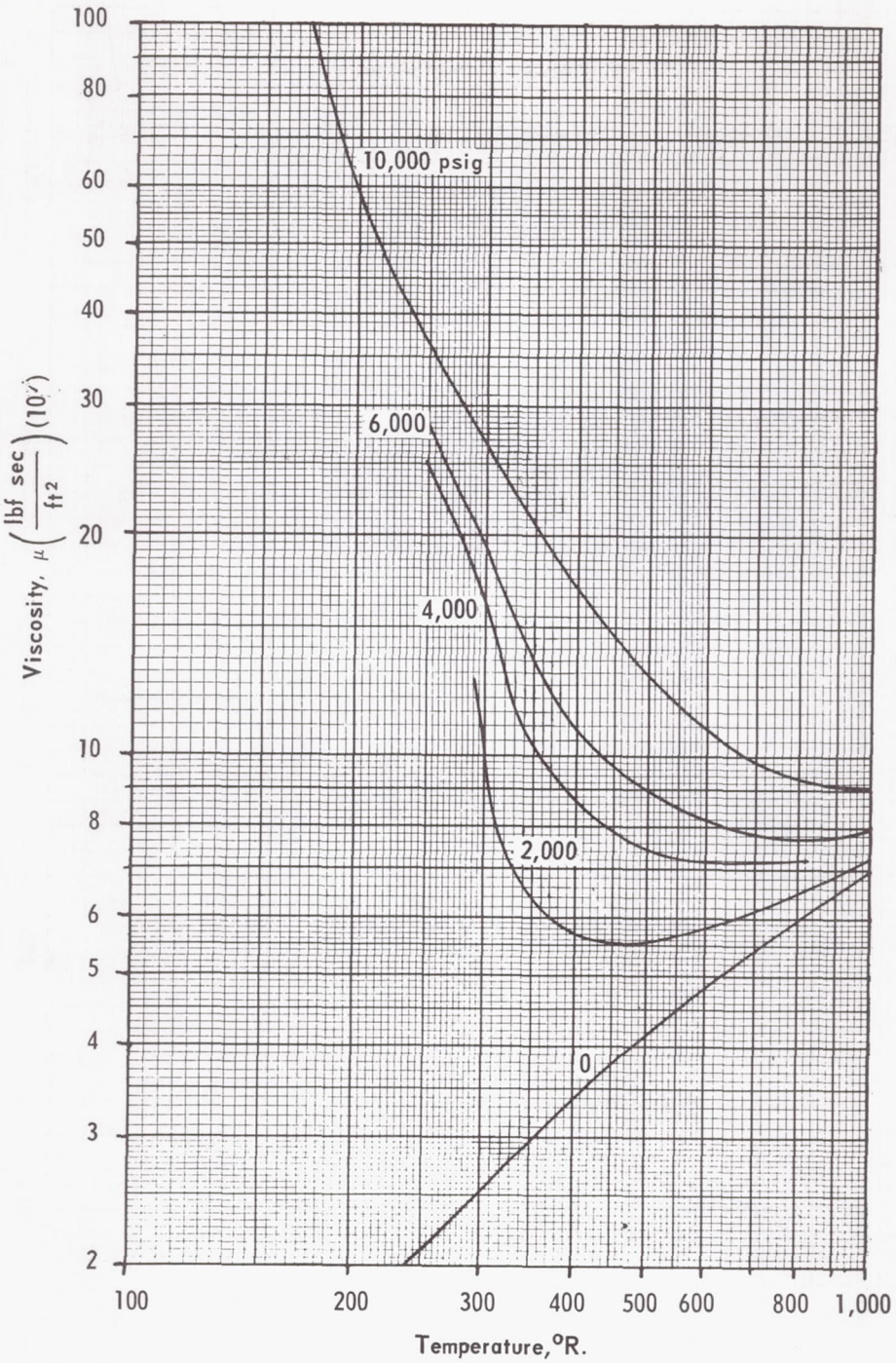


Figure F.8. Viscosity versus temperature for gaseous oxygen.—Concluded.

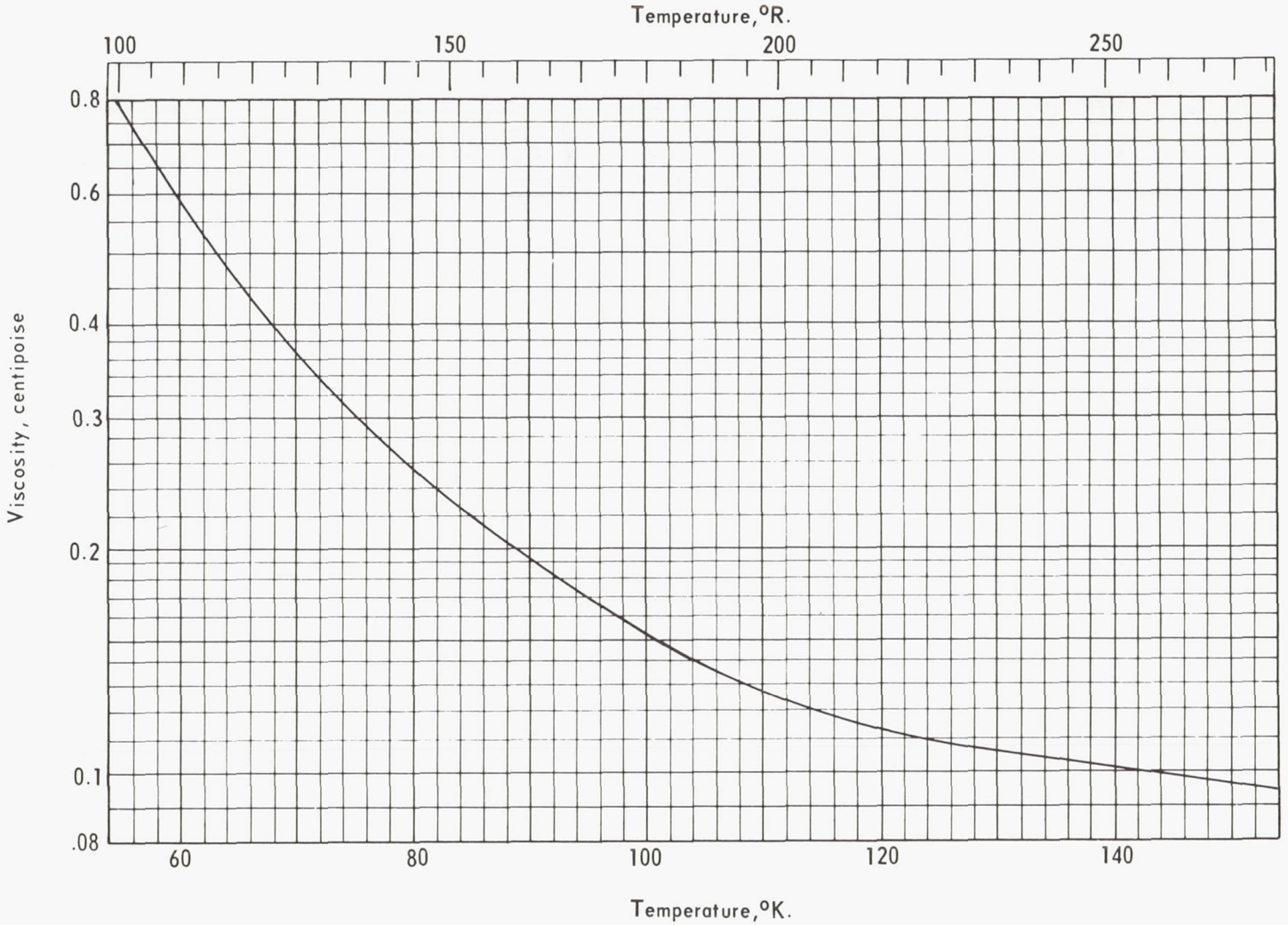


Figure F.9. Viscosity versus temperature for liquid oxygen. [*Reference WADD TR 60–56, Part I.*]

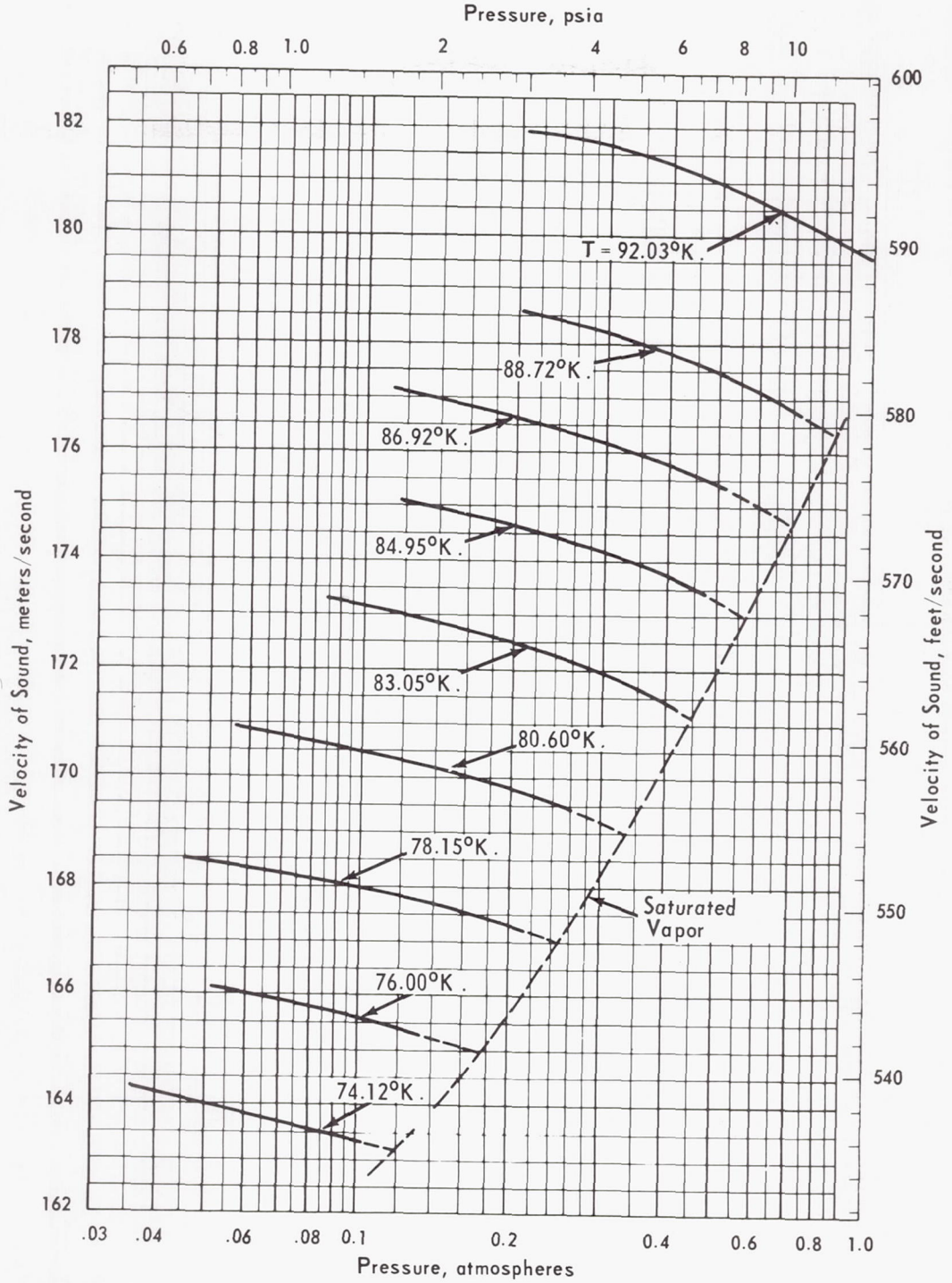


Figure F.10. Velocity of sound versus pressure in gaseous oxygen. [*Reference WADD TR 60–56, Part IV.*]

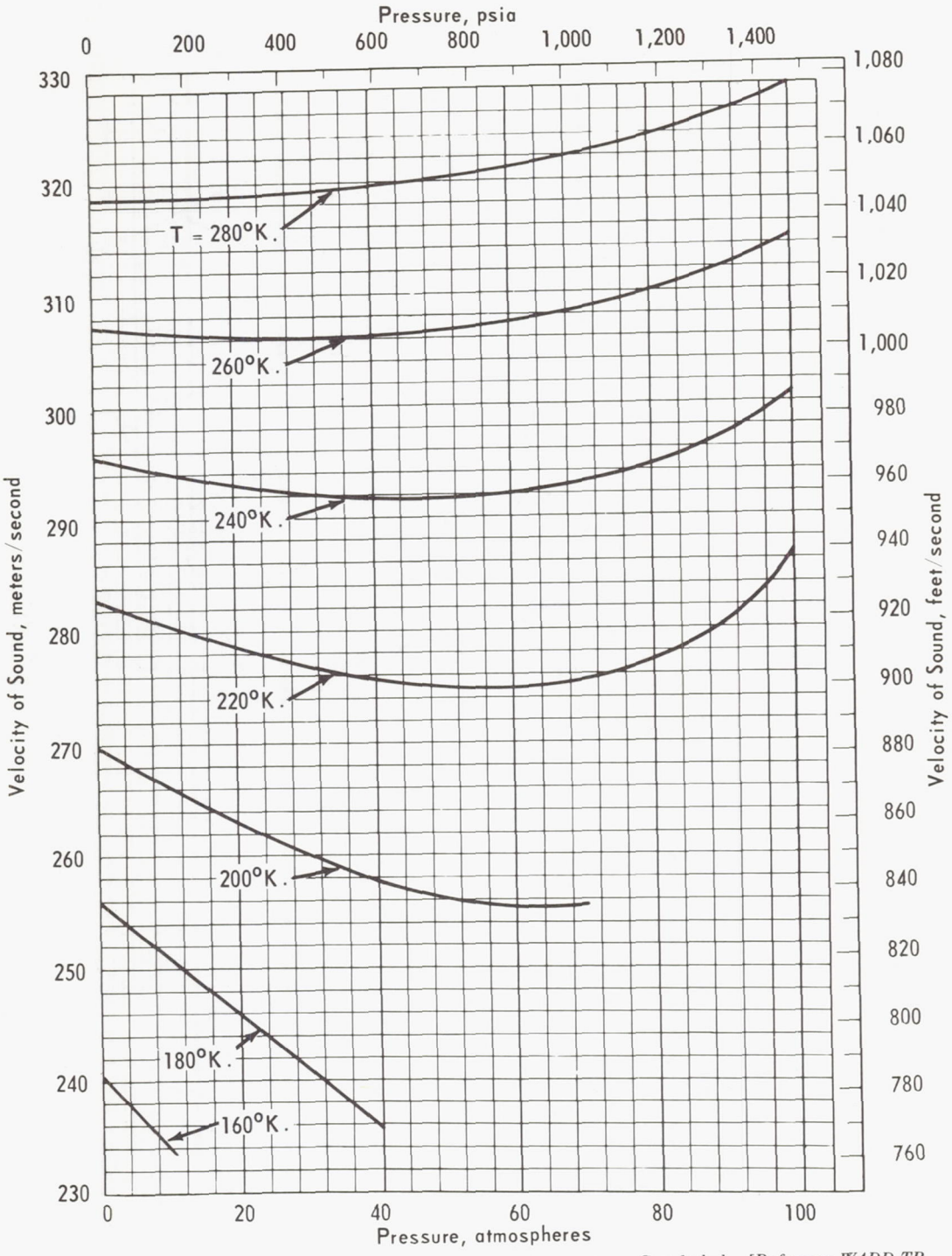


Figure F.10. Velocity of sound versus pressure in gaseous oxygen.—Concluded. [*Reference WADD TR 60–56, Part IV.*]

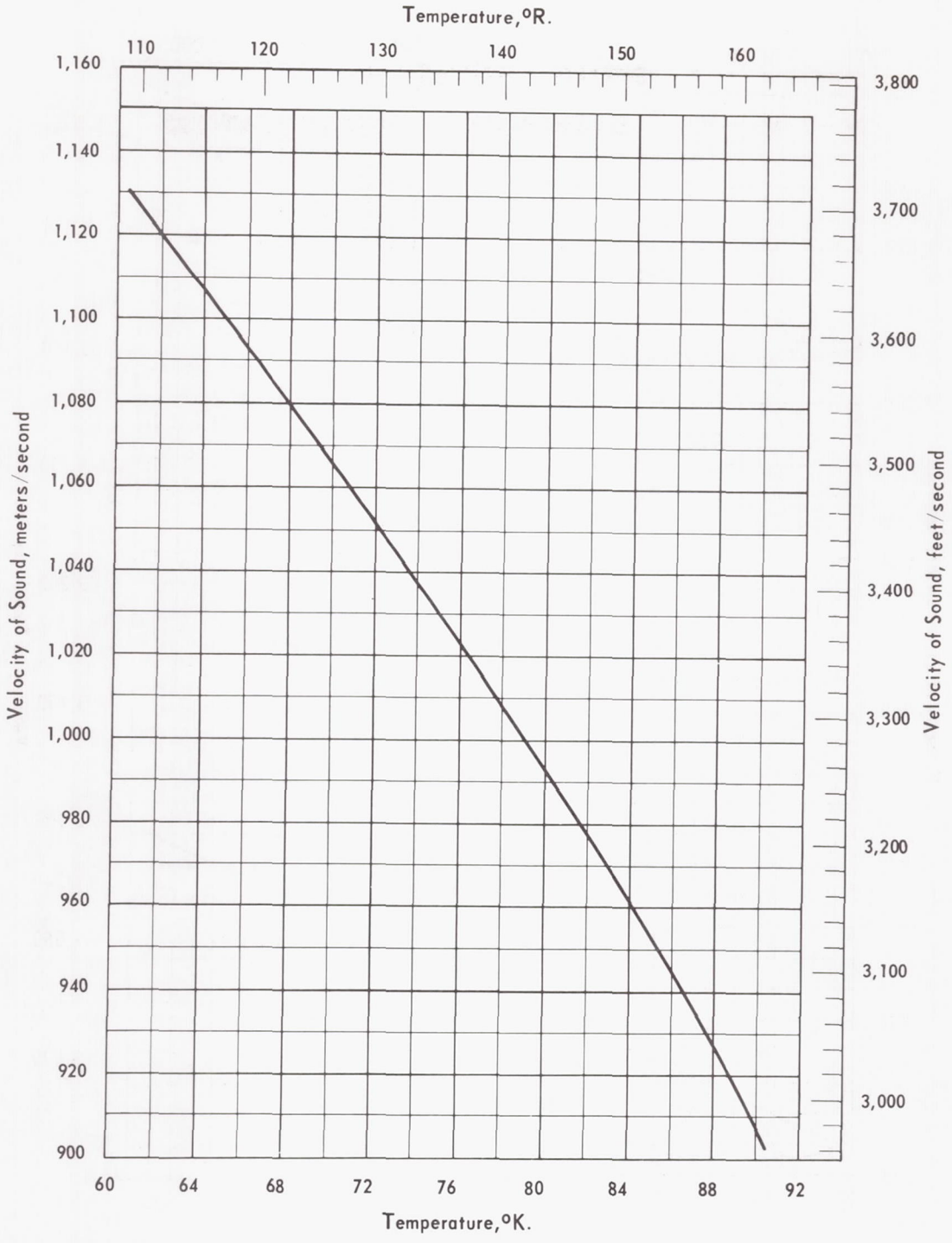


Figure F.11. Velocity of sound versus temperature in liquid oxygen. [*Reference WADD TR 60–56, Part IV.*]

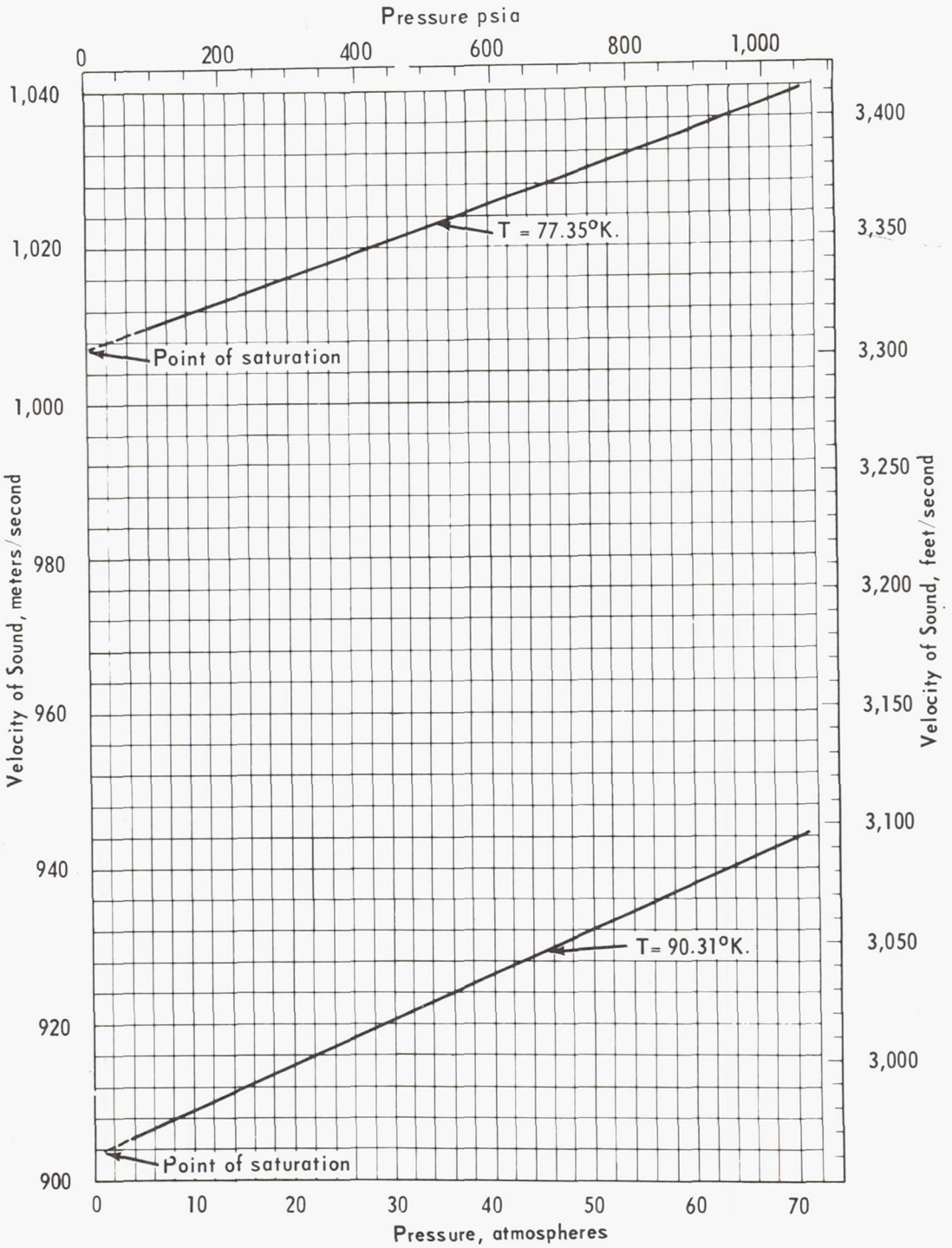


Figure F.12. Velocity of sound versus pressure in liquid oxygen. [*Reference WADD TR 60–56, Part IV.*]

U.S. GOVERNMENT PRINTING OFFICE : OL 1969—325–994